University of Glasgow

Hydrogenation and low temperature hydrodeoxygenation of oxygen-substituted aromatics over a Rh/SiO_2 catalyst

Kathleen Kirkwood

Submitted in fulfilment of the requirements for the Degree of PhD

School of Chemistry

College of Science and Engineering

University of Glasgow

April 2020

1 Abstract

One of the main areas of energy consumption is the transportation sector, where at present the vast majority of fuel comes from crude oil. Well documented environmental concerns over the use of fossil fuels has driven a search for alternative sources of energy and one focus is on second generation biofuels from agricultural waste. The most abundant source for candidate biofuels is lignocellulosic biomass which contains hemicellulose (25-35 %), cellulose (40-50 %) and lignin (15-20 %), with the exact composition dependent on the plant species present. The focus of this study is on the components of bio-oil derived from lignin and in particular the p-hydroxyphenyl and guaiacol based monomers. Lignocellulosic biomass can be converted into liquid bio-oil via fast pyrolysis at 673–873 K in the absence of air with multiple reactions taking place. The result is a bio-oil that contains over 300 individual compounds, many of them oxygenates, limiting their value as increased oxygen content is the cause of many of the negative properties of bio-oil such as low heating value, corrosiveness, high viscosity and instability. The challenge to try and selectively remove the oxygen has gathered considerable momentum, with efforts focused on catalytic hydrodeoxygenation (HDO) and hydrogenation. Currently, there is limited understanding of the mechanisms involved in this process and our study aims to increase knowledge in this area.

Hydrogenation of dihydroxybenzene, cresol and methoxyphenol isomers was studied over a Rh/SiO_2 catalyst at mild operating conditions (303-343 K, 3 barg H_2). Reaction temperature and substrate concentration were varied to assess their effect on reactivity and HDO activity. Isomers were reacted together to uncover the effect of the competitive environment on reaction rate and behaviour. To gain further insight into the reaction mechanism, substrates were reacted with deuterium to ascertain overall and product KIE values. TPO analysis was carried out on spent catalysts under standard conditions to investigate the extent of carbon laydown.

Dihydroxybenzene isomers were studied initially, and deoxygenated products (cyclohexanone, cyclohexanol and cyclohexane) were formed in significant amounts; the *meta* and *para* isomers (resorcinol and hydroquinone) favoured HDO product formation over conventional hydrogenated products (hydroxycyclohexanone and cyclohexanediol). The lack of any deoxygenation or isomerisation activity when the aromatic substrate was replaced by *cis*-cyclohexanediol led to the proposal of an independent and direct route for both HDO and hydrogenated products. The HDO products are believed to form via highly reactive surface intermediates whereby the position of the double-bond β-γ to hydroxyl

group facilitates the C-OH bond cleavage more readily. The *trans* isomer was shown not to occur via an isomerization mechanism, and instead was proposed to form exclusively from hydrogenation of the ketone intermediate product.

To understand the effect changing a substituent had on the hydrogenation reactivity and HDO favourability, the cresol isomers were tested under identical reaction conditions. In this instance, it was the *ortho* isomer which showed the greatest favourability towards the deoxygenated product (methylcyclohexane), however, all three isomers favoured the standard hydrogenated products (methylcyclohexanone and methylcyclohexanol) overall. A clear substituent effect was shown to exist, with a shift in the HDO favourability of each isomer and a change in overall order in reactivity apparent when a hydroxyl group was replaced with a methyl group. The methyl group on the *ortho* isomer was shown to interact directly with the catalyst surface through NMR analysis, this exchange was significantly reduced with both the *meta* and *para* isomers. This suggests the existence of a different mode of adsorption for the *ortho* isomer and may explain its increased favourability towards HDO.

The effect of substituent was investigated further by studying the hydrogenation of the methoxyphenol isomers under identical reaction conditions. Similar to the dihydroxybenzenes, the *meta* and *para* isomers favoured HDO products (cyclohexanone, cyclohexanol, cyclohexane and methoxycyclohexane) over conventional hydrogenated products (methoxycyclohexanone, methoxycyclohexanol). Order in reactivity was also in accordance with that observed for the dihydroxybenzenes indicating the presence of two oxygen-containing substituents resulted in similar substrate behaviour. The hydrogenation of 4-methoxyphenol was particularly interesting as secondary hydrogenation was completely absent: the only instance that this was observed. This is postulated to be a result of the adsorption/desorption kinetics when the bulky methoxy group and hydroxyl group are in the *para* position to one another.

A significant reduction in reactivity was observed for all substrates in the competitive environment. When combined, the three isomers of each substrate and the corresponding isomers from each set of substrates, gave a uniform rate constant, independent of substituent nature and position. This shows competition for limited surface hydrogen and active sites on the catalyst surface is the major factor influencing reactivity in these competitive situations. Calculated overall and product KIE values from competitive deuterated reactions showed a change in reaction mechanism from that observed during individual hydrogenation, and again highlights the complex nature of these reactions. This

substantial change in behaviour and reactivity observed in the competitive environment substantially limits the value of studying a single model compound as a route to understanding a true bio-oil feed.

It is notable that during the deuterated reaction of *ortho*-cresol, no *cis*-2-methylcyclohexanol was detected and formation of the HDO product, methylcyclohexane, was delayed until 60 minutes into the reaction; significantly different behaviour to that observed during the hydrogenation reaction.

Extended run reactions of the dihydroxybenzene isomers showed a substantial drop in conversion associated with deactivation of the catalyst; confirmed by spent catalyst TPO analysis to be a result of carbonaceous deposits. TPO analysis of post reaction catalysts from standard reactions for each substrate showed the existence of a direct relationship between percentage of carbon found and substituent nature. The post-reaction catalysts of those substrates that exhibited the highest levels of HDO showed the presence of additional carbon, phenolic in nature, arising from the formation of these products.

2 Acknowledgements

First and foremost, I would like to express my sincere gratitude to my supervisor Professor David Jackson. I am so thankful for you giving me the opportunity to do the PhD and for all your help with all my questions no matter how big or small. Thank you for everything!

I would like to thank my industrial sponsor, Innospec, for funding my PhD and in particular to Ian McRobbie for all his help and guidance throughout.

Andrew Monaghan I am particularly grateful for all your support and assistance throughout my PhD. Thank you so much for all the help, the well needed laughs, tea and chocolate and everything else and I know we will be friends for life!

Caitlin Moffat I will miss our lunch time break and working alongside you everyday, thank you for all the fun and laughter you brought me and for being an amazing friend. To all the past and present members of the Jackson and Hargreaves group thanks for everything.

Thanks so much to my mum and dad for always being there and pushing me on throughout my studies and helping me through it all in more ways than possible. My cousin, Katie, who is a sister to me, thank you for the constant support.

My best friends you have been amazing, and I am so grateful for you all in my life.

I would like to dedicate this thesis to my guardian angel brother, David, who has been with me every step of the way.

3 Declaration

I declare that, except where explicit reference is made to the contribution of others, that this thesis is the result of my own work and has not been submitted for any other degree at the University of Glasgow or any other institution.

Table of Contents

4 Introduction

4.1 Future Developments in Catalysis

The development of catalysts for the conversion of biomass has grown significantly in recent years, driven by increasing awareness of environmental issues. The drive for renewable, cleaner sources of energy as an alternative to fossil fuels dominates current research around the world with various renewable energy sources (*e.g.*, solar, wind and hydrogen) employed. [1] The issue has become even more prescient as world demand for energy is expected to double before 2050, due to the development of our society and population growth, in conjunction with depleting fossil fuel reserves. [2,3] Currently, 85 % of world energy production comes from fossil fuels with the resultant negative environmental and climatic effects from the emission of huge quantities of CO_2. One of the largest areas of energy consumption is transportation of both people and goods accounting for 1/5 of the total energy usage. Previous research in first generation biofuels, which focused on food sources, highlighted a number of serious concerns such as the impact on food availability resulting from crops being specifically grown as biofuels. As a response to these issues research has shifted towards the development of a second generation of biofuels sourced from agricultural waste. [4-11]

Lignocellulosic biomass is the most abundant of the potential new biofuel sources and the minimal environmental effects associated with its use make it an ideal carbon resource. [12] In addition, biomass shows significant potential as a carbon feedstock in the chemical industry opening further possibilities for the exploitation of this widely available, yet underutilized material. It is composed of hemicellulose (25-35 %), cellulose (40-50 %) and lignin (15-20 %), however the exact composition is dependent on the plant species present in the biomass feedstock and the pre-treatment conditions used. [13] The extremely complicated structure of lignin, which presently is still not fully understood, has led to it being the most under used of the three constituent parts. Lignin originates from oxidative polymerization of one or more of the 3 main types of hydroxycinnamyl alcohol precursors: 4-hydroxycinnamyl alcohol, coniferyl alcohol and sinapyl alcohol which in turn give rise to p-hydroxyphenyl, guaiacyl, and syringyl, referred to as H-unit, G-unit and S-unit as shown in Figure 1 below: [14]

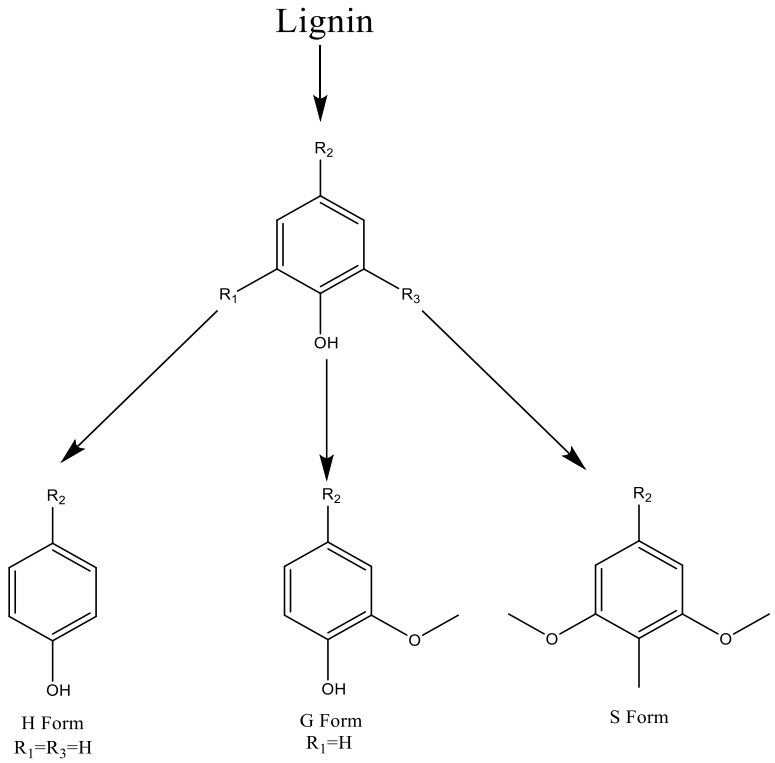

Figure 1. The 3 sub-units of lignin.

Biomass can be converted to liquid biofuels through thermochemical processes. In recent decades biomass fast pyrolysis has emerged as one of the most promising routes for the conversion of lignocellulosic biomass to liquid bio-fuels. In this process, lignin is converted to compounds such as phenol, catechol, anisole, guaiacol and cresol [7] through heating to 673–873K in the absence of air. During this procedure, multiple reactions take place including dehydration, depolymerisation, re-polymerization, fragmentation and rearrangement resulting in the production of a bio-oil containing over 300 individual compounds, of which large amounts are oxygenates. The crucial difference between bio-oil and crude oil is the elemental composition, most notably the concentration of oxygen; bio-oil ~ 28-40 %, crude oil < 1 %, [15] which results in an unstable, corrosive bio-oil with high viscosity, and low high heating value limiting its application as a bio-fuel. Commercial viability requires upgrading of the bio-oil by decreasing the oxygen content; however, the presence of such a wide variety of compounds and current lack of insight into the reaction mechanisms make this a difficult process.

4.2 Hydrodeoxygenation

The aim to selectively reduce the oxygen content of bio-oil is currently achieved via 2 catalytic processes: hydrodeoxygenation (HDO) and zeolite cracking. [16] The HDO reaction has gathered considerable attention in recent years and uses hydrodesulphurization (HDS) catalysts such as Co-MoS_2/Al_2O_3 or Ni-MoS_2/Al_2O_3. The most effective HDO

reactions involve a stabilisation step using mild hydrogenation to remove the most reactive components including the ketones and aldehydes; followed by high temperature (573-723 K) treatment to remove oxygen. [17-20] Issues with current zeolite cracking procedures, such as catalyst deactivation through carbon laydown and production of bio-oils with a heating value 25 % lower than crude oil, has resulted in a shift in research emphasis towards HDO. [4,18] Currently there is limited insight into the complex mechanisms involved in the HDO process; an increased understanding of these is vital to successful upscaling of the process. [21]

As previously mentioned, $CoMo/Al_2O_3$ and $NiMo/Al_2O_3$ catalysts are those favoured for HDO, where Mo acts as the active element and Co or Ni play the role of promoters. [4,22] In recent years there has been a shift from conventional sulfide catalysts to noble metals; known to be active at activating hydrogen under mild conditions and exhibiting increased activity and selectivity when supported. [23] The greatest challenge with HDO is catalyst deactivation due to coking, sintering and interaction with water and sulfides. [24-27] Of these the commonest route is from coking, where carbon formed by polymerization and polycondensation reactions blocks the catalyst pores and results in a decrease in the available active sites. The extent of this coking is influenced by reaction operating conditions, the type of oxy-compounds and the catalyst employed. [28]

A deactivation study was carried out by Bouxin *et al.* [21] on the hydrodeoxygenation of *para*-methylguaiacol over silica supported rhodium and platinum catalysts, with *para*-methylguaiacol employed as a model compound for the G-unit of lignin. Numerous reactions, including demethylation, demethoxylation and hydrogenation, can occur during this process and the mechanisms for many of these are still not fully understood. An example of the reaction scheme that can take place for *para*-methyl guaiacol is shown below in Figure 2:

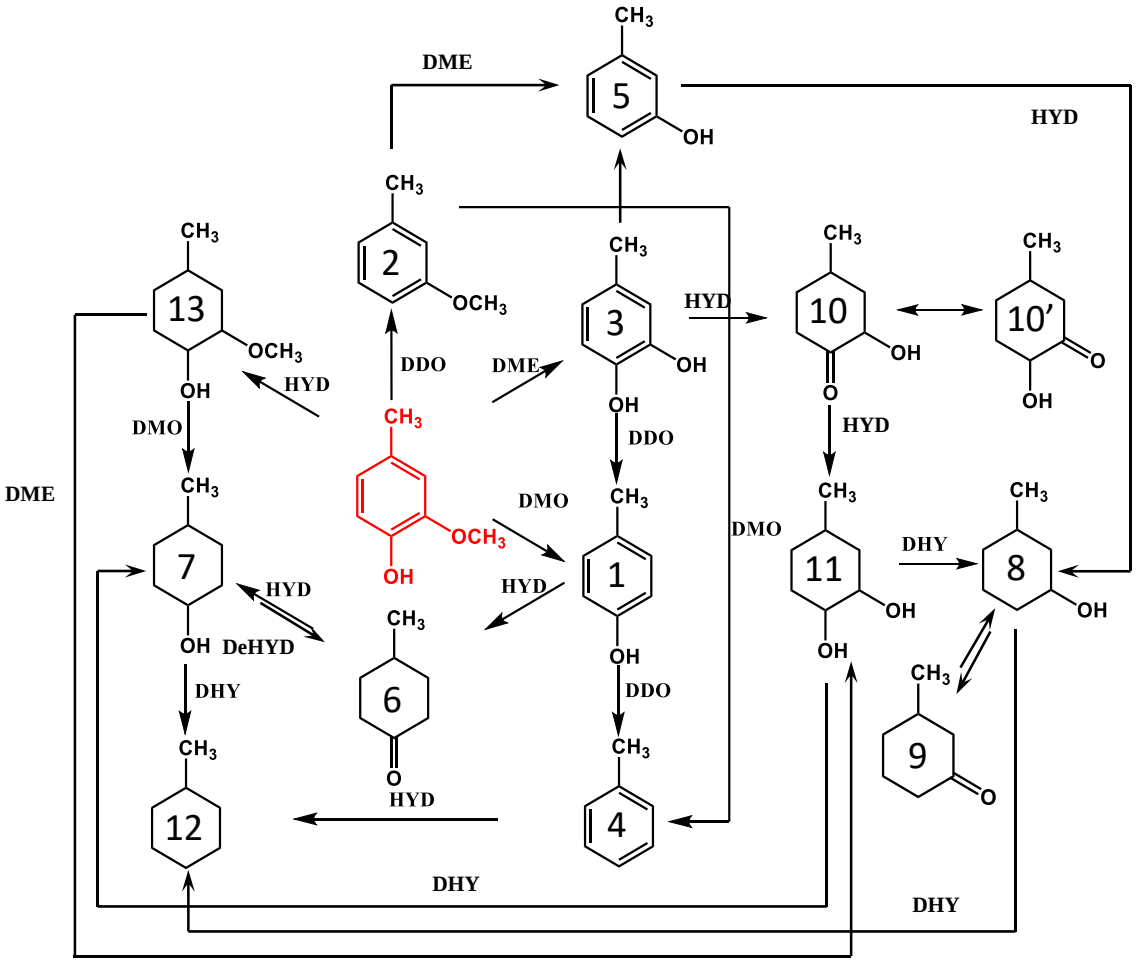

Figure 2. Reaction pathways for the HDO of para-methylguaiacol. [DMO : demethoxylation, DME: demethylation, DDO: direct deoxygenation, HYD: hydrogenation, DeHYD : dehydrogenation, DHY: dehydration][21]

From Figure 2, the complexity of reaction pathways is apparent, with numerous possible routes available. It should be noted, the methyl group in the *para* position of guaiacol is consistently present throughout all reactions. Catalysts tested included: a commercial Johnson Matthey (JM) 2.5 % Rh/silica and a 2.5 % Rh/silica and 1.55 % Pt/silica prepared by the authors. The rhodium catalysts showed higher HDO activity, whilst the platinum catalyst favoured hydrogenation; only at low temperature (323 K) was hydrogenation observed with the rhodium catalysts. The JM catalyst exhibited greatest stability, with reaction reaching steady state after 10 hours and a constant activity maintained over 3 days on stream. In contrast, reactions carried out using catalysts prepared by the authors failed to reach steady state and catalyst deactivation was observed. Both rhodium catalysts selectivity favoured cresol, in contrast to the platinum catalyst which displayed higher selectivity towards 4-methyl catechol.

The choice of support should ensure minimal carbon formation and facilitate activation of the oxy-compounds via hydrogen bonds. For many years the most commonly used support

was Al_2O_3, however, recent research has thrown up questions around its suitability for HDO. A number of studies have found that following the formation of water through the reaction between hydrogen and bio-oil, the Al_2O_3 can convert to boemite (AlO(OH)) resulting in oxidation of nickel and a reduction in catalyst activity. [29-31] Furthermore, Propev *et al.* [32] postulated that phenolic species were present on up to 2/3 of the alumina, giving an increased propensity towards carbon laydown. This is believed to be due to the high acidity of the Al_2O_3 and resulted in a movement towards more pH neutral supports such as SiO_2, which was found to have a concentration of adsorbed phenol species just 12 % of that on Al_2O_3.

4.3 Catalytic Hydrogenation

Catalytic hydrogenation continues to have widespread industrial applications in the production of pharmaceuticals, agrochemicals, fine chemicals, flavours, and fragrances; between 10-20 % of reactions today use this process for chemical production. [33] Although recent years has seen a substantial shift in interest towards HDO, increased insight into the role played by hydrogenation is vital to our overall understanding of the complex mechanisms involved in the HDO process. In recent years catalytic hydrogenation of aromatics has gathered renewed interest due to the demand for lower levels of aromatics in diesel fuels driven by environmental concerns and EU legislation. [34]

An important role of hydrogenation in the HDO upgrading of bio-oil may be as a route to facilitating deoxygenation more readily. Below, relevant bond dissociation energies are summarised:

Table 1. Bond dissociation energies (kJ/mol).

	Bond dissociation energies (kJ/mol)
$R_{aliphatic}$–OR	339
$R_{aromatic}$–OR	422
$R_{aliphatic}$–OH	385
$R_{aromatic}$–OH	468

From Table 1 it can be seen that, in the case of ethers and alcohols the bond strength of the oxygen when attached to the aromatic carbon in comparison to the aliphatic carbon increases by ~83 kJ/mol. Hence, initial hydrogenation of the aromatic to aliphatic ring will reduce the C-O bond energy and potentially enhance the removal of oxygen allowing deoxygenation to

take place more readily. [35] However, steric constraints of cleaving the aliphatic carbon-oxygen bond are higher than for the equivalent aromatic bond. [36]

A long history of research into aromatic hydrogenation exists, with Sabatier and Senderens reporting the first catalytic hydrogenation of the aromatic ring in their work with benzene in 1905. [37] They established the use of nickel-based hydrogenation of unsaturated molecules to their saturated equivalent, including the reaction of benzene to cyclohexane, for which Sabatier was awarded a Nobel Prize in 1912. In the intervening 100 plus years many studies have been carried out on aromatic hydrogenation with no clear consensus reached on the exact nature of what occurs on the catalyst surface. [34]

Benzene, the simplest aromatic molecule, is stabilised by the simultaneous involvement of three sets of π- electrons and therefore hard to disrupt. Due to the heats of hydrogenation, under most circumstances cyclohexane is the only product when benzene is hydrogenated. [38,39] Investigations of the different activation energies and ionisation potentials have provided evidence that the mechanism of benzene hydrogenation proceeds through an associatively π-adsorbed complex which is accepted by many in literature. There is ambiguity, however, regarding the number and type of intermediates that form during the hydrogenation process. Scholten and co-workers suggested the stepwise mechanism presented in Figure 3 below: [40-42]

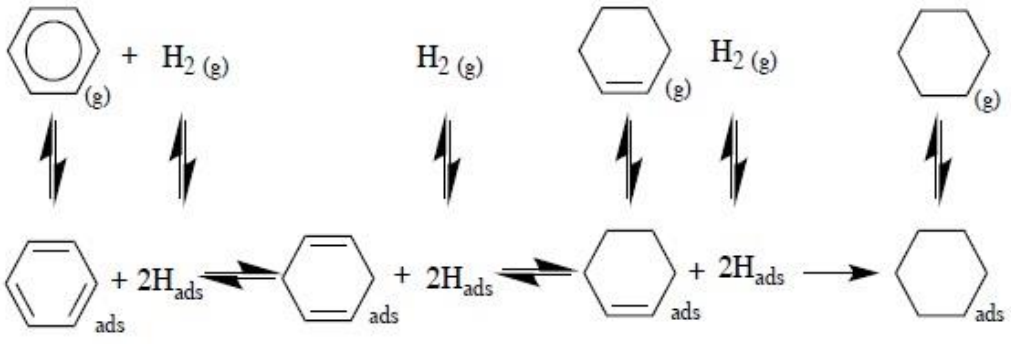

Figure 3. Stepwise hydrogenation mechanism of benzene.

This shows the different states of chemisorbed benzene and the desorption process of the aromatic species. Cyclohexadiene is believed to adsorb too strongly to the catalyst surface for the desorption of this intermediate to occur. A definitive mechanism for the hydrogenation of benzene is still to be fully understood, however, those involving Langmuir-Hinshelwood kinetics and Eley-Rideal kinetics are the most commonly proposed. [43-45] The greatest area of debate is precisely how the hydrogen adsorbs on the

catalyst surface during aromatic hydrogenation. This all underlines that despite over a century passing since the original hydrogenation of benzene a full understanding of the simplest aromatic does not yet exist.

4.4 Phenol Hydrogenation/HDO

The addition of a single hydroxyl group to benzene brings us to phenol. The catalytic hydrogenation of phenol to cyclohexanone is of commercial significance. Cyclohexanone is a key raw material in the production of Nylon 6 and Nylon 66 and for the synthesis of other industrially important chemicals. [46] There are currently two main industrial processes in operation: the oxidation of cyclohexane under high temperature and pressure, and the more preferred hydrogenation of phenol, which suffers however, from low selectivity to cyclohexane under mild reaction conditions. [47,48] Sabatier and Senderens [37] carried out the first phenol hydrogenation and reported that the main product formed was a mixture of cyclohexanol/cyclohexanone in addition to fractional amounts of benzene, cyclohexane, and cyclohexene. Although, in the early stages of research into phenol hydrogenation the route of product formation was ambiguous, following kinetic studies by Jungers *et al.* [49,50] in 1950 it was widely accepted that cyclohexanone forms as a primary product in the liquid phase hydrogenation of phenol. The mechanism for phenol hydrogenation is shown in Figure 4 below:

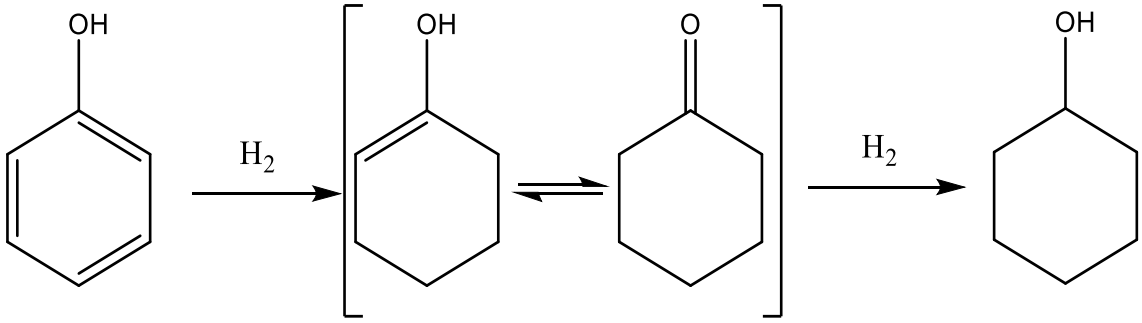

Figure 4. Phenol Hydrogenation.

The standard Gibbs free energy changes of the reactions of phenol are negative, with phenol to cyclohexanone giving $\Delta G = -145$ kJ mol^{-1} and phenol to cyclohexanol giving $\Delta G = -211$ kJ mol^{-1}, both are thermodynamically favourable products. [37, 51] As shown in Figure 4, the presence of ketones in the reaction can be explained by tautomerization - the keto form is 18 kcal more stable than the enol. Smith and Stump in 1961 [52] proposed that phenol was adsorbed on the catalyst surface where hydrogenation occurred with the production of hydroxycylohexenes as short-lived intermediates. These may or may not be

desorbed from the catalyst surface: hydroxycyclohexene, for example, may react with an additional mole of hydrogen to form cyclohexanol without entering the reaction medium where it would compete with unreacted phenol; the intermediate may undergo cleavage to cyclohexene and water, or ring hydrogenation to cyclohexanol. It is believed that these reactions can occur simultaneously until all double bonds are saturated.

Hydrogenation of phenol occurs between activated H_2 molecules and chemisorbed phenol molecules, where phenol is adsorbed on the catalyst surface via the oxygen atom of the hydroxy group in the form of phenolate. [53,54] It is believed to be able to adopt two different modes of adsorption depending on the nature of the support: on a basic support phenol can be chemisorbed in a non-planar manner, which facilitates the production of cyclohexanone, or on acidic supports where it is adsorbed in a co-planar arrangement favouring cyclohexanol formation. [36]

The occurrence of phenol in bio-oil makes it a commonly used model compound. Belonging to the *p*-hydroxyphenyl lignin subunit, it is the simplest model compound with only an aromatic ring and single hydroxyl group present.[32] Research carried out investigating the HDO of phenol has proposed a bi-functional reaction, utilizing metal sites on the catalyst for hydrogenation and dehydrogenation, and acidic sites for polymerization and alkylation. [55-57] A number of reaction pathways have been proposed for phenol HDO, one major route is direct deoxygenation (DDO) involving hydrogenolysis of the stable $C(sp^2)$-O bond; however, this is seen as a difficult reaction to achieve under conventional conditions, due to the stability of the aromatic ring. An alternative proposal is through metal-catalysed ring hydrogenation, which reduces the energy required to scission the C-O bond. [37,58] Regardless of the catalyst employed, whether conventional NiMo or CoMo or the noble metals, the two main routes for phenol HDO have been hydrogenolysis and hydrogenation. [18]

A recent study by Alsheri *et al.* examined phenol hydrogenation over rhodium in a batch reactor (< 343 K, 2-5 barg H_2). [59] The principal product at the early stages of the reaction was found to be cyclohexanone, with cyclohexanol formed as a secondary product from cyclohexanone. The conditions employed were significantly milder than those commonly used for HDO; however, hydrogenolysis was still seen to occur at relatively high levels with around 20 % yield of cyclohexane recorded. The study also replaced deuterium for hydrogen and found an inverse kinetic isotope effect for cyclohexanone, the ring hydrogenated product of the reaction, indicating hydrogen addition is not the rate determining step for phenol hydrogenation to cyclohexanone. However, it was found that

cyclohexane, the hydrogenolysis product, gave a positive kinetic isotope effect. Calculation of KIE values during reactions carried out with deuterium as the active gas can result in the three possible outcomes shown below:

- KIE value equals 1 then there is no KIE effect
- KIE > 1 yields a positive KIE effect
- KIE < 1 yields a negative KIE effect

A positive KIE value indicates that the addition of hydrogen is involved in the RDS of the reaction mechanism, whilst an inverse KIE implies the hydrogen addition is not involved in the RDS. This highlights the significance that determination of KIE value can have on understanding the mechanism of a reaction.

The addition of a second hydroxyl group to phenol results in the dihydroxybenzenes, made up of catechol, resorcinol and hydroquinone, with catechol (the *ortho* isomer) the most commonly studied as a bio-oil model compound. It is generally thought, that for compounds with the same number of substituents those with symmetrical arrangement had the highest reactivity, with the dihydroxybenzenes believed to follow the pattern recorded for xylene isomers by Vannice and Rahman: *para* > *meta* > > *ortho*-xylene. [60,61] To the best of our knowledge Smith and Stump in 1961 are the only researchers to study the isomers of the dihydroxybenzenes as a group. [52] They also recorded the order of reactivity as *para* > *meta* > *ortho* over both a Rh and Pt catalyst. A mechanism was proposed whereby the dihydroxybenzene is adsorbed to the catalyst surface where hydrogenation takes place to give hydroxycyclohexenes as short-lived intermediates which may or may not desorb from the catalyst surface. [62] These intermediates can then undergo hydrogenation to give *cis*/*trans*-cyclohexanediol and hydroxycyclohexanone or hydrogenation coupled with hydrogenolysis to form cyclohexanol, cyclohexanone and cyclohexane. They reported that the least level of cleavage occurred with the *ortho*-isomer (catechol) quoting steric hindrance as the reason behind this. The reactivity order of *para* > *meta* > *ortho* is by no means uniform across all substituted aromatic hydrogenation studies, Odebunmi and Ollis for example, in a study of methyl substituted aromatics, reported an order of *meta* > *para* > *ortho* and attributed the low reactivity of the *ortho* isomer to be a result of steric-interactions. [63,64]

Song *et al.* [65] carried out HDO of catechol at high temperature and elevated pressure (473K, 30 barg H_2) and found the ring hydrogenated 1,2-cyclohexanediol to be the major product. Two possible mechanisms were proposed: hydrogenolysis to phenol, followed by

subsequent hydrogenation to cyclohexanone and cyclohexanol; or an initial hydrogenation to 2-hydroxycyclohexanone, with further hydrogenation to the *cis*/*trans*-1,2-cyclohexanediol. In the latter route the diol is thought to be capable of undergoing hydrogenolysis to cyclohexanone and cyclohexanol under even harsher conditions.

4.5 Alkyl substituted hydrogenation

It has been found that the addition of substituents to the aromatic ring can significantly influence the process of hydrogenation, bringing changes in electron density which affect adsorption. The addition of an alkyl group, which are electron donating in nature, increases the electron density of the aromatic ring by an inductive effect. [66] An additional steric effect can also exist which could influence the formation of the transient state between the substrate and the catalyst surface and dictate whether the substrate will adsorb in a horizontal or vertical manner. Studies by Toppineen *et al.* [67,68] found that the hydrogenation rate increased as number of substituents increased (xylenes < toluene < benzene), and length of substituent decreased (ethylbenzene < toluene < benzene).

Vannice and Rahman [60,61] studied the hydrogenation of xylenes and toluene over palladium and compared these to benzene to determine the effect alkyl groups have on hydrogenation. They postulated the following sequence*: ortho*-xylene < *meta*-xylene ≤ *para*-xylene < toluene < benzene, where the position and number of methyl groups have an effect on the rate of hydrogenation. The lower rate of toluene hydrogenation than that of benzene hydrogenation may be explained when we consider the electron density of the adsorbate. In toluene, the induction effect from the methyl group to the aromatic ring increases the π-electron density, thus a stronger bond is formed between the aromatic substrate and the catalyst surface. The resultant increased stability of toluene with the catalyst surface would result in a lower reactivity than that recorded with benzene. Smith and Rader, during competitive hydrogenation studies of substituted aromatics, postulated the relative reduction in rate of methyl substituted aromatics was not a direct consequence of the ease in which the nucleus is chemisorbed to the catalyst surface. [69] They argued instead, that the ease of adsorption is fundamentally a result of the mode of adsorption adopted by the aromatic substrate. If we have an unsubstituted aromatic, i.e. benzene, we assume a flat mode of adsorption, any additional substituents to the aromatic ring would be on the side pointing away from the catalyst surface. If the substituent bulkiness is increased, the steric strain during adsorption would also increase with a resultant decrease in the ease of adsorption. Smith and Rader [69] categorized the steric strain for alkyl-substituted aromatics into two categories: frontal strain, which is mutual repulsion between

the nuclear substituent and catalyst surface; and back strain, which is due to the close proximity of substituents and would mainly affect the *ortho* isomer, although in some instances the *meta* isomer may also be influenced.

The xylenes when compared with toluene and benzene show the lowest reactivity. This may be expected as the addition of a further methyl group and subsequent increase in the electron density would result in even greater stability when xylene is adsorbed on the catalyst surface. [67,68] The lower hydrogenation rate for the *ortho* isomer of the xylenes is widely believed to be a result of steric hindrance caused by the neighbouring methyl substituents on the aromatic ring. However, a study by Alshehri *et al.* [70] of xylene hydrogenation at low temperature found the order to be *para*-xylene > *ortho*-xylene > *meta*-xylene, casting doubt on the role of steric hindrance in determining xylene hydrogenation reactivity. The same study found the rate of hydrogenation decreased as alkyl chain length increased, in line with much of the current literature. They proposed that this inhibition of reaction rate was due to the inductive effect of the alkyl chain, increasing the electron density of the ring and resulting in a stronger π-bond to the surface; a decrease from zero to negative first order from toluene to propylbenzene was reported.

Any discussion of di-substituted aromatic hydrogenation must consider the role of stereoselectivity, as both *cis* and *trans* isomers can be formed. Since 1922, it has been hypothesized that the *cis* isomer is preferentially formed over the *trans* isomer, a theory confirmed through experimental findings. [71] Indeed, if the assumption is that hydrogenation occurs via a flat mode of adsorption then it would be difficult to see how the *trans* isomer could form at all. Any attempt at stereochemical control during hydrogenation reactions requires an understanding of how the unsaturated hydrocarbons are adsorbed on the catalyst surface to begin with. It is widely believed a π-complex exists in which a net charge transfer from the aromatic to the metal exists. The hydrogenation of the aromatic is believed to occur via this π-complexed aromatic system through a series of intermediates until a π-adsorbed cyclohexene is formed. [72,73] The σ-1,2-diadsorbed complex differs from the π-complex in that, upon formation of the π-complex groups attached to the former double bond must assume a *cis* configuration and the ring probably exists in the chair conformation. The groups attached to the former double bond assume a position directed away from the surface. When the olefin is symmetrically substituted, only the *cis* configuration should be possible as both sides of the ring are equivalent. However, this has been shown not to be the case as the *cis* isomer is not selectivity formed when studying *ortho*-substituted aromatics, and hence, the formation of the *trans* isomer must be via a

different mechanism. Many such as Siegal and co-workers [74] in a study on 1,2-dimethylcyclohexane and 1,2-dimethylcyclopentane hydrogenation over Pt have proposed the *cis*-olefin substrate must undergo isomerization when it desorbs from the catalyst surface as the *trans*-olefin. A recent study of *ortho*-xylene hydrogenation by Alshehri *et al*.[69], however, observed two intermediate cycloalkenes: 1,2-dimethylcyclohexene and 1,6-dimethylcyclohexene, it was proposed that hydrogenation of 1,2-dimethylcyclohexene gave *cis*-1,2-dimethylcyclohexane while hydrogenation of 1,6-dimethylcyclohexene gave *trans*-1,2-dimethylcyclohexane indicating a different means of the *trans* isomer formation. As of yet, this route of formation remains unclear.

The cresol substrates, containing both a hydroxyl and methyl group, are another widely used bio-oil model compound. Massoth *et al.* [75] showed during his study with methyl substituted phenols that the presence of the methyl group resulted in an increased yield of aromatic products when compared with phenol. Their work also suggested that *ortho*-cresol gave the lowest activity of the three isomers and postulated this as being a result of the adjacent hydroxyl and methyl groups inhibiting adsorption on the catalyst surface.

The reaction pathways of the cresol isomers have been studied by Shafaghat *et al.* [76] over a Pd/C catalyst at 15 bar H_2 and 550 K. Three distinct pathways were hypothesised for *ortho*-cresol: the direct HDO of cresol to toluene; alkylation of cresol to 2,6-dimethylphenol; and initial hydrogenation to 2-methylcyclohexanone/2-methylcyclohexanol followed by hydrogenolysis to methylcyclohexane. The hydrogenation pathway was found to be dominant using a Pd/C catalyst. The observed pathways for *meta*-cresol showed only direct HDO and hydrogenation with no alkylation recorded, suggesting the methyl group adjacent to the hydroxyl group promotes the dealkylation reaction. The study concluded that the presence of the methyl groups in the bio-oil model compounds favoured hydrogenolysis in the hydrogenation reaction.

Work by Nie *et al.* [77] focused on maximizing selectivity during cresol hydrogenation to their corresponding cyclohexanol (*cis* or *trans*). This is of industrial importance, especially for the *cis*-isomers, which are useful intermediates in the fragrance and perfume industries. Their work achieved high selectivity to the *cis* isomer with a ratio of 96:4 *cis* to *trans* alcohol, however, it was discovered that the *cis*:*trans* ratio decreased over time with lower selectivity to the *cis* isomer following conversion of 4-methylcylcohexanone.

Odebunmi and Ollis [63,64] studied the HDO of the cresol isomers over $CoMo/Al_2O_3$ catalysts at high temperature (498-673 K) and high pressure (30-130 bar H_2) in a

continuous flow microreactor and found an order in reactivity of *meta* > *para* > *ortho*. This was in agreement with work by Shin and Keane over a Ni/SiO_2 catalyst who concluded that the steric effect was independent of catalyst type. Studies of cresol HDO have suggested the existence of two different pathways, using *para*-cresol as an example they proposed either direct deoxygenation (DDO) to toluene or hydrogenation (HYD) to 4-methylcyclohexanol. Romero *et al.* [81] during a study of 4-ethyl phenol HDO over a MoS_2 catalyst suggested the favourability of each pathway is dependent on the mode of adsorption adopted by the aromatic. A vertical adsorption (η1) via the -OH group on 4-ethyl phenol would favour the DDO pathway, whilst a planar mode of adsorption (η5) via the aromatic ring and the hydroxyl group would favour the HYD pathway.

4.6 Anisole Hydrogenation/HDO

The single substituted anisole containing the aromatic ring and methoxy group is another commonly used bio-oil model compound. Many different reaction pathways have been proposed for the HDO of anisole and include: an initial demethylation to produce phenol, which then undergoes hydrogenolysis to benzene with a subsequent hydrogenation step resulting in the formation of cyclohexane; hydrogenation and hydrogenolysis, where anisole is hydrogenated to methoxycyclohexane which then undergoes hydrogenolysis to give cyclohexane; and methyl group transfer, where anisole is hydrogenated to cresol through the methyl group from the methoxy transferring to another position on the aromatic ring. [33,37,82-83] From this list the number and complexity of possible reaction pathways available when reacting anisole in the presence of hydrogen and a catalyst is evident. The proposed mechanism from which deoxygenation occurs from anisole has been proposed by Thompson as follows: anisole is adsorbed on the catalyst surface to give methoxycyclohexene as a short-lived intermediate which may undergo cleavage and hydrogenation to cyclohexane and methanol, or simple hydrogenation to methoxycylohexane. [84]

A recent study examined anisole hydrogenation over rhodium in a batch reactor (< 343 K, 2-5 barg H_2). [59] The major product of the reaction was found to be the ring hydrogenated methoxycyclohexane. Cyclohexanone was formed as an intermediate via keto-enol tautomerization, and only when anisole was fully consumed did the cyclohexanone hydrogenate further to cyclohexanol. This was postulated to be a result of anisole blocking the ability of cyclohexanone to re-adsorb onto the catalyst surface and inhibiting subsequent hydrogenation to cyclohexanol.

The methoxyphenol substrates, with the addition of a hydroxyl group to anisole, is another group of highly studied bio-oil model compounds. Research has been almost exclusively focused on the 2-methoxyphenol isomer, commonly known as guaiacol. [85] The HDO of this substrate is thought to occur by two main routes: hydrogenolysis to catechol, and subsequent deoxygenation to phenol, and/or demethoxylation to form phenol and methanol, followed by hydrogenolysis to benzene or hydrogenation to cyclohexanol. [86]

The hydrogenation of 4-methoxyphenol was documented by Alshehri *et al.* [70] who employed a rhodium/silica catalyst at 323 K and 3 barg H_2. They found the major product of the reaction to be the ring hydrogenated 4-methoxycyclohexanone, with formation of methoxycyclohexane, cyclohexanol, cyclohexanone and cyclohexane also recorded. Surprisingly, further hydrogenation of the 4-methoxycyclohexanone to 4-methoxycyclohexanol was not observed and it was suggested that this was a result of the larger cross-sectional area occupied by 4-methoxycyclohexanone when compared to cyclohexanone. It is notable, that significant hydrogenolysis was reported under these conditions, with around ~ 35 % cumulative yield of the HDO products formed by the end of reaction, indicating a clear propensity for bond cleavage to occur with these bio-oil model compounds at mild conditions over a Rh catalyst.

Smith and Stump [52] in their studies on the hydrogenation of dihydroxybenzene and methoxyphenols reported a higher reactivity for the former and proposed that the following factors were responsible: the difference in size of -OH in comparison to -OCH_3, the extensive formation of ketones from hydroxybenzenes, and the presence of the methyl group in methoxybenzene decreasing the likelihood of oxygen donation.

The choice of metal has a significant effect on whether HDO or hydrogenation is favoured. It is well known rhodium is an excellent ring hydrogenation catalyst and it has been postulated that over rhodium [39], hydrogenation of the ring to 2-methoxycyclohexanol occurs first, followed by demethoxylation to methoxycyclohexane with a final hydrogenation step to cyclohexane or methylcyclohexane. [87,88] Gutierrez *et al.* [89] investigated different noble metals for the HDO reaction and found that activity decreased in the following order: Rh/ZrO_2 > $Co\text{-}MoS_2/Al_2O_3$ > Pd/ ZrO_2 > Pt/ZrO_2, providing further evidence that supported rhodium is a more effective catalyst for the HDO reaction than the conventional HDS catalysts that have been employed for many years.

4.7 Exchange Reactions with Deuterium

Research involving mechanistic studies and preparation of labelled substrates can use deuterium exchange reactions to gain crucial information. Research into the exchange processes of bio-oil model compounds has been limited, and as such, our study will attempt to increase knowledge and understanding in this area. The exchange reaction is not just a simple stepwise addition of deuterium for hydrogen, each addition of the deuterium can appear as an individual product and alkyl substituted aromatics further increase the number of positions on the molecule where exchange can occur. The mean number of exchanged deuterium atoms is dependent on the metal catalyst employed and the temperature at which the reaction is performed. [37]

The H/D exchange of aromatics has been studied extensively, with the dissociative and associative mechanisms those most commonly proposed. The associative mechanism was originally advanced by Farkas and Farkas [90] who proposed that exchange and hydrogenation occur by two unrelated mechanisms. They stated that, hydrogenation occurs via the simultaneous addition of 2H atoms to the adsorbed hydrocarbon, whilst the exchange process involves prior dissociation of the hydrocarbon on the catalyst surface to form a σ-phenyl complex and hydrogen atom. This σ-phenyl complex combines with the deuterium atom and the benzene-d1 desorbs. The associative mechanism, initially proposed by Horiuti and Polanyi, [91] suggests that a common intermediate must be involved in both the hydrogenation and exchange processes. However, inconsistences in both these proposed mechanisms resulted in the development of a new adsorption theory centred on the major role the π-complex plays in the presence of D_2 gas. This is the adsorption mechanism believed to take place when Pt is used as the metal catalyst.

Deuterium isotope exchange studies over alkylbenzenes, anisole and phenol have been useful in helping to understand these complex reaction mechanisms. [38] Alsherhri *et al.* [70] found the alkylbenzenes had an overall inverse kinetic isotope effect, in contrast to phenol and anisole where a normal kinetic isotope effect was observed. There is debate over the exact nature of inverse kinetic isotope effects, however, it has been suggested it involves the change of hybridisation from sp^2 to sp^3, such as that which occurs during ring hydrogenation from the aromatic to the aliphatic carbon. Interestingly, selectivity during anisole hydrogenation differed between deuterium and hydrogen with the hydrogenated product, methoxycyclohexane, showing an increase in selectivity from 65 % to 70 % and the hydrogenolysis product, cyclohexane, a decrease from 25 % to 20 % when deuterium replaced hydrogen. These changes indicate that under deuterium the breaking of the Ar-

OCH_3 bond is slower (reduction in yield of cyclohexane) and hydrogenation faster (increased yield of methoxycyclohexane).

Deuterium work by Alsherhri *et al.* [59] with toluene hydrogenation over a Rh catalyst established a faster rate of exchange for protons in the methyl group than with the aromatic protons. They postulated the H/D exchange is a separate process from hydrogenation and the rate at which it takes place indicates that no loss of aromatic stability is likely to occur, suggesting the existence of a dissociative mechanism. The exchange of methyl group protons with deuterium indicates direct interaction with the methyl group and catalyst surface, in addition to the strong interaction with the aromatic ring. This is in agreement with the proposal by Webb and Orozco [92] that toluene adsorbed to the surface via both the methyl group and the aromatic ring. Harper and Kemball, [93] in a study of *para*-xylene hydrogenation over Pt, observed substantially more exchange in the methyl groups than with that of the aromatic ring protons. A further study found H/D exchange with both the aromatic ring and methyl group protons when a Ni catalyst was used, however, when a Pd catalyst was employed exchange occurred only with the aromatic protons.[94] This suggests the H/D exchange process on methyl substituted aromatics is dependent on the catalytic metal.

The H/D exchange of alkyl substituted aromatics over a Pd catalyst was studied by Esaki *et al.* [95] using D_2O as the deuterium source. They found that for the methyl substituted aromatics, deuterium was incorporated, whilst for the methoxy groups no exchange took place within the substituent protons. The efficiency of deuterium exchange was postulated to be lower as the distance from the benzene ring and substituent increased, and a direct connection between the aromatic ring and alkyl group on the catalyst surface was a significant prerequisite for efficient H/D exchange.

4.8 Competitive Hydrogenation

Up until now the upgrading of bio-oil has been carried out using single model compounds to represent a true bio-oil feed. Although this has given good understanding of the reactivity and behaviour of these molecules individually it has not provided us with information on how they would behave when reacted together. In all probability, successful upscaling of the process would result in a multi-component feedstock, and as such, in addition to individual hydrogenation we have focused on competitive hydrogenation of the bio-oil model compounds. As it has not been studied previously to the best of our knowledge, there is no literature in respect to the competitive hydrogenation of bio-oils.

Alshehri *et al.* [70] studied competitive hydrogenation of toluene, ethylbenzene, propylbenzene and the xlyenes. The pair combination of toluene and ethylbenzene was found to increase the reactivity of both, indicating each aromatic had a unique adsorption site. This enhancement in reactivity is not something that is commonly reported during competitive reactions, in fact, the expectation is that an increase in aromatics would result in a decrease in reactivitiy due to greater competition for active sites on the catalyst surface. This increase was proposed to be a result of enhanced hydrogen transfer from hydrocarbonaceous depositis on the catalyst surface. When toluene or ethylbenzene was paired with propylbenzene, both experienced a reduction in reactivity, with a near 60 % drop recorded, this was in agreement with the strong negative order in substrate concentration recorded for propylbenzene. Unexpectedly, an increase in propylbenzene reactivity during these paired combinations was reported. Alsherhri *et al.* [70] postulated that this was a result of a decrease in the strength of adsorption for propylbenzene when competition for catalytic surface sites exists in the competitive environment. Competitive reactions with the double substituted aromatics (xylenes) did not follow the same pattern to that observed with the single substituted aromatics. During all xylene isomer competitive reactions the reactivity of each substrate decreased. The reported order for each xylene isomer was negative and, as such, this decrease in rate when concentration of xylene and competition for active sites is increased is not unexpected. It is clear when studying alkyl aromatics unpredictable behaviour can occur in the competitive environment.

Rader and Smith [69] found during their 1961 study of xylene competitive hydrogenation that the ease of adsorption on the active surface of the catalyst followed the order *ortho* > *meta* > *para*; the exact reverse of the relative reduction rate of the individual xylenes (*para*> *meta*> *ortho*). The relative reduction rate and ease of adsoption of the aromatic are two different phenomenas, the former is a kinetic effect, determined by the relative stability of the transition state of the rate-determining step. In contrast, the ease of adsorption is a thermodynamic effect based on the stability of the chemisorbed nucleus. For substituted aromatics it is dependent on the mode of adsorption and molecular structure of the aromatic compound on the catalyst surface. This is difficult to interpret as the exact nature of the catalyst surface is still unknown.

Although research into competitive hydrogenation is sparse, those studies that exist generally report a decrease in reactivity in comparison to the individual environment. Hamilton *et al.* [96] for example, in their study on the competitive hydrogenation of 1-pentyne, phenyl acetylene, 2-pentyne, and 1-phenyl-1-propyne over a Pd/C catalyst

reported a decrease in reaction rate when all four were reacted together. There was, however, a rate enhancement observed for both alkynes when 1-pentyne and 2-pentyne were reacted together. This was postulated to be a result of enhanced hydrogen transfer on the surface with each adsorbed alkyne acting as a hydrogen transfer agent for the other. Generally, however, it was found that competitive hydrogenation resulted in a significant reduction in rate when compared to individual hydrogenation, with the decrease in hydrogen concentration on the surface of the catalyst given as the reason. As well as the significant reduction in reactivity, changes in alkene selectivity were observed; the presence of an alkyne in the system, resulted in no secondary hydrogenation of the alkene to the alkane.

It is apparent from this literature search that a complete understanding of oxygen-substituted aromatic hydrogenation does not yet exist. Our study will attempt to address some of the current gaps in knowledge in this area, specifically those outlined in the following Project Aims Section.

5 Project Aims

The HDO of single bio-oil model compounds, over a variety of catalysts, has been widely studied; however, no real understanding of the complex reaction mechanisms involved or the factors that favour hydrogenolysis exists. Most current studies have employed the use of high temperature and high hydrogen pressure (>573-723 K, 75-300 barg H_2) to achieve HDO. In this thesis we aim to show that HDO can occur at low-temperature and pressure (323 K, 3 barg H_2) on these oxygen-substituted aromatics present in bio-oil. Furthermore, competitive studies will be carried out as a route to understanding whether a single model compound can be used to represent a multi-component bio-oil feed.

The specific aims of this project are to investigate:

i) The effect nature of substituent and ring position has on the hydrogenation of oxygen substituted aromatics.
ii) The order of reactivity and the product distribution for all model compounds with a view to identify the reaction mechanism for each.
iii) The factors which influence the occurrence of HDO.
iv) The effect on reactivity and product distribution of the competitive environment.
v) H/D exchange reactions and identify the overall and product KIE values for each model compound in the individual and competitive environment.

The scope of this thesis will involve the hydrogenation of the following groups of substrates:

- Dihydroxybenzenes
- Cresols
- Methoxyphenols

The *ortho*, *meta* and *para* isomer of each set of substrates will be tested.

6 Experimental

6.1 Catalyst characterization

6.1.1 Properties of Commercial Rh/Silica Catalyst

The catalyst used throughout this study (2.5 % Rh/silica, M01078) was supplied and characterised by Johnson Matthey and the main properties are listed below:

- Pore size: 13.2 nm
- Average Metal Crystallite Size: 2.6 nm
- Surface Area: 321 $m^2 g^{-1}$
- Rhodium Dispersion: 50 %
- Rhodium Surface Area: 5.5 $m^2 g^{-1}$

The catalyst was prepared by employing an incipient-wetness technique using aqueous rhodium chloride salts and a silica support supplied by Davison Catalysts. The catalyst was dried overnight at 333 K and reduced in flowing hydrogen at 473 K for 2 hours before being cooled and exposed to air. The surface area of the catalyst was 321 m^2g^{-1} with a pore size of 13.2 nm, measured using standard BET methodology. The metal surface area was measured by hydrogen chemisorption (reproducibility ±0.5 $m^2.g^{-1}$) and gave an area of 5.5 $m^2.g^{-1}$ and a dispersion of 50 %, from which an average metal crystallite size of 2.6 nm was calculated.

6.1.2 BET

To determine the overall surface area and pore diameter of the catalyst the Brunauer-Emmett Teller (BET) method was used. Analysis was carried out on a Micrometrics

Gemini III 2375 Surface Area Analyser with helium used as a calibrant and nitrogen as the absorbent. Approximately 0.03-0.05 g of catalyst was dried overnight at 383 K under a flow of nitrogen prior to nitrogen physisorption at 77 K.

The overall equation using the BET method is as shown below,

Equation 1. BET Equation

$$\frac{P}{V(P_0 - P)} = \frac{1}{V_m C} + \frac{C-1}{V_m C} \times \frac{P}{P_0}$$

Where:

- V_m is the monolayer volume of nitrogen,
- C is the BET constant,
- P and V are the pressure adsorbed and measured throughout the experiment,
- P_0 is the saturated vapour pressure of nitrogen,
- $\frac{P}{P_0}$ is the relative pressure.

Thereby, plotting of $\frac{P}{V(P_0-P)}$ against $\frac{P}{P_0}$ yields a straight line, with slope equal to $\frac{C-1}{V_m C}$ and intercept equal to $\frac{1}{V_m C}$. Finally, the overall surface area is governed from the monolayer volume shown below,

Equation 2. Surface Area Determination

$$SA = \frac{V_m L a_m}{V_0}$$

Where:

- V_m is the monolayer volume of nitrogen,
- L is Avogadro's constant,
- a_m is the cross-sectional area of the nitrogen molecule,
- V_0 is the molar volume of gas.

6.1.3 Thermo-gravimetric analysis

Thermo-gravimetric analysis was performed on post-reaction catalysts using a TA Instruments combined TGA/DSC SDT Q600 thermal analyser coupled to an ESS mass spectrometer for evolved gas analysis to investigate catalyst deactivation, specifically carbon deposition on the catalyst. A sample 10-15 mg was heated to a maximum temperature of 1000 ℃ at a ramp rate of 10 ℃/min under a 100ml/min flow of 2% O_2/Argon. For mass spectrometric analysis, mass fragments: 2 (H_2), 18 (H_2O), 28 (CO), 32 (O_2) and 44 (CO_2) were followed.

6.2 Experimental Procedure for Hydrogenation Reactions

6.2.1 Reactor

Hydrogenation reactions were performed in a 500 cm^3 three-phase Büchi autoclave stirred tank reactor, shown below in Figure 5.

The Büchi autoclave stirred tank is composed of three separate parts:

1. Büchi autoclave
2. Büchi press-flow gas controller
3. The Julabo temperature control system

The reactor is constructed of glass with stainless steel tubing and connections for gas delivery. Ports on the cover plate of the autoclave allow access to the reactor vessel for the addition of the substrate and sample collection as well as enabling the catalyst and solvent to be loaded pre-reaction. Reaction temperature is controlled using a Julabo oil pump system, with oil delivered to a glass jacket around the reaction vessel by a pressure pump and circulated back to the oil bath via a suction pump. Temperature is measured by a thermocouple within the reaction mixture. A motor attached to the stirrer shaft allows variable speed transmissions to be applied. Hydrogen and argon (inert) are supplied directly to the reactor vessel via the press-flow gas controller. The regulated and delivered pressure is monitored by the gas controller, with 5.5 bar the maximum pressure used throughout reactions.

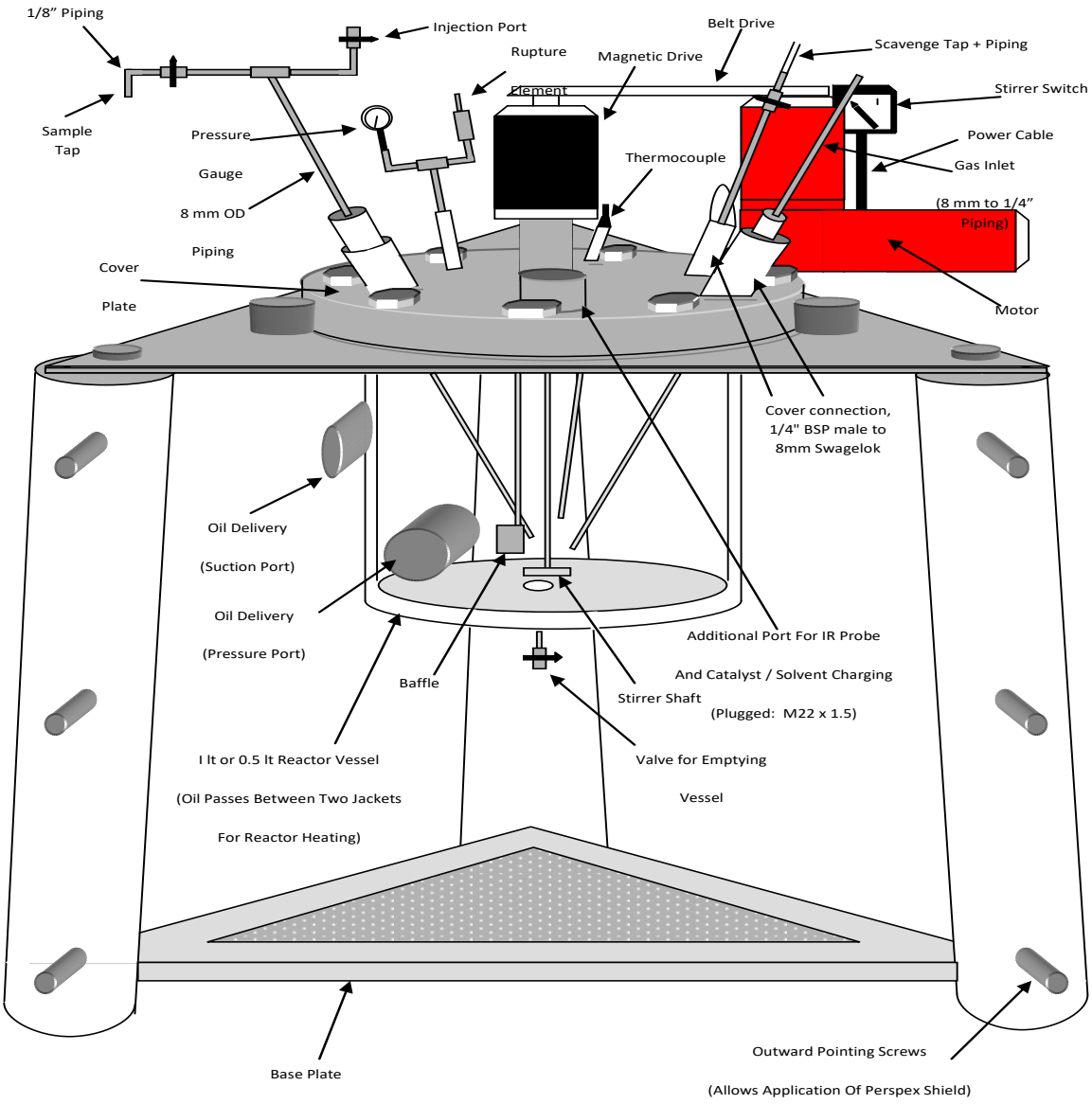

Figure 5. Büchi autoclave stirred tank reactor.

6.2.2 Reaction Procedure

The reaction procedure involved the addition of the catalyst (100 mg Rh/SiO_2) and 310 cm^3 of 2-propanol (IPA) into the reactor. The autoclave was purged with argon and the catalyst was then reduced *in situ* at 343 K by sparging hydrogen gas (280 cm^3 min^{-1}) through the mixture for 0.5 h, whilst stirring at 300 rpm. Once reduction procedure was complete, the hydrogen gas and stirrer were turned off and the reactor purged with argon twice prior to being pressurized to 1 barg. The gas controller measured the flow of hydrogen and inert gas to the reactor. Once at the desired temperature (303 – 343 K) the agitator was turned to 0 rpm and 10 mmol bio-oil model compound added to the reactor in 25 cm^3 IPA. This was followed by an IPA flush to ensure all reactants entered the reaction mixture, giving a total volume of 350 ml. The solution was thoroughly mixed by increasing

the agitator to 1000 rpm and a sample (2.5 cm^3) was withdrawn for analysis. The reactor was flushed with argon before being purged twice with hydrogen and pressurized to the desired level (3 barg). The reaction was started by setting the stirrer speed to 1000 rpm and the reaction profile followed by withdrawing samples of 2.5 cm^3 over a 180-minute time period. For the first 30 minutes a sample was taken every 5 minutes, this was increased to every 10 and 20 minutes for the following 30 and 120 minutes respectively. The moles of hydrogen gas consumed during the reaction were also recorded. The reaction procedure described was also carried out in the presence of deuterium gas in place of hydrogen.

Of importance, it should be stated that errors related to experimental results were low, as determined via replicated measurements.

6.2.3 Post Reaction Procedure

Following completion of each run, the reactor was vented, and the oil bath, stirrer and gas handling system switched off. The reactant mixture was drained via the valve at the bottom of the reactor vessel and once cooled, the vessel removed to allow thorough cleaning of the reactor vessel and injection and sample ports with IPA.

6.3 Competitive Reaction

Substrates were hydrogenated together to investigate the effect of the presence of more than one compound on the catalytic hydrogenation of bio-oil. Model compounds were tested as groups of two and as a group of three, for example in the scheme below, where A=Catechol, B=Resorcinol and C=Hydroquinone the 4 reactions carried out would be as follows:

- 10 mmol A + 10 mmol B
- 10 mmol B + 10 mmol C
- 10 mmol A+ 10 mmol C
- 10 mmol A + 10 mmol B + 10 mmol C

The reaction conditions for competitive hydrogenation were the same as individual hydrogenation (333 K, 3 barg H_2, 10 mmol substrate). Of note, the overall moles of aromatic have increased relative to the standard individual hydrogenation. Further reactions under identical conditions were carried out in the presence of deuterium.

6.4 Analysis

6.4.1 Gas Chromatography

Reaction samples were analysed on a Focus GC equipped with a flame ionization detector (FID). Separation was achieved using a 1701 column with the following dimensions:

length: 30.0 m, diameter: 0.25 mm and film thickness: 1.0 μm. Stationary phase was a mix of cyano and phenyl functional groups for increased polarity.

The separation of different molecules is based on the partition of the analytes between the stationery and mobile phase. The mobile phase, helium, transports the sample through the column. The liquid sample (~ 1mg), injected through a self-sealing silicone-rubber septum, passes through the columns mobile phase then enters the stationary phase where separation occurs. The separated molecules re-enter the mobile phase and are detected by the FID as they exit the column at their unique retention times. The method used throughout the reactions is shown below in Table 2,

Table 2. Method for Gas Chromatography.

	Rate (°C per min)	Temperature (°C)	Hold Time (min)
Initial	-	50	20.00
Ramp	20.0	230	11.00

6.4.2 GC Reference Standards

Reference standards for all substrates and expected products were prepared over a range of concentrations and analysed by GC. For each substrate, the measured peak areas were plotted against concentrations and a linear equation obtained; the resultant calibration factor was used to calculate unknown concentrations of reactants and products during reaction. Calibration plot examples for dihydroxybenzene and cresol isomers are shown below in Figure 6 and 7.

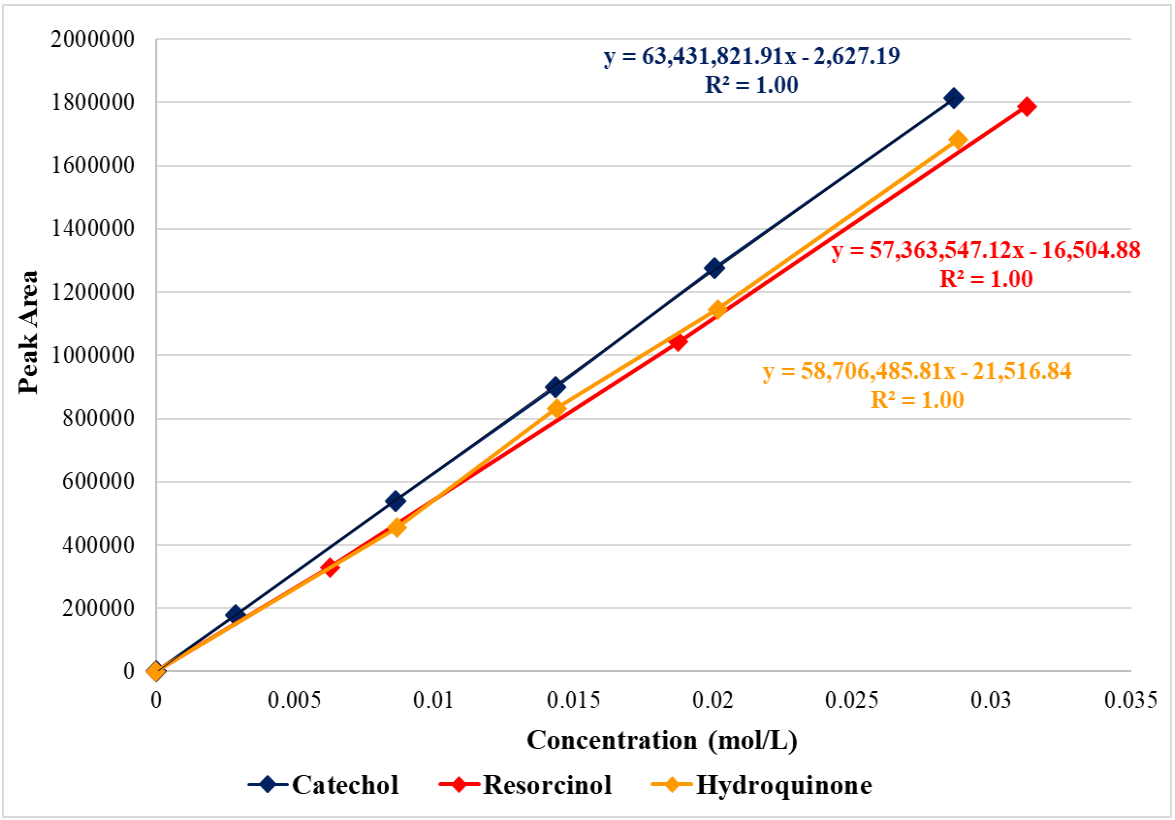

Figure 6. GC Reference standards for dihydroxybenzene isomers.

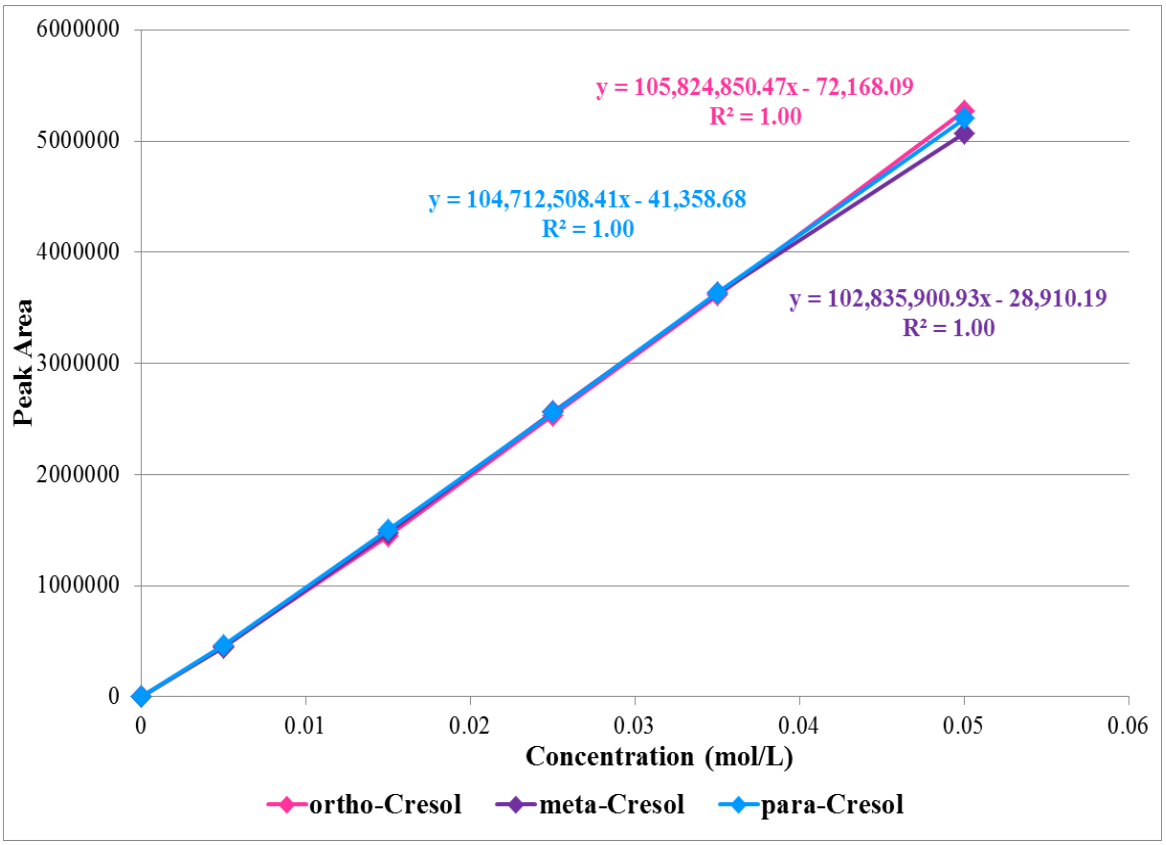

Figure 7. GC Reference standards for cresol isomers.

6.4.3 Deuterium NMR

Deuterium NMR analysis through a Bruker 500 Ultra Shield-NMR system was performed on selected deuteration reactions to investigate hydrogen-deuterium exchange. Data analysis was via a deuterium-lock data channel on the Bruker AU-programme.

6.5 Data Analysis

For each reaction, the concentration in mol/L of all reactants and products was ascertained and a mass balance calculated for each sample point. Mass balance for all reactions was 100±5 % or better. From this, a mole fraction percentage was calculated and plotted for reactants and products, which removed the need for an internal standard.

6.5.1 Rate Constant

The zero and first order rate constants were calculated for each reactant to identify the best fit. The integrated equation for a zero-order reaction is of the form shown below and applies when one or more of the species appearing in the rate law concentration remain fairly constant. Therefore, in a zero-order reaction a plot of concentration against time yields a straight line with slope equal to (–k).

Equation 3. Zero Order Integrated Rate Equation

$$A - A_0 = -kt$$

In comparison, first order reactions show an exponential decrease in reactant concentration with increasing time as outlined below:

Equation 4. Exponential Form of First Order Equation

$$A = A_0 e^{-kt}$$

Where:

- A_0 is the initial concentration of reactant A, mol L^{-1}
- t is the time, s
- k is the rate constant, s^{-1}

The integrated equation for a first order reaction is shown below:

Equation 5. Integrated First Order Equation

$$ln\frac{A_0}{A} = kt$$

Whereby a plot of the logarithm of concentration ($\frac{A_0}{A}$) verus time yields a straight line graph with slope equal to the rate constant, k.

6.5.2 Activation Energy

Reactions were carried out for each substrate between 303 and 343 K at 10 K increments to measure an activation energy. The effect of temperature on the rate of reaction can be expressed by the Arrhenius equation shown below:

Equation 6. Arrhenius Equation

$$k = Ae^{-Ea/RT}$$

Where:

- k is the rate constant
- A is the pre-exponential factor
- R is the gas constant; 8.314 J K^{-1} mol^{-1}
- T is the absolute temperature of the reaction K
- Ea is the activation energy J mol^{-1}

For each reaction, the rate constant values were calculated as shown in Section 6.5.1. From using the integrated form of the Arrhenius equation shown in Equation 7, ln k was plotted against ($\frac{1}{T}$).

Equation 7. Integrated Form of the Arrhenius Equation

$$\ln k = -\frac{Ea}{R}\left(\frac{1}{T}\right) + \ln A$$

Where the parameters are as described previously, this form of the Arrhenius equation gives a straight line with a slope equal to $-\frac{Ea}{R}$ which upon multiplication by the gas constant gives an activation energy for the reaction.

6.6 Concentration Variation

The concentration of substrate (5, 10, 15 and 20 mmol) was varied to investigate the effect on the rate of reaction and the results used to calculate an order in reactant using a simple rate equation shown below:

Equation 8. Experimental Rate Equation

$$Rate = k[A]^x[B]^y$$

Where:

- k is the rate constant
- [A] and [B] are the concentrations of the reactants
- x is the partial order of reaction with respect to concentration of A
- y is the partial order of reaction with respect to concentration of B

Whereby taking the natural log of Equation 8 the equation becomes:

Equation 9. Natural log of rate equation

$$\ln(rate) = \ln k + x \ln[A] + y \ln[B]$$

Where in our case, [A] = hydrogen and is assumed to be first order. [70] When the concentration of [A] is kept constant, the equation can be simplified and the plot of ln(rate) against ln[B] will yield a straight line, with the gradient equal to the order of substrate [B]. The sum of the partial orders of the reaction x and y gives the overall order of the reaction.

6.7 Substrates under study

All materials studied are shown below in Table 3 and Figure 8 and were used as received with no further purification.

Table 3. List of substrates tested for hydrogenation.

Chemical	**Supplier**	**Purity**
Hydrogen	BOC	99.99 %
Deuterium	BOC	100 %
Argon	BOC	99.99 %
2-Propanol	Sigma-Aldrich	99.5 %
Catechol	Sigma Aldrich	≥ 99 %
Resorcinol	Sigma Aldrich	99 %
Hydroquinone	Sigma Aldrich	99 %
ortho-Cresol	Sigma Aldrich	98 %
meta-Cresol	Sigma Aldrich	99 %
para-Cresol	Sigma Aldrich	99 %
2-Methoxyphenol	Sigma Aldrich	99 %
3-Methoxyphenol	Sigma Aldrich	99 %
4-Methoxyphenol	Sigma Aldrich	98 %

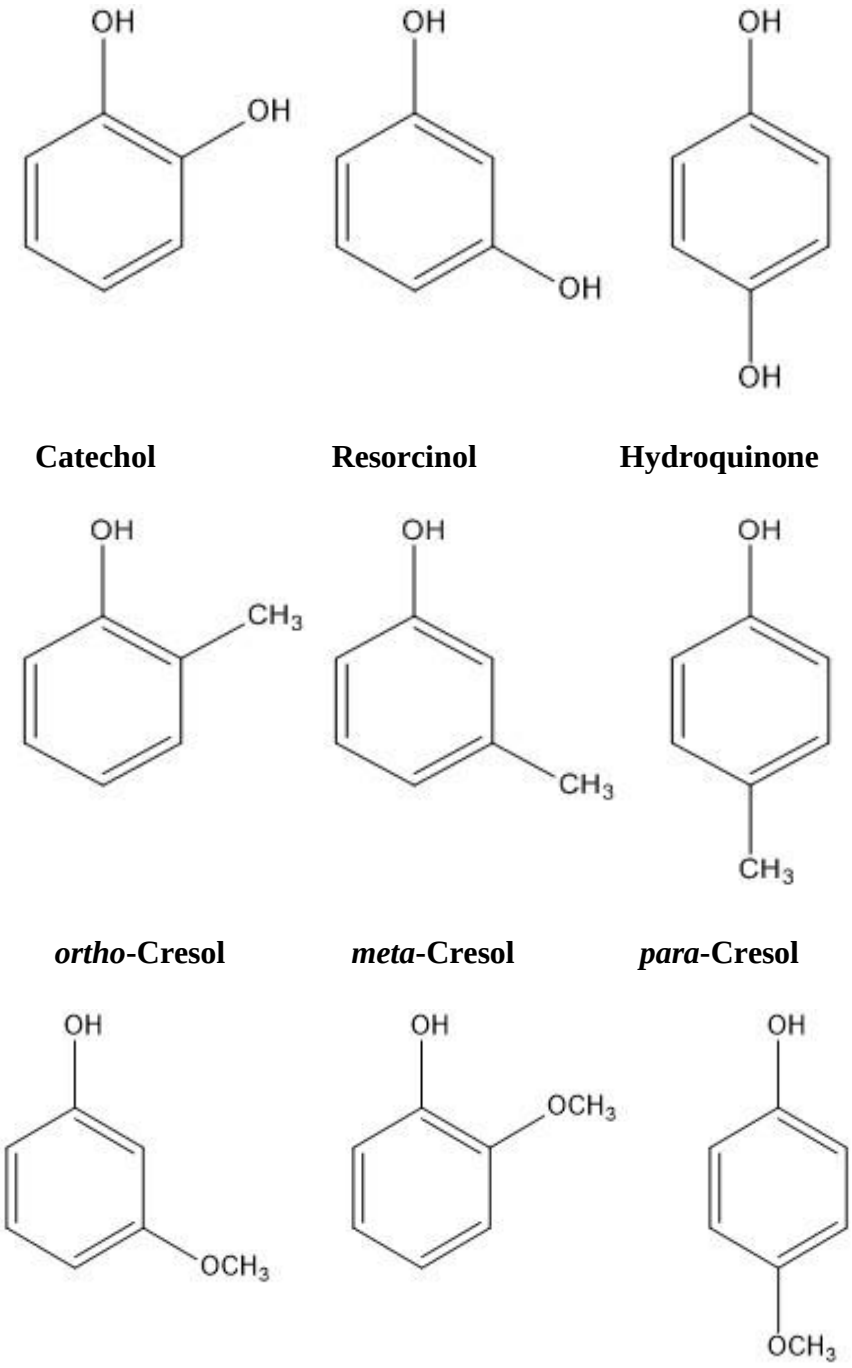

Catechol **Resorcinol** **Hydroquinone**

***ortho*-Cresol** ***meta*-Cresol** ***para*-Cresol**

3-Methoxyphenol **2-Methoxyphenol** **4-Methoxyphenol**

Figure 8. Oxygen-substituted aromatics under study for hydrogenation.

6.8 Diffusion Control

Prior to commencing experimental work, the mass transfer limitation of our hydrogenation reaction was tested through investigation of the effect of stirrer speed on the rate of reaction. As the substrate with the fastest reactivity, *para*-cresol was used for these reactions. All experiments were carried out as described in Section 6.2, with stirrer speed varied to encompass 250 rpm, 500 rpm, 1000 rpm (standard) and 1200 rpm.

No liquid samples were taken, with hydrogen consumption (mol) recorded and used to calculate the rate constant value for each reaction, as shown in Table 4 below:

Table 4. Initial rate constants for tested stirrer speeds.

Stirrer speed (rpm)	Rate constant ($x10^{-5}$, $molmin^{-1}$)
250	10.0
500	11.4
750	11.3
1000	11.3
1200	11.2

From above, it can be seen that the rate constant plateaued between 500 and 1200 rpm and as such it can be confirmed that our standard stirrer speed of 1000 rpm ensured we are operating under kinetic control.

6.9 Solvent

In advance of carrying out experimental work, the possibility of H-transfer from our standard solvent (isopropanol) was investigated. Catechol was tested over Rh/SiO_2 for 5 hours, with deuterium used as the reductant gas to ensure any hydrogenation that occurred would be a result of H-transfer from the solvent. The result of this experiment is shown in Figure 9:

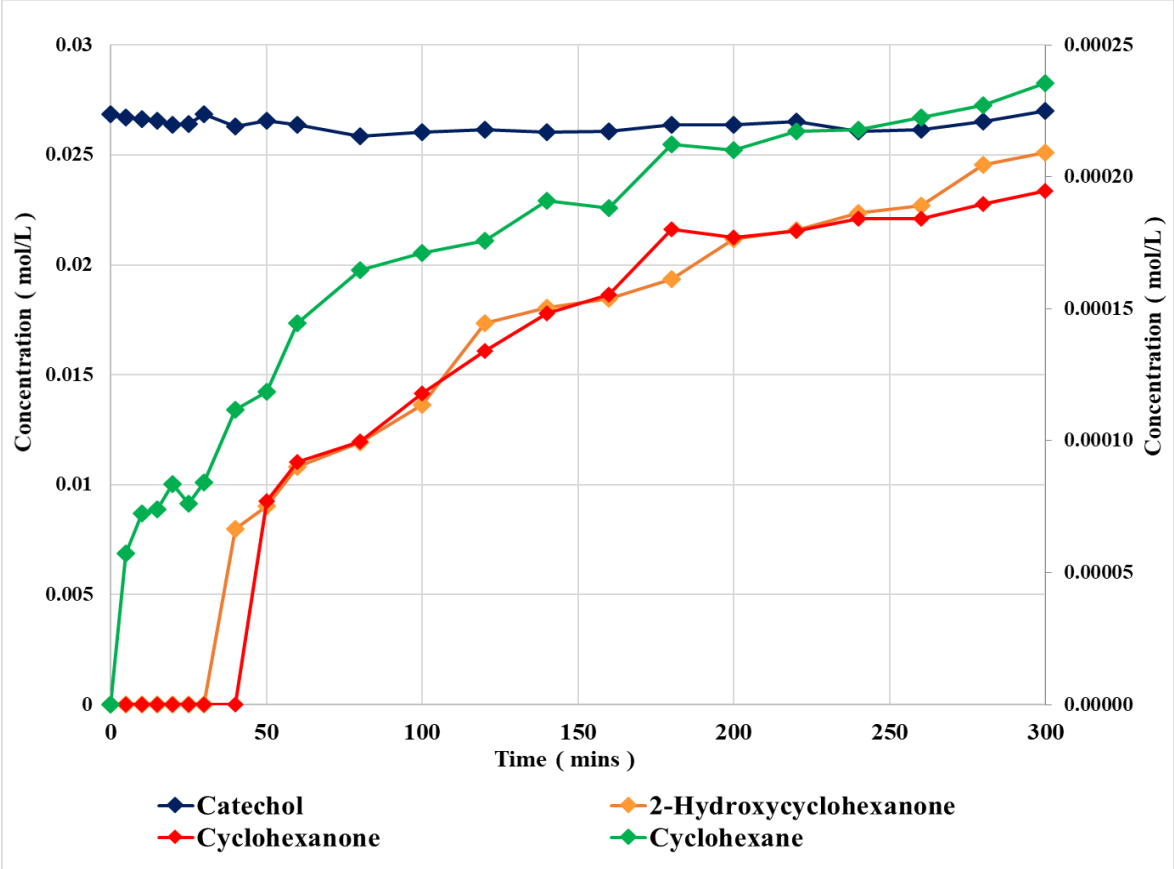

Figure 9. Catechol solvent test reaction, 323 K, 3 barg Ar, 0.1 g Rh/SiO_2.

It is clear from Figure 9 that minimal conversion of catechol occurred; a negligible cumulative yield of product, ~3%, was measured by the end of the reaction. From this result it can be stated that H-transfer from the solvent is minimal and can be disregarded during our study.

A deuterium NMR was carried out on the sample at 180 minutes reaction time to test for the occurrence of H/D exchange with the aromatic substrate. The spectrum from this is shown in Figure 10 below:

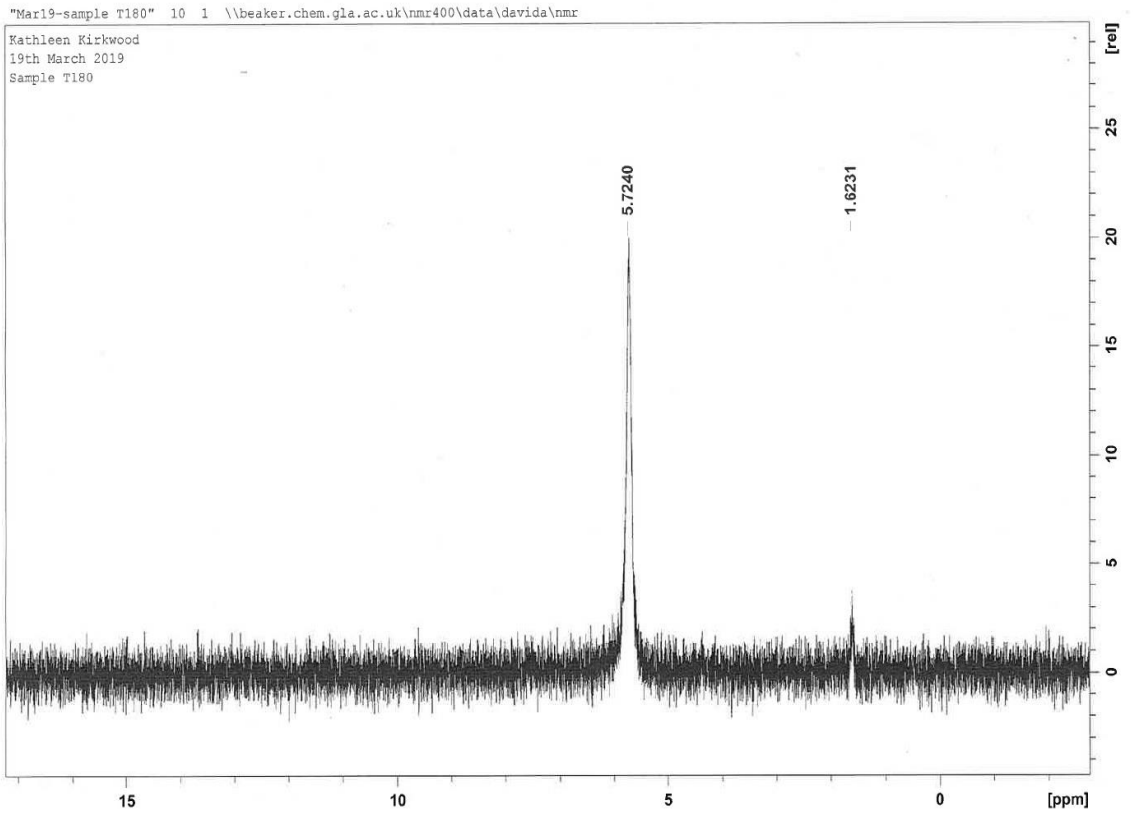

Figure 10. NMR Sample ran on T180 sample during catechol solvent test reaction.

It is clear that no proton exchange took place with the aromatic substrate. H/D exchange did occur with the -OH from the isopropanol solvent and with cyclohexane formed on the surface of the catalyst from the hydrogenation of catechol, as shown in the peaks at 5.71 ppm and 1.62 ppm respectively.

7 Results

7.1 Dihydroxybenzene Isomers

This section contains all results from hydrogenation of dihydroxybenzene isomers and covers the following sets of reactions: individual hydrogenation of catechol, resorcinol and hydroquinone including temperature and concentration variations; competitive hydrogenation reactions where the isomers were reacted in pairs and as a set of three; individual and competitive reactions with deuterium in place of hydrogen, and extended run time reactions. In addition, post catalyst thermal analysis data will be presented.

7.1.1 Individual Hydrogenation Standard Reactions

In this set of reactions catechol, resorcinol and hydroquinone hydrogenation will be shown at our standard reaction conditions of 323 K, 10 mmol substrate and 3 barg hydrogen. Catechol is shown below in Figure 11:

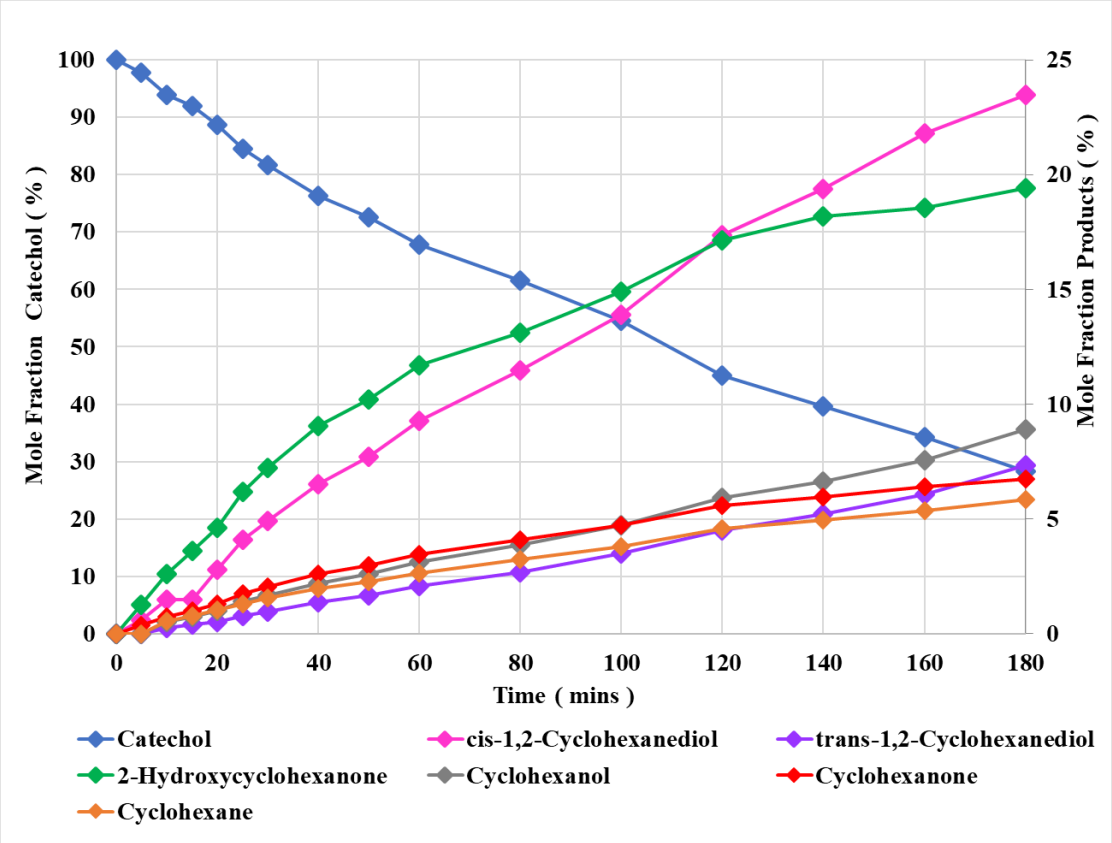

Figure 11. Reaction profile of catechol hydrogenation. Conditions, 323 K, 10 mmol, 3 barg.

It can be seen that ~ 76 % conversion of catechol occurred by 180 min. Formation of all products was observed from the initial stages of the reaction with the ring hydrogenated, *cis*-1,2-cyclohexanediol and 2-hydroxycyclohexanone, formed to the greatest extent, with a mole fraction percentage of 25 % and 20 % respectively. HDO products, cyclohexanone,

cyclohexanol and cyclohexane, were all observed, although to a lesser degree than that of the hydrogenated products, with cyclohexanol recording the highest mole fraction at ~ 10 %.

For resorcinol at identical conditions, the reaction profile is shown below in Figure 12:

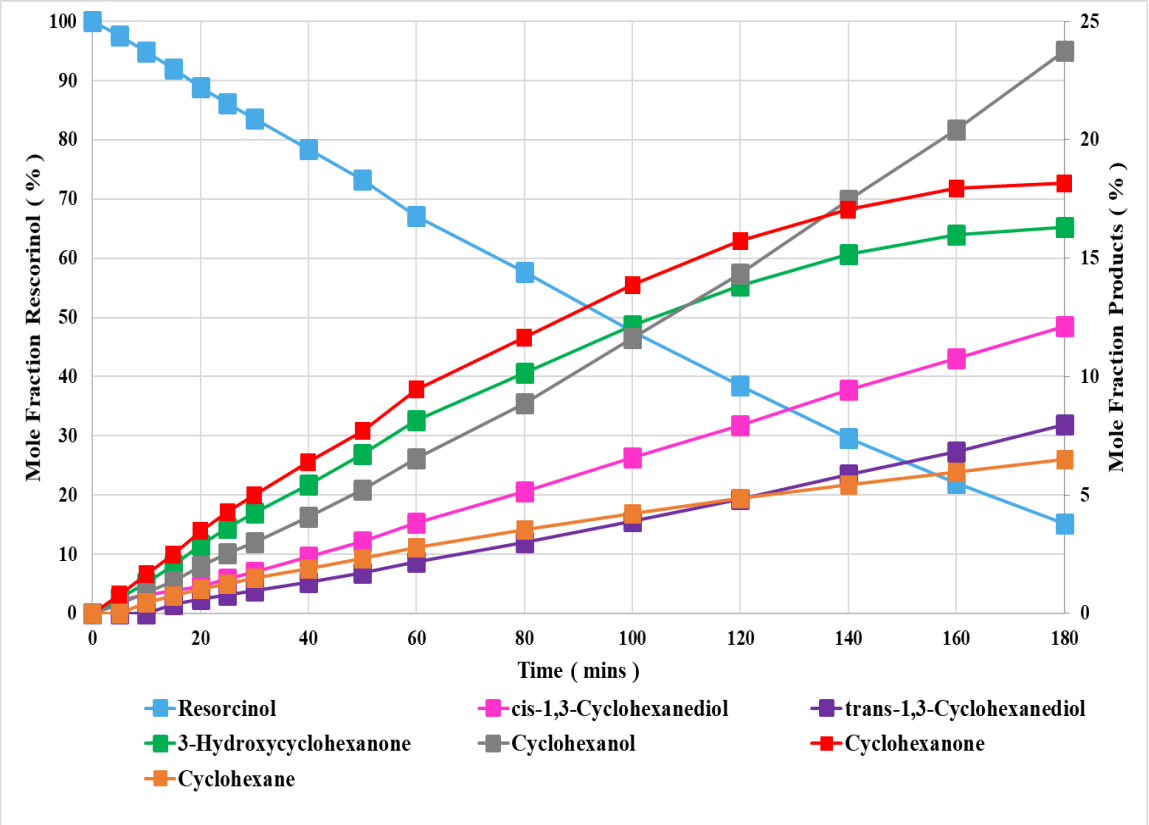

Figure 12. Reaction profile of resorcinol hydrogenation. Conditions, 323 K, 10 mmol, 3 barg.

It can be seen that ~ 86 % conversion of resorcinol occurred by 180 min a figure 10 % greater than that observed with catechol hydrogenation. In contrast with catechol, the HDO product cyclohexanol was formed to the greatest extent with a mole fraction of ~ 26 % at 180 minutes. The formation of the other HDO products, cyclohexanone and cyclohexane, were observed at ~ 17 % and ~ 6 % respectively. In this instance, 3-hydroxycyclohexanone was the major ring hydrogenated product at ~ 17 % mole fraction, with a decrease in formation of the *cis*-cyclohexanediol observed when compared with catechol.

For hydroquinone under identical conditions, the reaction profile is shown below in Figure 13:

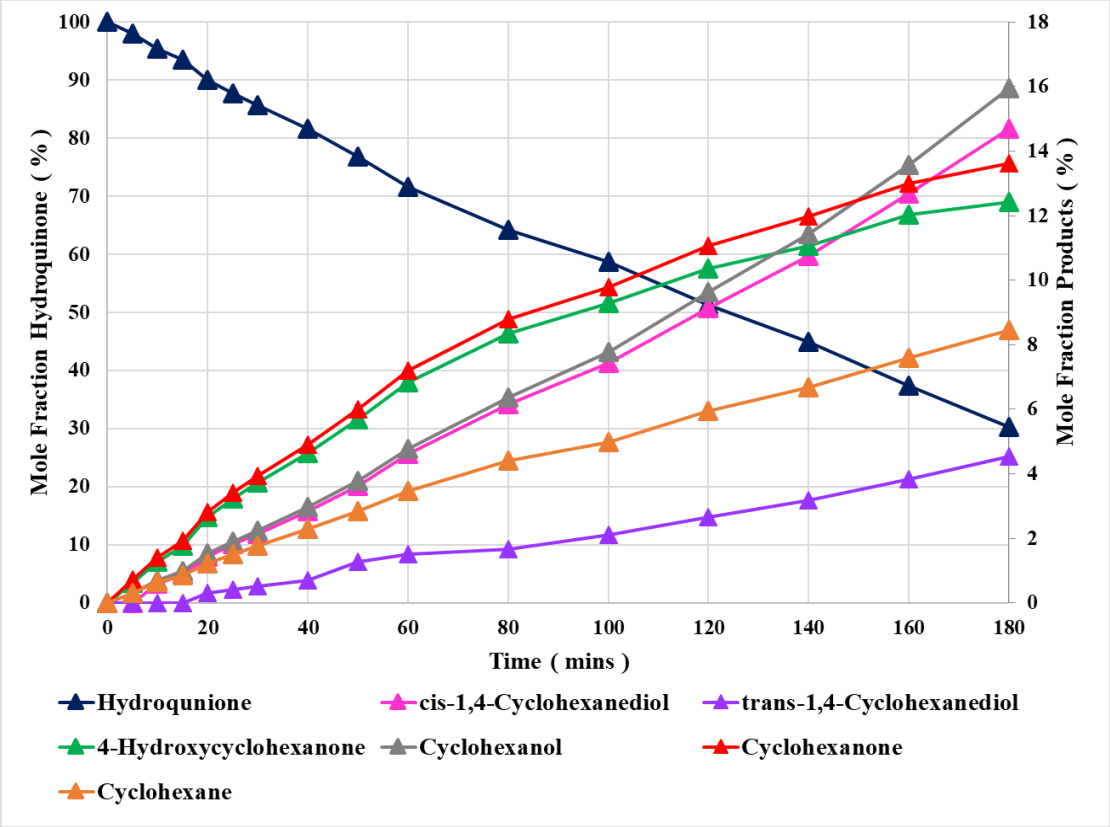

Figure 13. Reaction profile of hydroquinone hydrogenation. Conditions, 323 K, 10 mmol, 3 barg.

It can be seen that at ~ 71 % conversion at 180 minutes hydroquinone exhibited the slowest reaction rate of all three isomers. As with resorcinol, the major product formed was the HDO product, cyclohexanol, with a mole fraction of ~ 16 % at 180 minutes. The other HDO products, cyclohexanone and cyclohexane, were observed at ~ 14 % and ~ 8 % respectively. The major ring hydrogenated product was the *cis*-cyclohexanediol, similar to that observed with catechol.

7.1.2 Temperature Variations of Dihydroxybenzene Isomers

7.1.2.1 Catechol Temperature Variations

In this set of reactions, catechol was hydrogenated at 10 K increments from 303 to 343 K, with 323 K taken as the standard reaction. Hydrogen pressure (3 barg) and reactant concentration (10 mmol) were kept constant to understand the effect temperature had on catechol hydrogenation. The graphs shown below are in increasing order of temperature:

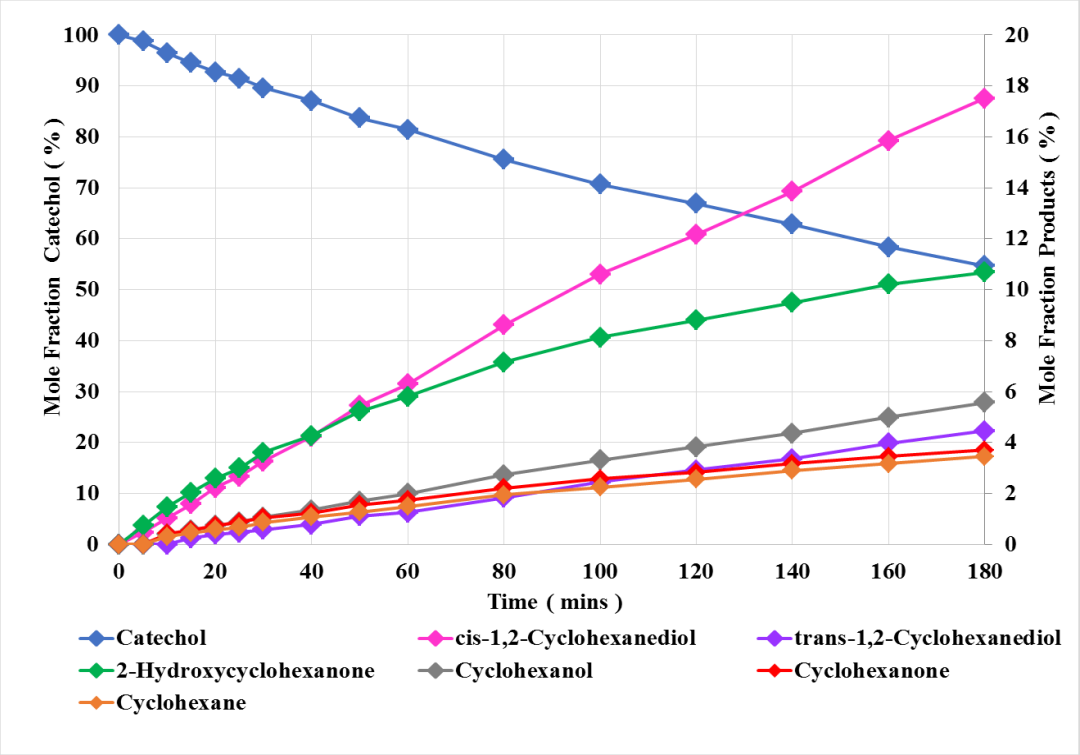

Figure 14. Reaction profile of catechol hydrogenation. Conditions, 303 K, 10 mmol, 3 barg.

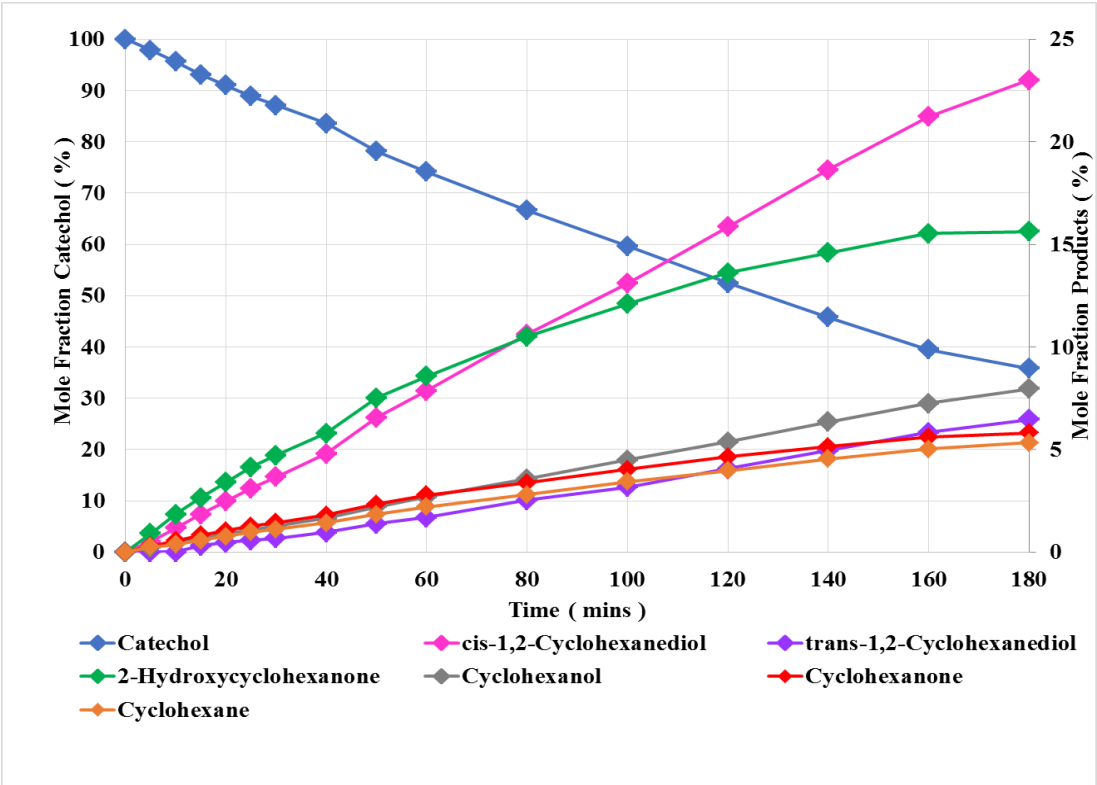

Figure 15. Reaction profile of catechol hydrogenation. Conditions, 313 K, 10 mmol, 3 barg.

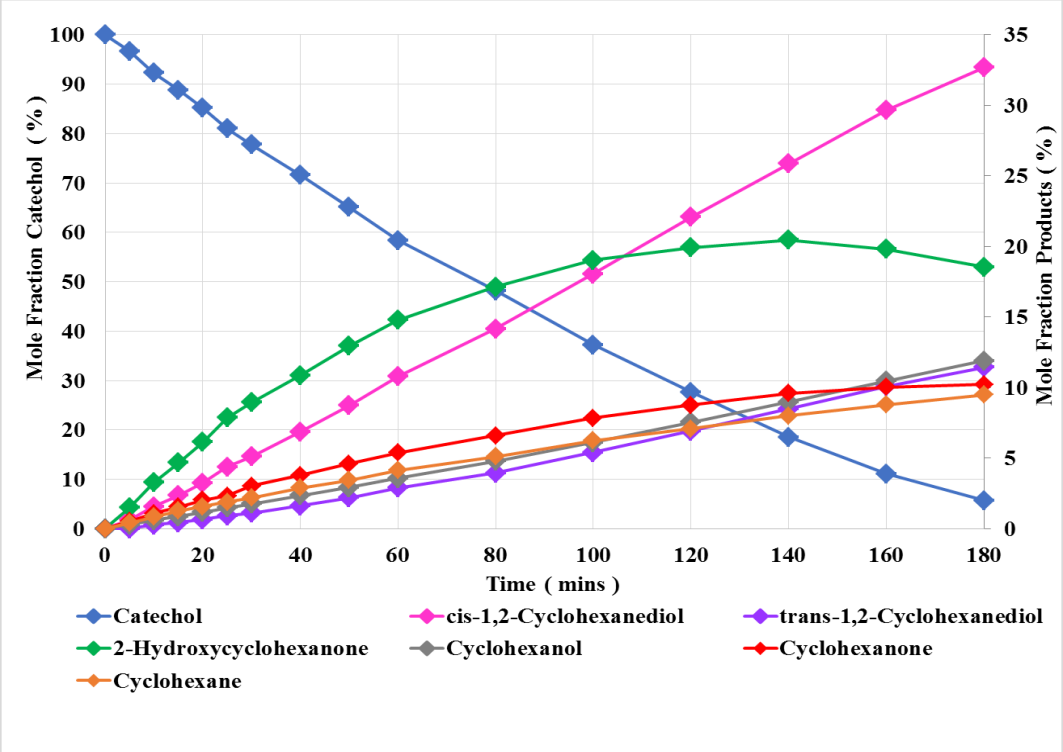

Figure 16. Reaction profile of catechol hydrogenation. Conditions, 333 K, 10 mmol, 3 barg.

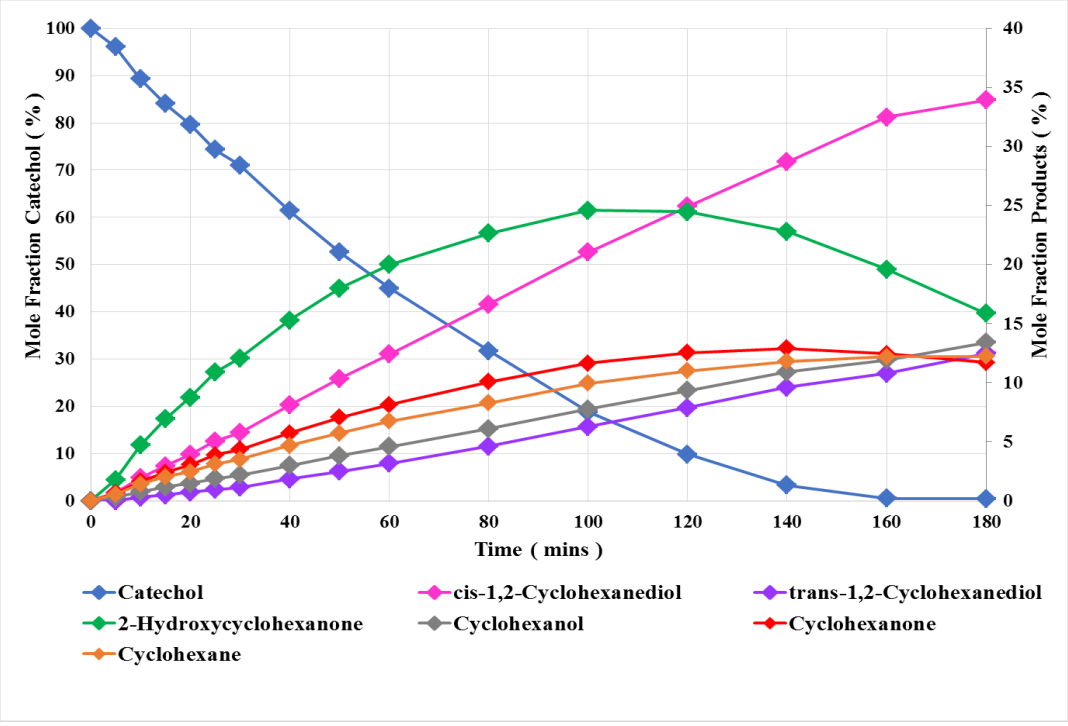

Figure 17. Reaction profile of catechol hydrogenation. Conditions, 343 K, 10 mmol, 3 barg.

From Figures 14-17 above, it can be clearly seen as temperature was increased, the reaction rate increased. The rate constant at 303 K was 3.1 $x10^{-3}min^{-1}$ compared with 11.3 $x10^{-3}min^{-1}$ at 343 K; an almost fourfold increase in rate from a 40 K increase in

temperature. The main catechol hydrogenation product, *cis*-1,2-cyclohexanediol, formed at ~ 17.5 % at 303 K by reaction end, compared with ~ 34 % at 343 K, showing a near doubling of product yield over the temperature range measured. The HDO product, cyclohexanol, also showed an increase with temperature: from ~ 6 % to ~ 15 % at 180 minutes over the 40 K measured range. The product distribution of the hydrogenated (*cis*+*trans*-1,2-cyclohexanedioland 2-hydroxycyclohexanone) and hydrodeoxygenated products (cyclohexanone, cyclohexanol and cyclohexane) at ~ 35 % conversion is shown below in Figure 18:

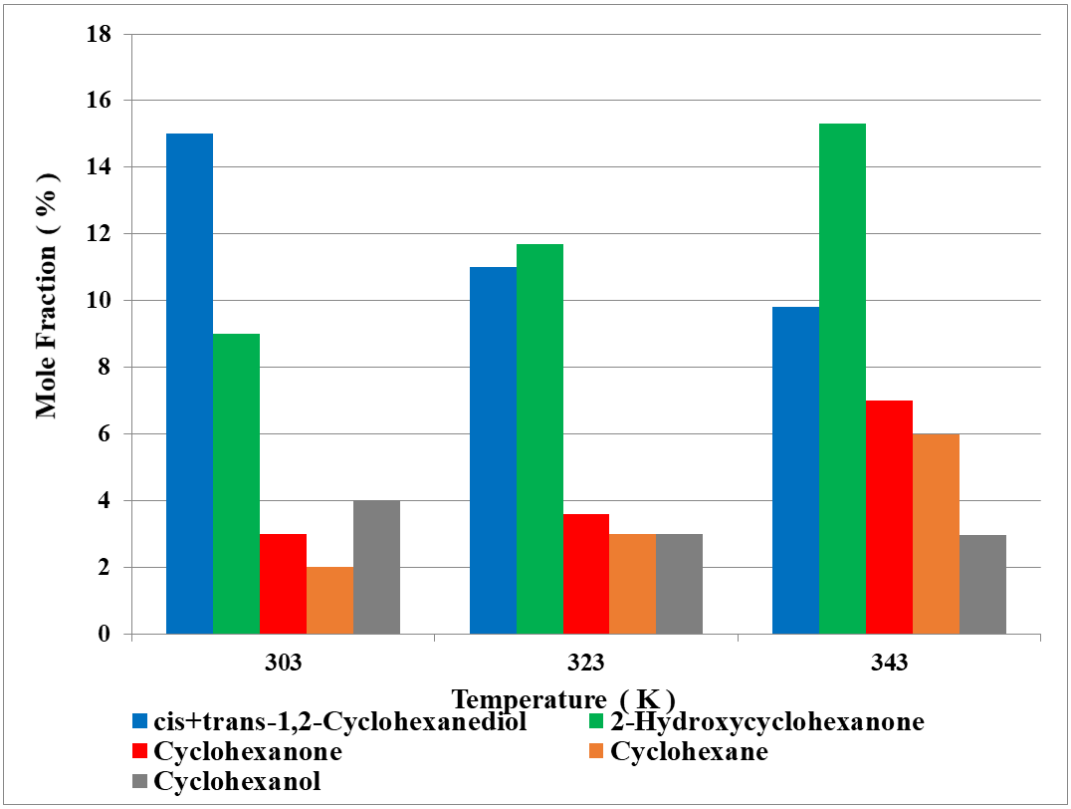

Figure 18. Product distribution at ~ 35 % conversion for catechol hydrogenation.

It can be seen from Figure 18 that as temperature was increased formation of the intermediate hydrogenated product, 2-hydroxycyclohexanone, increased whilst that of the *cis*/*trans*-cyclohexanediol decreased. Of the HDO products, cyclohexanone formation was seen to increase with temperature, whilst that of cyclohexanol decreased. Cyclohexane, which has undergone two –OH bond cleavages, increased across the temperature range. The relationship between temperature and conversion of catechol is shown below in Figure 19:

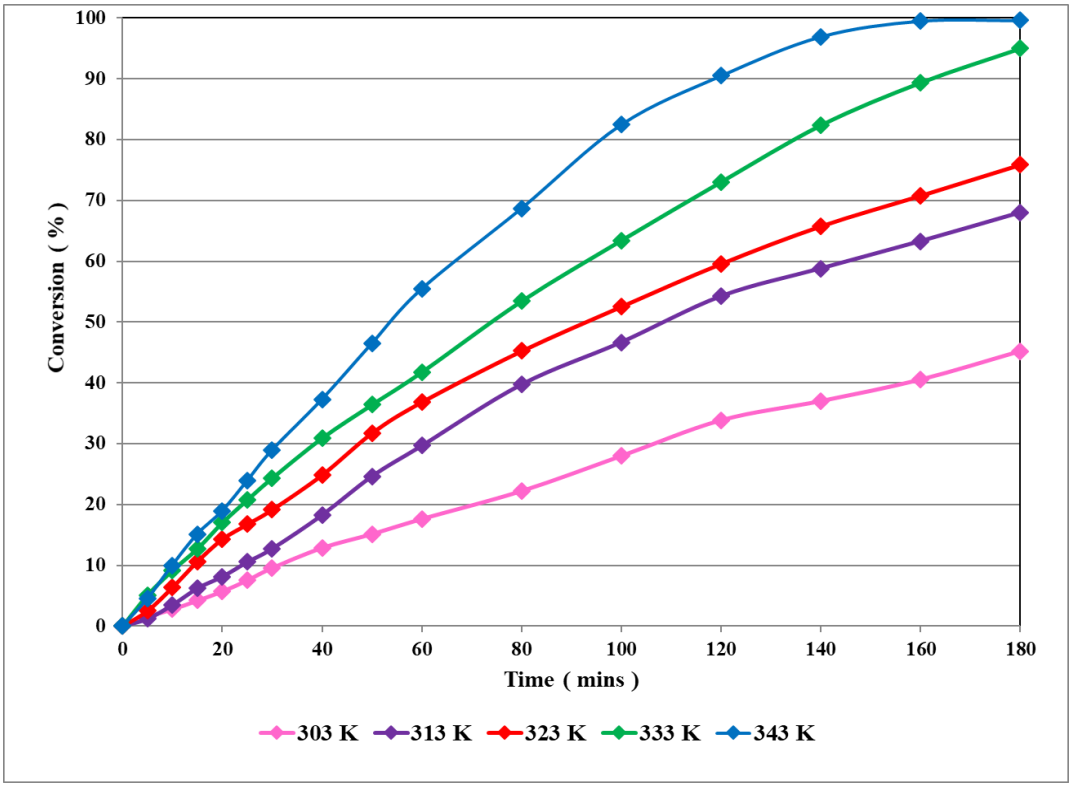

Figure 19. Effect of temperature on the conversion of catechol hydrogenation.

It can be seen from Figure 19 that an increase in temperature results in a significant effect on catechol conversion with an increase from ~ 45 % to full conversion observed over the 303 – 343 K temperature range.

For each temperature reaction, the rate constant was calculated and an example of this, at 333 K, is shown below in Figure 20:

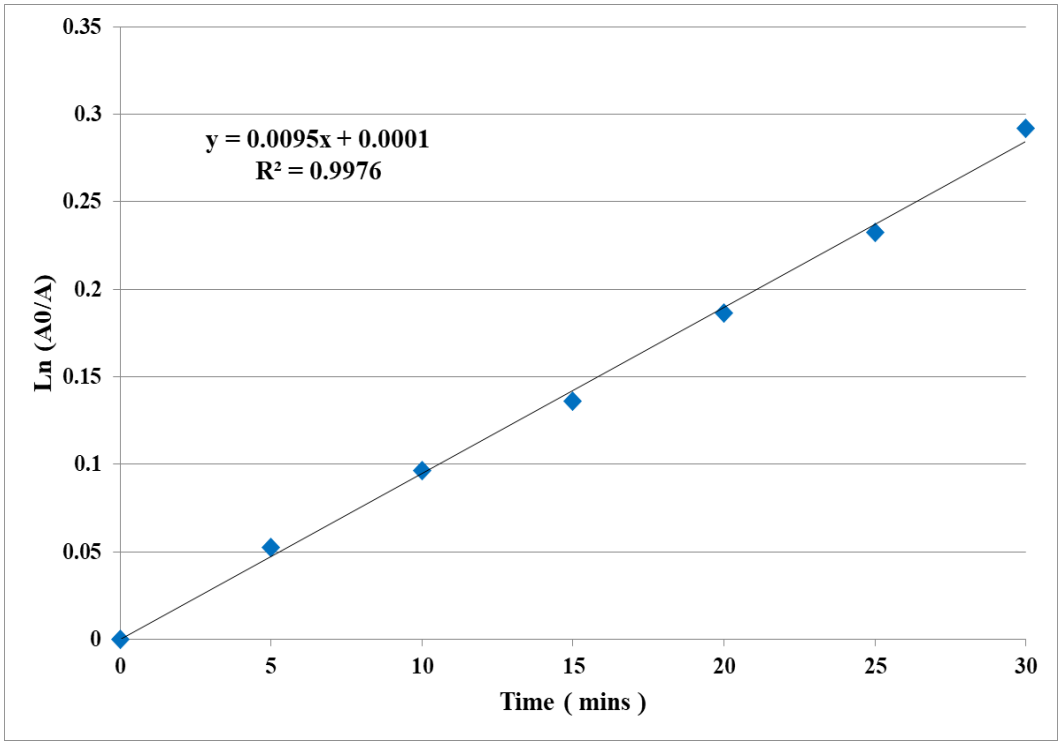

Figure 20. Rate constant graph for catechol hydrogenation at 333 K.

From the integrated form of the Arrhenius equation shown in Equation 7 of the Experimental Section, ln k was plotted against ($\frac{1}{T}$) using the values in Table 5 below:

Table 5. Summary of data for catechol activation energy.

Temperature (K)	k (x10^{-3}min^{-1})	1/T (x- axis)	Ln k (y-axis)
303	3.3	0.00330	-5.7138
313	4.6	0.00319	-5.3816
323	8.3	0.00309	-4.9062
333	9.5	0.00300	-4.6564

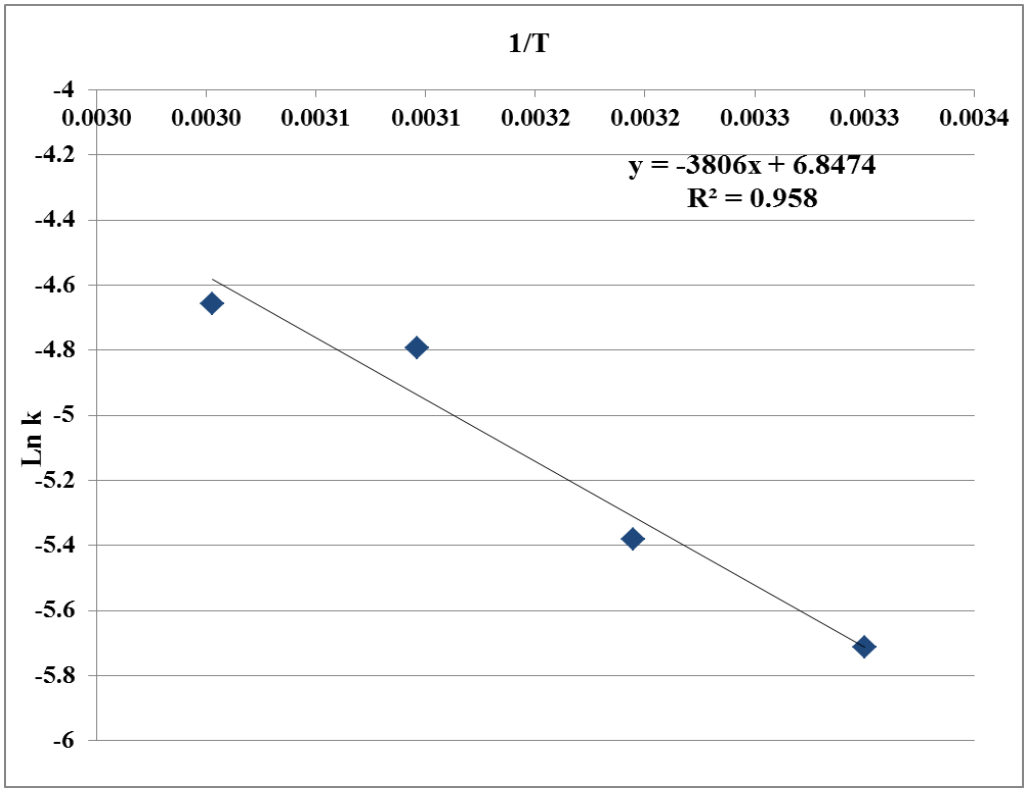

Figure 21. Activation energy plot for catechol.

Therefore, the gradient of ln k against 1/T equals $-\frac{Ea}{RT}$ and can be expressed for Ea as:

- Ea = -mR
- -(-3806 x 8.314)/1000
- = 31.6 kJmol^{-1}

From this, an overall activation energy for catechol hydrogenation of 31.6 kJmol^{-1} was measured.

7.1.2.2 Resorcinol Temperature Variations

In this set of reactions, resorcinol was hydrogenated at 10 K increments from 303 to 343 K, with 323 K taken as the standard reaction. Hydrogen pressure (3 barg) and reactant concentration (10 mmol) were kept constant to understand the effect temperature had on resorcinol hydrogenation. The graphs of these are shown below in increasing order of temperature:

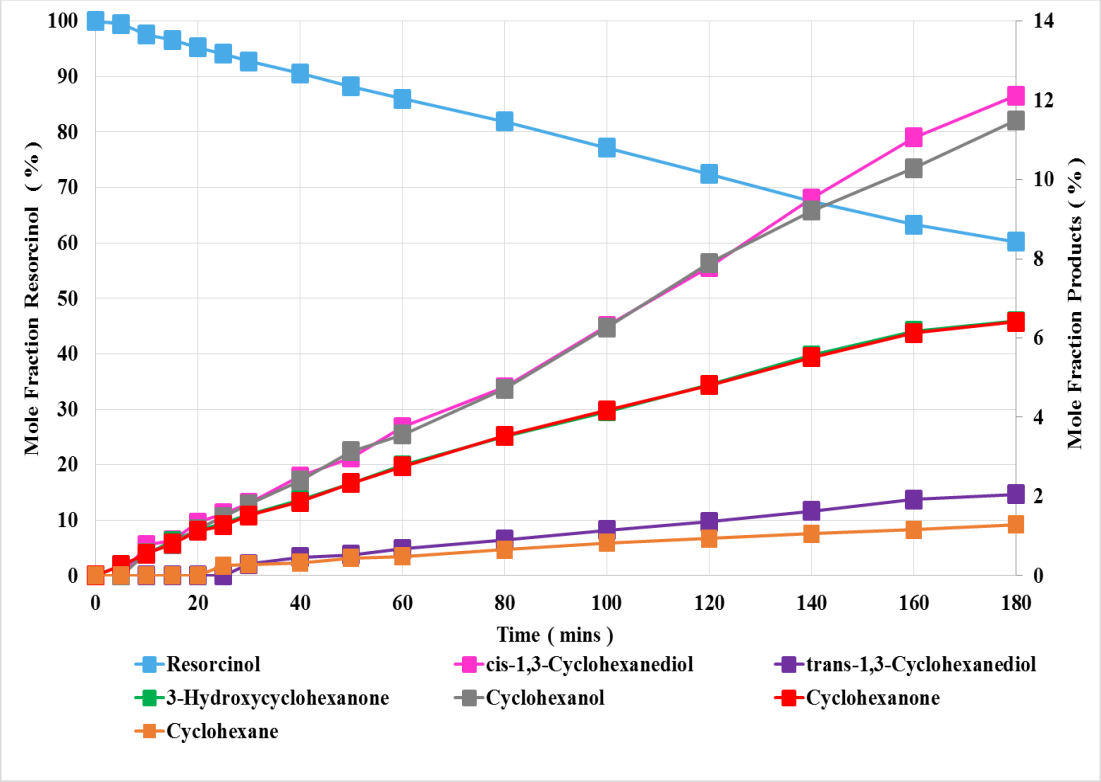

Figure 22. Reaction profile of resorcinol hydrogenation. Conditions, 303 K, 10 mmol, 3 barg.

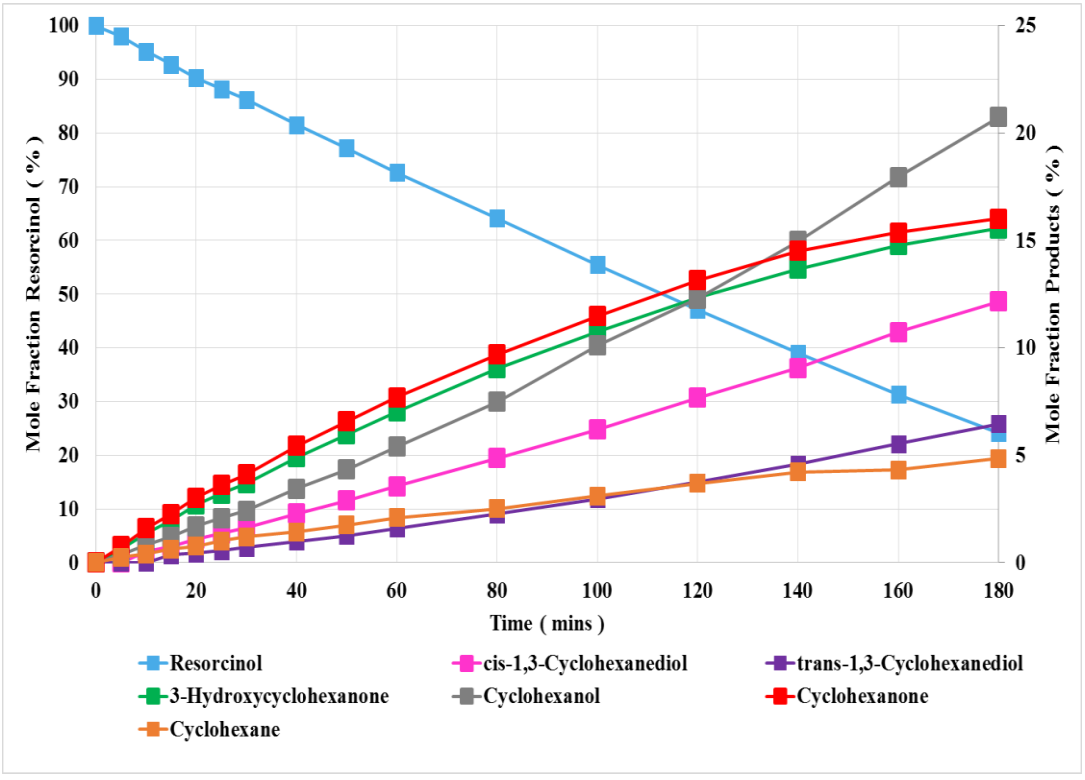

Figure 23. Reaction profile of resorcinol hydrogenation. Conditions, 313 K, 10 mmol, 3 barg.

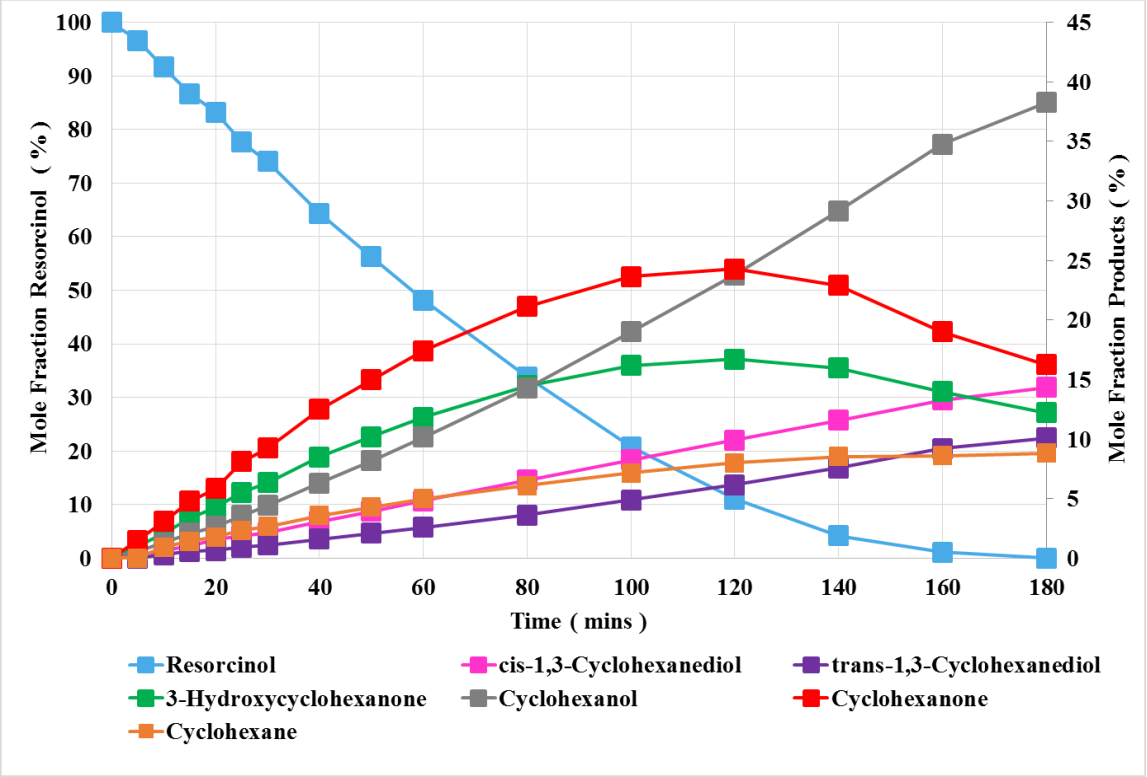

Figure 24. Reaction profile of resorcinol hydrogenation. Conditions, 333 K, 10 mmol, 3 barg.

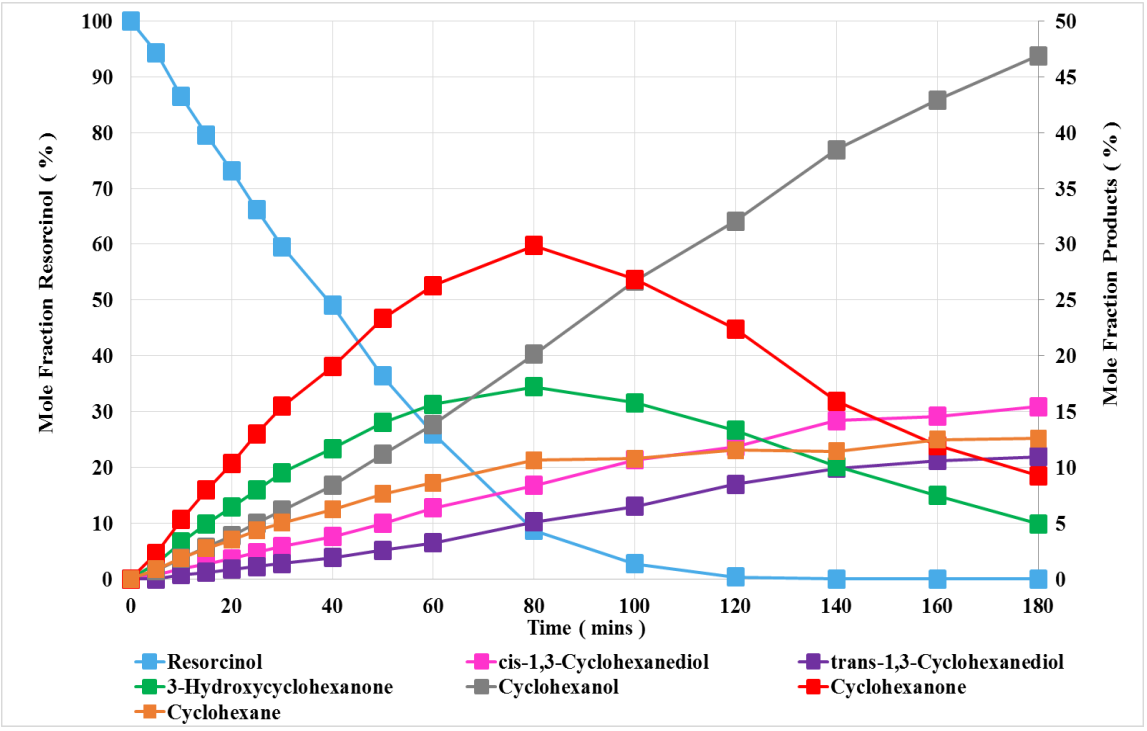

Figure 25. Reaction profile of resorcinol hydrogenation. Conditions, 343 K, 10 mmol, 3 barg.

From Figures 22-25 above the formation of HDO products increased with temperature, with a cumulative yield of ~ 66 % at 343 K compared to ~ 18 % at 303 K at 180 minutes. The rate of reaction increased significantly with temperature showing a six fold increase

between 303 K (3.3 x$10^{-3}$$min^{-1}$) and 343 K (21.0 x$10^{-3}$$min^{-1}$). The product distribution of the hydrogenated (*cis*/*trans*-cyclohexanediol and 2-hydroxycyclohexanone) and hydrodeoxygenated products (cyclohexanol, cyclohexanone and cyclohexane) at ~ 35 % conversion is shown below in Figure 26:

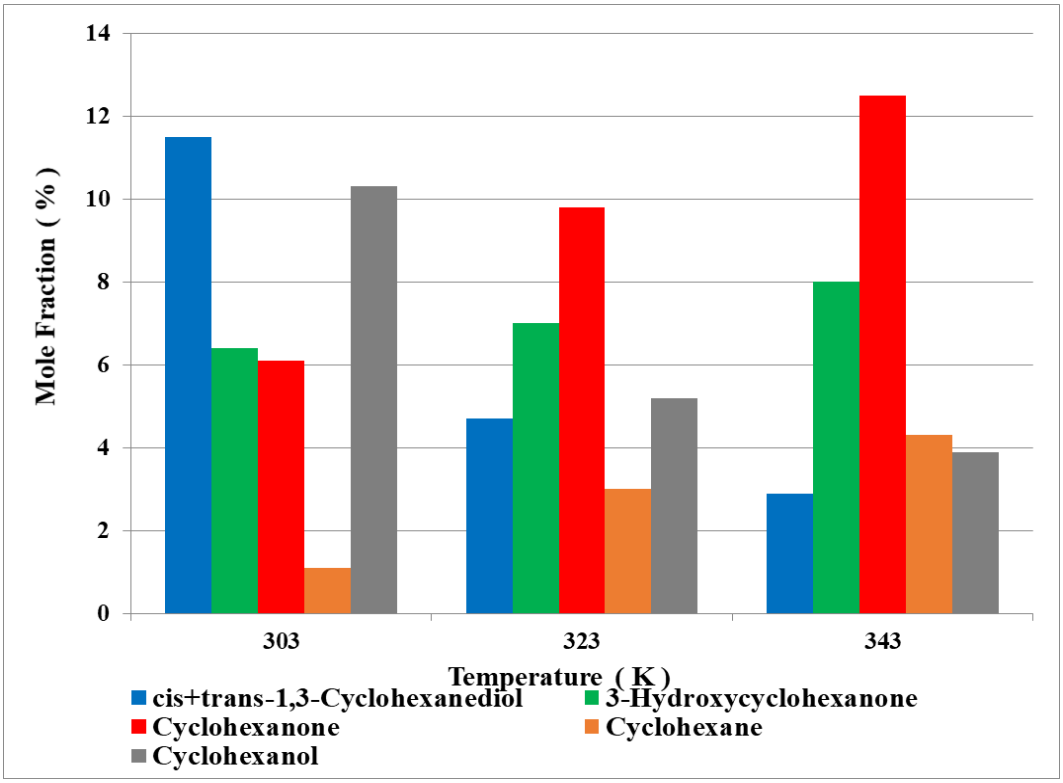

Figure 26. Product distribution at ~ 35 % conversion for resorcinol hydrogenation.

It can be seen from Figure 26 that temperature had a significant effect on the product distribution for resorcinol hydrogenation. A substantial decrease in the formation of the hydrogenated products, *cis*+*trans*-cyclohexanediol, was observed, 3-hydroxycyclohexanone, however, showed a slight increase over the measured temperature range. For the HDO products, a doubling (6 to ~ 12 %) in the observed levels of cyclohexanone and an increase from 1 to 4 % for cyclohexane was observed between 303 and 343 K. Cyclohexanol formation however, showed a 50 % decrease (10 to ~ 4 %) over the same temperature range. The effect of temperature on the conversion of resorcinol is shown below in Figure 27:

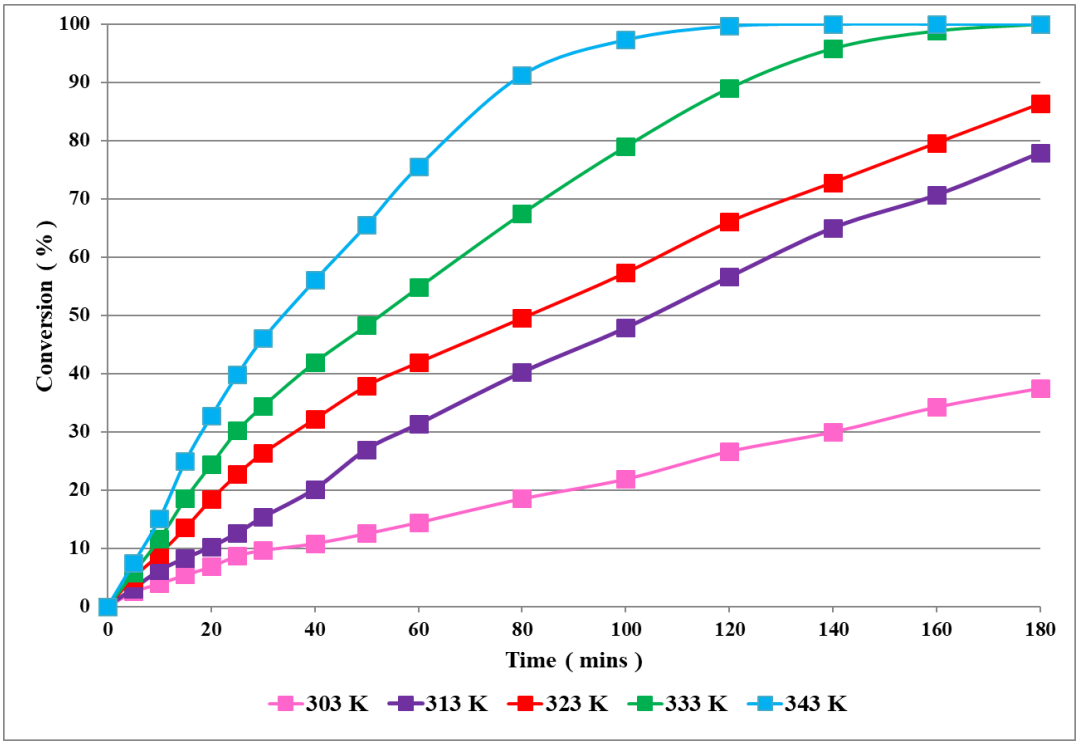

Figure 27. Temperature effect on conversion of resorcinol hydrogenation.

It is apparent from Figure 27 that the increase in temperature from 303 K to 343 K had a significant effect on the conversion of resorcinol. Increasing from ~ 37 % conversion at 303 K at the end of the reaction to full conversion for the 343 K at ~ 120 minutes.

For each temperature, the rate constant was calculated and an example of this at 313 K is shown below in Figure 28:

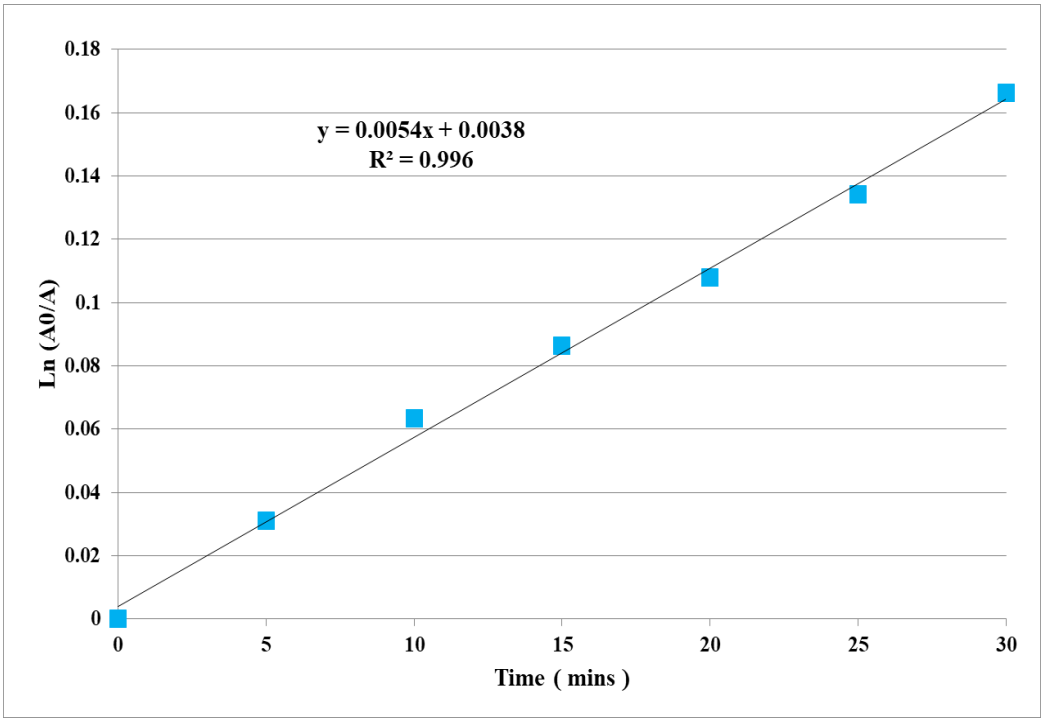

Figure 28. Rate constant graph for hydrogenation at 313 K.

From the integrated form of the Arrhenius equation shown in Equation 7 of the Experimental Section, ln k was plotted against ($\frac{1}{T}$) using the values in the Table 6 below:

Table 6. Data used to calculate activation energy for resorcinol.

Temperature (K)	**k ($x10^{-3}min^{-1}$)**	**1/T (x- axis)**	**Ln k (y-axis)**
303	3.3	0.00330	-5.7138
313	5.4	0.00319	-5.2213
323	11.9	0.00309	-4.8283
333	14.6	0.00300	-4.2267
343	21.9	0.00291	-3.8212

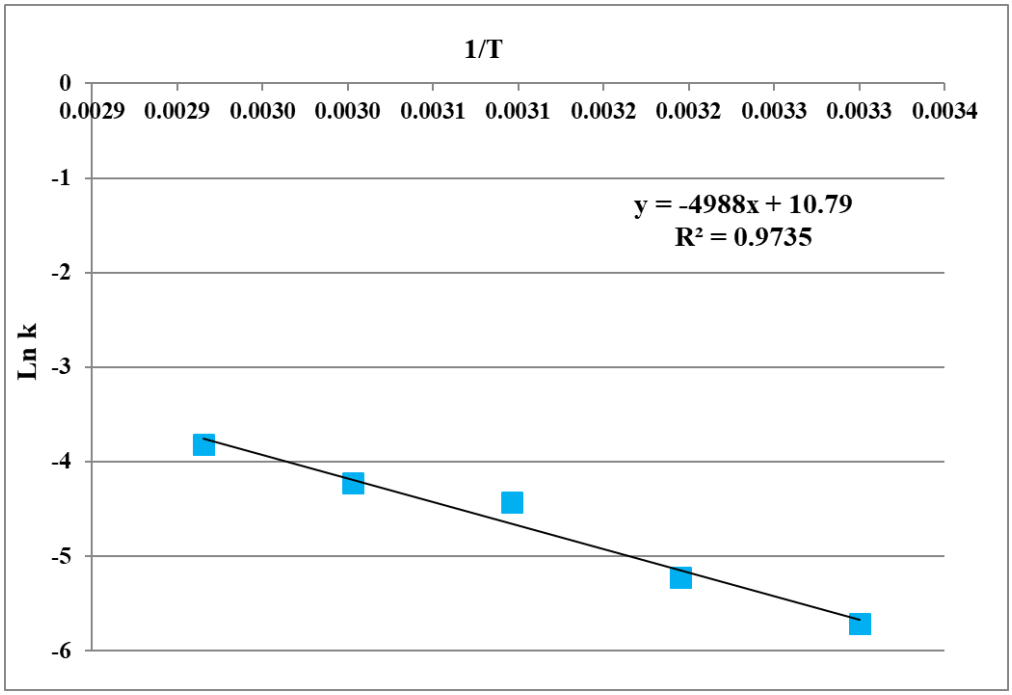

Figure 29. Activation energy plot for resorcinol hydrogenation.

Therefore, the gradient of ln k against 1/T equals $-\frac{Ea}{RT}$ and can be expressed for Ea as:

- Ea= -mR
- -(-4988*8.314)/1000
- = 41.47 kJmol^{-1}

From this, an overall activation energy for catechol hydrogenation of 41.3 kJmol^{-1} was measured.

7.1.2.3 Hydroquinone Temperature Variations

In this set of reactions, hydroquinone was hydrogenated at 10 K increments from 303 to 343 K, with 323 K taken as the standard reaction. Hydrogen pressure (3 barg) and reactant concentration (10 mmol) were kept constant to understand the effect temperature had on hydroquinone hydrogenation. The graphs of these are shown below in increasing order of temperature:

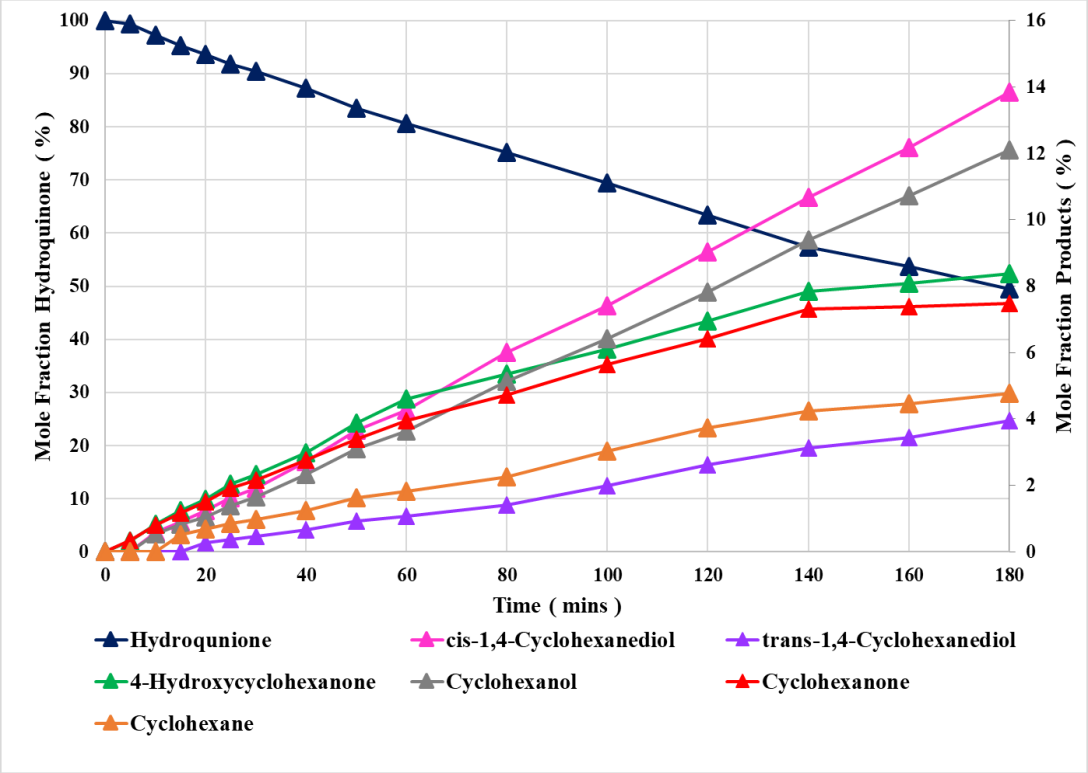

Figure 30. Reaction profile of hydroquinone hydrogenation. Conditions, 303 K, 10 mmol, 3 barg.

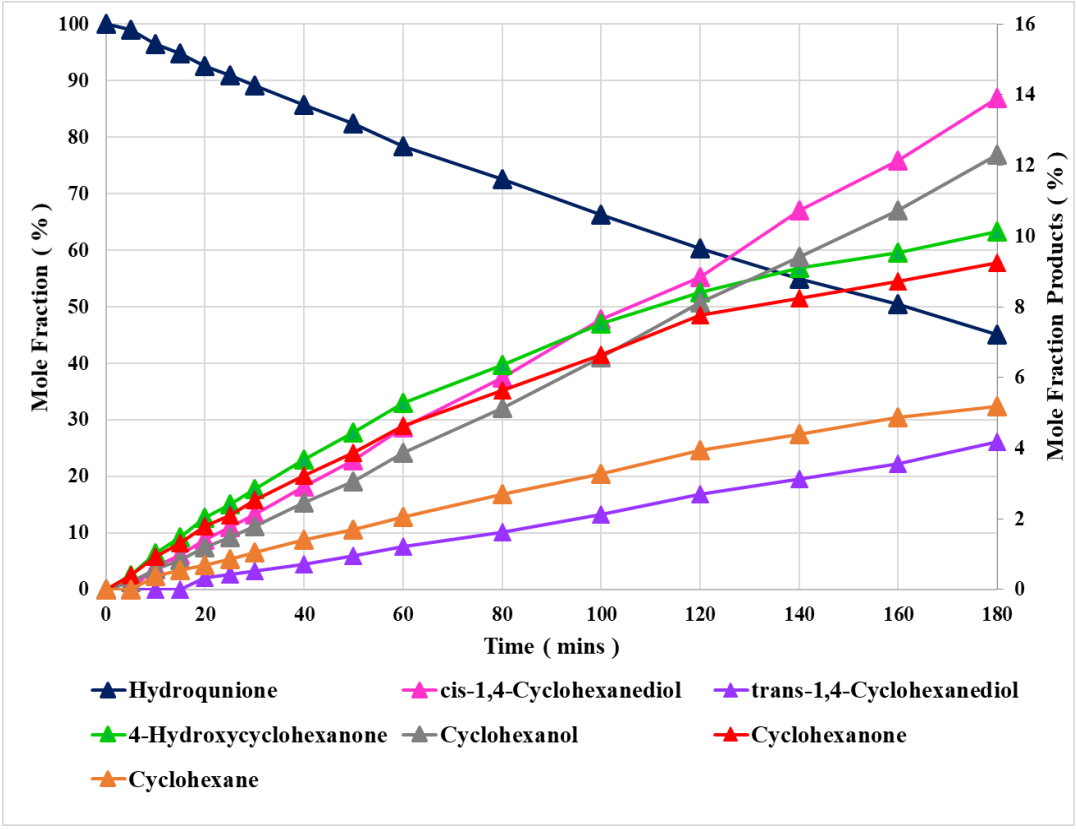

Figure 31. Reaction profile of hydroquinone hydrogenation. Conditions, 313 K, 10 mmol, 3 barg.

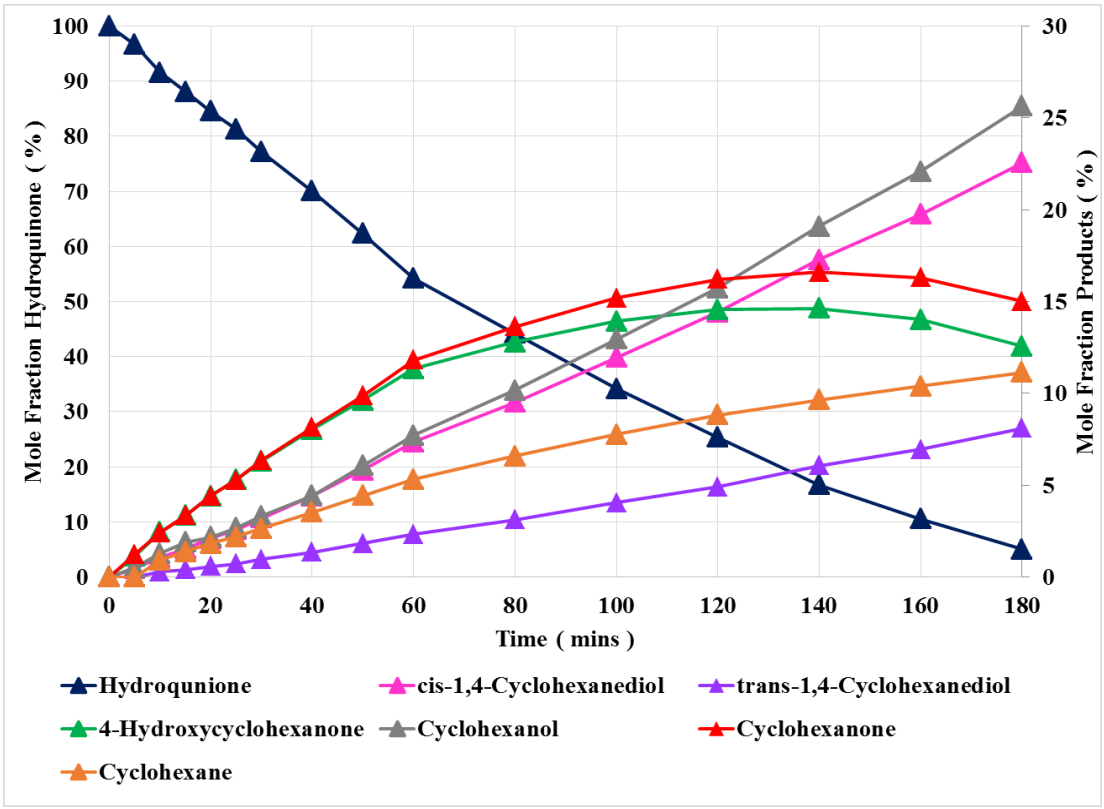

Figure 32. Reaction profile of hydroquinone hydrogenation. Conditions, 333 K, 10 mmol, 3 barg.

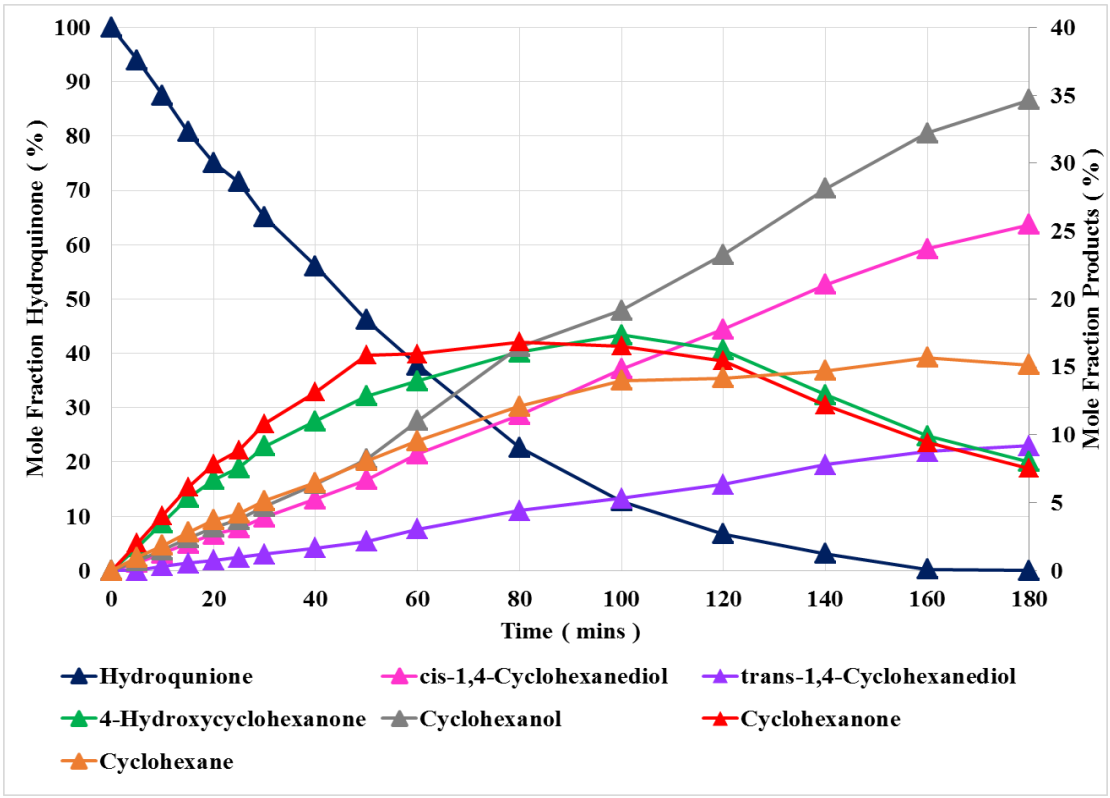

Figure 33. Reaction profile of hydroquinone hydrogenation. Conditions, 343 K, 10 mmol, 3 barg.

From Figures 30 – 33 above it can be seen that the rate of reaction had an almost fourfold increase from 3.3 x$10^{-3}$$min^{-1}$ to 12.5 x$10^{-3}$$min^{-1}$ after a 40 K rise in temperature. The cumulative yield of the HDO products at reaction end was ~ 57 % at 343 K compared to ~ 27 % at 303 K. The product distribution of the hydrogenated (*cis*/*trans*-cyclohexanediol and 4-hydroxycyclohexanone) and hydrodeoxygenated products (cyclohexanol, cyclohexanone and cyclohexane) at ~ 35 % conversion is shown below in Figure 34:

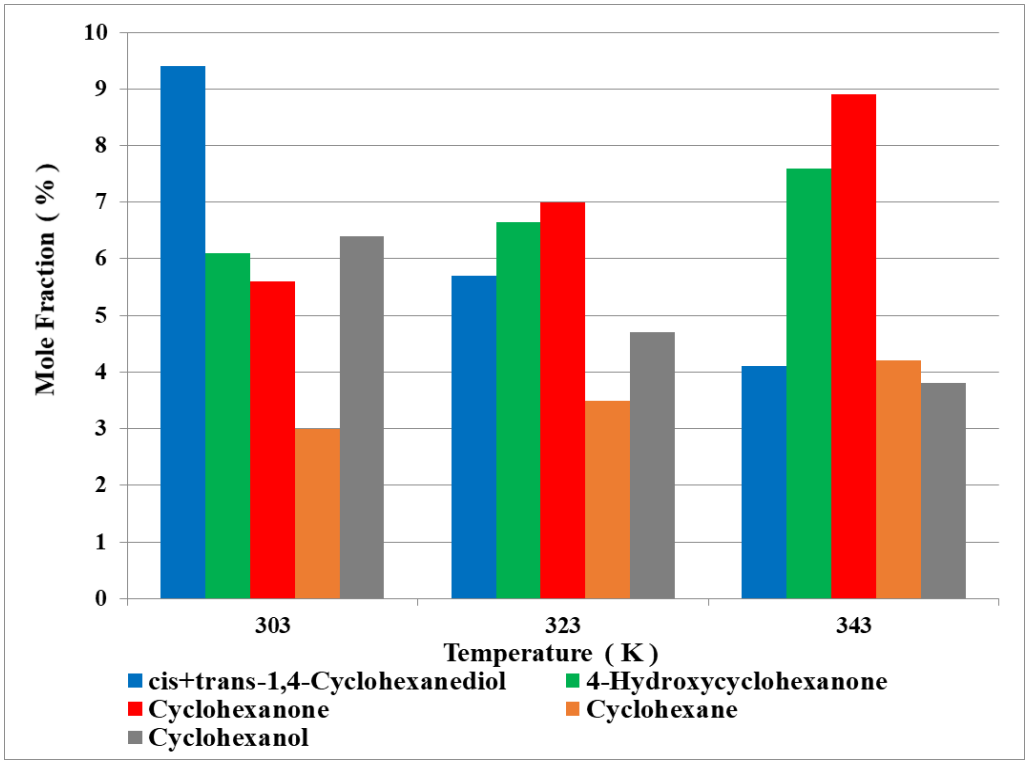

Figure 34. Product distribution at ~ 35 % conversion for hydroquinone hydrogenation.

It can be seen from Figure 34 that the formation of the hydrogenated products *cis* and *trans*-cyclohexanediol decreased whilst 4-hydroxycyclohexanone increased as the temperature was elevated. Analysis of the HDO products showed an increase in production of cyclohexanone and cyclohexane and a decrease in cyclohexanol between 303 and 343 K. The effect of temperature on the conversion of hydroquinone is shown below in Figure 35:

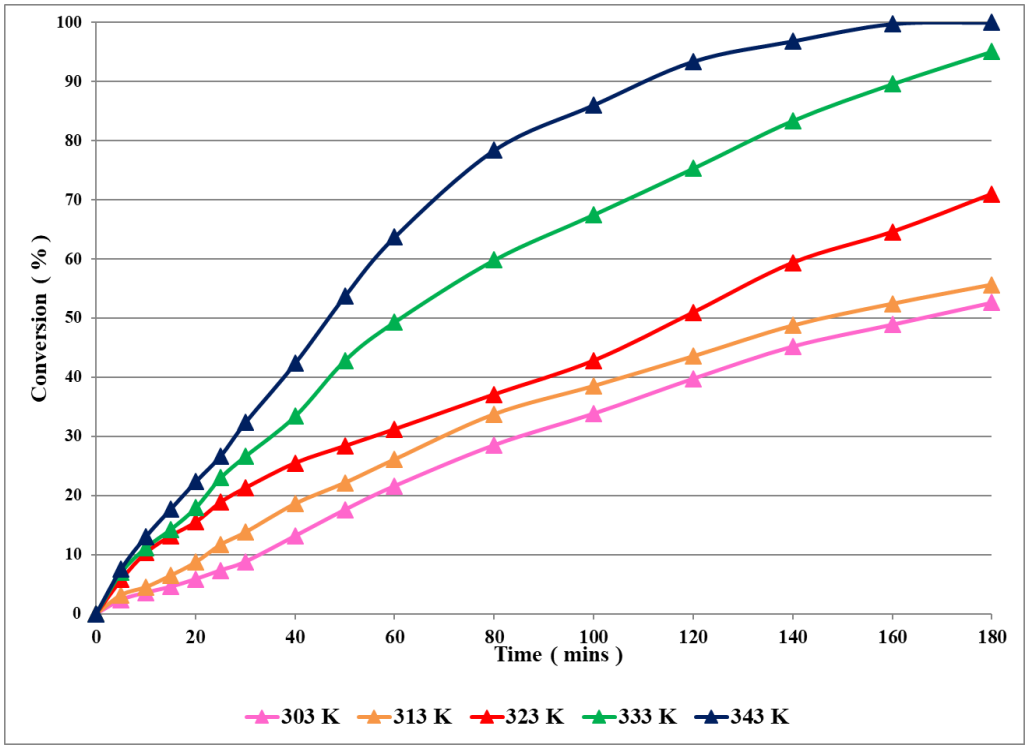

Figure 35. Temperature effect on conversion of hydroquinone hydrogenation.

It can be seen as the temperature increased the conversion of hydroquinone increased. The conversion at 303 K was ~ 50 % by reaction end, whereas at 343 K hydroquinone was at full conversion by 160 minutes.

For each temperature, the rate constant was calculated and an example of this at 343 K is shown below in Figure 36:

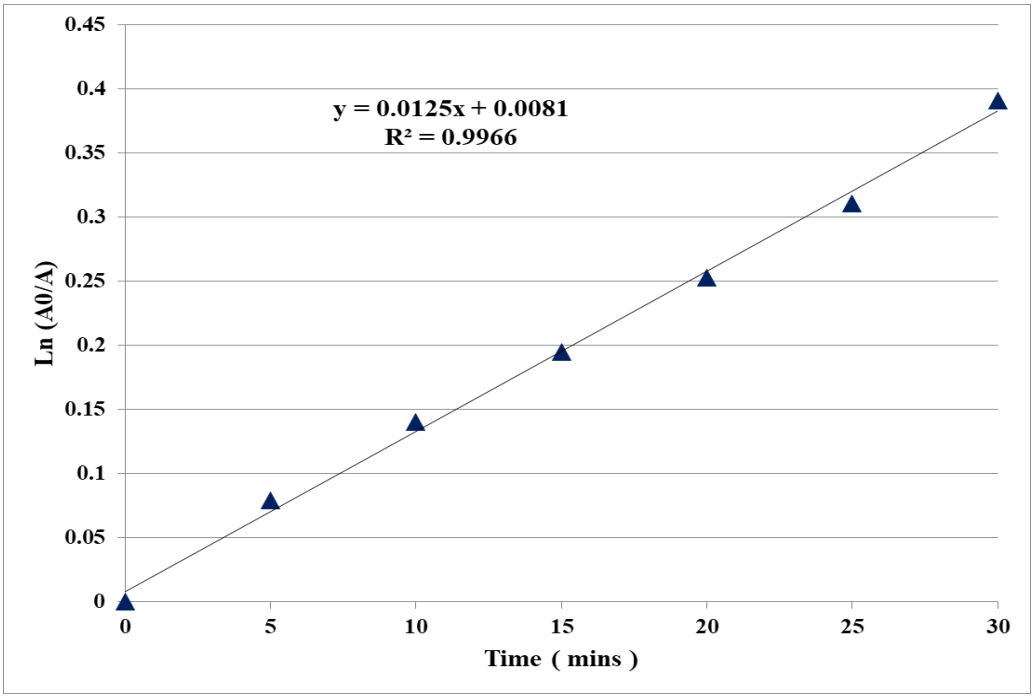

Figure 36. Rate constant graph for hydroquinone hydrogenation at 343 K.

From the integrated form of the Arrhenius equation shown in Equation 7 of the Experimental Section, ln k was plotted against ($\frac{1}{T}$) using the values in Table 7 below:

Table 7. Data used to calculate activation energy for hydroquinone.

Temperature (K)	k (x10^{-3}min^{-1})	1/T (x- axis)	Ln k (y-axis)
303	2.9	0.00330	-5.71383
313	3.9	0.00319	-5.38170
323	4.2	0.00309	-4.79150
333	8.1	0.00300	-4.65646
343	12.5	0.00291	-4.56595

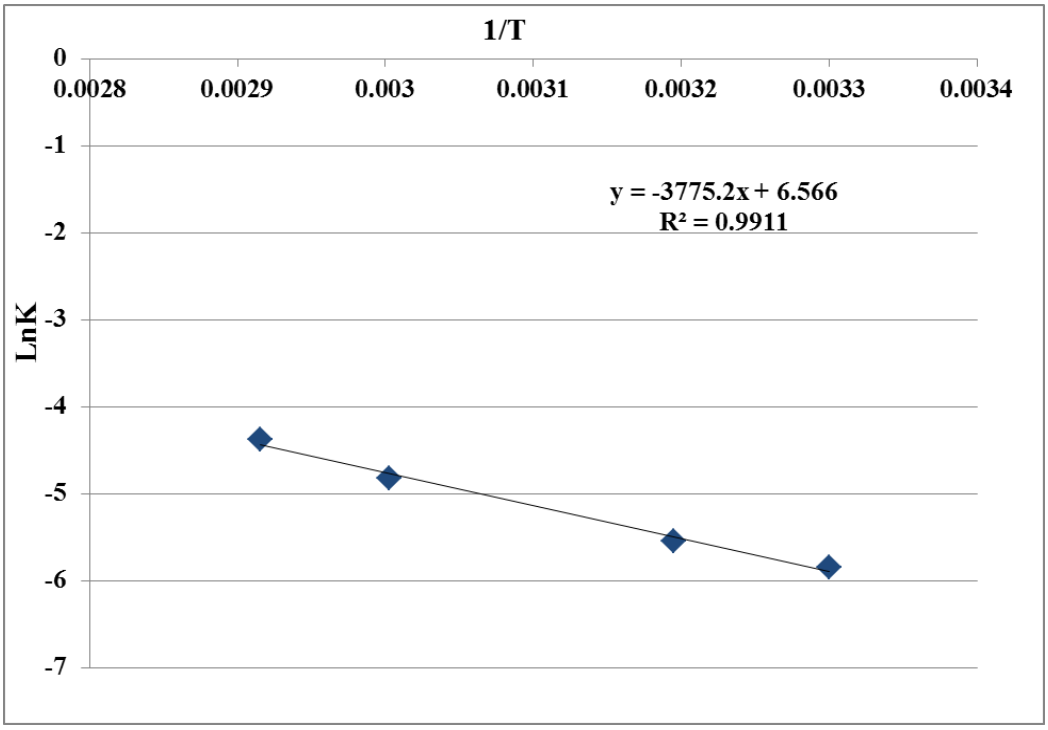

Figure 37. Activation energy plot for hydroquinone hydrogenation.

Therefore, the gradient of ln k against 1/T equals $-\frac{Ea}{RT}$ and can be expressed for Ea as:

- Ea= -mR
- -(-3775.2*8.314)/1000
- = 31.39 kJmol^{-1}

From this, an overall activation energy for hydroquinone hydrogenation of 31.4 kJmol^{-1} was measured.

The activation energies calculated for each isomer of the dihydroxybenzenes are summarised below in Table 8:

Table 8. Activation energies of dihydroxybenzene isomers.

Substrate	Activation Energy ($kJmol^{-1}$)
Catechol	31.6
Resorcinol	41.2
Hydroquinone	31.4

From Table 8 it can be seen the activation energies of catechol and hydroquinone were similar at ~ 31 $kJmol^{-1}$, whilst resorcinol was higher at ~ 41 $kJmol^{-1}$.

7.1.3 Concentration Variations of Dihydroxybenzene Isomers

Dihydroxybenzene concentration was varied to investigate reaction order of the organic.

7.1.3.1 Catechol Concentration Variations

In this set of reactions catechol was hydrogenated at 5, 10, 15 and 20 mmol to test the effect of substrate concentration on the hydrogenation activity, with 10 mmol taken as the standard reaction. The temperature (323 K) and hydrogen pressure (3 barg) were kept constant throughout. These results in order of increasing concentration are shown below:

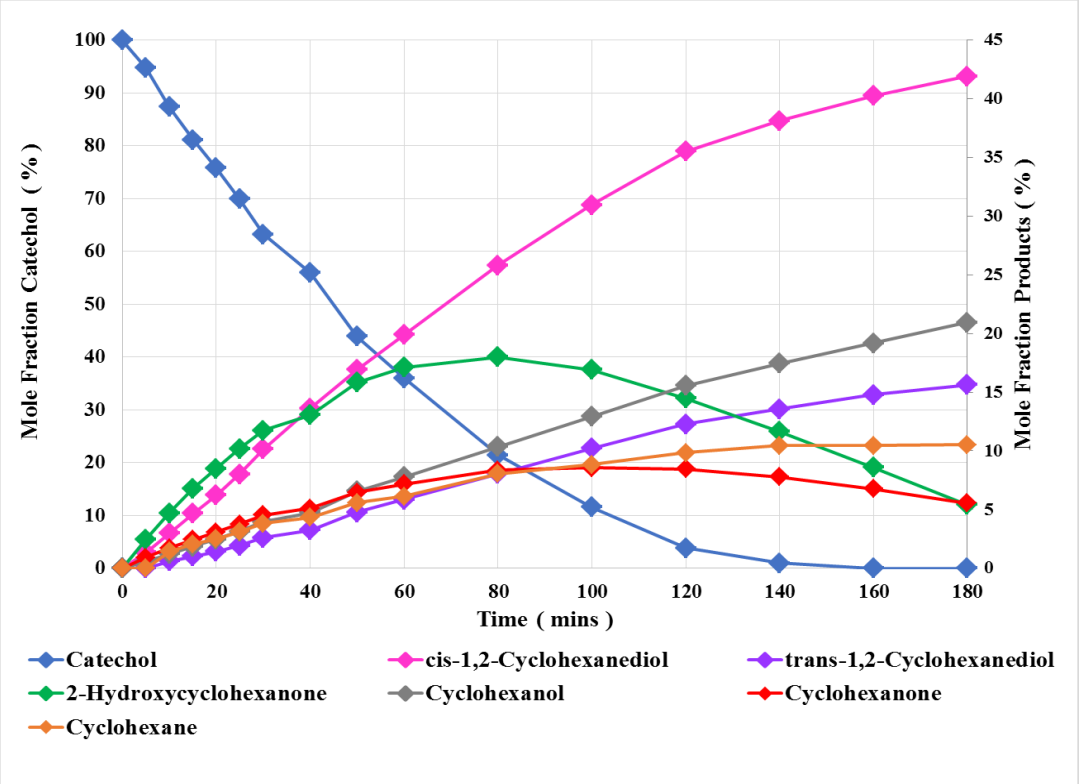

Figure 38. Reaction profile of catechol hydrogenation. Conditions, 323 K, 5 mmol, 3 barg.

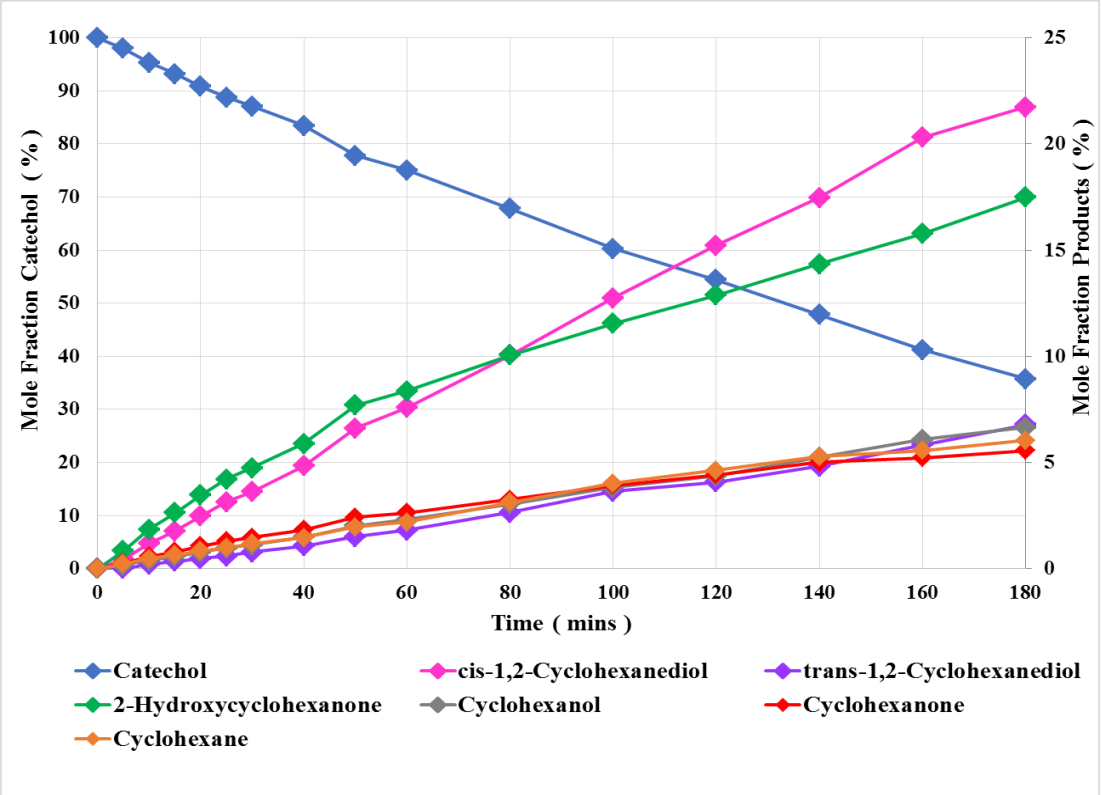

Figure 39. Reaction profile of catechol hydrogenation. Conditions, 323 K, 15 mmol, 3 barg.

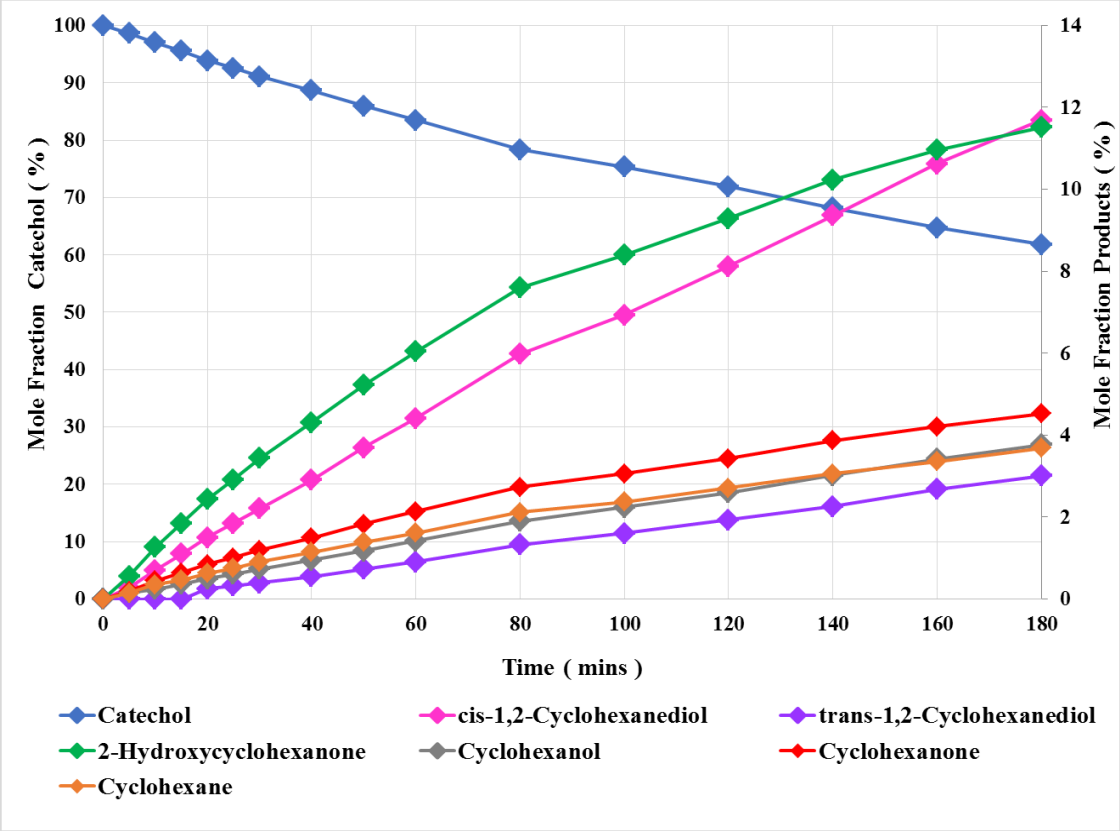

Figure 40. Reaction profile of catechol hydrogenation. Conditions, 323 K, 20 mmol, 3 barg.

Calculation of the initial rates of each concentration reaction shown above, found a decrease in catechol reactivity with an increase in concentration; a change in rate from 0.0163 mol $L^{-1}min^{-1}$ using 5 mmol substrate to 0.0108 mol $L^{-1}min^{-1}$ using 20 mmol. The product distribution of the hydrogenated (*cis*+*trans*-1,2-cyclohexanedioland 2-hydroxycyclohexanone) and hydrodeoxygenated products (cyclohexanone, cyclohexanol and cyclohexane) at ~ 35 % conversion is shown below in Figure 41:

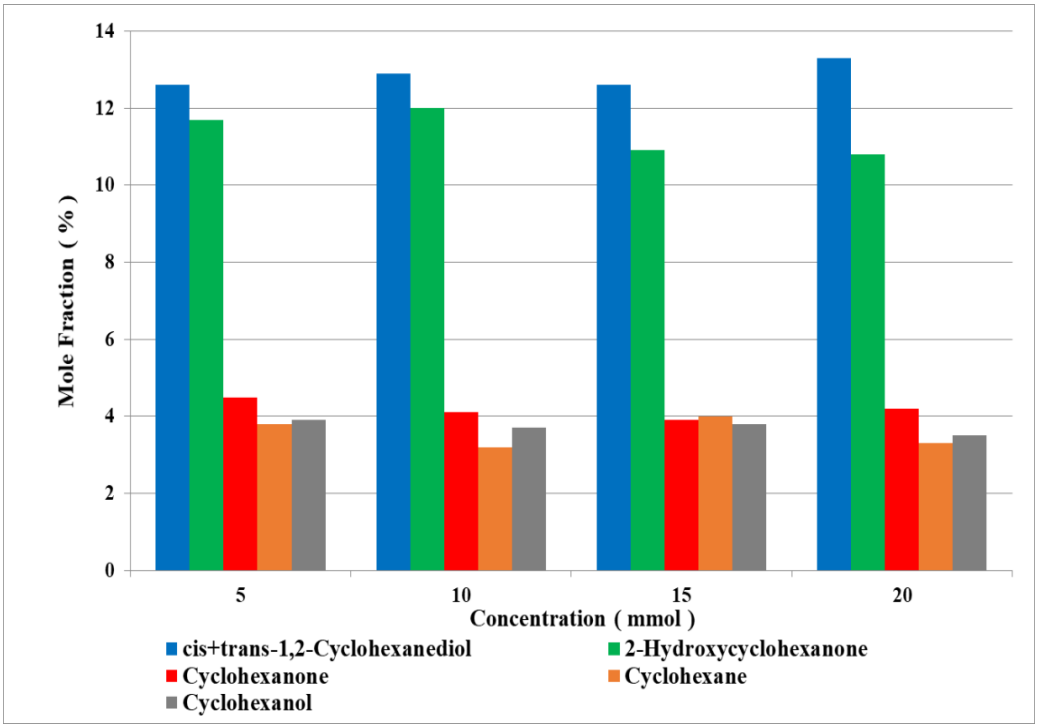

Figure 41. Product distribution for catechol concentration reactions at ~ 35 % conversion.

From Figure 41 above, it can be seen that the mole fraction percentages for both the hydrogenated and hydrodeoxygenated products remain constant over the concentration range tested signifying the concentration of catechol has an effect only on rate and not on product distribution.

To calculate an overall order in catechol Ln [A] against Ln [rate] was plotted using the data in Table 9 below:

Table 9. Data used to calculate order in substrate for catechol hydrogenation.

Reactant concentration (mol L^{-1})	**Rate (mol L^{-1} min^{-1})**	**Ln concentration**	**Ln rate**
0.015	0.0163	-4.12	-4.53
0.030	0.0130	-3.50	-4.44
0.045	0.0118	-3.10	-4.34
0.060	0.0108	-2.81	-4.12

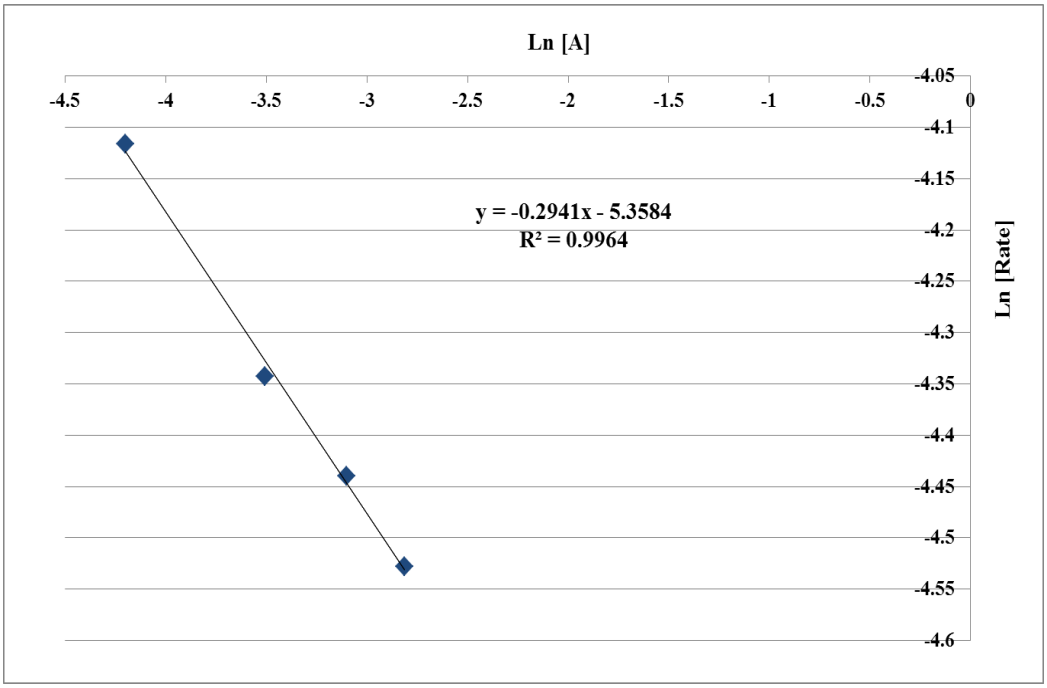

Figure 42. Substrate order plot for catechol hydrogenation.

Using the equations presented in Section 6.6 of the Experimental Section, the order in catechol was taken from the gradient of the straight line in Figure 42 above and found to be -0.3.

7.1.3.2 Resorcinol Concentration Variations

In this set of reactions resorcinol was hydrogenated using 5, 10, 15 and 20 mmol to test the effect this would have on the hydrogenation reaction, with 10 mmol taken as the standard reaction. The temperature (323 K) and hydrogen pressure (3 barg) were kept constant. The graphs of these in increasing order of concentration are shown below:

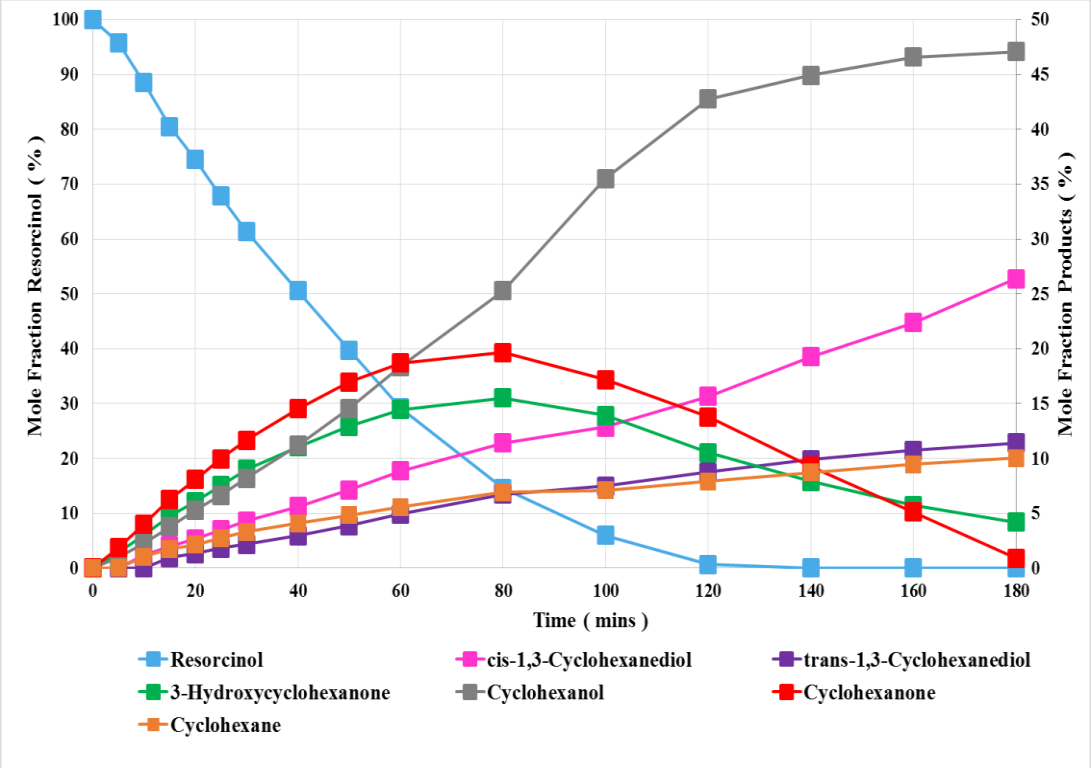

Figure 43. Reaction profile of resorcinol hydrogenation. Conditions, 323 K, 5 mmol, 3 barg.

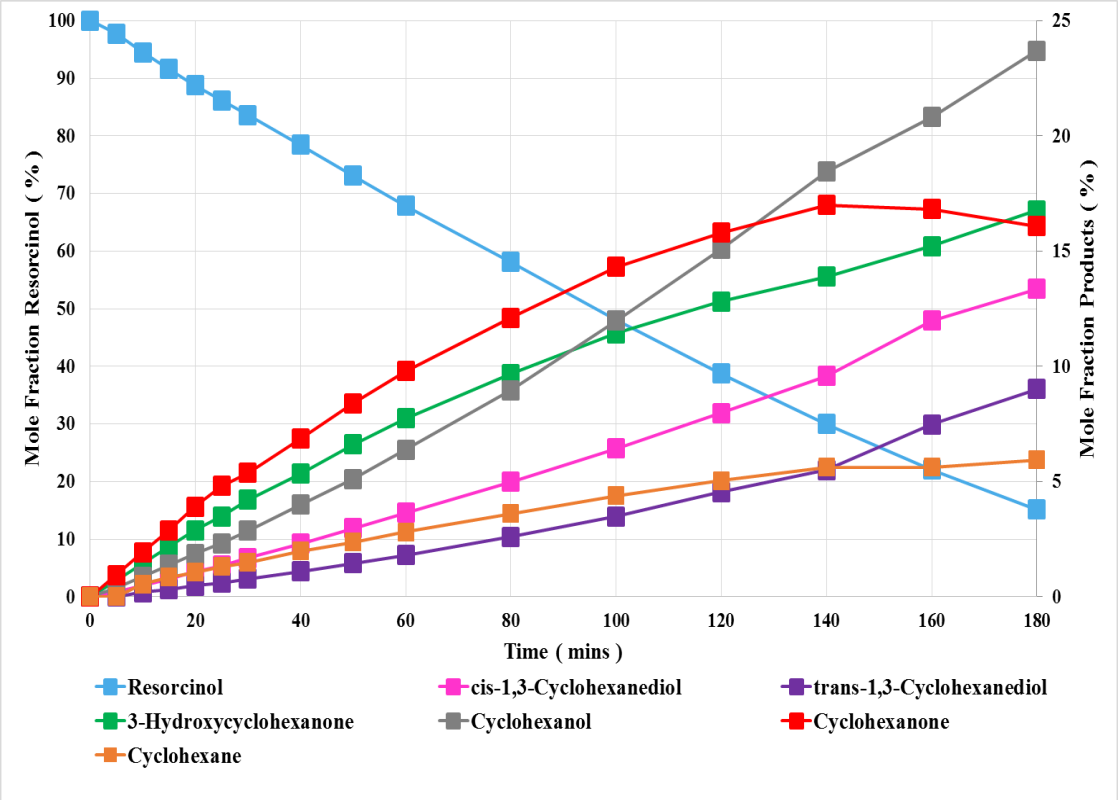

Figure 44. Reaction profile of resorcinol hydrogenation. Conditions, 323 K, 15 mmol, 3 barg.

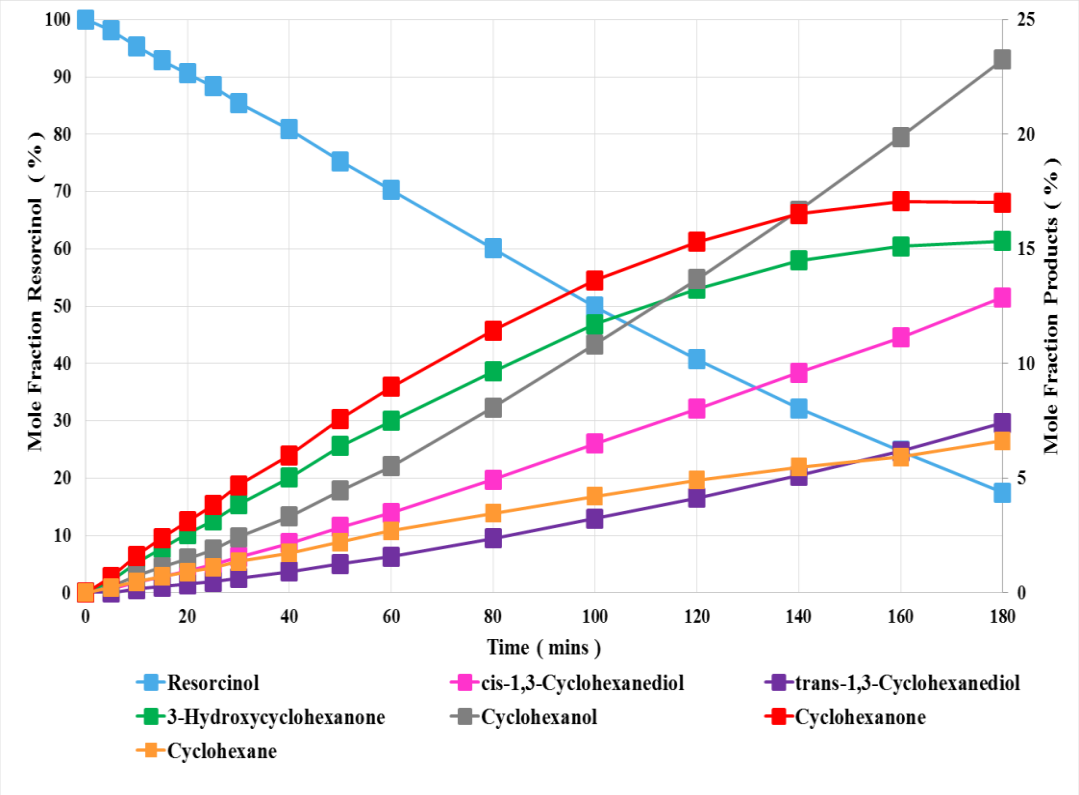

Figure 45. Reaction profile of resorcinol hydrogenation. Conditions, 323 K, 20 mmol, 3 barg.

Calculation of the initial rates of each concentration reaction shown above, found an increase in resorcinol reactivity with an increase in concentration; a change in rate from 0.0095 mol $L^{-1}min^{-1}$ using 5 mmol substrate to 0.0214 mol $L^{-1}min^{-1}$ using 20 mmol. The product distribution of the hydrogenated (*cis*+*trans*-1,2-cyclohexanedioland 2-hydroxycyclohexanone) and hydrodeoxygenated products (cyclohexanone, cyclohexanol and cyclohexane) at ~ 35 % conversion is shown below in Figure 46:

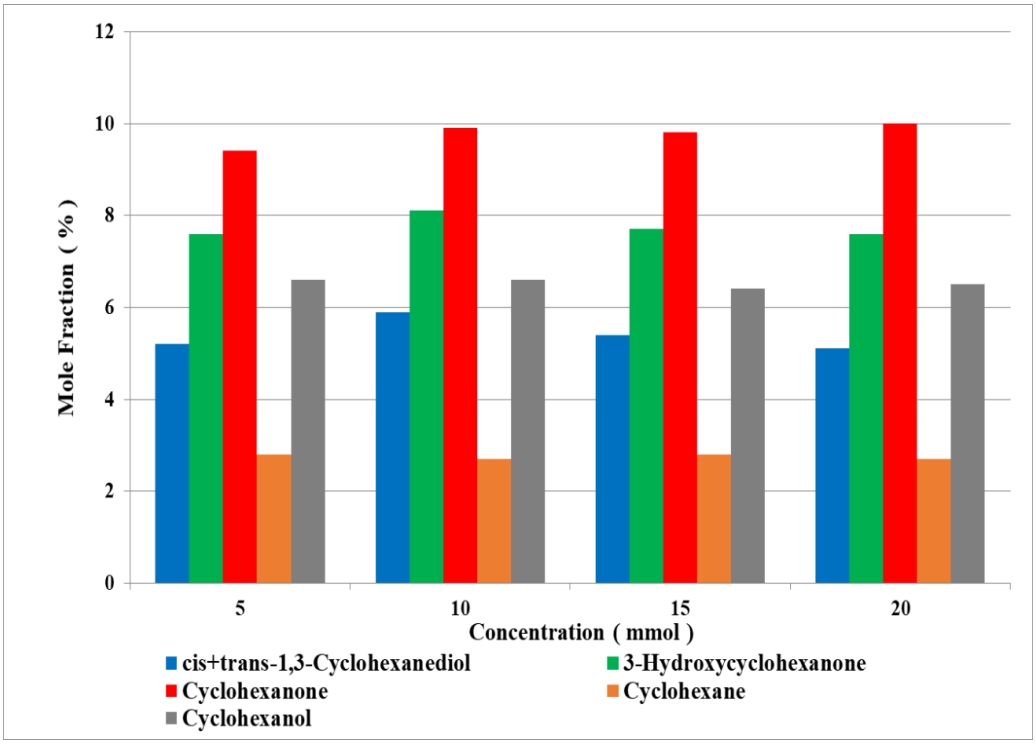

Figure 46. Product distribution for resorcinol concentration reactions at ~ 35 % conversion.

From Figure 46 above it can be seen that the mole fraction percentages of both the hydrogenated and hydrodeoxygenated products were unchanged over the concentration range tested. This suggests the concentration effect is limited to the rate of reaction and has no influence on product distribution.

To calculate an overall order in resorcinol Ln [A] against Ln [rate] was plotted using the data in Table 10 below:

Table 10. Data used to calculate the order in resorcinol.

Reactant concentration (mol L^{-1})	**Rate (mol L^{-1} min^{-1})**	**Ln concentration**	**Ln rate**
0.015	0.0095	-4.12	-4.65
0.030	0.0167	-3.50	-4.09
0.045	0.0197	-3.10	-3.93
0.060	0.0214	-2.81	-4.39

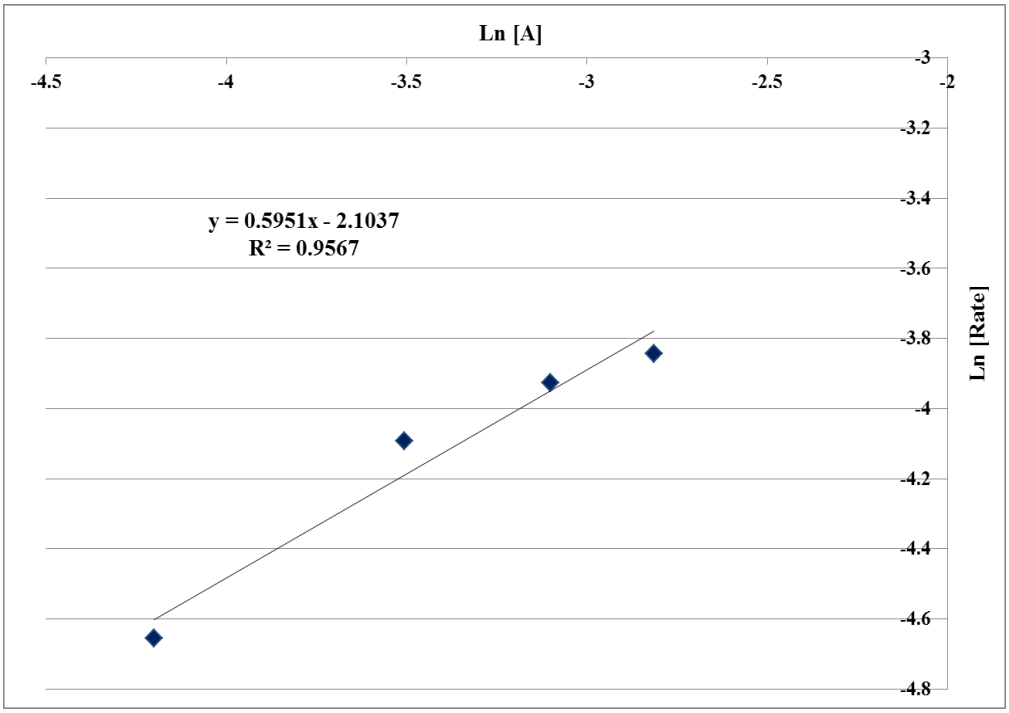

Figure 47. Order plot for resorcinol hydrogenation.

From the gradient of the line in Figure 47, the order for resorcinol was found to be 0.6.

7.1.3.3 Hydroquinone Concentration Variations

In this set of reactions hydroquinone was hydrogenated at different concentrations using 5, 10, 15 and 20 mmol of substrate, with 10 mmol the standard reaction. The temperature (323 K) and hydrogen pressure (3 barg) were kept constant to understand the effect hydroquinone concentration had on the hydrogenation reaction. The reaction profile graphs are shown below in increasing order of concentration:

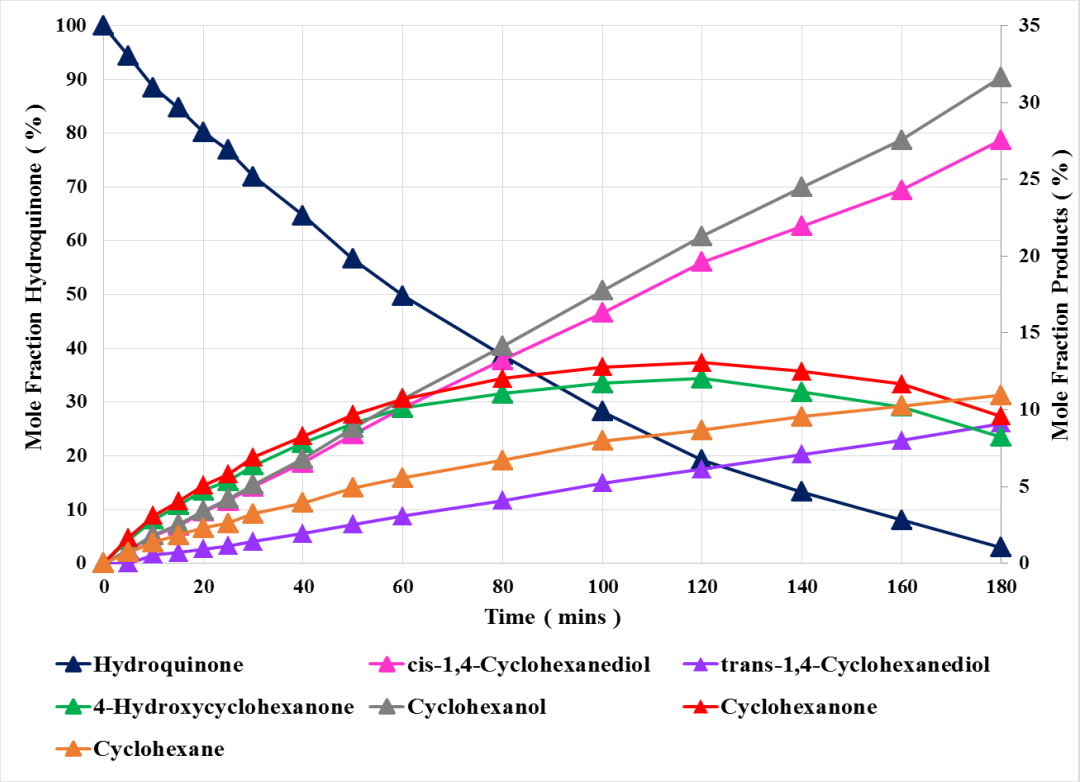

Figure 48. Reaction profile of hydroquinone hydrogenation. Conditions, 323 K, 5 mmol, 3 barg.

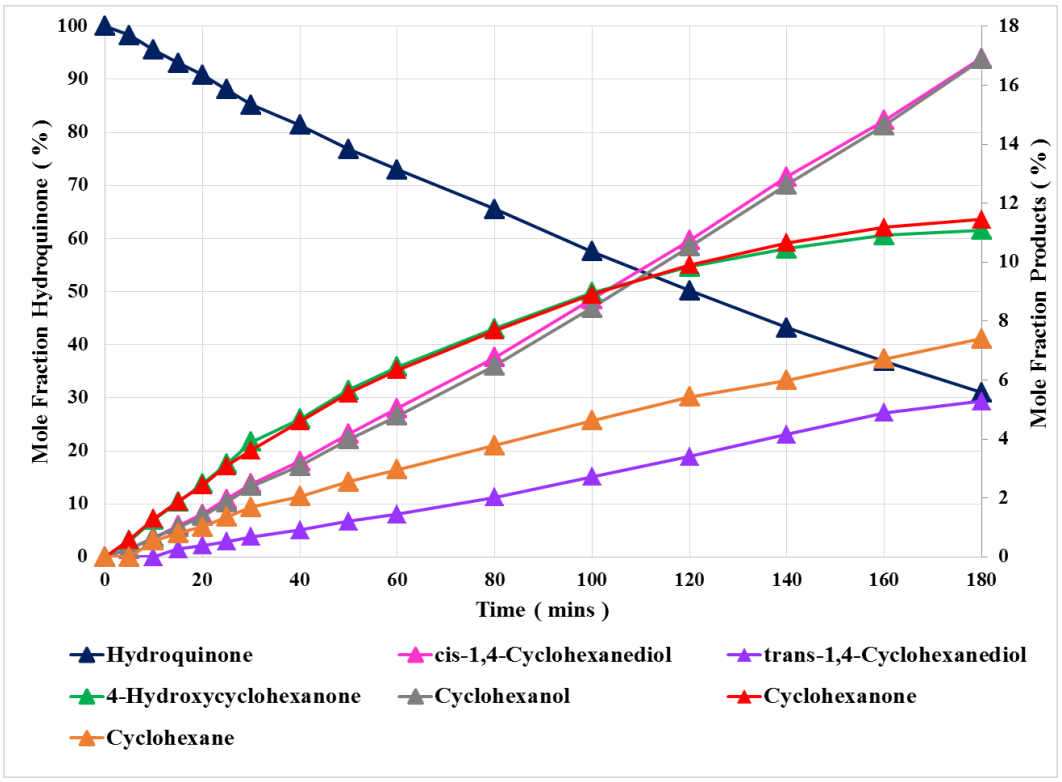

Figure 49. Reaction profile of hydroquinone hydrogenation. Conditions, 323 K, 15 mmol, 3 barg.

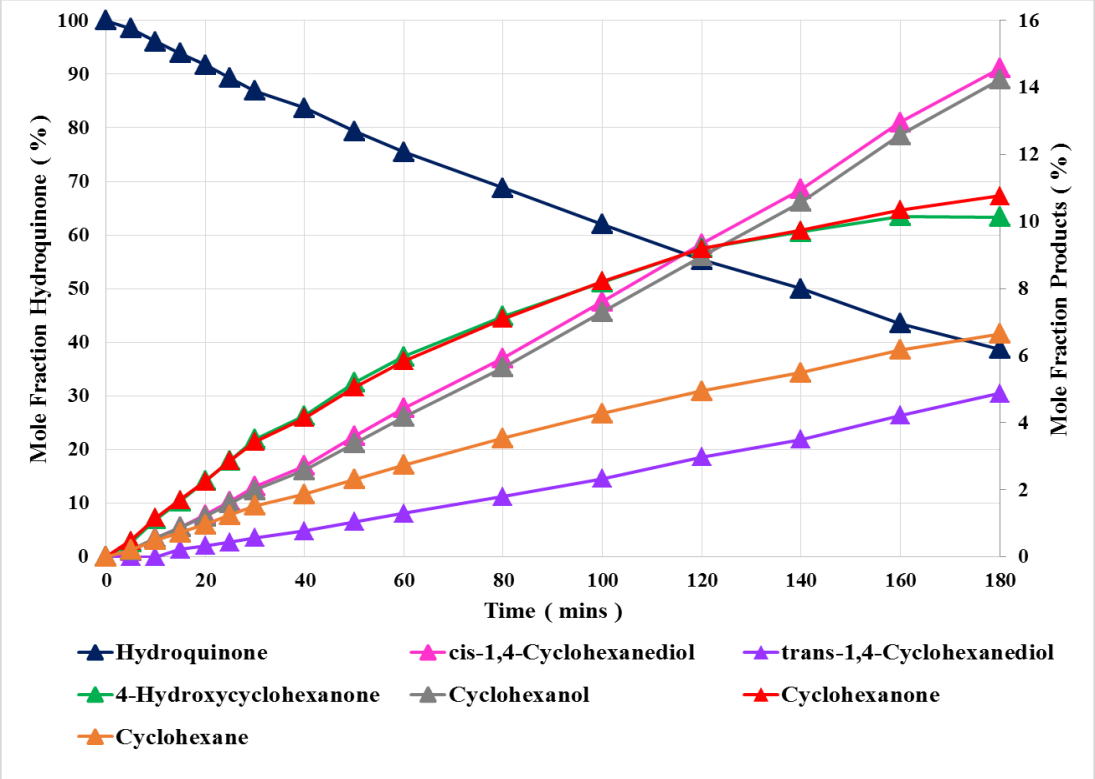

Figure 50. Reaction profile of hydroquinone hydrogenation. Conditions, 323 K, 20 mmol, 3 barg.

Calculation of the initial rates of each concentration reaction shown above, found an increase in hydroquinone reactivity with an increase in concentration; a change in rate from 0.0059 mol $L^{-1}min^{-1}$ using 5 mmol substrate to 0.0107 mol $L^{-1}min^{-1}$ using 20 mmol. The product distribution of the hydrogenated (*cis*+*trans*-1,2-cyclohexanedioland 2-hydroxycyclohexanone) and hydrodeoxygenated products (cyclohexanone, cyclohexanol and cyclohexane) at ~ 35 % conversion is shown below in Figure 51:

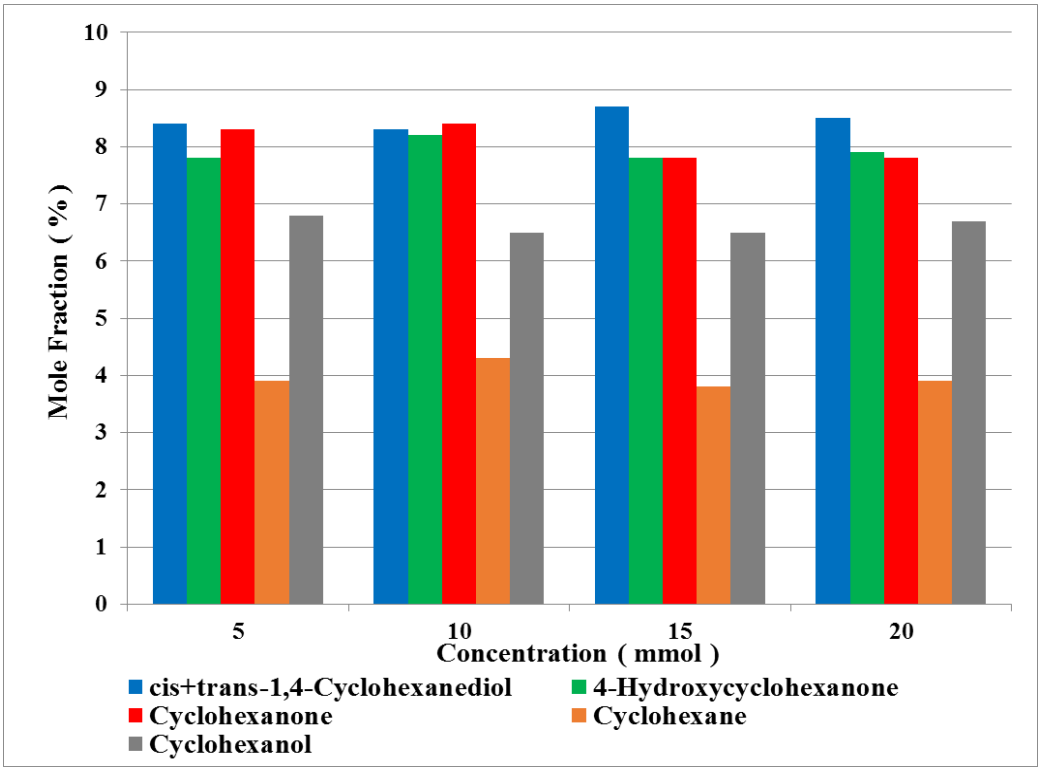

Figure 51. Product distribution for hydroquinone concentration reactions at ~ 35 % conversion.

Figure 51 above shows minimal change in product distribution across the concentration range tested indicating quantity of substrate present has an effect only on reaction rate.

To calculate an overall order in hydroquinone Ln [A] against Ln [rate] was plotted using the data below in Table 11:

Table 11. Data used to calculate order in substrate for hydroquinone hydrogenation.

Reactant concentration (mol L^{-1})	**Rate (mol L^{-1} min^{-1})**	**Ln concentration**	**Ln rate**
0.015	0.0059	-4.12	-5.13
0.030	0.0073	-3.50	-4.92
0.045	0.0087	-3.10	-4.74
0.060	0.0107	-2.81	-4.54

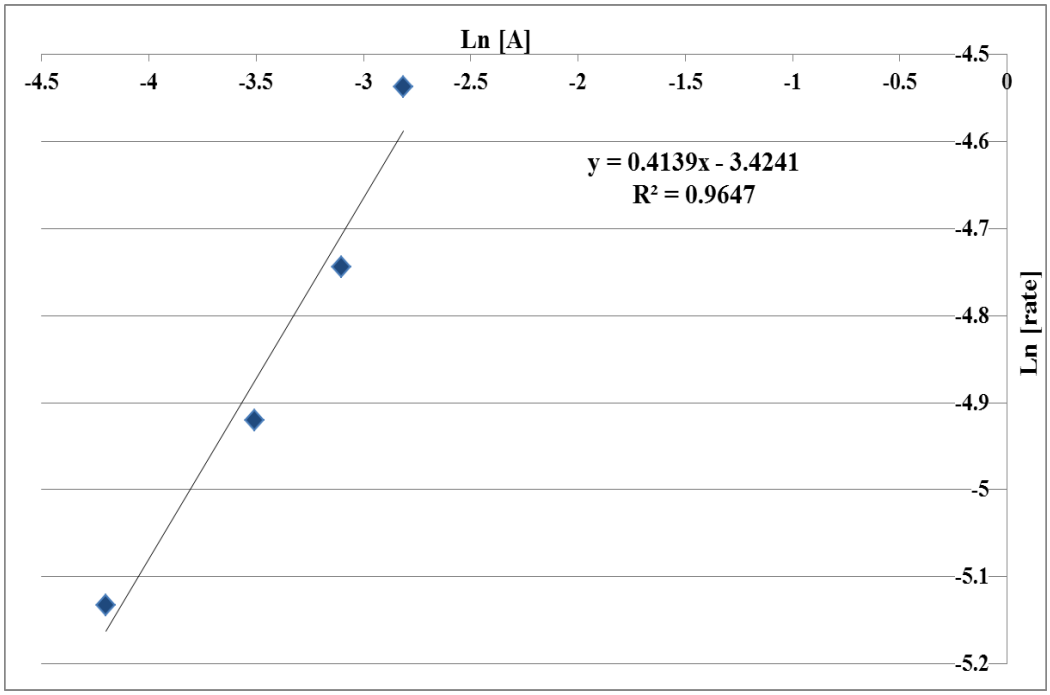

Figure 52. Order plot for hydroquinone hydrogenation.

Therefore, from the equation of the straight line above the order in hydroquinone is 0.41. The order for each substrate of the dihydroxybenzene isomers is summarised below:

Table 12. Orders in dihydroxybenzene isomer.

Substrate	Order
Catechol	-0.3
Resorcinol	0.6
Hydroquinone	0.4

From Table 12 above it can be seen the following order of strength of adsorption exists: catechol > hydroquinone > resorcinol.

7.1.4 Competitive Hydrogenation

Competitive testing of the dihydroxybenzene isomers in pairs and as a group of three was carried out and the results are detailed in this section.

The competitive reaction of catechol and resorcinol resulted in a significant decrease in the rate of reaction for both isomers as can be seen in Figure 53 below:

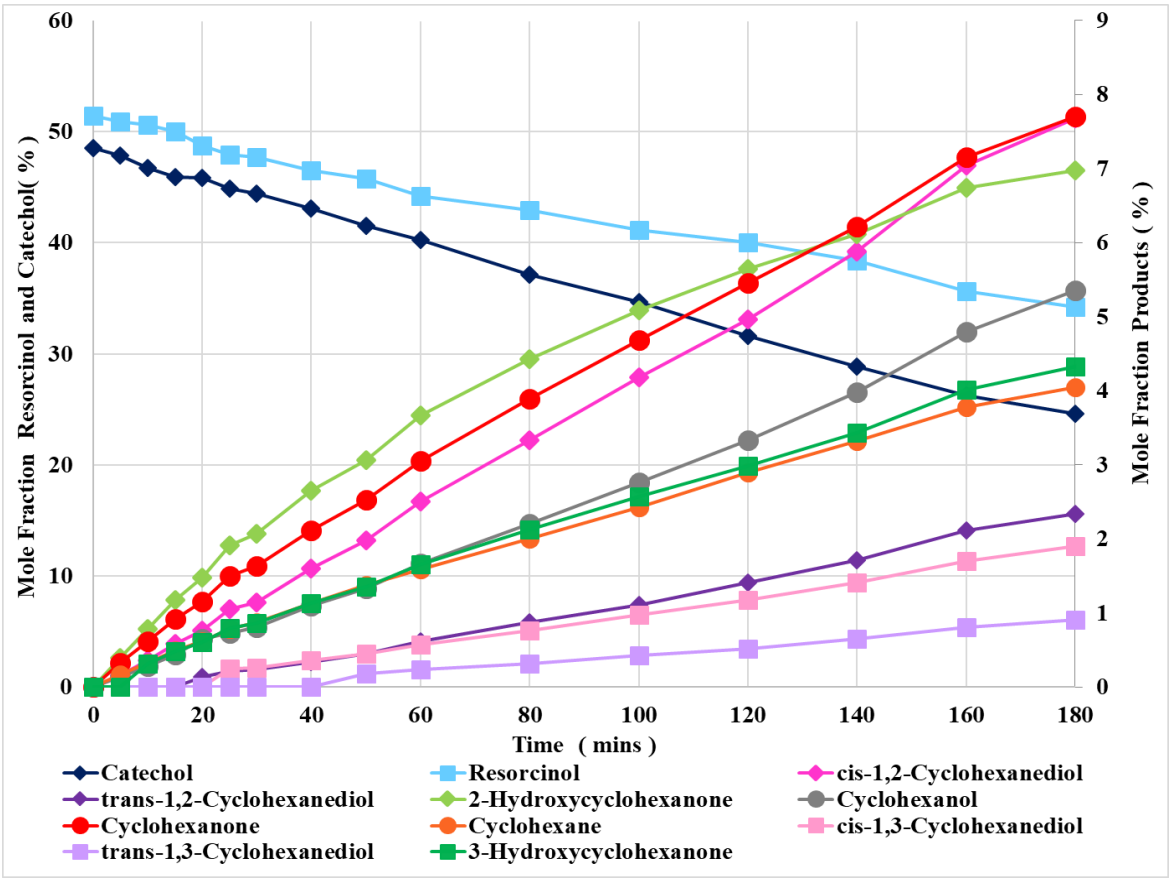

Figure 53. Competitive reaction of catechol and resorcinol. Conditions: 323 K, 3 barg, concentrations as per single reactions.

From Figure 53 it can be seen that slight inhibition of resorcinol occurred with no reaction taking place in the initial five minutes, whereas catechol reacted immediately. The hydrogenated products from catechol were favoured over those from resorcinol. The formation of the resorcinol ring hydrogenated products, 3-hydroxycyclohexanone and *cis*-1,3-cyclohexanediol, were delayed, not forming until five and twenty-five minutes respectively. This is in marked contrast to individual hydrogenation where both form from the outset. No evidence of the second component influencing reaction selectivity was observed; the product distributions remained constant between individual and competitive hydrogenation as shown below in Figure 54.

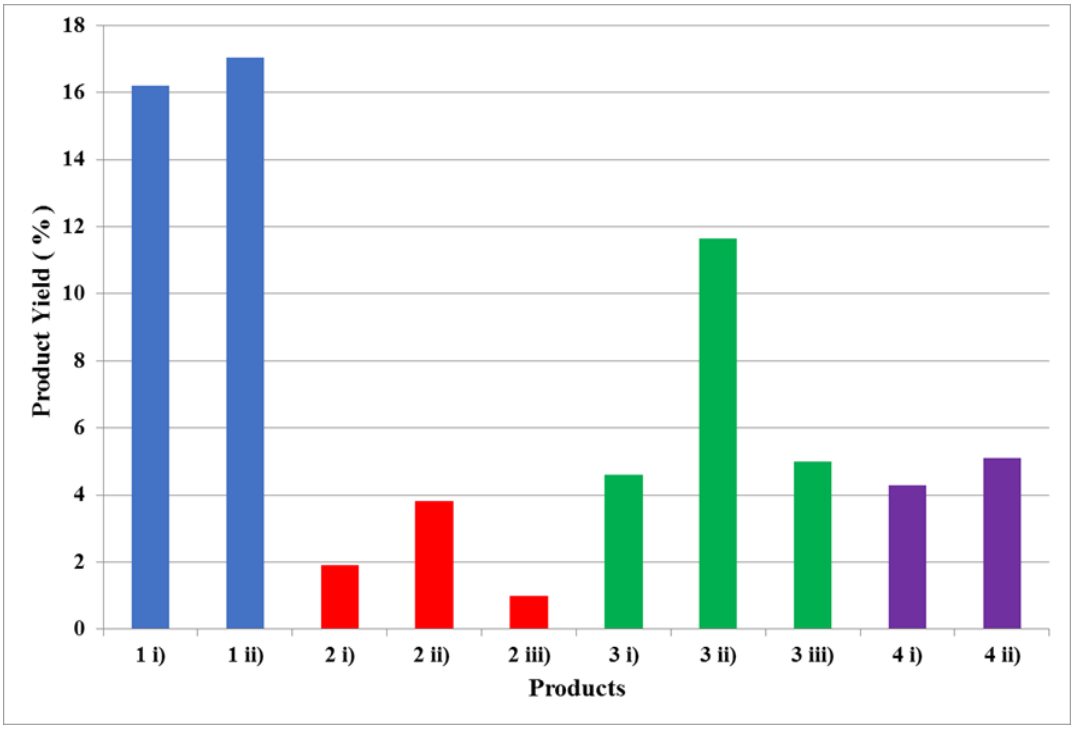

Figure 54. Comparison of product yield for individual and competitive hydrogenation of catechol and resorcinol. Data taken at 20 % conversion of resorcinol and 27 % conversion of catechol.

Key: 1 HYD products i) Individual catechol ii) Competitive catechol

2 Cyclohexane i) Individual catechol ii) Competitive catechol + resorcinol iii) Individual resorcinol

3 Cyclohexanol + Cyclohexanone i) Individual catechol ii) Competitive catechol + resorcinol iii) Individual resorcinol

4 HYD products i) Individual resorcinol ii) Competitive resorcinol

Similar findings were recorded for the competitive hydrogenation of catechol and hydroquinone as shown in Figures 55 and 56 below,

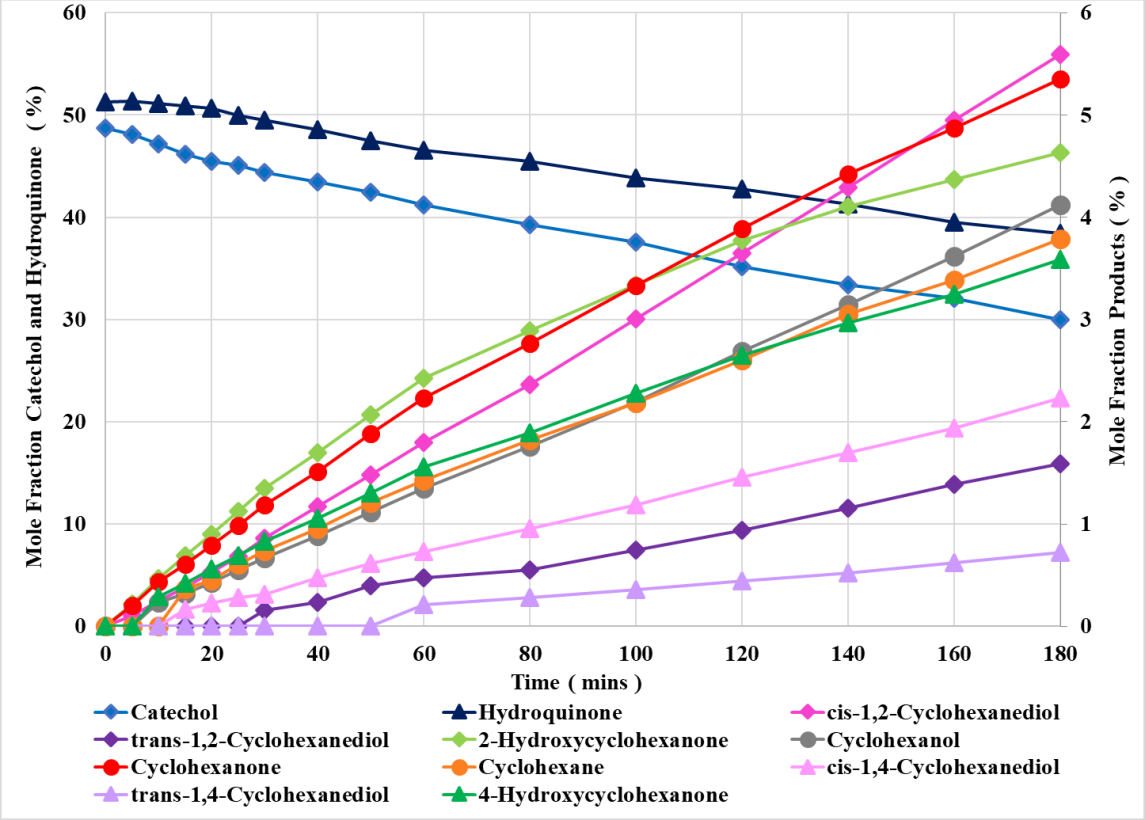

Figure 55. Competitive reaction of catechol and hydroquinone. Conditions: 323 K, 3 barg, concentrations as per single reactions.

Figure 55 shows that a substantial drop in reactivity occurred with both substrates. The inhibition effect observed with resorcinol was apparent with hydroquinone; both major ring hydrogenated products, 3-hydroxycyclohexanone and *cis*-1,3-cyclohexanediol, did not form until ten and fifteen minutes into the reaction respectively. As observed with the previous substrate combination, reaction product yields for hydroquinone and catechol were unchanged in the competitive environment.

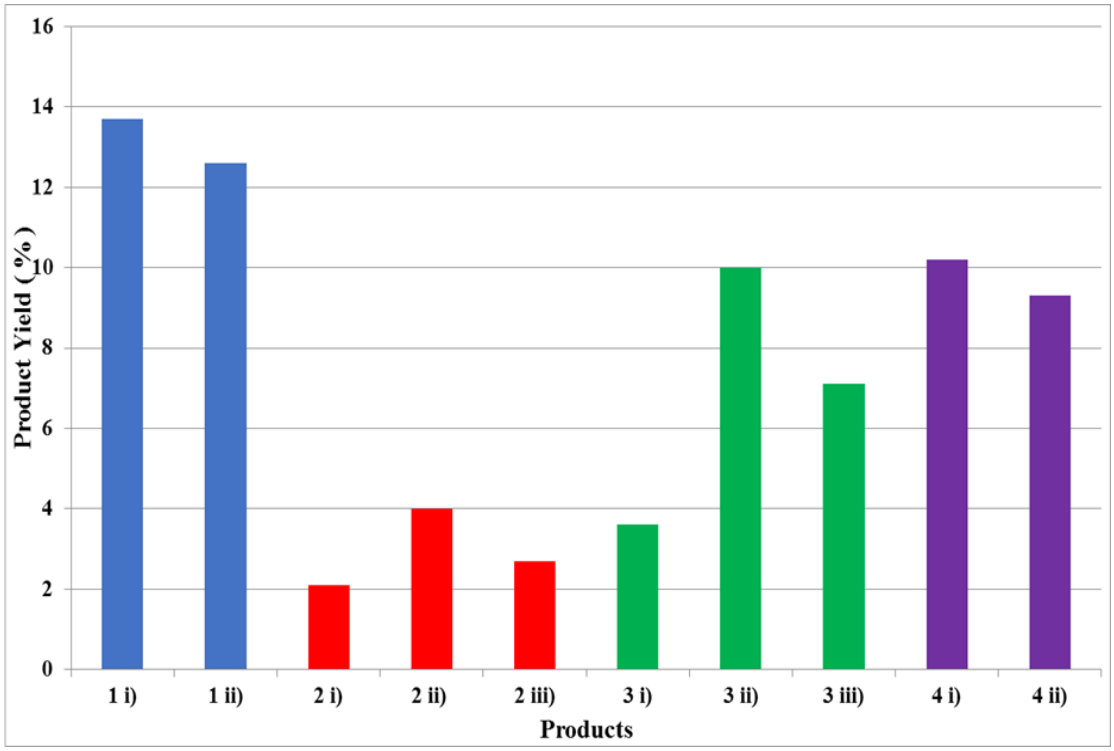

Figure 56. Comparison of product yield for individual and competitive hydrogenation of catechol and hydroquinone. Data taken at 30 % conversion of catechol and 25 % conversion of hydroquinone

Key : 1 HYD products i) individual catechol 1 ii) competitive catechol

2 Cyclohexane i) Individual catechol ii) Competitive catechol + hydroquinone iii) Individual hydroquinone

3 Cyclohexanol + Cyclohexanone i) Individual catechol ii) Competitive catechol + hydroquinone iii) Individual hydroquinone

4 HYD products i) Individual resorcinol ii) Competitive hydroquinone

The competitive hydrogenation of resorcinol and hydroquinone is shown in Figure 57 below:

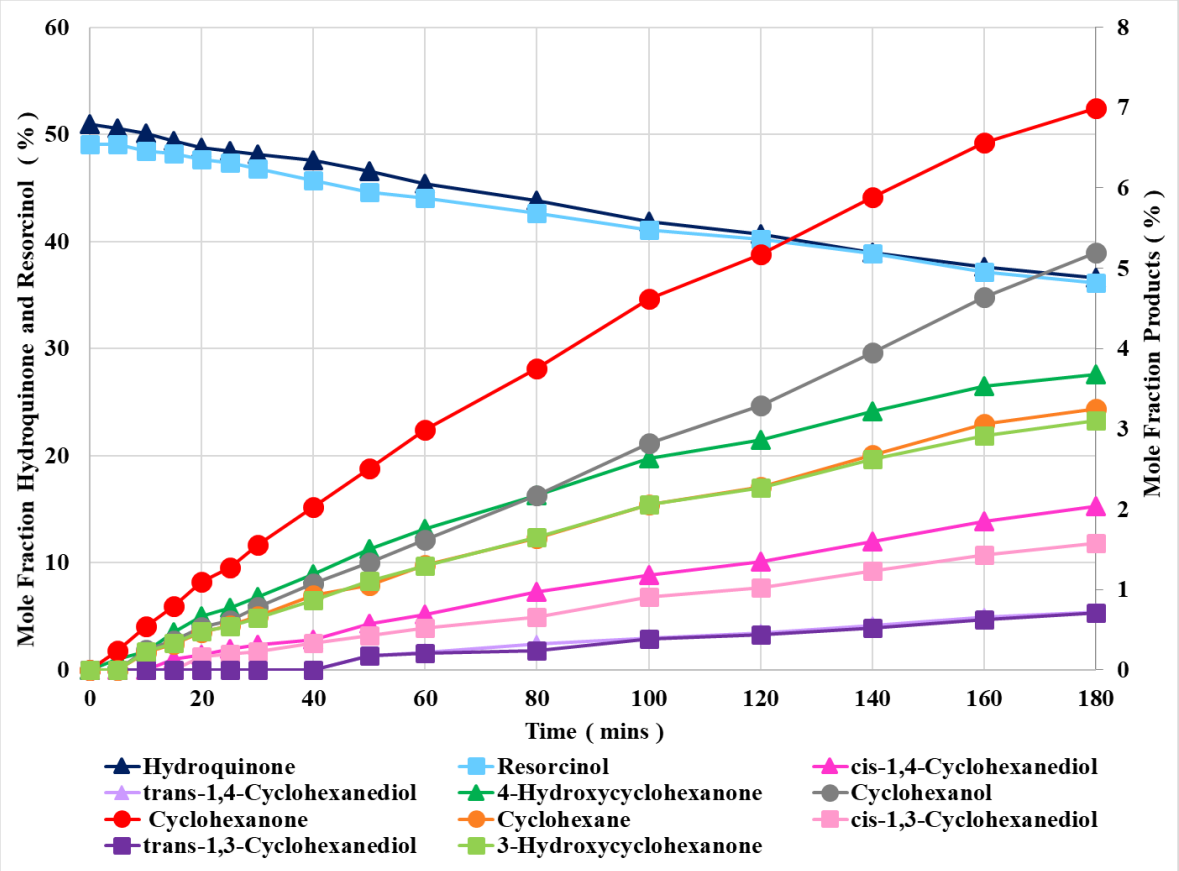

Figure 57. Competitive reaction of hydroquinone and resorcinol. Conditions: 323 K, 3 barg, concentrations as per single reactions.

From Figure 57 it can be seen that of all pairs of substrates tested competitively, resorcinol and hydroquinone showed the greatest decrease in rate of reaction. The major hydrogenated product for both substrates, hydroxycyclohexanone, formed initially with the hydrogenated products from hydroquinone favoured over those from resorcinol. The HDO products, cyclohexanone and cyclohexanol, were those formed to the greatest extent by reaction end. As with both previous substrate combinations, selectivity was unaffected when individual and competitive reactions were compared, as outlined in Figure 58 below:

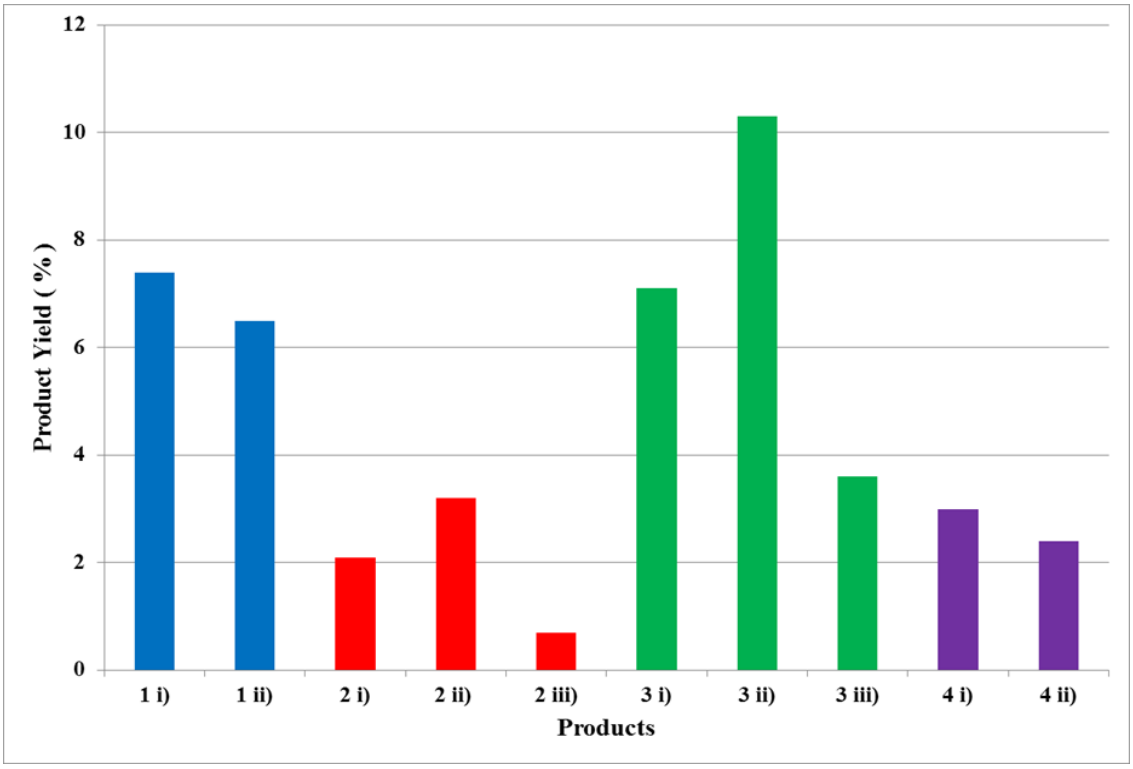

Figure 58. Comparison of product yield for individual and competitive hydrogenation of resorcinol and hydroquinone. Data taken at 17 % conversion of hydroquinone and 16.5 % conversion of resorcinol

Key: 1 HYD products i) Individual hydroquinone1 ii) Competitive hydroquinone

2 Cyclohexane i) Individual hydroquinone ii) Competitive hydroquinone + resorcinol iii) Individual resorcinol

3 Cyclohexanol + Cyclohexanone i) Individual hydroquinone ii) Competitive hydroquinone + resorcinol iii) Individual resorcinol

4 HYD products i) Individual resorcinol ii) Competitive resorcinol

The competitive hydrogenation with all three substrates present is shown in Figure 59 below, in addition to the conversion of each during individual and competitive hydrogenation shown in Figure 60:

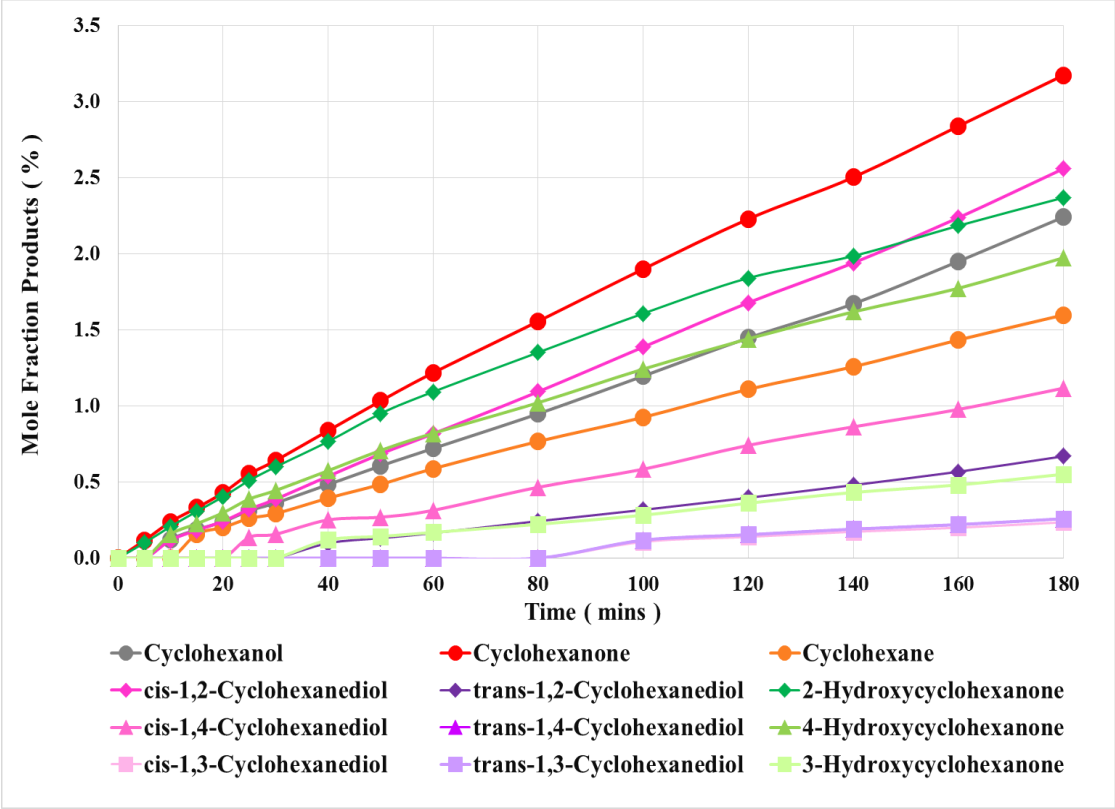

Figure 59. Competitive reactions of catechol, hydroquinone and resorcinol. Conditions: 323 K, 3 barg, concentrations as per single reactions.

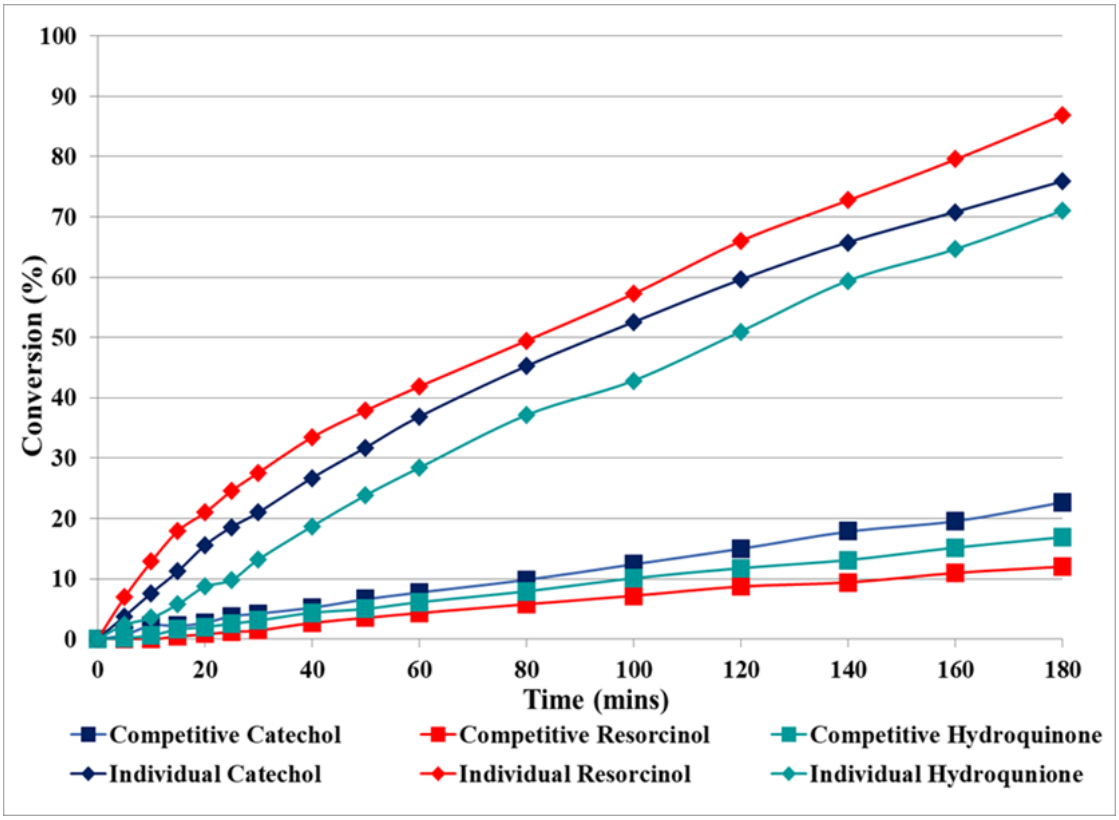

Figure 60. Individual hydrogenation and competitive hydrogenation conversions.

From Figure 59 and 60 it is apparent that the reaction rate for all three substrates was suppressed to a greater extent than observed with previous competitive reactions. The main product of the reaction was the HDO product, cyclohexanone, whilst for the hydrogenated products those from catechol, *cis*-1,2-cyclohexanediol and 2-hydroxycyclohexanone, are formed to the greatest extent, again emphasising the dominance of catechol in the competitive situation. As before, inhibition of the main hydrogenated products of hydroquinone and resorcinol occurs with the formation of 4-hydroxycyclohexanone and 3-hydroxycyclohexanone delayed until ten and forty minutes respectively. From Figure 60 it is clear to see the effect the competitive reaction has had on the conversion of all three dihydroxybenzenes. The most marked effect was observed with resorcinol where during individual hydrogenation conversion reached ~ 90% by the end of the reaction, compared with during the competitive reaction where it only reached ~ 20 % by 180 minutes.

The kinetic data gathered from competitive reaction combinations is outlined in Table 13 below:

Table 13. Competitive hydrogenation at 323 K, 3 barg and 10 mmol.

Reactant	First order rate constant, k (min^{-1}, $x10^{-3}$)				
	Single reactant	Catechol/ resorcinol	Catechol /hydroquinone	Resorcinol/ hydroquinone	Catechol/resorcinol /hydroquinone
Catechol	8.3	5.2	6.7	-	3.8
Resorcinol	11.2	5.0	-	3.5	3.5
Hydroquinone	4.2	-	4.8	3.8	3.0

It can be seen that catechol had the highest reactivity in all competitive reactions in contrast to individual hydrogenations where resorcinol was the fastest.

7.1.5 Deuteration Reactions

In the following set of reactions, deuterium was used in place of hydrogen for both the reduction and reaction procedure. All other parameters were set for standard conditions (323 K and 10 mmol substrate). Comparison of the rate constants from reactions carried out in deuterium and hydrogen was used to calculate the kinetic isotope effect for each substrate. All graphs and data from individual and competitive reactions are shown in Figures 61 - 73 below:

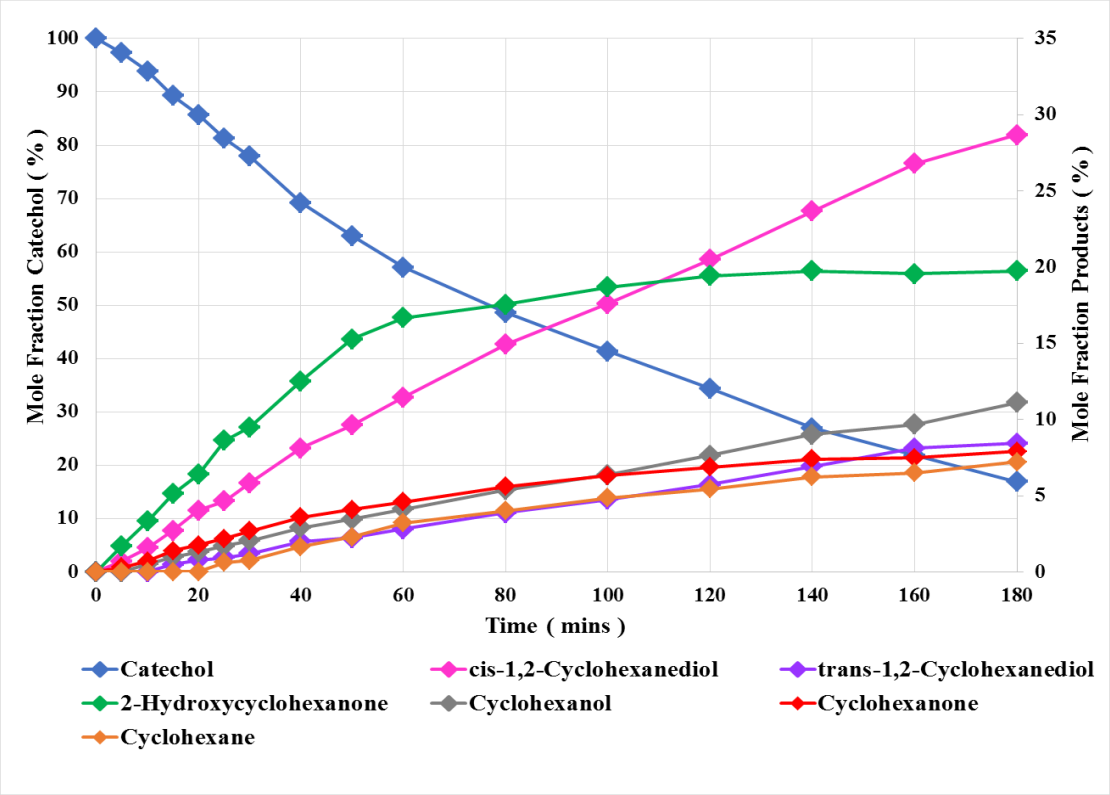

Figure 61. Reaction profile of catechol deuteration. Conditions, 323 K, 10 mmol, 3 barg.

From Figure 61 above it can be seen that the rate of catechol deuteration was significantly higher than that of hydrogenation with an increase observed in the rate constant from $8.3x10^{-3}$ to $12.8x10^{-3}$ min^{-1}. A marked inhibition of cyclohexane occurred with a delay in formation of 25 minutes against initial production under standard hydrogenation conditions. The product distribution for hydrogenated and hydrodeoxygenated products at the same conversion (35 %) is shown below in Figure 62:

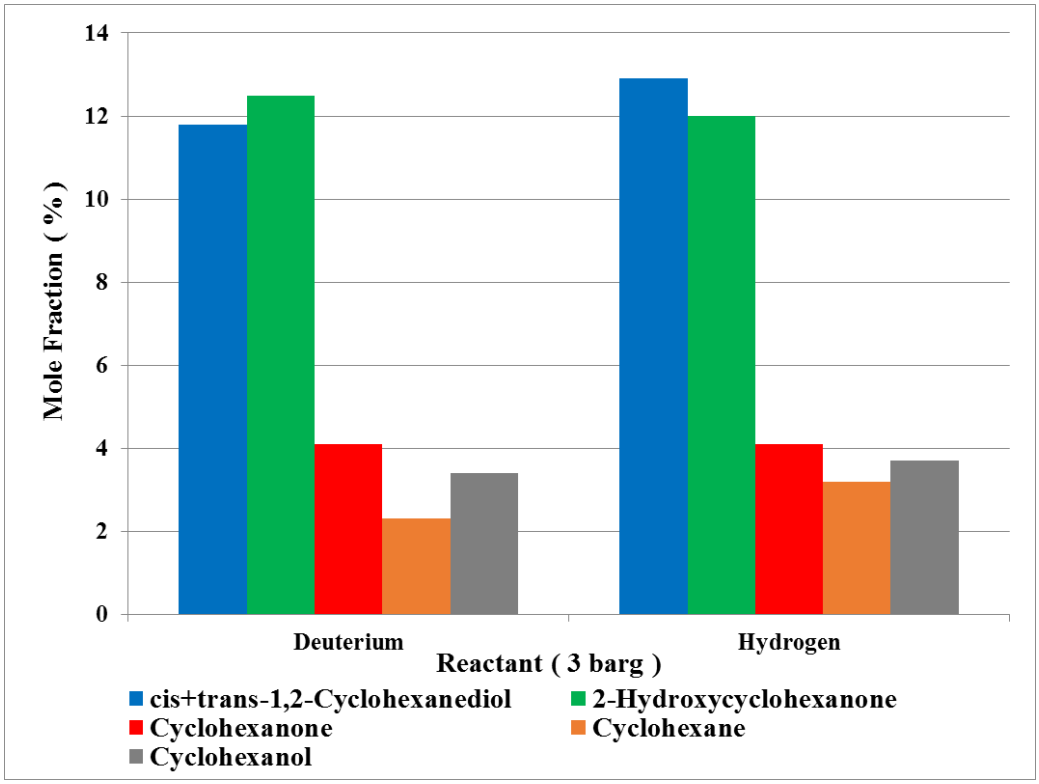

Figure 62. Product distribution of deuterium against hydrogen at 35 % conversion of catechol.

From Figure 62 it can be seen that with the exception of a decrease in formation of cyclohexane, product distribution was unaffected by the change from hydrogen to deuterium.

Resorcinol deuteration was carried out and is shown below in Figure 63:

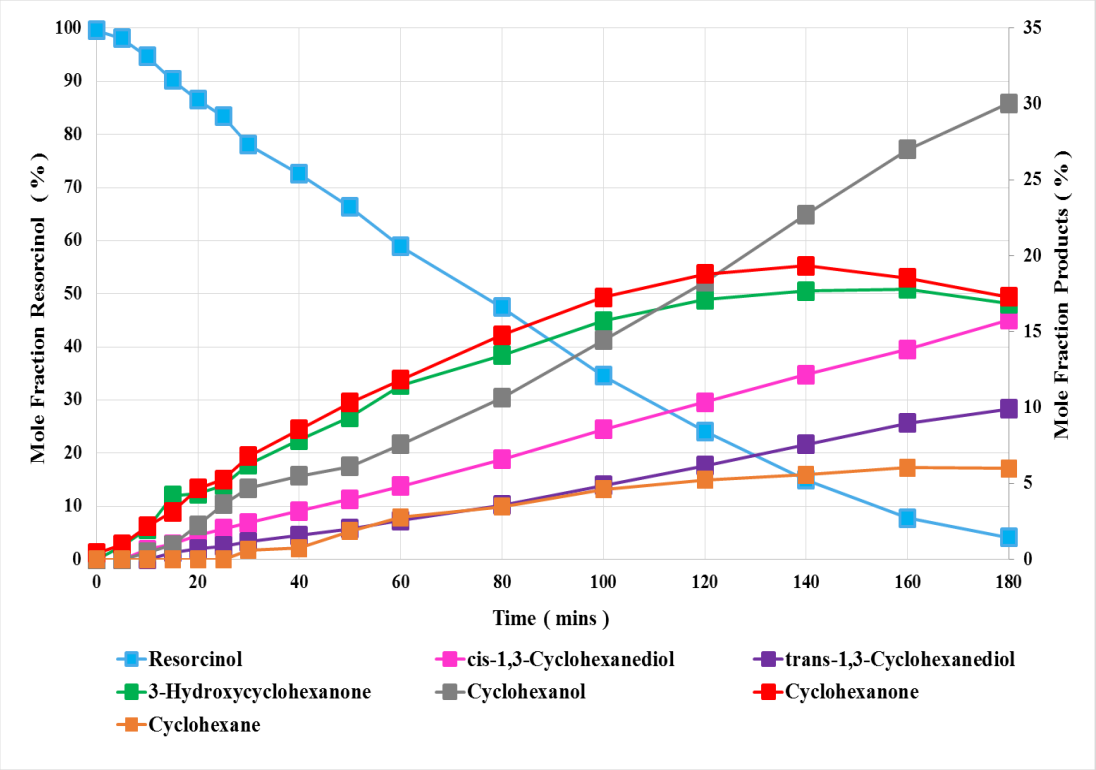

Figure 63. Reaction profile of resorcinol deuteration. Conditions, 323 K, 10 mmol, 3 barg.

From Figure 63 it is clear that as with catechol, resorcinol showed a faster rate of reaction under deuterium conditions, however, the change in measured rate constant ($11.9x10^{-3}$ to $12.5x10^{-3}$ min^{-1}) was less than that observed with catechol. As before, formation of cyclohexane was delayed; in this instance until 30 minutes reaction time against initial formation under hydrogenation conditions. A slight product distribution effect was observed when comparing the hydrogenated and hydrodeoxygenated products at the same conversion (~ 35 %) as shown below in Figure 64:

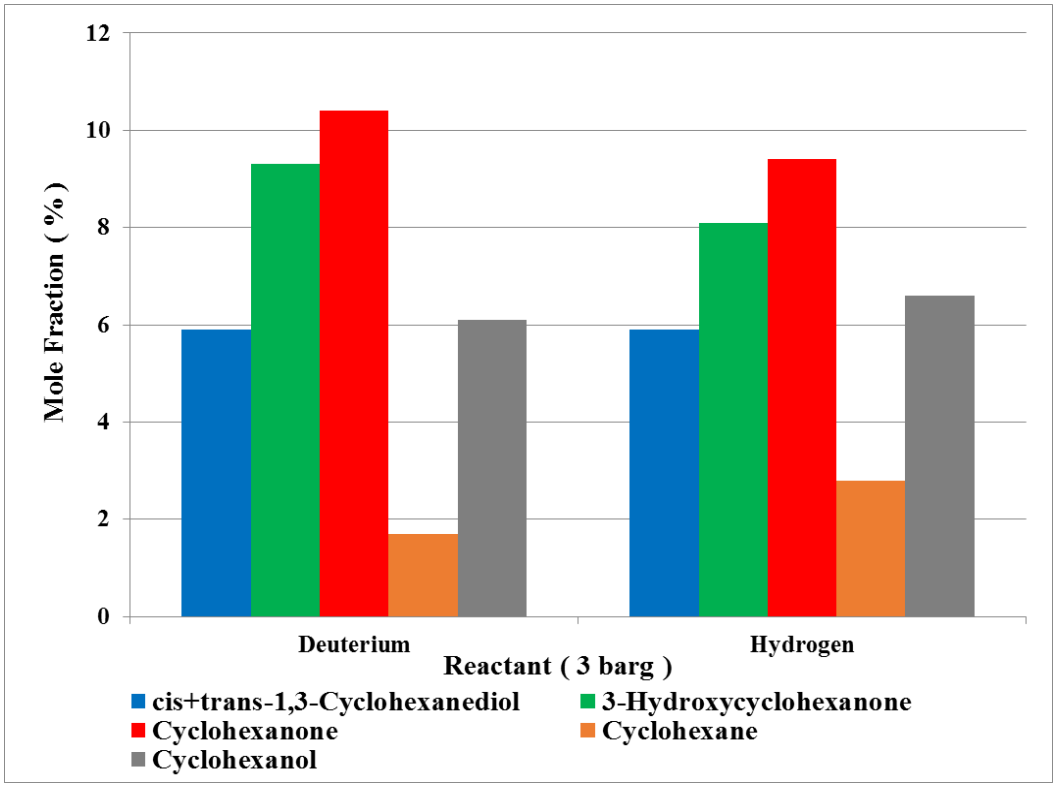

Figure 64. Product distribution of deuterium against hydrogen at 35 % conversion of resorcinol.

From Figure 64 it is clear that under deuterated conditions there was an increase in 3-hydroxycyclohexanone and cyclohexanone production with a concomitant decrease in the formation of cyclohexanol and cyclohexane. No change was observed with the *cis* and *trans*-cyclohexanediol isomers.

The deuterated reaction of hydroquinone is shown below in Figure 65:

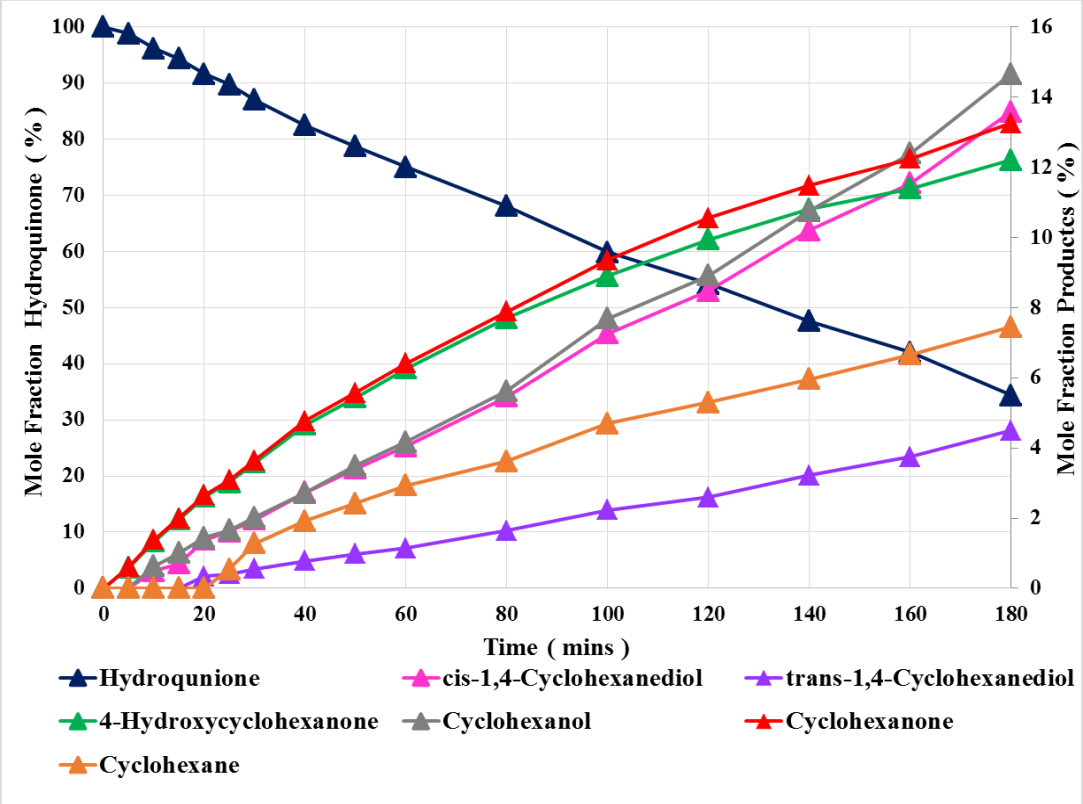

Figure 65. Reaction profile of hydroquinone deuteration. Conditions, 323 K, 10 mmol, 3 barg.

From Figure 65, in contrast to catechol and resorcinol, the deuterated hydroquinone reaction shows a slower rate than that observed with the hydrogenation, with a rate constant decrease from 4.2 $x10^{-3}$ to 3.5 $x10^{-3}$ min^{-1} recorded. Inhibition of cyclohexane formation until around 25 minutes reaction time was again observed. As with resorcinol, a mild product distribution effect was apparent when comparing the hydrogenated and hydrodeoxygenated products at the same conversion (~ 35 %) as shown below in Figure 66:

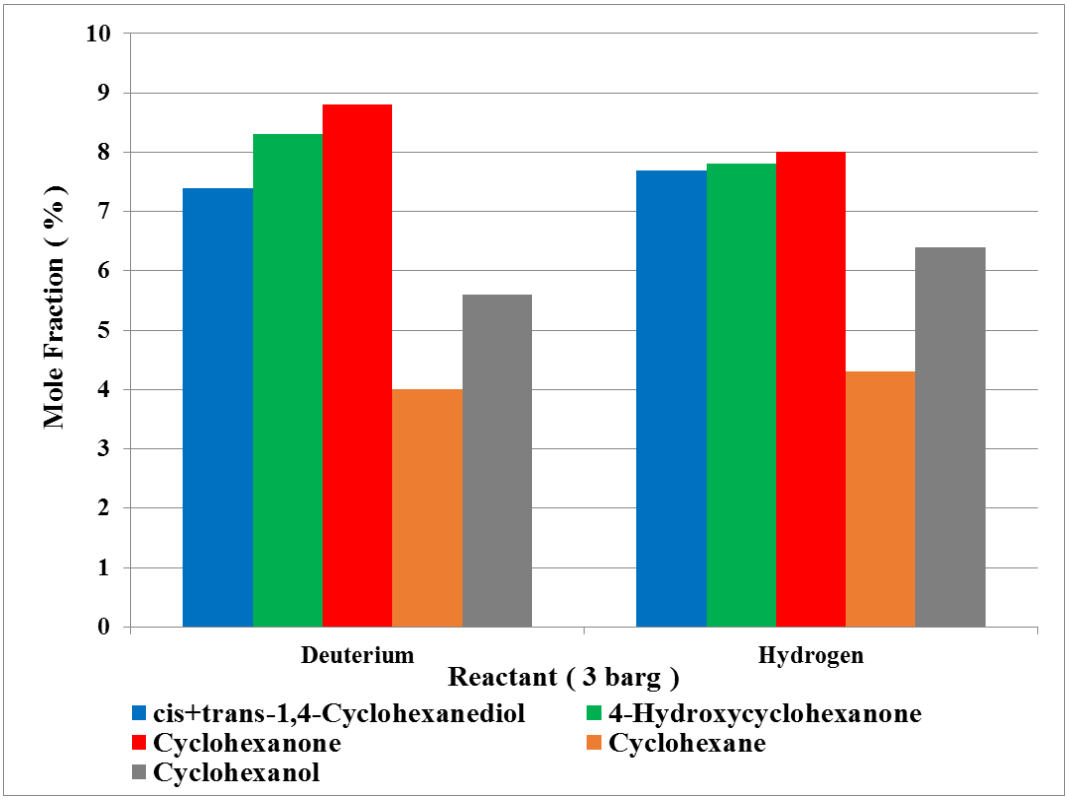

Figure 66. Product distribution of deuterium against hydrogen at 35 % conversion of hydroquinone.

From Figure 66 it can be seen that there was an increase in 3-hydroxycyclohexanone and cyclohexanone production with an associated decrease in the formation of cyclohexanol and cyclohexane. Again, no change with the *cis* and *trans*-cyclohexanediol isomers was observed.

The kinetic data gathered from the deuteration reactions is outlined in Table

14 below:

Table 14. KIE's for the individual dihydroxybenzene isomer reactions.

Substrate	kH	kD	KIE = $\frac{kH}{kD}$
Catechol	8.3	12.8	0.6
Resorcinol	11.9	12.5	0.9
Hydroquinone	4.2	3.5	1.2

Calculation of KIE can result in three possible outcomes as shown below:

- KIE value equals 1 then there is no KIE effect
- KIE > 1 yields a *positive* KIE effect

- KIE < 1 yields a *negative* KIE effect

From Table 14 above, it can be seen that a negative KIE was calculated for catechol and resorcinol, whereas hydroquinone gave a positive KIE.

Catechol and resorcinol were reacted under competitive conditions with deuterium and the results are shown in Figure 67 below:

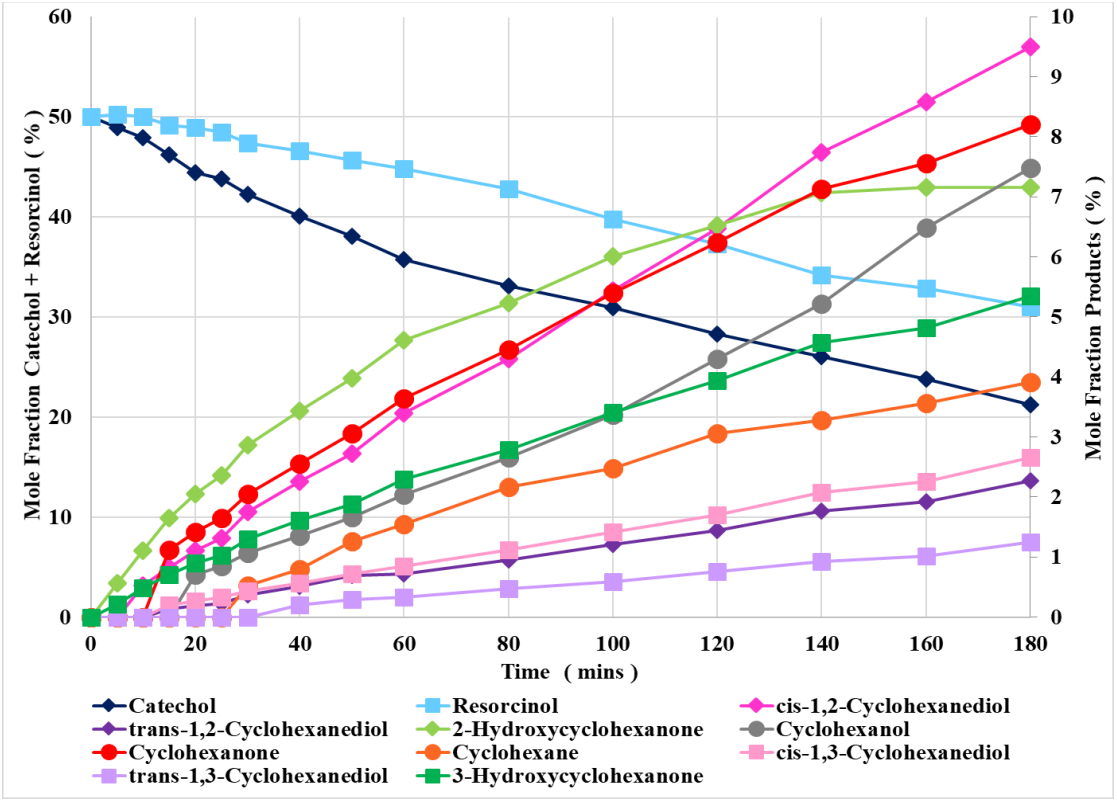

Figure 67. Reaction profile of catechol and resorcinol deuteration. Conditions, 323 K, 10 mmol, 3 barg.

From Figure 67 it is apparent that as with the hydrogenation reaction the two major products were *cis*-1,2-cyclohexanediol and cyclohexanone with a clear bias towards the formation of the catechol hydrogenated products. The inhibition of cyclohexane observed with individual deuteration reactions was again present under competitive conditions. The competitive reaction of catechol and resorcinol found an increase in catechol reactivity with no effect observed with resorcinol reactivity under deuterated conditions. The change in KIE between individual and competitive conditions is shown in Figure 68:

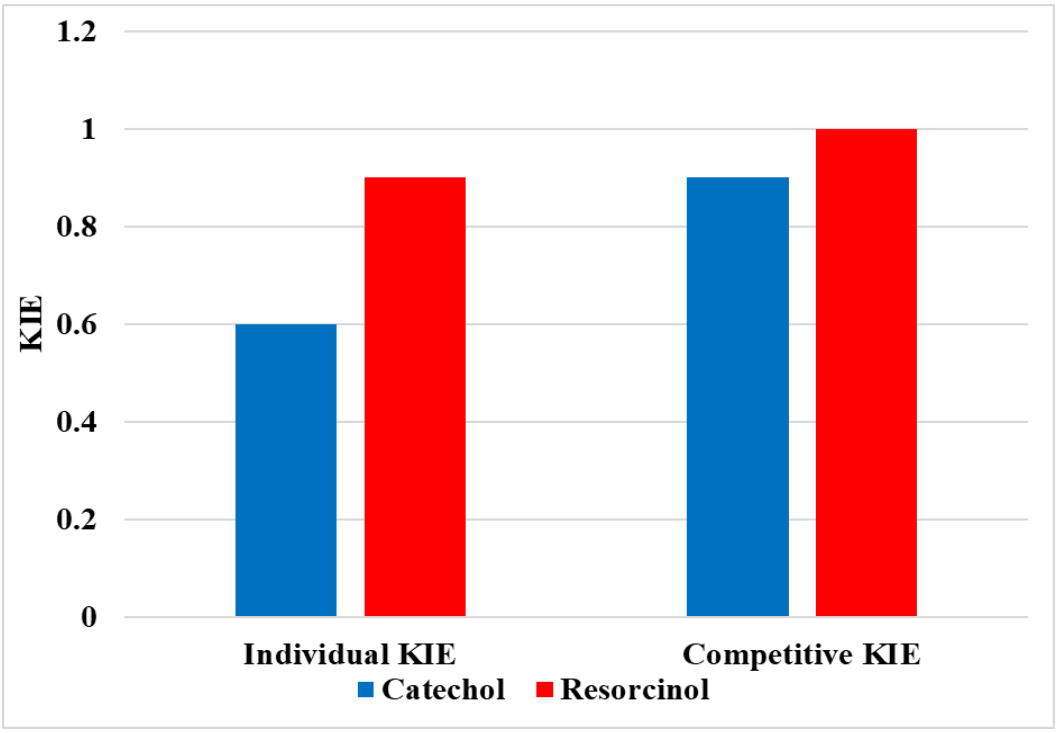

Figure 68. KIE for catechol and resorcinol individual versus competitive hydrogenation.

From Figure 68 it can be seen that across individual and competitive environments the negative KIE for catechol remained, whilst resorcinol registered no effect in the presence of deuterium during the competitive reaction with catechol.

The competitive deuteration of catechol and hydroquinone is shown below in Figure 69:

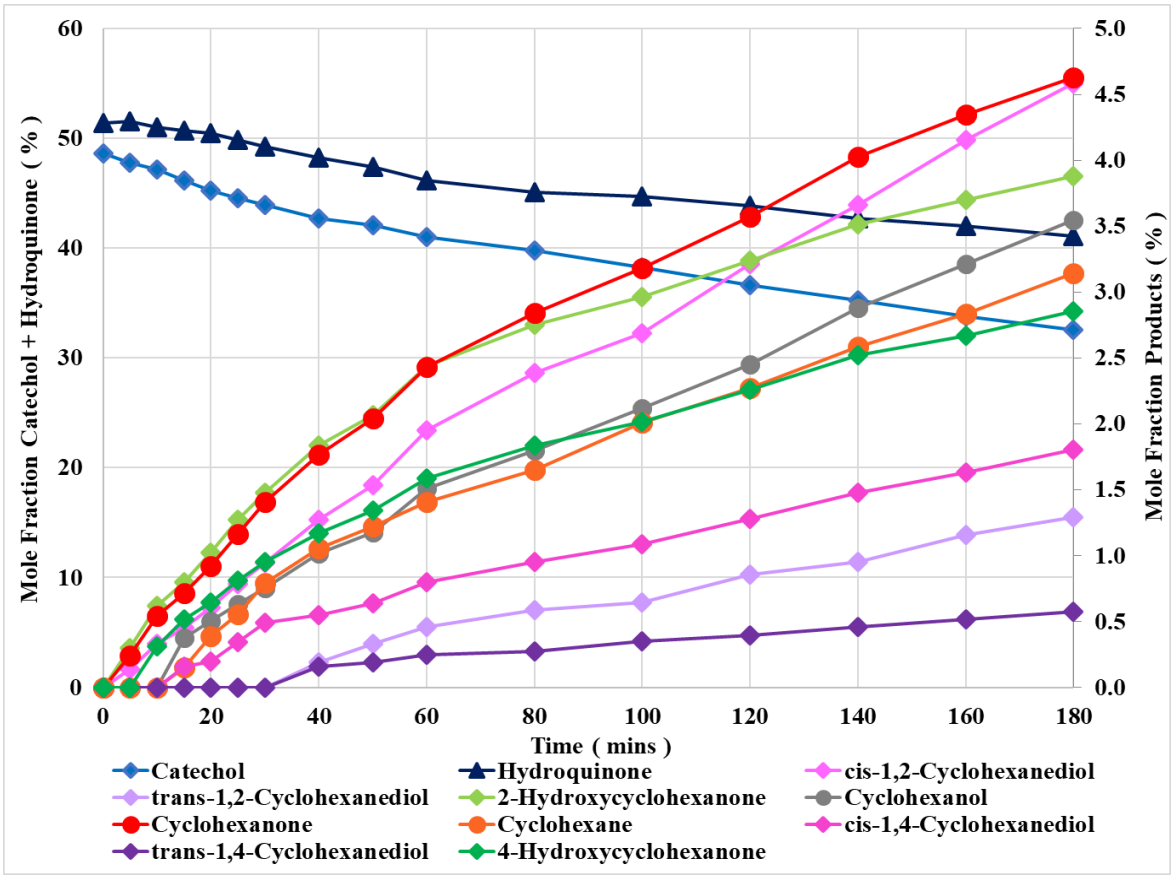

Figure 69. Reaction profile of catechol and hydroquinone deuteriation. Conditions, 323 K, 10 mmol, 3 barg.

From Figure 69, compared with hydrogenation the competitive deuteration reaction of catechol and hydroquinone showed a significant reduction in rate for both substrates. The major products at the end of reaction were cyclohexanone and *cis*-1-2-cyclohexanediol, followed by 2-hydroxycyclohexanone and as with the competitive deuteration of catechol and resorcinol, hydrogenated products from catechol are formed to the greatest extent. The KIE values for both substrates was calculated and compared against their respective individual KIE's and is shown in Figure 70 below:

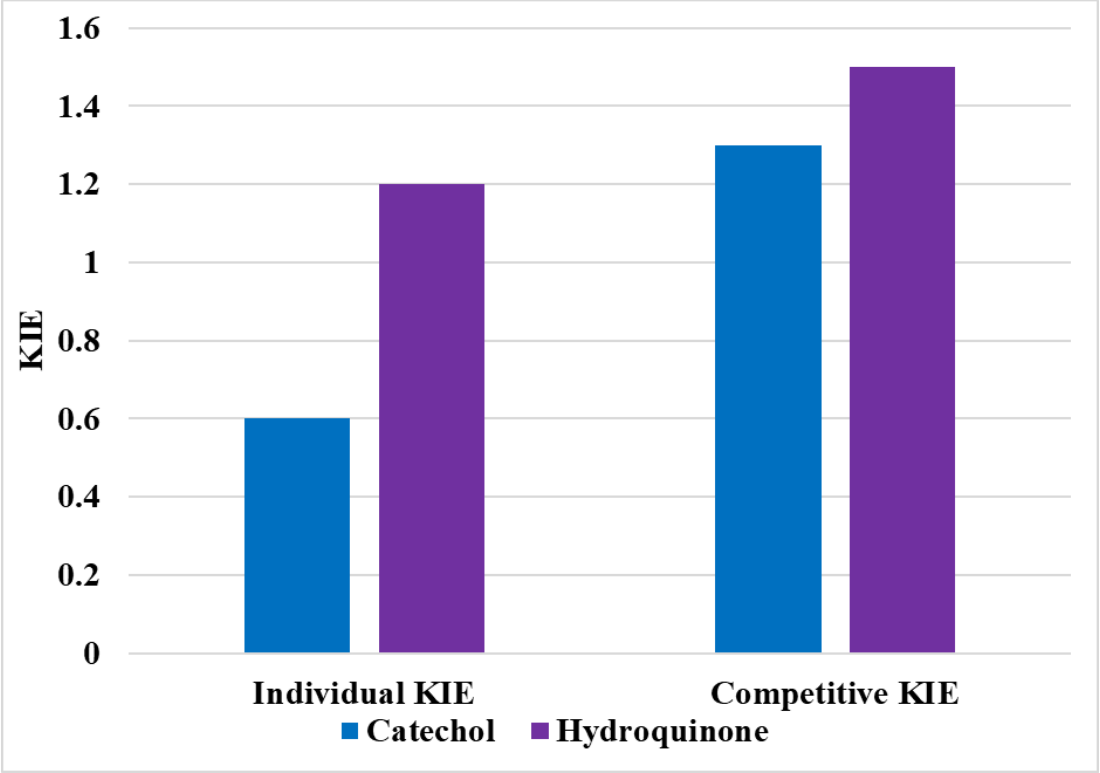

Figure 70. KIE for catechol and hydroquinone individual versus competitive hydrogenation.

From Figure 70 it can be seen that catechol changed from an inverse KIE to a positive KIE going from individual to competitive hydrogenation, whilst hydroquinone maintained a positive KIE throughout.

The deuteration reaction of resorcinol and hydroquinone is shown in Figure 71 below:

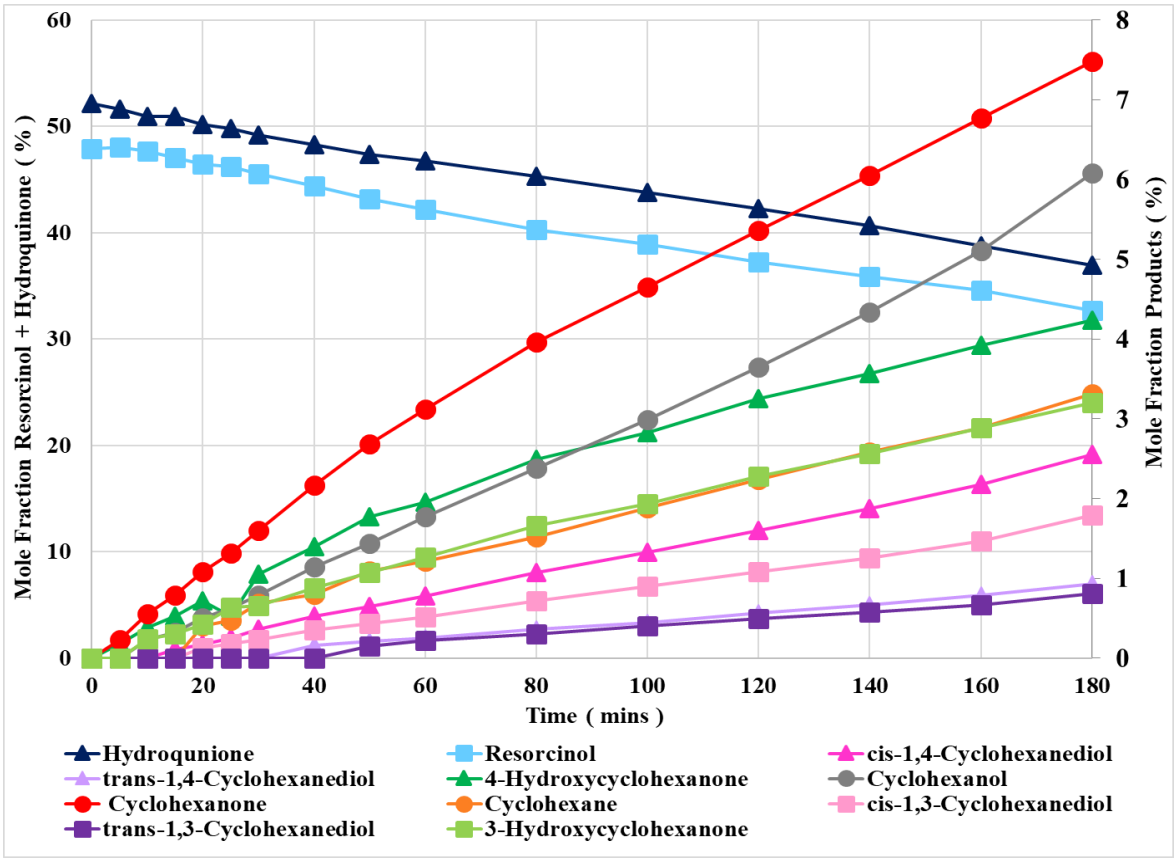

Figure 71. Reaction profile of hydroquinone and resorcinol deuteration. Conditions, 323 K, 10 mmol, 3 barg.

From Figure 71 it can be seen that under deuterated conditions an increase in reactivity was observed when compared with the respective hydrogenation reaction. As with competitive hydrogenation, the HDO products, cyclohexanone and cyclohexanol, were those formed to the greatest extent. The major ring hydrogenated product of hydroquinone, 4-hydroxycyclohexanone, was favoured over that of resorcinol. The rate constants of both substrates were used to calculate the KIE for the reaction and are compared with the individual KIE values in Figure 72 below:

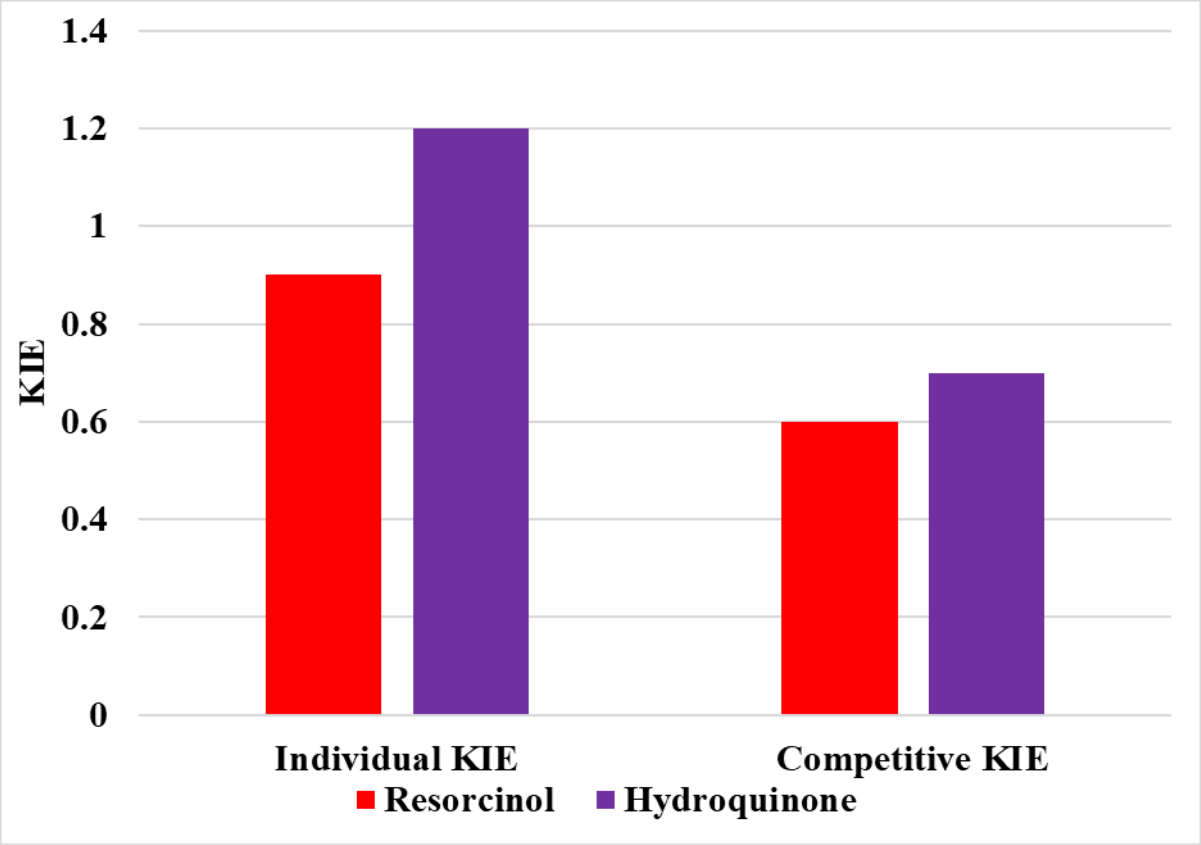

Figure 72. KIE for resorcinol and hydroquinone individual versus competitive hydrogenation.

It can be seen from Figure 72 that resorcinol and hydroquinone when reacted together found no change in the resorcinol negative KIE, whilst hydroquinone switched from positive to a negative KIE.

The competitive deuteration reaction of all three substrates reacted together is shown in Figure 73 below:

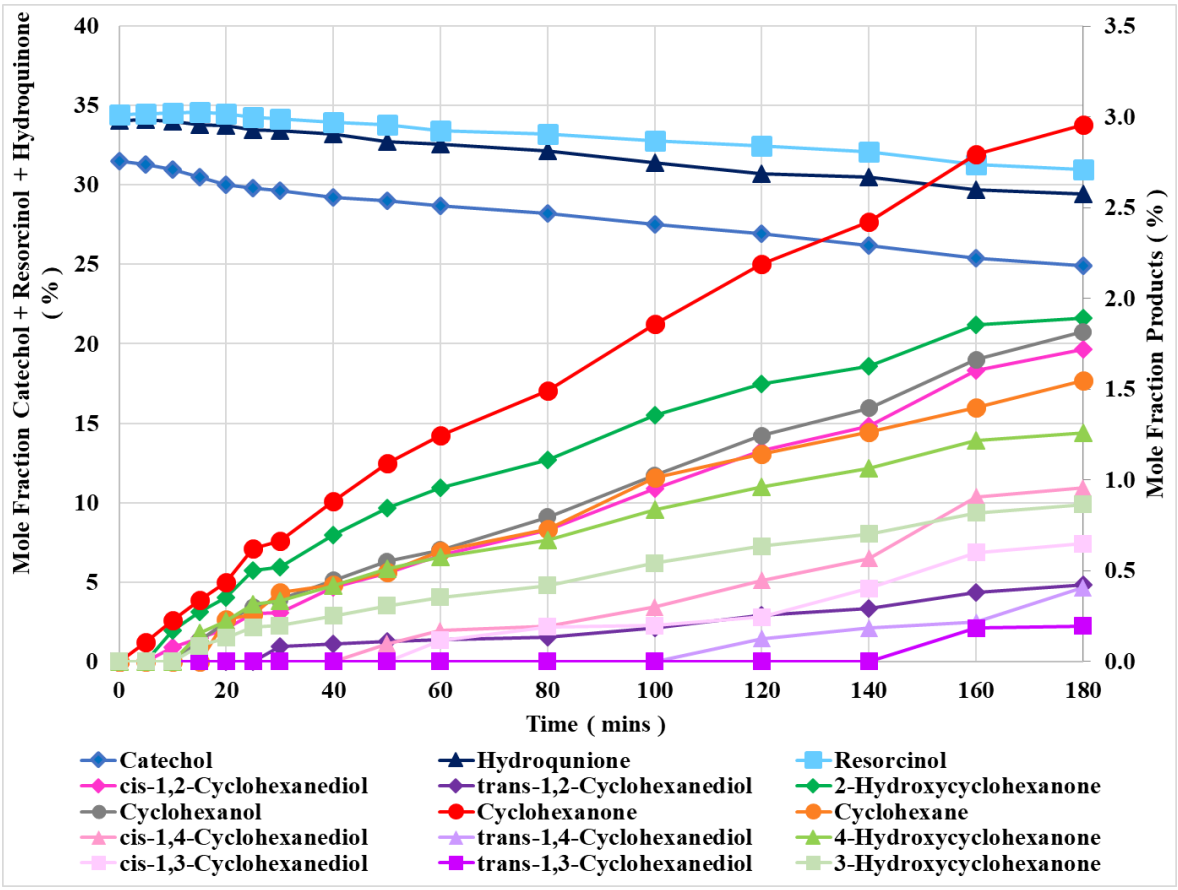

Figure 73. Reaction profile of catechol, hydroquinone and resorcinol deuteriation. Conditions, 323 K, 10 mmol, 3 barg.

From Figure 73 it was found that all isomers exhibited a decrease in reactivity under deuteration conditions. When compared with hydrogenation, cyclohexanone remained the major product under deuterium, however, 2-hydroxycyclohexanone replaced *cis*-1,2-cyclohexanediol as the second major product. The delay in formation of the *trans* isomer product was prolonged for each substrate when compared against the hydrogenation reaction.

The kinetic isotope effects calculated during the competitive reactions are summarised below in Table 15:

Table 15. KIE's for the dihydroxybenzene competitive reactions.

	Catechol/ Resorcinol	Catechol /Hydroquinone	Resorcinol/ Hydroquinone	Catechol/Resorcinol /Hydroquinone
KIE = $\frac{kH}{kD}$	**0.9, 1.0**	**1.3, 1.5**	**0.6, 0.7**	**1.1, 1.2, 1.4**

From Table 15 above it can be seen that no clear correlation between substrate and KIE exists, with each competitive reaction registering unique KIE values for each isomer.

7.1.6 Extended hydrogenation reaction

To test for catalyst activity and deactivation individual hydrogenation reactions were carried out on each of the three substrates over a six-hour time period. An initial addition of 10 mmol substrate was followed by a second 10 mmol addition after 3 hours reaction run time. All other parameters were set for standard conditions (323 K, 3 barg H_2).

The conversion plots for catechol from first and second additions are shown separately in Figure 74 below:

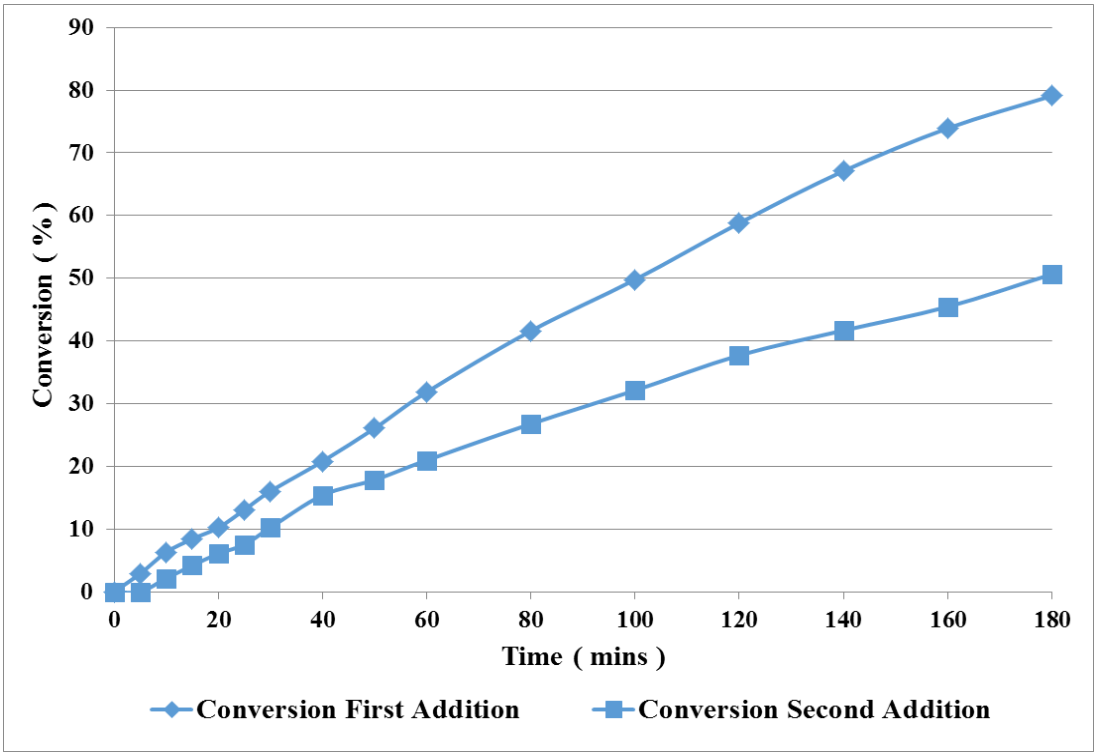

Figure 74. Catechol conversion for first and second addition of substrate.

From above it can be seen that over the six-hour time frame the catalyst has underwent significant deactivation with a drop-in conversion of ~ 80 % to ~ 50 % between the first and second additions of catechol.

The conversion plots for resorcinol from first and second additions are shown separately in Figure 75 below:

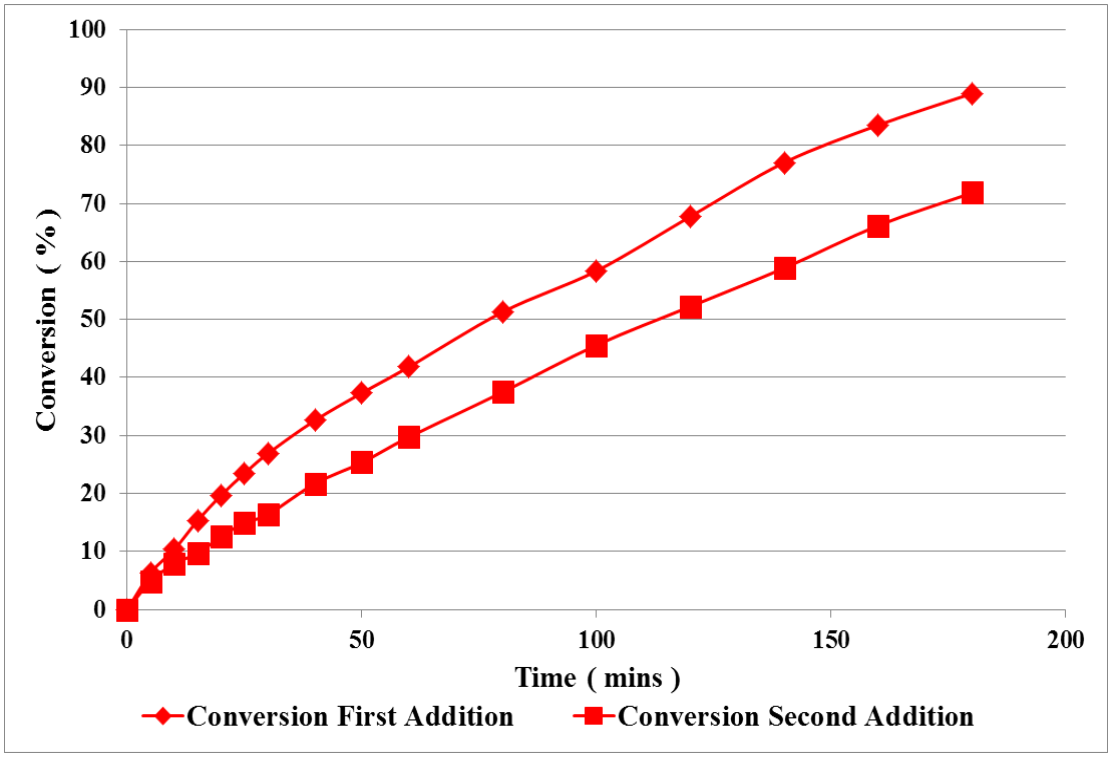

Figure 75. Resorcinol conversion after 3 hour versus 6-hour hydrogenation.

From Figure 75 deactivation of the catalyst is evident, with a drop-in conversion from 90 % to 70 % between the first and second addition.

The conversion plots for hydroquinone from first and second additions are shown separately in Figure 76 below:

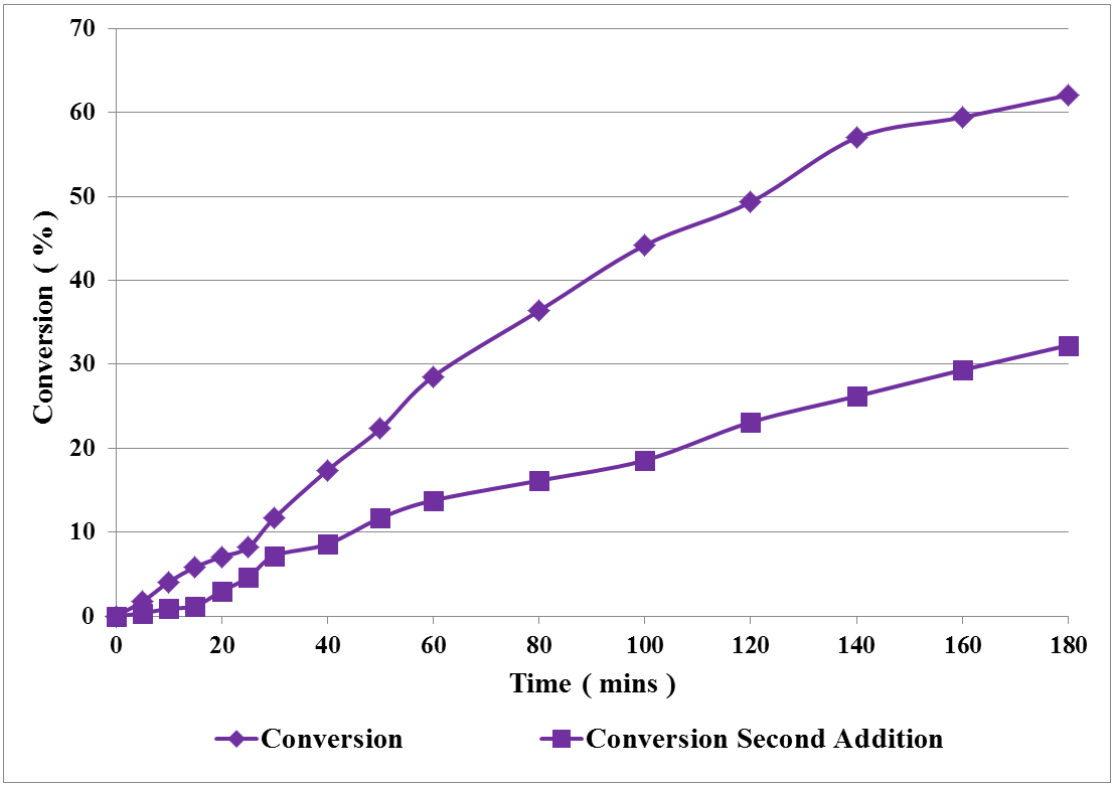

Figure 76. Hydroquinone conversion after 3 hour versus 6 hour hydrogenation.

From Figure 76 it can be seen that there is a substantial decrease in conversion between the first and second additions (60 to 30 %) indicating significant catalyst deactivation.

7.1.7 Post Reaction Catalyst Characterization

Thermogravimetric analysis (TGA) on the post reaction catalyst from the standard (3 hours) and extended hydrogenation (6 hours) reactions of all substrates was carried out.

7.1.7.1 Catechol

The thermal weight loss and associated evolved gas mass spectrometry data for the three- and six-hour post reaction catalysts are shown in Figures 77-80 below:

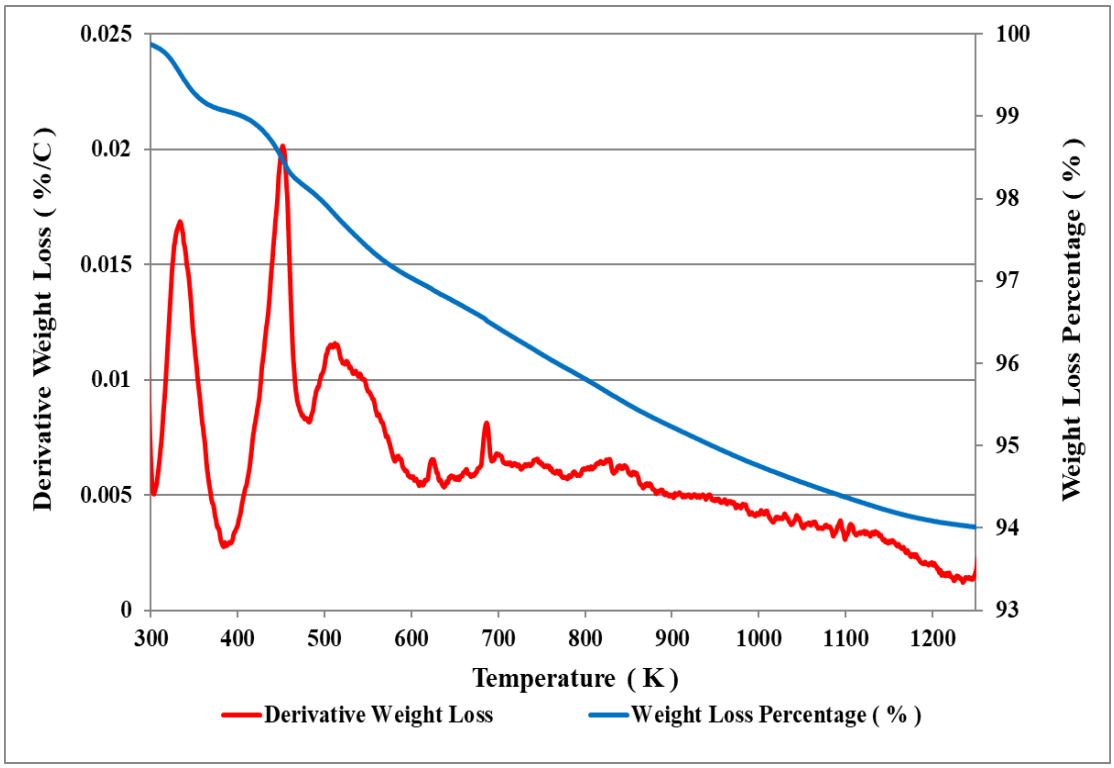

Figure 77. TGA of Rh/SiO_2 catalyst after 3-hour catechol hydrogenation reaction.

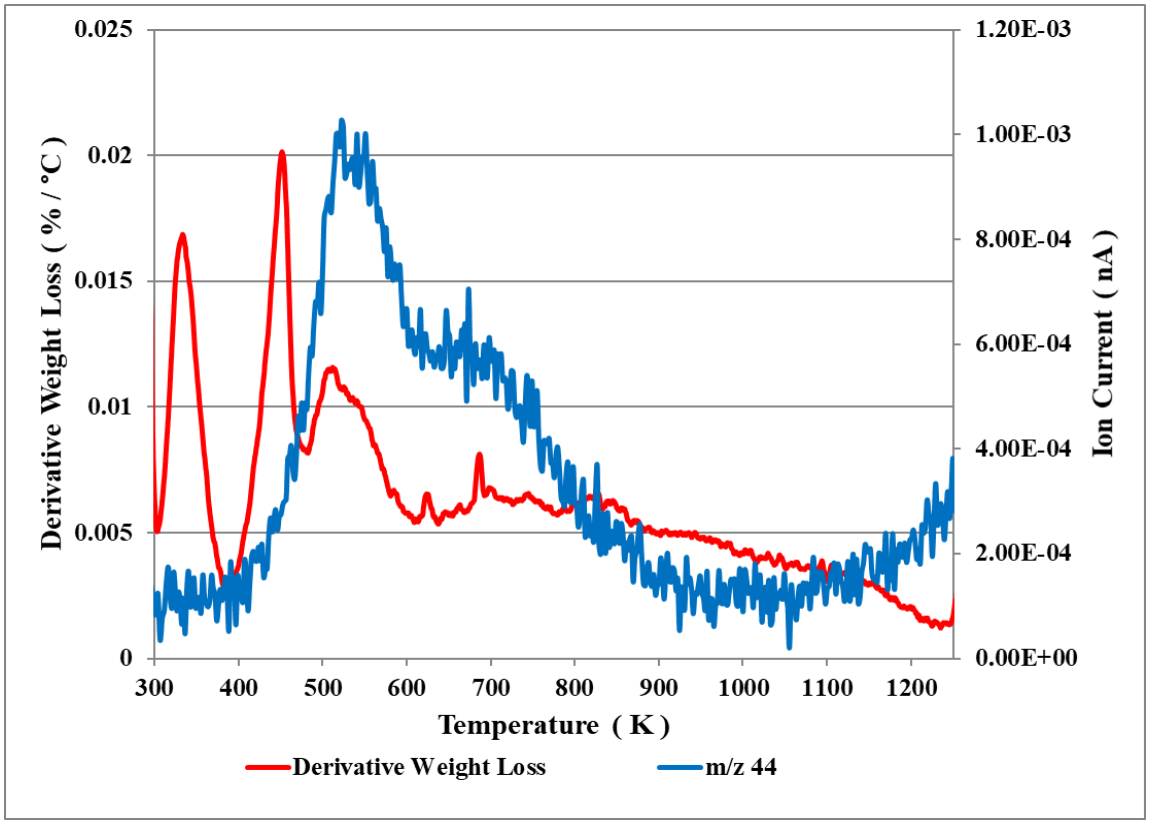

Figure 78. Derivative weight loss coupled with m/z of Rh/SiO2 catalyst after 3 hour catechol hydrogenation reaction.

From Figures 77 and 78 above it can be seen that the catalyst from the three hour reaction exhibited an overall weight loss of ~ 6 % with ~ 4 % of this attributed to the two high temperature weight losses confirmed as m/z = 44 (CO_2) from the mass spectrometry data. Initial weight loss events between 353 and 473 K are associated with the desorption of water and catechol.

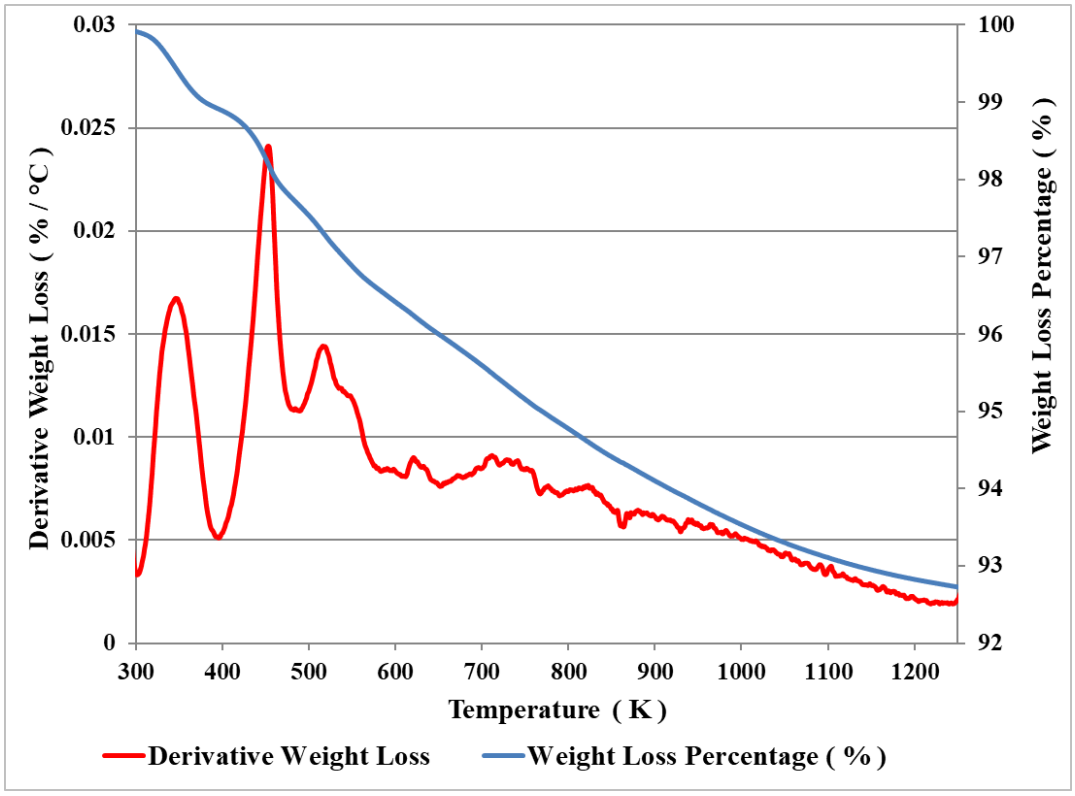

Figure 79. TGA of Rh/SiO_2 catalyst after 6-hour catechol hydrogenation reaction.

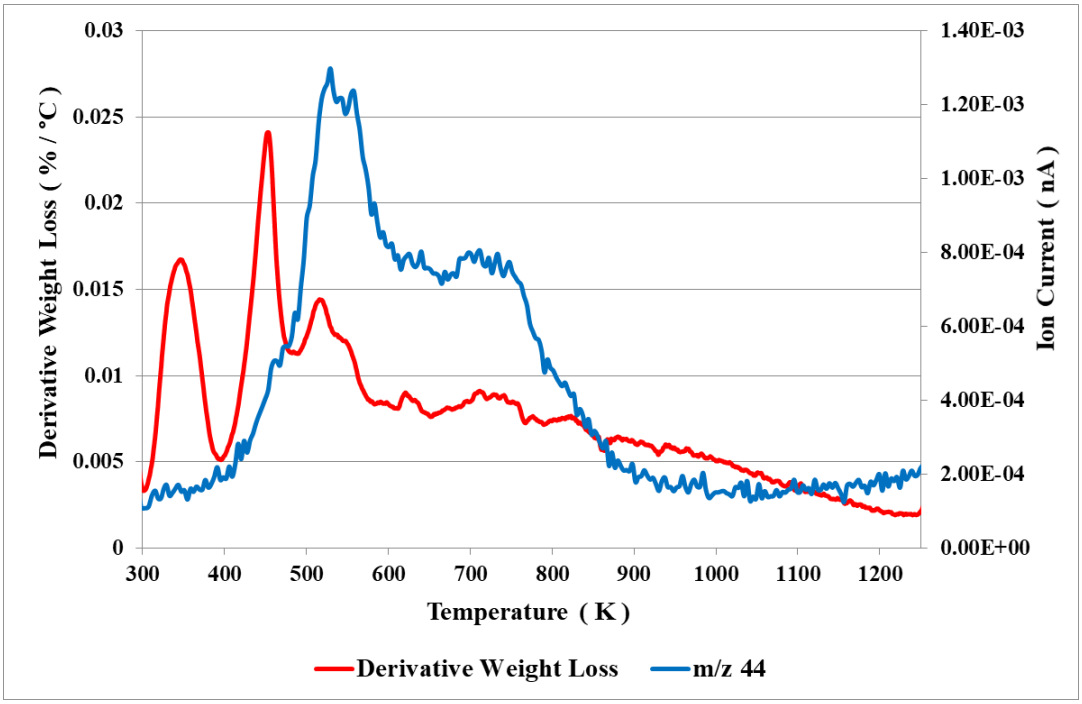

Figure 80. Derivative weight loss coupled with m/z of Rh/SiO_2 catalyst after 6-hour catechol hydrogenation reaction.

From Figure 79 and 80 it can be seen that following the six-hour reaction an increase in the overall catalyst weight loss to ~ 7 % occurred, with an increase from 4 to 5 % observed

with the weight loss events attributed to CO_2. As previously, low temperature weight loss events prior to 473 K are a result of the desorption of water and catechol.

7.1.7.2 Resorcinol

The thermal weight loss and associated evolved gas mass spectrometry data for the three- and six-hour post reaction catalysts are shown in Figures 81-84 below:

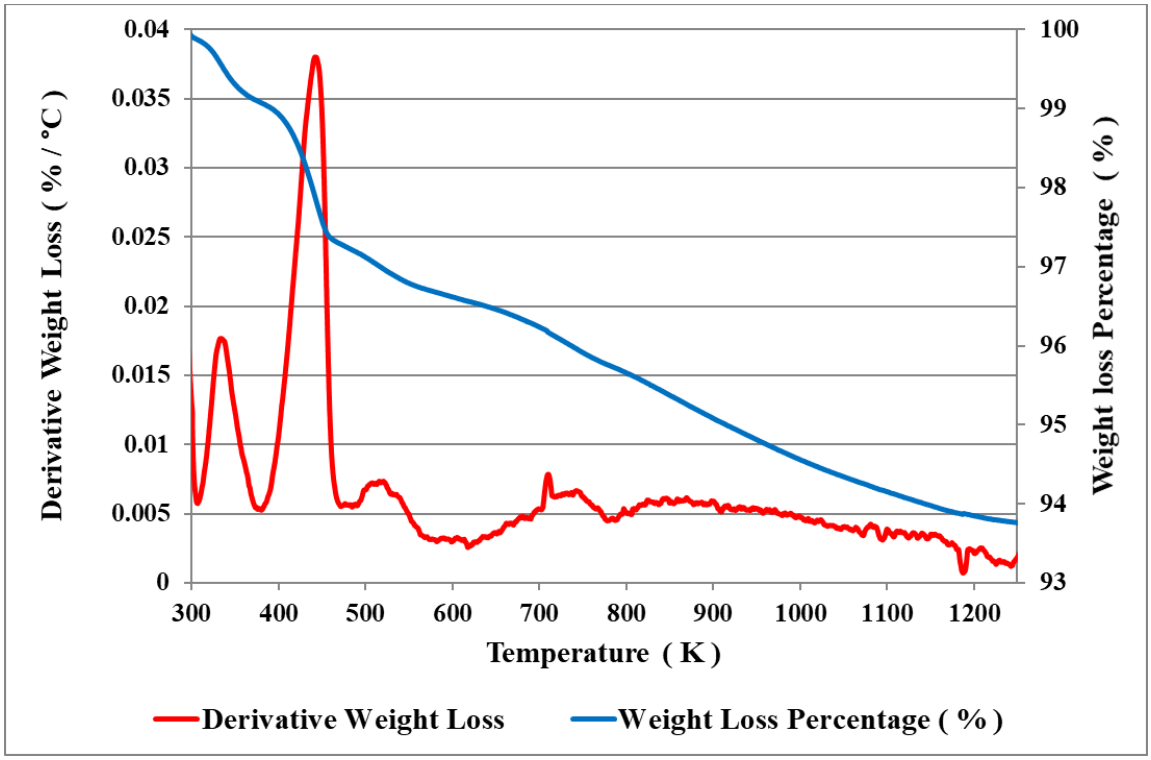

Figure 81. TGA of Rh/SiO_2 catalyst after 3-hour resorcinol hydrogenation reaction.

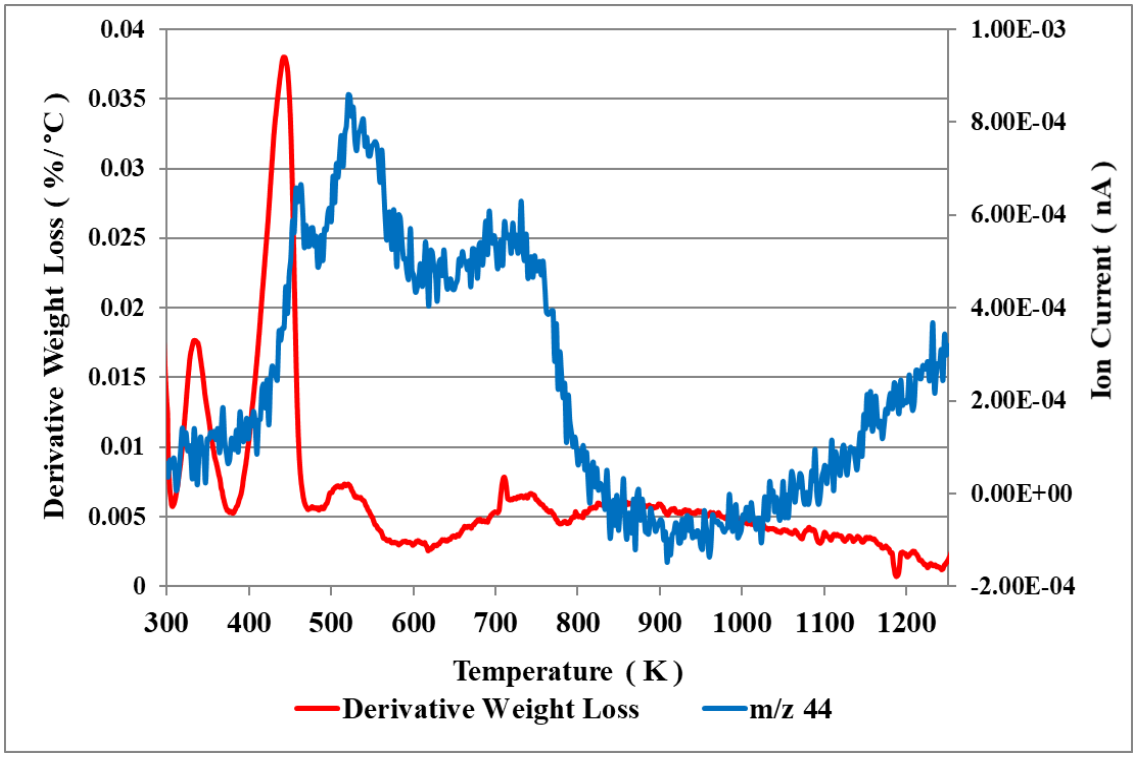

Figure 82. Derivative weight loss coupled with m/z of Rh/SiO_2 catalyst after 3 hour resorcinol hydrogenation reaction.

From Figures 81 and 82 above it can be seen that the catalyst from the three hour reaction showed an overall weight loss of ~ 6 % with ~ 3 % of this from the two high temperature weight losses confirmed as m/z = 44 (CO_2) from the mass spectrometry data. Initial weight loss events between 353 and 473 K are a result of water and resorcinol desorption.

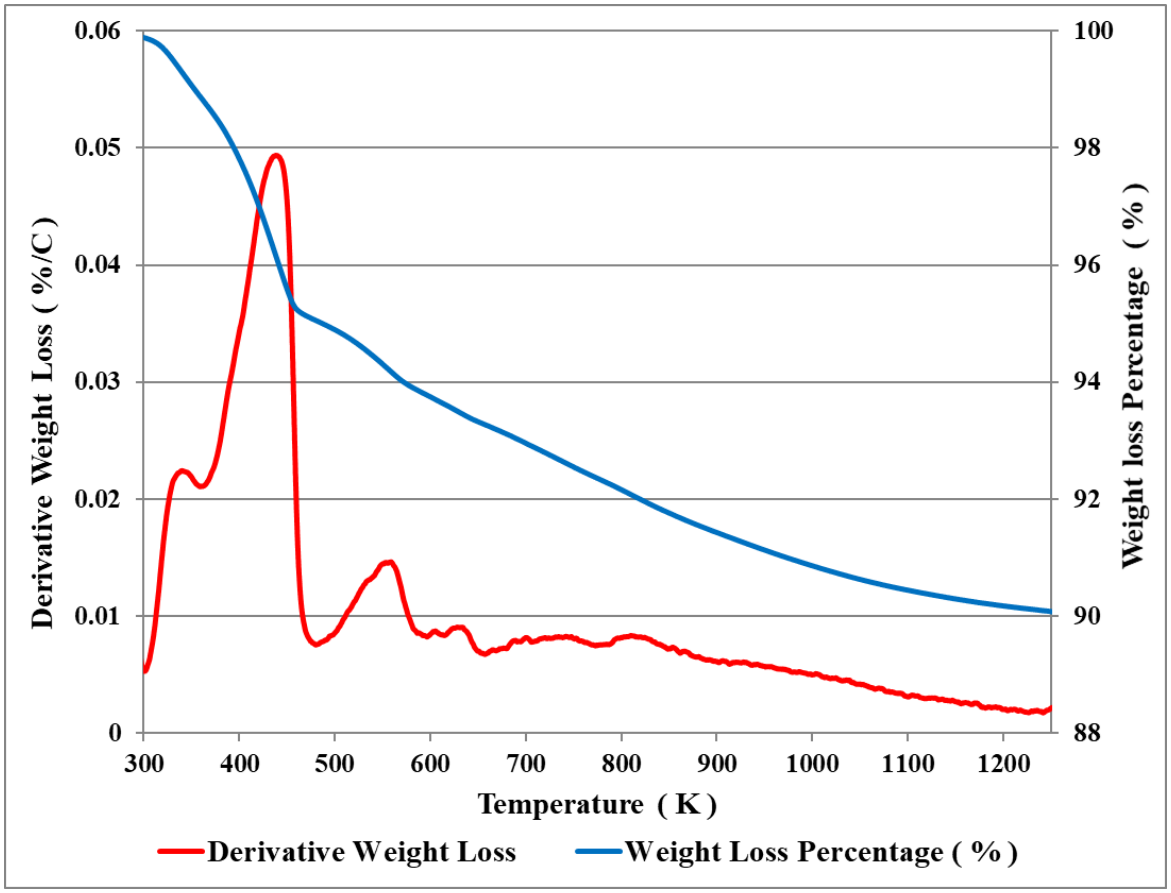

Figure 83. TGA of Rh/SiO_2 catalyst after 6-hour resorcinol hydrogenation reaction.

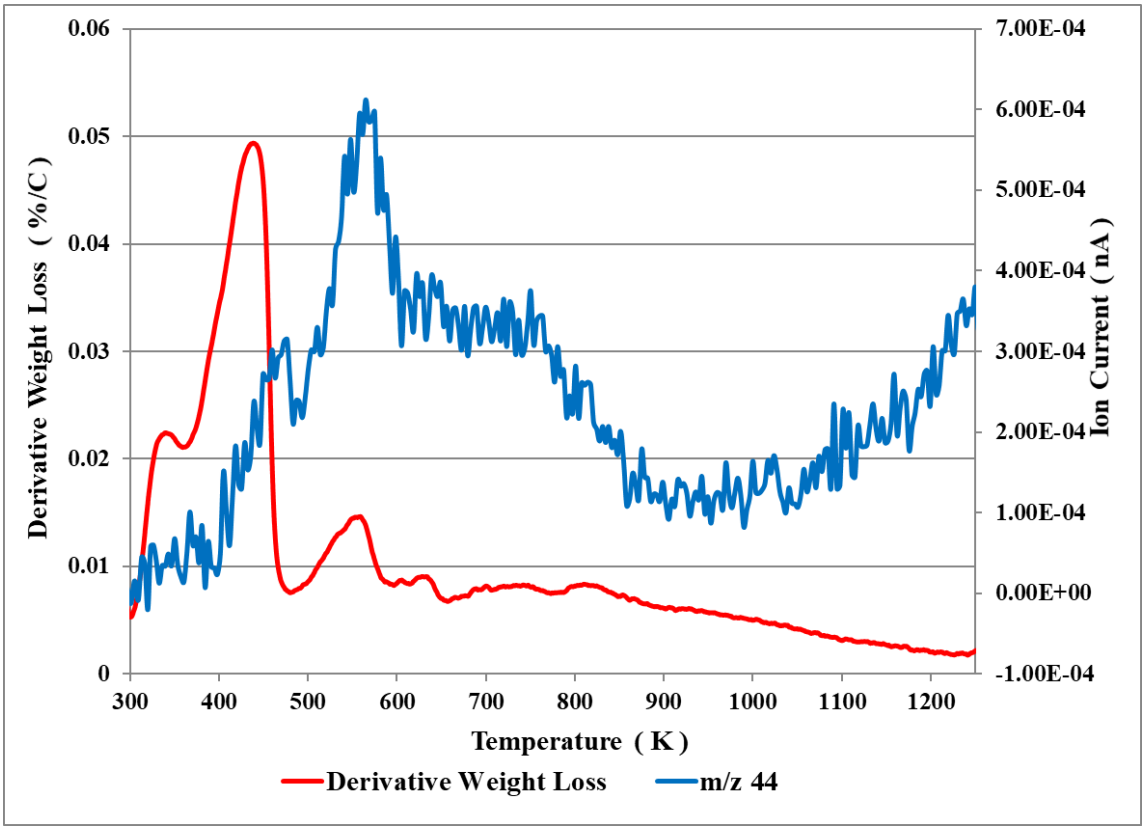

Figure 84. Derivative weight loss coupled with m/z of Rh/SiO_2 catalyst after 6-hour resorcinol hydrogenation reaction.

From Figure 83 and 84 it can be seen that following the six-hour reaction an increase in the overall catalyst weight loss to ~ 10 % occurred, with an increase from 3 to 5 % observed with the weight loss events attributed to the removal of carbon in the form of CO_2. As previously, those weight loss events below 473 K are a result of the desorption of water and resorcinol.

7.1.7.3 Hydroquinone

The thermal weight loss and associated evolved gas mass spectrometry data for the three- and six-hour post reaction catalysts are shown in Figures 85-88 below:

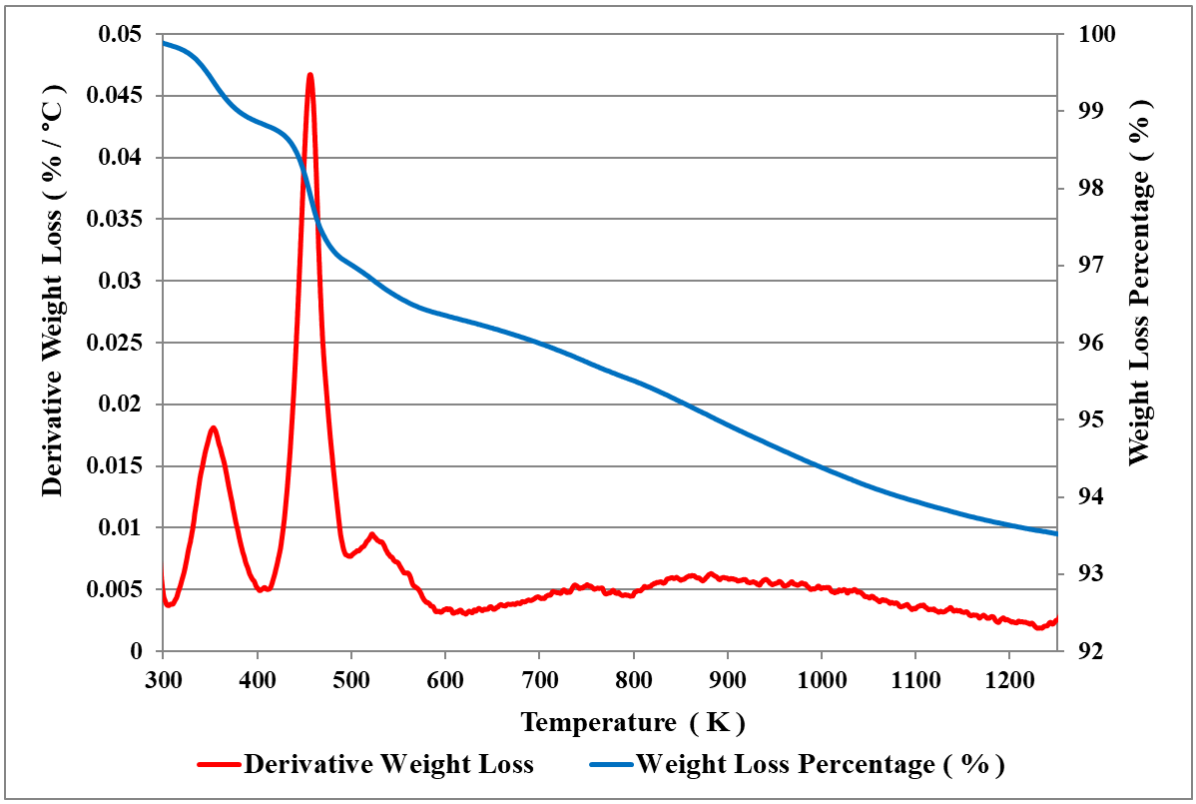

Figure 85. TGA of R/SiO_2 catalyst after 3-hour hydroquinone hydrogenation reaction.

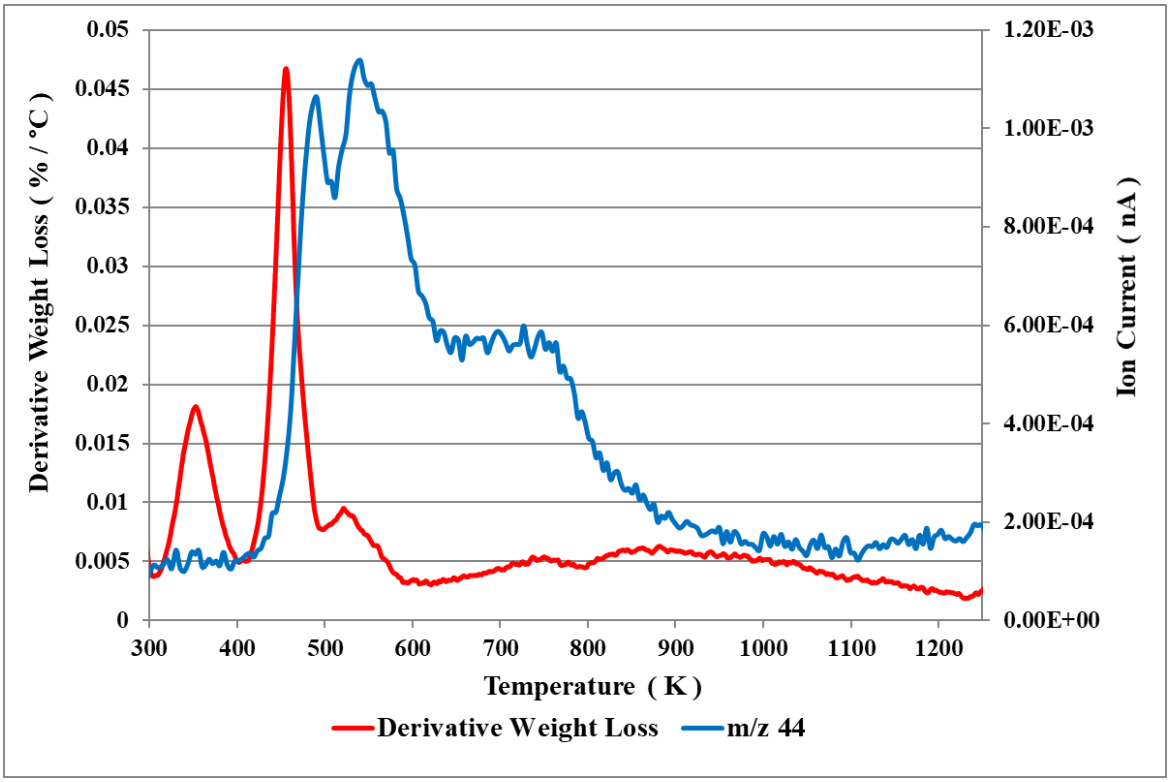

Figure 86. Derivative weight loss coupled with m/z of Rh/SiO_2 catalyst after 3-hour hydroquinone hydrogenation reaction.

From Figures 85 and 86 above it can be seen that the catalyst from the three hour reaction exhibited a total weight loss of ~ 6 % with ~ 3.5 % of this attributed to the two high temperature weight losses confirmed as m/z = 44 (CO_2) from the mass spectrometry data.

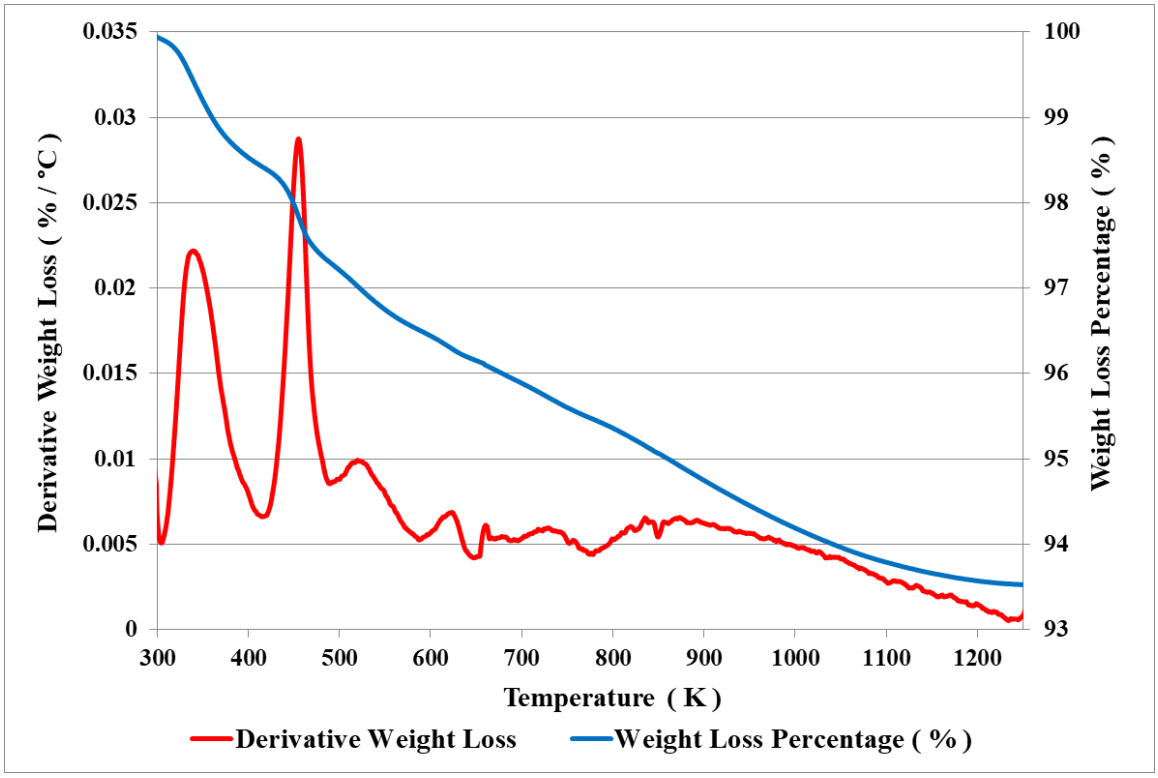

Figure 87. TGA of Rh/SiO_2 catalyst after 6-hour hydroquinone hydrogenation reaction.

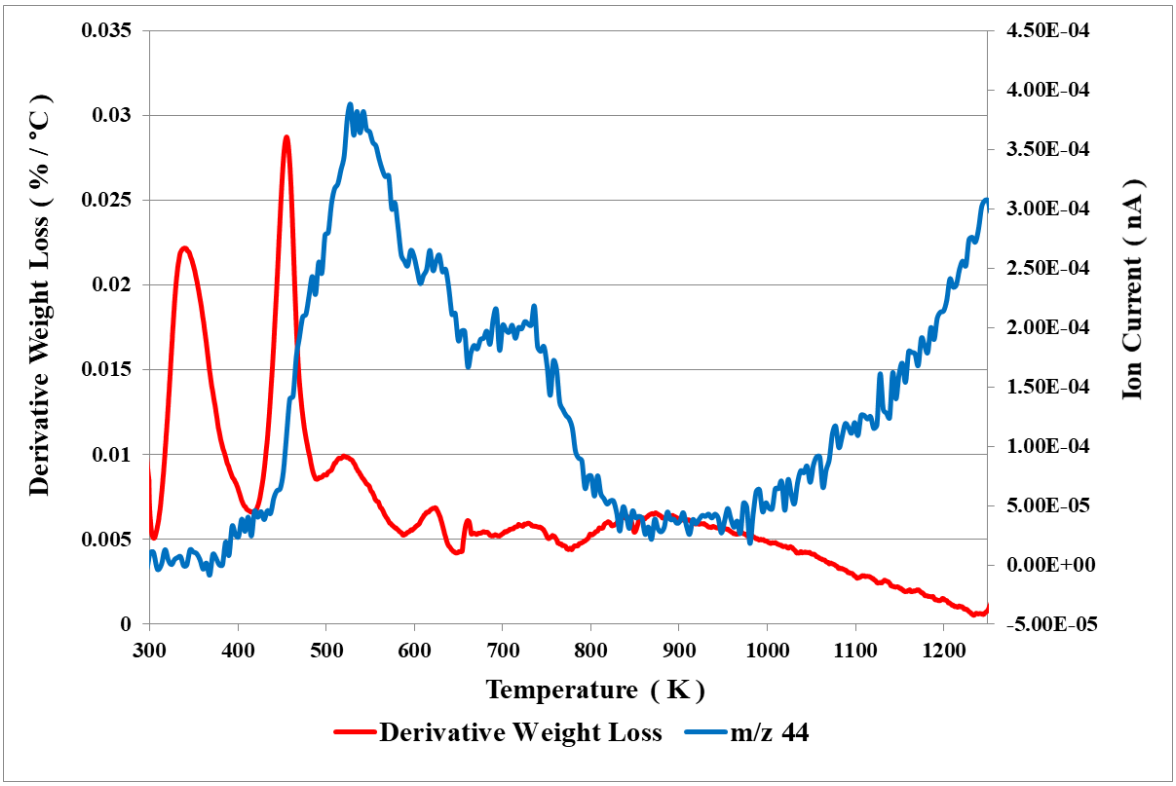

Figure 88. Derivative weight loss coupled with m/z of Rh/SiO_2 catalyst after 6-hour hydroquinone hydrogenation reaction.

From Figure 87 and 88 it can be seen that following the six-hour reaction both the overall catalyst weight loss at ~ 6 % and that of the weight loss attributed to the removal of carbon

in the form of CO_2 were broadly similar. As previously, low temperature weight loss events prior to 473 K are a result of the desorption of water and hydroquinone.

7.2 Cresol Isomers

This section contains all results from the cresol isomers and covers the following sets of reactions: individual hydrogenation of *ortho*-, *meta*- and *para*-cresol including temperature variations and competitive hydrogenation reactions where the isomers were reacted in pairs and as a set of three.

7.2.1 Individual Hydrogenation Standard Reactions

In this set of reactions *ortho*, *meta* and *para*-cresol hydrogenation will be shown at our standard reaction conditions of 323 K, 10 mmol substrate and 3 barg hydrogen. *ortho*-Cresol is shown below in Figure 89:

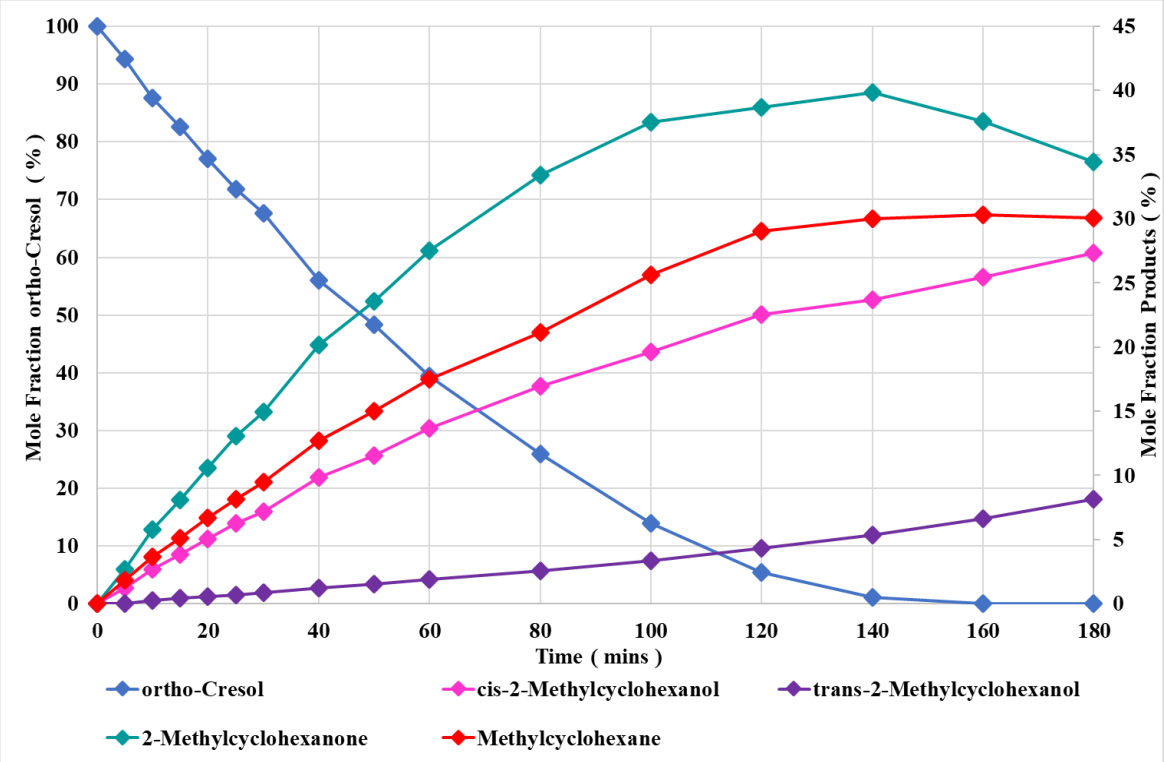

Figure 89. Reaction profile of *ortho*-cresol hydrogenation. Conditions, 323 K, 10 mmol, 3 barg.

From Figure 89 it can be seen, that full conversion of *ortho*-cresol was achieved by ~ 140 minutes. Formation of the two major ring hydrogenated products, 2-methylcyclohexanone and *cis*-2-methylcyclohexanol, was observed from the initial stages of the reaction with 2-methylcyclohexanone the main product at the end of reaction. The *trans*-2-methylcyclohexanol did not form until 10 minutes into the reaction and remained low throughout (<10%). Significant levels of the sole HDO product, methylcyclohexane, were formed ~ 30% total mole fraction by140 minutes; the second largest reaction product overall. It should be noted that at this point yield plateaued in conjunction with total consumption of the aromatic.

For *meta*-cresol at identical conditions, the reaction profile is shown below in Figure 90:

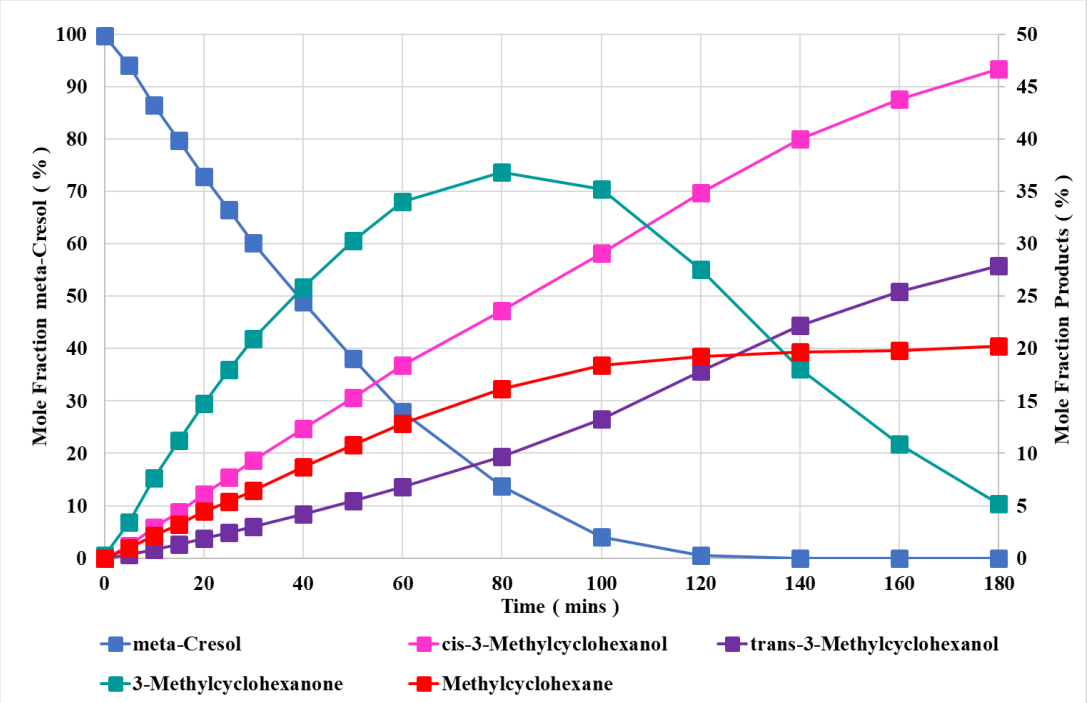

Figure 90. Reaction profile of *meta*-cresol hydrogenation. Conditions, 323 K, 10 mmol, 3 barg.

From Figure 90 it is apparent that full conversion of *meta*-cresol occurs by ~ 120 minutes. Again, both major ring hydrogenated products, 3-methylcyclohexanone and *cis*-3-methylcyclohexanol, formed initially whilst in this instance the major product by the end of reaction was the *cis*-3-methylcyclohexanol. It is evident that the 3-methylcyclohexanone is behaving as an intermediate in the reaction, forming to ~ 35 % as the major product by 80 minutes followed by a decline to < 5 % by the end of reaction. Hydrogenation to the *trans*-2-methylcyclohexanol was observed from the early stages of the reaction and it ended as the second major product. Significant formation of the HDO product, methylcyclohexane, again occurred, ~ 20 % by 120 minutes upon where it clearly plateaued, that of the secondary hydrogenated products however continued to rise until end of reaction.

For *para*-cresol at identical conditions, the reaction profile is shown below in Figure 91:

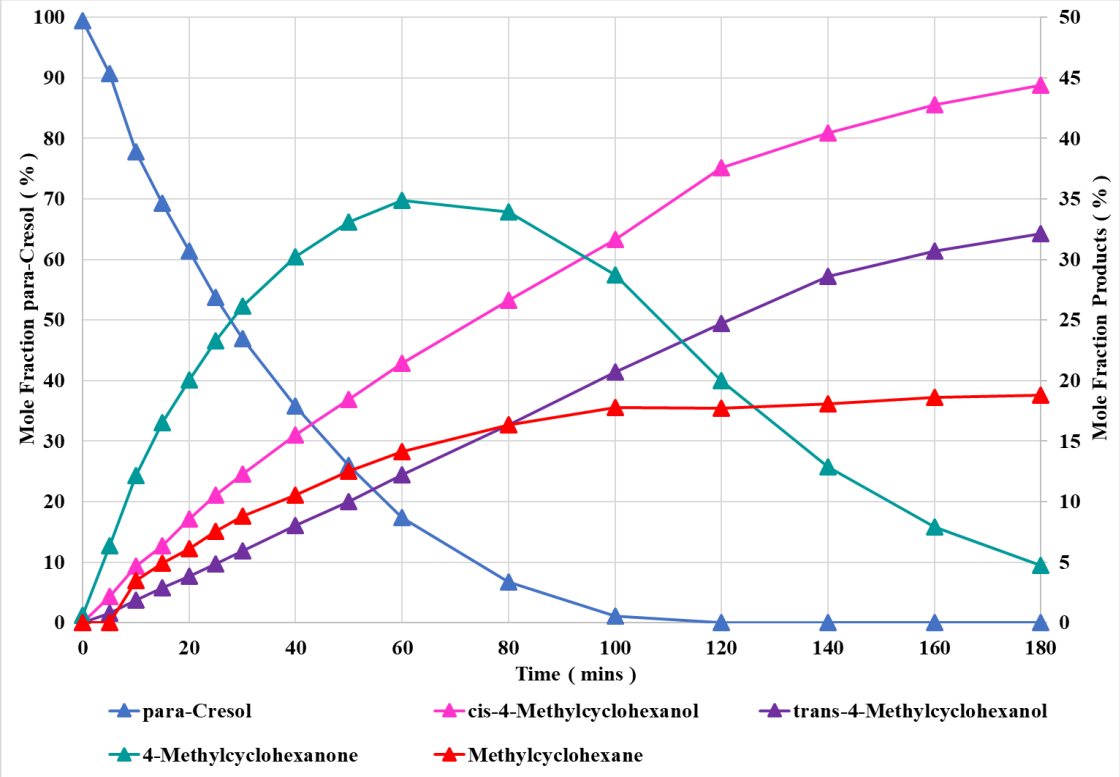

Figure 91. Reaction profile of *para*-cresol hydrogenation. Conditions, 323 K, 10 mmol, 3 barg.

It can be seen from Figure 91 that *para*-cresol achieved full conversion by ~ 100 minutes; the fastest of all three isomers. The major products at the end of reaction were the ring hydrogenated, *cis*-4-methylcyclohexanol, with ~ 45% mole fraction followed by the *trans*-4-methylcyclohexanol at ~ 30 %. It is notable, that as with *meta*-cresol the 4-hydroxycyclohexanone exhibited a rapid increase in formation to ~35 % followed by a steady decline to ~5% by the end of reaction. The methylcyclohexane also showed a similar profile to that observed during *meta*-cresol hydrogenation, with ~ 20 % formed by the end of reaction.

7.2.2 Temperature Variations of Cresol Isomers

7.2.2.1 *ortho*-Cresol Temperature Variations

In this set of reactions, *ortho*-cresol was hydrogenated at 10 K increments from 303 to 343 K, with 323 K taken as the standard reaction. Hydrogen pressure (3 barg) and reactant concentration (10 mmol) were kept constant to understand the effect temperature had on *ortho*-cresol hydrogenation. The graphs are shown below in increasing order of temperature:

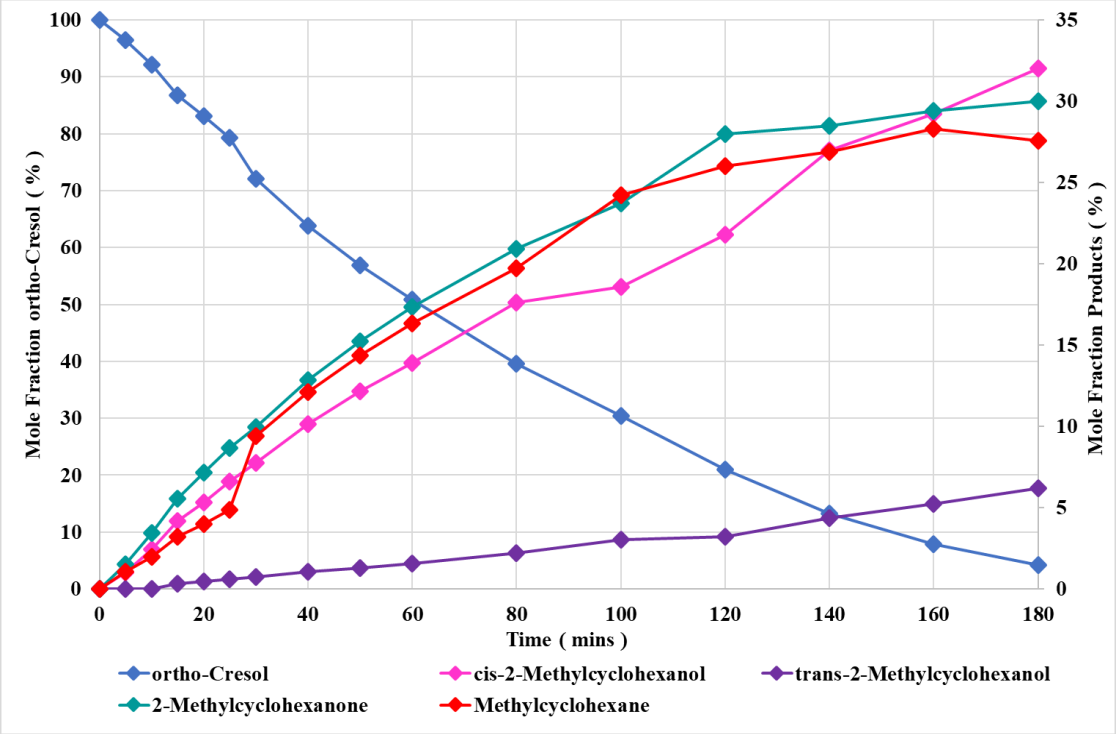

Figure 92. Reaction profile of *ortho*-cresol hydrogenation. Conditions, 303 K, 10 mmol, 3 barg.

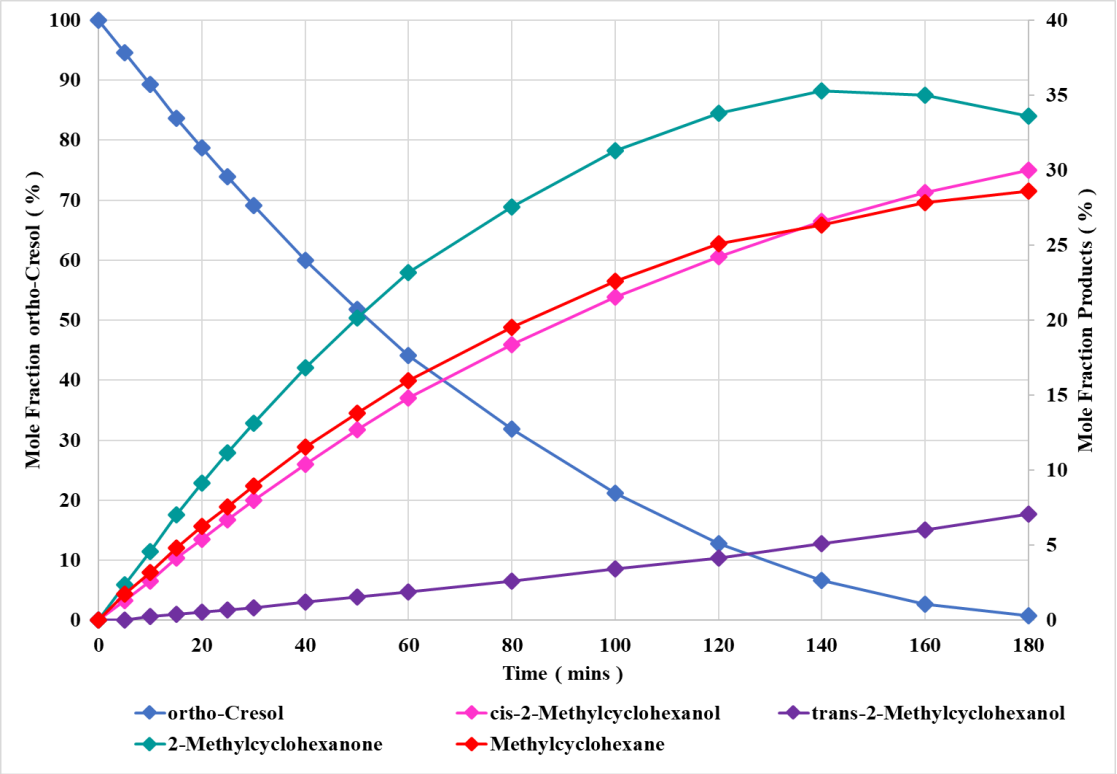

Figure 93. Reaction profile of *ortho*-cresol hydrogenation. Conditions, 313 K, 10 mmol, 3 barg.

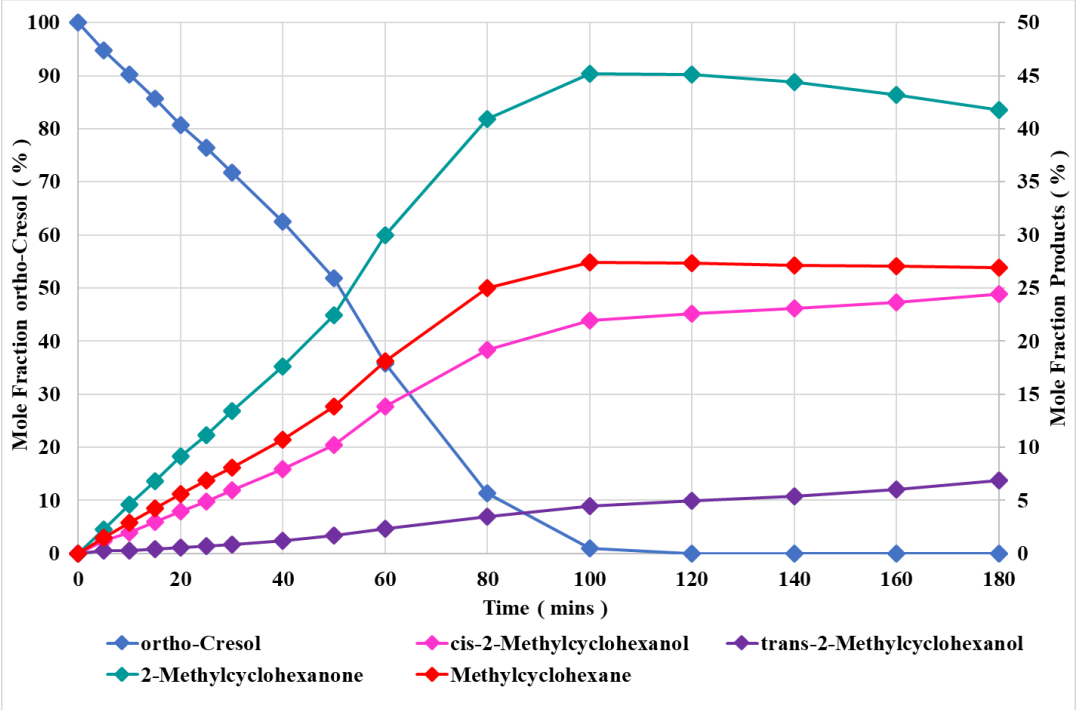

Figure 94. Reaction profile of *ortho*-cresol hydrogenation. Conditions, 333 K, 10 mmol, 3 barg.

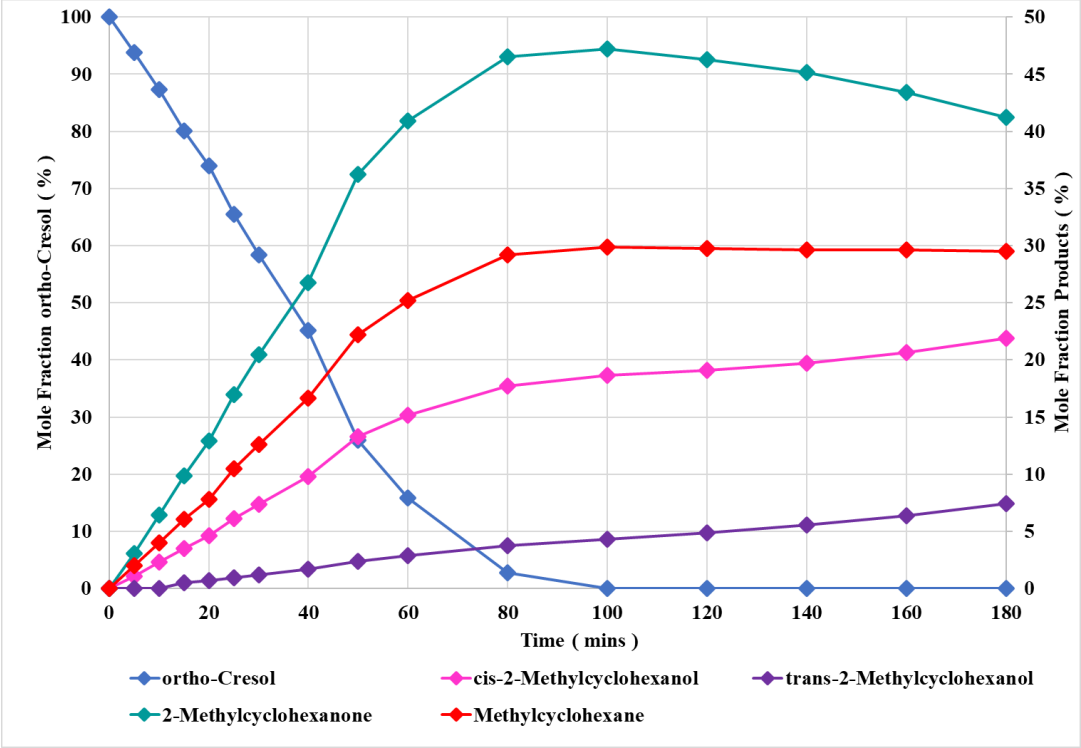

Figure 95. Reaction profile of *ortho*-cresol hydrogenation. Conditions, 343 K, 10 mmol, 3 barg.

From Figures 92-95 above, it is clear that reaction rate increased with temperature with a measured rate constant of 1.1 x$10^{-2}$$min^{-1}$ at 303 K compared with 2.5 x$10^{-3}$$min^{-1}$ at 343 K; an almost doubling of reaction rate. At 303 K the main product, *cis*-2-methylcyclohexanol, was formed at ~ 32% by the end of reaction compared with ~ 26 % at 343 K, showing a

decrease in the formation of this product over the temperature range. The HDO product methylcyclohexane, however, showed an increase with temperature from ~ 27 % to ~ 34 % at the end of reaction over the 40 K measured range. The product distribution of the hydrogenated (*cis*+*trans*-2-methylcyclohexanol and 2-methylcyclohexanone) and hydrodeoxygenated (methylcyclohexane) products at ~ 90 % conversion is shown below in Figure 96:

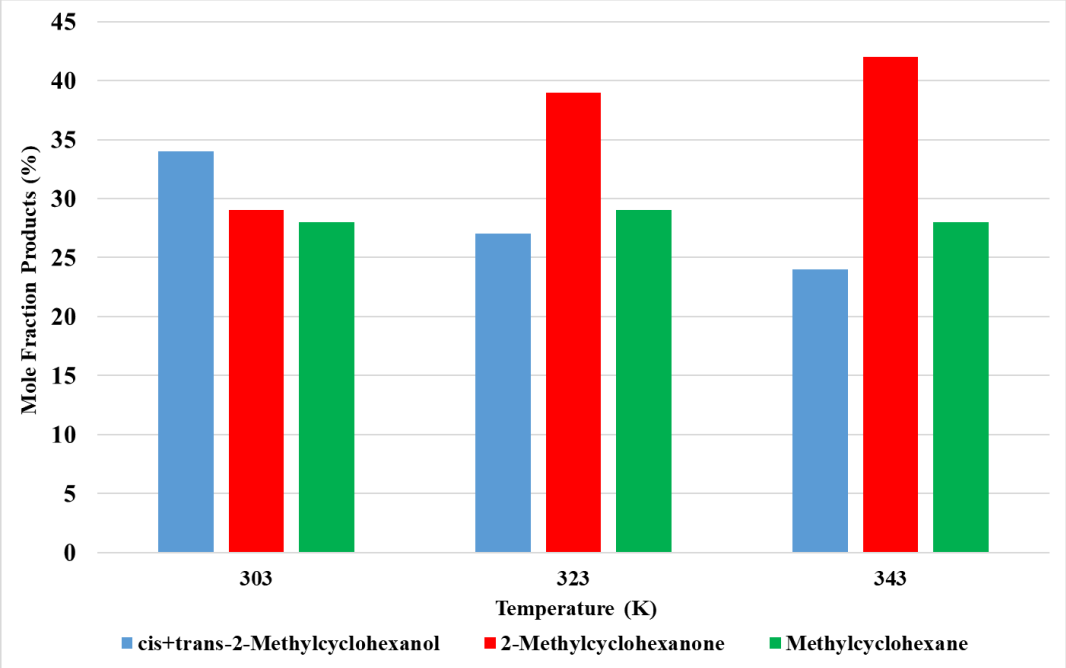

Figure 96. Product distribution at ~ 90 % conversion for *ortho*-cresol hydrogenation.

It can be seen from Figure 96 that as temperature was increased formation of the intermediate hydrogenated product, 2-methylcyclohexanone, increased whilst that of the *cis*+*trans*-2-methylcyclohexanol decreased. The HDO product, methylcyclohexane, remained constant over the temperature range. The relationship between temperature and conversion of *ortho*-cresol is shown below in Figure 97:

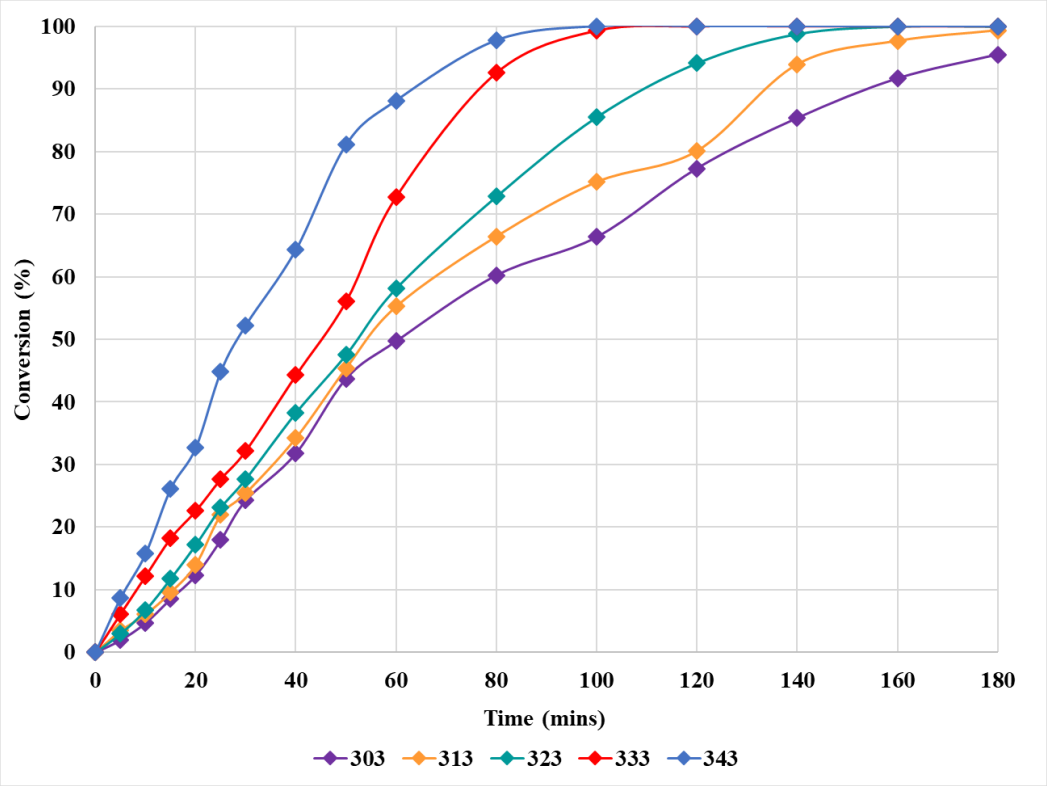

Figure 97. Temperature effect on *ortho*-cresol conversion.

It can be seen from Figure 97 that an increase in temperature resulted in an increase in *ortho*-cresol conversion, with full conversion by ~ 100 minutes at 343 K against ~ 95 % at the end of reaction for 303 K.

For each temperature reaction the rate constant was calculated and an example of this, at 333 K, is shown below in Figure 98:

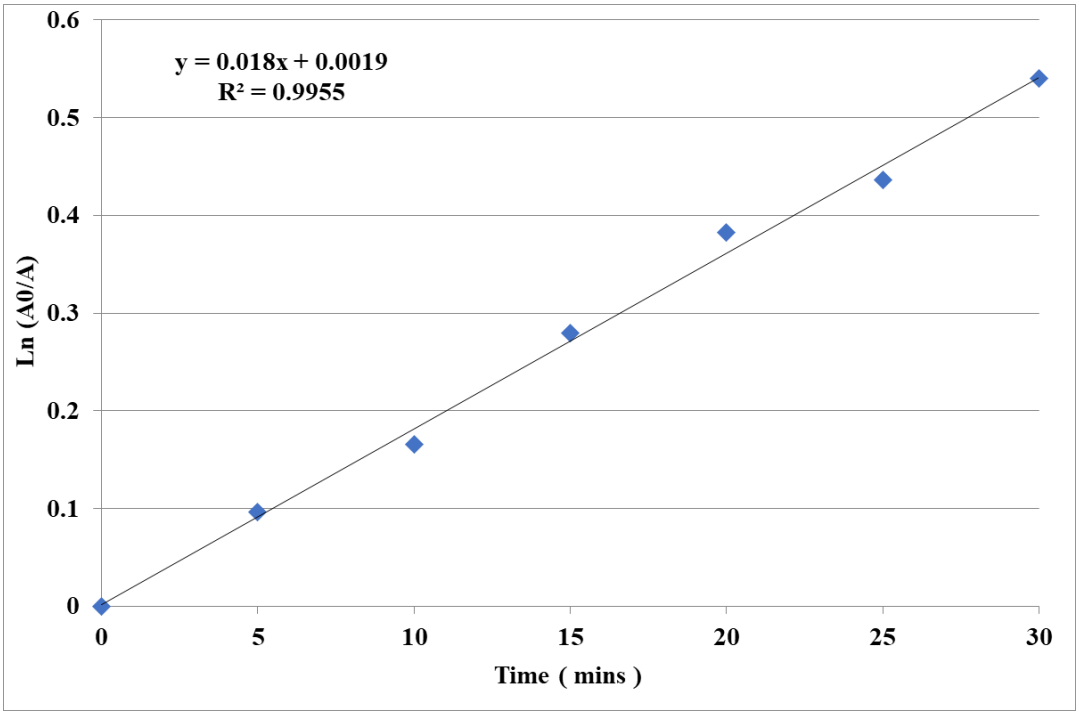

Figure 98. Rate constant graph for *ortho*-cresol hydrogenation at 333 K.

From the integrated form of the Arrhenius equation shown in Equation 7 of the Experimental Section, ln k was plotted against ($\frac{1}{T}$) using the values in Table 16 below:

Table 16. Summary of data for activation energy.

Temperature (K)	k (x10^{-3}min^{-1})	1/T (x- axis)	Ln k (y-axis)
313	10.0	0.00319	-4.6051
323	11.1	0.00309	-4.5098
333	18.0	0.00300	-4.0398
343	24.6	0.00291	-3.6888

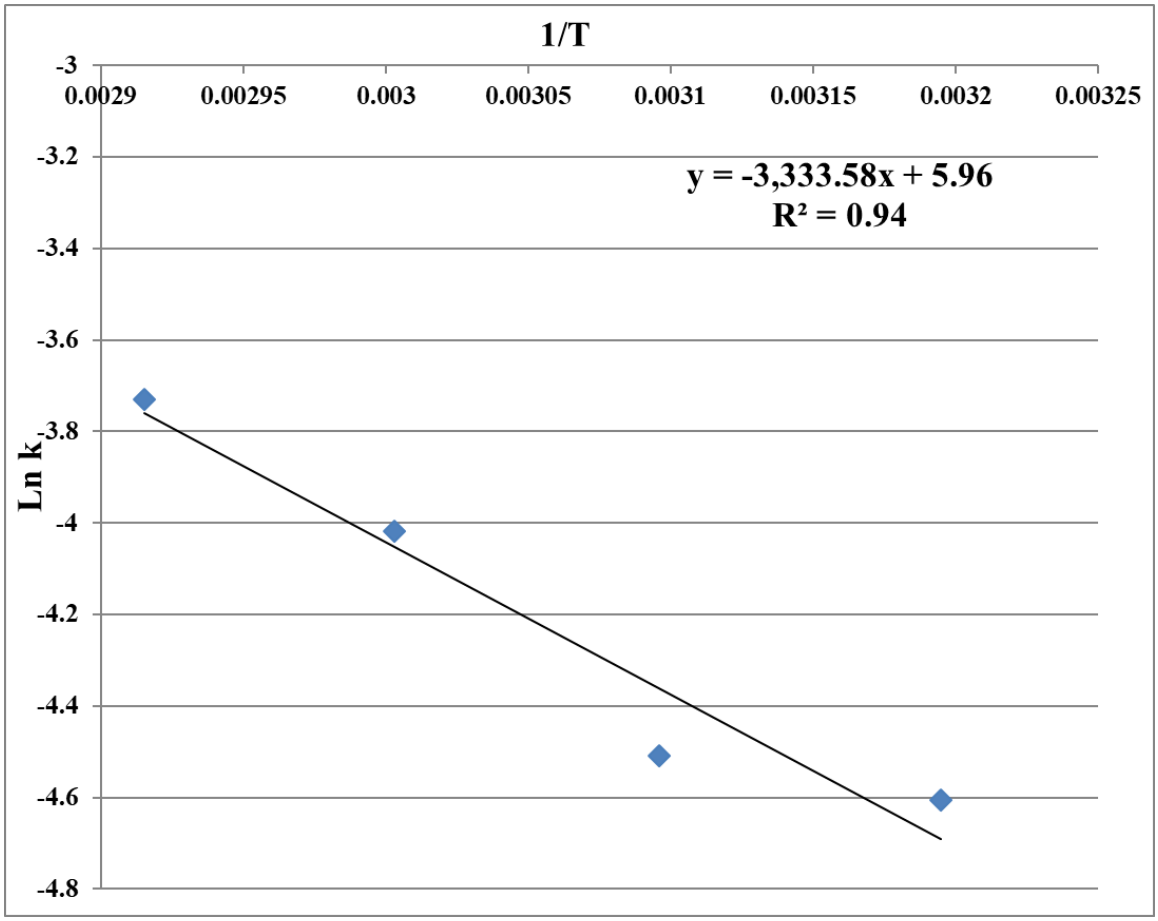

Figure 99. Activation energy plot for *ortho*-cresol hydrogenation.

Therefore, the gradient of ln k against 1/T equals $-\frac{Ea}{RT}$ and can be expressed for Ea as:

- Ea= -mR
- -(-3333.58*8.314)/1000
- = 27.7 kJmol^{-1}

From this, an overall activation energy for *ortho*-cresol hydrogenation of 27.7 kJmol^{-1} was measured.

7.2.2.2 *meta*-Cresol Temperature Variations

In this set of reactions, *meta*-cresol was hydrogenated at 10 K increments from 303 to 343 K, with 323 K taken as the standard reaction. Hydrogen pressure (3 barg) and reactant concentration (10 mmol) were kept constant to understand the effect temperature had on *meta*-cresol hydrogenation. The graphs of these are shown below in increasing order of temperature:

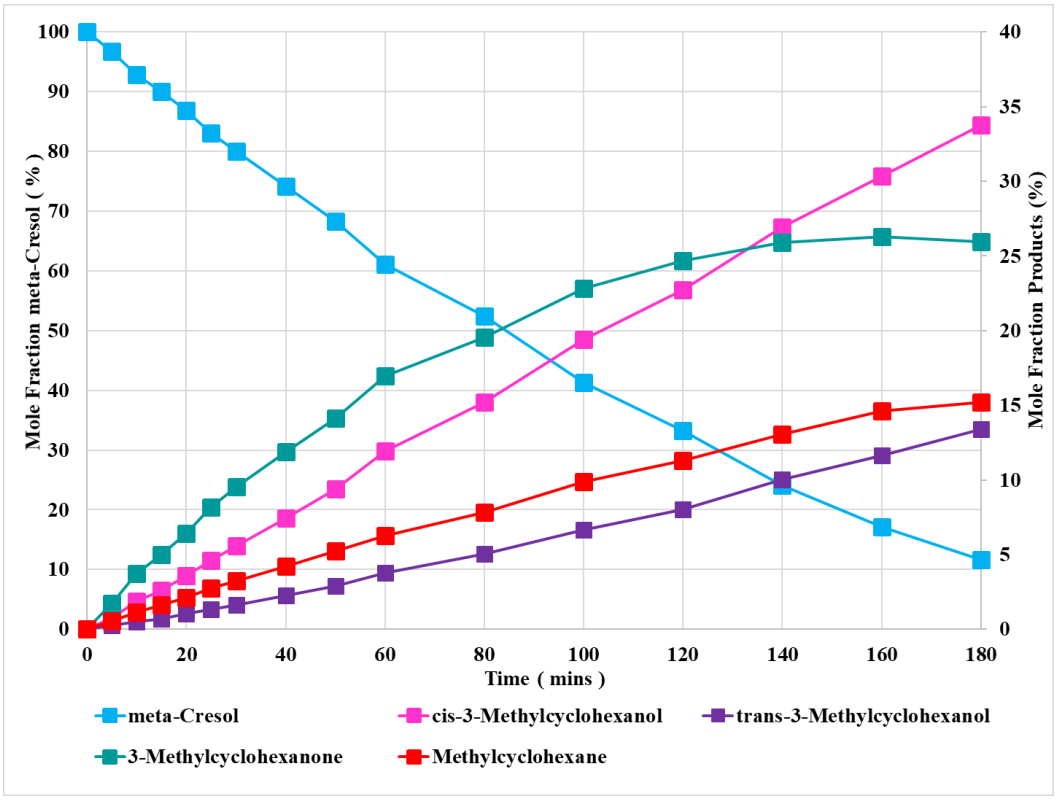

Figure 100. Reaction profile of *meta*-cresol hydrogenation. Conditions, 303 K, 10 mmol, 3 barg.

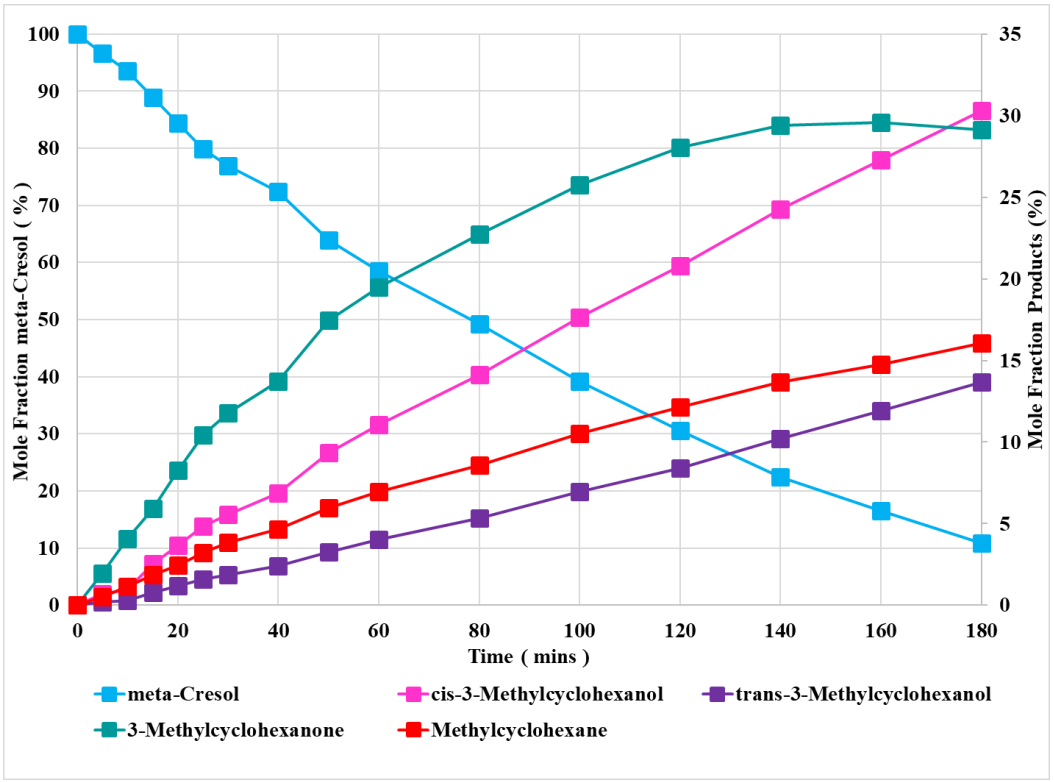

Figure 101. Reaction profile of *meta*-cresol hydrogenation. Conditions, 313 K, 10 mmol, 3 barg.

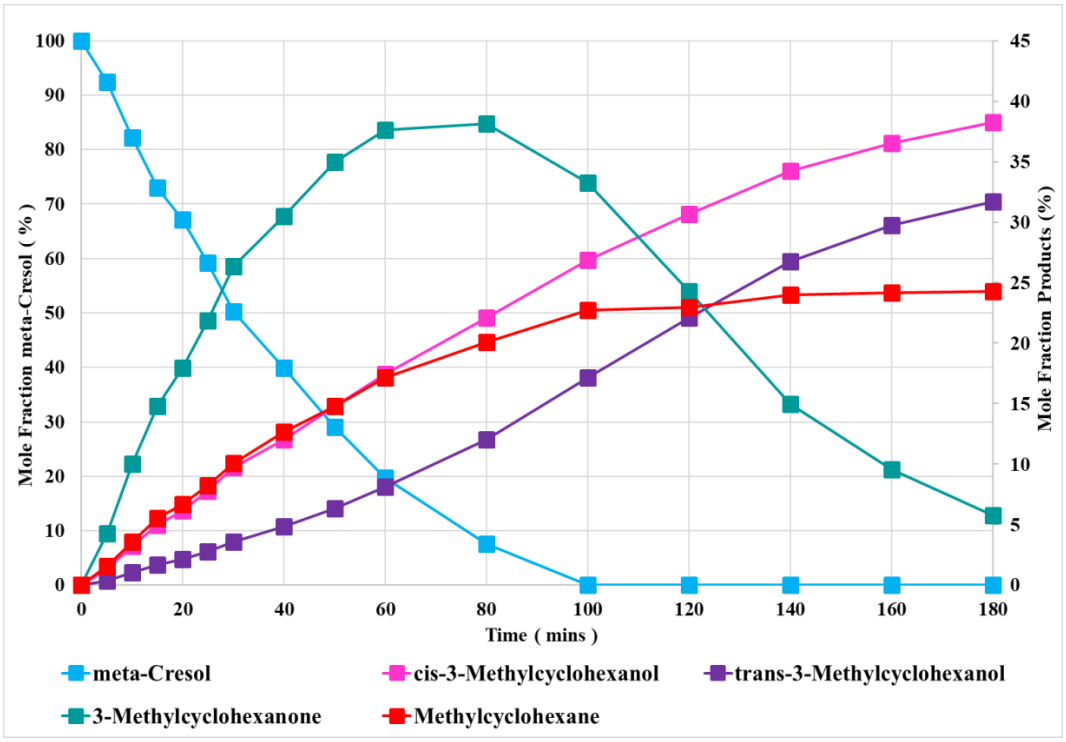

Figure 102. Reaction profile of *meta*-cresol hydrogenation. Conditions, 333 K, 10 mmol, 3 barg.

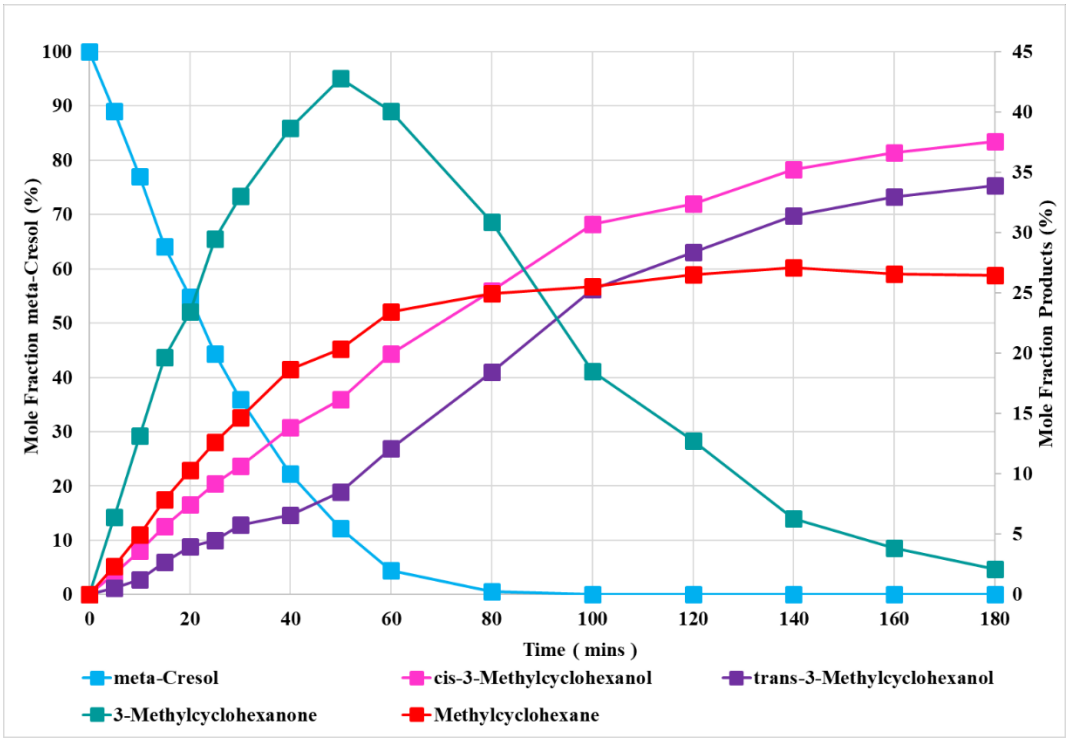

Figure 103. Reaction profile of *meta*-cresol hydrogenation. Conditions, 343 K, 10 mmol, 3 barg.

From Figures 100-103 above, it can be clearly seen that reaction rate increased with temperature. The rate constant at 303 K was 11.6 $x10^{-3}min^{-1}$ compared with 41.2 $x10^{-3}min^{-1}$ at 343 K; an almost fourfold increase in rate over a 40 K elevation in temperature. The

major hydrogenated product, *cis*-3-methylcyclohexanol, remained broadly constant at reaction end ~ 35 %, over the temperature range measured; however, *trans*-3-methylcyclohexanol increased from ~ 15 % to ~ 35 % over the same range. A decrease at end of reaction from ~ 25 % to < 5 % was observed for the initially formed 3-methylcyclohexanone between 303 K and 343 K. The HDO product, methylcyclohexane, showed an end of reaction increase from ~ 15 % to ~ 25 %. The product distribution of the hydrogenated (*cis*+*trans*-3-methylcyclohexanol and 3-methylcyclohexanone) and hydrodeoxygenated (methylcyclohexane) products at ~ 90 % conversion is shown below in Figure 104:

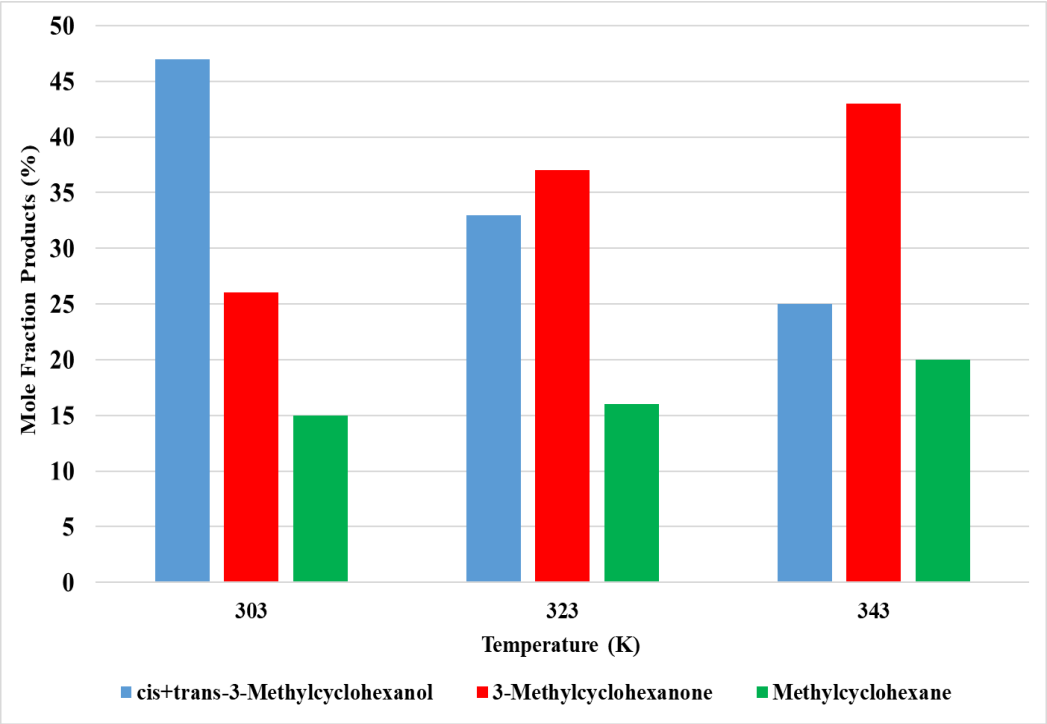

Figure 104. Product distribution at ~ 90 % conversion for *meta*-cresol hydrogenation.

It can be seen from Figure 104 that, as observed with *meta*-cresol, when temperature was increased formation of the hydrogenated product, 3-methylcyclohexanone, increased whilst that of the *cis*+*trans*-3-methylcyclohexanol decreased. The HDO product, methylcyclohexane, increased over the temperature range. The relationship between temperature and conversion of *meta*-cresol is shown below in Figure 105:

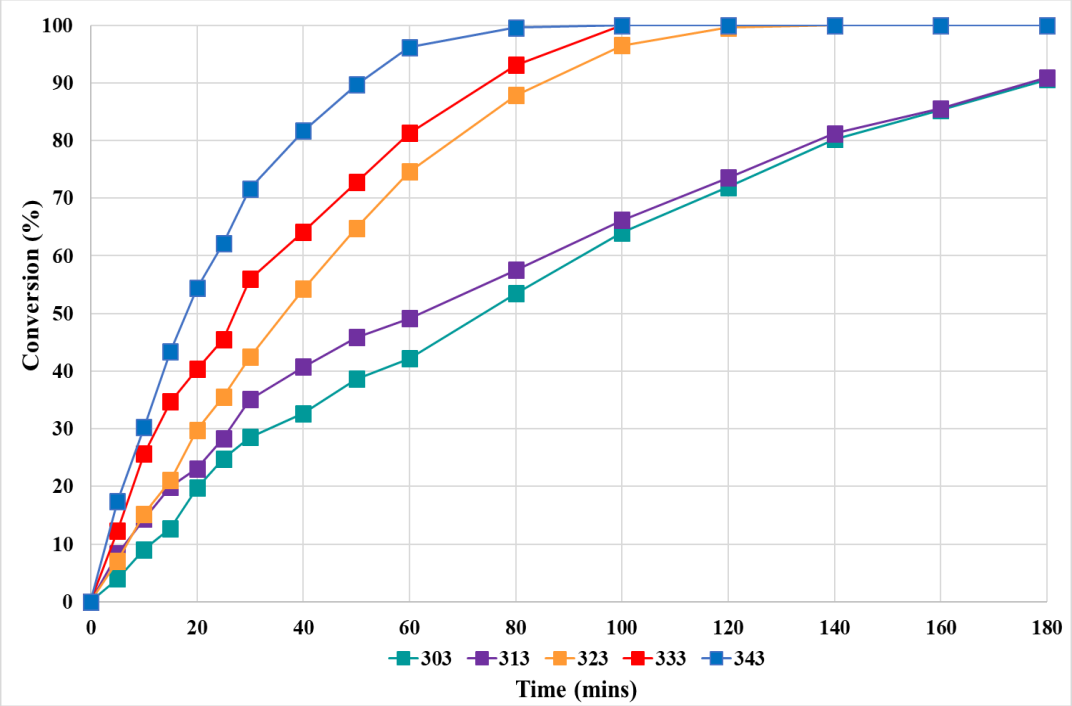

Figure 105. Temperature effect on *meta*-cresol conversion.

It can be seen from Figure 105 that an increase in temperature results in a concomitant increase on *meta*-cresol conversion, from ~ 90 % at reaction end for 303 K to full conversion by ~ 80 minutes at 343 K.

For each temperature reaction, the rate constant was calculated and an example of this, at 333 K, is shown below in Figure 106:

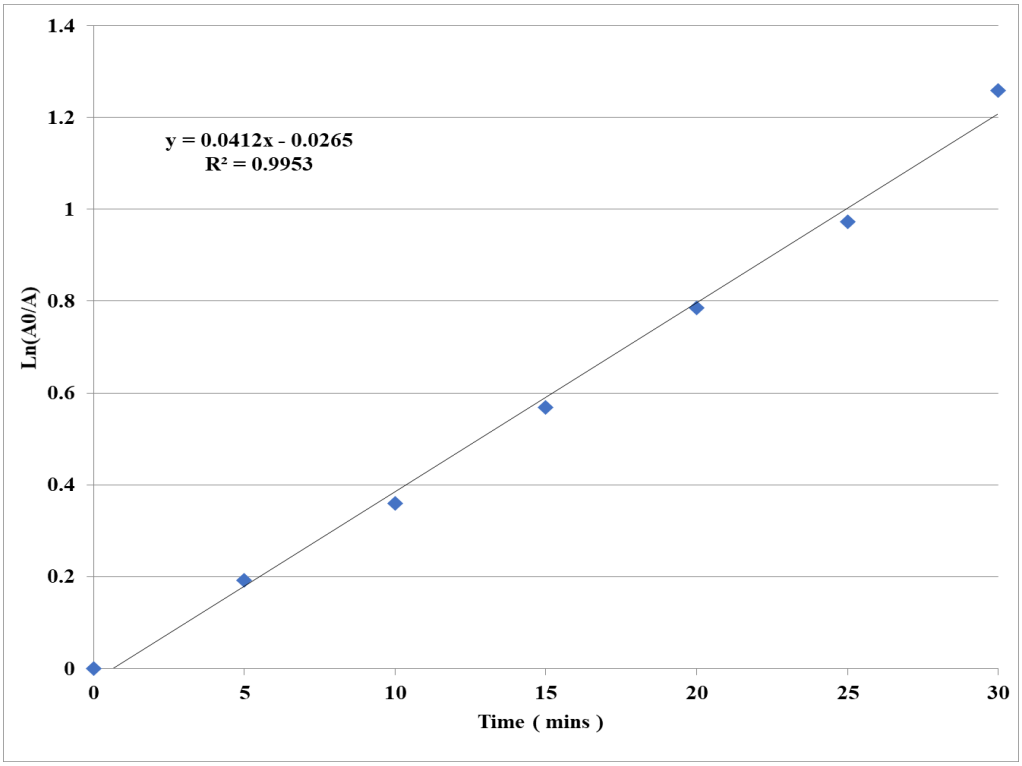

Figure 106. Rate constant graph for *meta*-cresol hydrogenation at 343 K.

From the integrated form of the Arrhenius equation shown in Equation 7 of the Experimental Section, ln k was plotted against ($\frac{1}{T}$) using the values in Table 17 below:

Table 17. Summary of data for activation energy.

Temperature (K)	k ($x10^{-3}min^{-1}$)	1/T (x- axis)	Ln k (y-axis)
313	12.7	0.00319	-4.36615
323	18.4	0.00309	-3.99540
333	26.0	0.00300	-3.64965
343	41.0	0.00291	-3.19418

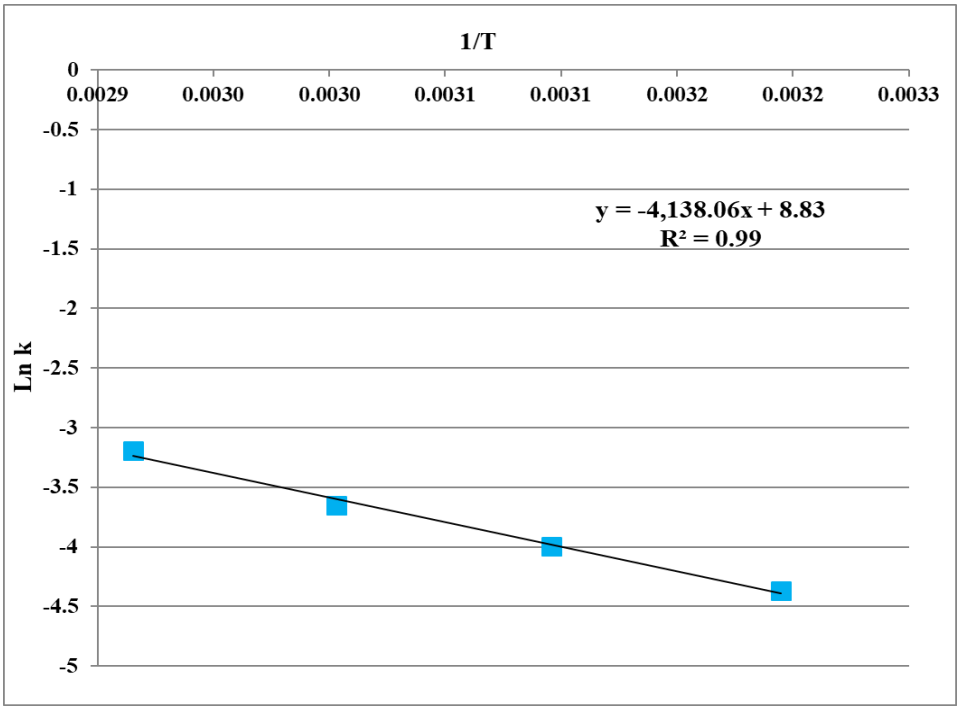

Figure 107. Activation energy plot for *meta*-cresol hydrogenation.

Therefore, the gradient of ln k against 1/T equals $-\frac{Ea}{RT}$ and can be expressed for Ea as:

- Ea= -mR
- -(-4138*8.314)/1000
- = 34.4 kJmol^{-1}

From this, an overall activation energy for *meta*-cresol hydrogenation of 34.4 kJmol^{-1} was measured.

7.2.2.3 *para*-Cresol Temperature Variations

In this set of reactions, *para*-cresol was hydrogenated at 10 K increments from 303 to 343 K, with 323 K taken as the standard reaction. Hydrogen pressure (3 barg) and reactant concentration (10 mmol) were kept constant to understand the effect temperature had on *para*-cresol hydrogenation. The graphs of these are shown below in increasing order of temperature:

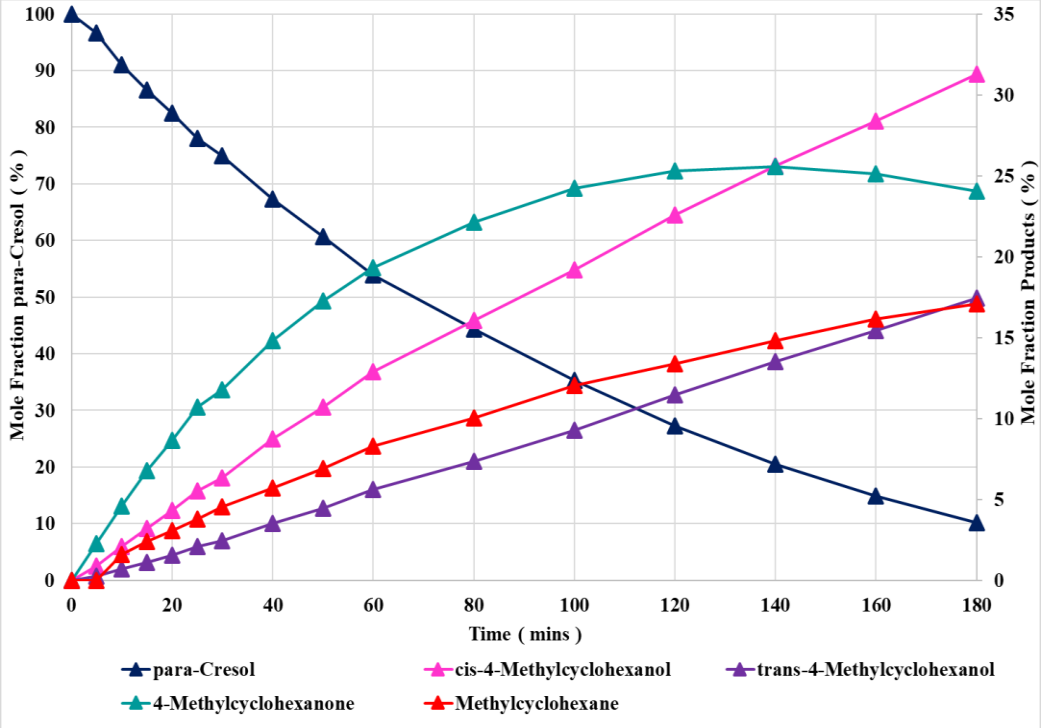

Figure 108. Reaction profile of *para*-cresol hydrogenation. Conditions, 303 K, 10 mmol, 3 barg.

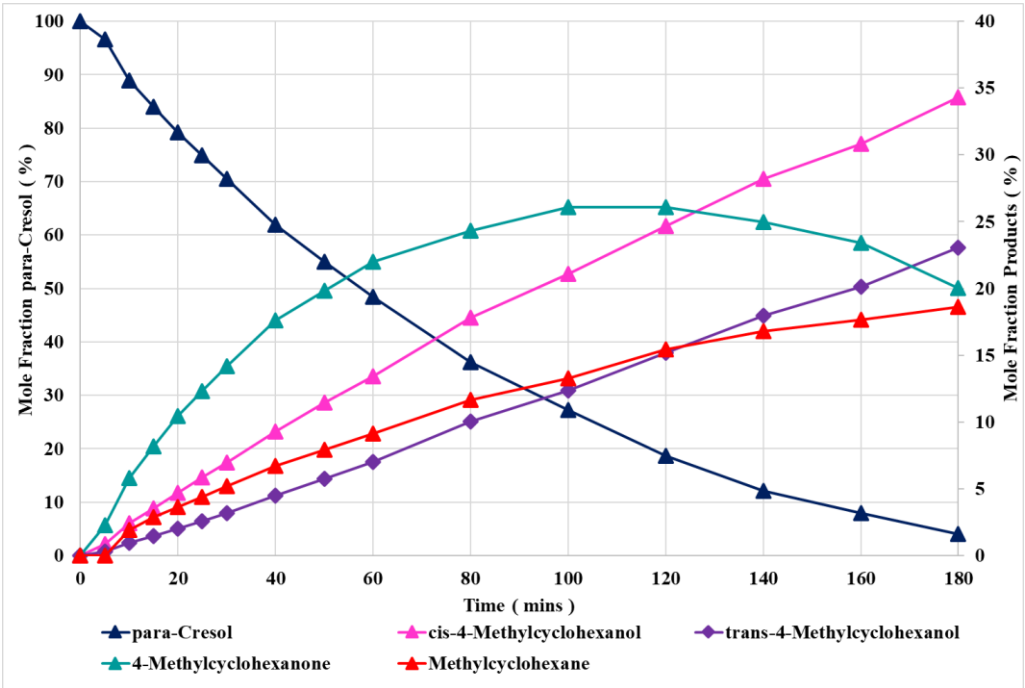

Figure 109. Reaction profile of *para*-cresol hydrogenation. Conditions, 313 K, 10 mmol, 3 barg.

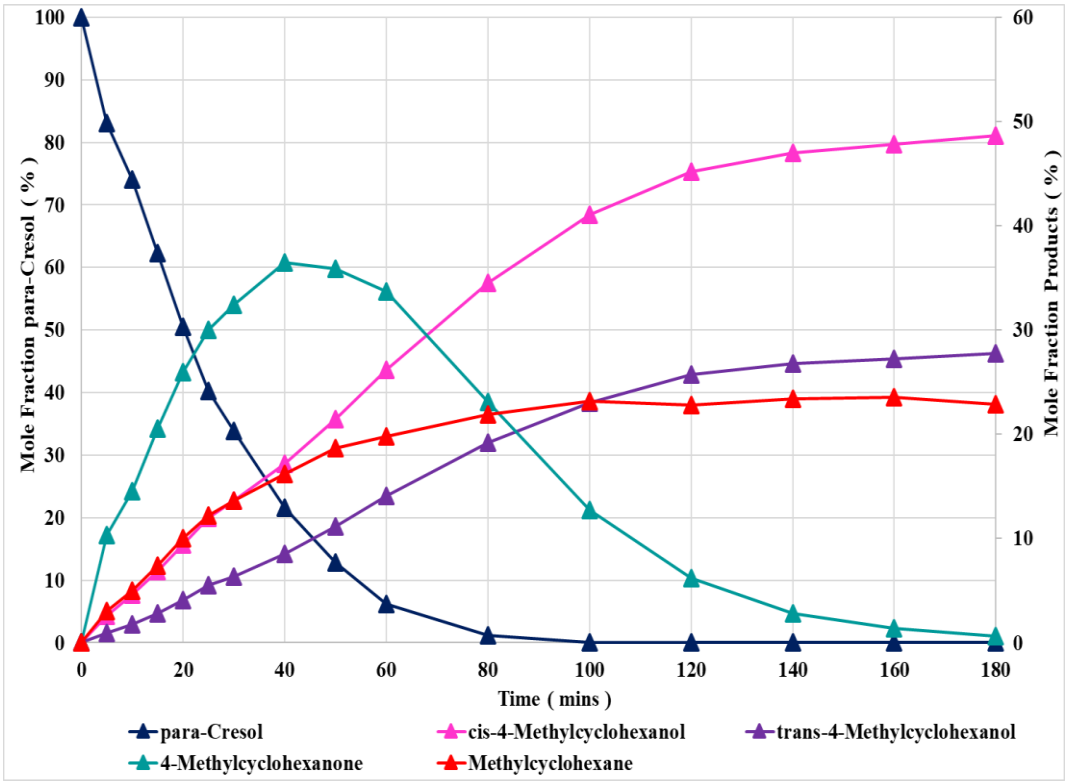

Figure 110. Reaction profile of *para*-cresol hydrogenation. Conditions, 333 K, 10 mmol, 3 barg.

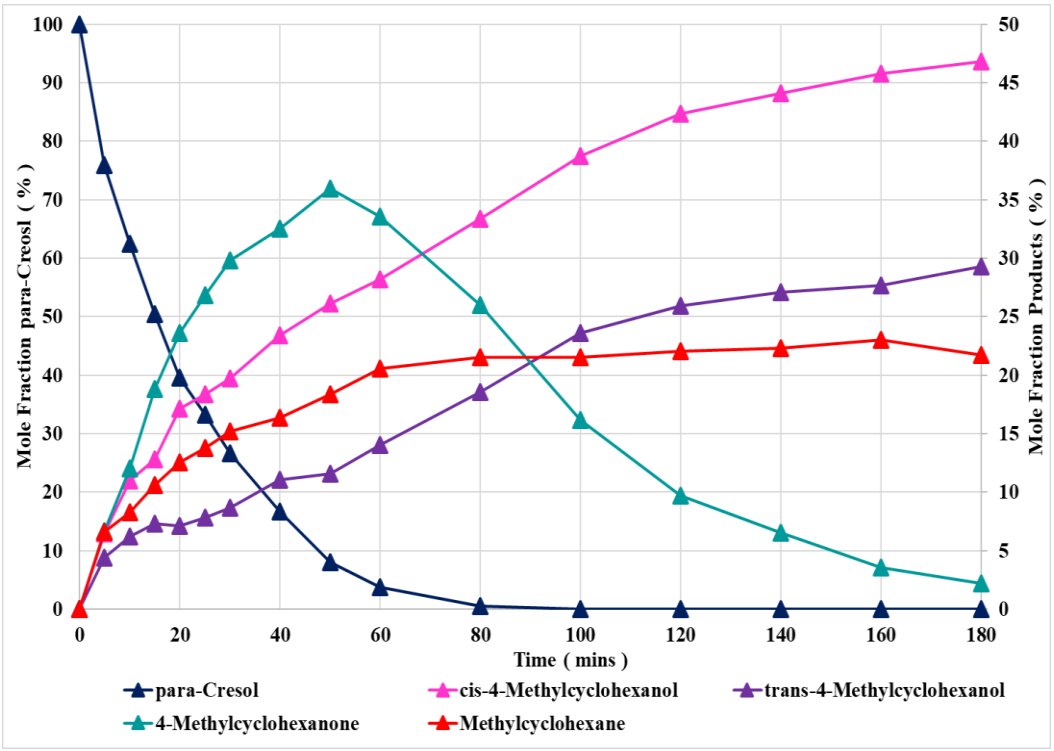

Figure 111. Reaction profile of *para*-cresol hydrogenation. Conditions, 343 K, 10 mmol, 3 barg.

From Figures 108-111 above, as observed with both the *ortho* and *meta* isomer an increase in temperature resulted in an increase in the rate of reaction. The measured rate constant

almost quadrupled from 8.6 x$10^{-3}$$min^{-1}$ at 303 K to 40.7 x$10^{-3}$$min^{-1}$ at 343 K. Over the same temperature range, both the major final hydrogenated products, *cis*-4-methylcyclohexanol and *trans*-4-methylcyclohexanol, showed an end of reaction increase, from ~ 30 % to > 45 % and ~ 17 % to ~ 30 % respectively. A less pronounced increase of ~ 17 % to ~ 20 % at end of reaction was recorded for the HDO product methylcyclohexane. The product distribution of the hydrogenated (*cis*+*trans*-4-methylcyclohexanol and 4-methylcyclohexanone) and hydrodeoxygenated (methylcyclohexane) products at ~ 90 % conversion is shown below in Figure 112:

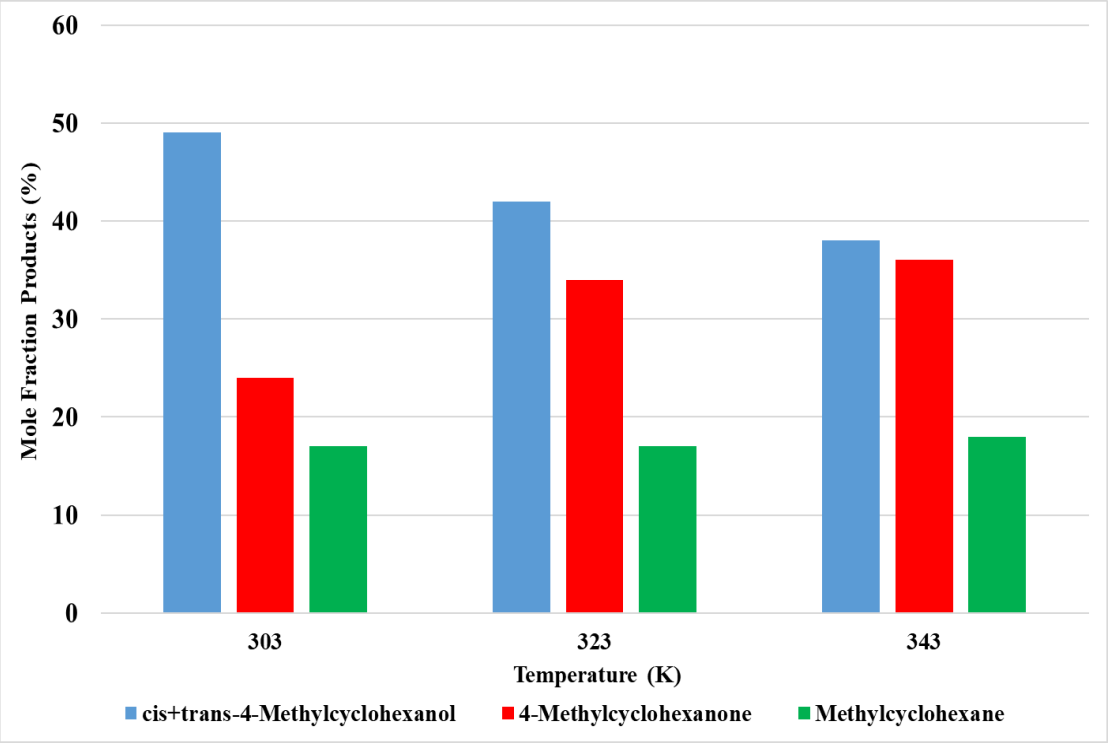

Figure 112. Product distribution at ~ 90 % conversion for *para*-cresol hydrogenation.

It can be seen from Figure 112 that as temperature was increased formation of the intermediate hydrogenated product, 4-methylcyclohexanone, increased whilst that of the *cis*+*trans*-4-methylcyclohexanol decreased; an identical trend to that observed with the *ortho* and *meta* isomers. Methylcyclohexane again showed a minor increase in production over the temperature range. The relationship between temperature and conversion of *para*-cresol is shown below in Figure 113:

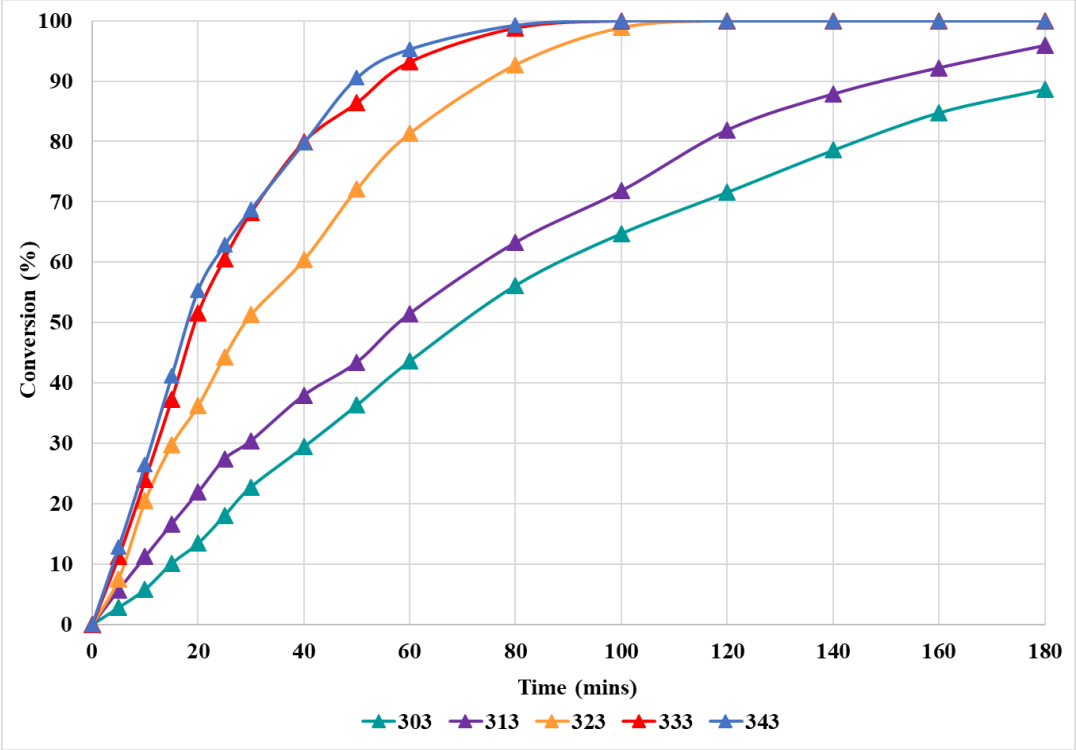

Figure 113. Temperature effect on *para*-cresol conversion.

It can be seen from Figure 113 that an increase in temperature resulted in an increase in *para*-cresol conversion, from ~ 90 % at the end of reaction at 303 K to full conversion by ~ 80 minutes at 343 K.

For each temperature reaction, the rate constant was calculated and an example of this, at 313 K, is shown below in Figure 114:

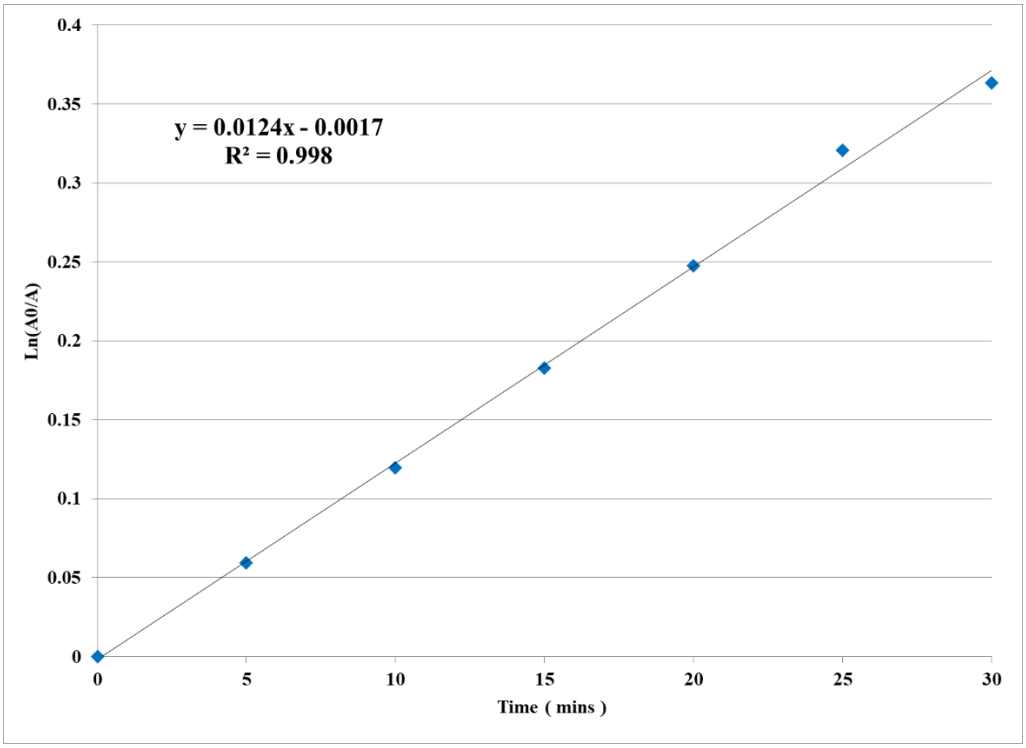

Figure 114. Rate constant graph for *para*-cresol hydrogenation at 313 K.

From the integrated form of the Arrhenius equation shown in Equation 7 of the Experimental Section, ln k was plotted against ($\frac{1}{T}$) using the values in Table 18 below:

Table 18. Summary of data for activation energy.

Temperature (K)	k (x10^{-3}min^{-1})	1/T (x- axis)	Ln k (y-axis)
303	8.6	0.00330	-4.755993076
313	12.4	0.00319	-4.390058806
323	24.2	0.00309	-3.721402646
333	39.4	0.00300	-3.233989463

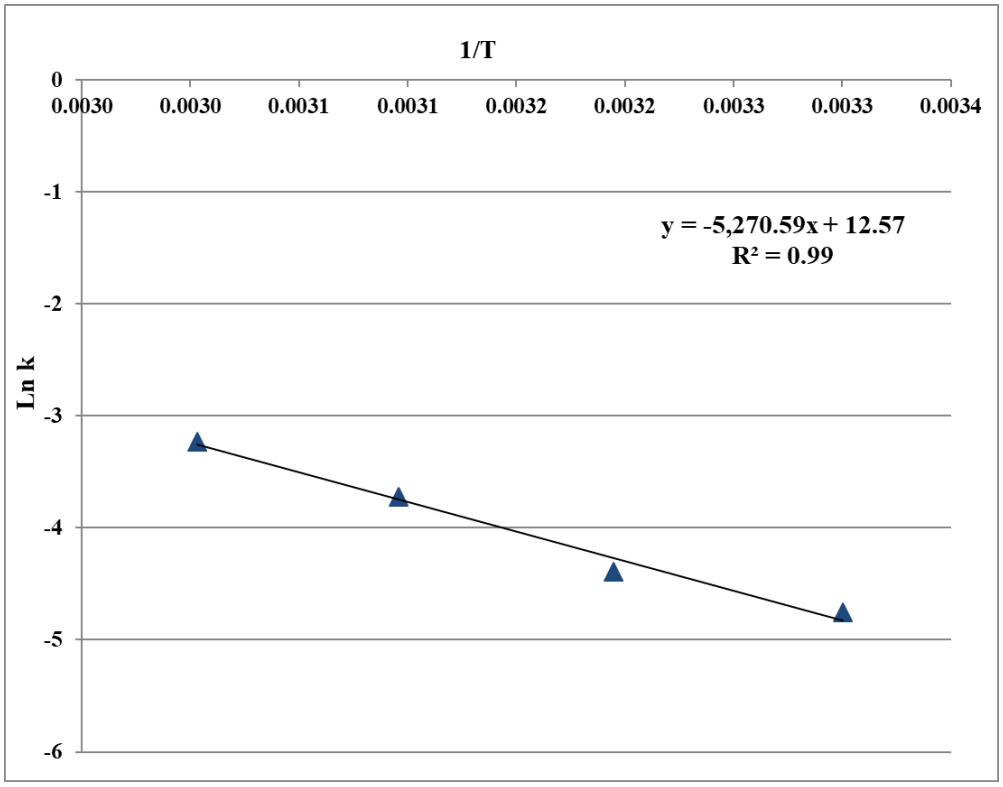

Figure 115. Activation energy plot for *para*-cresol hydrogenation.

Therefore, the gradient of ln k against 1/T equals $-\frac{Ea}{RT}$ and can be expressed for Ea as:

- Ea= -mR
- -(-5270.59*8.314)/1000
- = 37.04 kJmol^{-1}

From this, an overall activation energy for *para*-cresol hydrogenation of 37.0 kJmol^{-1} was measured.

The activation energies calculated for each isomer of the cresols are summarised below in Table 19:

Table 19. Activation energies of the cresol isomers.

Substrate	Activation Energy (kJmol^{-1})
ortho-Cresol	28.6
meta-Cresol	34.4
para-Cresol	37.0

From Table 19 it can be seen the activation energies varied for all three isomers, with *para*-cresol exhibiting the highest value of 37.0 kJmol^{-1}.

7.2.3 Concentration Variations of Cresol Isomers

Concentration of the cresol isomers was varied to investigate reaction order of the substrate.

7.2.3.1 *ortho*-Cresol Concentration Variations

In this set of reactions *ortho*-cresol was hydrogenated at 5, 10, 15 and 20 mmol to test the effect of substrate concentration on the hydrogenation activity, with 10 mmol taken as the standard reaction. The temperature (323 K) and hydrogen pressure (3 barg) were kept constant throughout. These results in order of increasing concentration are shown below:

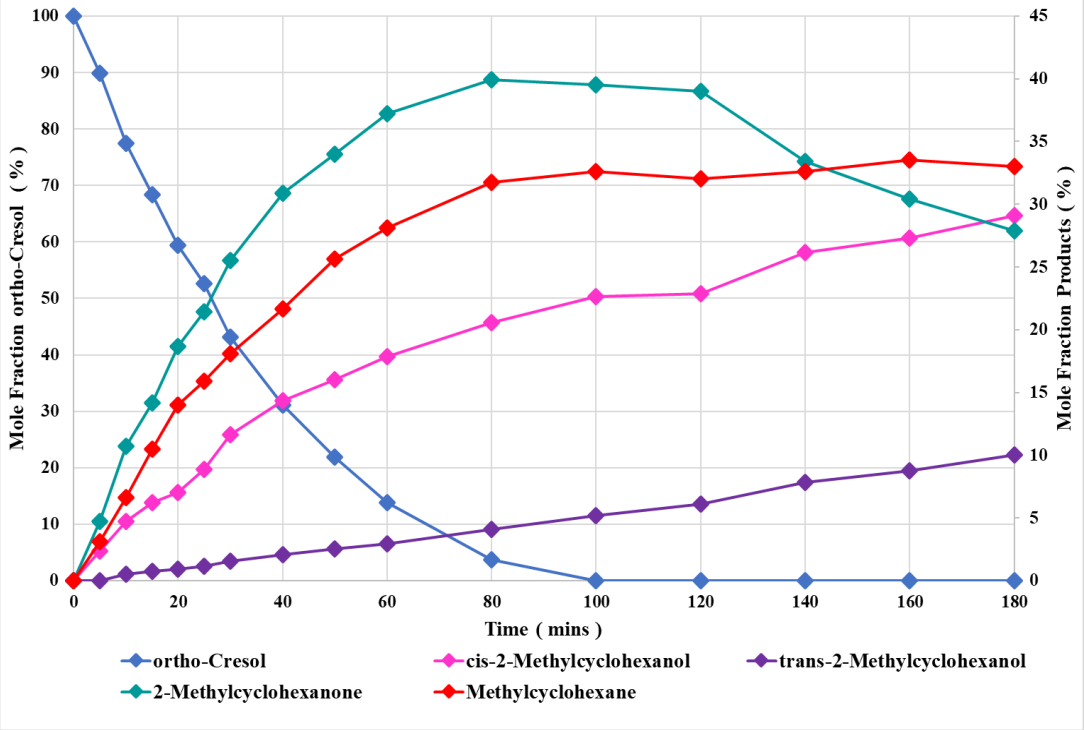

Figure 116. Reaction profile of *ortho*-cresol hydrogenation. Conditions, 323 K, 5 mmol, 3 barg.

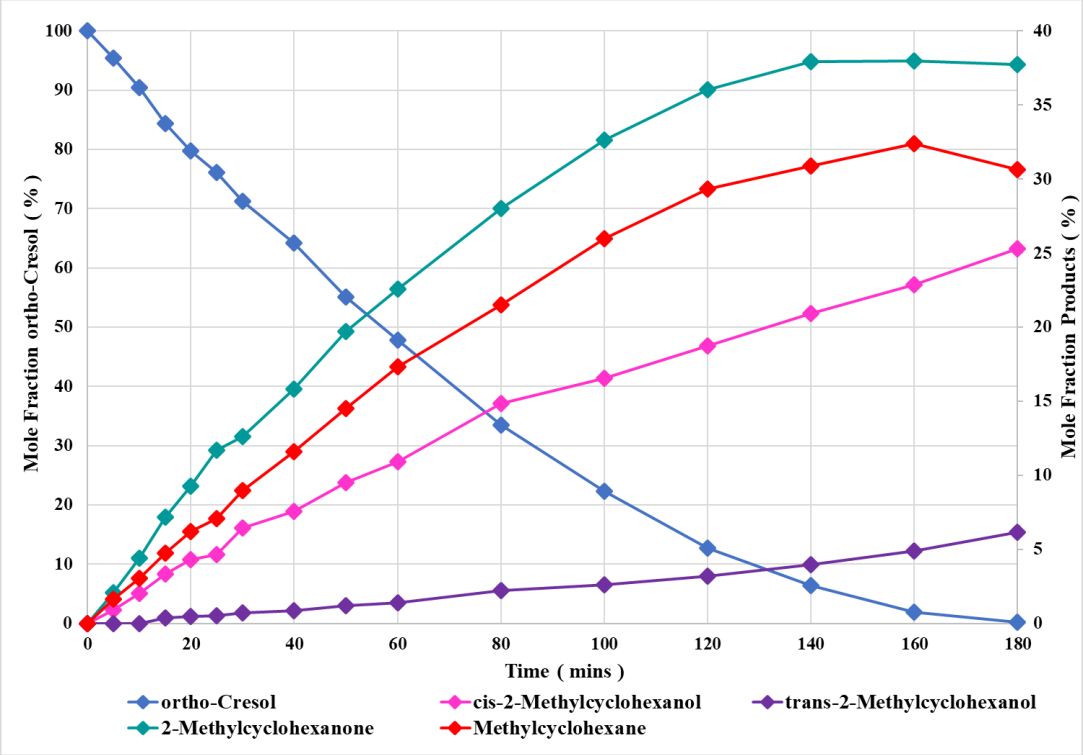

Figure 117. Reaction profile of ortho-cresol hydrogenation. Conditions, 323 K, 15 mmol, 3 barg.

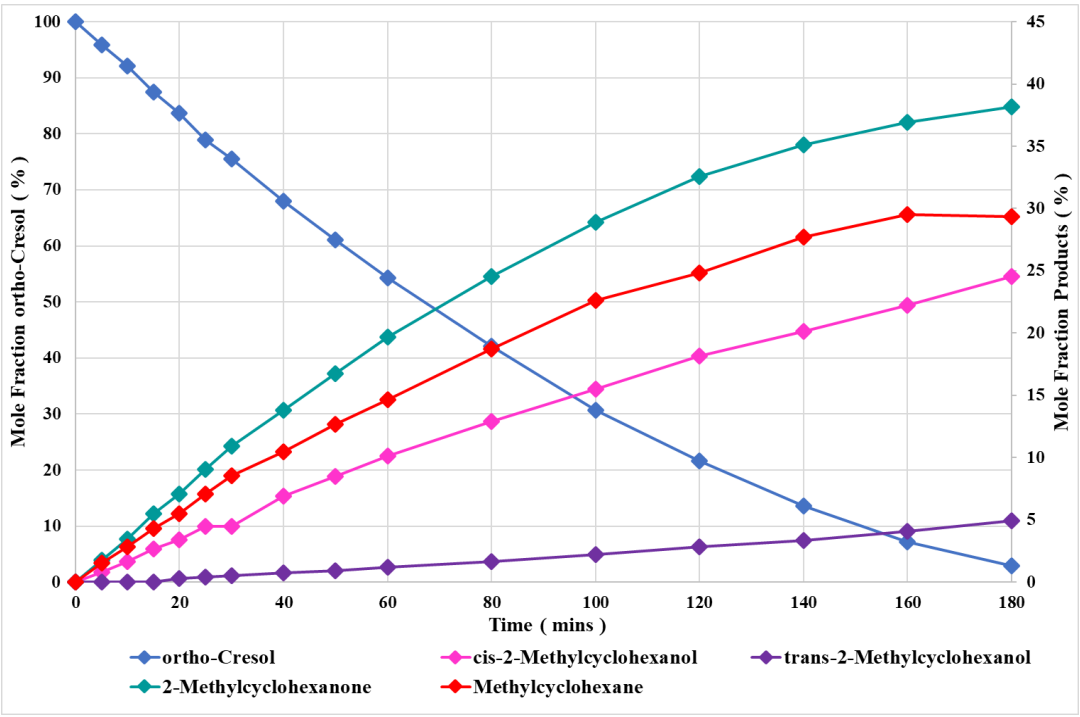

Figure 118. Reaction profile of *ortho*-cresol hydrogenation. Conditions, 323 K, 20 mmol, 3 barg.

Calculation of the initial rates of each concentration reaction shown above found the reactivity of the *ortho* isomer increased with concentration; a change in rate from 0.0093 mol $L^{-1}min^{-1}$ using 5 mmol substrate to 0.0319 mol $L^{-1}min^{-1}$ using 20 mmol. The product

distribution of the hydrogenated (*cis*+*trans*-2-methylcyclohexanol and 2-methylcyclohexanone) and hydrodeoxygenated (methylcyclohexane) products at ~ 95 % conversion is shown below in Figure 119:

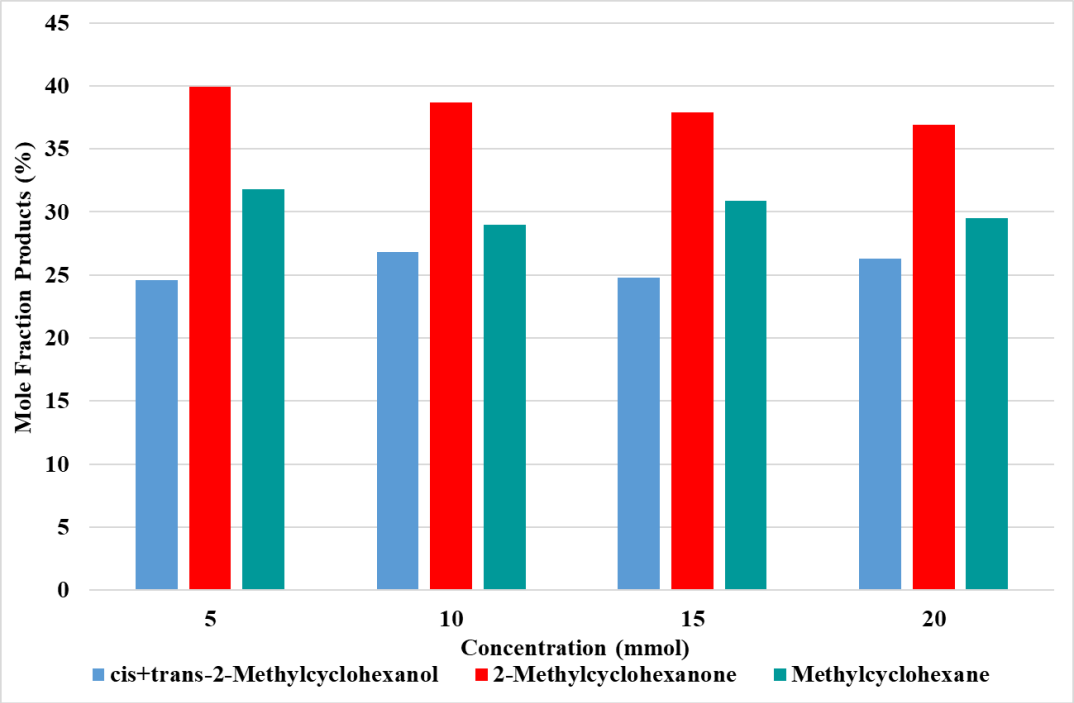

Figure 119. Product distribution for ortho-cresol concentration reactions at ~ 95 % conversion.

From Figure 119 above, the mole fraction percentages for the *cis*+*trans*-2-methylcyclohexanol and methylcyclohexane remained constant over the concentration range, whilst that of 2-methylcyclohexanone decreased.

To calculate an overall order in *ortho*-cresol Ln [A] against Ln [rate] was plotted using the data in Table 20 below:

Table 20. Data used to calculate order in substrate for the *ortho*-cresol hydrogenation.

Reactant concentration (mol L^{-1})	Rate (mol L^{-1} min^{-1})	Ln concentration	Ln rate
0.015	0.0093	-4.12	-4.67
0.030	0.0129	-3.50	-4.35
0.045	0.0169	-3.10	-4.08

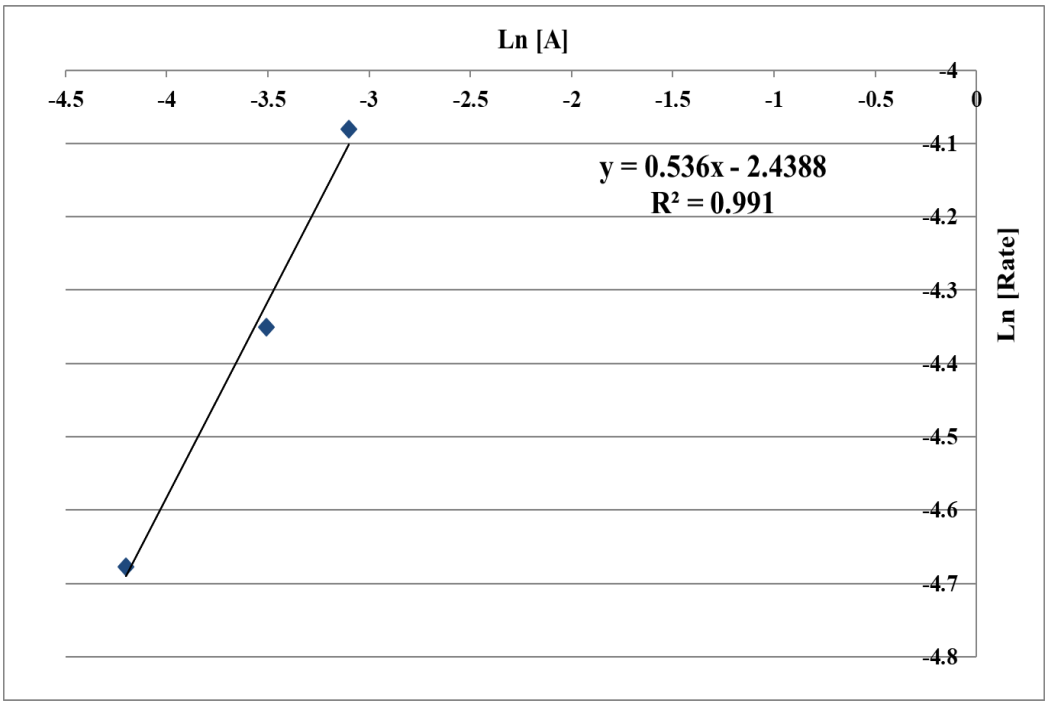

Figure 120. Substrate order plot for *ortho*-cresol hydrogenation.

Using the equations presented in Section 6.6 of the Experimental Section, the order in *ortho*-cresol was taken from the gradient of the straight line in Figure 120 above and found to be 0.54.

7.2.3.2 *meta*-Cresol Concentration Variations

In this set of reactions *meta*-cresol was hydrogenated using 10, 15 and 20 mmol to test the effect this would have on the hydrogenation reaction, with 10 mmol taken as the standard reaction. The temperature (323 K) and hydrogen pressure (3 barg) were kept constant. The graphs of these in increasing order of concentration are shown below:

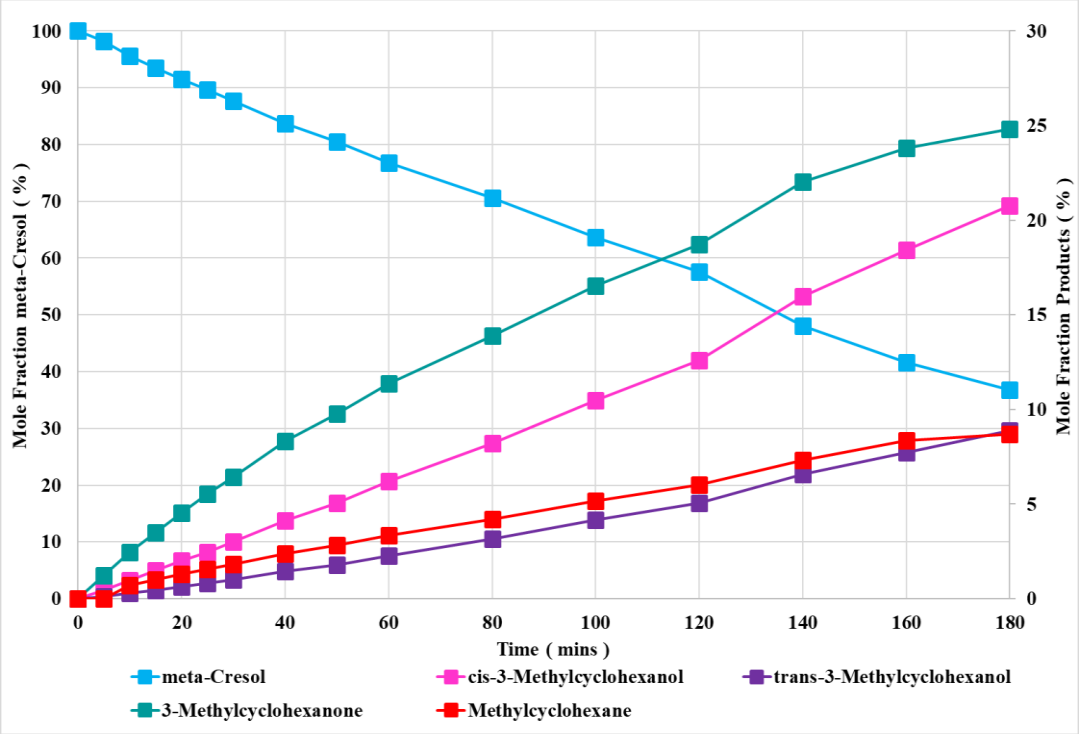

Figure 121. Reaction profile of *meta*-cresol hydrogenation. Conditions, 323 K, 15 mmol, 3 barg.

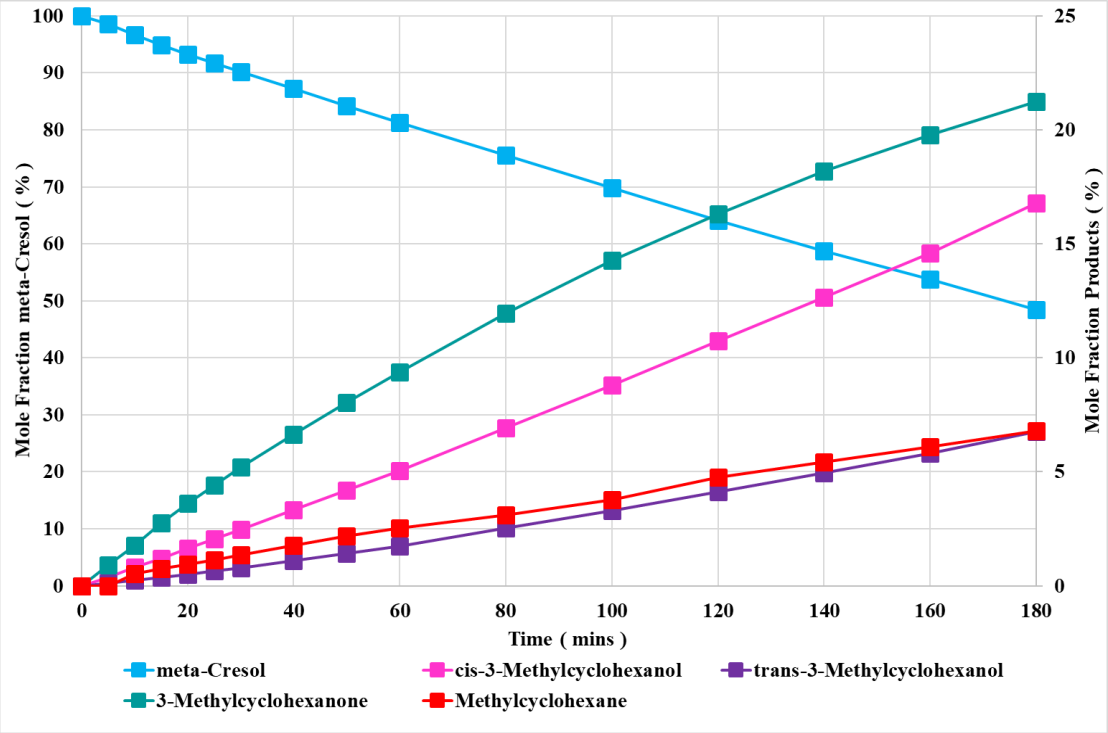

Figure 122. Reaction profile of *meta*-cresol hydrogenation. Conditions, 323 K, 20 mmol, 3 barg.

Calculation of the initial rates of each concentration reaction shown above, found a decrease in *meta*-cresol reactivity with an increase in concentration; a change in rate from 0.0241 mol $L^{-1}min^{-1}$ using 10 mmol substrate to 0.0088 mol $L^{-1}min^{-1}$ using 20 mmol. The product distribution of the hydrogenated (*cis*+*trans*-3-methylcyclohexanol and 2-

methylcyclohexanone) and hydrodeoxygenated products (methylcyclohexane) at ~ 50 % conversion is shown below in Figure 123:

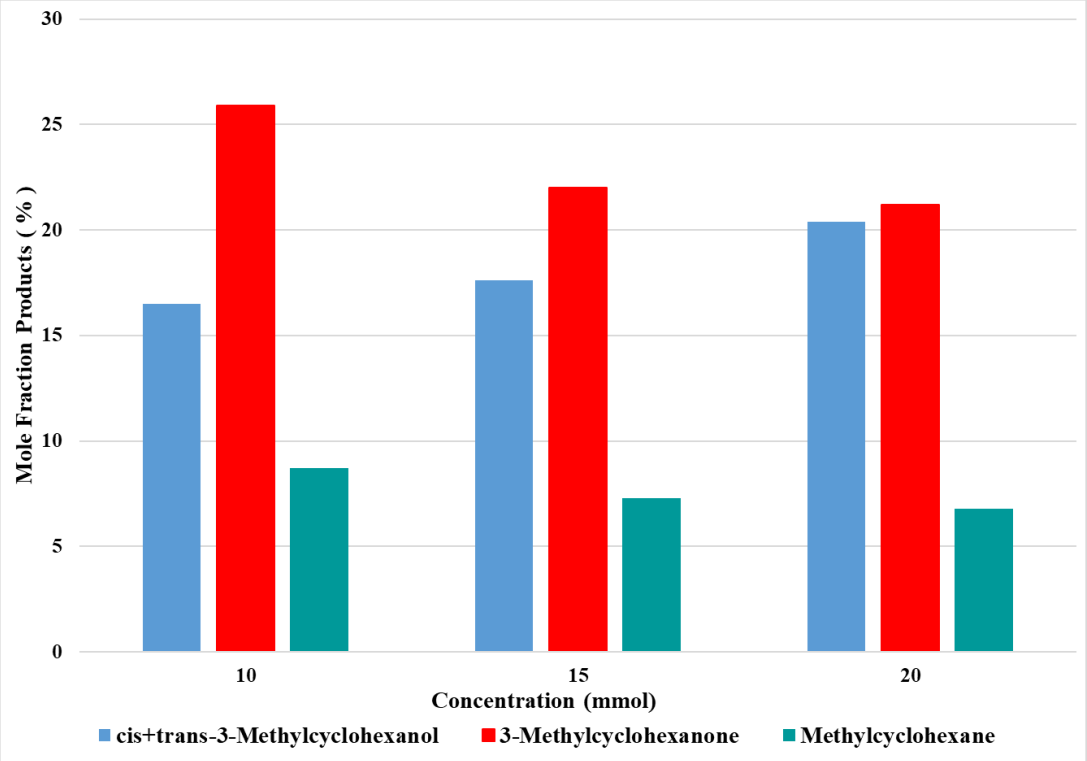

Figure 123. Product distribution for meta-cresol concentration reactions at ~ 50 % conversion.

From Figure 123 above, over the concentration range tested, the mole fraction percentages of 3-methycyclohexanone and methylcyclohexane showed a decrease whilst that of the *cis+trans*-3-methylcyclohexanol exhibited an increase, indicating a *meta*-cresol concentration effect on both rate and product distribution.

To calculate an overall order in *meta*-cresol Ln [A] against Ln [rate] was plotted using the data in Table 21 below:

Table 21. Data used to calculate the order in *meta*-cresol.

Reactant concentration (mol L^{-1})	**Rate (mol L^{-1} min^{-1})**	**Ln concentration**	**Ln rate**
0.030	0.0241	-3.50	-3.725
0.045	0.0127	-3.10	-4.366
0.060	0.0080	-2.81	-4.828

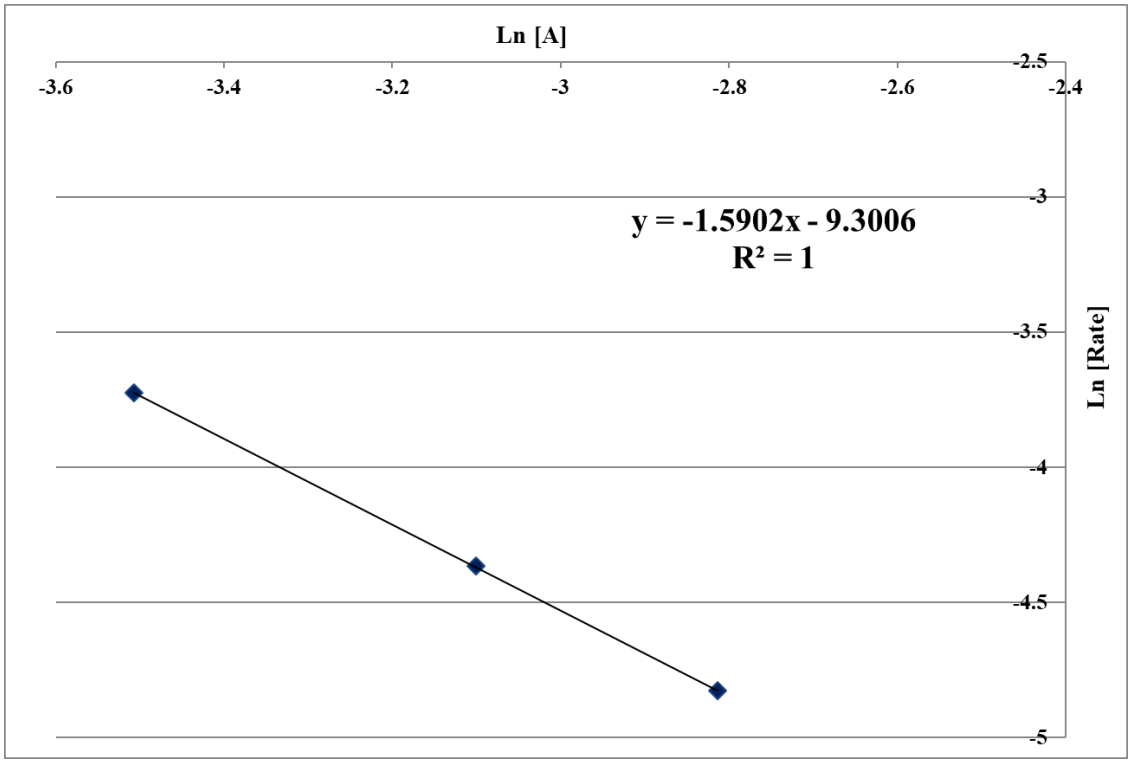

Figure 124. Substrate order plot for *meta*-cresol hydrogenation.

Using the equations presented in Section 6.6 of the Experimental Section, the order in *meta*-cresol was taken from the gradient of the straight line in Figure 124 above and found to be -1.6.

7.2.3.3 *para*-Cresol Concentration Variations

In this set of reactions *para*-cresol was hydrogenated using 5, 10, 15 and 20 mmol to test the effect this would have on the hydrogenation reaction, with 10 mmol taken as the standard reaction. The temperature (323 K) and hydrogen pressure (3 barg) were kept constant. The graphs of these in increasing order of concentration are shown below:

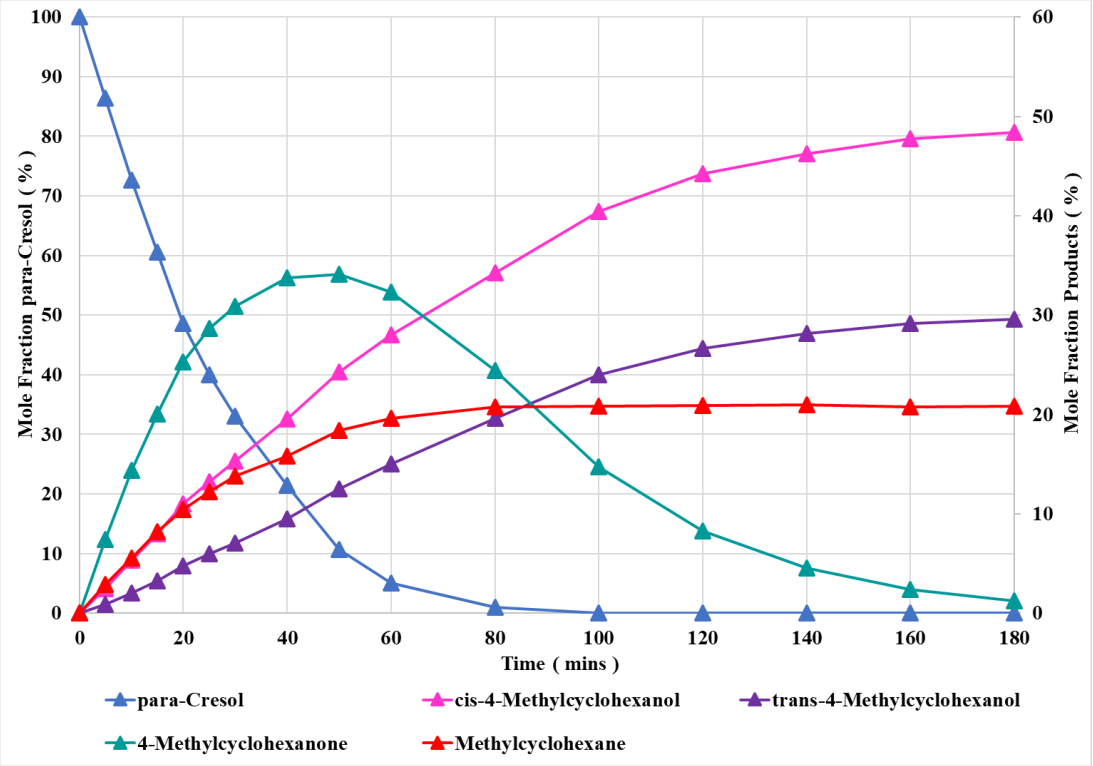

Figure 125. Reaction profile of *para*-cresol hydrogenation. Conditions, 323 K, 5 mmol, 3 barg.

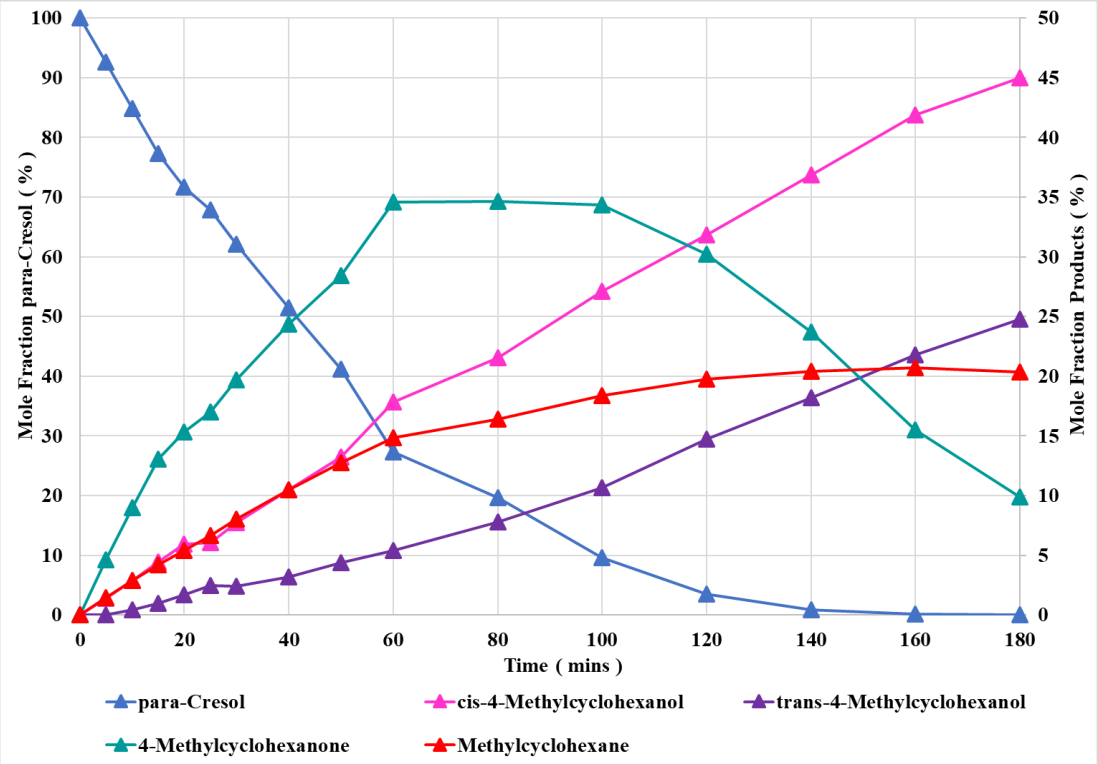

Figure 126. Reaction profile of para-cresol hydrogenation. Conditions, 323 K, 15 mmol, 3 barg.

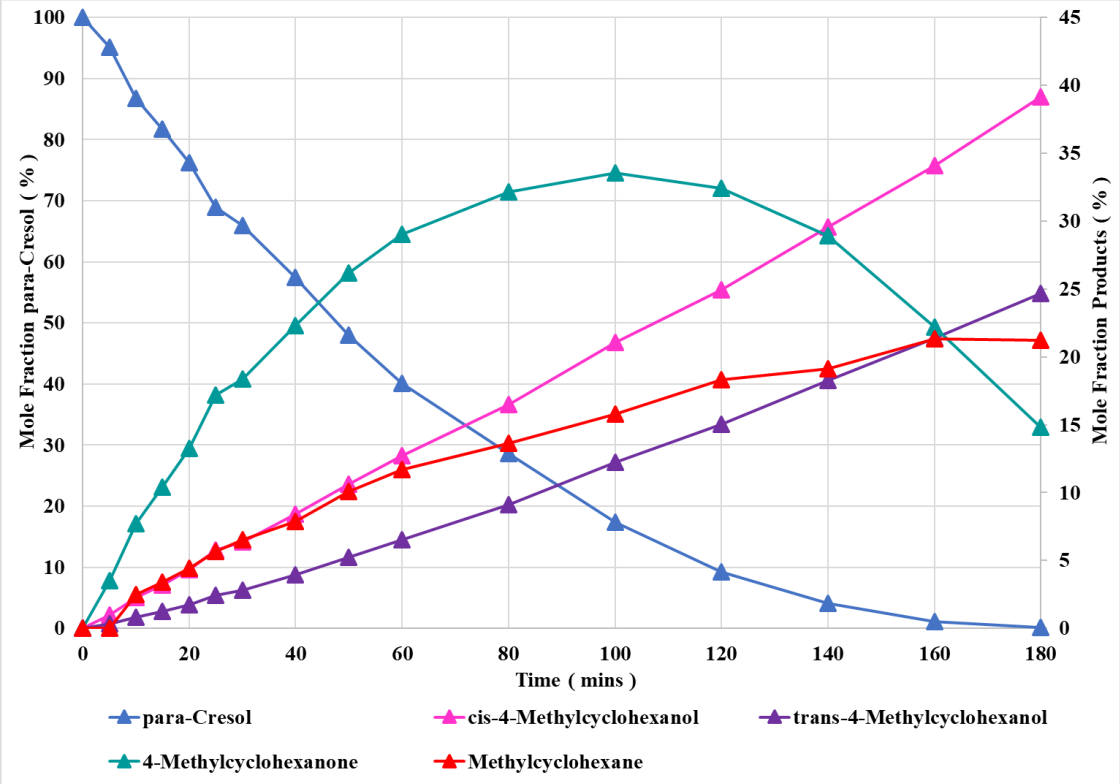

Figure 127. Reaction profile of *para*-cresol hydrogenation. Conditions, 323 K, 15 mmol, 3 barg.

Calculation of the initial rates of each concentration reaction shown above found an increase in *para*-cresol reactivity with an increase in concentration; a change in rate from 0.0205 mol $L^{-1}min^{-1}$ using 5 mmol substrate to 0.0362 mol $L^{-1}min^{-1}$ using 20 mmol. The product distribution of the hydrogenated (*cis*+*trans*-4-methylcyclohexanol and 4-methylcyclohexanone) and hydrodeoxygenated (methylcyclohexane) products at ~ 95 % conversion is shown below in Figure 128:

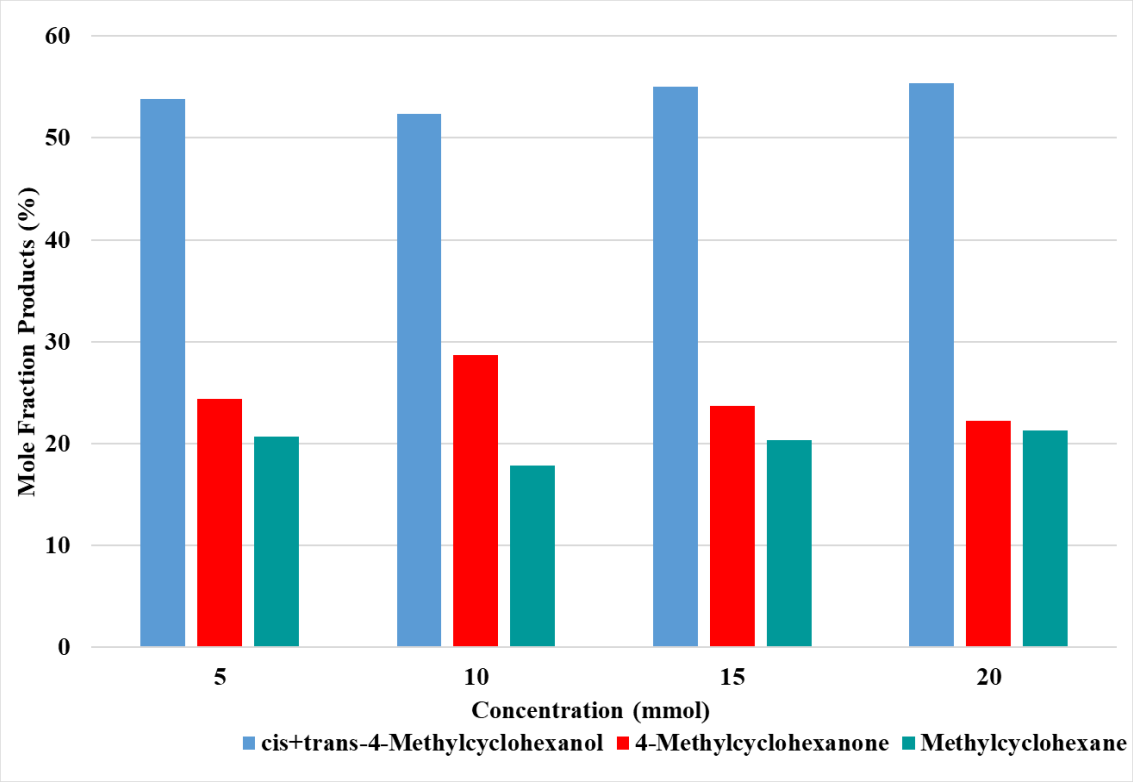

Figure 128. Product distribution for *para*-cresol concentration reactions at ~ 95 % conversion.

From Figure 128 above, the mole fraction percentages for all products remain broadly constant over the concentration range tested signifying the concentration of the *para*-cresol has an effect only on rate and not on the product distribution.

To calculate an overall order in *para*-cresol Ln [A] against Ln [rate] was plotted using the data in Table 22 below:

Table 22. Data used to calculate the order in *para*-cresol.

Reactant concentration (mol L^{-1})	**Rate (mol L^{-1} min^{-1})**	**Ln concentration**	**Ln rate**
0.015	0.0205	-4.12	-2.81
0.030	0.0250	-3.50	-3.50
0.045	0.0308	-3.10	-3.10
0.060	0.0362	-2.81	-2.81

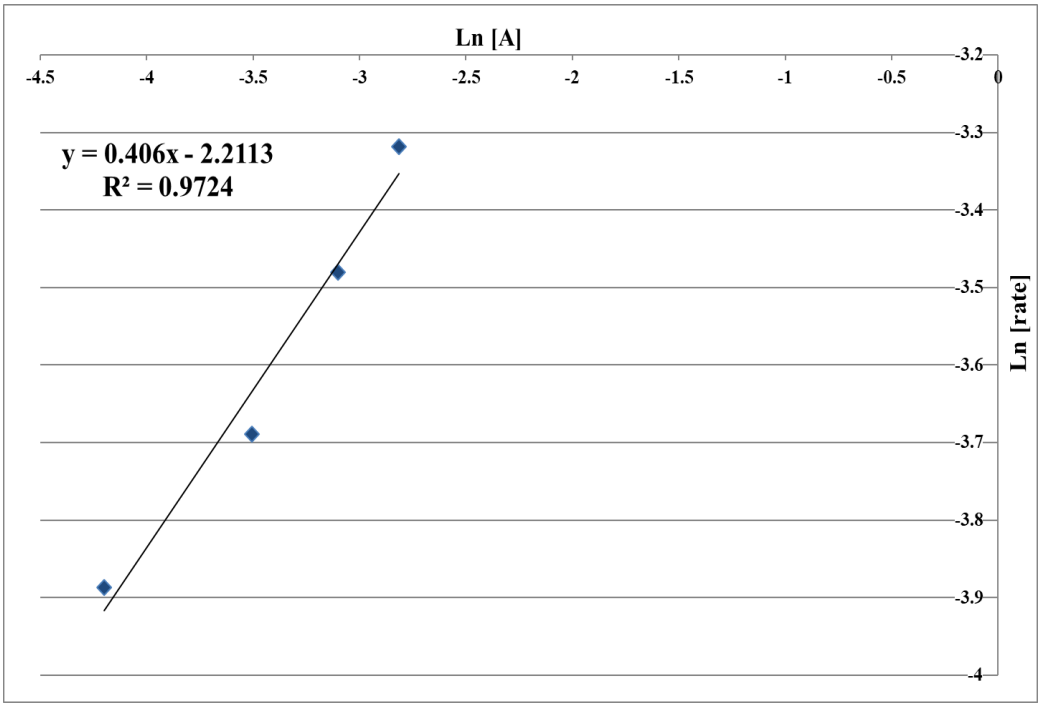

Figure 129. Substrate order plot for *para*-cresol hydrogenation.

Using the equations presented in Section 6.6 of the Experimental Section, the order in *para*-cresol was taken from the gradient of the straight line in Figure 129 above and found to be 0.40. The order for each substrate of the cresol isomers is summarised below:

Table 23. Orders in cresol isomer.

Substrate	Order
ortho-	0.5
meta-	-1.6
para-	0.4

From Table 23 above it can be seen the following order of strength of adsorption exists: *meta*- > *para*- > *ortho*-cresol.

7.2.4 Competitive Hydrogenation

Competitive testing of the cresol isomers in pairs and as a group of three was carried out and the results are detailed in this section.

The competitive reaction of the *ortho*- and *meta*- cresol resulted in a significant decrease in the rate of reaction for both isomers as can be seen in Figure 130 below:

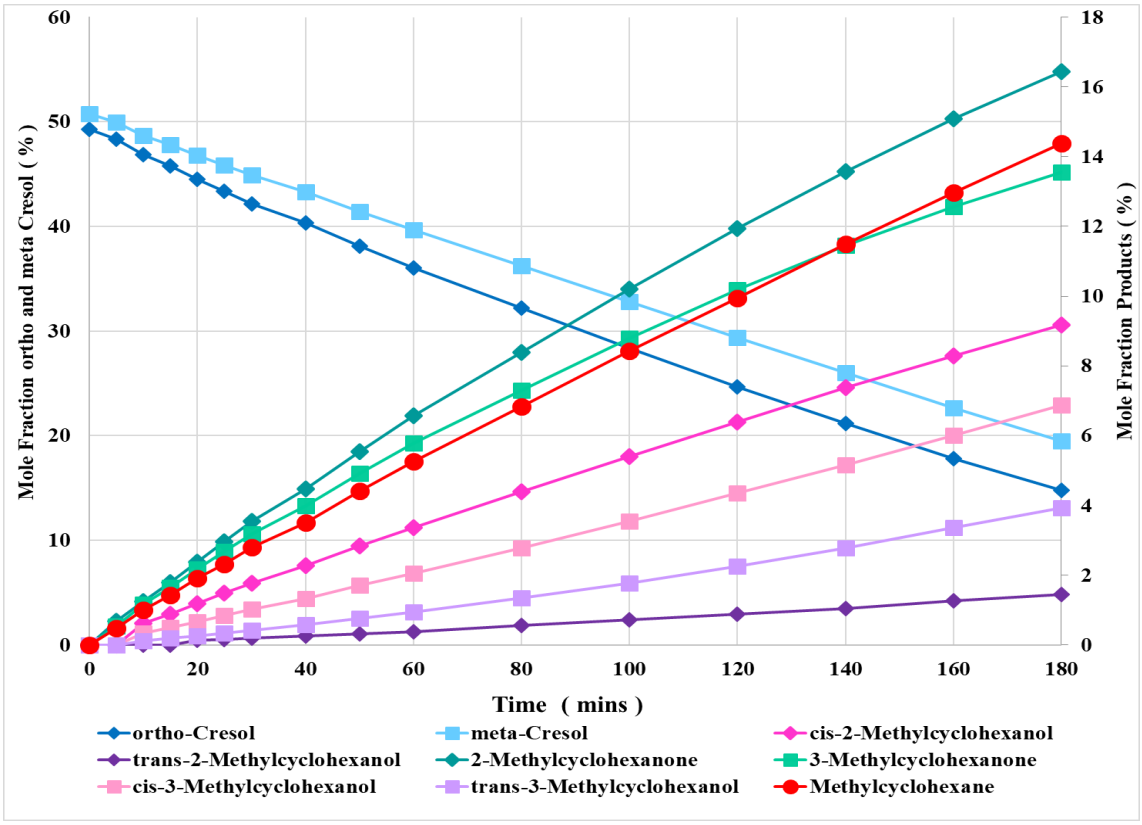

Figure 130. Competitive reaction of *ortho*- and *meta*-cresol. Conditions: 323 K, 3 barg, concentrations as per single reactions.

From Figure 130, it can be seen that both *ortho*- and *meta*- cresol underwent a significant reduction in rate when reacted together. The two isomers behaved similarly, parallel formation of their initial hydrogenated products, 2/3-methylcyclohexanone, was observed until ~ 30 minutes when divergence occurred and formation of the 2-methylcyclohexanone outstripped that of the 3-methylcyclohexanone. Immediate formation of the HDO product, methylcyclohexane, was observed and reached ~ 14 % by the end of reaction.

From Figure 131 below it can be seen that a slight effect on selectivity occurred with an increase registered in the hydrogenated products of *ortho*-cresol and a decrease in that of *meta*-cresol during the competitive reaction. The HDO product, methylcyclohexane, remained unaffected.

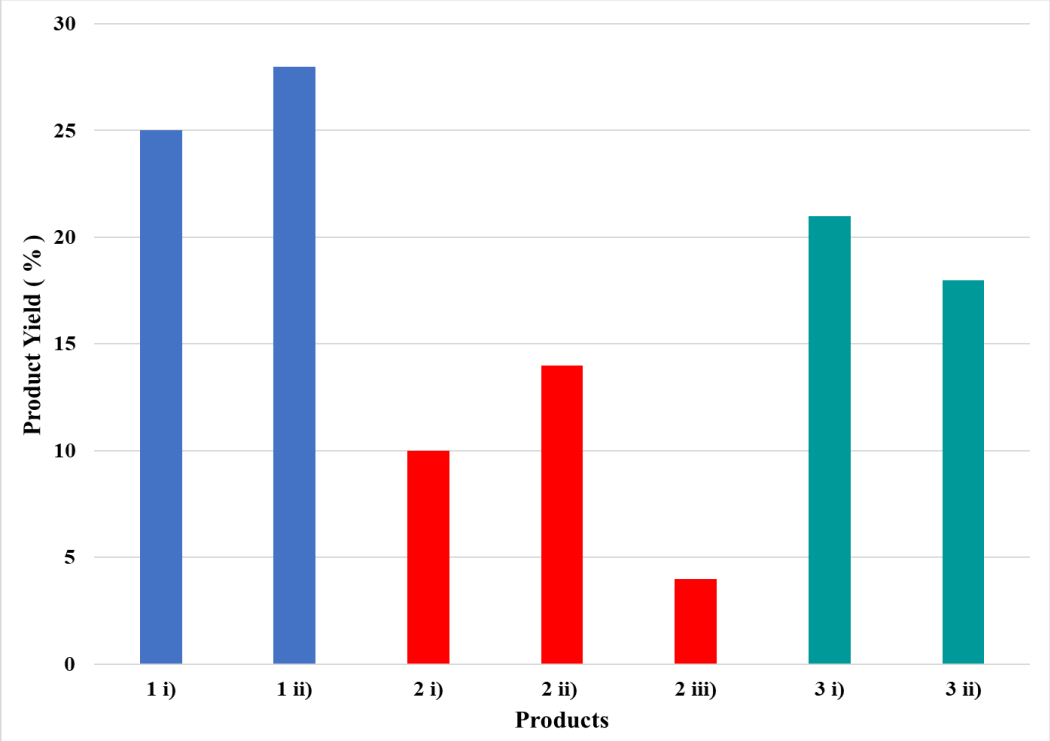

Figure 131.Comparison of product yield for individual and competitive hydrogenation of *ortho*- and *meta*-cresol. Data taken at 33 % conversion of *ortho*-cresol and 27 % conversion of *meta*-cresol.

Key : 1 HYD products i) Individual ortho-cresol 1 ii) Competitive ortho-cresol

2 Methylcyclohexane i) Individual ortho-cresol ii) Competitive ortho + meta cresol iii) Individual meta-cresol

3 HYD products i) Individual meta-cresol ii) Competitive meta-cresol

The competitive hydrogenation of *ortho*- and *para*-cresol is shown in Figure 132 below:

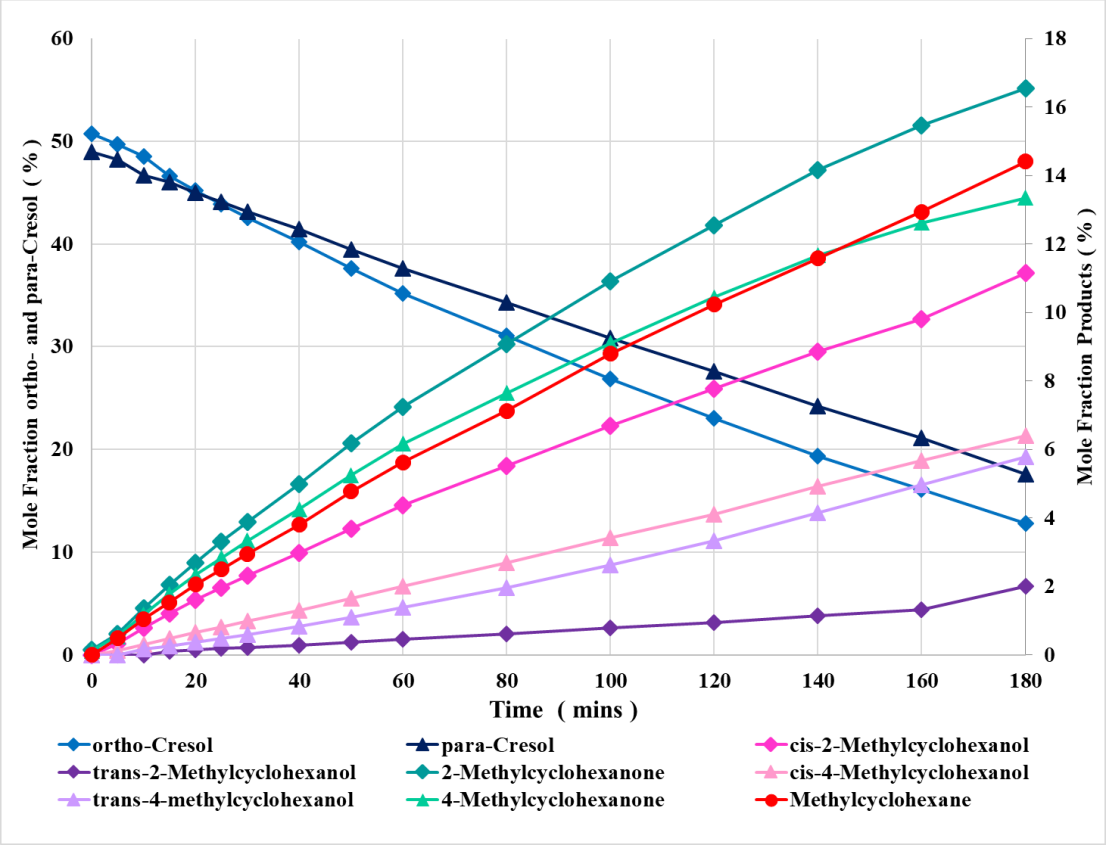

Figure 132. Competitive reaction of *ortho*- and *para*-cresol. Conditions: 323 K, 3 barg, concentrations as per single reactions.

Again, a significant reduction in rate was observed for both isomers during the competitive reaction, as with the previous pair combination the inhibitive effect on the *ortho* isomer was less pronounced. Initial formation of the hydrogenated products, 2-methylcyclohexanone and 4-methylcyclohexanone, was evident until ~ 15 minutes when divergence occurred and formation of the 2-methylcyclohexanone outstripped that of the 4-methylcyclohexanone. Similar to that observed with the *ortho* and *meta* combination, formation of the HDO product, methylcyclohexane, occurred from reaction outset and reached ~ 14 % by the end of reaction. It is of note, that the formation of both *cis*-4-methylcyclohexanol and *trans*-4-methycyclohexanol occurred at similar levels, in sharp contrast to the clear preference exhibited for *cis*-2-methylcyclohexanol over *trans*-2-methylcyclohexanol.

As observed with the *ortho* and *meta* pair combination a slight selectivity effect occurred, with the hydrogenated products of *ortho*-cresol and *para*-cresol registering an increase and decrease respectively. The HDO product, methylcyclohexane, was again unaffected. The product yield comparison between individual and competitive reactions is shown below in Figure 133.

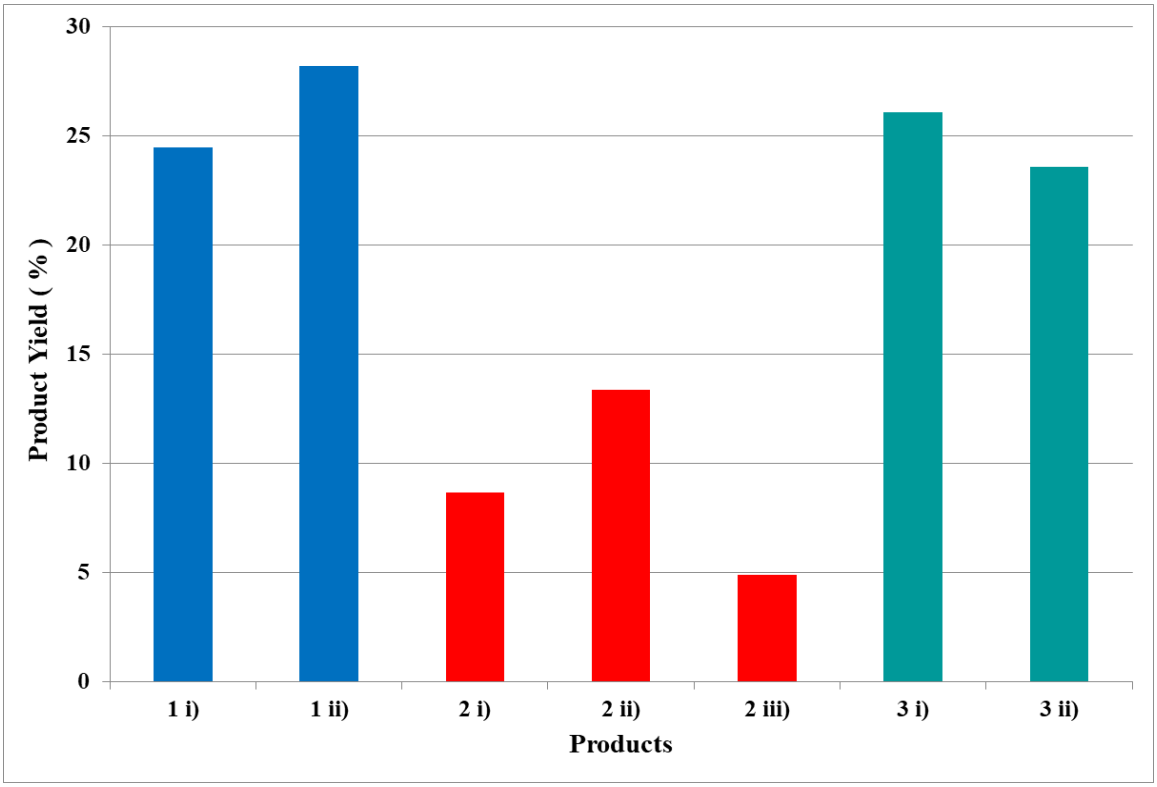

Figure 133. Comparison of product yield for individual and competitive hydrogenation of *ortho*- and *para*-cresol. Data taken at 42 % conversion of *ortho*-cresol and 34 % conversion of *para*-cresol.

Key : 1 HYD products i) Individual ortho-cresol 1 ii) Competitive ortho-cresol

2 Methylcyclohexane i) Individual ortho-cresol ii) Competitive ortho + para cresol iii) Individual para-cresol

3 HYD products i) Individual para-cresol ii) Competitive para-cresol

The competitive hydrogenation of *meta*- and *para*-cresol is shown in Figure 134 below:

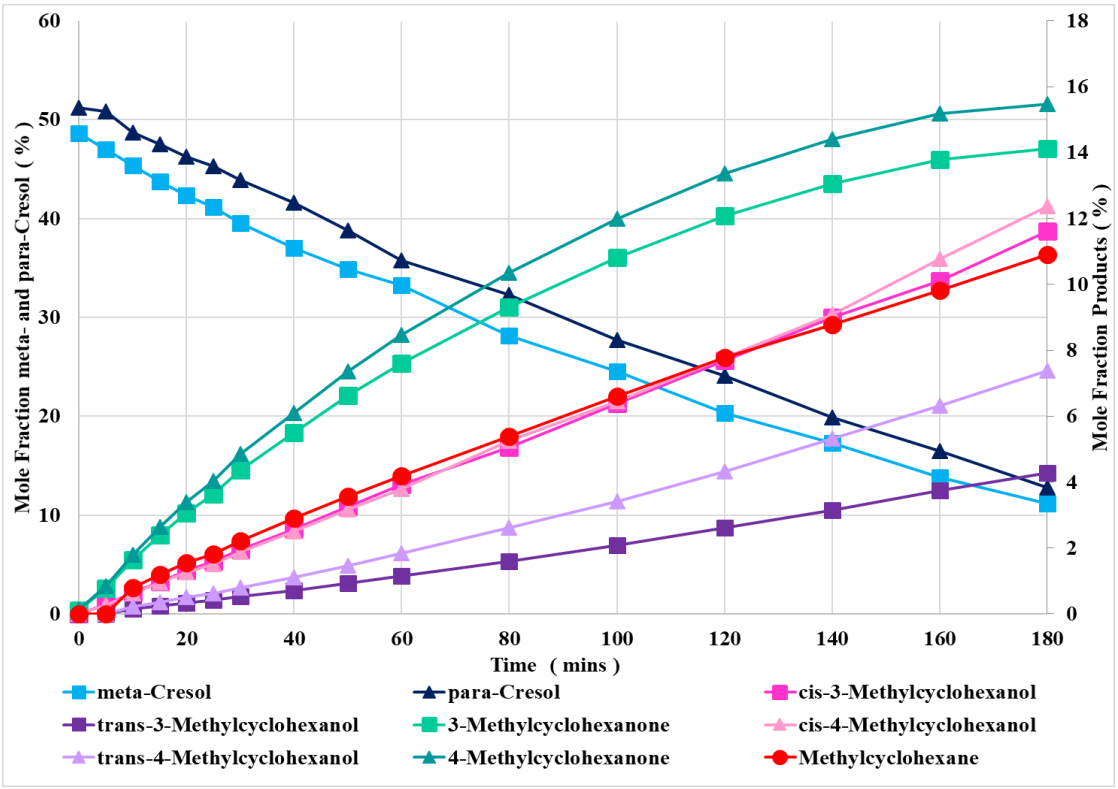

Figure 134. Competitive reaction of *meta*- and *para*-cresol. Conditions: 323 K, 3 barg, concentrations as per single reactions.

It is clear from the graph above that the *meta* and the *para* isomers behave similarly when reacted together, with a close correlation in both rate of reaction, and the formation of their major hydrogenated products (3/4-methylcyclohexanone and *cis*-2/3-methylcyclohexanone). Overall, product formation from *para*-cresol was slightly favoured over that from *meta*-cresol. Formation of methylcyclohexane occurred at the lowest level of all pair combinations at ~ 11 % by end of reaction.

The *meta* and *para* pair combination showed an effect on selectivity, with the hydrogenated products from each registering an increase in the competitive environment. The HDO product, methylcyclohexane, however, had a reduction in formation when compared with individual hydrogenation. The product yield comparison between individual and competitive reactions is shown below in Figure 135.

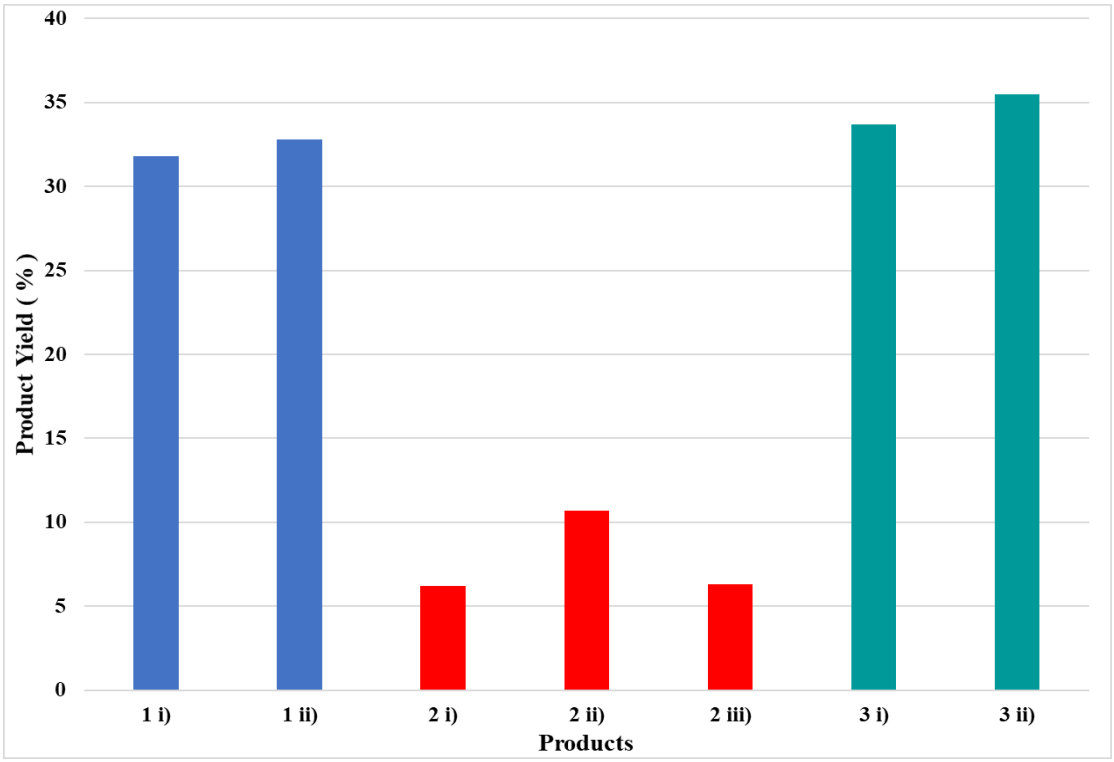

Figure 135. Comparison of product yield for individual and competitive hydrogenation of *meta*- and *para*-cresol. Data taken at 42 % conversion of *meta*-cresol and 37 % conversion of *para*-cresol.

Key : 1 HYD products i) Individual meta-cresol 1 ii) Competitive meta-cresol

2 Methylcyclohexane i) Individual meta-cresol ii) Competitive meta + para cresol iii) Individual para-cresol

3 HYD products i) Individual para-cresol ii) Competitive para-cresol

Data for all three substrates reacted together in the competitive environment is shown in the figures below. Figure 136 shows product formation. Figure 137 outlines substrate conversion and a comparison with hydrogenation of the individual substrates.

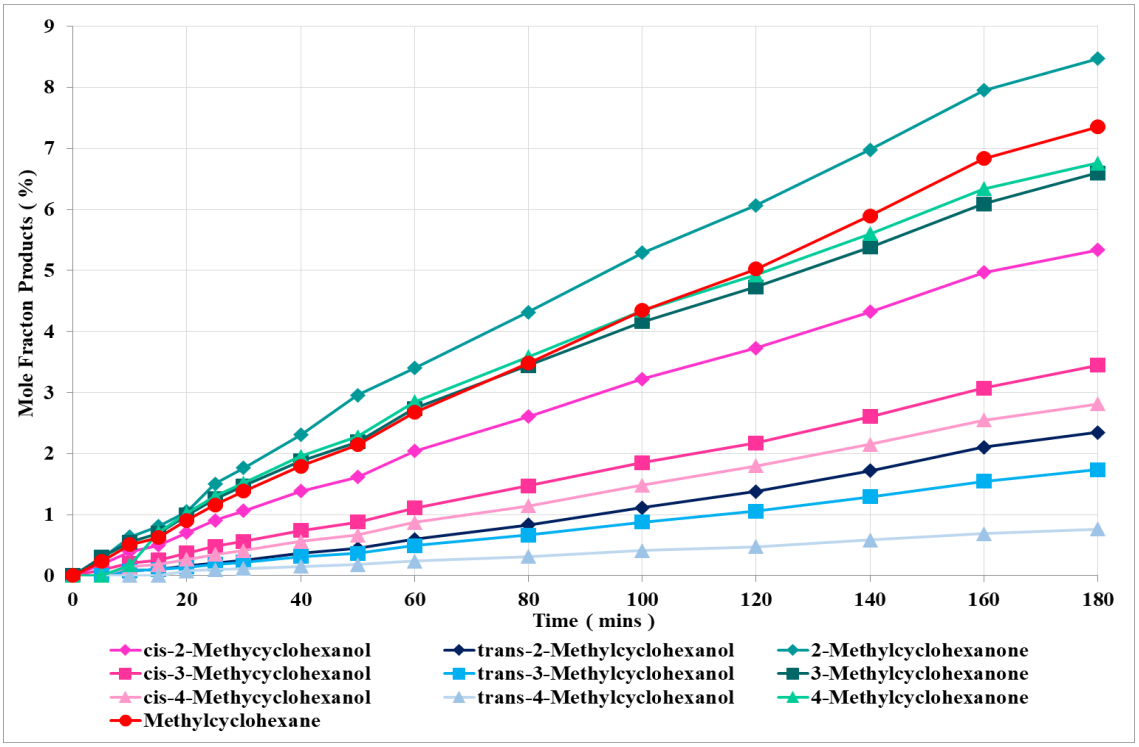

Figure 136. Competitive reactions of *ortho*, *meta* and *para*-cresol. Conditions, 323 K, 3 barg, concentrations as per single reactions.

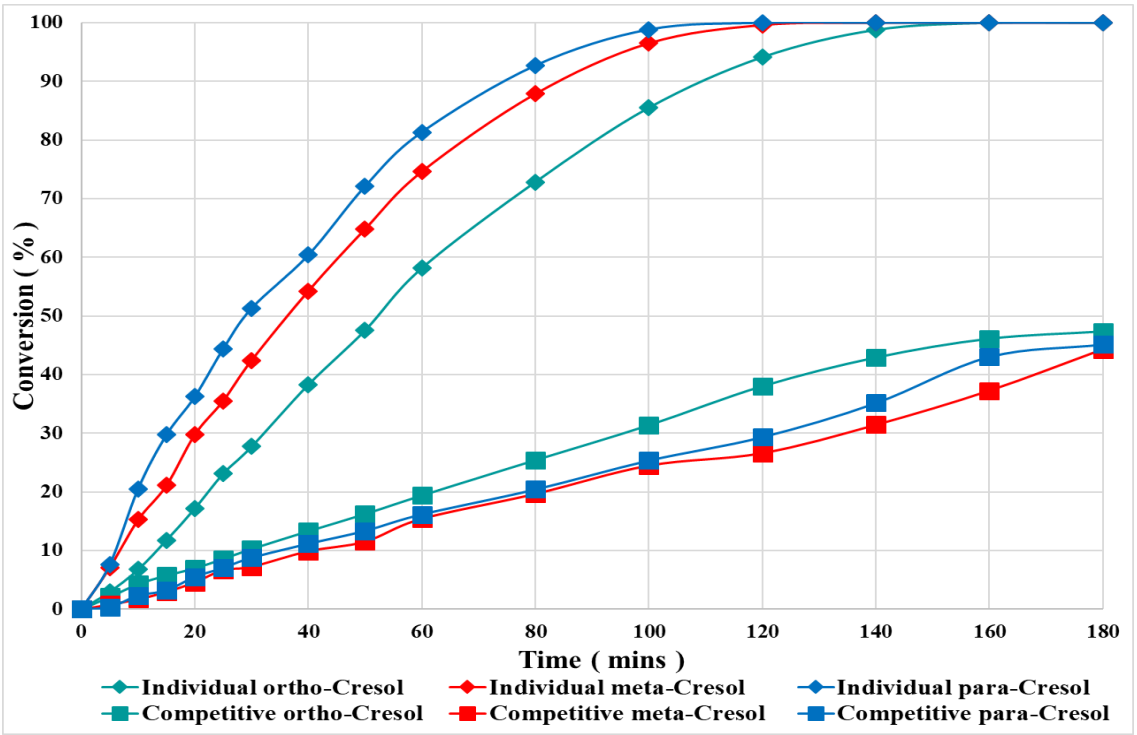

Figure 137. Conversion of the three isomers in the competitive environment compared with that during individual hydrogenation.

From Figure 136 and 137 it is apparent that the reaction rate for all three substrates was suppressed to a greater extent than that observed during previous competitive reactions. The hydrogenated products from *ortho*-cresol, *cis*-2-methylcyclohexanol and 2-

methylcyclohexanone, are formed to the greatest extent, again emphasising its dominance in the competitive environment. A slight inhibition in formation of the initial hydrogenated products from both *meta*- and *para*-cresol occurs; formation of 3-hydroxycyclohexanone is delayed until 5 minutes and that of 4-hydroxycyclohexanone until after 10 minutes. The delay in formation of the *trans*-3-methylcyclohexanol and *trans*-4-methylcyclohexanol observed during individual hydrogenation is exacerbated to 10 and 20 minutes respectively. From Figure 49 it is clear that when reacted together, all three isomers show a significant decrease in conversion. This is most pronounced with the *meta* and *para* isomers where full conversion by ~120 minutes in the individual environment is reduced to only ~ 45 % by end of reaction.

The kinetic data gathered from competitive reaction combinations is outlined in Table 24 below:

Table 24. Competitive hydrogenation of cresol isomers at 323 K, 3 barg and 10 mmol.

Reactant	First order rate constant, k (min^{-1}, $x10^{-3}$)				
	Single reactant	ortho/ meta	ortho/ para	meta/ para	ortho/meta/ para
ortho-	11.1	3.8	5.0	-	3.9
meta-	18.4	2.6	-	7.1	3.1
para-	24.2	-	3.2	5.6	3.6

It can be seen that across all competitive reactions *ortho*-cresol had the highest reactivity, in marked contrast to the individual hydrogenations where it exhibited the lowest rate.

7.2.5 Deuteration Reactions

In the following set of reactions, deuterium was used in place of hydrogen for both the reduction and reaction procedure. All other parameters were set for standard conditions (323 K and 10 mmol substrate). Comparison of the rate constants from reactions carried out in deuterium and hydrogen was used to calculate the kinetic isotope effect for each substrate. All graphs and data from individual and competitive reactions are shown in Figures 138 - 150 below:

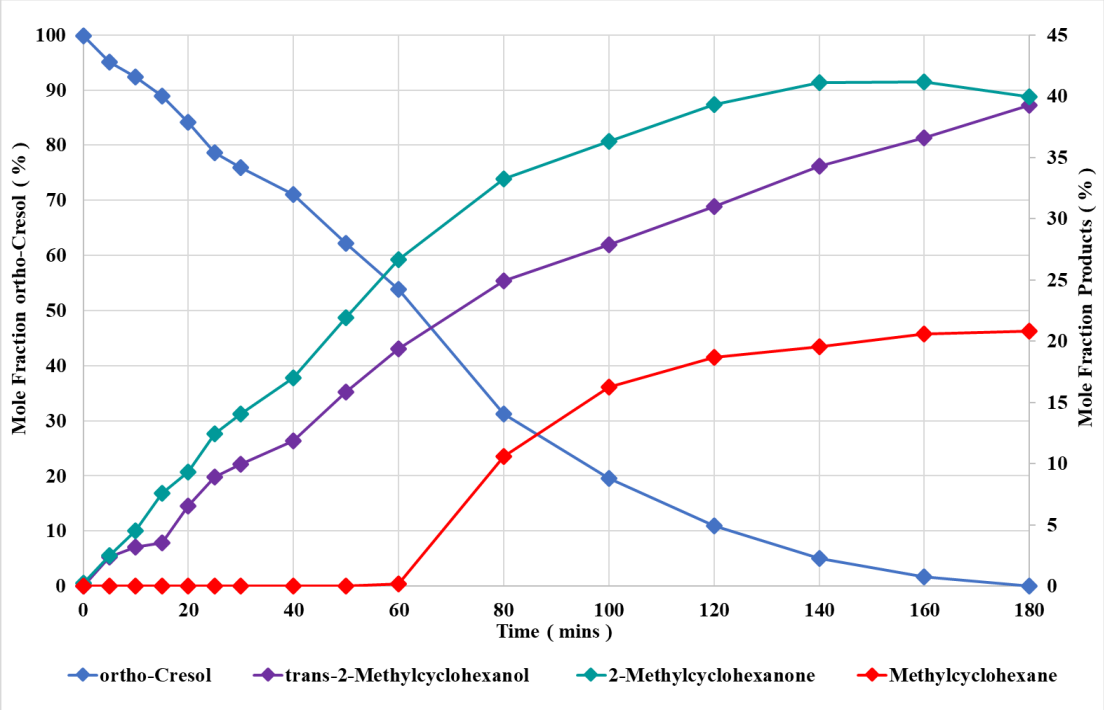

Figure 138. Reaction profile of *ortho*-cresol deuteration. Conditions, 323 K, 10 mmol, 3 barg.

From Figure 138 above it can be seen that the rate of *ortho*-cresol deuteration was lower than that of hydrogenation with a decrease observed in the rate constant from 11.1×10^{-3} to 8.8×10^{-3} min^{-1}. Of note is the complete absence of the formation of *cis*-2-methylcyclohexanol over the duration of the reaction. A marked inhibition effect was seen for the HDO product, methylcyclohexane, with formation delayed until 80 minutes against initial production under standard hydrogenation conditions. The product distribution for hydrogenated and hydrodeoxygenated products at the same conversion (90 %) is shown below in Figure 139:

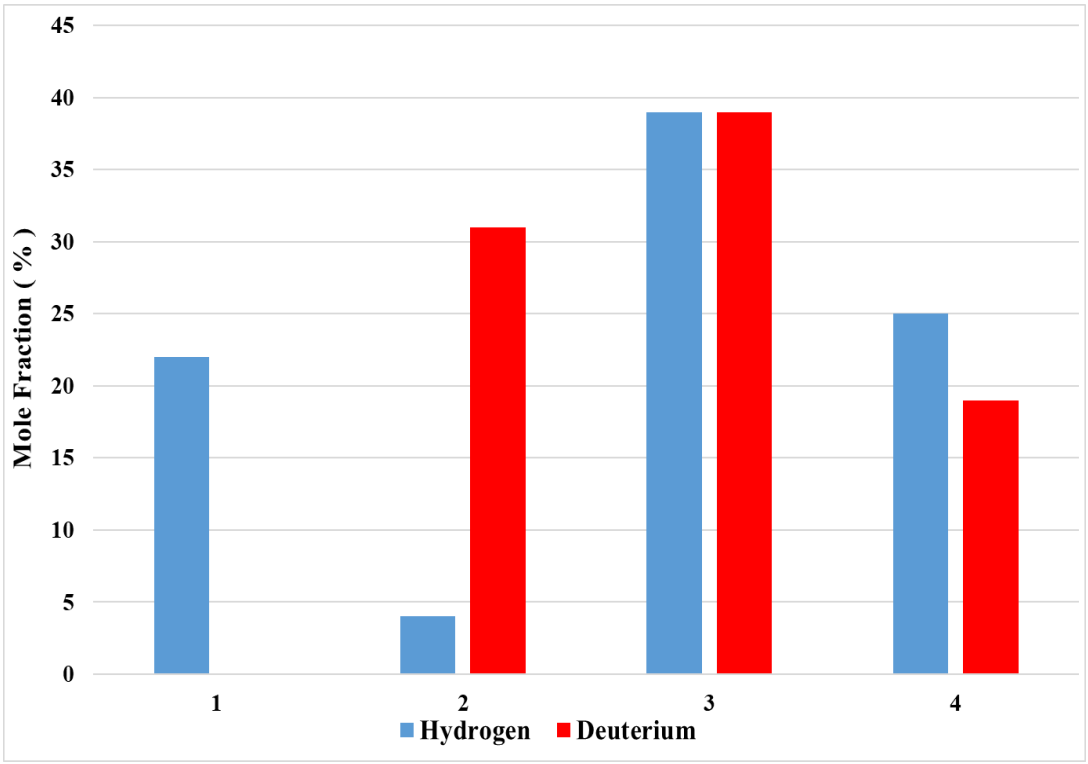

Figure 139. Product distribution of deuterium against hydrogen at 90 % conversion of *ortho*-cresol

Key: 1: cis-2-Methylcyclohexanol **2:** trans-2-Methylcyclohexanol **3:** 2-Methylcyclohexanone **4:** Methylcyclohexane

From Figure 139 it is immediately apparent that significant differences in product distribution exist between the hydrogenation and deuterated reactions for *ortho*-cresol. This is most pronounced with the *cis*-2-methylcyclohexanol where no formation occurred in the presence of deuterium. A significant effect was also observed on the *trans*-2-methylcyclohexanol, increasing from ~ 5 % with hydrogen to ~ 30 % with deuterium. A slight inhibition in the presence of deuterium was observed with methylcyclohexane, a decrease of ~ 6 % mole fraction, whilst the 2-methylcyclohexanone remained constant with both gas reactants.

meta-Cresol deuteration was carried out and is shown below in Figure 140:

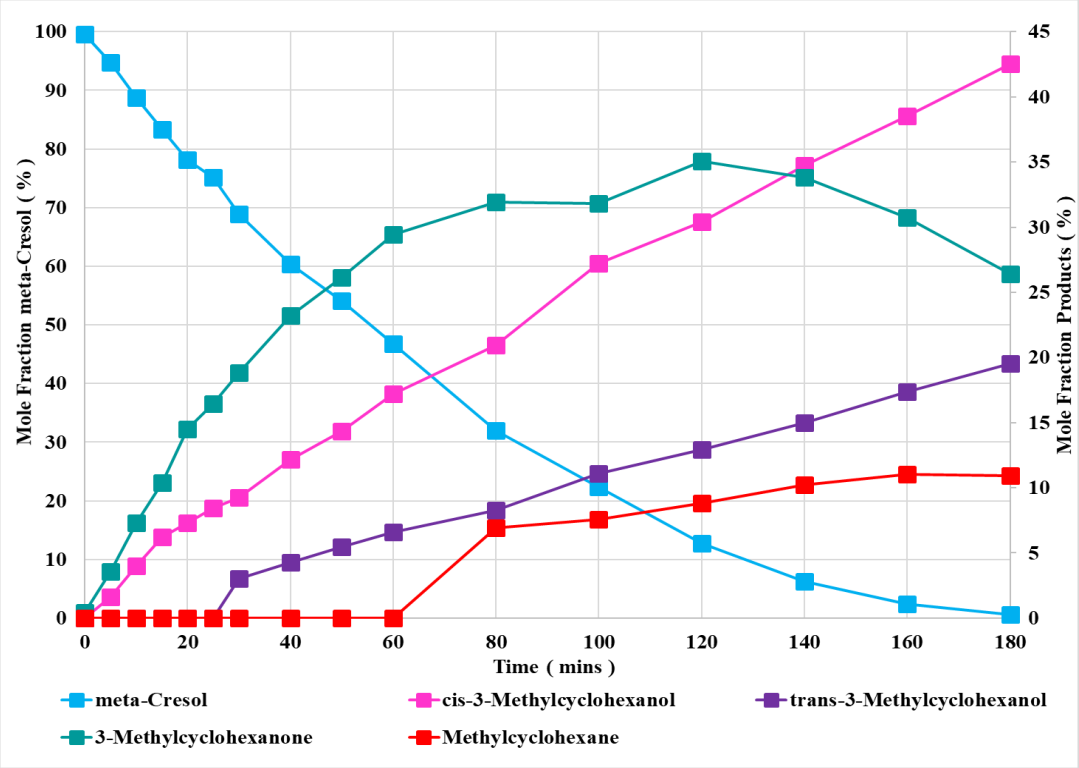

Figure 140. Reaction profile of *meta*-cresol deuteration. Conditions, 323 K, 10 mmol, 3 barg.

Figure 140 above shows a slower reaction rate of *meta*-cresol deuteration to that observed for the hydrogenation reaction with measured rate constants of 18.4×10^{-3} to 14.4×10^{-3} min^{-1} respectively. Formation of the *cis*-3-methylcyclohexanol occurred immediately, whilst a significant inhibition of 25 minutes was observed for the *trans*-3-methylcyclohexanol. An even greater suppression in formation occurred for the methylcyclohexane which remained undetected until 80 minutes reaction time. The product distribution for hydrogenated and hydrodeoxygenated products at the same conversion (90 %) is shown below in Figure 141:

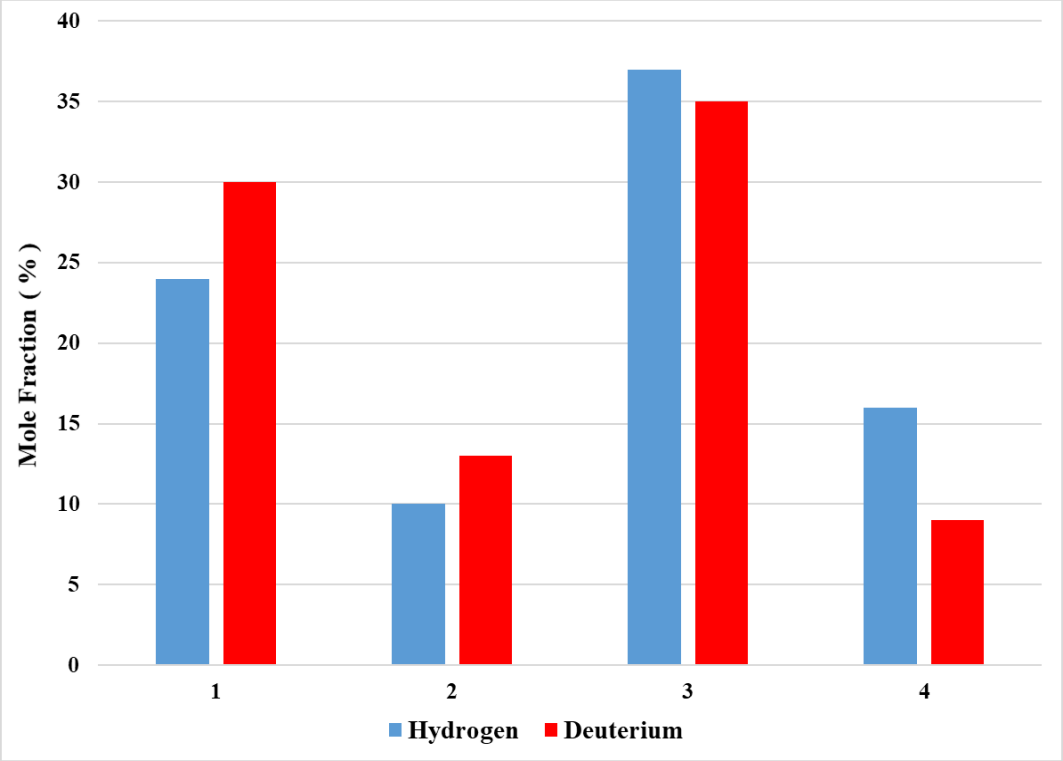

Figure 141. Product distribution of deuterium against hydrogen at 90 % conversion of *meta*-cresol.

Key: 1: cis-3-Methylcyclohexanol **2:** trans-3-Methylcyclohexanol **3:** 3-Methylcyclohexanone **4:** Methylcyclohexane

From Figure 141, differences between the hydrogenation and deuterated reaction for *meta*-cresol are apparent. Both the *cis* and *trans*-3-methylcyclohexanol show an increase in the presence of deuterium, whilst the 3-methylcyclohexanone and methylcyclohexane exhibit a decrease.

para-Cresol deuteration was carried out and is shown below in Figure 142:

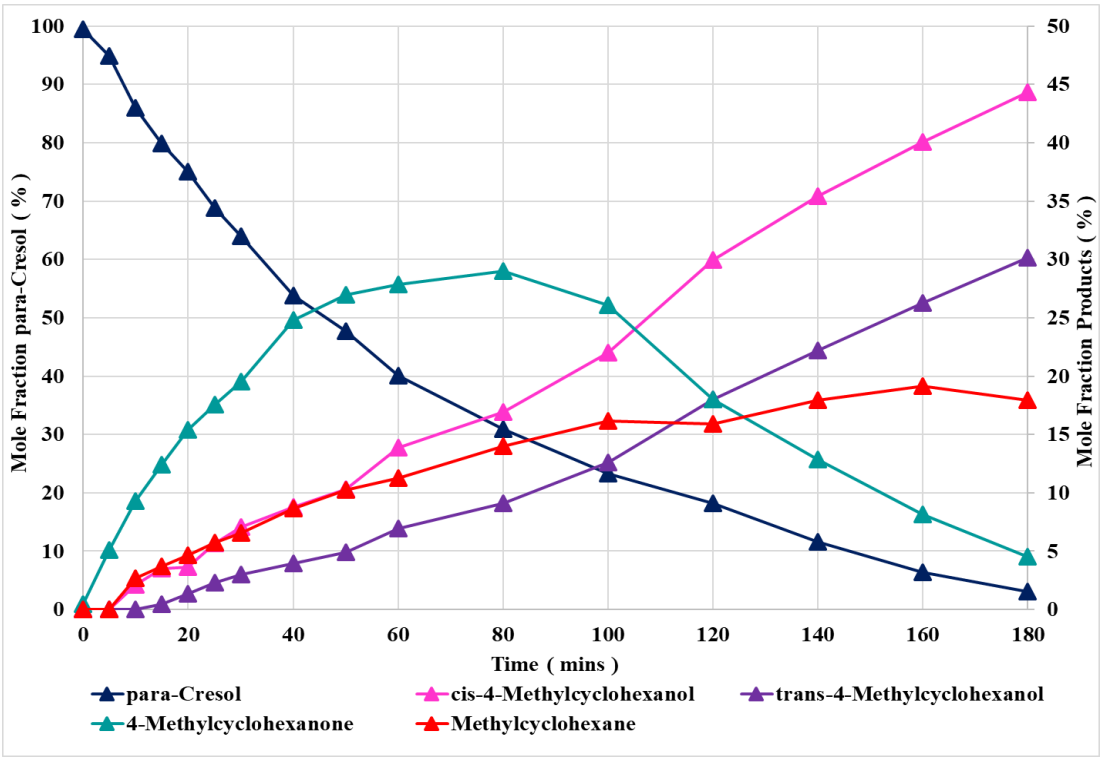

Figure 142. Reaction profile of *para*-cresol deuteration. Conditions, 323 K, 10 mmol, 3 barg.

Figure 142 above shows a significant reduction in the rate of *para*-cresol deuteration to that observed with the hydrogenation reaction; a measured rate constant decrease from 24.2×10^{-3} to 11.9×10^{-3} min^{-1}. Immediate formation of the hydrogenated product, 4-methylcyclohexanone, was observed whilst both the *cis*-4-methylcyclohexanol and methylcyclohexane exhibited a delay of 10 minutes. A more pronounced inhibitive effect occurred for the *trans*-4-methylcyclohexanol which remained undetected until around 20 minutes reaction time.

The product distribution for hydrogenated and hydrodeoxygenated products at the same conversion (90 %) is shown below in Figure 143:

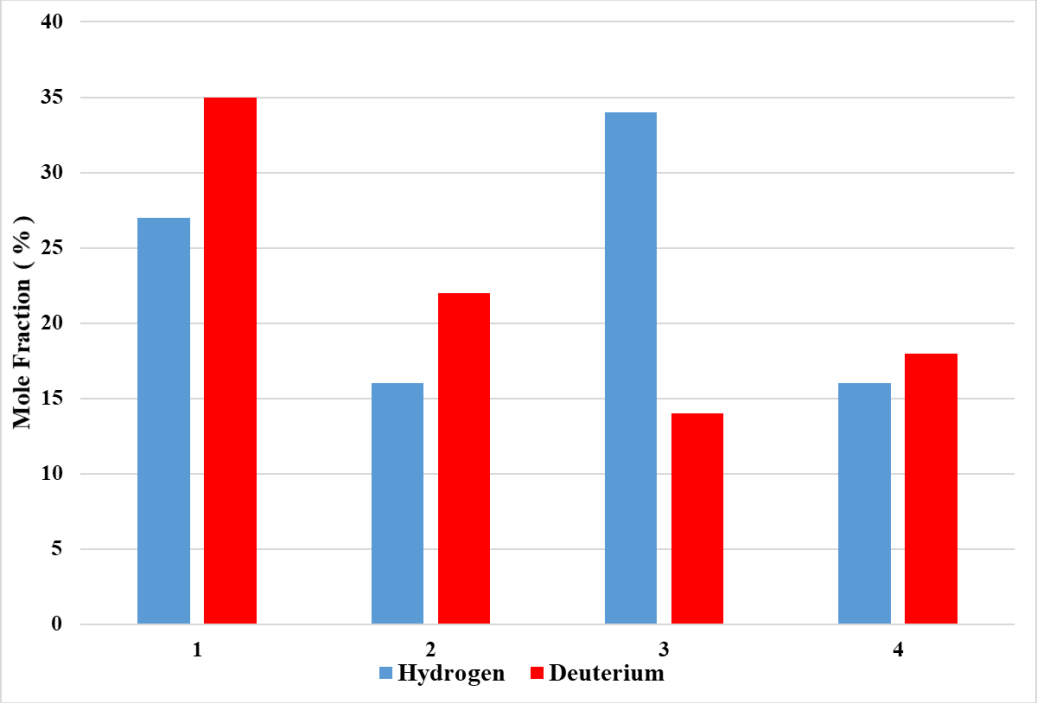

Figure 143. Product distribution of deuterium against hydrogen at 90 % conversion of *para*-cresol.

Key: 1: cis-4-Methylcyclohexanol **2:** trans-4-Methylcyclohexanol **3:** 4-Methylcyclohexanone **4:** Methylcyclohexane

From Figure 143 it can be seen that clear differences exist between the hydrogenation and deuterated reactions for *para*-cresol. In the presence of deuterium, both *cis* and *trans*-3-methylcyclohexanol showed a significant increase whilst the 4-methylcyclohexanone exhibited a marked decrease. A slight rise in the formation of methylcyclohexane was detected when hydrogen was replaced with deuterium.

The kinetic data gathered from the deuteration reactions is outlined in Table 25 below:

Table 25. KIE's for the individual the cresol isomer reactions.

Substrate	kH	kD	KIE = $\frac{kH}{kD}$
ortho-	11.3	17.3	1.3
meta-	18.4	14.4	1.3
para-	24.2	11.9	2.0

Calculation of KIE can result in three possible outcomes as shown below:

- KIE value equals 1 then there is no KIE effect
- KIE > 1 yields a *positive* KIE effect

- KIE < 1 yields a *negative* KIE effect

Table 25 above shows a positive KIE calculated for *ortho*-, *meta*- and *para*-cresol.

ortho-Cresol and *meta*-Cresol were reacted under competitive conditions with deuterium and the results are shown in Figure 144 below:

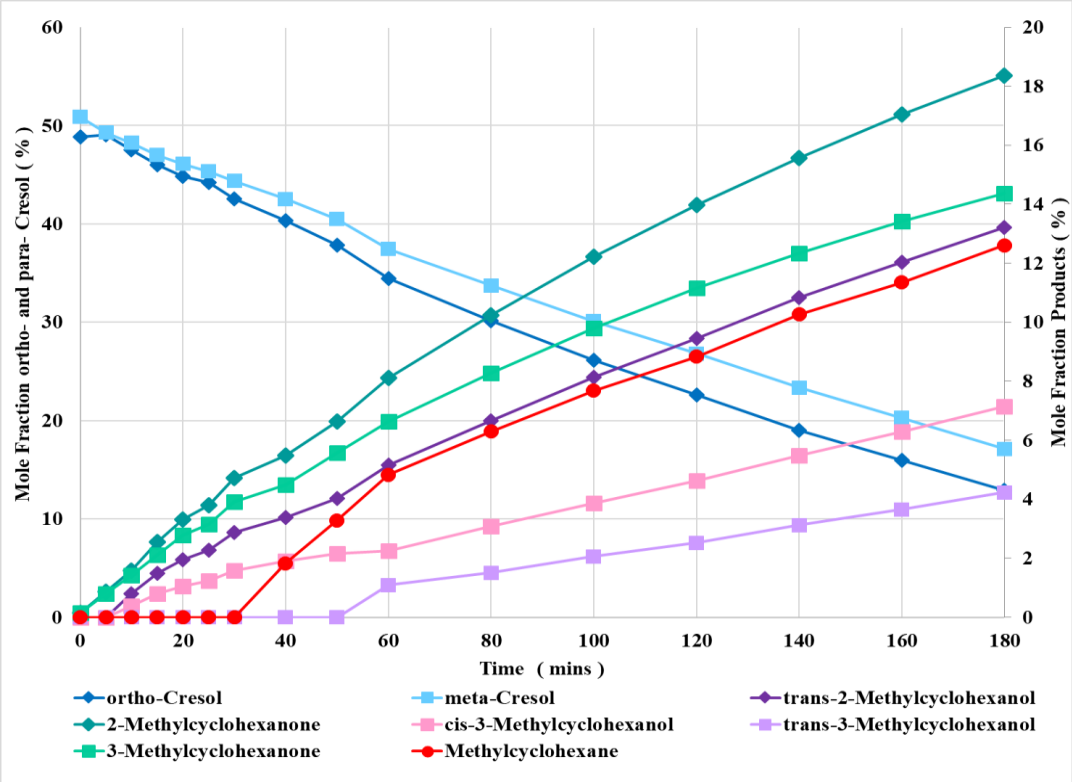

Figure 144. Reaction profile of *ortho*- and *meta*-Cresol deuteration. Conditions, 323 K, 10 mmol, 3 barg.

From Figure 144 it can be seen that the major products of the reaction, 2-methylcyclohexanone and 3-methylcyclohexanone, were those formed through initial hydrogenation of each isomer. As observed with individual deuteration, complete inhibition of the *cis*-2-methylcyclohexanol occurred. Formation of the *trans*-2-methylcyclohexanol was significantly greater than that observed during the competitive reaction in the presence of hydrogen; ~ 14 % against ~ 2 % by end of reaction. As with the *ortho* and *meta* individual deuterated reactions, a significant inhibition of methylcyclohexane (~40 minutes) was apparent. The competitive reaction of *ortho*- and *meta*-cresol under deuterated conditions found *ortho*-cresol had no effect in the presence of deuterium, whilst *meta*-cresol underwent an increase in reactivity. The change in KIE between individual and competitive conditions is shown in Figure 145 below:

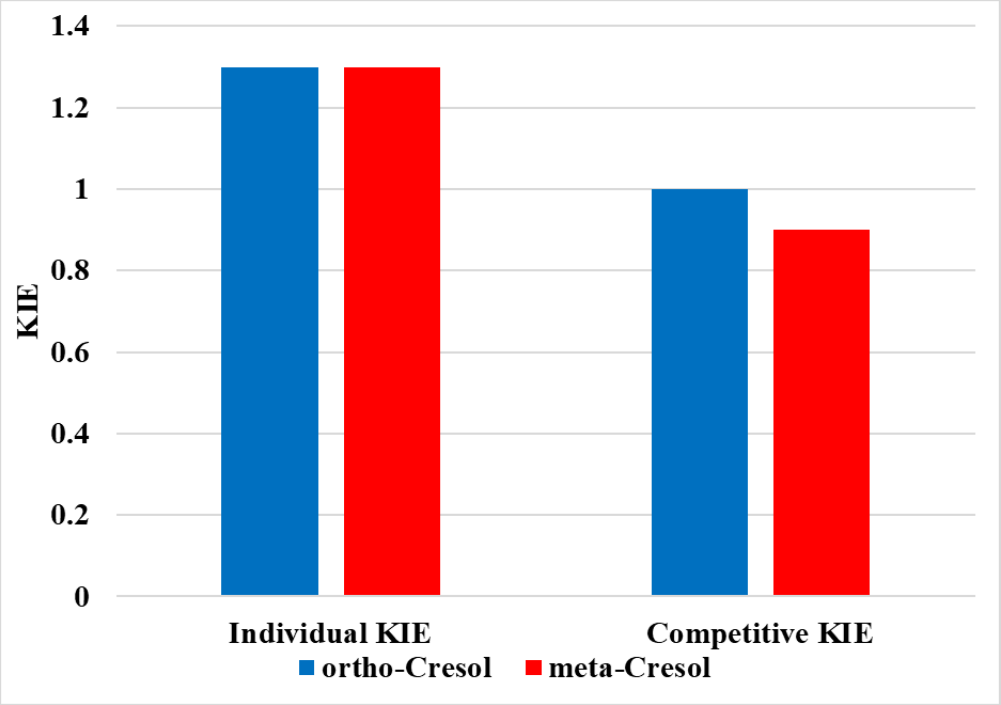

Figure 145. KIE for *ortho*- and *meta*-cresol individual versus competitive hydrogenation.

From Figure 145 it is clear KIE values changed between the individual and competitive environments: *ortho*-cresol changed from a positive effect to no effect, whilst *meta*-cresol went from a positive effect to an inverse KIE.

The competitive deuteration of *ortho*- and *para*-cresol is shown below in Figure 146:

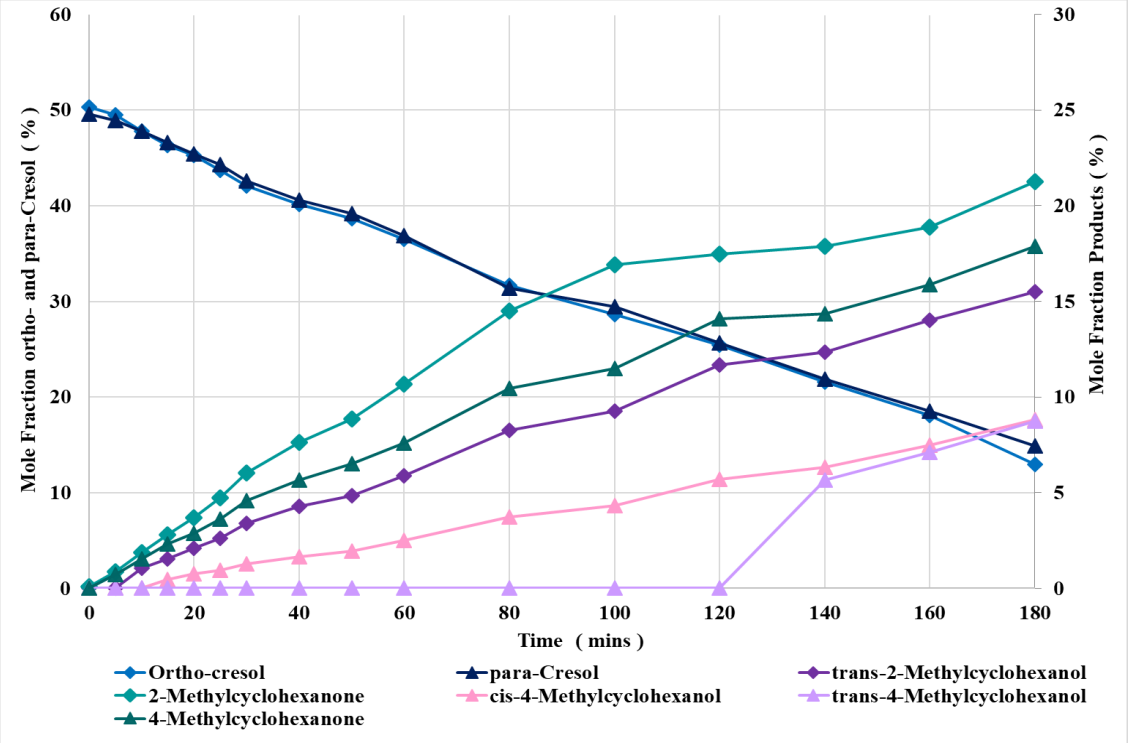

Figure 146. Reaction profile of *ortho*- and *para*-cresol deuteration. Conditions, 323 K, 10 mmol, 3 barg.

From Figure 146 it is apparent that the major products of the reaction are the initial hydrogenated products from each isomer, 2-methylcyclohexanone and 4-methylcyclohexanone. In accordance with the *ortho* and *meta* reaction, formation of the *cis*-2-methylcyclohexanol did not occur, whilst the *trans*-2-methylcyclohexanol reached a level of ~ 15 % by the end of reaction. Of particular note, is the complete lack of the HDO product, methylcyclohexane, throughout the 180-minute time period. The competitive reaction of *ortho*- and *para*-cresol under deuterated conditions found *ortho*-cresol had no effect in the presence of deuterium, whilst *para*-cresol underwent an increase in reactivity. The change in calculated KIE values between individual and competitive reactions is shown in Figure 147 below:

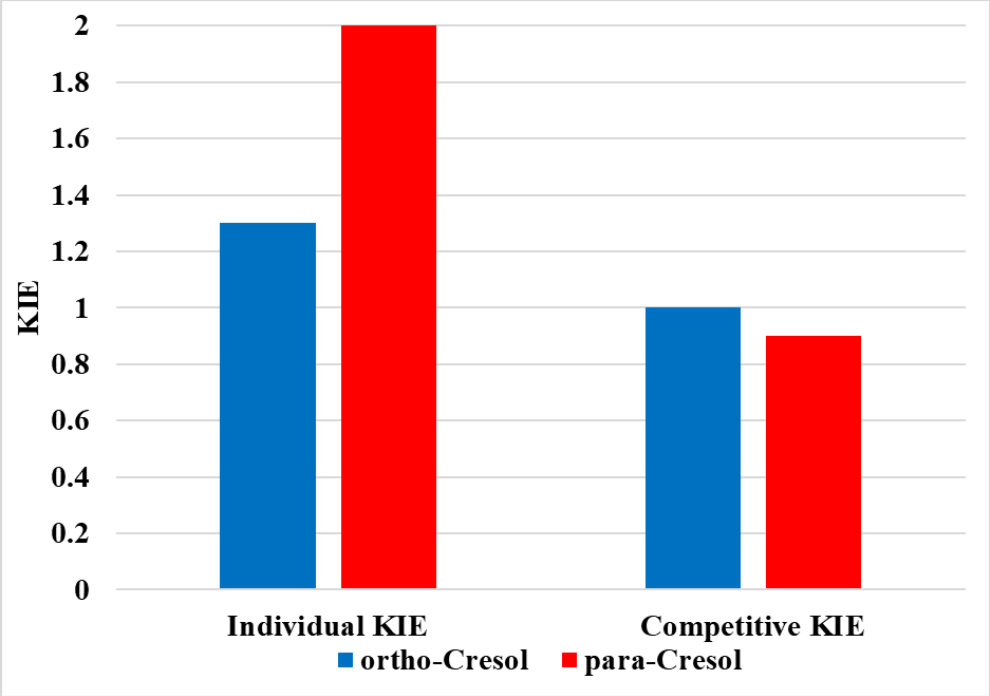

Figure 147. KIE for *ortho*- and *para*-cresol individual versus competitive hydrogenation.

From Figure 147 it can be seen that across individual and competitive environments both KIE values changed: *ortho*-cresol moved from a positive effect to no effect, whilst that of *para*-cresol went from a positive to an inverse KIE.

The competitive deuteration of *meta*- and *para*-cresol is shown below in Figure 148:

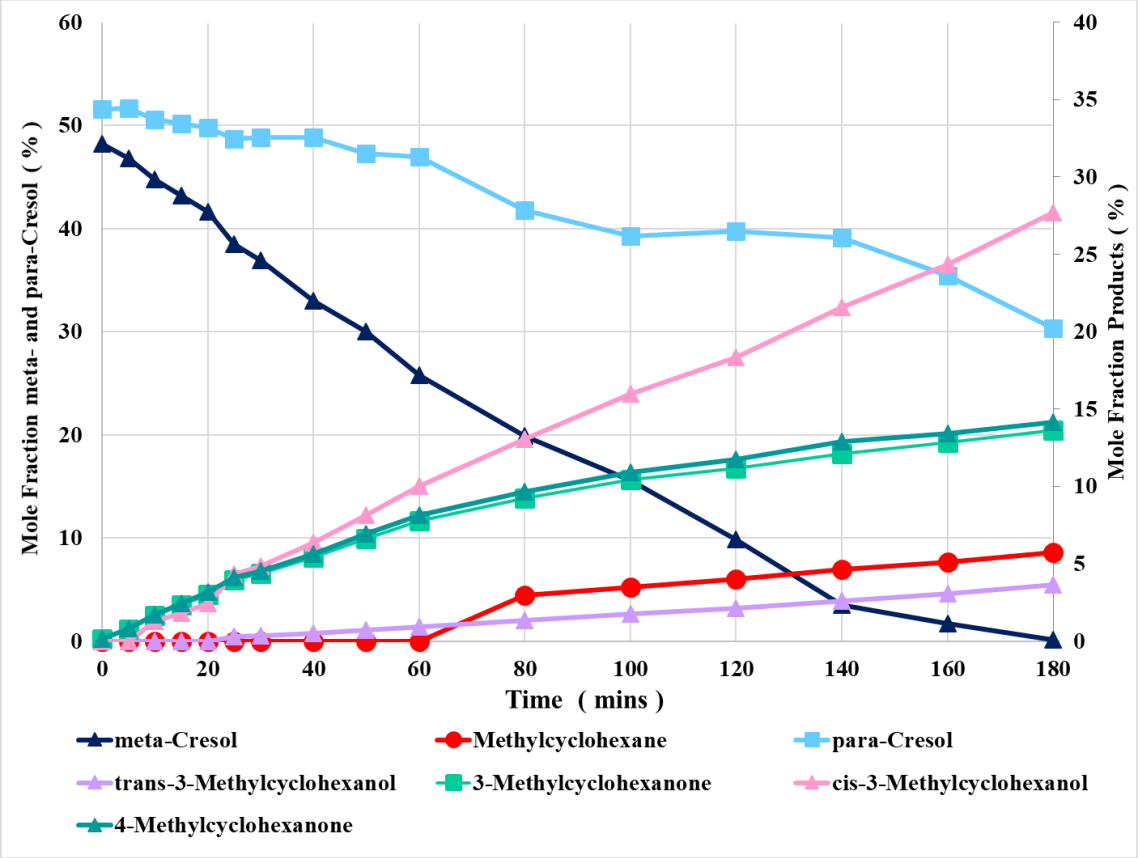

Figure 148. Reaction profile of meta- and para-cresol deuteration. Conditions, 323 K, 10 mmol, 3 barg.

From Figure 148 it is apparent that *cis*-3-methylcyclohexanol was the major reaction product. Formation of *cis*-4-methylcyclohexanol and *trans*-4-methylcyclohexanol was absent throughout the reaction. Similar behaviour for 3-methycyclohexanone and 4-methylcyclohexanone occurred with both forming immediately and achieving ~ 15 % by the end of reaction. Substantial inhibition was observed with the HDO product, methylcyclohexane, with no formation registered until 80 minutes reaction time. The competitive reaction of *meta*- and *para*-cresol under deuterated conditions found *meta*-cresol experienced an increase reactivity in the presence of deuterium, whilst *para*-cresol underwent a decrease in reactivity. The change in calculated KIE values between individual and competitive conditions is shown in Figure 149 below:

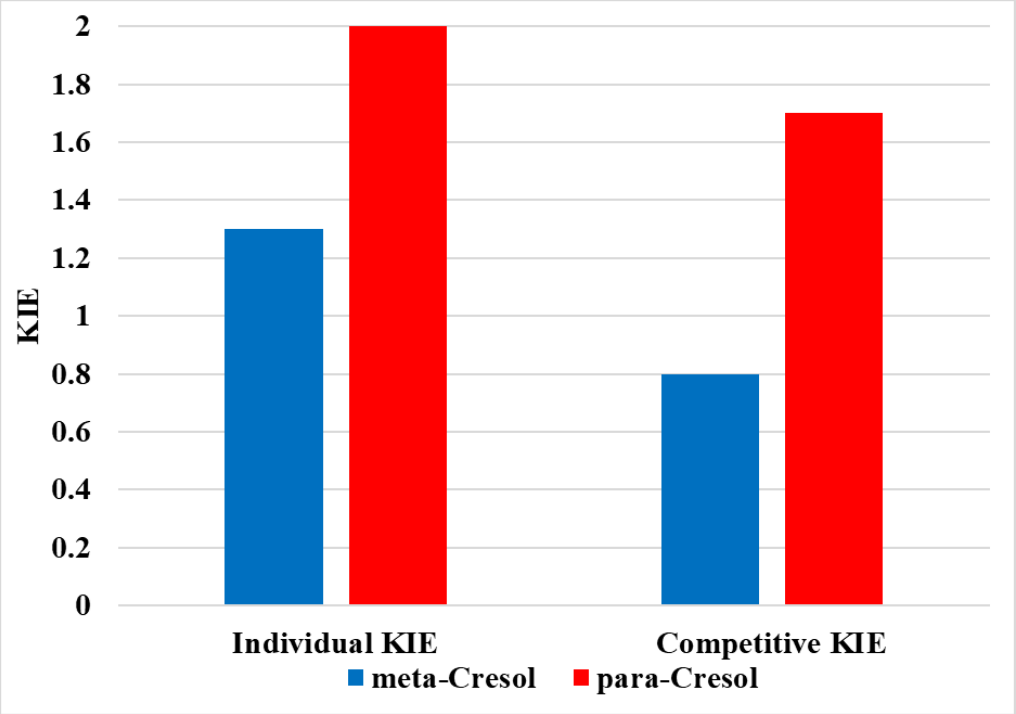

Figure 149. KIE for *meta*- and *para*-cresol individual versus competitive hydrogenation.

From Figure 149 it can be seen that across individual and competitive environments only the overall KIE value for *meta*-cresol changed from a positive effect to an inverse effect, whilst that of *para*-cresol remained positive throughout.

The competitive deuteriation reaction of all three substrates reacted together is shown in Figure 150 below:

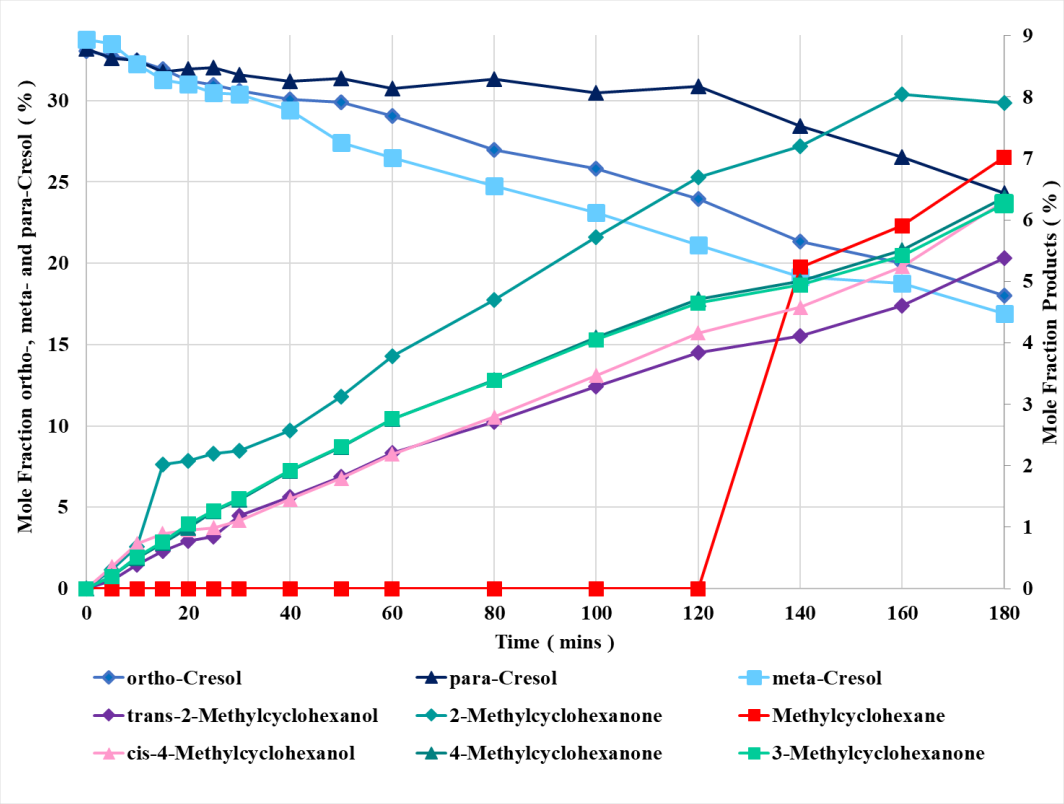

Figure 150. Reaction profile of *ortho*-, *meta*- and *para*-cresol. Conditions, 323 K, 10 mmol, 3 barg.

From Figure 150 it was found that *ortho*-cresol exhibited a similar reaction rate during the deuterated reaction with *meta*- and *para*-cresol, *meta*-cresol underwent an increase whilst that of *para*-cresol decreased in reactivity. It is of note that neither *cis*-2-methylcyclohexanol from *ortho*-cresol or *trans*-4-methylcyclohexanol from *para*-cresol were formed during the reaction. Furthermore, both methylcyclohexanol isomers from *meta*-cresol were absent. The HDO product, methylcyclohexane, showed significant inhibition with no detection prior to 140 minutes, following that however, it was present as the second major reaction product.

The kinetic isotope effects are summarised below in Table 26:

Table 26. KIE's for the cresol isomers competitive reactions.

	ortho/meta	*ortho/para*	*meta/para*	*ortho/meta/para*
KIE = $\frac{kH}{kD}$	**1.0, 0.9**	**1.0, 0.9**	**0.7, 1.5**	**1.0, 0.9, 1.6**

From Table 26 above it can be seen that over all competitive reactions tested *ortho*-cresol exhibited no effect with deuterium in contrast to the positive effect observed during individual hydrogenation. Both *meta*- and *para*-cresol showed the same effect when reacted competitively with *ortho*-cresol: their positive individual KIE values changed to an

inverse KIE. The competitive reaction of *meta*- and *para*-cresol showed a change with *meta*-cresol only - shifting from a positive KIE to an inverse KIE; *para*-cresol remained positive. The competitive reaction with all three isomers present found no effect observed with *ortho*-cresol whilst *para*-cresol remained positive and *meta*-cresol witnessed a change from a positive KIE to an inverse KIE when compared against their individual values.

7.2.6 Post Reaction Catalyst Characterization

Thermogravimetric analysis (TGA) on the post reaction catalyst from the standard (3 hours) hydrogenation of all substrates was carried out.

7.2.6.1 *ortho*-Cresol

The thermal weight loss and associated evolved gas mass spectrometry data for the post *ortho*-cresol reaction catalyst is shown in Figures 151 and 152 below:

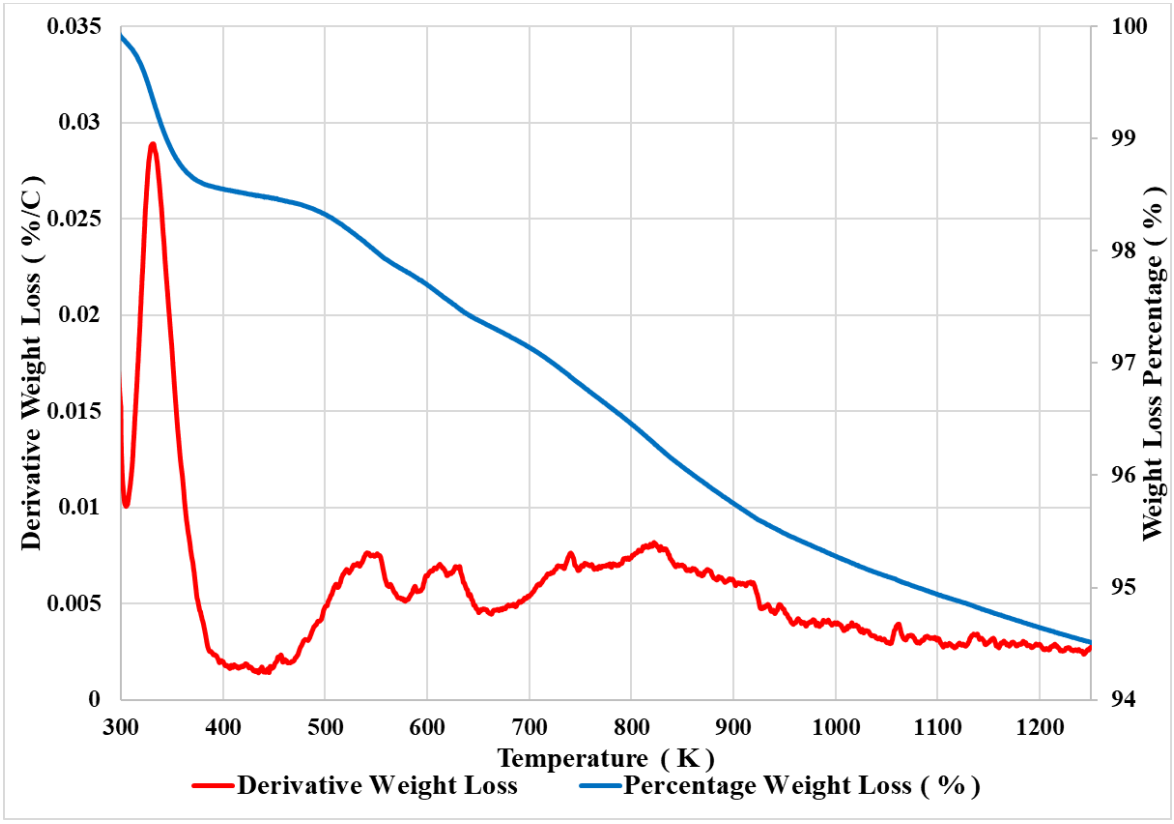

Figure 151. TGA of Rh/SiO_2 catalyst after 3-hour *ortho*-cresol hydrogenation reaction.

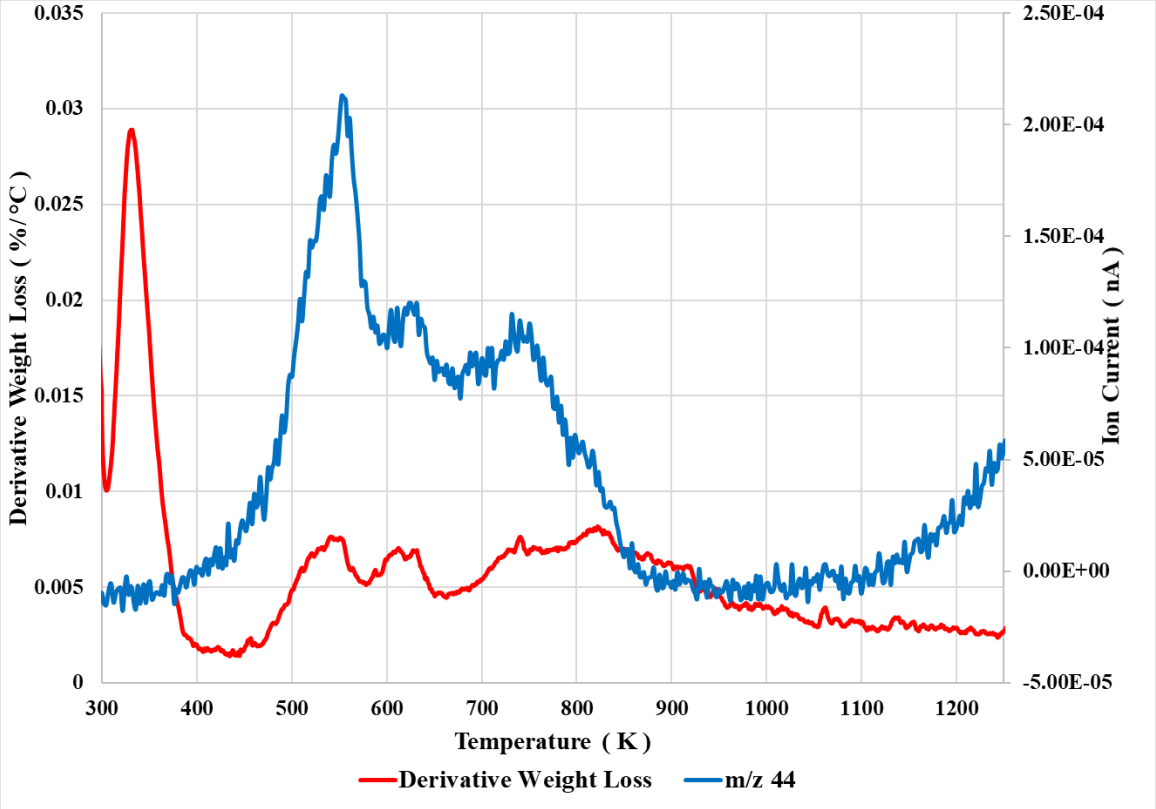

Figure 152. Derivative weight loss coupled with m/z of Rh/SiO_2 catalyst after 3-hour *ortho*-cresol hydrogenation reaction.

From Figures 151 and 152 above it can be seen that the total weight loss from the catalyst over the measured temperature range was 5.5 %. The three high temperature weight loss events (>490 K) account for around 3.5 % and are associated with the evolution of m/z = 44 (CO_2). The initial weight loss event between 290 and 390 K is a result of the evolution of water.

7.2.6.2 *meta*-Cresol

The thermal weight loss and associated evolved gas mass spectrometry data for the post *meta*-cresol reaction catalyst is shown in Figures 153 and 154 below:

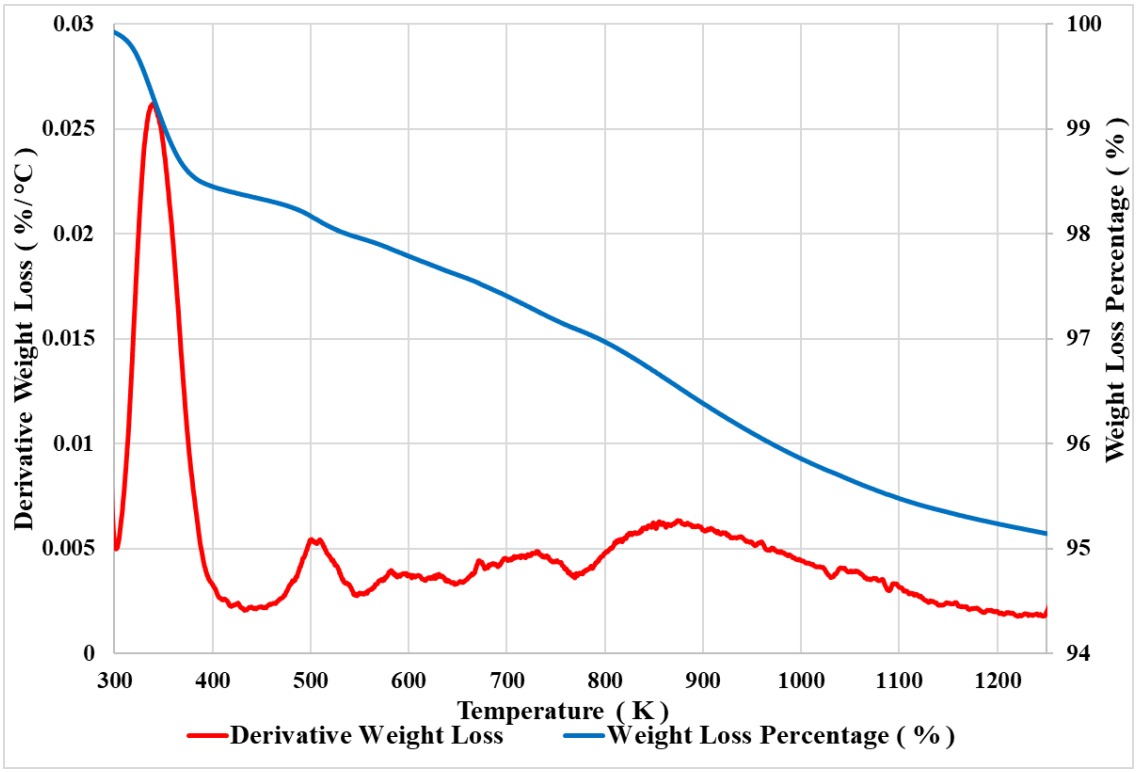

Figure 153. TGA of Rh/SiO_2 catalyst after 3-hour *meta*-cresol hydrogenation reaction.

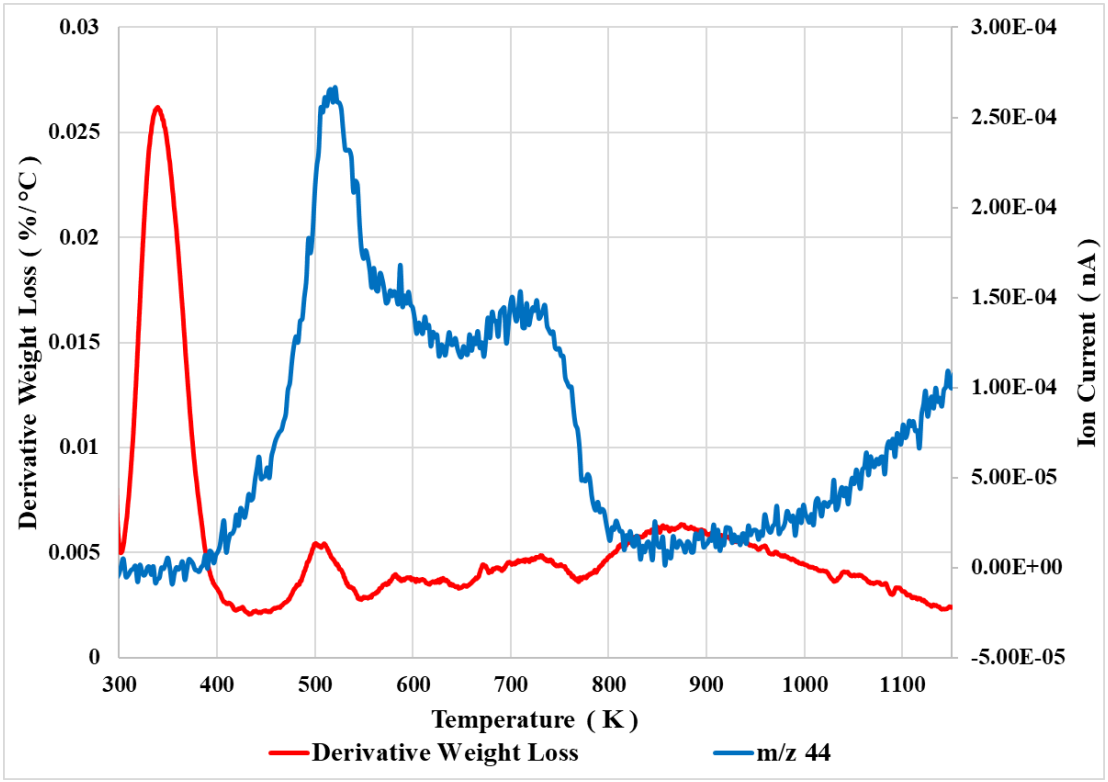

Figure 154. Derivative weight loss coupled with m/z of Rh/SiO_2 catalyst after 3-hour *meta*-cresol hydrogenation reaction.

From Figures 153 and 154 above it can be seen that the catalyst from the three-hour reaction showed an overall weight loss of 5 % with 3 % pertaining to the two high

temperature weight losses confirmed as m/z = 44 (CO_2) from the mass spectrometry data. The initial weight loss event between 290 and 390 K is a result of the evolution of water.

7.2.6.3 *para*-Cresol

The thermal weight loss and associated evolved gas mass spectrometry data for the post *para*-cresol reaction catalyst is shown in Figures 155 and 156 below:

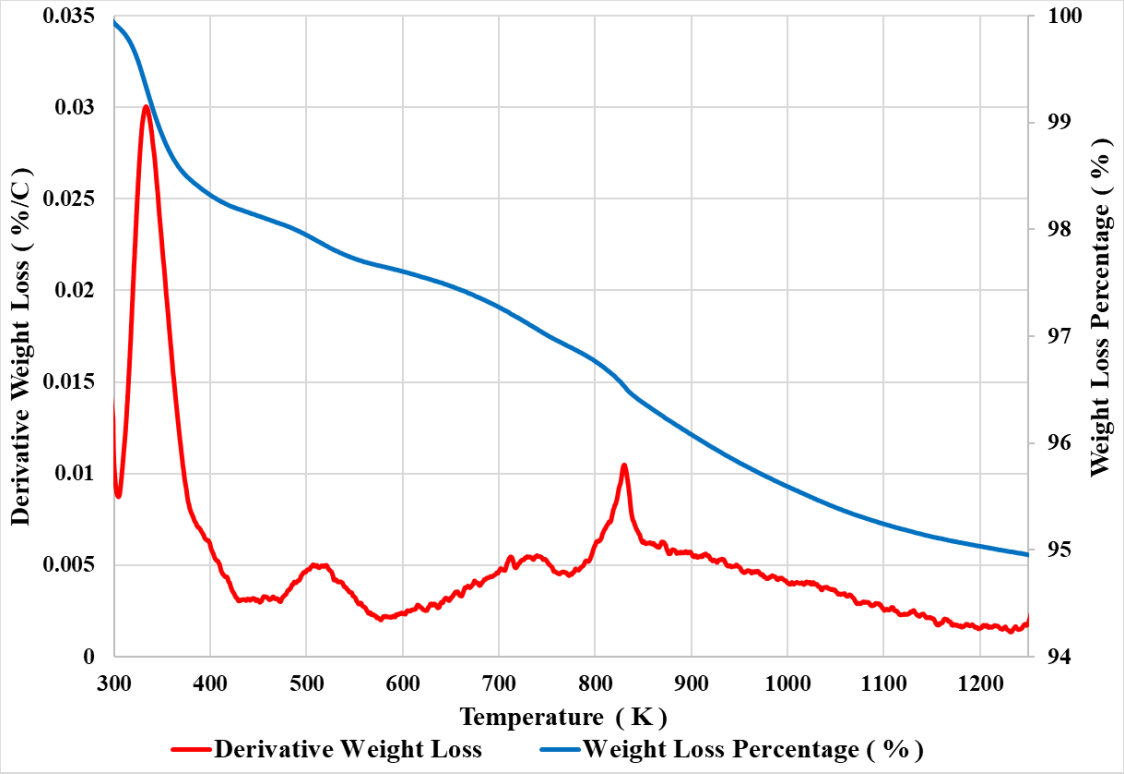

Figure 155. TGA of Rh/SiO_2 catalyst after 3-hour *para*-cresol hydrogenation reaction.

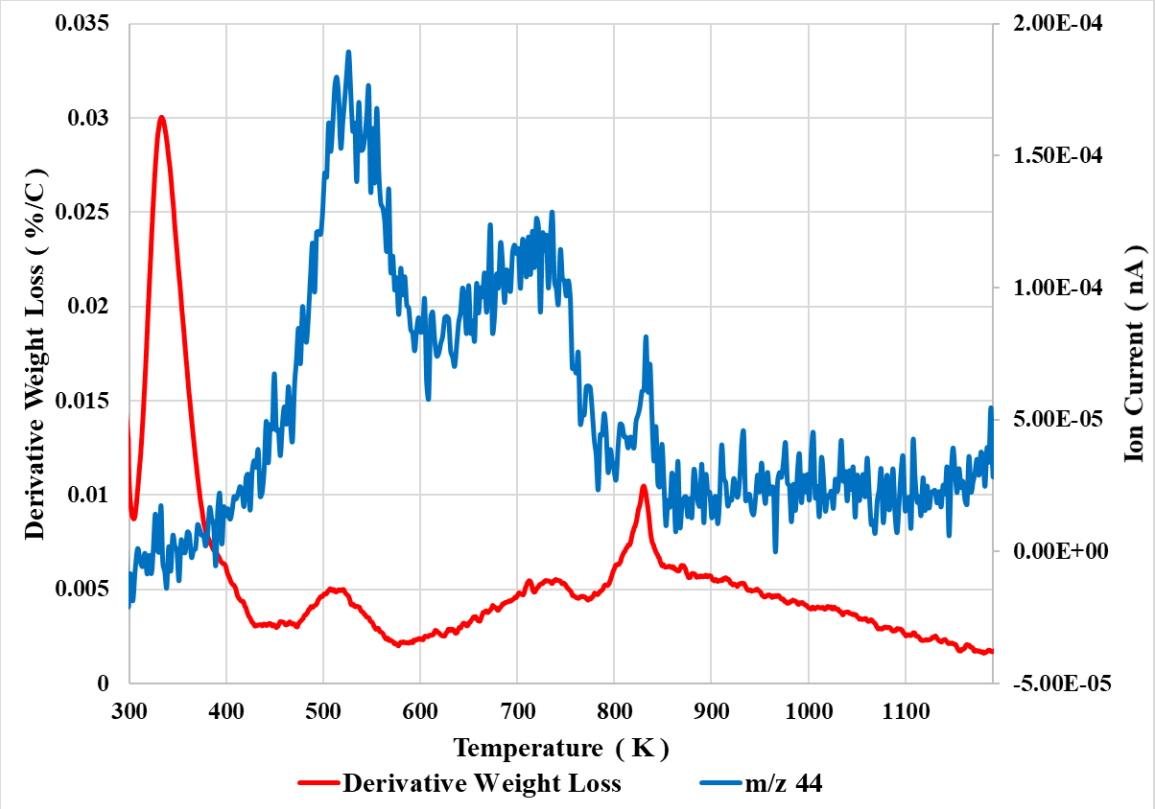

Figure 156. Derivative weight loss coupled with m/z of Rh/SiO_2 catalyst after 3-hour para-cresol hydrogenation reaction.

From Figures 155 and 156 above it can be seen that the catalyst showed an overall weight loss of 5 % with 3 % associated with the three high temperature weight loss events confirmed as m/z = 44 (CO_2) from the mass spectrometry data. The initial weight loss event between 290 and 390 K is a result of the evolution of water.

7.3 Methoxyphenol Isomers

This section contains all results from the methoxyphenol isomers and covers the following sets of reactions: individual hydrogenation of 2,3 and 4-methoxyphenol including temperature variations and competitive hydrogenation reactions where the isomers were reacted in pairs and as a set of three.

7.3.1 Individual Hydrogenation Standard Reactions

In this set of reactions 2,3 and 4-methoxyphenol hydrogenation will be shown at our standard reaction conditions of 323 K, 10 mmol substrate and 3 barg hydrogen. 2-Methoxyphenol is shown below in Figure 157:

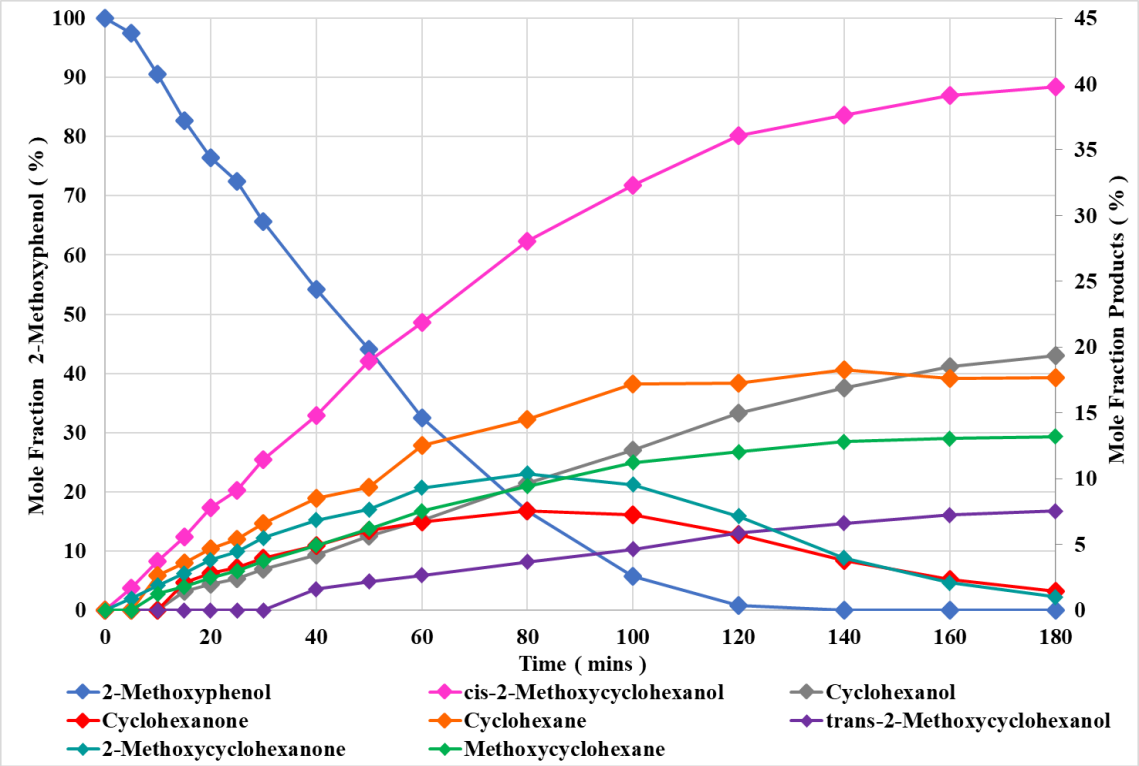

Figure 157. Reaction profile of 2-methoxyphenol hydrogenation. Conditions, 323 K, 10 mmol, 3 barg.

It can be seen that full conversion of 2-methoxyphenol was achieved by ~ 120 minutes. Formation of the two major ring hydrogenated products, *cis*-2-methoxycyclohexanol and 2-methoxycyclohexanone, was observed from the initial stages of the reaction, with the *cis*-2-methoxycyclohexanol the major product by end of reaction. The *trans*-2-methoxycyclohexanol did not form until 40 minutes into the reaction and remained low throughout (<10%). The HDO products, cyclohexanone, cyclohexanol, methoxycyclohexane and cyclohexane, gave a cumulative mole fraction of ~ 52 % by end of reaction.

For 3-methoxyphenol at identical conditions, the reaction profile is shown below in Figure 158:

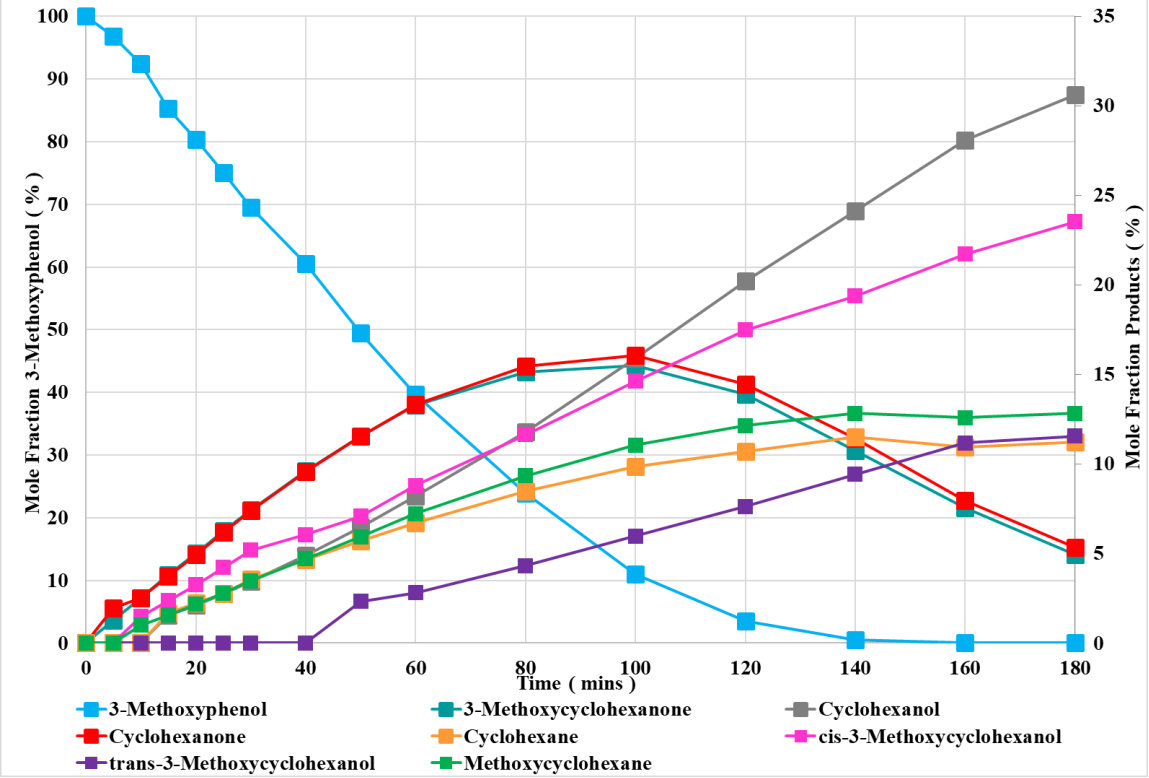

Figure 158. Reaction profile of 3-methoxyphenol hydrogenation. Conditions, 323 K, 10 mmol, 3 barg.

It can be seen that full conversion of 3-methoxyphenol was achieved by ~ 140 minutes. The major products by end of reaction was the HDO product, cyclohexanol, followed by the major ring hydrogenated product, *cis*-3-methoxycyclohexanol. It is evident from Figure 158 that both 3-methoxycyclohexanone and cyclohexanone are behaving as intermediates; a parallel rate of formation for both occurs, achieving ~ 15 % as the two major products by 100 minutes followed by a decline to ~ 5 % by end of reaction with concomitant increases observed for 3-methoxycyclohexanol and cyclohexanol. As seen with the 2-methoxyphenol reaction, *trans*-3-methoxycyclohexanol showed a significant delay in formation; in this instance until 50 minutes. The HDO products, cyclohexanone, cyclohexanol, methoxycyclohexane and cyclohexane, gave a cumulative mole fraction of ~ 60 % by end of reaction.

For 4-methoxyphenol at identical conditions, the reaction profile is shown below in Figure 159:

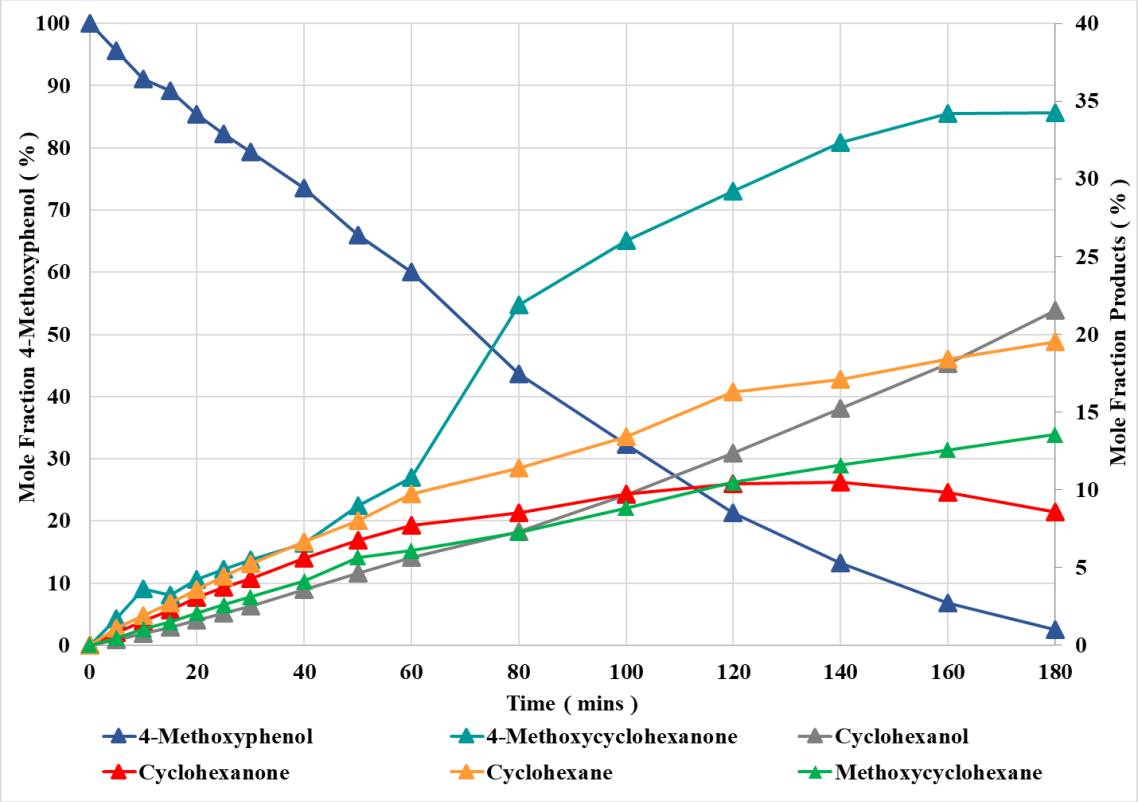

Figure 159. Reaction profile of 4-methoxyphenol hydrogenation. Conditions, 323 K, 10 mmol, 3 barg.

It can be seen that full conversion of 4-methoxyphenol was not achieved by reaction end; the slowest rate of reaction out of the three isomers tested. Of significance, is the absence of both secondary hydrogenated products, *cis*-4-methoxycyclohexanol and *trans*-4-methoxycyclohexanol, from this reaction. The major product at the end of reaction was 4-methoxycyclohexanone, with ~ 35 % mole fraction followed by the HDO product, cyclohexanol with ~20 %. The HDO products, cyclohexanone, cyclohexanol, methoxycyclohexane and cyclohexane, gave a cumulative mole fraction of ~ 63 % by the end of reaction.

7.3.2 Temperature Variations of Methoxyphenol Isomers

7.3.2.1 2-Methoxyphenol Temperature Variations

In this set of reactions, 2-methoxyphenol was hydrogenated at 10 K increments from 303 to 343 K, with 323 K taken as the standard reaction. Hydrogen pressure (3 barg) and reactant concentration (10 mmol) were kept constant to understand the effect temperature had on 2-methoxyphenol hydrogenation. The graphs of these are shown below in increasing order of temperature:

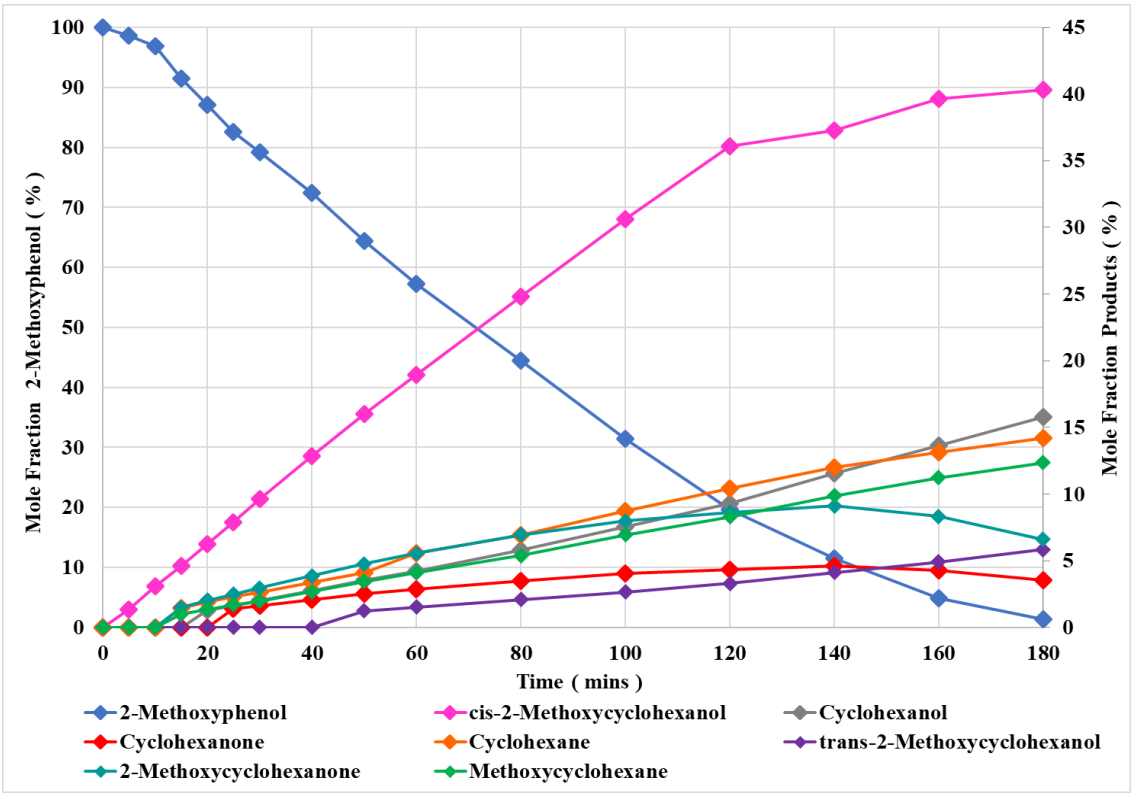

Figure 160. Reaction profile of 2-methoxyphenol hydrogenation. Conditions, 303 K, 10 mmol, 3 barg.

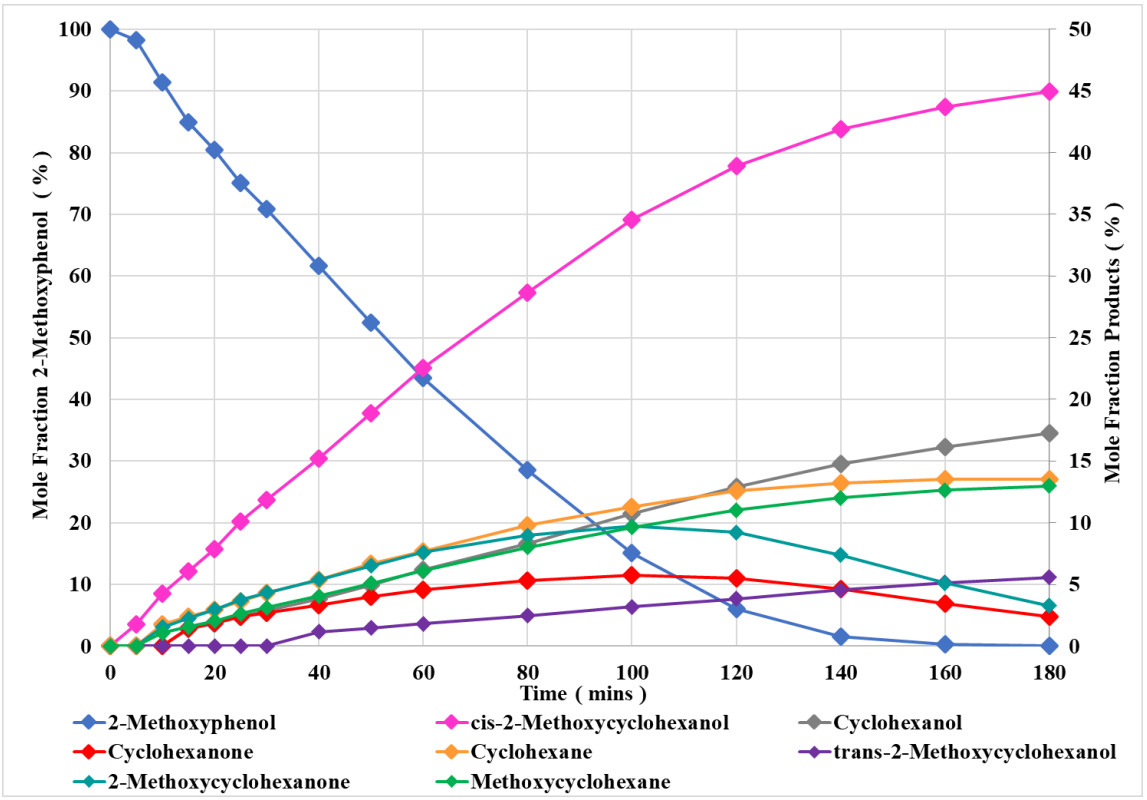

Figure 161. Reaction profile of 2-methoxyphenol hydrogenation. Conditions, 313 K, 10 mmol, 3 barg.

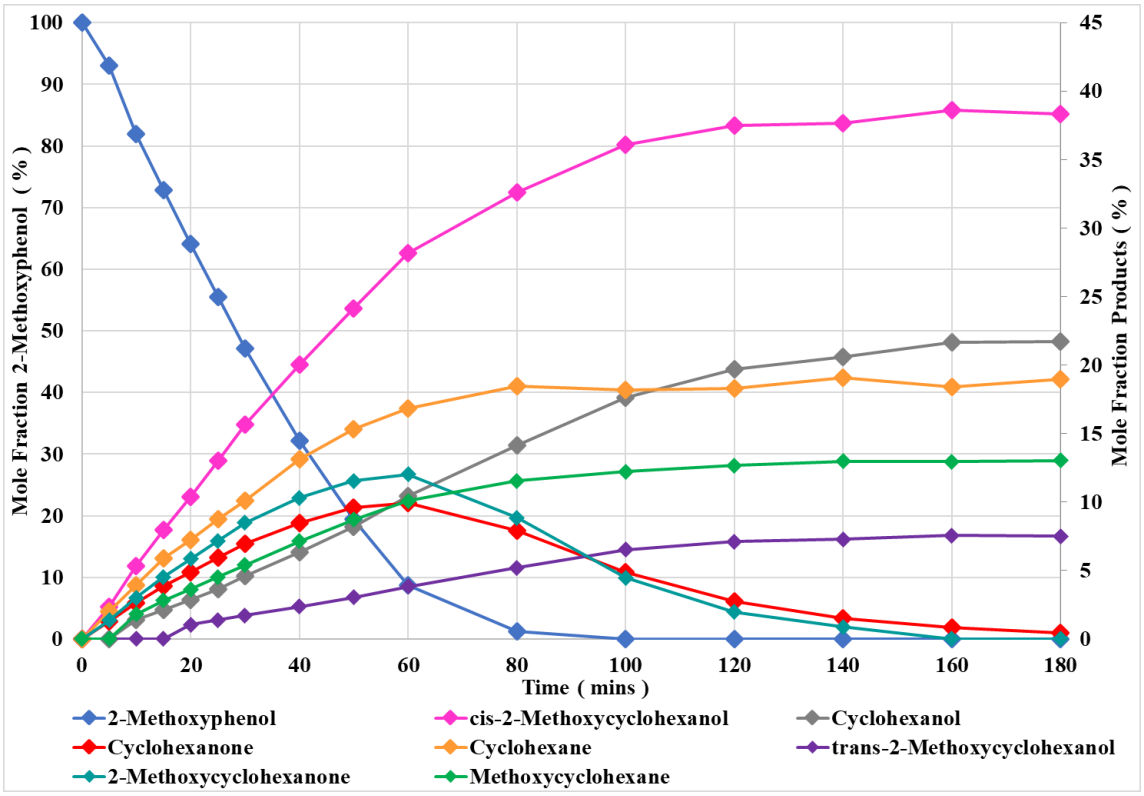

Figure 162. Reaction profile of 2-methoxyphenol hydrogenation. Conditions, 333 K, 10 mmol, 3 barg.

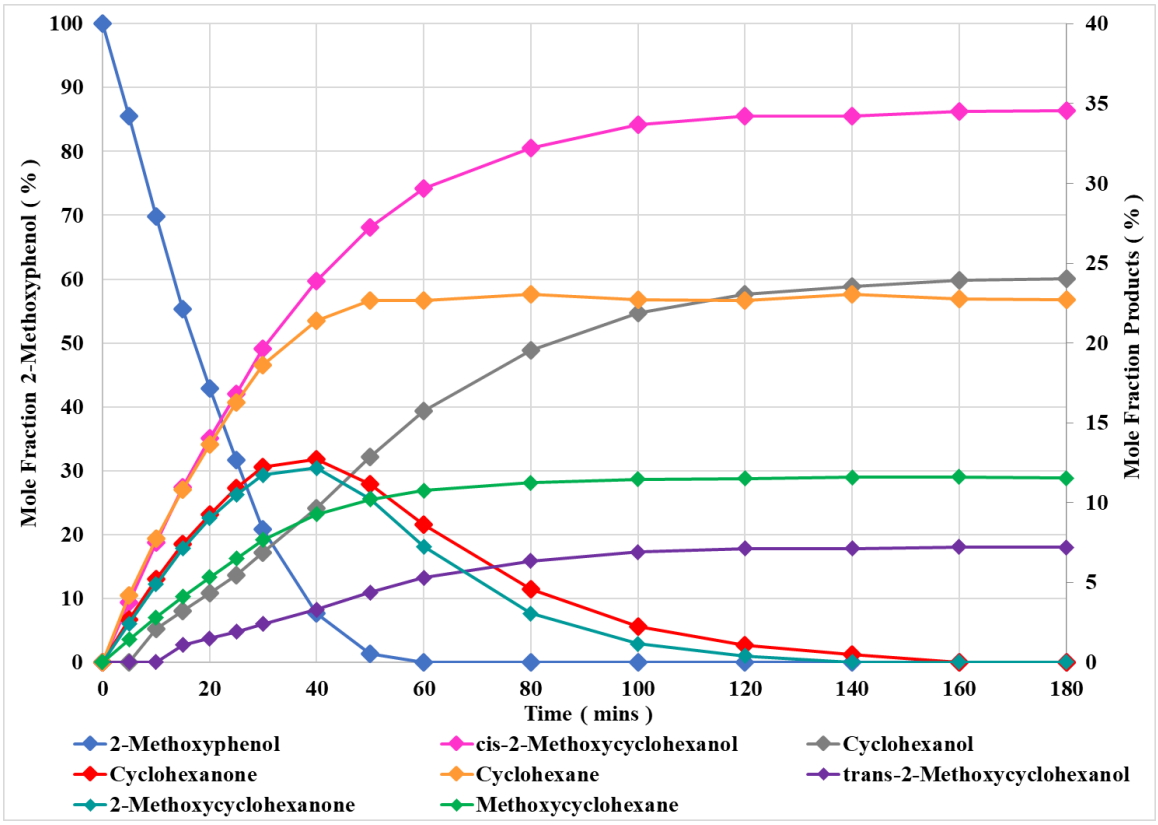

Figure 163. Reaction profile of 2-methoxyphenol hydrogenation. Conditions, 343 K, 10 mmol, 3 barg.

From Figures 160-163 above, it is clear that reaction rate increased with temperature, registering a measured rate constant of 8.5 $x10^{-2}min^{-1}$ at 303 K compared with 42.7 $x10^{-2}min^{-1}$ at 343 K. At 303 K the main product, *cis*-2-methoxycyclohexanol, was formed at ~ 40 % by the end of reaction against ~ 35 % at 343 K, showing a decrease in the formation of this product over the temperature range. The two most favoured HDO products, cyclohexanol and cyclohexane, however, increased with temperature from ~ 15 % to ~ 25 % at the end of reaction over the 40 K measured range. The product distribution of the hydrogenated (*cis*+*trans*-2-methoxycyclohexanol and 2-methoxycyclohexanone) and hydrodeoxygenated (cyclohexanone, cyclohexanol, methoxycyclohexane and cyclohexane) products at ~ 80 % conversion is shown below in Figure 164:

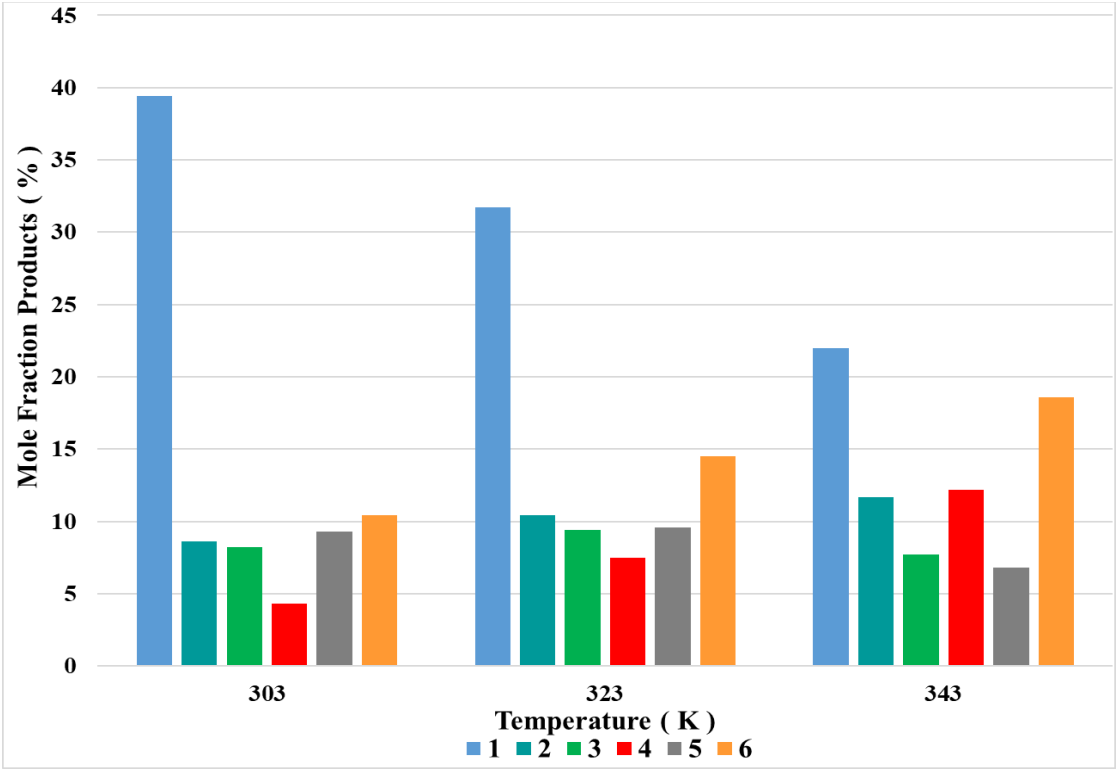

Figure 164. Product distribution at ~ 80 % conversion for 2-methoxyphenol hydrogenation.

Key: 1: cis+trans-2-Methoxycyclohexanol **2:** 2-Methoxycyclohexanone **3:** Methoxycyclohexane **4:** Cyclohexanone **5:** Cyclohexanol **6:** Cyclohexane

It can be seen from Figure 164, that as temperature was increased, formation of the secondary hydrogenated products, *cis*+*trans*-2-methoxycyclohexanol, decreased whilst that of the initial hydrogenated product, 2-methoxycyclohexanone, registered an increase. A similar relationship exists for the HDO products, cyclohexanol and cyclohexanone, with the alcohol decreasing and the ketone increasing with temperature. A significant increase

in formation of the complete HDO product, cyclohexane, occurred over the measured temperature range, doubling from 10 to ~ 20 %. Formation of methoxycyclohexane remained relatively stable with temperature. The relationship between temperature and conversion of 2-methoxyphenol is shown below in Figure 165:

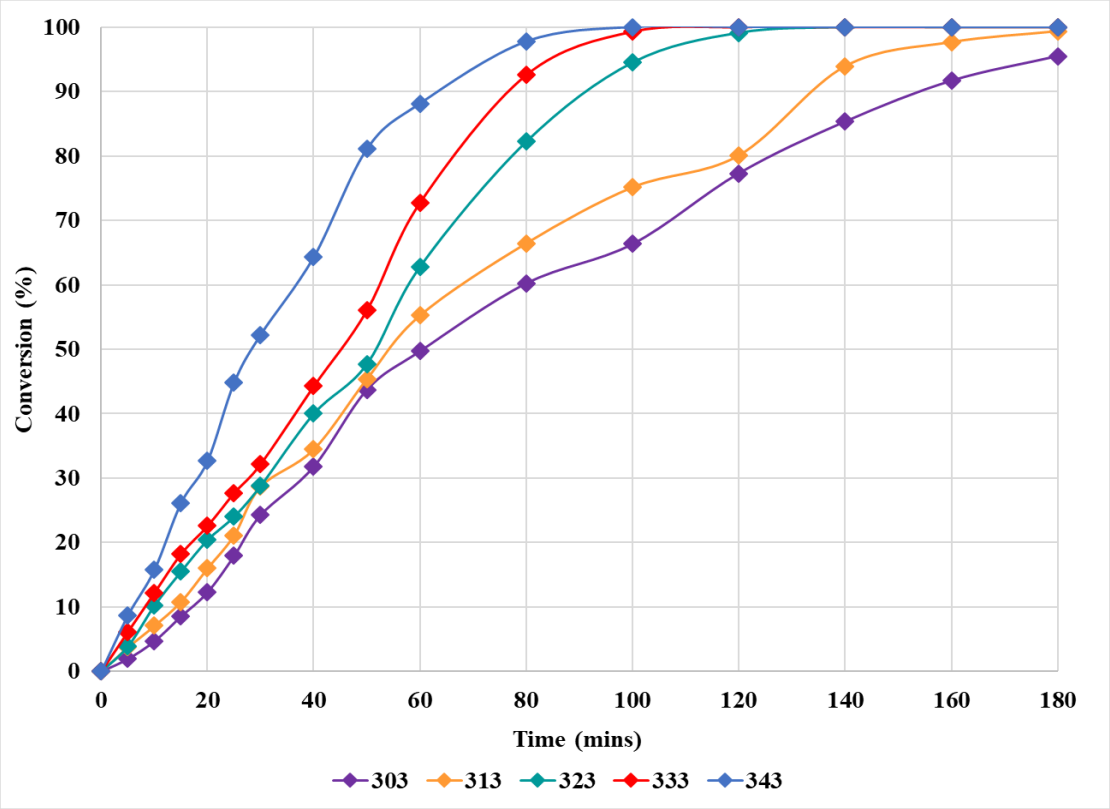

Figure 165. Temperature effect on 2-methoxyphenol conversion.

It can be seen from Figure 165 that an increase in temperature resulted in an increase in 2-methoxyphenol conversion, with full conversion by ~ 100 minutes at 343 K against ~ 95 % at the end of reaction for 303 K.

For each temperature reaction the rate constant was calculated and an example of this, at 323 K, is shown below in Figure 166:

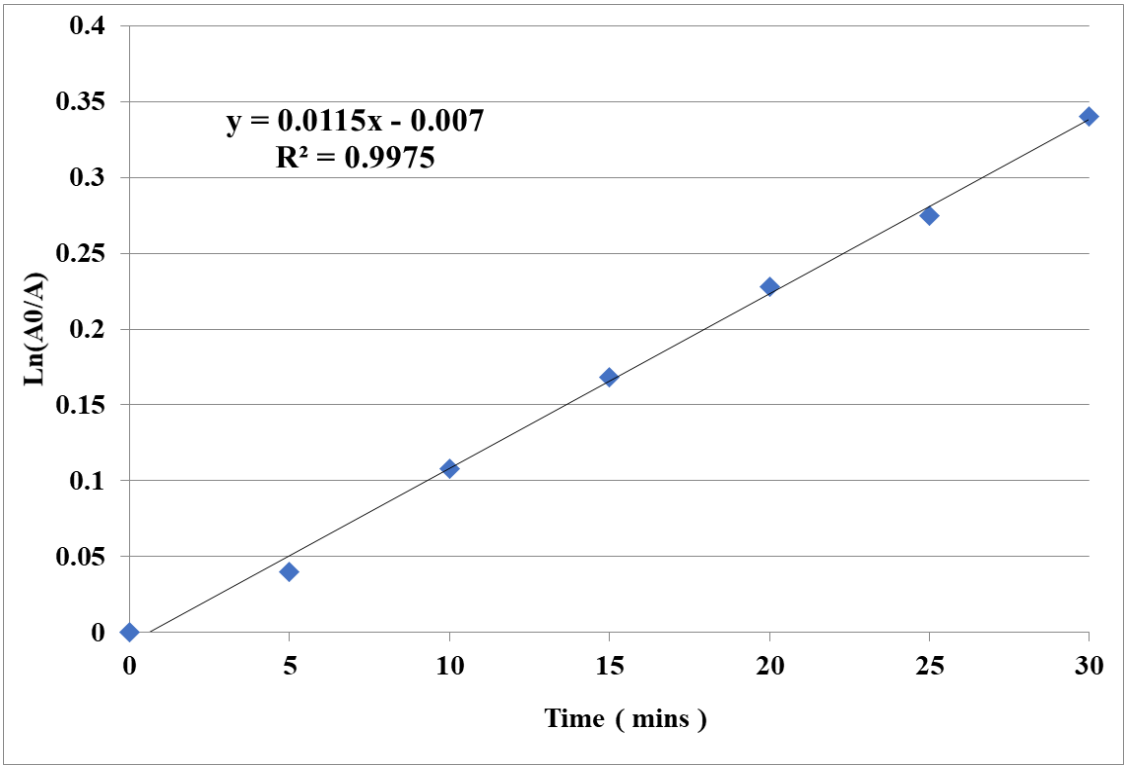

Figure 166. Rate constant graph for 2-methoxyphenol hydrogenation at 323 K.

From the integrated form of the Arrhenius equation shown in Equation 7 of the Experimental Section, ln k was plotted against ($\frac{1}{T}$) using the values in Table 27 below:

Table 27. Summary of data for activation energy.

Temperature (K)	k ($x10^{-3}min^{-1}$)	1/T (x- axis)	Ln k (y-axis)
303	8.5	0.00319	-4.7676
313	11.4	0.00309	-4.4741
333	25.7	0.00300	-3.6612
343	42.7	0.00291	-3.1535

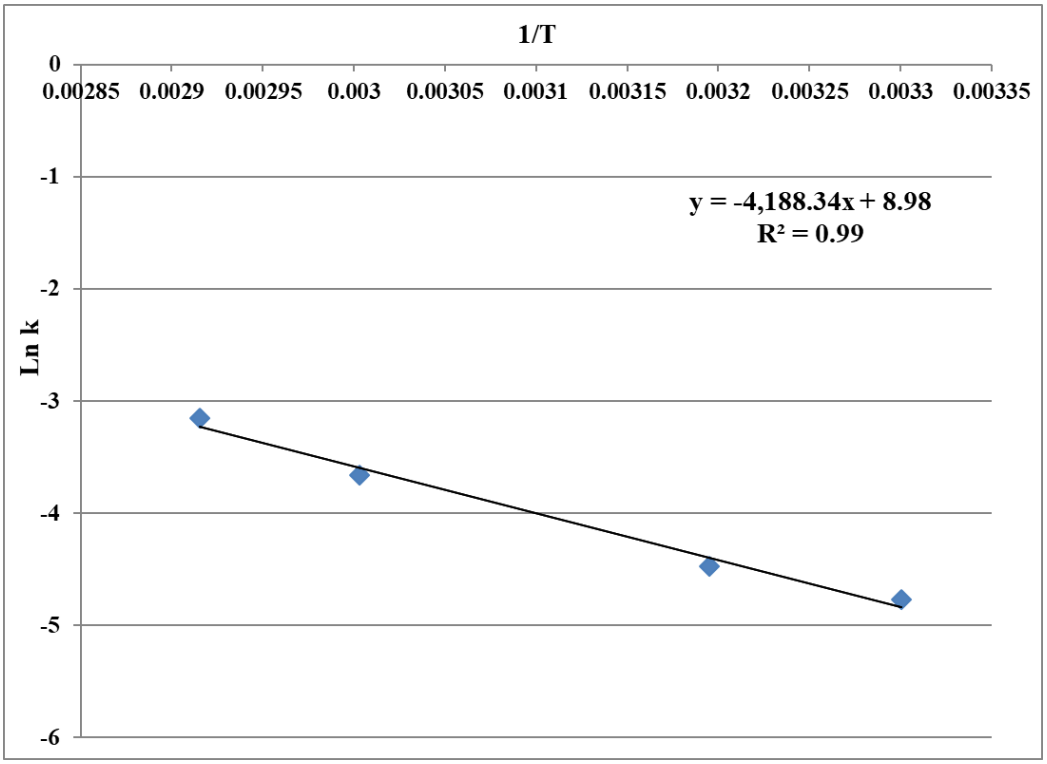

Figure 167. Activation energy plot for 2-methoxyphenol hydrogenation.

Therefore, the gradient of ln k against 1/T equals $-\frac{Ea}{RT}$ and can be expressed for Ea as:

- Ea= -mR
- -(-4188.3*8.314)/1000
- = 34.8 kJmol^{-1}

From this, an overall activation energy for 2-methoxyphenol hydrogenation of 34.8 kJmol^{-1} was measured.

7.3.2.2 3-Methoxyphenol Temperature Variations

In this set of reactions, 3-methoxyphenol was hydrogenated at 10 K increments from 303 to 343 K, with 323 K taken as the standard reaction. Hydrogen pressure (3 barg) and reactant concentration (10 mmol) were kept constant to understand the effect temperature had on 3-methoxyphenol hydrogenation. The graphs of these are shown below in increasing order of temperature:

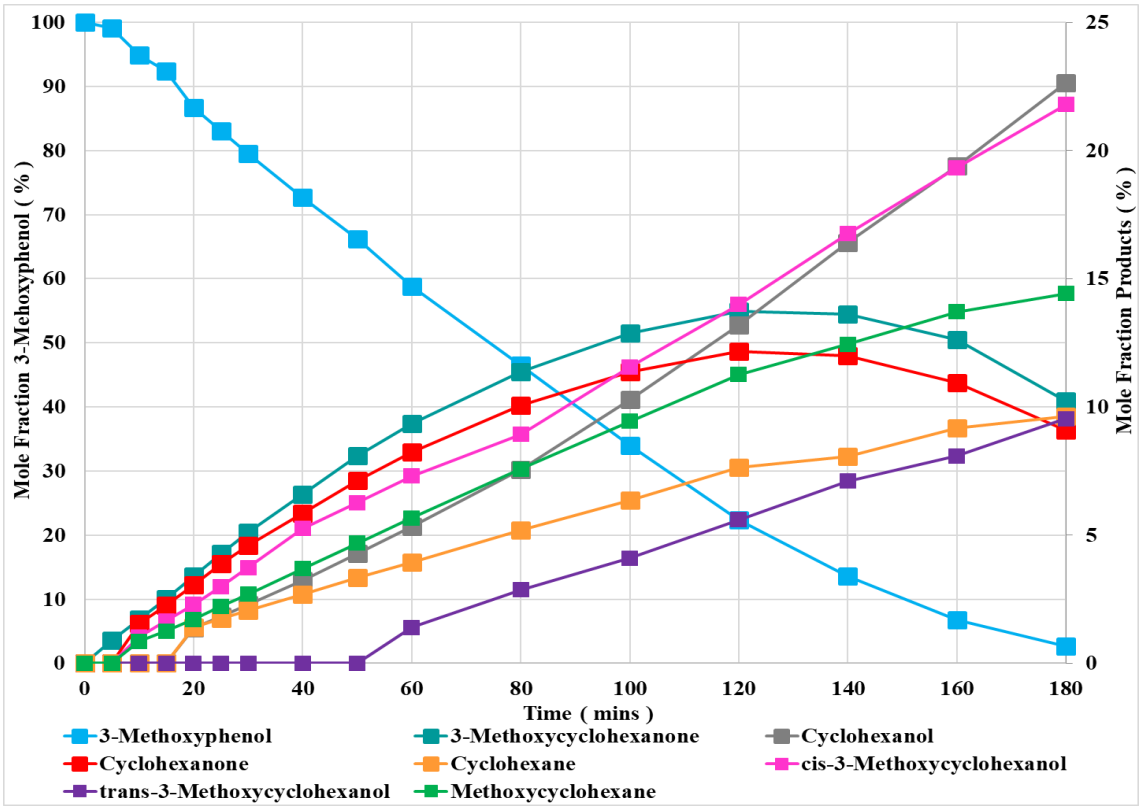

Figure 168. Reaction profile of 3-methoxyphenol hydrogenation. Conditions, 303 K, 10 mmol, 3 barg.

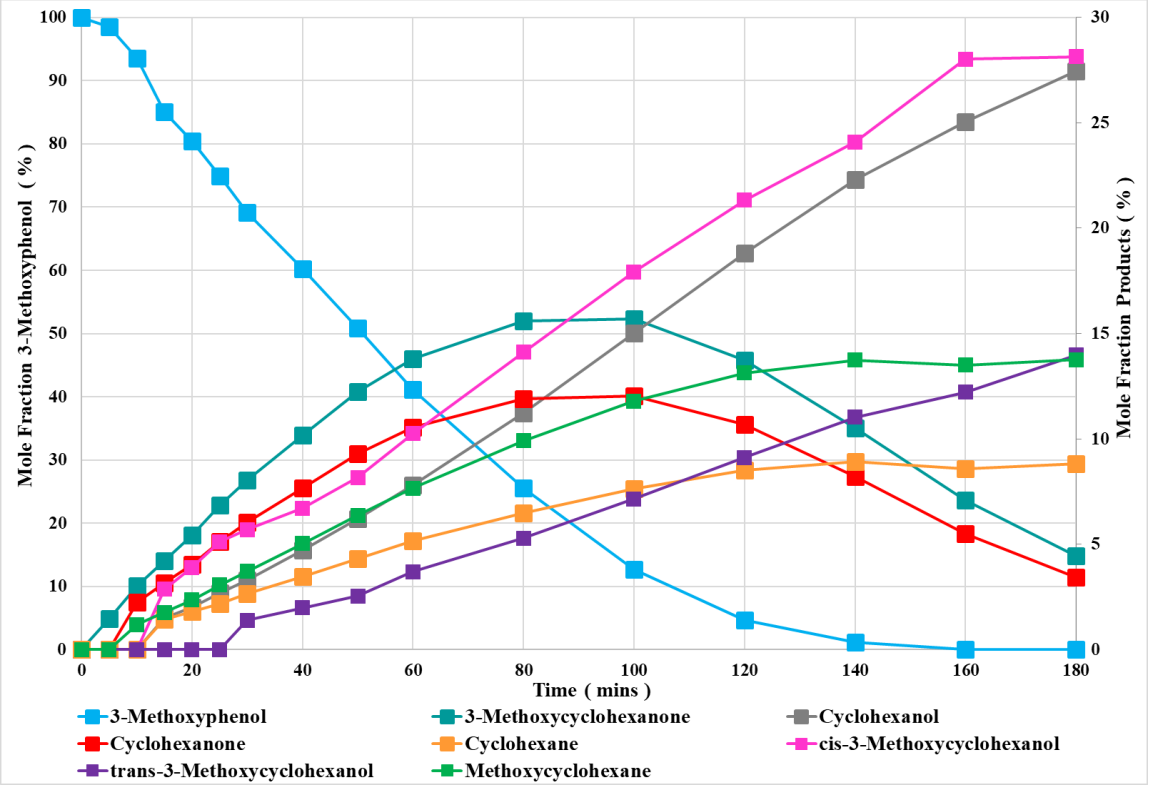

Figure 169. Reaction profile of 3-methoxyphenol hydrogenation. Conditions, 313 K, 10 mmol, 3 barg.

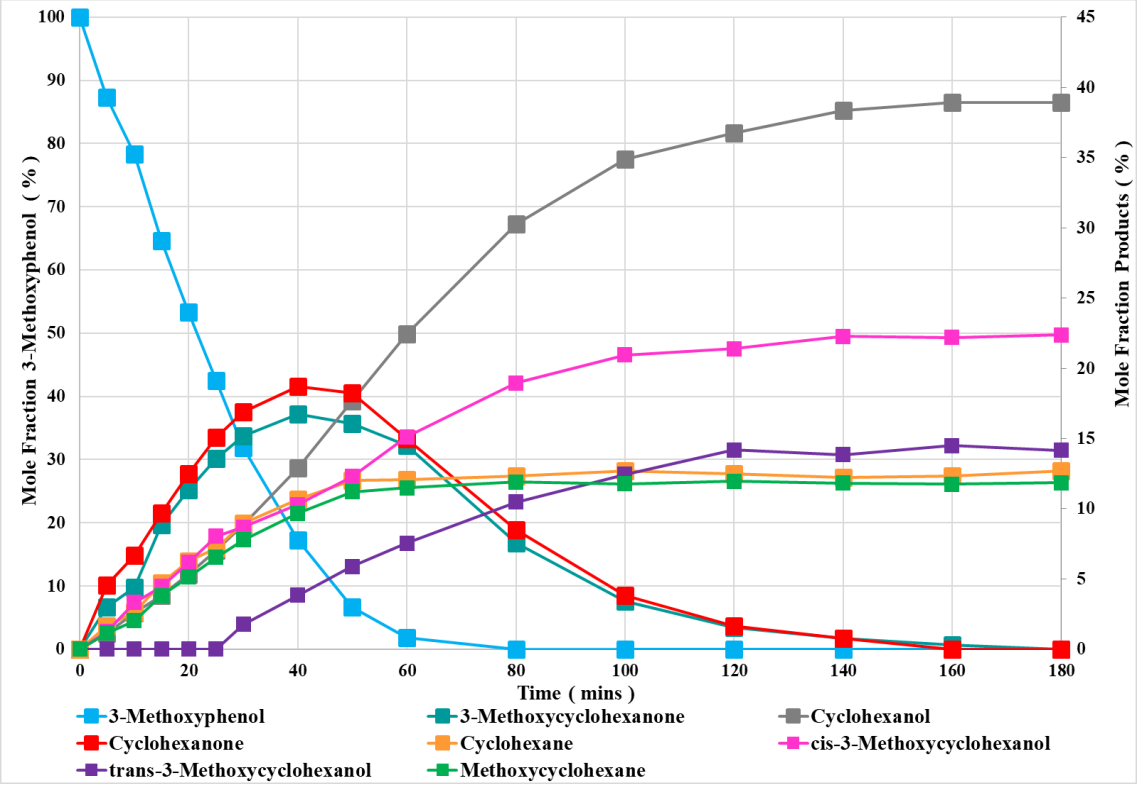

Figure 170. Reaction profile of 3-methoxyphenol hydrogenation. Conditions, 333 K, 10 mmol, 3 barg.

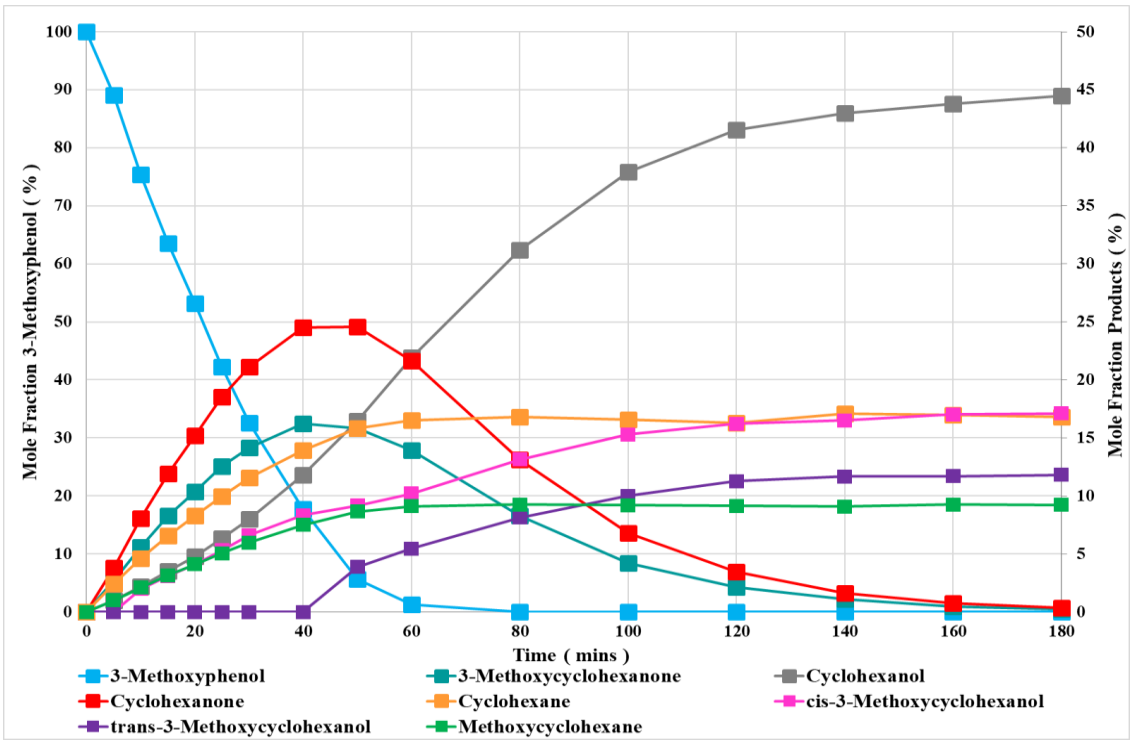

Figure 171. Reaction profile of 3-methoxyphenol hydrogenation. Conditions, 343 K, 10 mmol, 3 barg.

From Figures 168-171 above, it is clear that reaction rate increased with temperature, with a measured rate constant of 8.5 x$10^{-2}$$min^{-1}$ at 303 K compared with 42.7 x$10^{-2}$$min^{-1}$ at 343

K. At 303 K the main product, *cis*-3-methylcyclohexanol, at end of reaction registered a mole fraction of ~ 40 % compared with ~ 35 % at 343 K, showing a decrease in the formation of this product over the temperature range. Both major HDO products, cyclohexanol and cyclohexane showed an increase with temperature from ~ 15 % to ~ 25 % at the end of reaction over the 40 K measured range. The product distribution of the hydrogenated (*cis*+*trans*-3-methoxycyclohexanol and 3-methoxycyclohexanone) and hydrodeoxygenated (cyclohexanone, cyclohexanol, methoxycyclohexane and cyclohexane) products at ~ 80 % conversion is shown below in Figure 172:

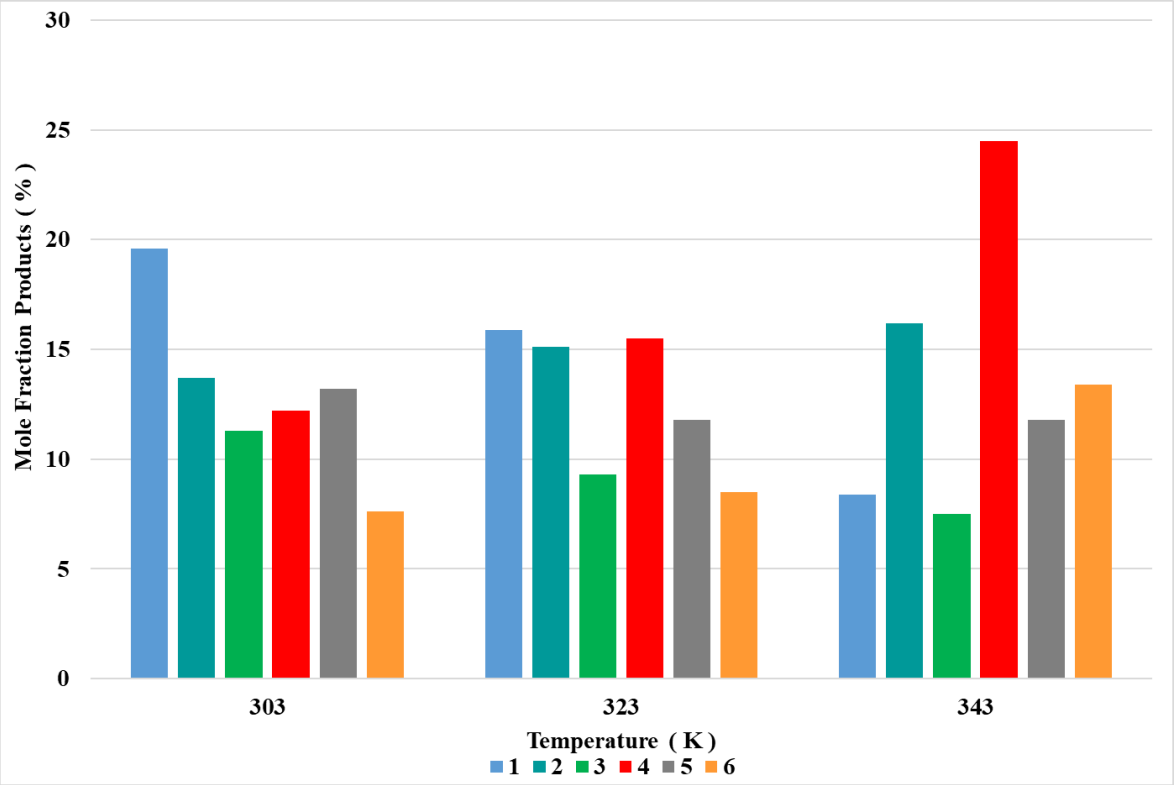

Figure 172. Product distribution at ~ 80 % conversion for 3-methoxyphenol hydrogenation.

Key: 1: cis+trans-3-Methoxycyclohexanol **2:** 3-Methoxycyclohexanone **3:** Methoxycyclohexane **4:** Cyclohexanone **5:** Cyclohexanol **6:** Cyclohexane

It can be seen from Figure 172 that as temperature was increased formation of the secondary hydrogenated products, *cis*+*trans*-3-methoxycyclohexanol, decreased whilst that of the initial hydrogenated product, 3-methoxycyclohexanone, increased. The HDO product, cyclohexanol, exhibited a decrease with temperature, with a concomitant increase in formation of cyclohexanone observed. Formation of methoxycyclohexane decreased over the temperature range, whilst cyclohexane increased. The relationship between temperature and conversion of 3-methoxyphenol is shown below in Figure 173:

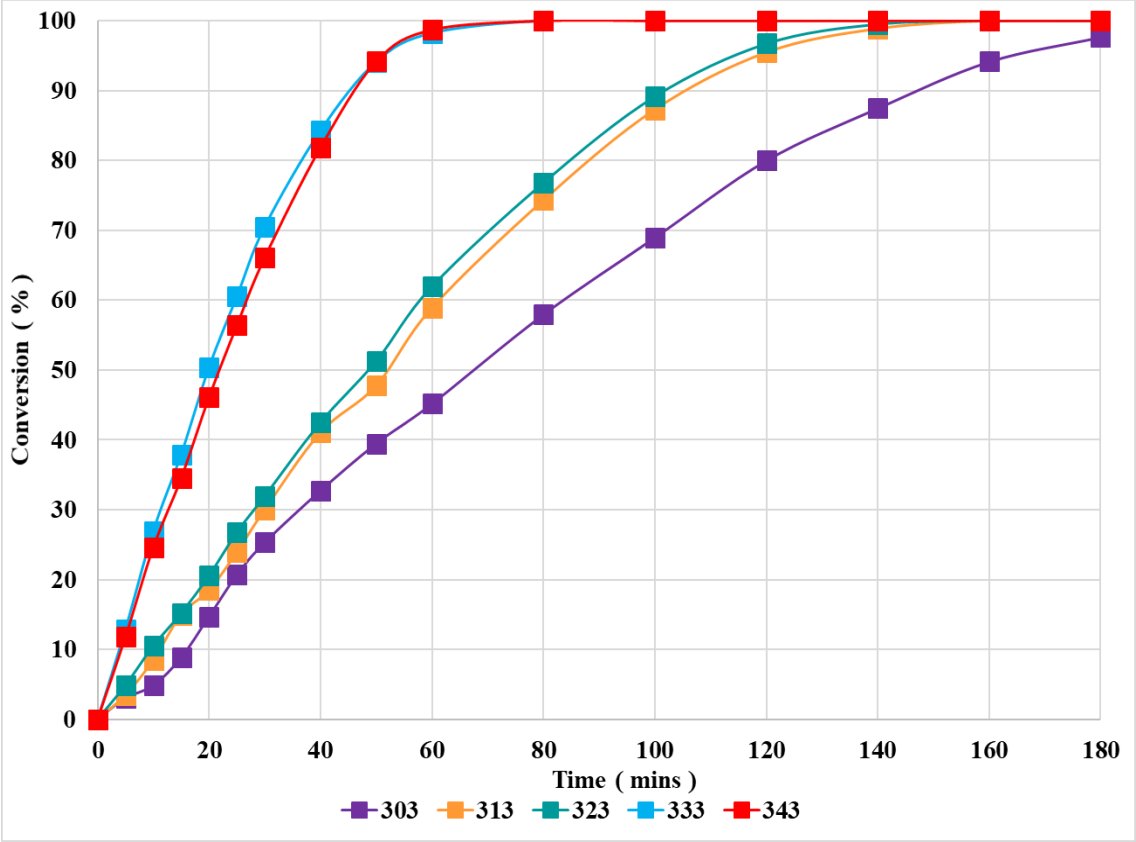

Figure 173. Temperature effect on 3-methoxyphenol conversion.

It can be seen from Figure 173 that an increase in temperature resulted in an increase in 3-methoxyphenol conversion, with full conversion by ~ 60 minutes at 333 and 343 K against ~ 96 % at the end of reaction for 303 K.

For each temperature reaction the rate constant was calculated and an example of this, at 323 K, is shown below in Figure 174:

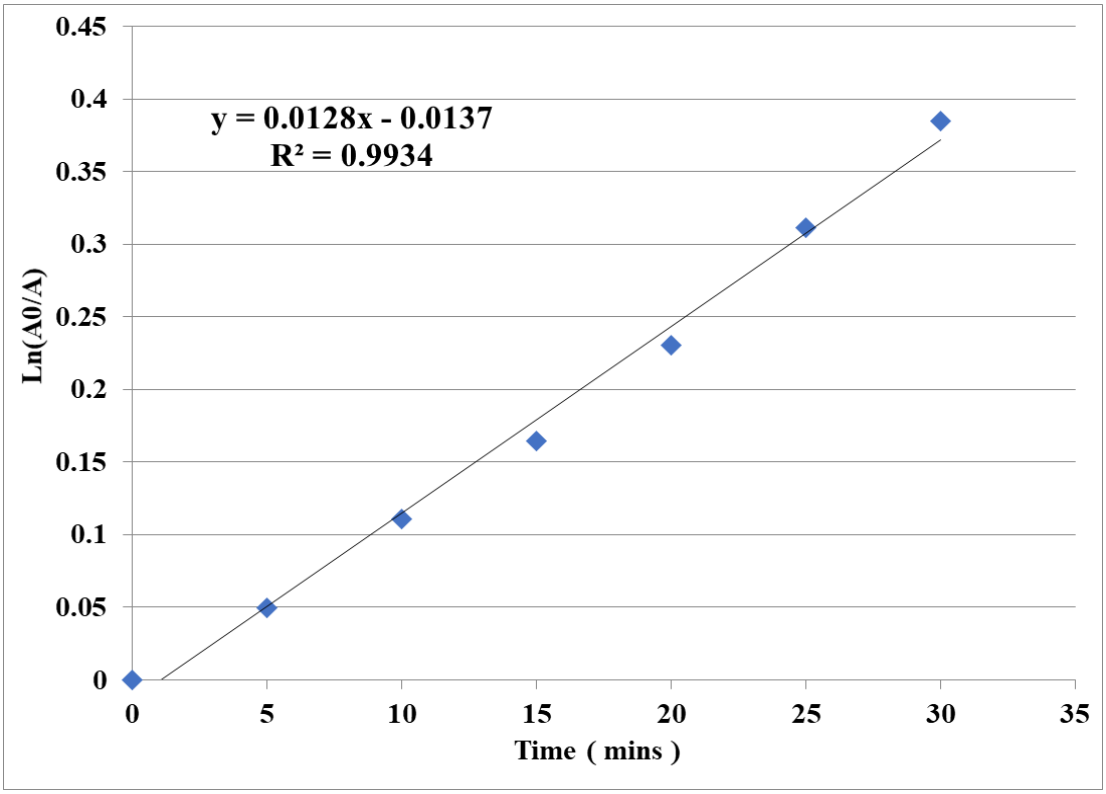

Figure 174. Rate constant graph for 3-methoxyphenol hydrogenation at 323 K.

From the integrated form of the Arrhenius equation shown in Equation 7 of the Experimental Section, ln k was plotted against ($\frac{1}{T}$) using the values in Table 28 below:

Table 28. Summary of data for activation energy.

Temperature (K)	k (x10^{-3}min^{-1})	1/T (x- axis)	Ln k (y-axis)
303	9.1	0.00319	-4.7676
313	11.1	0.00309	-4.4741
333	37.1	0.00300	-3.6612

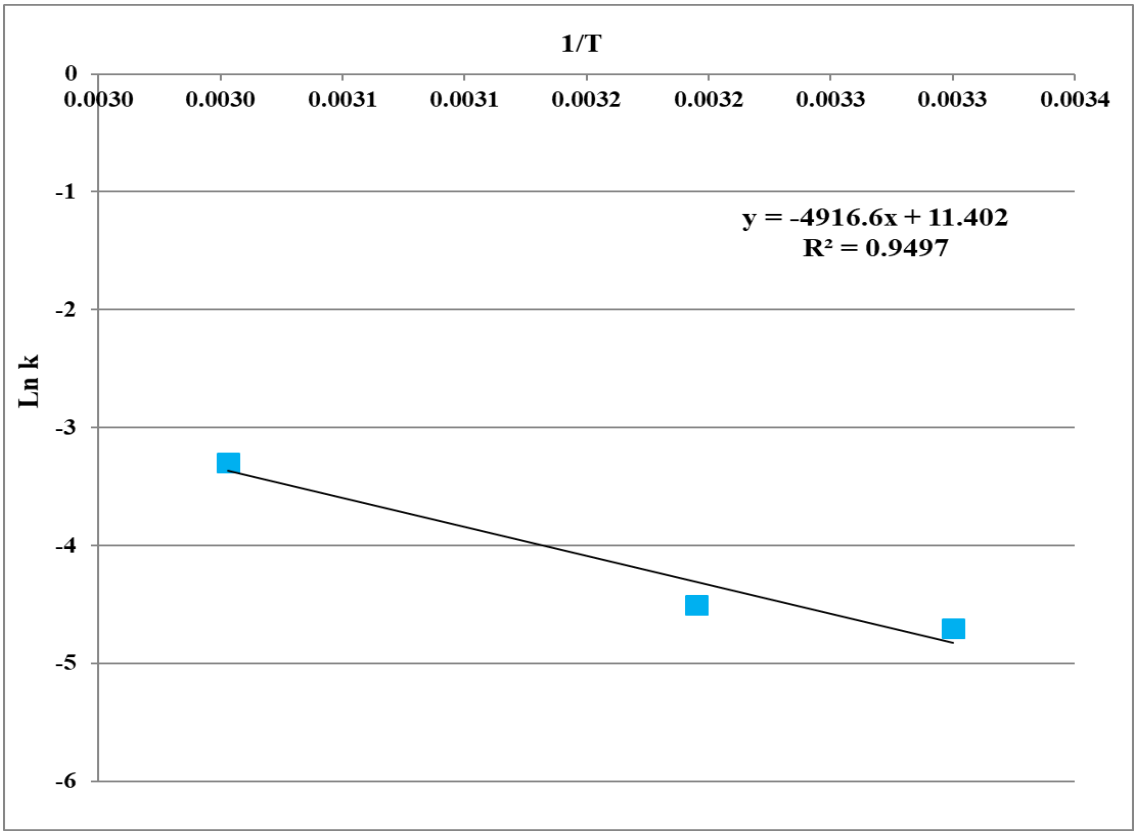

Figure 175. Activation energy plot for 3-methoxyphenol hydrogenation.

Therefore, the gradient of ln k against 1/T equals $-\frac{Ea}{RT}$ and can be expressed for Ea as:

- Ea= -mR
- -(-4916.6*8.314)/1000
- = 40.9 kJmol^{-1}

From this, an overall activation energy for 3-methoxyphenol hydrogenation of 40.9 kJmol^{-1} was measured.

7.3.2.3 4-Methoxyphenol Temperature Variations

In this set of reactions, 4-methoxyphenol was hydrogenated at 10 K increments from 303 to 343 K, with 323 K taken as the standard reaction. Hydrogen pressure (3 barg) and reactant concentration (10 mmol) were kept constant to understand the effect temperature had on 4-methoxyphenol hydrogenation. The graphs of these are shown below in increasing order of temperature:

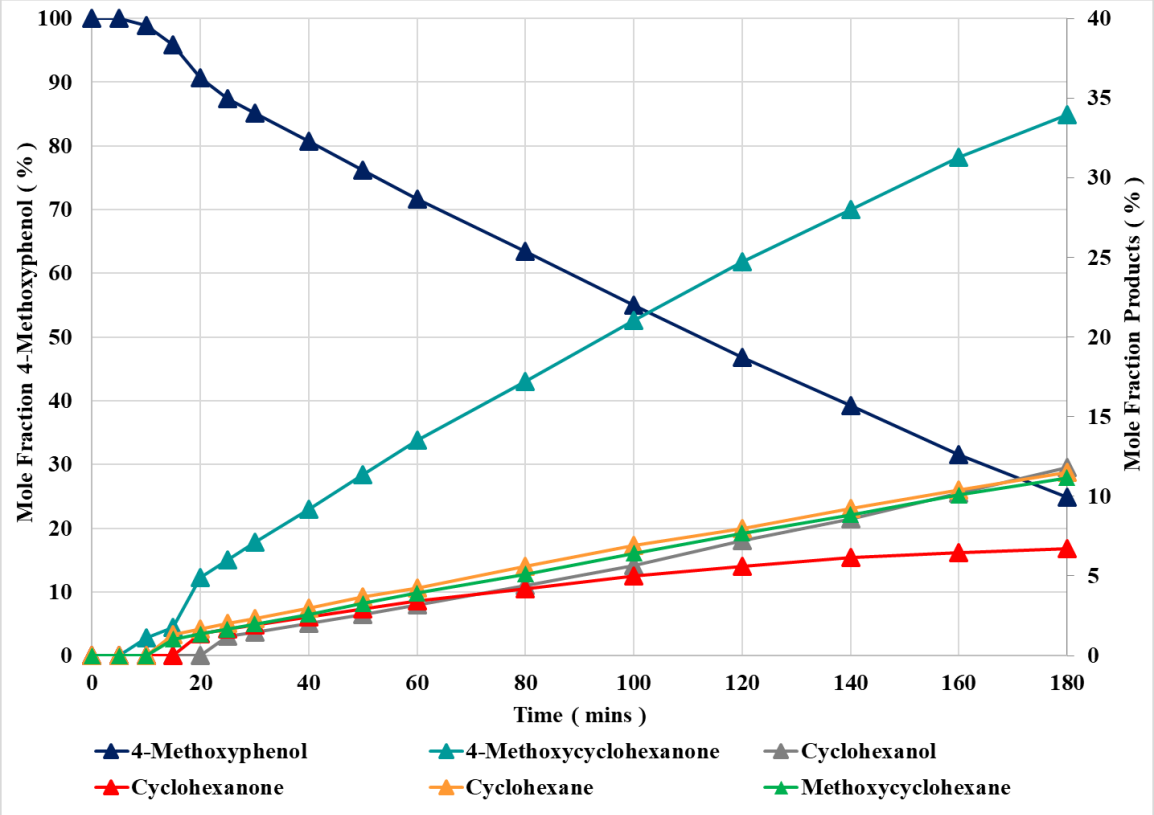

Figure 176. Reaction profile of 4-methoxyphenol hydrogenation. Conditions, 303 K, 10 mmol, 3 barg.

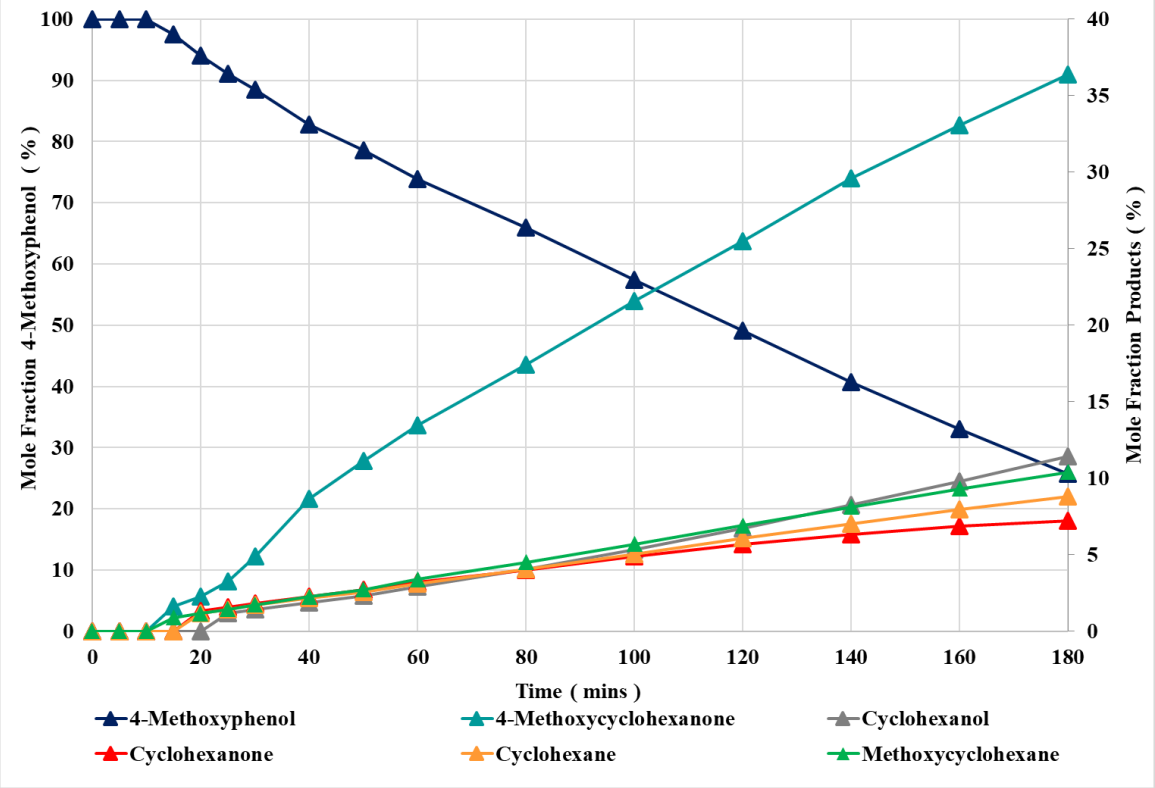

Figure 177. Reaction profile of 4-methoxyphenol hydrogenation. Conditions, 313 K, 10 mmol, 3 barg.

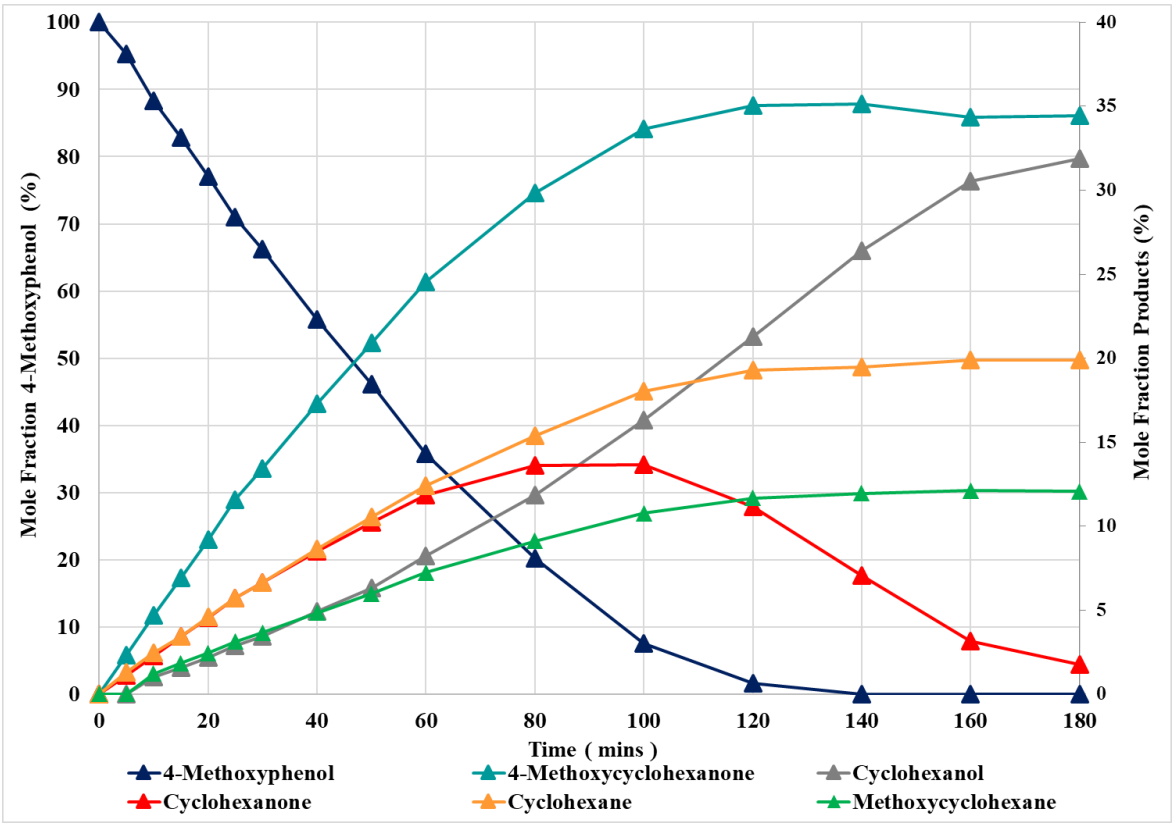

Figure 178. Reaction profile of 4-methoxyphenol hydrogenation. Conditions, 333 K, 10 mmol, 3 barg.

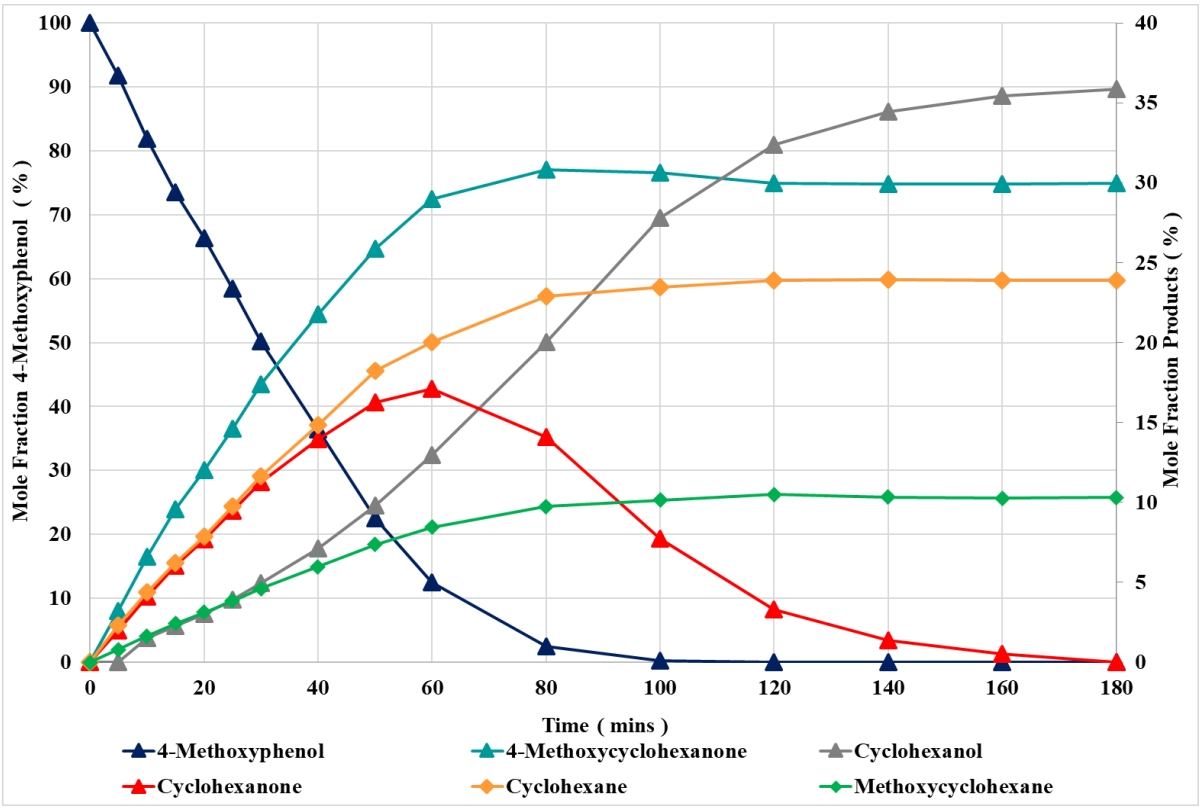

Figure 179. Reaction profile of 4-methoxyphenol hydrogenation. Conditions, 343 K, 10 mmol, 3 barg.

From Figures 176-179 above, it is clear that reaction rate increased with temperature with a measured rate constant of 7.3 x$10^{-2}$$min^{-1}$ at 303 K compared with 24.2 x$10^{-2}$$min^{-1}$ at 343 K. A significant increase in the formation of the HDO products, cyclohexanol and cyclohexane, was observed from ~10 % at 303 K to > 25 % at 343 K, where cyclohexanol was the major product by end of reaction. The initial hydrogenated product, 4-methoxycyclohexanone, decreased in formation over the temperature range. It is of note that as a result of full consumption of the aromatic at the higher temperatures – 333 and 343 K – 4-methoxycyclohexanone exhibits a plateau affect. The product distribution of the hydrogenated (4-methoxycyclohexanone) and hydrodeoxygenated (cyclohexanone, cyclohexanol, methoxycyclohexane and cyclohexane) products at ~ 80 % conversion is shown below in Figure 180:

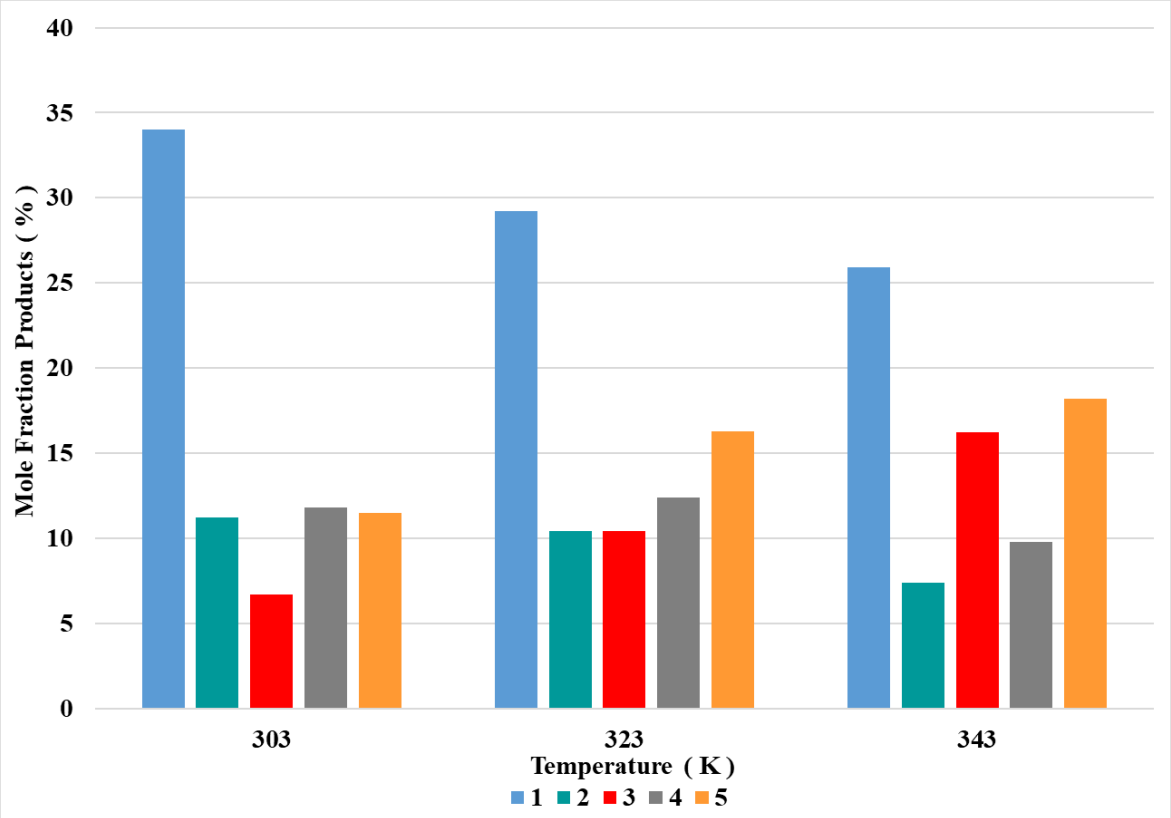

Figure 180. Product distribution at ~ 80 % conversion for 4-methoxyphenol hydrogenation.

Key: 1: 4-Methoxycyclohexanone **2:** Methoxycyclohexane **3:** Cyclohexanone **4:** Cyclohexanol **5:** Cyclohexane

It can be seen from Figure 180 that as temperature was increased formation of the initial hydrogenated product, 4-methoxycyclohexanone, decreased. Analysis of the HDO products show cyclohexanone and cyclohexane increased over the temperature range

whilst methoxycyclohexane and cyclohexanol decreased. The relationship between temperature and conversion of 4-methoxyphenol is shown below in Figure 181:

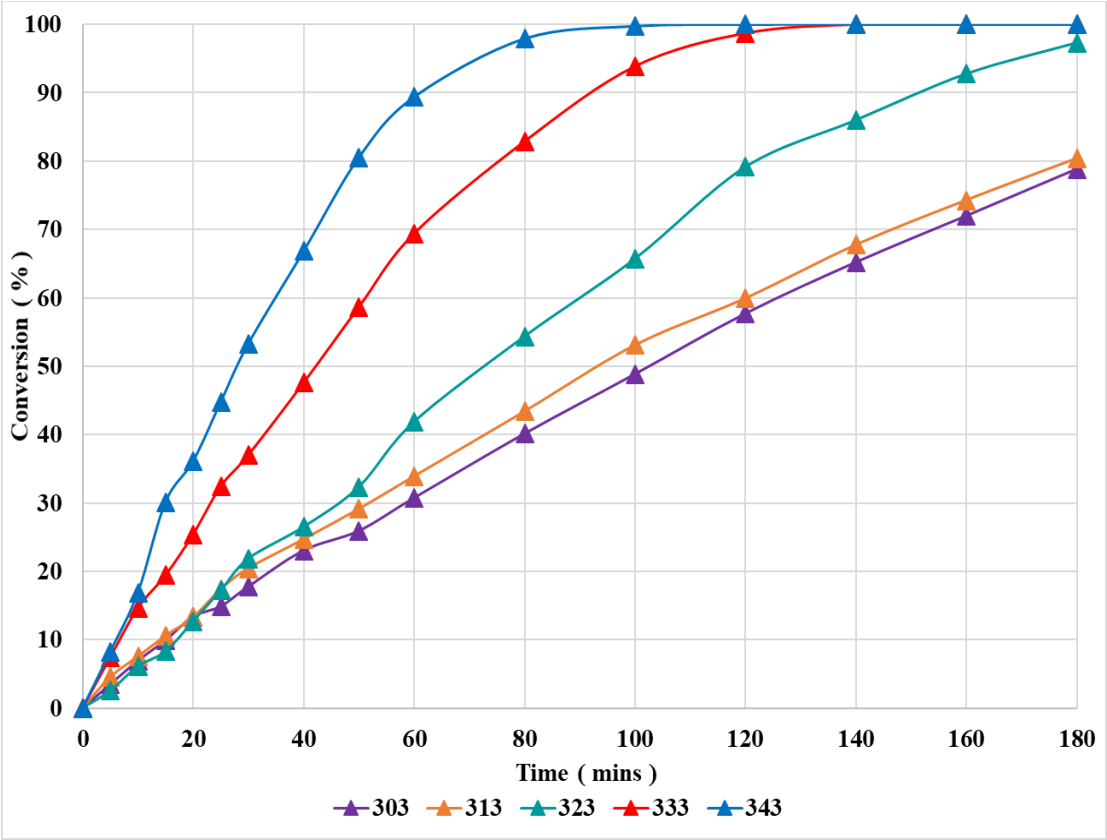

Figure 181. Temperature effect on 4-methoxyphenol conversion.

It can be seen from Figure 181 that an increase in temperature resulted in an increase in 4-methoxyphenol conversion, with full conversion by ~ 100 minutes at 343 K against ~ 80 % at the end of reaction for 303 and 313 K.

For each temperature reaction, the rate constant was calculated and an example of this, at 343 K, is shown below in Figure 182:

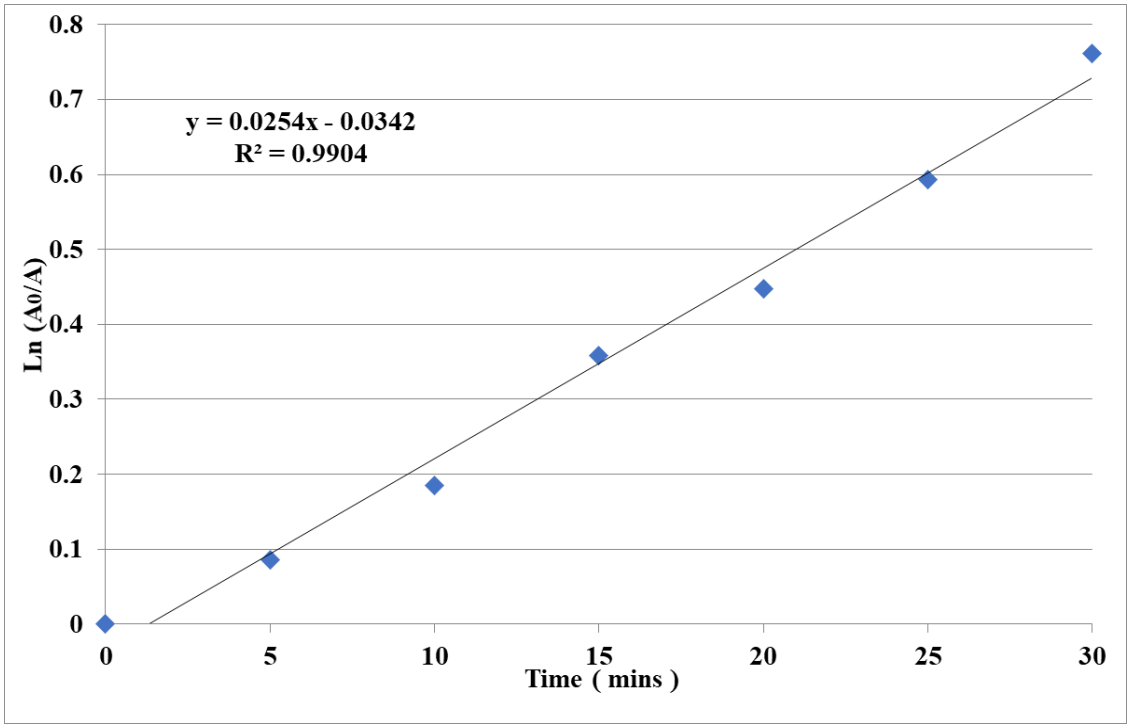

Figure 182. Rate constant graph for 4-methoxyphenol hydrogenation at 343 K.

From the integrated form of the Arrhenius equation shown in Equation 7 of the Experimental Section, ln k was plotted against ($\frac{1}{T}$) using the values in Table 29 below:

Table 29. Summary of data for 4-methoxyphenol activation energy.

Temperature (K)	k (x$10^{-3}$$min^{-1}$)	1/T (x- axis)	Ln k (y-axis)
313	9.1	0.00319	-5.0206
333	11.1	0.00300	-4.1864
343	37.1	0.00291	-3.7214

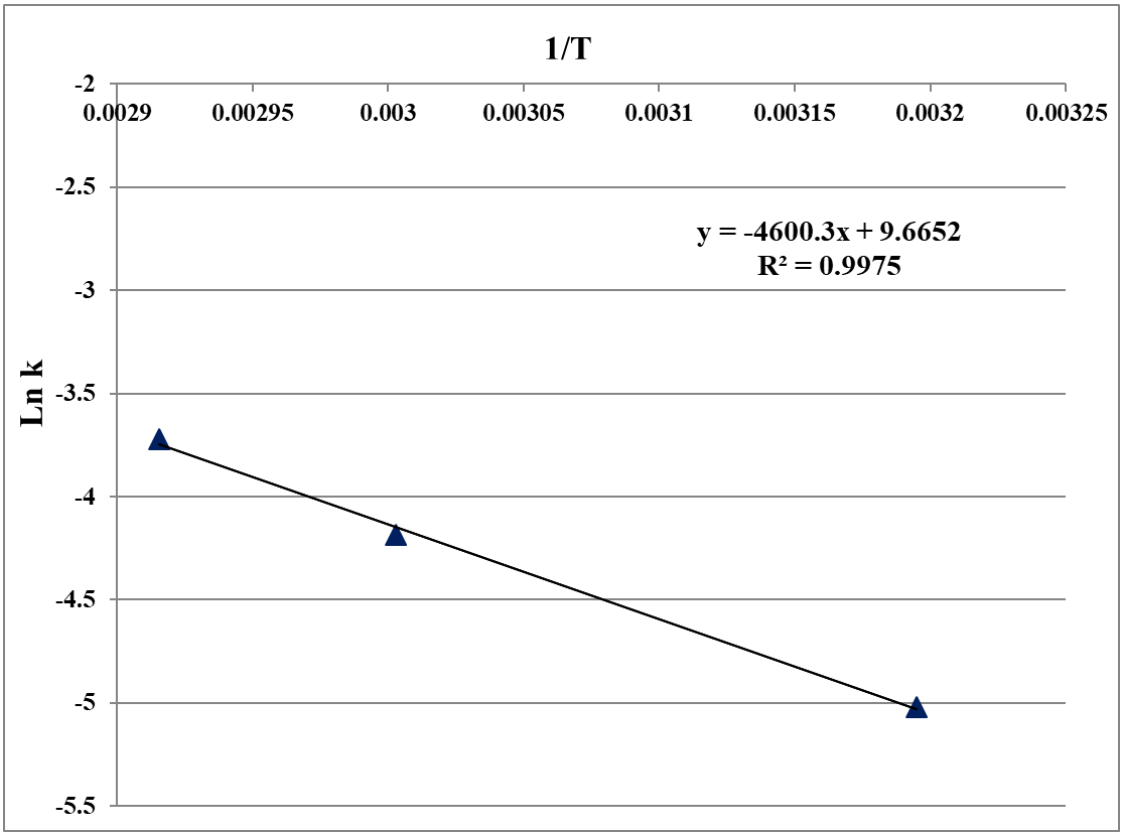

Figure 183. Activation energy plot for 4-methoxyphenol hydrogenation.

Therefore, the gradient of ln k against 1/T equals $-\frac{Ea}{RT}$ and can be expressed for Ea as:

- Ea= -mR
- -(-4600.3*8.314)/1000
- = 38.2 kJmol^{-1}

From this, an overall activation energy for 4-methoxyphenol hydrogenation of 38.2 kJmol^{-1} was measured.

7.3.3 Concentration Variations of Methoxyphenol Isomers

Concentration of the methoxyphenol isomers was varied to investigate reaction order of the substrate.

7.3.3.1 2-Methoxyphenol Concentration Variations

In this set of reactions 2-methoxyphenol was hydrogenated at 5, 10, 15 and 20 mmol to test the effect of substrate concentration on the hydrogenation activity, with 10 mmol taken as the standard reaction. The temperature (323 K) and hydrogen pressure (3 barg) were kept constant throughout. These results in order of increasing concentration are shown below:

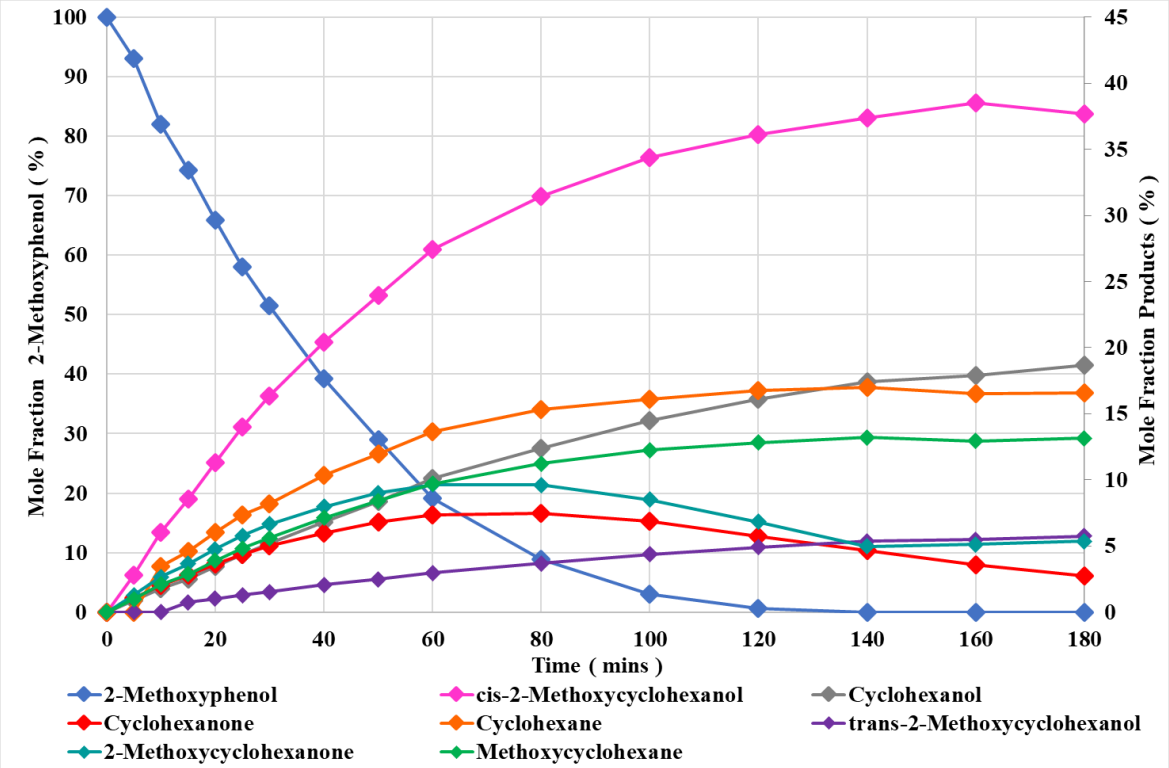

Figure 184. Reaction profile of 2-methoxyphenol hydrogenation. Conditions, 323 K, 5 mmol, 3 barg.

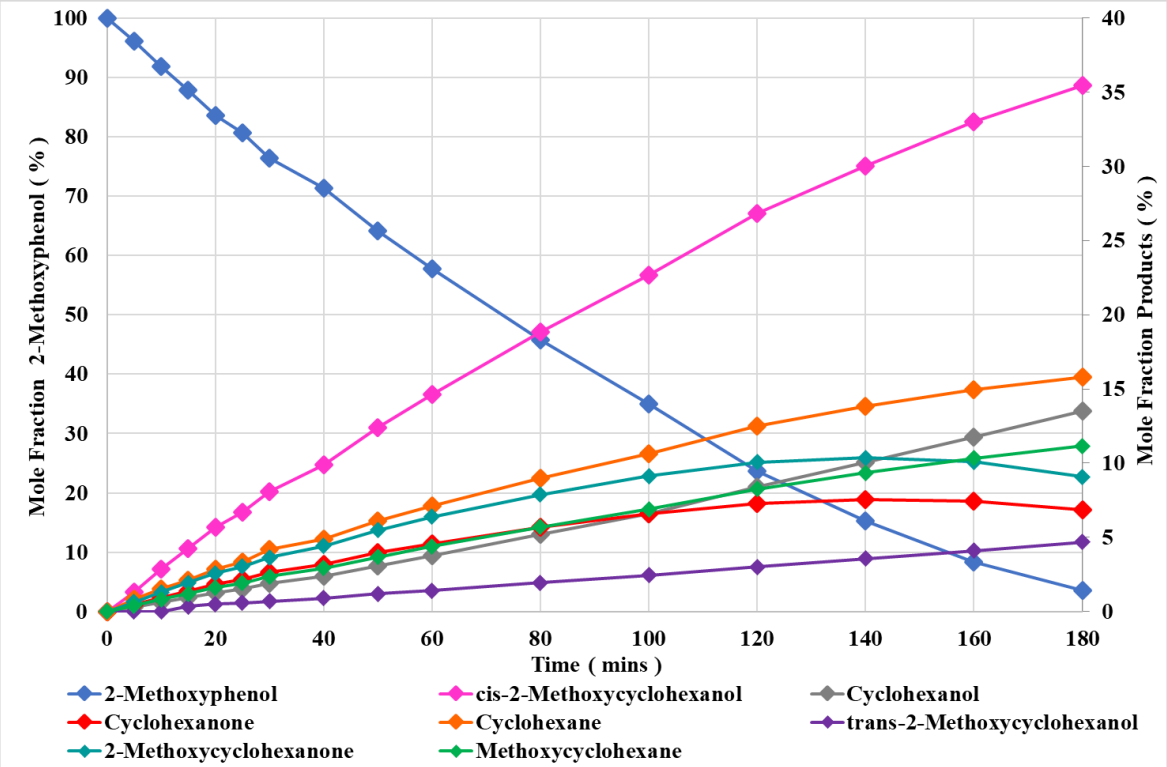

Figure 185. Reaction profile of 2-methoxyphenol hydrogenation. Conditions, 323 K, 15 mmol, 3 barg.

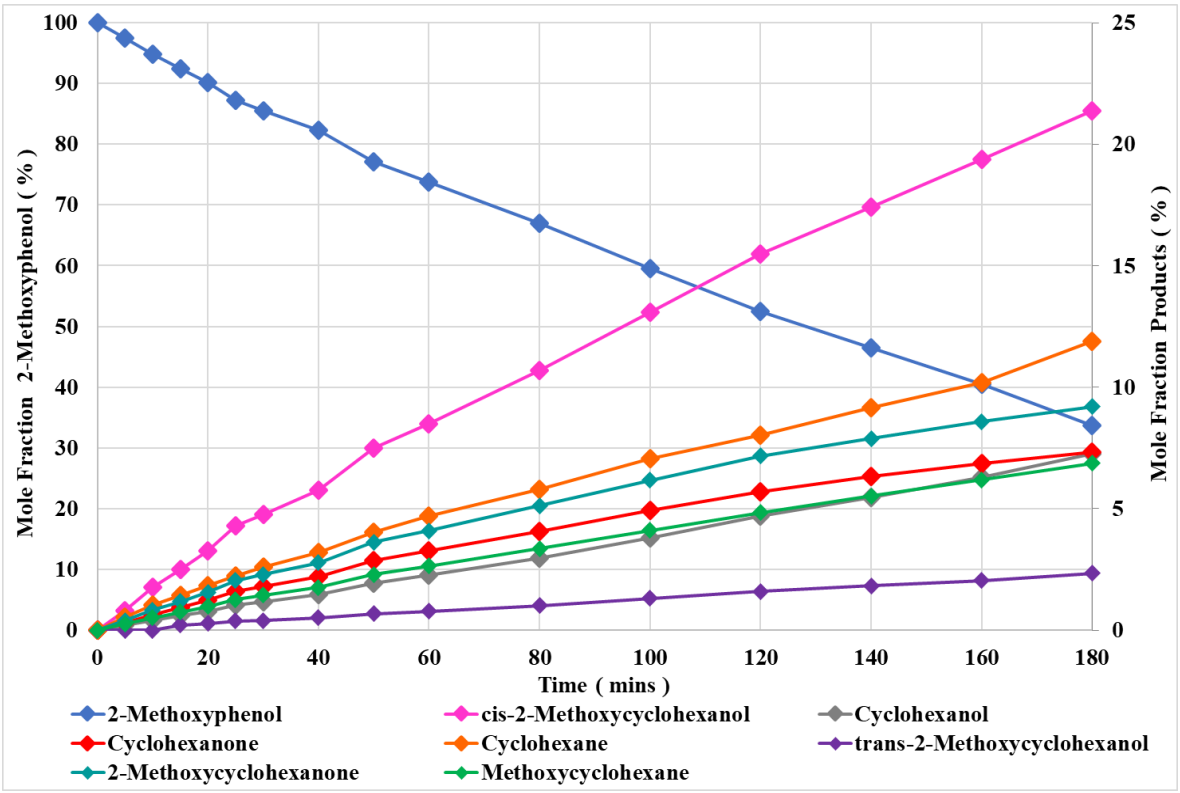

Figure 186. Reaction profile of 2-methoxyphenol hydrogenation. Conditions, 323 K, 20 mmol, 3 barg.

Calculation of the initial rates of each concentration reaction shown above found the reactivity of 2-methoxyphenol increased with concentration; a change in rate from 0.0131 mol $L^{-1}min^{-1}$ using 5 mmol substrate to 0.0205 mol $L^{-1}min^{-1}$ using 20 mmol. The product distribution of the hydrogenated (*cis*+*trans*-2-methoxycyclohexanol and 2-methoxycyclohexanone) and hydrodeoxygenated (cyclohexanol, cyclohexanone, methoxycyclohexane and cyclohexane) products at ~ 50 % conversion is shown below in Figure 187:

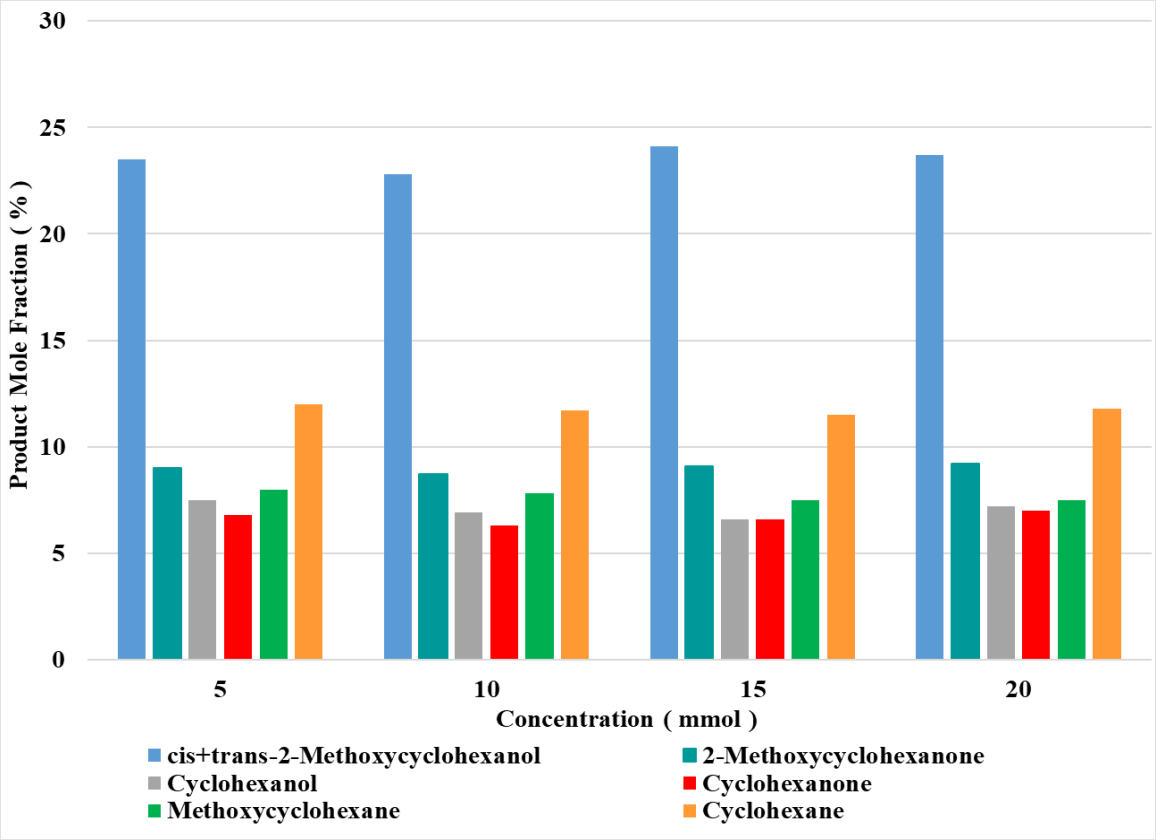

Figure 187. Product distribution for 2-methoxyphenol concentration reactions at ~ 50 % conversion.

From Figure 187 above, over the concentration range tested, the mole fraction percentages of all products remained broadly constant, indicating the effect of 2-methoxyphenol concentration is limited to the rate of reaction and does not affect product distribution.

To calculate an overall order in 2-methoxyphenol Ln [A] against Ln [rate] was plotted using the data in Table 30 below:

Table 30. Data used to calculate the order in 2-methoxyphenol.

Reactant concentration (mol L^{-1})	**Rate (mol L^{-1} min^{-1})**	**Ln concentration**	**Ln rate**
0.015	0.0131	-4.199705078	-4.3351
0.045	0.0188	-3.101092789	-3.9738
0.060	0.0205	-2.813410717	-3.8873

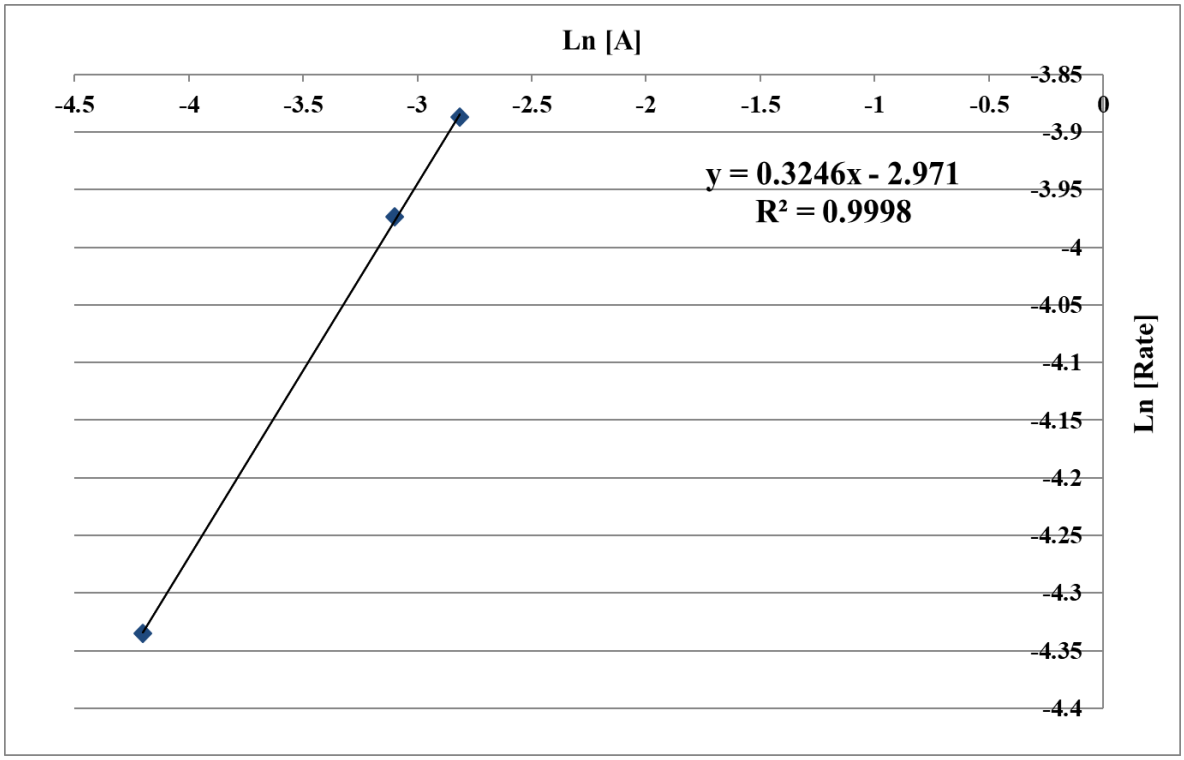

Figure 188. Substrate order plot for 2-methoxyphenol hydrogenation.

Using the equations presented in Section 6.6 of the Experimental Section, the order in 2-methoxyphenol was taken from the gradient of the straight line in Figure 188 above and found to be 0.32.

7.3.3.2 3-Methoxyphenol Concentration Variations

In this set of reactions 3-methoxyphenol was hydrogenated using 5, 10, 15 and 20 mmol to test the effect this would have on the hydrogenation reaction, with 10 mmol taken as the standard reaction. The temperature (323 K) and hydrogen pressure (3 barg) were kept constant. The graphs of these in increasing order of concentration are shown below:

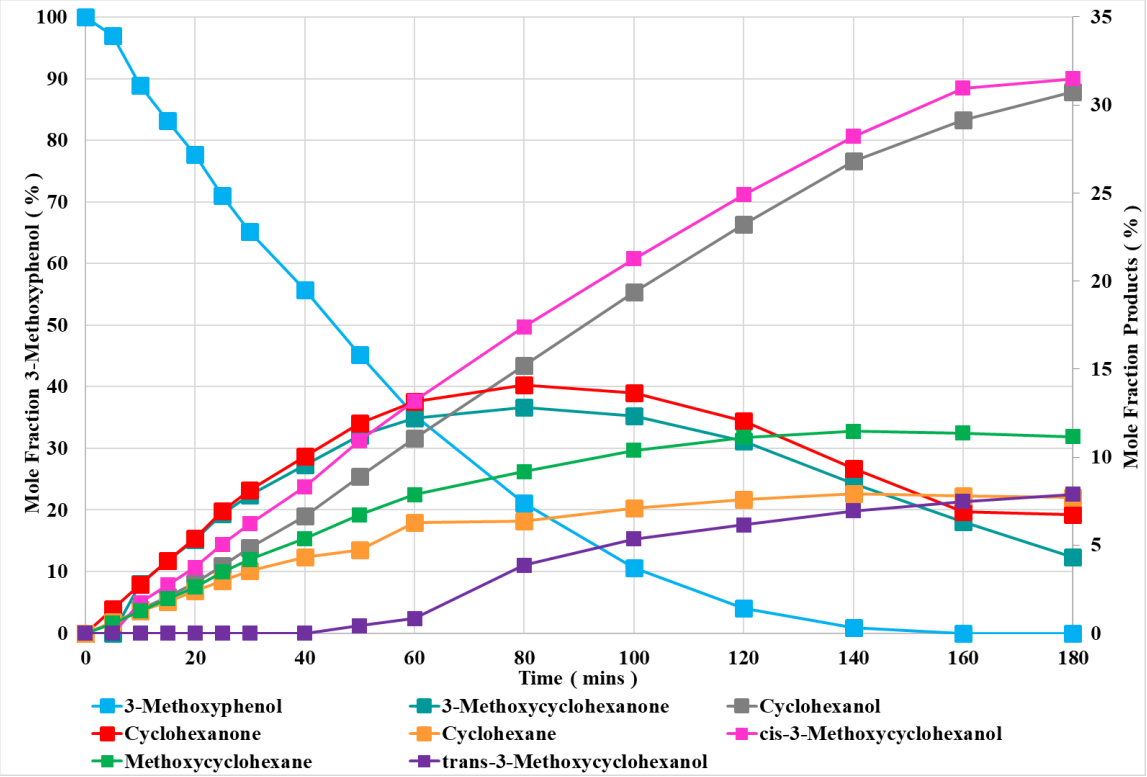

Figure 189. Reaction profile of 3-methoxyphenol hydrogenation. Conditions, 323 K, 5 mmol, 3 barg.

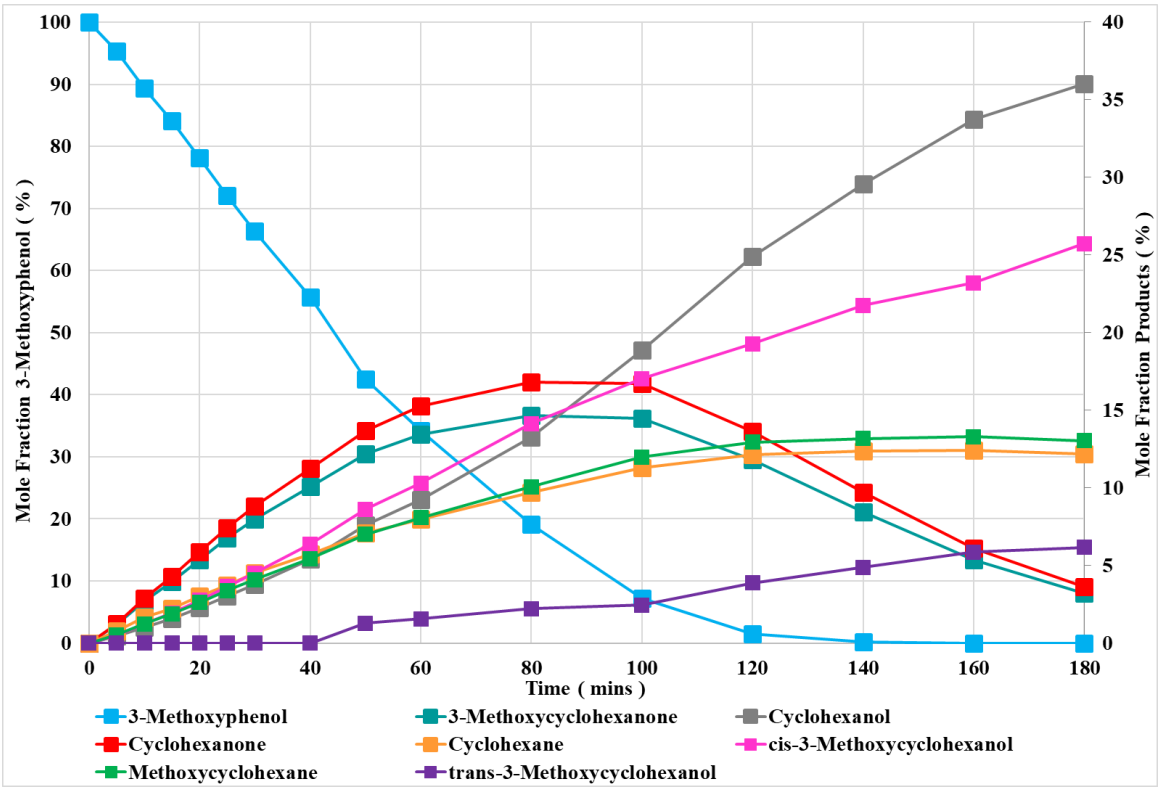

Figure 190. Reaction profile of 3-methoxyphenol hydrogenation. Conditions, 323 K, 15 mmol, 3 barg.

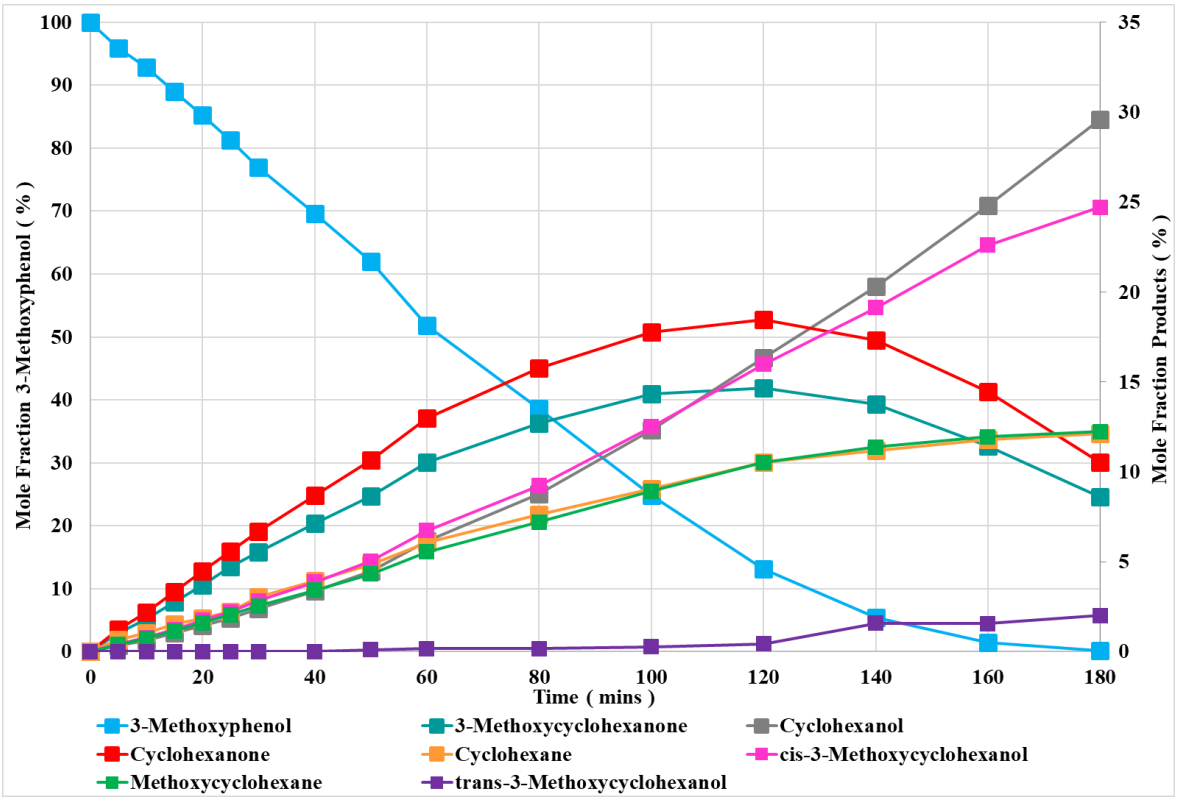

Figure 191. Reaction profile of 3-methoxyphenol hydrogenation. Conditions, 323 K, 20 mmol, 3 barg.

Calculation of the initial rates of each concentration reaction shown above found the reactivity of the 3-methoxyphenol increased with concentration; a change in rate from 0.011 mol $L^{-1}min^{-1}$ using 5 mmol substrate to 0.0301 mol $L^{-1}min^{-1}$ using 20 mmol. The product distribution of the hydrogenated (*cis*+*trans*-3-methoxycyclohexanol and 2-methoxycyclohexanone) and hydrodeoxygenated (cyclohexanol, cyclohexanone, methoxycyclohexane and cyclohexane) products at ~ 75 % conversion is shown below in Figure 192:

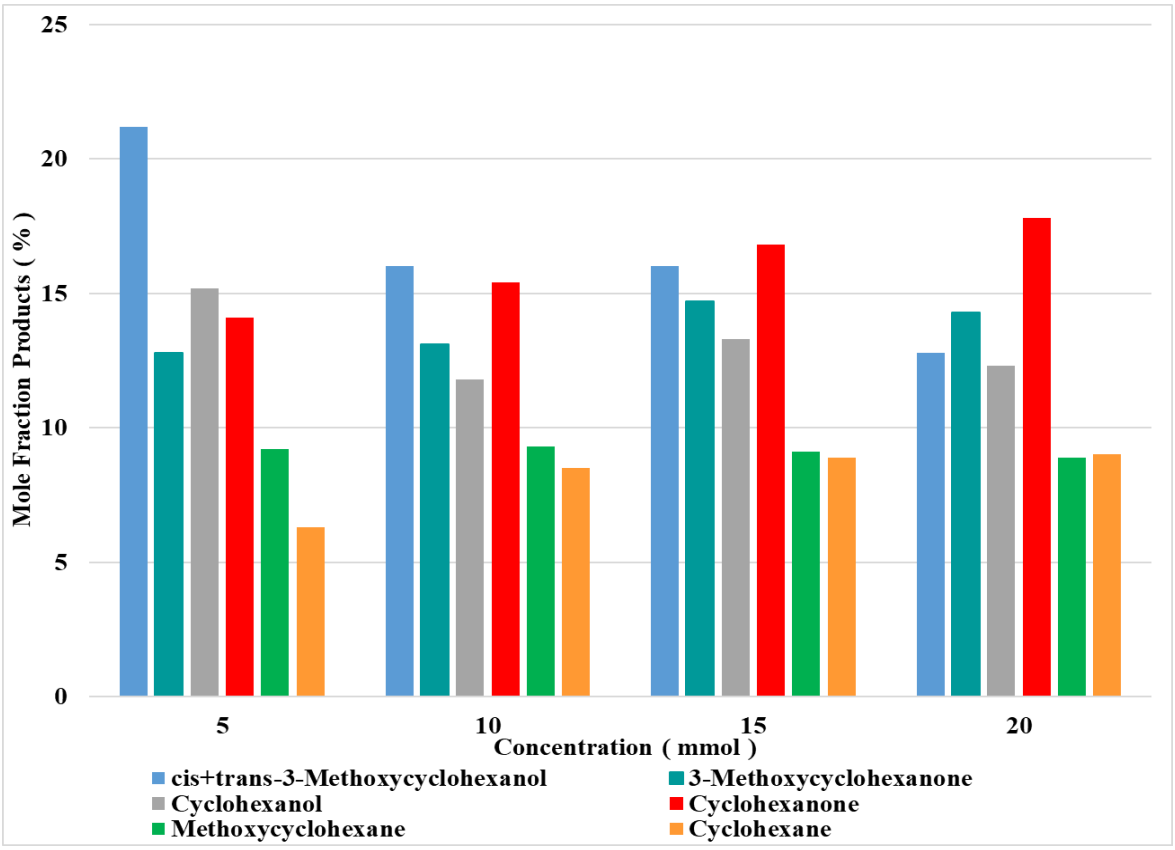

Figure 192. Product distribution for 3-methoxyphenol concentration reactions at ~ 75 % conversion.

From Figure 192 above it can be seen, that over the concentration range tested a change in the mole fraction percentage of the products occurs. The *cis*+*trans*-3-methoxycyclohexanol exhibited a noticeable decrease as concentration was increased whilst 3-methoxycyclohexanone showed a moderate increase before levelling off at the higher concentrations. The equivalent alcohol and ketone HDO products, cyclohexanol and cyclohexanone, showed a moderate decrease and increase respectively. Formation of the methoxycyclohexane remained constant, whilst that of cyclohexane showed an initial increase between 5-10 mmol, then remained constant as concentration was further increased.

To calculate an overall order in 3-methoxyphenol Ln [A] against Ln [rate] was plotted using the data in Table 31 below:

Table 31. Data used to calculate the order in 3-methoxyphenol.

Reactant concentration (mol L^{-1})	Rate (mol L^{-1} min^{-1})	Ln concentration	Ln rate
0.015	0.0111	-4.19	-4.500
0.030	0.0184	-3.50	-3.995
0.045	0.0286	-3.10	-3.554
0.060	0.0301	-2.81	-3.503

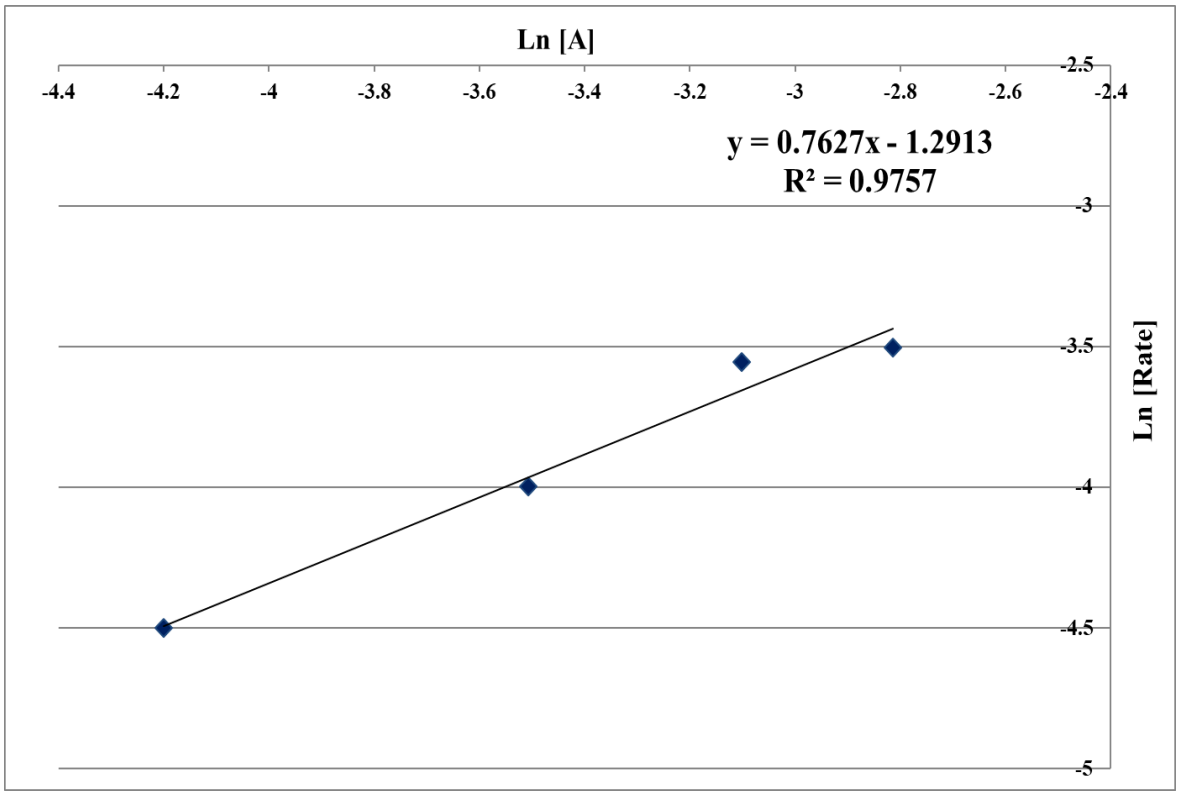

Figure 193. Substrate order plot for 3-methoxyphenol hydrogenation.

Using the equations presented in Section 6.6 of the Experimental Section, the order in 3-methoxyphenol was taken from the gradient of the straight line in Figure 193 above and found to be 0.8.

7.3.3.3 4-Methoxyphenol Concentration Variations

In this set of reactions 4-methoxyphenol was hydrogenated at 5, 10, 15 and 20 mmol to test the effect of substrate concentration on the hydrogenation activity, with 10 mmol taken as the standard reaction. The temperature (323 K) and hydrogen pressure (3 barg) were kept constant throughout. These results in order of increasing concentration are shown below:

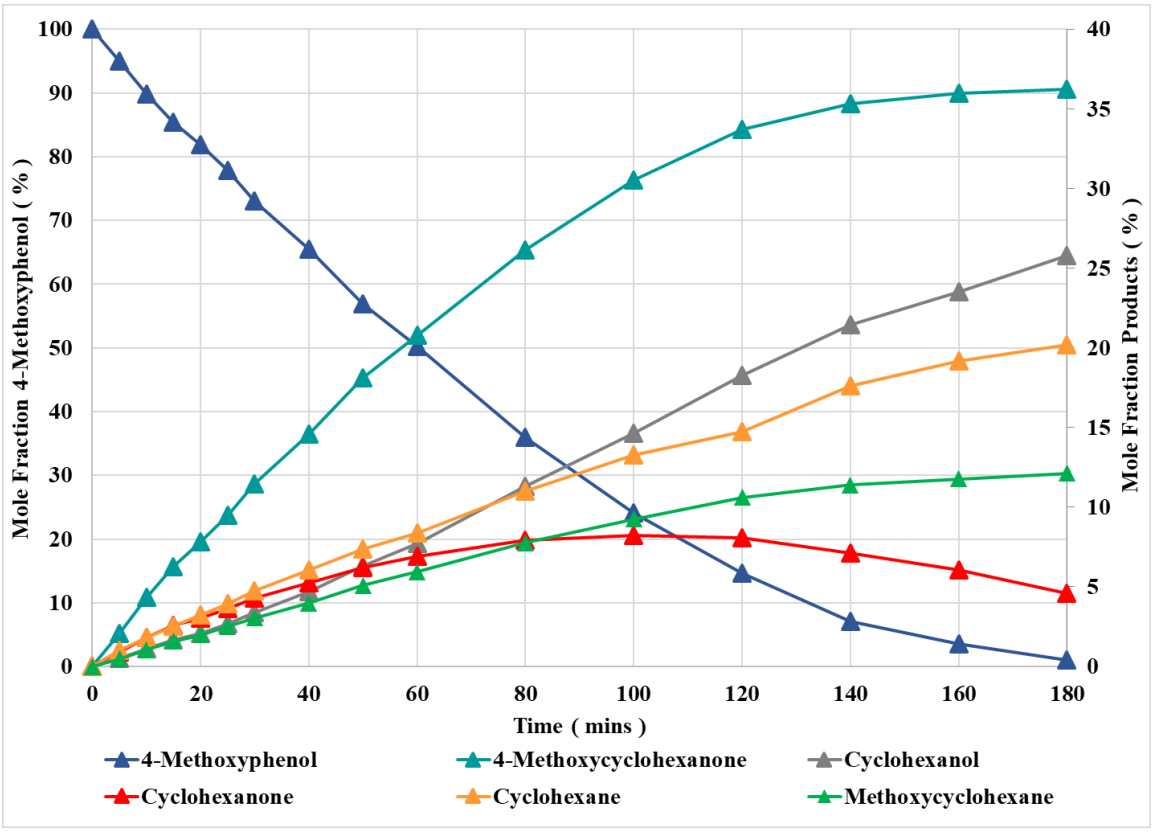

Figure 194. Reaction profile of 4-methoxyphenol hydrogenation. Conditions, 323 K, 5 mmol, 3 barg.

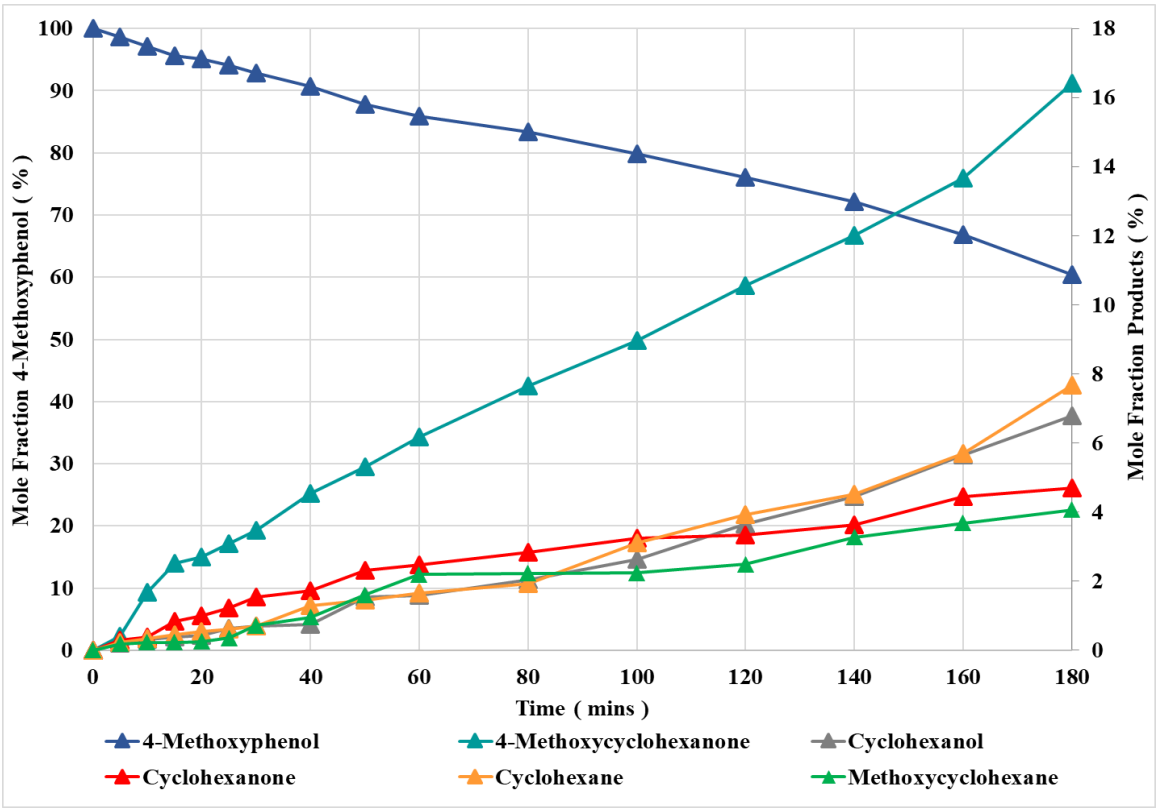

Figure 195. Reaction profile of 4-methoxyphenol hydrogenation. Conditions, 323 K, 15 mmol, 3 barg.

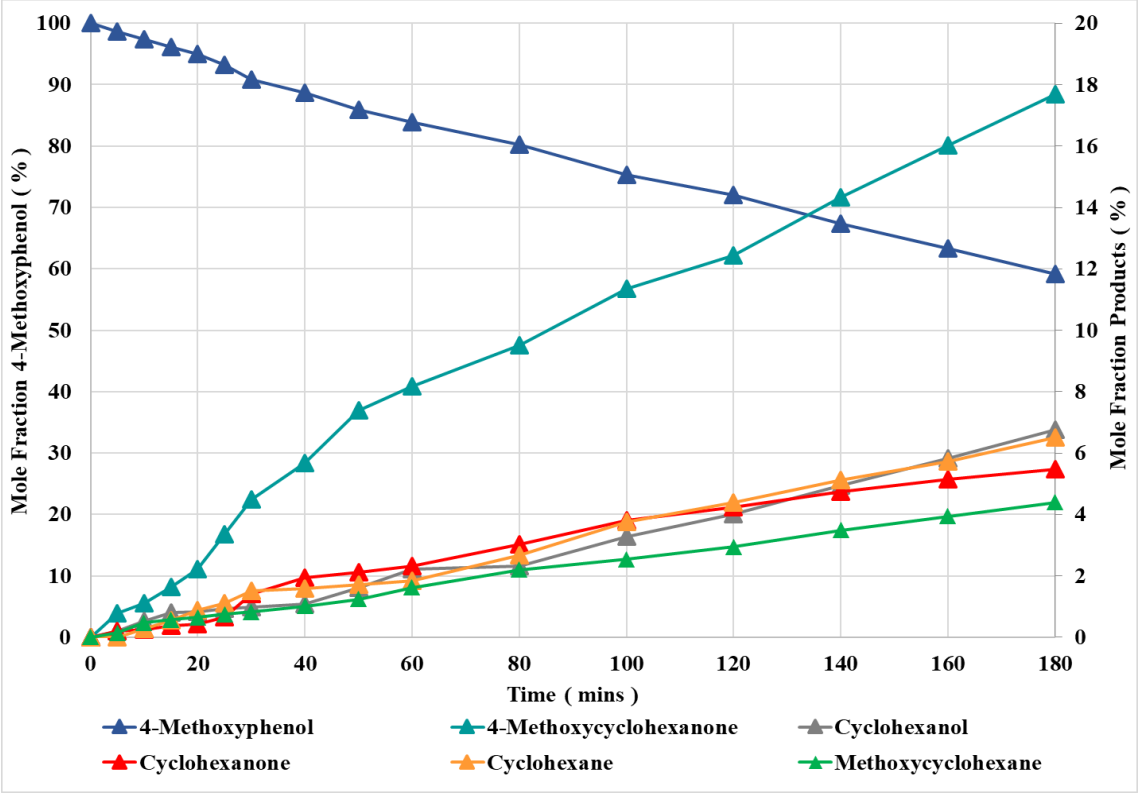

Figure 196. Reaction profile of 4-methoxyphenol hydrogenation. Conditions, 323 K, 20 mmol, 3 barg.

Calculation of the initial rates of each concentration reaction shown above found the reactivity of the 4-methoxyphenol increased with concentration; a change in rate from 0.0106 mol $L^{-1}min^{-1}$ using 5 mmol substrate to 0.0197 mol $L^{-1}min^{-1}$ using 20 mmol. The product distribution of the hydrogenated (*cis*+*trans*-4-methoxycyclohexanol and 4-methoxycyclohexanone) and hydrodeoxygenated (cyclohexanol, cyclohexanone, methoxycyclohexane and cyclohexane) products at ~ 35 % conversion is shown below in Figure 197:

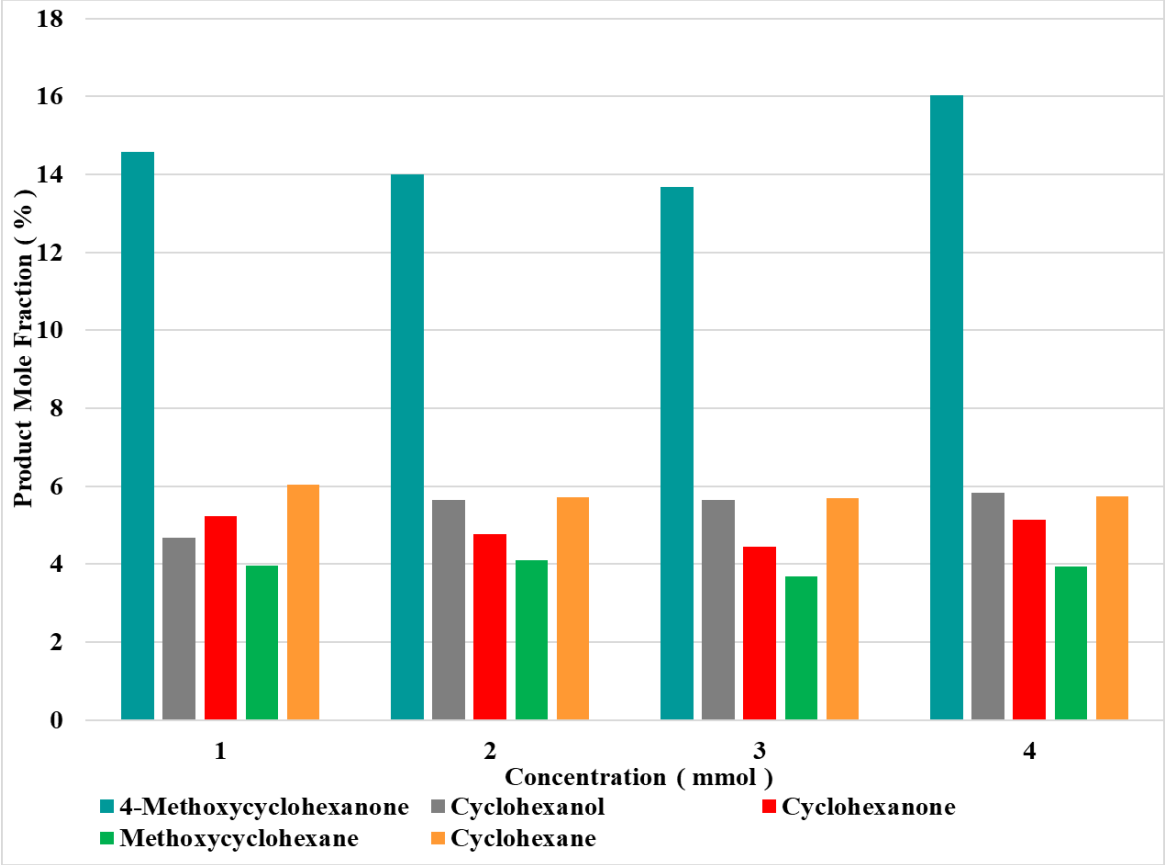

Figure 197. Product distribution for 4-methoxyphenol concentration reactions at ~ 35 % conversion.

From Figure 41 above, over the concentration range tested, the mole fraction percentages of all products remained broadly constant, indicating the effect of 4-methoxyphenol concentration is limited to the rate of reaction and does not affect product distribution.

To calculate an overall order in 4-methoxyphenol Ln [A] against Ln [rate] was plotted using the data in Table 32 below:

Table 32. Data used to calculate the order in 4-methoxyphenol.

Reactant concentration (mol L^{-1})	**Rate (mol L^{-1} min^{-1})**	**Ln concentration**	**Ln rate**
0.015	0.0106	-4.19	-4.546
0.030	0.0138	-3.50	-4.283
0.045	0.0150	-3.10	-4.199

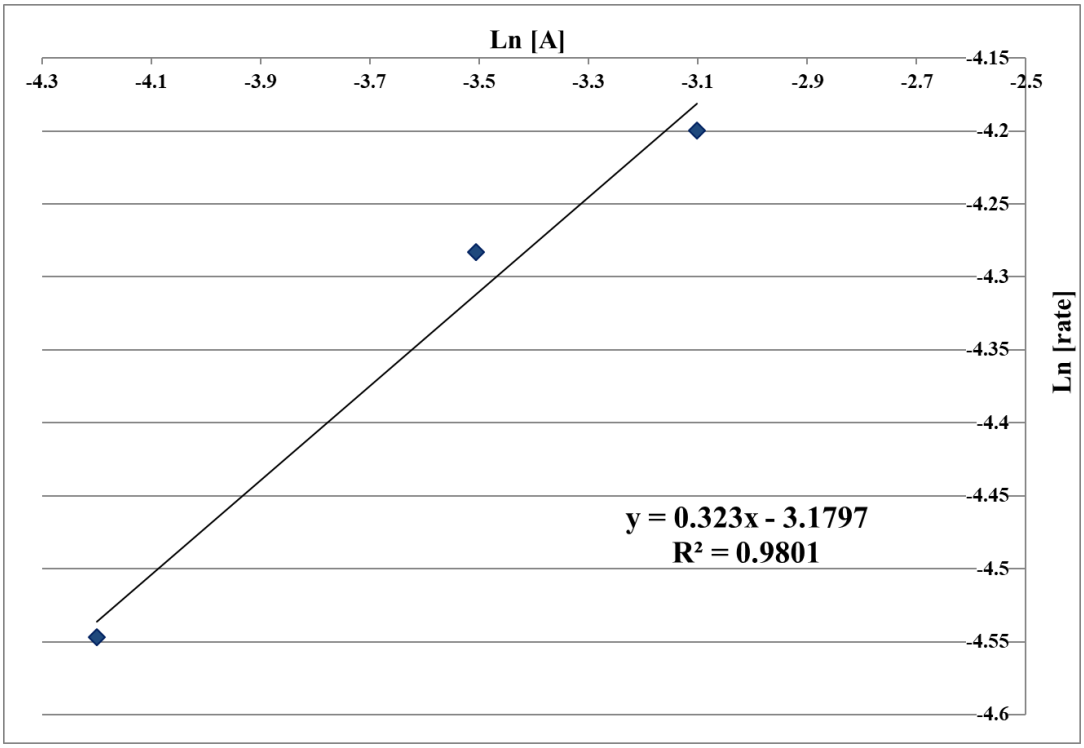

Figure 198. Substrate order plot for 4-methoxyphenol hydrogenation.

Using the equations presented in Section 6.6 of the Experimental Section, the order in 4-methoxyphenol was taken from the gradient of the straight line in Figure 198 above and found to be 0.3. The order for each substrate of the methoxyphenol isomers is summarised below:

Table 33. Orders in methoxyphenol isomer.

Substrate	Order
2-Methoxyphenol	0.3
3-Methoxyphenol	0.8
4-Methoxyphenol	0.3

From Table 33 above it can be seen the following order of strength of adsorption exists: 2-/4- > 3-methoxyphenol.

7.3.4 Competitive Hydrogenation

Competitive testing of the methoxyphenol in pairs and as a group of three was carried out and the results are detailed in this section.

The competitive reaction of the 2- and 3-methoxyphenol resulted in a noticeable decrease in the rate of reaction for both isomers, as can be seen in Figure 199 below:

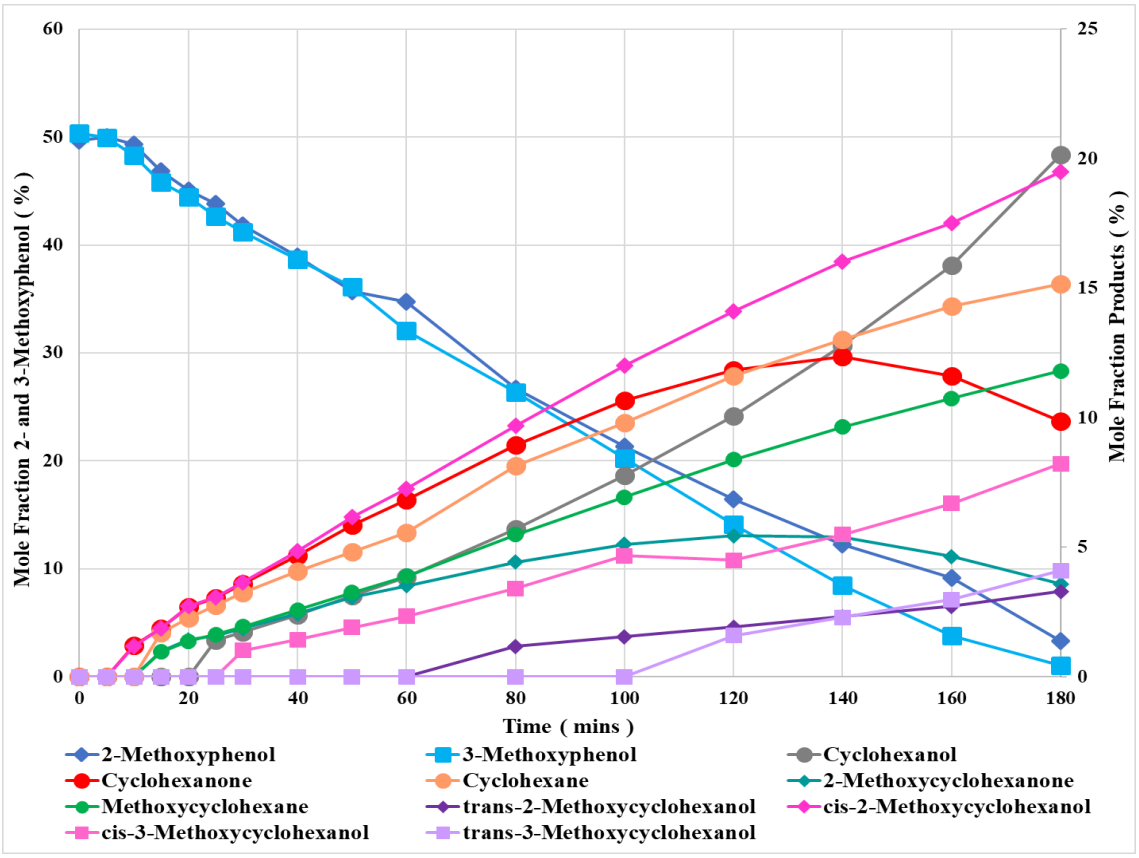

Figure 199. Competitive reaction of 2- and 3-methoxyphenol. Conditions: 323 K, 3 barg, concentrations as per single reactions.

From Figure 199, it can be seen that both isomers exhibit a similar rate of decay and each showed a decrease in rate of reaction from individual hydrogenation. A delay in formation of at least 10 minutes occurred for all products at which point cyclohexanone and *cis*-2-methoxycyclohexanol exhibited a shared rate of formation until around 60 minutes. The initial 2-methoxyphenol hydrogenated product, 2-methoxycyclohexanone, did not form until 15 minutes reaction time and remained low throughout, whilst complete inhibition of the initial hydrogenated product from 3-methoxyphenol occurred. The greatest inhibitive effect was observed with the *trans*-methoxycyclohexanol from both substrates: 80 minutes and 120 minutes from 2- and 3-methoxyphenol respectively. Significant formation of all HDO products occurred with a cumulative mole fraction of ~ 57 % by end of reaction.

This pair combination showed an effect on selectivity solely on the hydrogenated products from 3-methoxyphenol which experienced a reduction in formation in the competitive environment. Formation of HDO products and hydrogenated products from 2-methoxyphenol were unaffected. The product yield comparison between individual and competitive reactions is shown below in Figure 200:

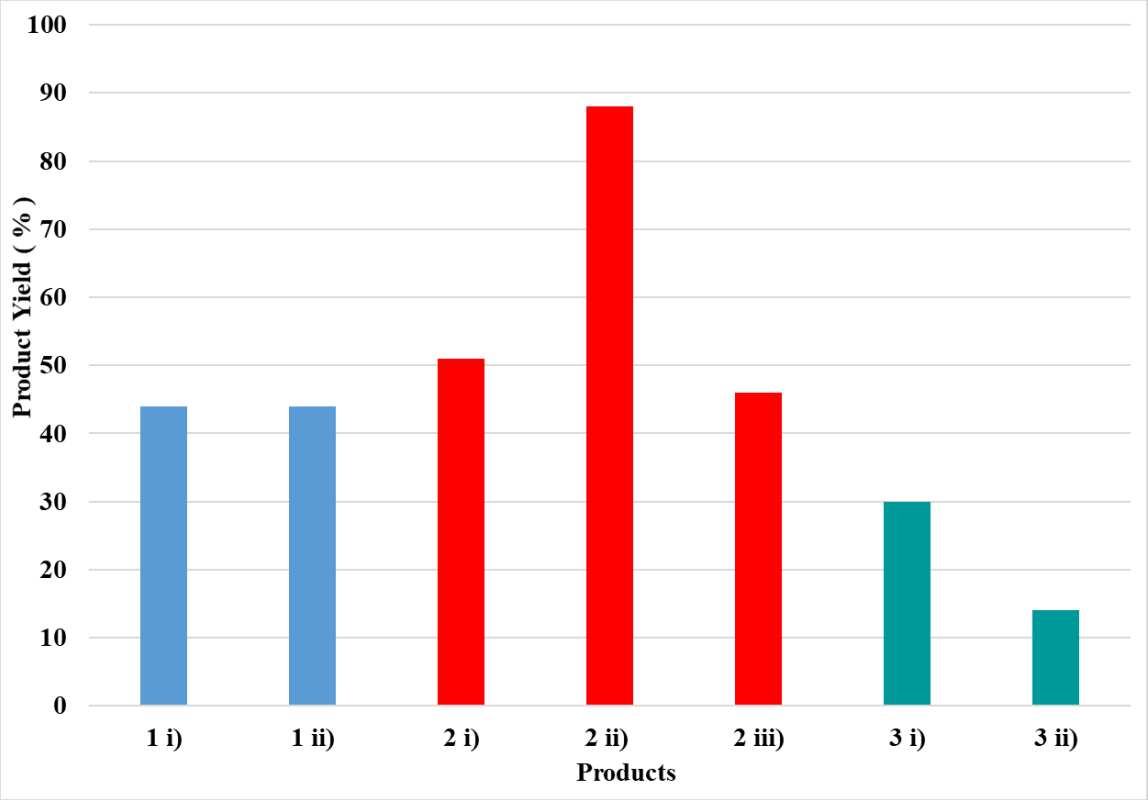

Figure 200. Comparison of product yield for individual and competitive hydrogenation of 2- and 3-methoxyphenol. Data taken at 80 % conversion of 2-methoxyphenol and 85 % conversion of 3-methoxyphenol.

Key: 1 HYD products i) Individual 2-methoxyphenol 1 ii) Competitive 2-methoxyphenol

2 HDO products (cyclohexanol + cyclohexanone + methoxycyclohexane + cyclohexane)

i) Individual 2-methoxyphenol ii) Competitive 2- + 3-methoxyphenol iii) Individual 3-methoxyphenol

3 HYD products i) Individual 3-methoxyphenol ii) Competitive 3-methoxyphenol

The competitive hydrogenation of 2- and 4-methoxyphenol is shown in Figure 201 below:

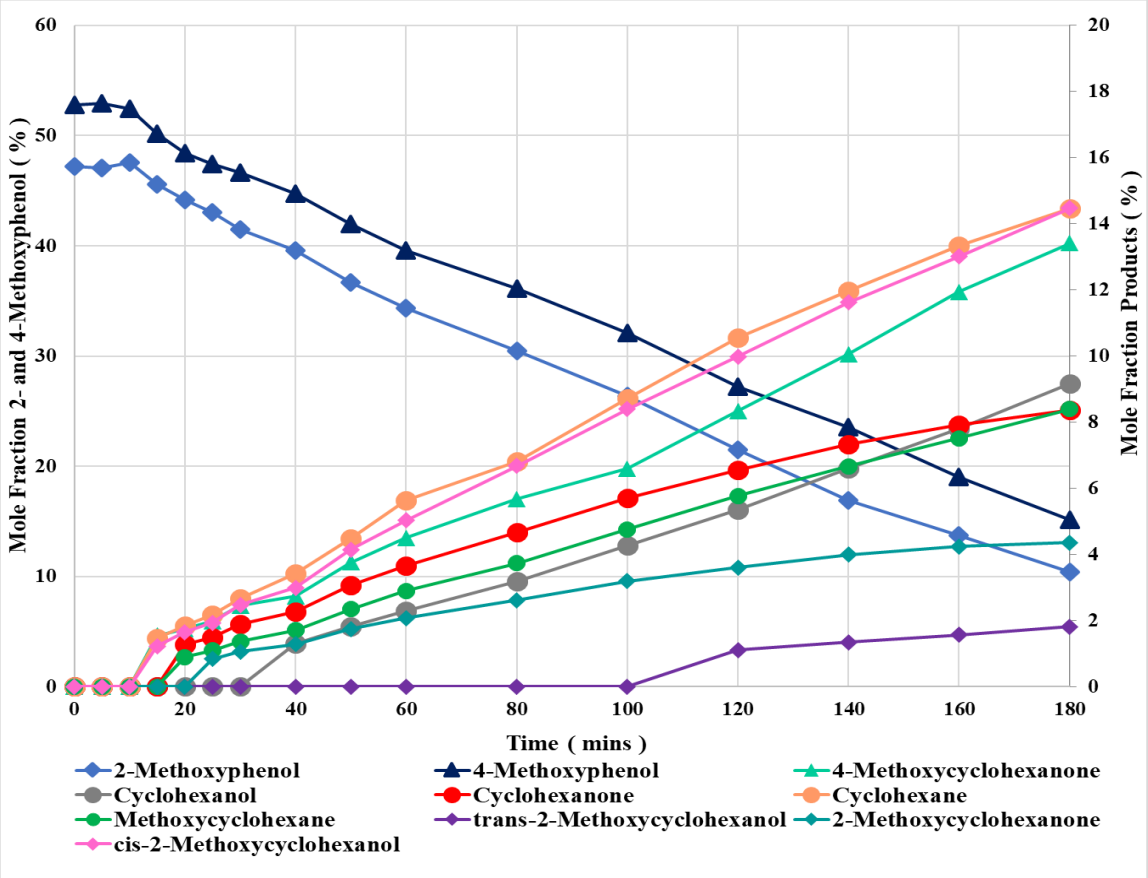

Figure 201. Competitive reaction of 2- and 4-methoxyphenol. Conditions: 323 K, 3 barg, concentrations as per single reactions.

Again, a significant reduction in rate was observed for both isomers in the competitive environment with a similar rate of decay for both, as observed with the previous pair combination. In this instance, a delay of at least 15 minutes occurred for all products at which point *cis*-2-methoxycyclohexanol, cyclohexane and 4-methoxycyclohexanone formed simultaneously and followed a similar rate of formation until 30 minutes. As with individual hydrogenation, no secondary hydrogenated products from 4-methoxyphenol were observed; however, the significant delay in formation of the *trans*-2-methoxycyclohexanol noted previously was again present, in this instance until 120 minutes reaction time. Formation of the HDO products was still significant during this pair combination with a cumulative mole fraction by reaction end of ~ 40 %.

The 2- and 4-methoxyphenol pair combination showed no effect on product selectivity during the reaction. The product yield comparison between individual and competitive reactions is shown below in Figure 202.

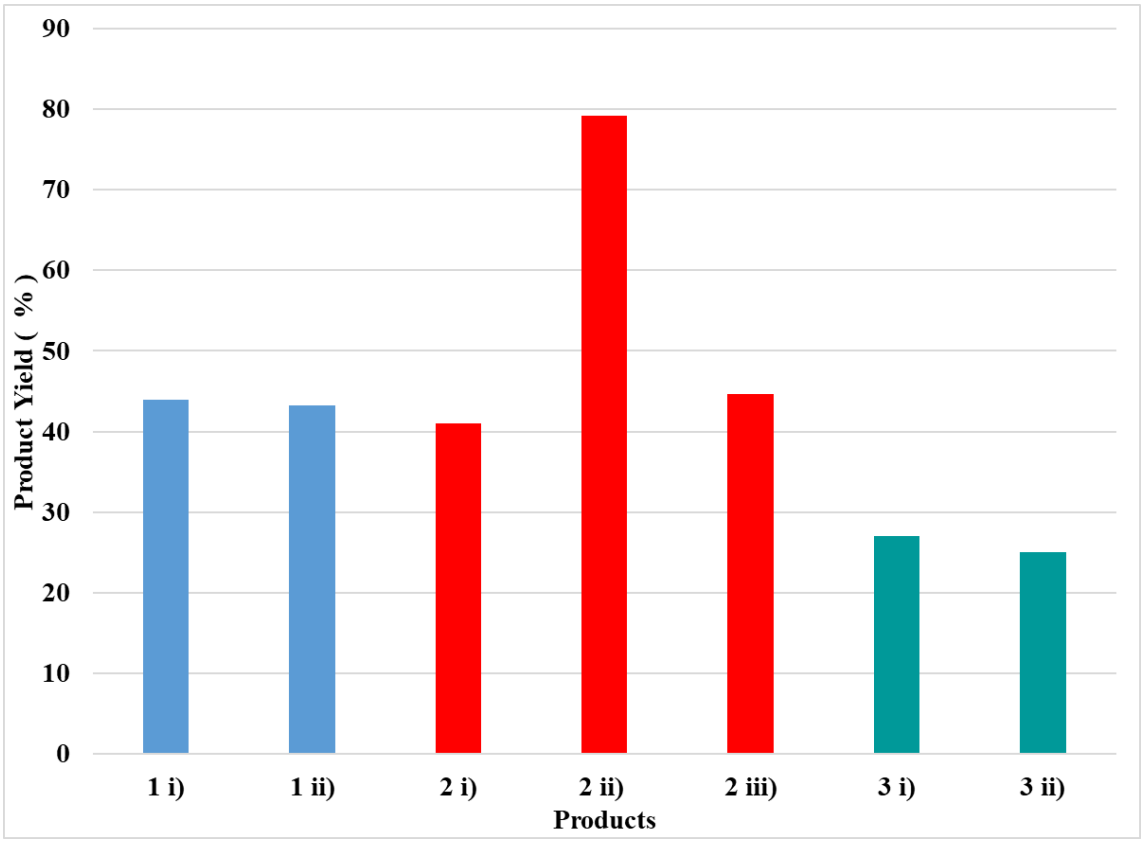

Figure 202. Comparison of product yield for individual and competitive hydrogenation of 2- and 4-methoxyphenol. Data taken at ~ 80 % conversion of 2-methoxyphenol and ~ 70 % conversion of 4-methoxyphenol.

Key: 1 HYD products i) Individual 2-methoxyphenol 1 ii) Competitive 2-methoxyphenol

2 HDO products (cyclohexanol + cyclohexanone + methoxycyclohexane + cyclohexane)

i) Individual 2-methoxyphenol ii) Competitive 2- + 4-methoxyphenol iii) Individual 4-methoxyphenol

3 HYD products i) Individual 4-methoxyphenol ii) Competitive 4-methoxyphenol

The competitive hydrogenation of 3- and 4-methoxyphenol is shown in Figure 203 below:

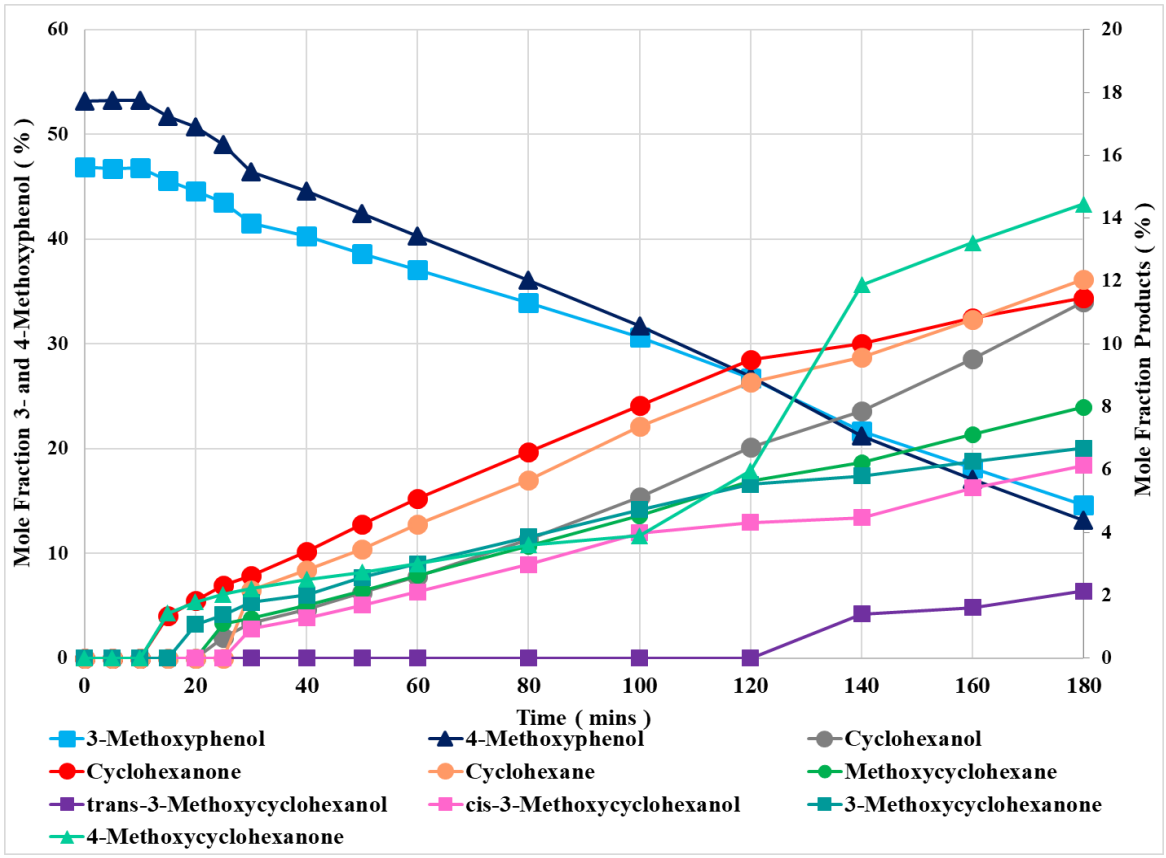

Figure 203. Competitive reaction of 3- and 4-methoxyphenol. Conditions: 323 K, 3 barg, concentrations as per single reactions.

From Figure 203 above it is apparent that, when reacted together, 4-methoxyphenol exhibits a slightly faster rate of decay than that of 3-methoxyphenol. As with both previous pair combinations a delay in formation of all products is present, in this instance until around 15 minutes at which point the cyclohexanone and 4-methoxycyclohexanone are present. A sharp increase in the rate of formation of 4-methoxycyclohexanone is present at 120 minutes leading to it becoming the major product of the reaction. Significant levels of HDO product formation was again recorded with ~ 42 % mole fraction by end of reaction.

The 3- and 4-methoxyphenol pair combination resulted in an increase in the hydrogenated products from 3-methoxyphenol and no change in those from 4-methoxyphenol. A decrease in formation of HDO products occurred. The product yield comparison between individual and competitive reactions is shown below in Figure 204.

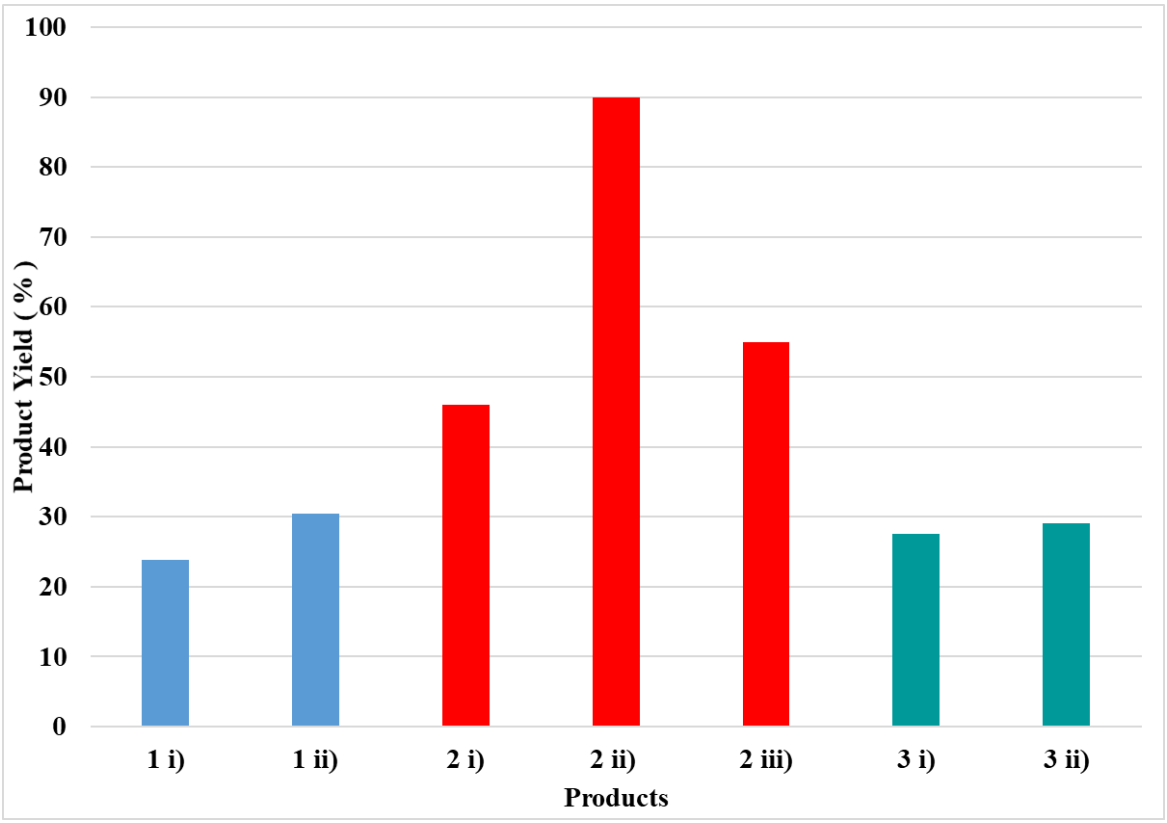

Figure 204. Comparison of product yield for individual and competitive hydrogenation of 3- and 4-methoxyphenol. Data taken at ~ 73 % conversion of 3-methoxyphenol and ~ 77 % conversion of 4-methoxyphenol.

Key: 1 HYD products i) Individual 3-methoxyphenol 1 ii) Competitive 3-methoxyphenol

2 HDO products (cyclohexanol + cyclohexanone + methoxycyclohexane + cyclohexane)

i) Individual 3-methoxyphenol ii) Competitive 3- + 4-methoxyphenol iii) Individual 4-methoxyphenol

3 HYD products i) Individual 4-methoxyphenol ii) Competitive 4-methoxyphenol

Data for all three substrates reacted together in the competitive environment is shown in the figures below. Figure 205 shows reaction graph. Figure 206 outlines substrate conversion and a comparison with hydrogenation of the individual substrates.

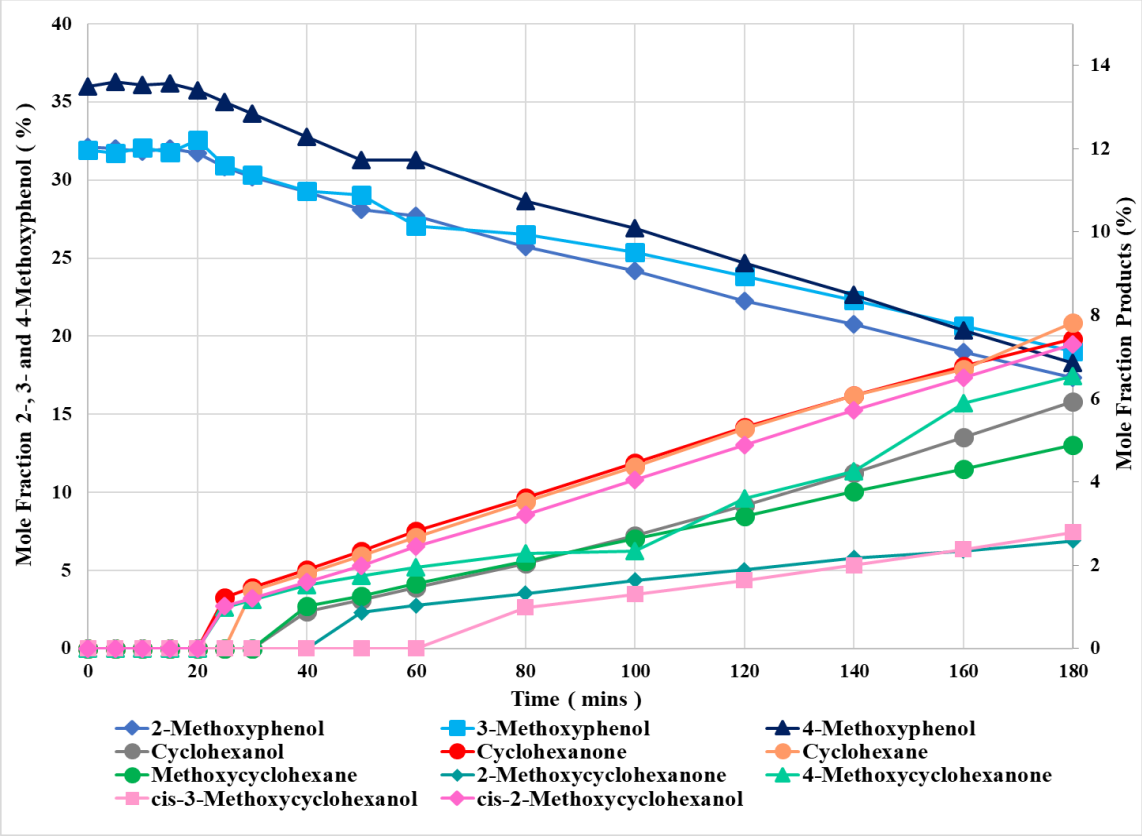

Figure 205. Competitive reactions of 2-, 3- and 4-methoxyphenol. Conditions, 323 K, 3 barg, concentrations as per single reactions.

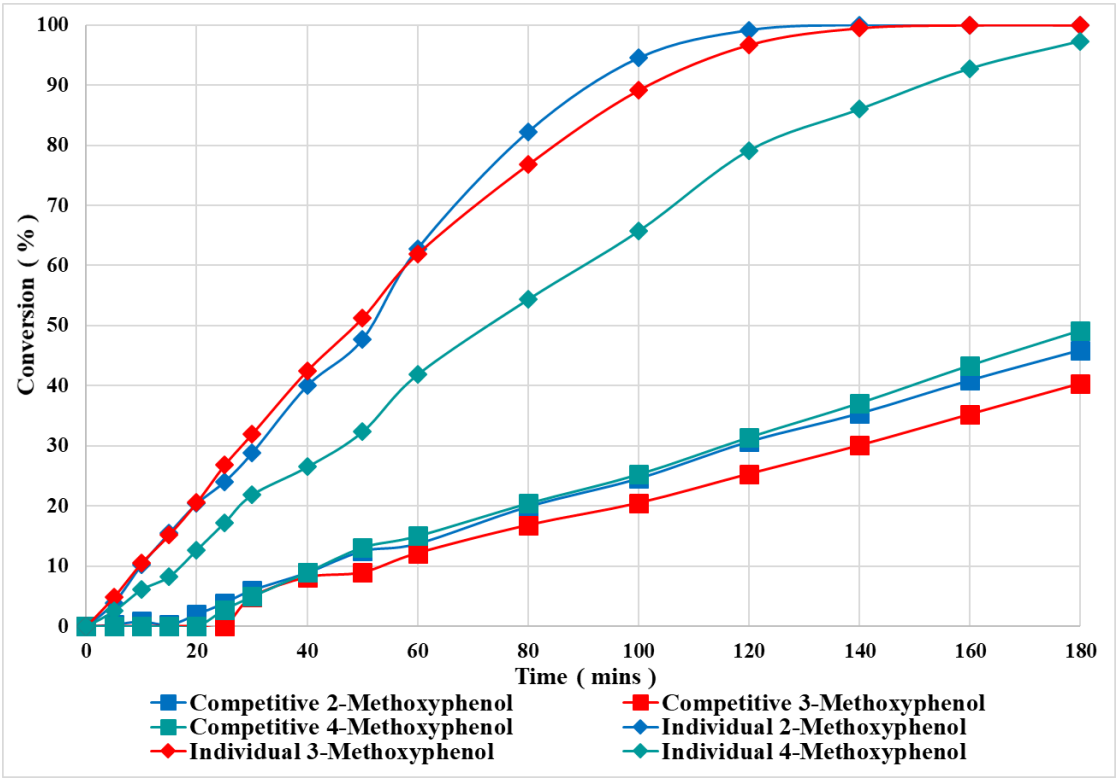

Figure 206. Conversion of the three isomers in the competitive environment compared with that during individual hydrogenation.

From Figure 205 and 206 it is apparent that the reaction rate for all three substrates was suppressed to a greater extent than that observed during previous competitive reactions. Of the products formed solely from hydrogenation, *cis*-2-methoxycyclohexanol, was present to the greatest extent with 4-methoxycyclohexanone, the initial hydrogenated product, from 4-methoxyphenol, the next most favoured. The HDO products, cyclohexane and cyclohexanone, were those formed to the greatest extent at the end of reaction. In this instance the inhibition of *trans*-methoxycyclohexanol from all three substrates was complete, with no formation throughout the 180 minutes. The delay in formation of *cis*-3-methoxycyclohexanol reported in the previous pair combinations is further prolonged to around 80 minutes. Closer analysis of the effect on conversion between competitive and individual hydrogenation, from Figure 49, showed the greatest detrimental effect occurred on 3-methoxyphenol where full conversion by ~140 minutes in the individual environment is reduced to ~ 45 % by end of reaction.

The kinetic data gathered from competitive reaction combinations is outlined in Table 34 below:

Table 34. Competitive hydrogenation at 323 K, 3 barg and 10 mmol.

Reactant	First order rate constant, k (min^{-1}, $x10^{-3}$)				
	Single	2-/3-MP	2-/4-MP	3-/4-MP	2-/3-/4-MP
2-Methoxphenol	11.5	10.6	3.8	-	6.6
3-Methoxyphenol	12.8	12.0	-	5.8	5.9
4-Methoxyphenol	7.4		4.7	4.7	6.4

MP, methoxyphenol

It can be seen, that across the pair combinations 3-methoxyphenol had the highest reactivity, which correlates with its higher reactivity observed during individual hydrogenation. During the competitive reaction of all three however, it exhibited the lowest reactivity, although all three substrates recorded similar rate constants.

7.3.5 Deuteration Reactions

In the following set of reactions, deuterium was used in place of hydrogen for both the reduction and reaction procedure. All other parameters were set for standard conditions (323 K and 10 mmol substrate). Comparison of the rate constants from reactions carried out in deuterium and hydrogen was used to calculate the kinetic isotope effect for each substrate. All graphs and data from individual reactions are shown in Figures 207 – 212 below:

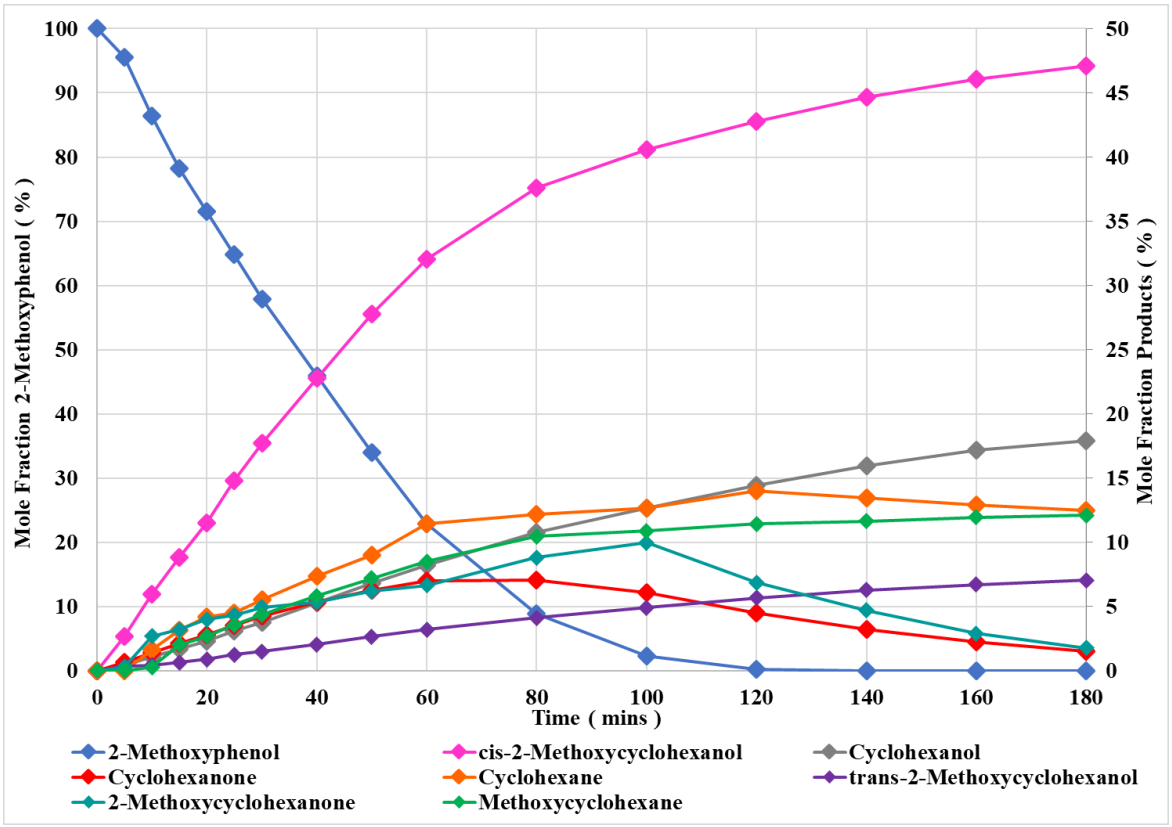

Figure 207. Reaction profile of 2-methoxyphenol deuteration. Conditions, 323 K, 10 mmol, 3 barg.

From Figure 207 above it can be seen that the rate of 2-methoxyphenol deuteration was higher than that of hydrogenation with an increase observed in the rate constant from 11.5×10^{-3} to 16.3×10^{-3} min^{-1}. Of note, is the initial formation of *trans*-2-methoxycyclohexanol in the presence of deuterium in contrast to the 40-minute delay observed during reaction with hydrogen. The product distribution for the hydrogenated and hydrodeoxygenated products at the same conversion (80 %) is shown below in Figure 208:

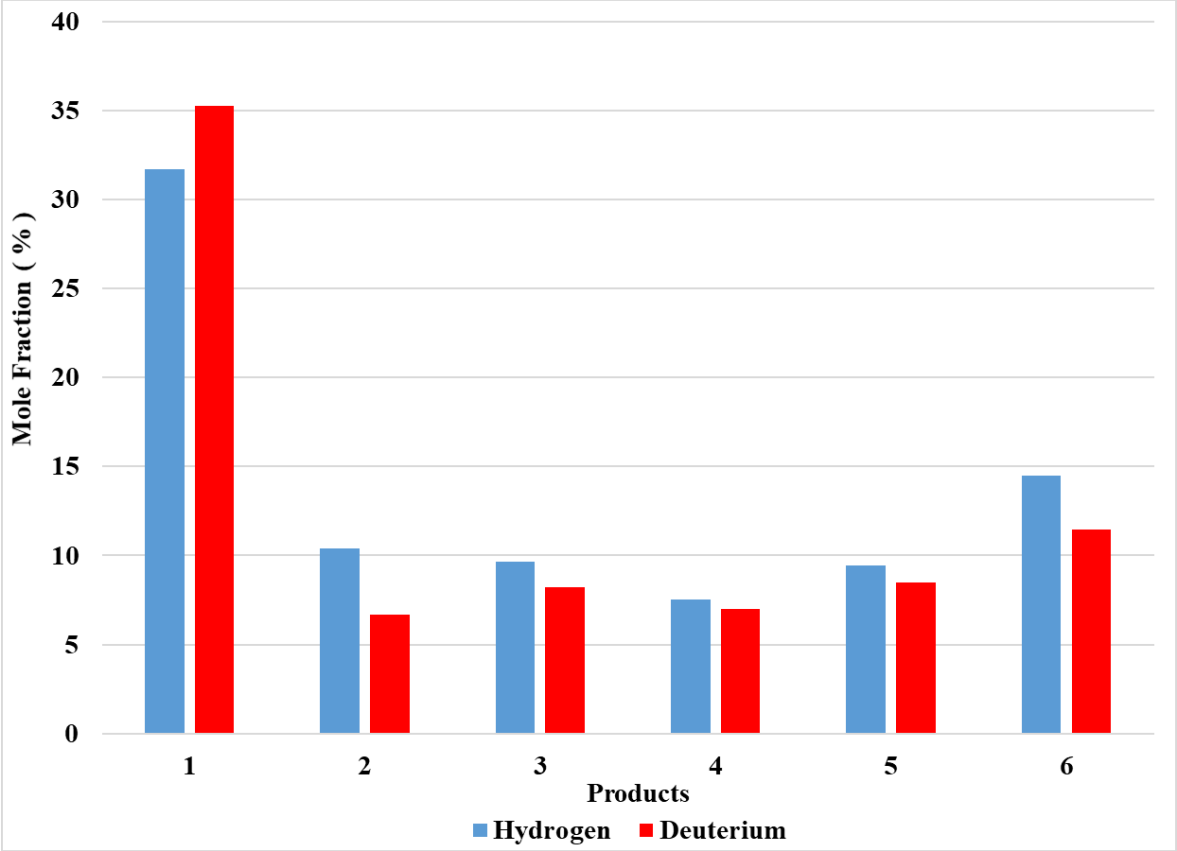

Figure 208. Product distribution of deuterium against hydrogen at ~80 % conversion of 2-methoxyphenol.

Key: 1: cis+trans-2-Methoxycyclohexanol **2:** 2-Methoxycyclohexanone **3:** Cyclohexanol **4:** Cyclohexanone **5:** Methoxycyclohexane **6:** Cyclohexane

From Figure 208 it can be seen that, in the presence of deuterium, the formation of the secondary hydrogenated products, *cis* and *trans*-methoxycyclohexanol, increased whilst that of 2-methoxycyclohexanone and cyclohexane decreased. The product distributions for cyclohexanol, cyclohexanone and methoxycyclohexane remained broadly constant with both gas reactants.

3-Methoxyphenol deuteration was carried out and is shown below in Figure 209:

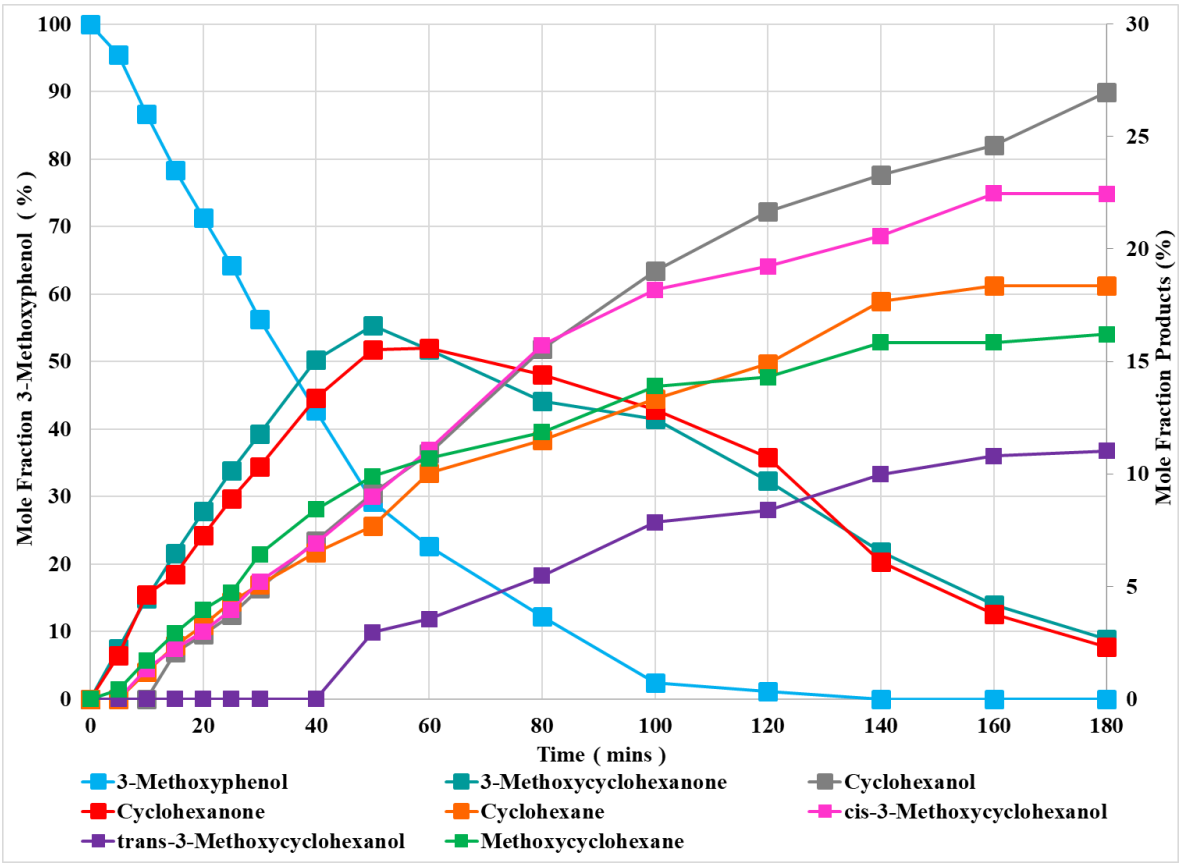

Figure 209. Reaction profile of 3-methoxyphenol deuteration. Conditions, 323 K, 10 mmol, 3 barg.

From Figure 209 above it can be seen that, the rate of 3-methoxyphenol deuteration was higher than that of hydrogenation with an increase observed in the rate constant from 12.8×10^{-3} to 18.0×10^{-3} min^{-1}. The presence of cyclohexanol as the major product followed by *cis*-2-methoxycyclohexanol was in accordance with that found during hydrogenation. Again, as when reacted with hydrogen, the *trans*-3-methoxycyclohexanol underwent a delay in formation of 50 minutes. The product distribution for the hydrogenated and hydrodeoxygenated products at the same conversion (90 %) is shown below in Figure 210:

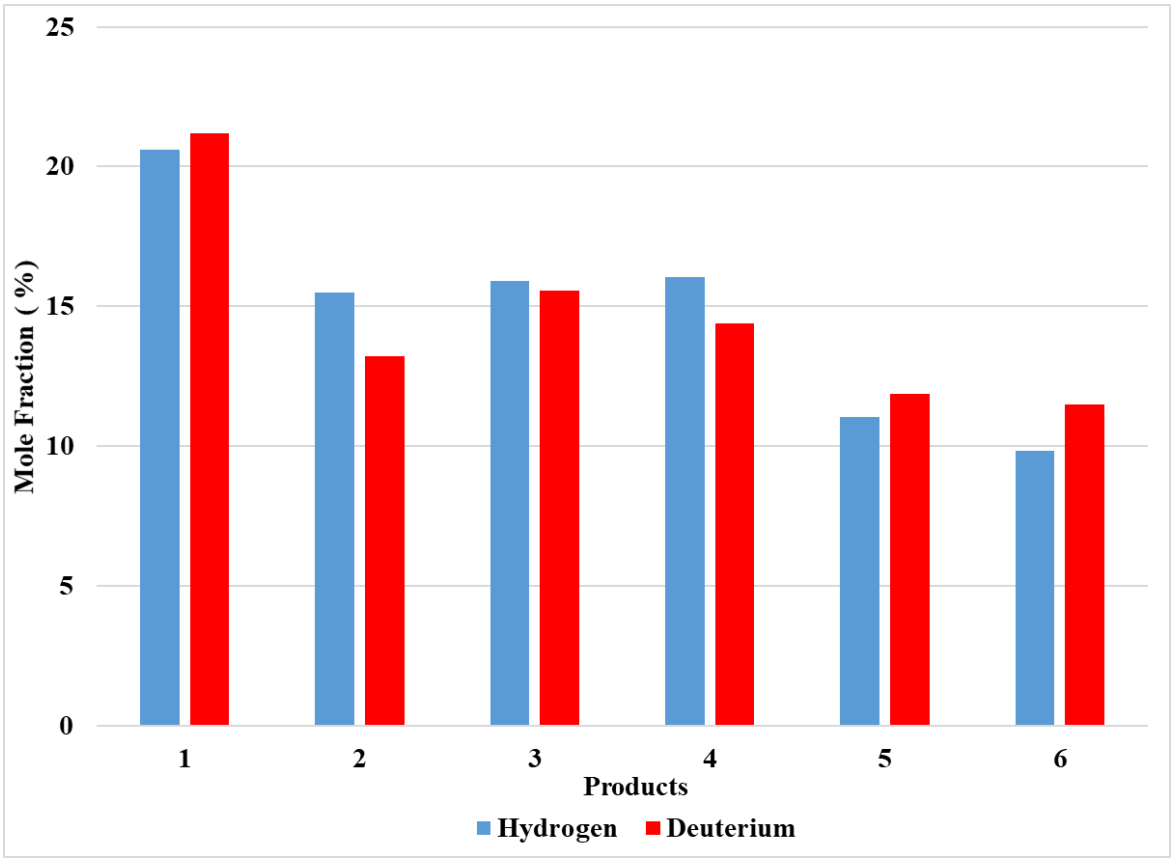

Figure 210. Product distribution of deuterium against hydrogen at 90 % conversion of 3-methoxyphenol.

Key: 1: cis+trans-3-Methoxycyclohexanol **2:** 3-Methoxycyclohexanone **3:** Cyclohexanol **4:** Cyclohexanone **5:** Methoxycyclohexane **6:** Cyclohexane

From Figure 210 it is apparent that formation of the initial hydrogenated product, 3-methoxycyclohexanone, and cyclohexanone decreased whilst that of cyclohexane increased. The product distributions for *cis*+*trans*-3-methoxycyclohexanol, cyclohexanol and methoxycyclohexane remained broadly constant with both gas reactants.

4-Methoxyphenol deuteration was carried out and is shown below in Figure 211:

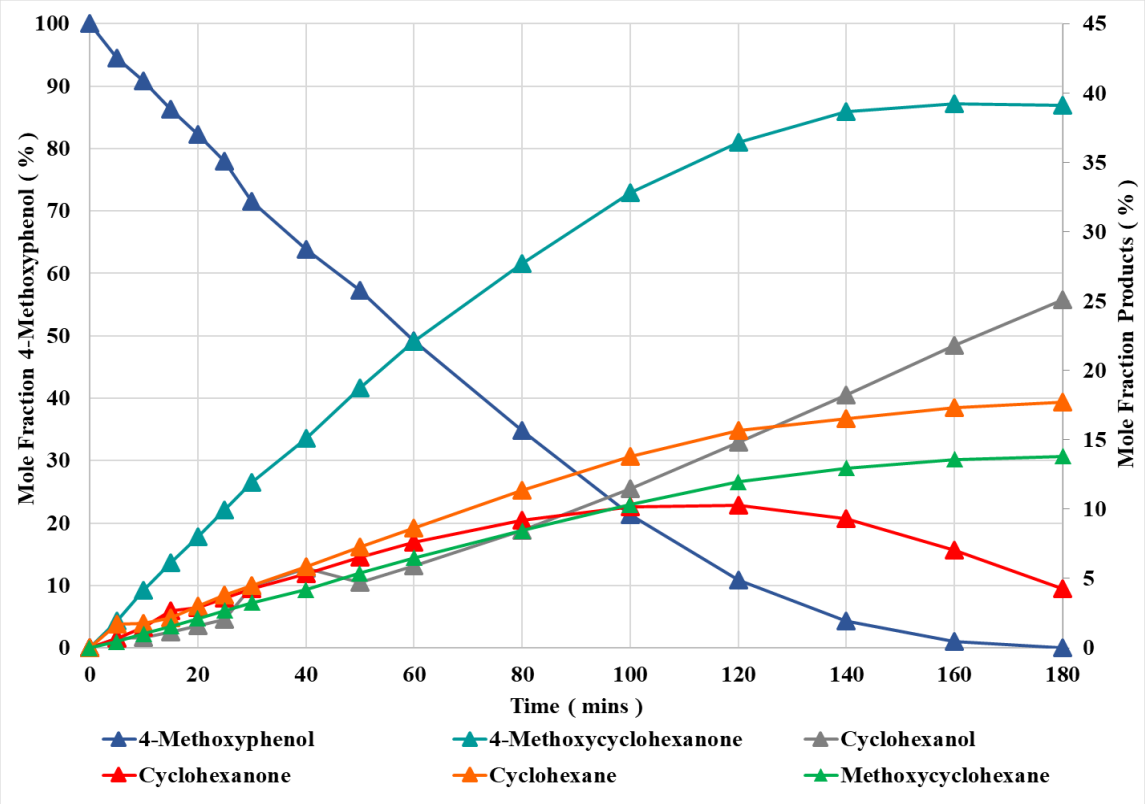

Figure 211. Reaction profile of 4-methoxyphenol deuteration. Conditions, 323 K, 10 mmol, 3 barg.

From Figure 211 above it can be seen that the rate of 4-methoxyphenol deuteration was higher than that of hydrogenation; an increase in the calculated rate constant from $7.4x10^{-3}$ to $11.3x10^{-3}$ min^{-1}. As with the hydrogenation reaction, 4-methoxycyclohexaone was the major product followed by cyclohexanol and again the secondary hydrogenated products were absent. The product distribution for the hydrogenated and hydrodeoxygenated products at the same conversion (90 %) is shown below in Figure 212:

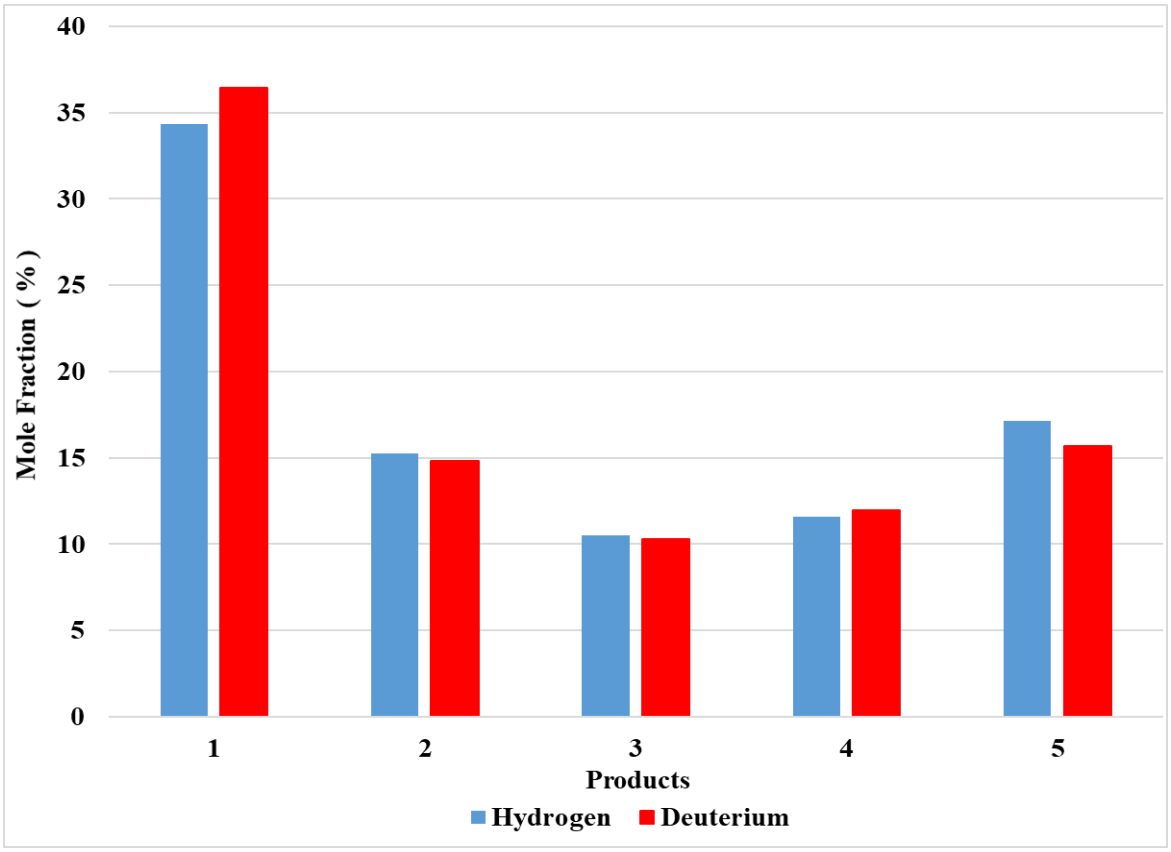

Figure 212. Product distribution of deuterium against hydrogen at 90 % conversion of 4-methoxyphenol.

Key: 1: 4-Methoxycyclohexanone **2:** Cyclohexanol **3:** Cyclohexanone **4:** Methoxycyclohexane **5:** Cyclohexane

From Figure 212 it can be seen that, except for a small increase in 4-methoxycyclohexanone and a small decrease in cyclohexane under deuterated conditions, all product distribution remained broadly constant with both gas reactants.

The kinetic data gathered from the deuteration reactions is outlined in Table 35 below:

Table 35. KIE's for the individual the methoxyphenol isomer reactions.

Substrate	kH	kD	KIE = $\frac{kH}{kD}$
2-Methoxyphenol	11.5	16.3	0.7
3-Methoxyphenol	12.8	18.0	0.7
4-Methoxyphenol	7.4	11.3	0.7

Calculation of KIE can result in three possible outcomes as shown below:

- KIE value equals 1 then there is no KIE effect
- KIE > 1 yields a *positive* KIE effect
- KIE < 1 yields a *negative* KIE effect

Table 35 above shows all three substrates recorded an inverse KIE of 0.7.

7.3.6 Post Reaction Catalyst Characterization

Thermogravimetric analysis (TGA) on the post reaction catalyst from the standard hydrogenation (3 hours) of all substrates was carried out.

7.3.6.1 2-Methoxyphenol

The thermal weight loss and associated evolved gas mass spectrometry data for the post 2-methoxyphenol reaction catalyst is shown in Figures 213 and 214 below:

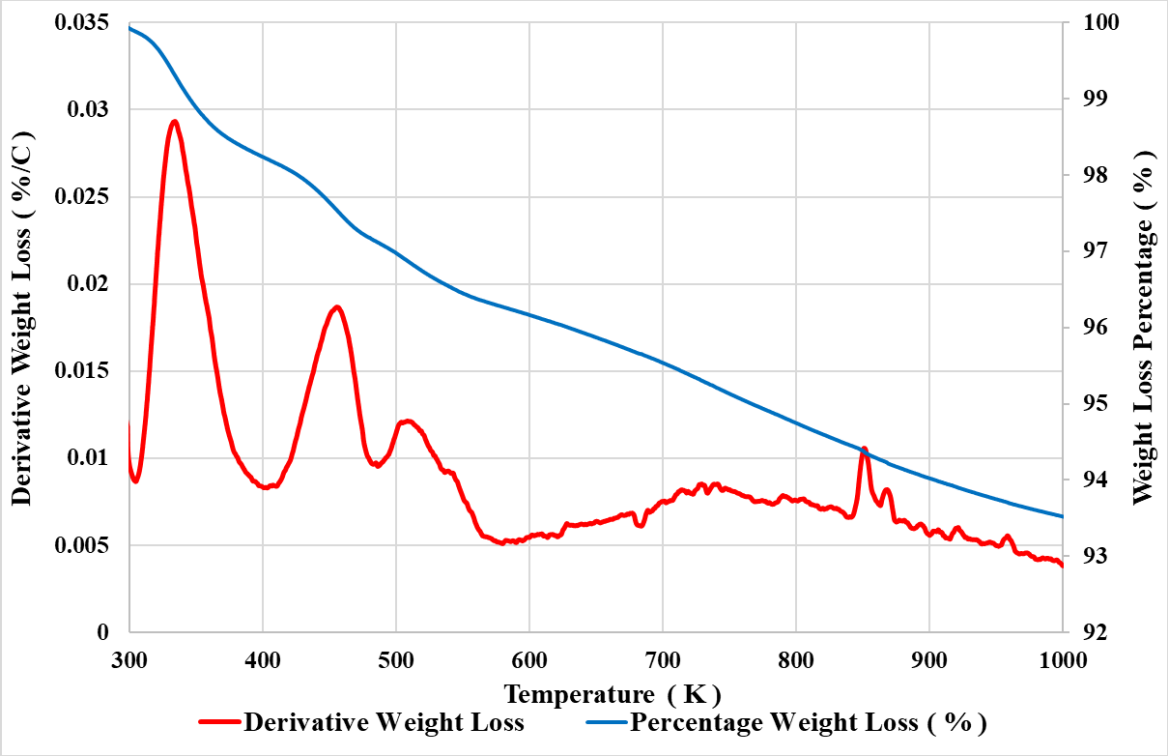

Figure 213. TGA of Rh/SiO_2 catalyst after 3-hour 2-methoxyphenol hydrogenation reaction.

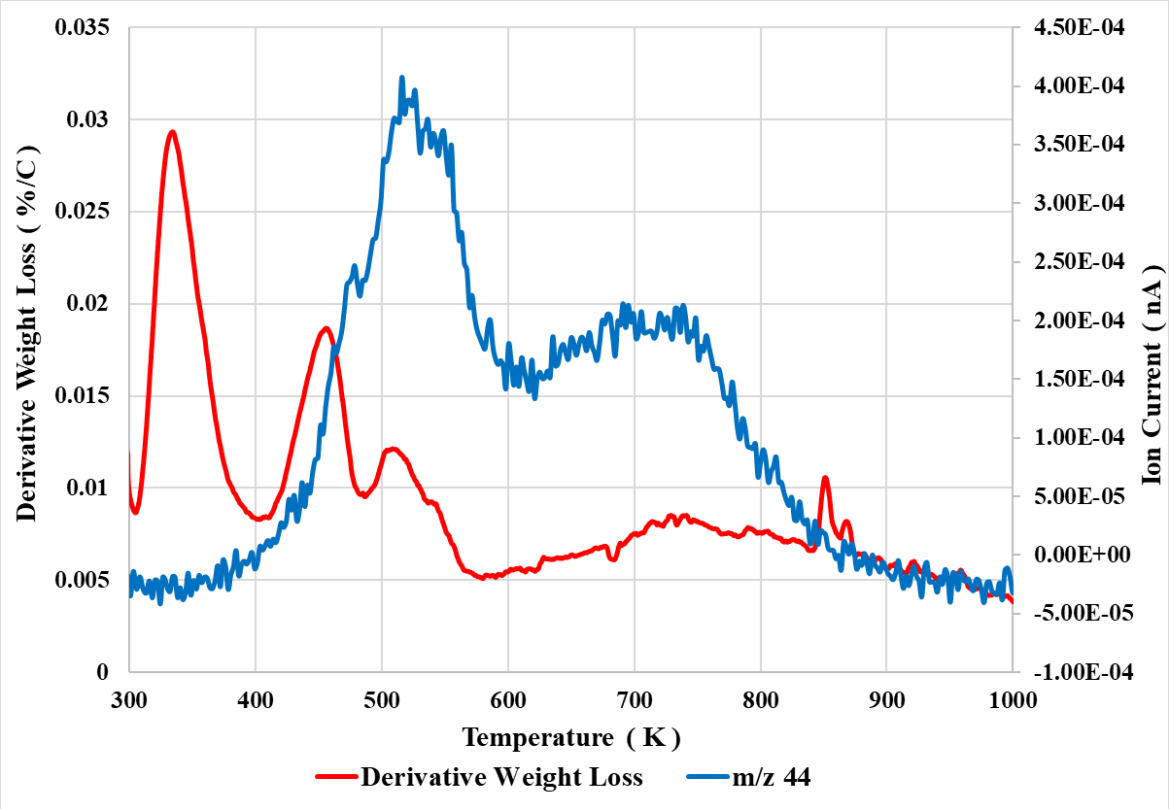

Figure 214. Derivative weight loss coupled with m/z of Rh/SiO_2 catalyst after 3-hour 2-methoxyphenol hydrogenation reaction.

From Figures 213 and 214 above it can be seen that, the total weight loss from the catalyst over the measured temperature range was 6.5 %, of which 5 % is accounted for by the three high temperature weight loss events (>460 K) associated with the evolution of m/z = 44 (CO_2). The initial weight loss event between 300 and 400 K is a result of the evolution of water.

7.3.6.2 3-Methoxyphenol

The thermal weight loss and associated evolved gas mass spectrometry data for the post 3-methoxyphenol reaction catalyst is shown in Figures 215 and 216 below:

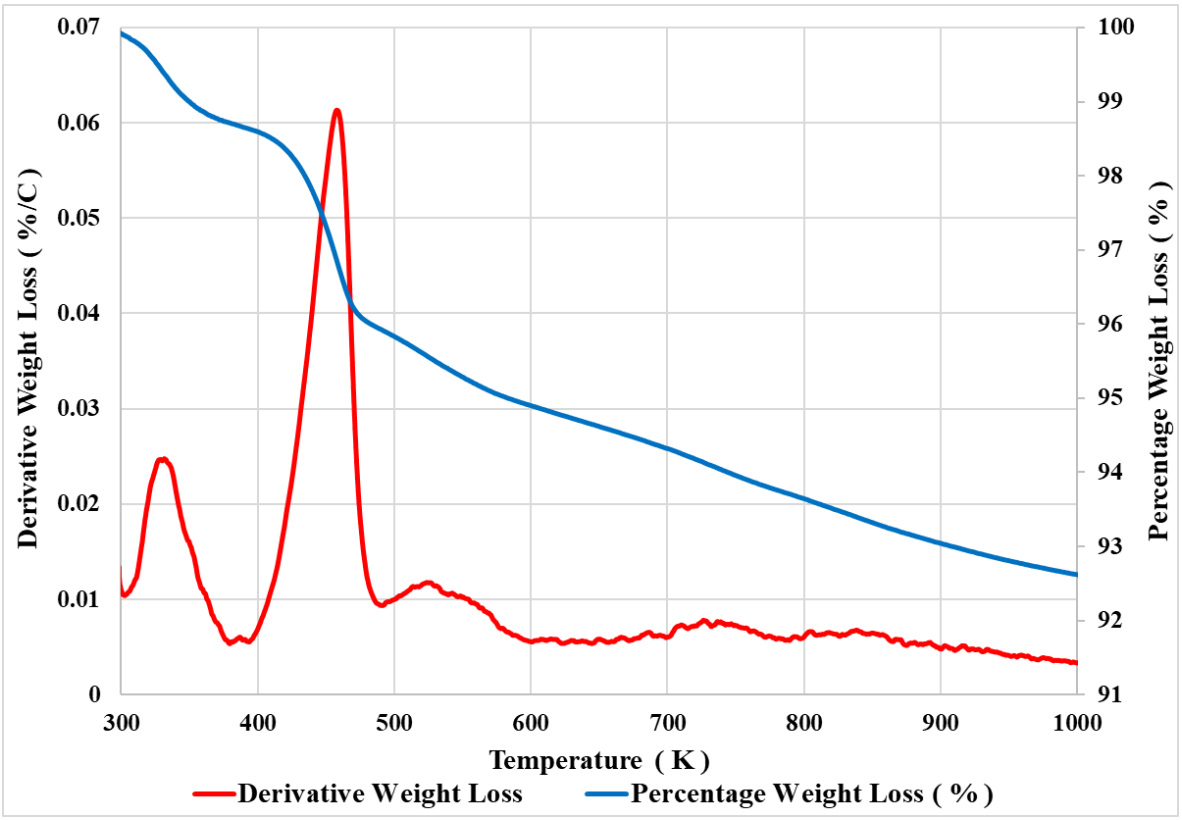

Figure 215. TGA of Rh/SiO_2 catalyst after 3-hour 3-methoxyphenol hydrogenation reaction.

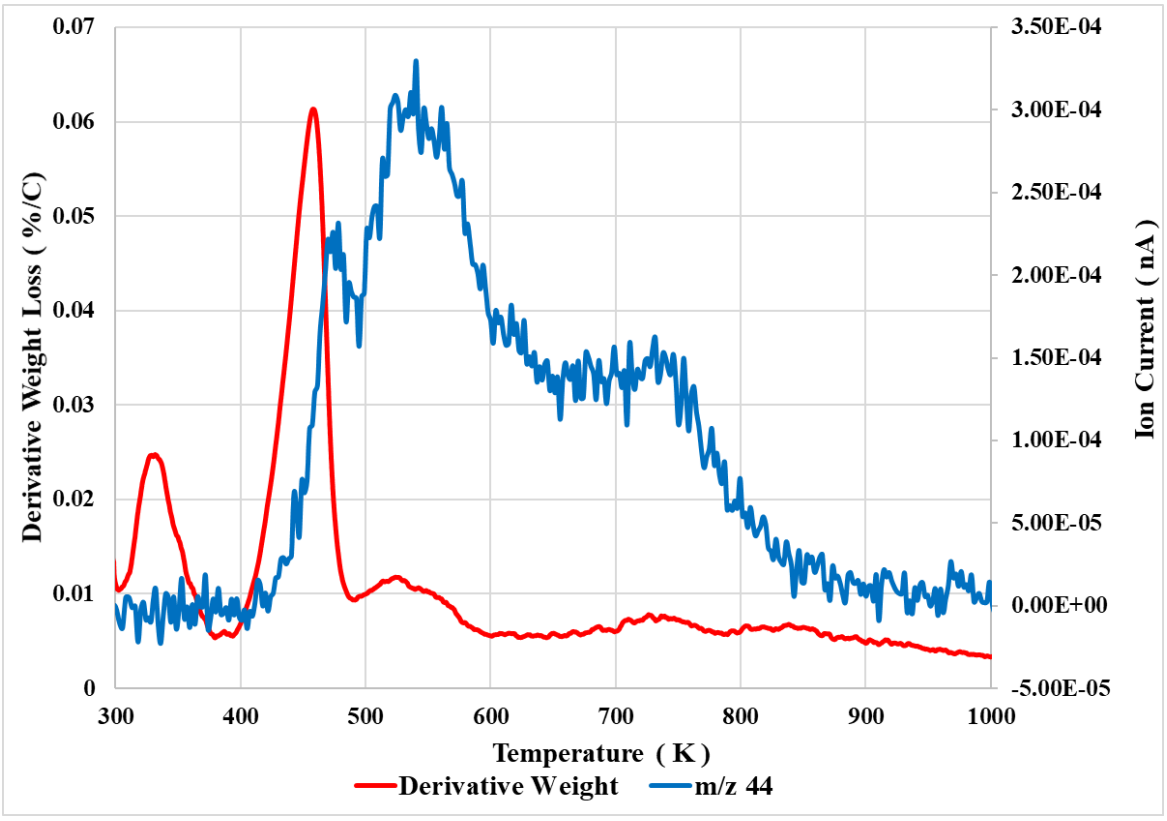

Figure 216. Derivative weight loss coupled with m/z of Rh/SiO_2 catalyst after 3-hour 3-methoxyphenol hydrogenation reaction.

From Figures 215 and 216 above it can be seen that the total weight loss from the catalyst over the measured temperature range was ~7 %. The three high temperature weight loss events (>460 K) account for around 6 % and are associated with the evolution of m/z = 44 (CO_2). The initial weight loss event between 300 and 400 K is a result of the evolution of water.

7.3.6.3 4-Methoxyphenol

The thermal weight loss and associated evolved gas mass spectrometry data for the post 4-methoxyphenol reaction catalyst is shown in Figures 217 and 218 below:

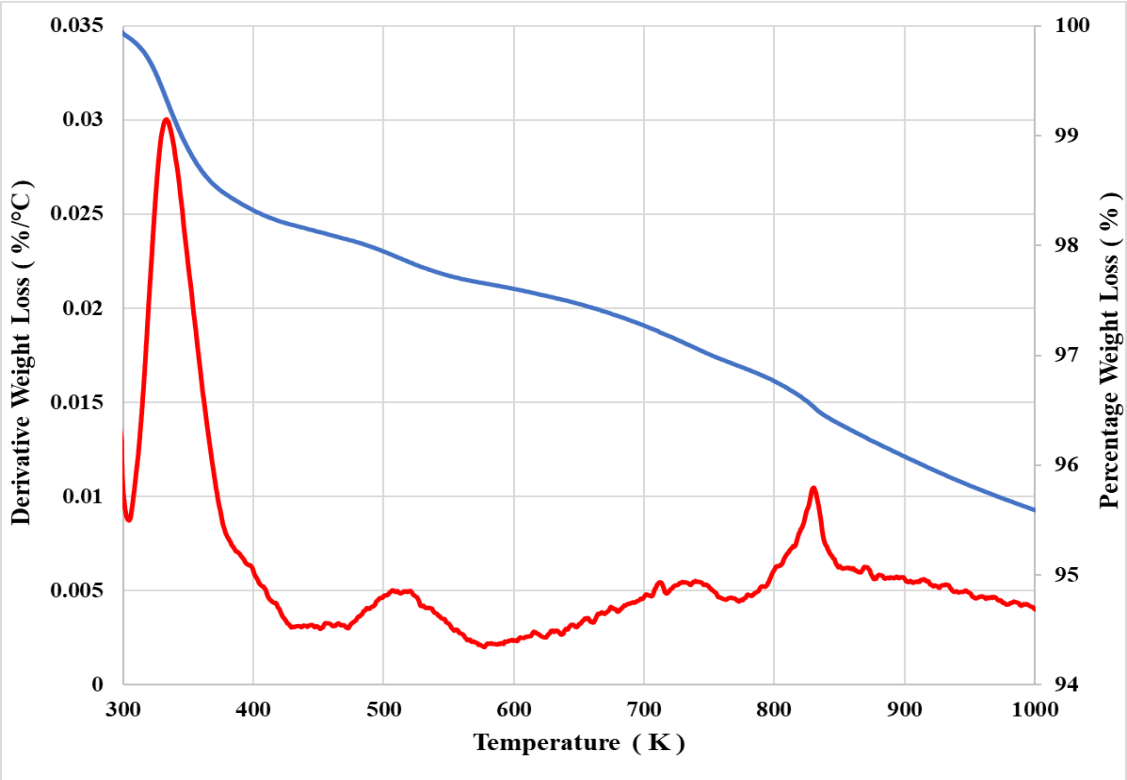

Figure 217. TGA of Rh/SiO_2 catalyst after 3-hour 4-methoxyphenol hydrogenation reaction.

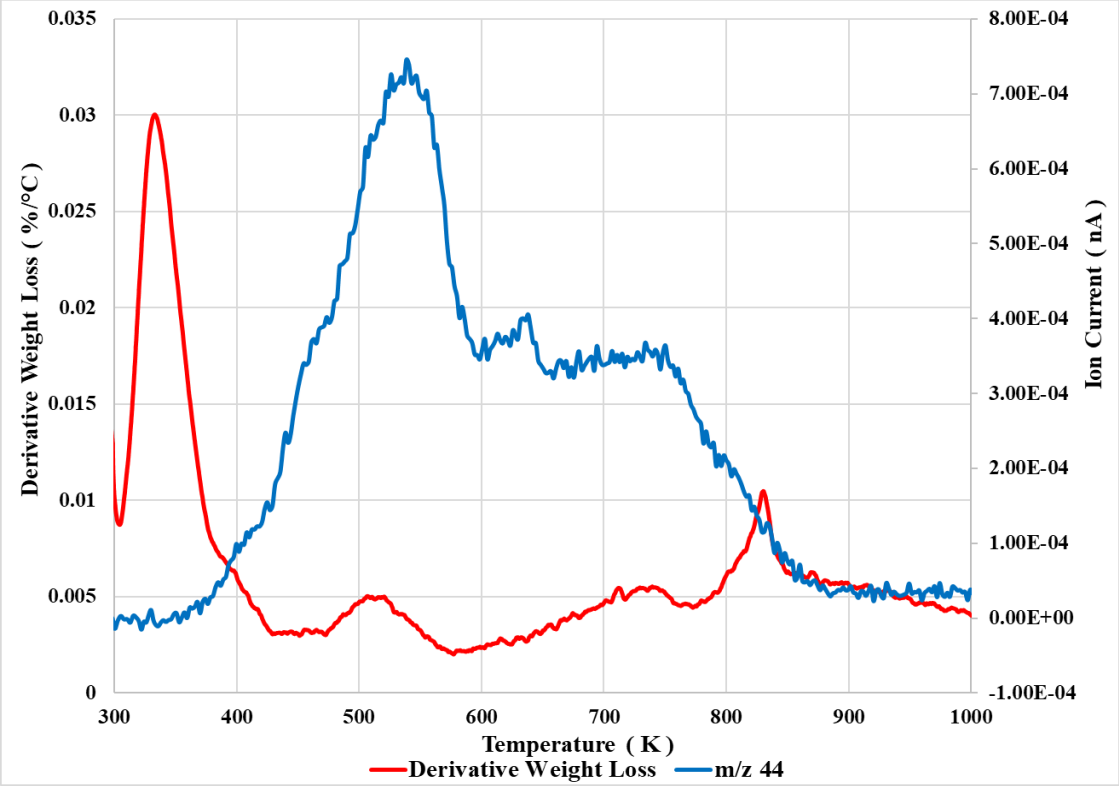

Figure 218. Derivative weight loss coupled with m/z of Rh/SiO_2 catalyst after 3-hour 4-methoxyphenol hydrogenation reaction.

From Figures 217 and 218 above it can be seen that the total weight loss from the catalyst over the measured temperature range was ~5 %. The three high temperature weight loss events (>460 K) account for around 3 % and are associated with the evolution of m/z = 44 (CO_2). The initial weight loss event between 300 and 400 K is a result of the evolution of water. The weight loss event >800 K and accounting for ~ 1 % is unique to the 4-methoxyphenol post reaction catalyst.

7.4 Combination of isomers

This section contains the results from three competitive reactions where the comparative isomers from each set of substrates were reacted together under standard conditions.

7.4.1 *ortho*-Isomer combinations

The competitive reaction of the *ortho* isomers: catechol, *ortho*-cresol and 2-methoxyphenol was carried out under standard reaction conditions of 323 K, 10 mmol substrate each and 3 barg hydrogen and is shown below in Figure 219:

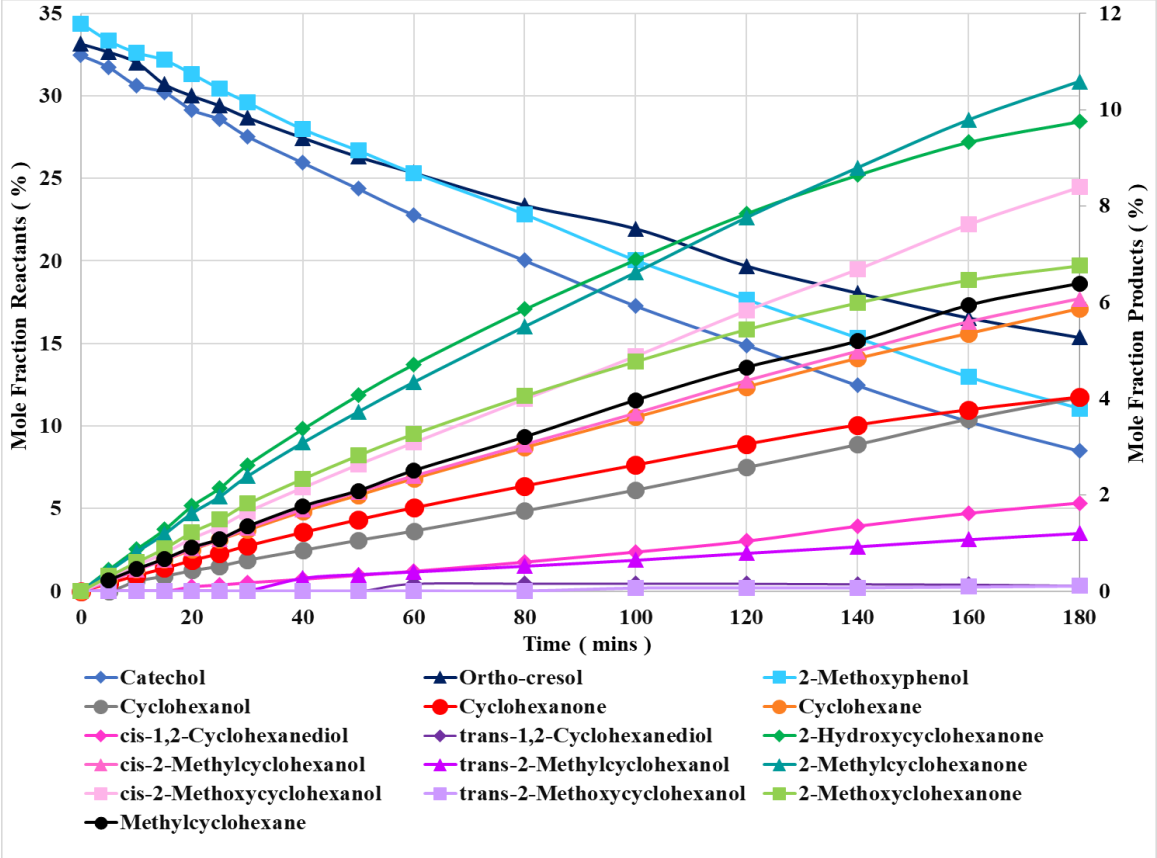

Figure 219. *ortho*-Isomer combination, 323 K, 10 mmol substrate, 3 barg H_2.

From Figure 219 it is clear, that no substrate achieved full conversion by end of reaction, with catechol recording the highest conversion of 70 %. All three isomers showed similar levels of reactivity, giving calculated rate constants of 3.8, 3.5 and 3.2x$10^3$$min^{-1}$ for catechol, *ortho*-cresol and 2-methoxyphenol respectively. At end of reaction the major products were the initial hydrogenated products from *ortho*-cresol (2-methylcyclohexanone) and catechol (2-hydroxycyclohexanone) followed by the secondary hydrogenated product from 2-methoxyphenol (*cis*-2-methoxycyclohexanol), slightly favoured over its initial hydrogenated product (2-methoxycyclohexanone). All HDO products, with the exception of methoxycyclohexane from 2-methoxyphenol, were observed, with the highest mole fraction recorded for methylcyclohexane, only formed via

ortho-cresol. Formation of the trans isomer from all three substrates was delayed, to 40, 50 and 100 minutes for *ortho*-cresol, catechol and 2-methoxyphenol respectively.

7.4.2 *meta*-Isomer combinations

The competitive reaction of the *meta* isomers: resorcinol, *meta*-cresol and 3-methoxyphenol was carried out under standard reaction conditions of 323 K, 10 mmol substrate each and 3 barg hydrogen and is shown below in Figure 220:

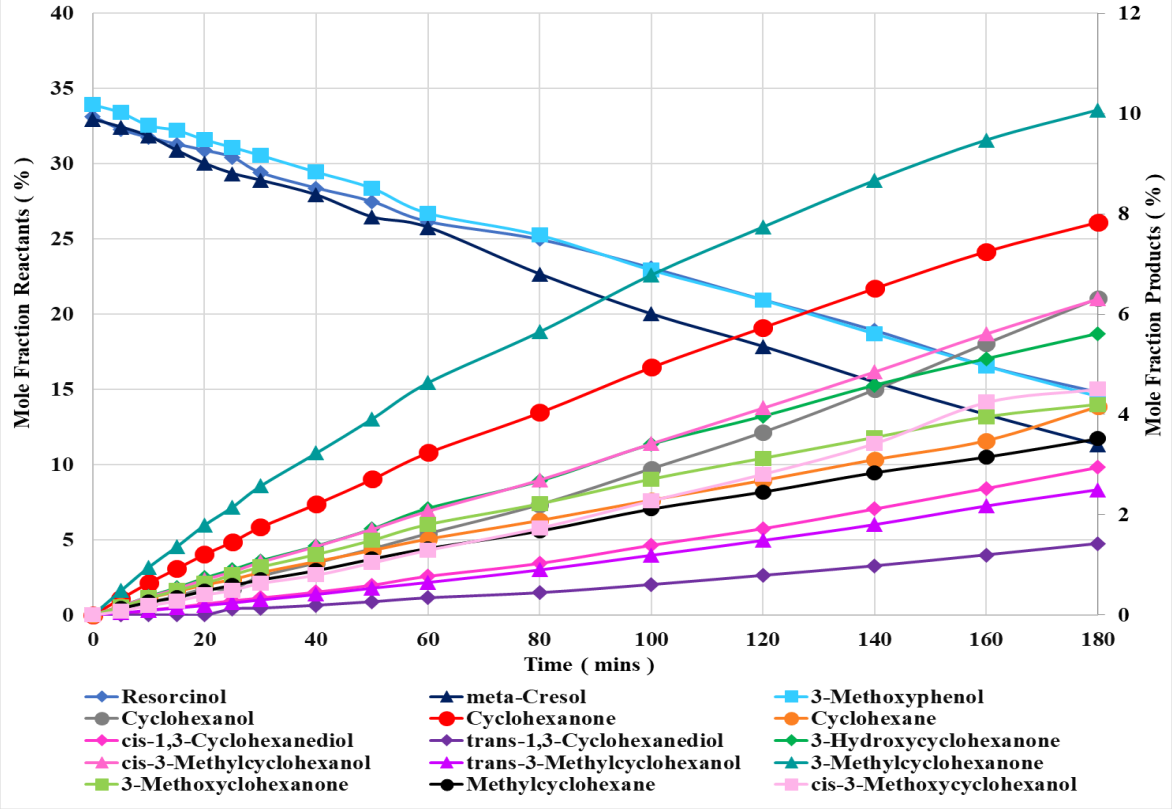

Figure 220. *meta*-Isomer combination, 323 K, 10 mmol substrate, 3 barg H_2.

From Figure 220 it is clear that no substrate achieved full conversion by end of reaction, with *meta*-cresol recording the highest conversion of 66 %. The highest reactivity was recorded for *meta*-cresol with a calculated rate constant of $4.8 \times 10^{3} min^{-1}$, both 3-methoxyphenol and resorcinol recorded similar values of 3.6 and 3.7 $\times 10^{3} min^{-1}$ respectively. The major product by reaction end was the initial hydrogenated product from *meta*-cresol (3-methylcyclohexanone) followed by the HDO product of both 3-methoxyphenol and resorcinol, cyclohexanone. As with the *ortho* isomer combination all HDO products were formed with the exception of methoxycyclohexane. Formation of the *trans* isomer from *meta*-cresol occurred initially, with that from resorcinol exhibiting a 25-minute delay. No formation of the *trans* isomer was detected from 3-methoxyphenol.

7.4.3 *para*-Isomer combinations

The competitive reaction of the *para* isomers: hydroquinone, *para*-cresol and 4-methoxyphenol was carried out under standard reaction conditions of 323 K, 10 mmol substrate each and 3 barg hydrogen and is shown below in Figure 221:

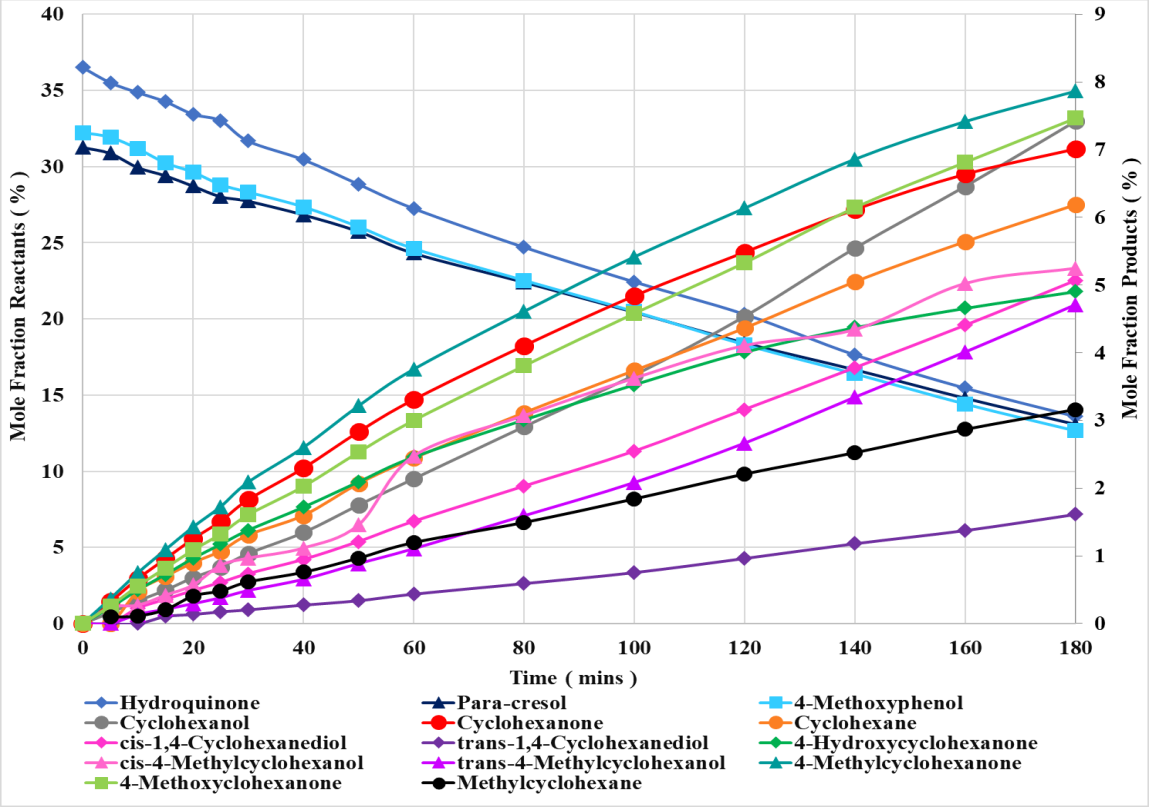

Figure 221. *para*-Isomer combination, 323 K, 10 mmol substrate, 3 barg H_2.

From Figure 221 it can be seen that all three substrates showed ~ 60 % conversion by end of the reaction, with calculated rate constants of 3.2, 3.1 and $3.4 \times 10^{3} min^{-1}$ found for hydroquinone, 4-methoxyphenol and *para*-cresol respectively. The major products by the end of reaction were the initial hydrogenated products from para-cresol (4-methylcyclohexanone) and 4-methoxyphenol (4-methoxycyclohexanone). Notable formation of the HDO products, cyclohexanol, cyclohexanone and cyclohexane, which can occur only via 4-methoxyphenol and hydroquinone was present. As with both the *ortho* and *meta* isomer combinations the HDO product, methoxycyclohexane, was absent from the reaction. Formation of the trans isomer was delayed to 10 and 15 minutes respectively from *para*-cresol and hydroquinone, whilst no formation was evidenced from 4-methoxyphenol.

8 Discussion

8.1 Dihydroxybenzene Isomers

8.1.1 Individual Hydrogenation

Hydrogenation of the individual substrates gave the following order of reactivity: resorcinol > catechol > hydroquinone (*meta* > *ortho* > *para*). This is in contrast to findings by Smith and Stump over rhodium and platinum catalysts who reported an order of hydroquinone > resorcinol > catechol. [52] The experimental conditions however were markedly different with 2.0 g of a 5 % rhodium on alumina catalyst used in comparison to the 0.1 g of a 2.5 % rhodium on silica catalyst employed in this study. This higher reactivity of resorcinol in comparison to catechol and hydroquinone has been previously documented by Maximov et al. using a ruthenium catalyst, with the favourable arrangement of the two-hydroxyl groups when in the *meta* position postulated as the reason behind the faster rate. [97] In addition, a study on HDO of methyl substituted phenols by Furimsky, et al. [35] found the *meta* isomer to be the most reactive isomer followed in this instance by the *para* isomer. Reasons why the *meta* position should be seen as a favourable arrangement was not proposed in either study. However, it is known that electrophilic aromatic substitution reactions are termed as '*ortho*- and *para*- directing' when a single electron donating substituent is present and are said to be '*meta*- directing' when the substituent is an electron withdrawing group. This is due to the increased stability of the resonance structures that can form when in the *ortho* and *para* position. Whilst not directly comparable with our work, the inability of the *meta* isomer to form the most stable resonance structure: whereby the electropositive charge is on the oxygen atom of the C=O bond, may offer an explanation as to why we see the enhanced reactivity with the *meta* isomer when compared to that of the *ortho* and *para* isomers. In the case of disubstituted aromatics, it is accepted that the inductive and resonance effects between two electron donating substituents can be either cooperative, when in the *meta* position, or conflictive in the *ortho* and *para* positions. This may offer a further explanation as to why we see an enhanced reactivity with the *meta* isomer.

An additional factor that may influence dihydroxybenzene reactivity is the substrate pKa value, which follows an order of 9.20, 9.25 and 9.91 for resorcinol, catechol and hydroquinone respectively. This indicates a possible relationship between pKa and order with the strongest acid, resorcinol, giving the highest reactivity and the weakest acid, hydroquinone, showing the least, therefore posing the question does the strength of the acid have an effect on the reactivity. [98] One answer could be that the lower pKa value of

resorcinol allows for easier dissociation of the -OH groups resulting in enhanced reactivity on the surface of the catalyst.

The product distribution for each of the substrates shows significant differences when comparing mole fraction at the same conversion as outlined in Figure 222 below:

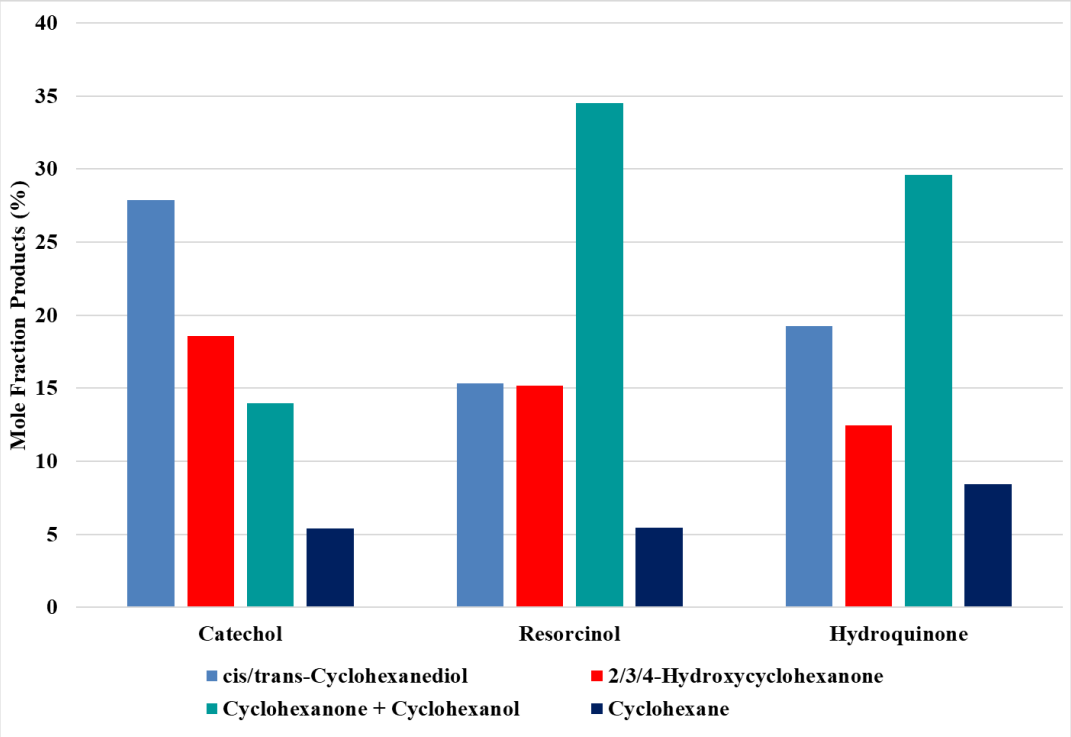

Figure 222. Product distribution for dihydroxybenzenes at ~ 70 % conversion.

It is apparent that resorcinol and hydroquinone have a clear preference towards HDO, with 40 % of the products having one of the hydroxyl groups cleaved against 30 % hydrogenated to the ring saturated products. In contrast, catechol, consisting of the same substituents as resorcinol and hydroquinone and differing only in their ring position, exhibited the opposite behaviour with just 19 % of products having a hydroxyl group cleaved against 46 % undergoing solely hydrogenation. Whilst literature on dihydroxybenzenes' adsorption is relatively sparse, this behaviour where the *ortho* isomer exhibited a greater resistance to HDO than *meta*/*para* isomers was reported by Odebunmi and Ollis in 1983 in a study of the HDO activity of methyl phenols [63,64].

The mode of adsorption has been put forward as one of the factors determining substrates deoxygenation ability. Bredenberg and Sarbak [99] in their study on the adsorption of dihydroxybenzenes, using chemisorption and infrared spectroscopy, proposed that the *para* and *meta* isomers both have a flat mode of adsorption whilst the *ortho* isomer adopts an inclined mode making deoxygenation less favourable. However, we postulate that when bonded strongly through the two oxygen atoms, with the hydrogen atoms pointing away

from the surface, the *ortho* position can adopt a flat mode of adsorption similar to that proposed in the *meta* and *para* positions and as such should be equally favourable to HDO. It may be instead that the position of the hydroxyl groups on the ring is the main factor when determining the substituents ability to undergo deoxygenation. The proximity of the two hydroxyl groups, when in the *ortho* position and their ability to interact via hydrogen bonding, would result in a significant suppression in cleavage of the –OH. Whilst in the *meta* and *para* position this would not be the case due to the nonadjacent ring position of the hydroxyl groups.

When we come to look at selectivity, these differences in favourability towards HDO between the isomers is further emphasised. Figure 223 below shows the selectivity of each product taken at ~ 70% conversion.

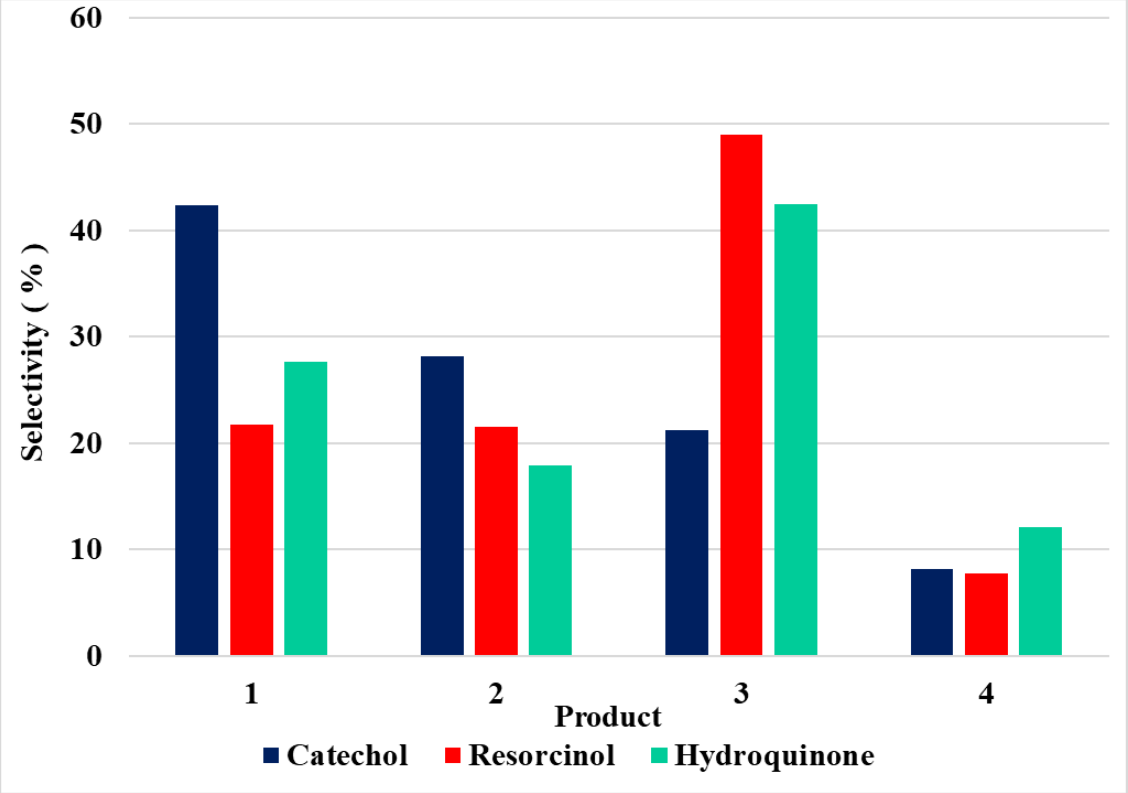

Figure 223. Product selectivities calculated at ~ 70 % conversion of substrate. Key: 1=cis+trans-cyclohexanediol 2=Hydroxycyclohexanone 3=Cyclohexanol+Cyclohexanone 4=Cyclohexane

It is evident that there are significant differences in the dominant reaction pathway for each of the substrates studied. As expected from the product distribution results shown previously, catechol has the highest selectivity towards the ring hydrogenated species; 42 % and 28 % to *cis+trans*-1,2-hydroxycyclohexane and 2-hydroxyclyclohexanone respectively. In contrast, resorcinol exhibited low selectivity for both *cis+trans*-1,3-hydroxycyclohexane and 3-hydroxycyclohexanone, with a higher selectivity towards

cyclohexanol and cyclohexanone of 49 %, reiterating the unexpected favourability of resorcinol to undergo HDO as seen in the product distribution. Hydroquinone, which shared a similar product distribution to resorcinol, also shows the expected higher selectivity towards hydrogenolysis products. It is of note, that a similar selectivity towards cyclohexane was observed for all three substrates. This may indicate that the ability to form this particular HDO product is independent of the hydroxyl groups' position on the ring, which leads us on to the important area of how the formation of products occur during the hydrogenation of dihydroxybenzenes.

For this purpose, we will focus on the product mole fraction graph, and that of hydroquinone is shown below in Figure 224:

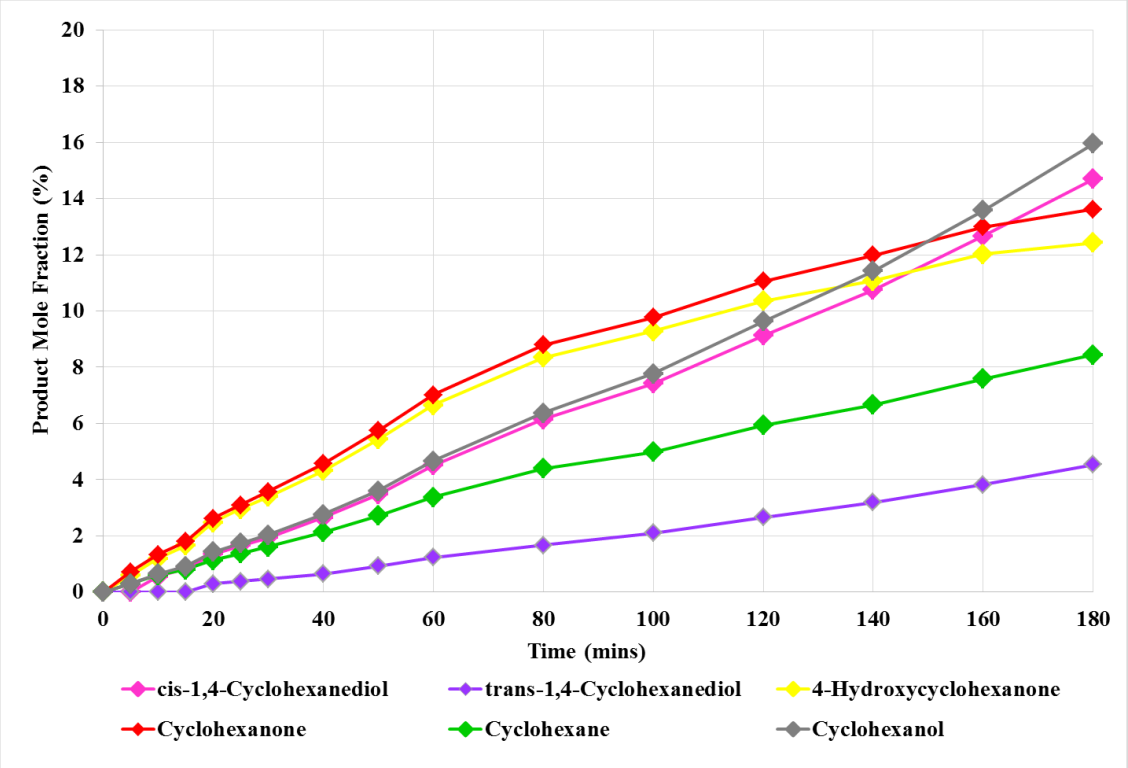

Figure 224. Product mole fraction graph of hydroquinone hydrogenation. Conditions, 323 K, 10 mmol, 3 barg

It is evident that, with the exception of *trans*-1,4-cyclohexanediol, all products are present from the start of the reaction suggesting a direct and independent route for each product. Whilst the graph refers to hydroquinone hydrogenation, these findings are applicable for both catechol and resorcinol. This independent route of product formation has been reported previously by Alshehri et al. [59] examining phenol hydrogenation. They also observed a delay in the formation of the *trans* isomer and suggested that this does not form directly from the substrate but instead via a desorption-readsorption mechanism from the *cis*-isomer. It could be assumed from the graph above where the presence of the *trans*

isomer only occurs after formation of the *cis* isomer that a similar mechanism is at play; however, we believe that this is not the case for the dihydroxybenzenes. The addition of the *cis*-1,2-cyclohexanediol under reaction conditions and the subsequent non formation of the *trans*-1,2-cyclohexanediol has shown that no isomerization takes place, as outlined in Figure 225 below.

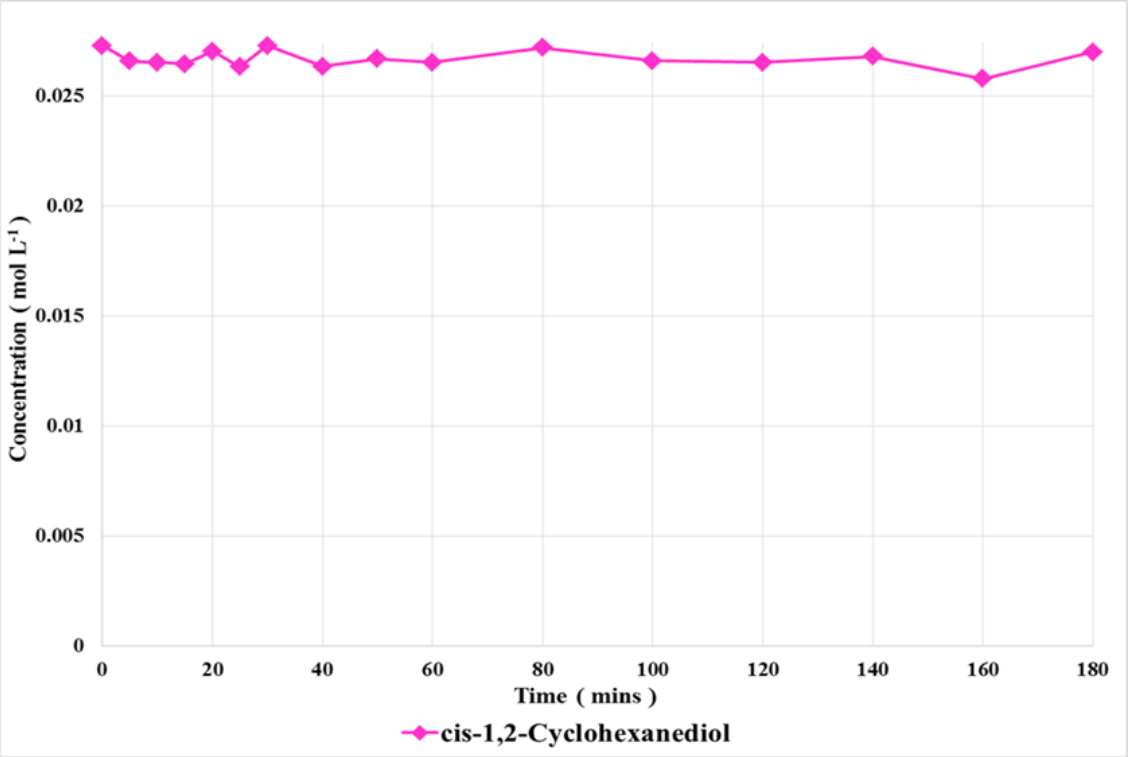

Figure 225. Reaction profile of cis-1,2-cyclohexanediol hydrogenation. Conditions, 333 K, 10 mmol, 3 barg.

cis-1,2-Cyclohexanediol is seen to be extremely unreactive under standard reaction conditions and as mentioned above no evidence of isomerization is present. Which begs the question what is the route of the *trans* isomer formation? We know the dihydroxybenzene undergoes hydrogenation to form both the keto and, the highly reactive and as such unobservable, enol product. Our previously postulated flat mode of adsorption for the dihydroxybenzenes would result in an enol product which could only undergo hydrogenation to the *cis* isomer. As such, we propose the formation of the *trans* isomer occurs solely via the keto product: initial formation of 2/3/4-hydroxycyclohexanone is followed by readsorption to the catalyst surface and subsequent desorption as the *trans* isomer. This extra step in the formation of the *trans* isomer may explain the delay in its detection.

In addition, this result also exposes an important insight into the mechanism of HDO; the failure of the hydrogenated product, *cis*-1,2-cyclohexanediol to form cyclohexanone or

cyclohexanol suggests a route of formation for these products directly from the aromatic substrate. The bond dissociation energies of aromatic and aliphatic C-O bonds at approximately 468 and 385 kJ/mol respectively would suggest that the *cis*-1,2-cyclohexanediol should cleave more readily than the substrates, however, this is shown not to be the case. [35] We instead propose the route of formation of the HDO products occurs via highly reactive surface intermediates formed directly from hydrogenation of the aromatic.

This idea of intermediates being linked to HDO activity was first stated by Smith and Stump in 1961 during their study on dihydroxybenzene hydrogenation. [52] Therefore, we propose that the initial hydrogenation of the aromatic results in the formation of highly reactive surface intermediates, containing double bonds, which facilitate the promotion of hydrogenolysis. Examining catechol as an example and considering the intermediates that can be formed (Figure 226) it is apparent

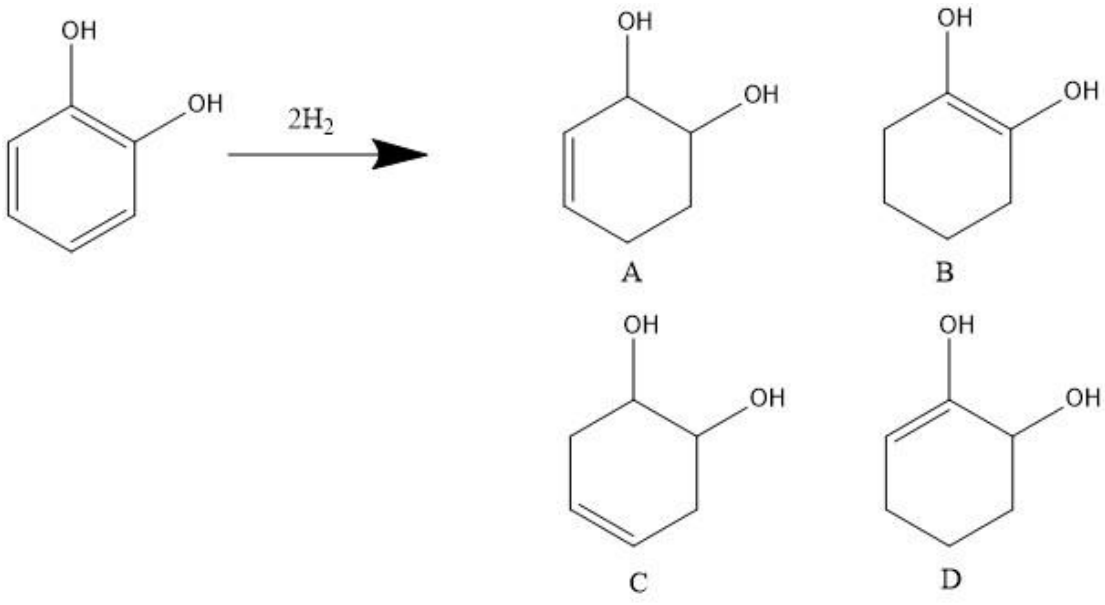

Figure 226. Catechol hydrogenation via highly reactive intermediates.

that intermediate A contains a double-bond β-γ to a hydroxyl group, rendering this group susceptible to hydrogenolysis, whilst in intermediates B and D the double bond position makes the formation of 2-hydroxcyclohexanone through keto-enol tautomerization more likely. Further hydrogenation of the 2-hydroxycyclohexanone would result in the formation of *cis*/*trans*-1,2-cyclohexanediol and as such, intermediates B and D are the most likely routes for hydrogenation. [52] It should be noted that although intermediate A can form the HDO products via hydrogenolysis, it can also form the hydrogenated products. Intermediate C is unlikely to contribute to the reaction due to the position of its

double bond making keto-enol tautomerization and HDO more difficult, it could however still exist as a surface intermediate. When studying the intermediate formation for resorcinol and hydroquinone it is apparent that a greater number of those with the double-bond β-γ to the hydroxyl group, as seen above in A, can be potentially formed, which may explain the increased bias towards hydrogenolysis observed with these two isomers.

However, analysis of selectivity of the HDO product, cyclohexane, showed similar levels for all three isomers indicating the variation in intermediates formed between the different isomers is having no effect. This may point to formation of cyclohexane occurring only when both hydroxyl groups, independent of ring position, are bonded to the surface and undergo simultaneous hydrogenolysis. It has been postulated in the literature that formation occurs via a step-wise process, with initial hydrogenation to the aliphatic hydroxycyclohexanone followed by hydrogenation to cyclohexanediol and subsequent hydrogenolysis to cyclohexane. The presence of cyclohexane, however, from the initial stages of the reaction in our study indicates that this theory is not applicable which corresponds with recent work studying phenol hydrogenation over the same catalyst as ours. [59,100] Their study showed that cyclohexane formation ceased when phenol was fully converted indicating a route of formation dependent on the presence of the aromatic substrate. Findings from the same study when cyclohexanone was used as the substrate recorded cyclohexanol as the sole product. Furthermore, cyclohexanol itself was shown to be stable under reaction conditions, with no cyclohexane formed. All this is in accordance with our earlier stated hypothesis that without the aromatic present there is no hydrogenolysis. The reaction scheme therefore proposed for the dihydroxybenzene isomers, using hydroquinone as an example, is shown below in Figure 227 below:

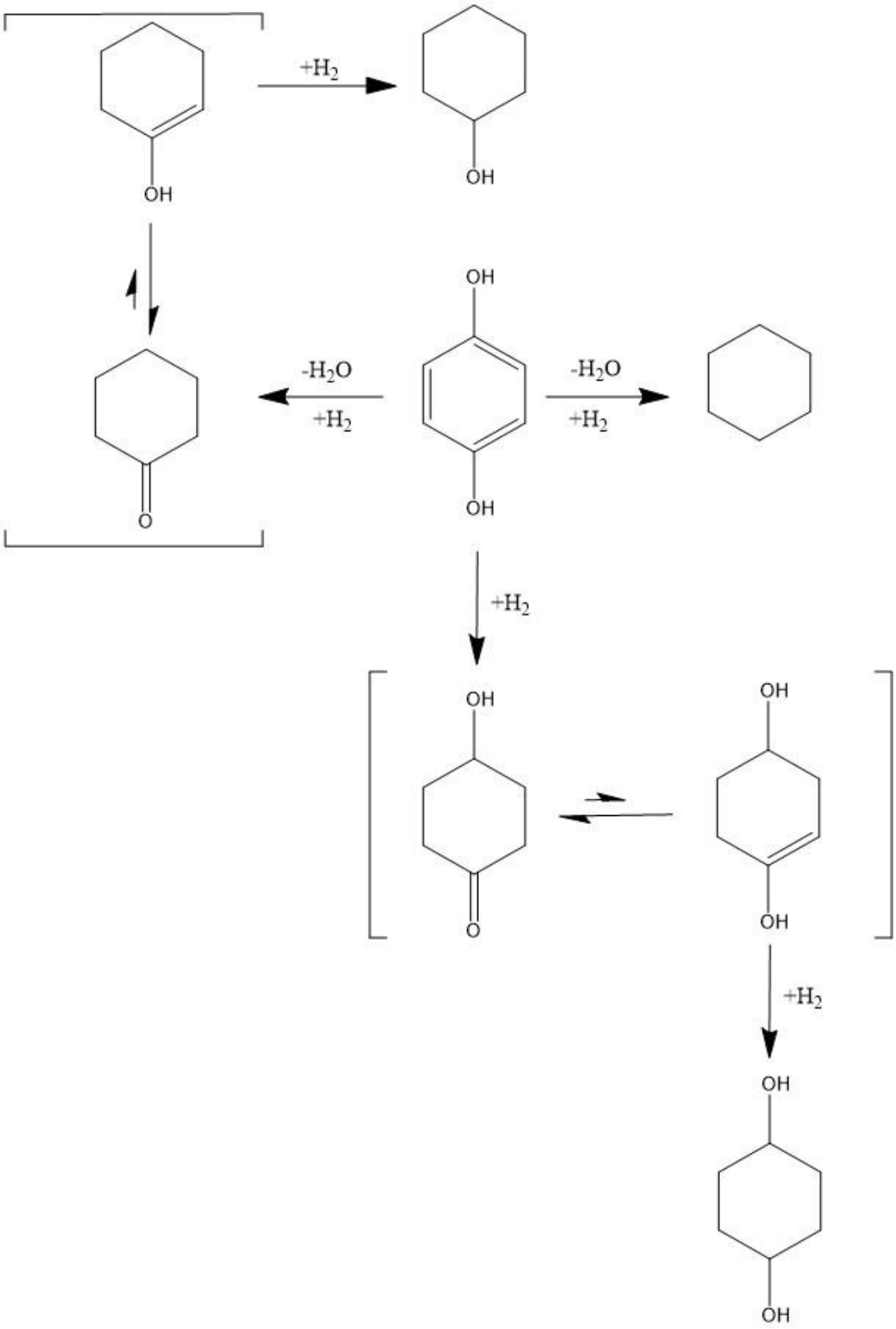

Figure 227. Hydroquinone Reaction Scheme.

The importance of high HDO activity under mild conditions as outlined in this study cannot be overstated. It is highly beneficial for the purpose of bio-oil upgrading that considerable amounts of oxygen are removed, and as such, the high selectivities shown

here towards the deoxygenated products are of real significance. In addition, cyclohexanol and cyclohexanone are vital intermediates in the preparation of caprolactam and adipic acid, the main ingredients in the production of Nylon 6 and Nylon 6,6 making them important products in their own right. [48,101] The high selectivity to the hydrogenated product, *cis*-1,2-hydroxycyclohexane, seen with catechol is also of importance as it plays a vital role as an intermediate in both the perfume and fragrance industry, and in drug and lubricant synthesis.[102]

8.1.2 Temperature Variations

As expected, all isomers of the dihydroxybenzenes showed an increase in rate with temperature; summarised in Table 36 below:

Table 36. Rate constants of dihydroxybenzene isomers over temperature range.

Temperature (K)	**Catechol: k ($x10^{-3}min^{-1}$)**	**Resorcinol: k ($x10^{-3}min^{-1}$)**	**Hydroquinone: k ($x10^{-3}min^{-1}$)**
303	3.3	3.3	2.9
313	4.6	5.4	3.9
323	8.3	11.9	4.2
333	9.5	14.6	8.1
343	10.4	21.9	12.5

From the calculated rate constants, it is clear that resorcinol experienced the most significant effect with temperature, a near 6-fold increase in rate over the 40 K temperature range. Both hydroquinone and catechol also exhibited a rate increase with temperature; however, this was less marked than seen with resorcinol. This may be due to the previously postulated 'reinforcing' favourable arrangement that exists when the two-hydroxyl groups are in the *meta* position having a more marked effect on the temperature dependence of resorcinol. The activation energies calculated followed the order: resorcinol > hydroquinone ~ catechol (41 > 31 ~ 31 $kJmol^{-1}$), whereby resorcinol displayed a unique activation energy whilst hydroquinone and catechol showed a similar dependence. The lower activation energy of catechol may be the result of a steric effect when adsorbed to the surface, however, with this said the hydroquinone value is similar and there would be

no steric inhibition for the *para* isomer. This order was documented previously by Smith and Stump [52] over Rh who also reported a different activation energy for resorcinol (33 $kJmol^{-1}$) from the shared value for catechol and hydroquinone of ~ 27 $kJmol^{-1}$. They offered no explanation as to why this was the case. A comparison with a study of phenol hydrogenation over the same catalyst, where an activation energy of 23 $kJmol^{-1}$ was reported, shows a stronger temperature dependence for the dihydroxybenzenes. This may be due to the presence of two hydroxyl groups in the dihydroxybenzenes, which when undergoing hydrogenolysis, would require significantly more energy than with phenol, as such an increase in temperature would facilitate cleavage to occur more readily.

When we come to look at the effect of temperature on the level of hydrogenolysis, it is apparent from the product distribution graphs that it becomes more favoured as temperature is increased with a rise in HDO products observed. Smith and Thompson [103] have stated the amount of cleavage of the hydroxyl group increases linearly with temperature; however, if we look at catechol shown in Figure 228:

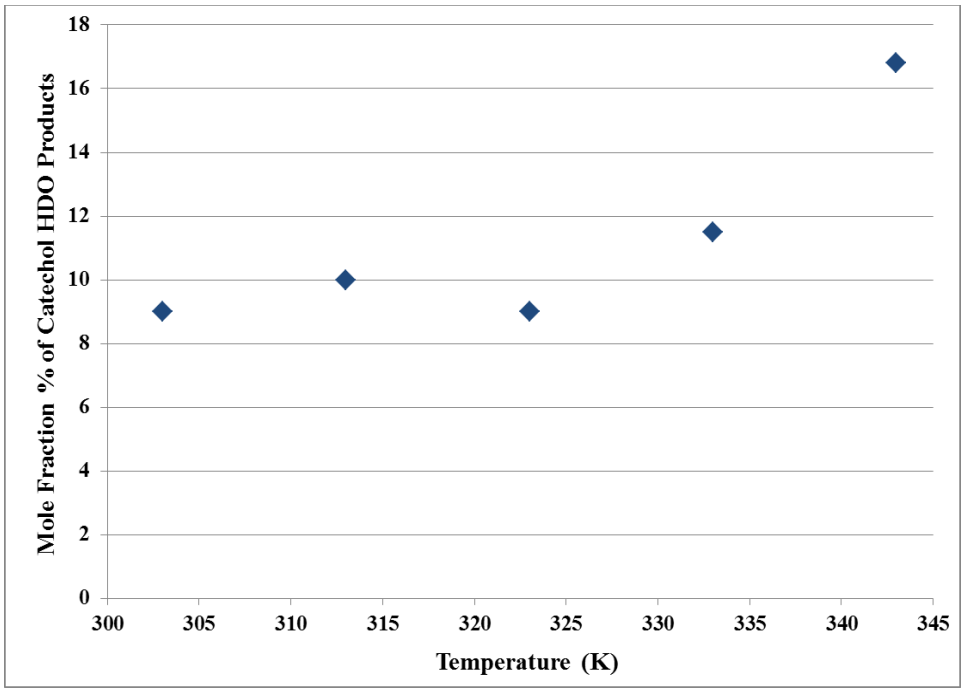

Figure 228. Mole fraction of catechol HDO products with temperature.

It is clear, that in our system, this is only evident between 323 and 343 K, with no linear relationship apparent below 323 K; an observation applicable for both resorcinol and hydroquinone. As we already witness the occurrence of HDO under mild conditions, it is not unexpected that an increase in temperature would result in even greater HDO activity.

Whilst an overall increase in hydrogenolysis activity and concomitant decrease in that of hydrogenation with temperature exists, there are divergent trends for the individual

reaction products. A closer examination of these shows that the initially formed hydroxycyclohexanone, exhibits an increase in formation with temperature, whilst the secondary hydrogenated product, *cis+trans*-cyclohexanediol, shows a decrease. This difference in behaviour with temperature was also present with the HDO products, where cyclohexanone increased and cyclohexanol decreased with temperature. We believe this is due to an increase in desorption of the ketone intermediate with an increase in temperature, as opposed to re-adsorption and hydrogenation to the alcohol product; hence the observed decrease in secondary hydrogenated products. The same behaviour is observed for both the hydrogenated and HDO products and indicates a commonality on the effect of temperature on the desorption of the ketones intermediates, independent of the presence of one or two substituents on the aromatic ring. The sole HDO product, cyclohexane, was found to increase with temperature again pointing to a route of formation directly from the aromatic. This relationship with temperature for resorcinol is outlined in Figure 229:

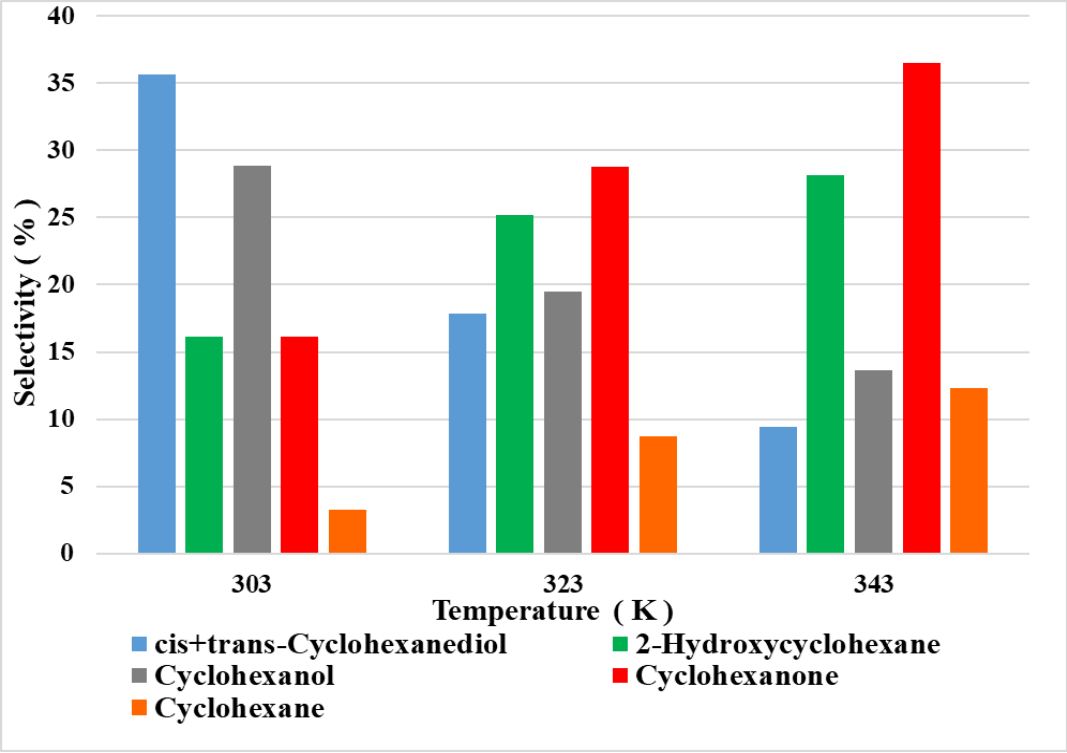

Figure 229. Resorcinol selectivity at ~ 35 % conversion.

A similar effect with temperature was reported in a study of phenol hydrogenation, where an increase in the initial hydrogenated product, cyclohexanone, and a decrease in the secondary hydrogenated product, cyclohexanol, was observed over the range studied. [59,100]

8.1.3 Concentration Variations

The effect of concentration showed a marked difference between the dihydroxybenzene substrates. Both resorcinol and hydroquinone showed an enhanced rate with increased concentration, whilst catechol showed the opposite effect. The negative order of catechol, -0.3, indicates a stronger adsorption to the catalyst surface compared with resorcinol and hydroquinone with their positive orders and explains this inhibitive effect. Why catechol adsorbs more strongly than resorcinol and hydroquinone is unclear, however the close proximity of the hydroxyl groups in catechol enables them to interact via H-bonding and may influence the strength of the adsorption; no H-bonding exists in resorcinol and hydroquinone.

Once again though, we see catechol exhibiting different behaviour from that of resorcinol and hydroquinone. It is worth considering the possibility that there is a link between strength of adsorption and ability of substrate to undergo hydrogenolysis. However, in a study of phenol and anisole hydrogenation, anisole showed significantly more hydrogenolysis than phenol, with both having a zero order in substrate. The higher strength of adsorption observed with catechol may be a result of the strong H-bonds that exist when adsorbed to the surface hindering cleavage of the –OH. A study of the chemical contamination of water by dihydroxybenzenes pollutants concluded catechol had the higher absorbability of the three isomers, with solubility, and position of –OH in the *ortho* position postulated as the reason. [104]

Across all isomers, the product distribution was found to be independent of concentration used. Whilst this was also true when looking at phenol hydrogenation, anisole again behaved in a different manner, with an increase in cyclohexanol and cyclohexanone and a decrease in methoxycyclohexane and cyclohexane observed. As with the unique behaviour of anisole when temperature is varied, the presence of the methoxy group and the resultant demethylation required to form cyclohexanone and cyclohexanol may be behind this disparity.

8.1.4 Competitive Substrate Hydrogenation

When substrates were reacted in a competitive environment, significantly different behaviour from that seen with the individual hydrogenation reactions occurred. Across all combinations of substrates, a marked decrease in rate was observed and a shift in order of reactivity from resorcinol > catechol > hydroquinone to catechol > hydroquinone > resorcinol witnessed. However, when we come to look at the effect of the competitive environment on each of the substrate combinations, a more nuanced picture emerges. A

comparison of the competitive resorcinol and catechol reaction with their individual hydrogenations is tabulated below:

Table 37. Individual and competitive conversion for resorcinol and catechol after 180 minutes.

Individual	**Conversion %**
Catechol	75.9
Resorcinol	86.9
Competitive	**Conversion %**
Catechol	54.8
Resorcinol	43.1

The shift in reactivity is clear to see, with the conversion of catechol now greater than that of resorcinol; further evidence catechol is the more strongly adsorbed isomer of the two. Smith [105] also highlighted these differences in behaviour under individual and competitive reaction conditions. He suggested catechol's place as the most reactive isomer in the competitive environment is due to the close proximity of the -OH groups on the aromatic ring, which interact with each other allowing hydrogenation to occur more readily. This opens the possibility that the position of the -OH group has even greater significance, as a factor in both, reactivity and our previously postulated ability to undergo hydrogenolysis.

The mode of adsorption is another factor worth considering when investigating this change in reactivity during competitive reactions. When more than one substrate is available to adsorb on the catalyst, competition for active sites can arise. It may be that, our previously postulated preferred planar mode of adsorption for the dihydroxybenzene isomers could switch to a non-planar mode in a competitive situation resulting in a decrease in reactivity. The higher electron donation of catechol, and subsequent increased strength of adsorption, may compensate, in part, for effects of this change in mode giving it a dominant position in the competitive environment. Abichandani and Jatkar, during a study of the addition of hydroxyl groups to benzoic acids at the *ortho, meta* and *para* positions, found a higher reactivity in the *ortho* position. [106] They again suggested this was due to the proximity of the adjacent hydroxyl group resulting in the weakening of the hydrogen bond and thus increasing the reactiveness of the *ortho* isomer.

The competitive reaction of catechol and hydroquinone again showed catechol as having the higher reactivity of the two isomers, in this instance matching the order observed when

hydrogenated individually. The inhibitive effect on catechol conversion was more pronounced when hydroquinone rather than resorcinol was present. Why this should be so is unclear at this stage.

The combination of resorcinol and hydroquinone showed the greatest detrimental effect on the rate of reaction of all three pairs. On the surface this would seem somewhat surprising as the negative ordered catechol is not present. It again however, suggests that additional factors beyond just the strength of adsorption must play a role in determining reactivity under competitive conditions. The comparable product distributions of resorcinol and hydroquinone recorded during individual hydrogenation would suggest competition for similar sites and thus this greater suppression of activity may be unsurprising. The less severe suppression of rate recorded with paired reactions involving catechol indicates that the strength of adsorption effect may be, in part, compensated for by the ability of catechol to access a limited number of alternative active sites, thus, lessening competition for the shared active sites. These limited number of sites may be accessible only when the two hydroxyl groups are in proximity and can interact with each other.

The competitive hydrogenation of all three isomers showed the greatest detrimental effect on reactivity, and a shift in order from: resorcinol > catechol > hydroquinone during individual hydrogenation to catechol > hydroquinone > resorcinol. All substrates exhibited the greatest inhibitive effect observed for any isomer combination; however, this was most pronounced with resorcinol with product formation delayed until 40 minutes. A less pronounced delay of around 10 minutes was observed for hydroquinone product formation, whereas reaction of catechol was immediate. This delay in product formation has been previously reported during a competitive reaction of anisole, phenol and 4-methoxphenol. In this instance anisole was seen to react immediately, with delays of 5 and 25 minutes found for phenol and 4-methoxyphenol respectively. [101] It was determined that anisole modified the adsorption mode of phenol resulting in a shift from an exponential decay when reacted alone to a linear decay in the presence of anisole. This shift in decay is not evident in the dihydroxybenzene reaction graphs.

Whilst we see an obvious effect on rate, when we come to look at product formation, we see that product distribution remains unaffected, with HDO products continuing to be formed from all three isomers as shown below in Figure 230:

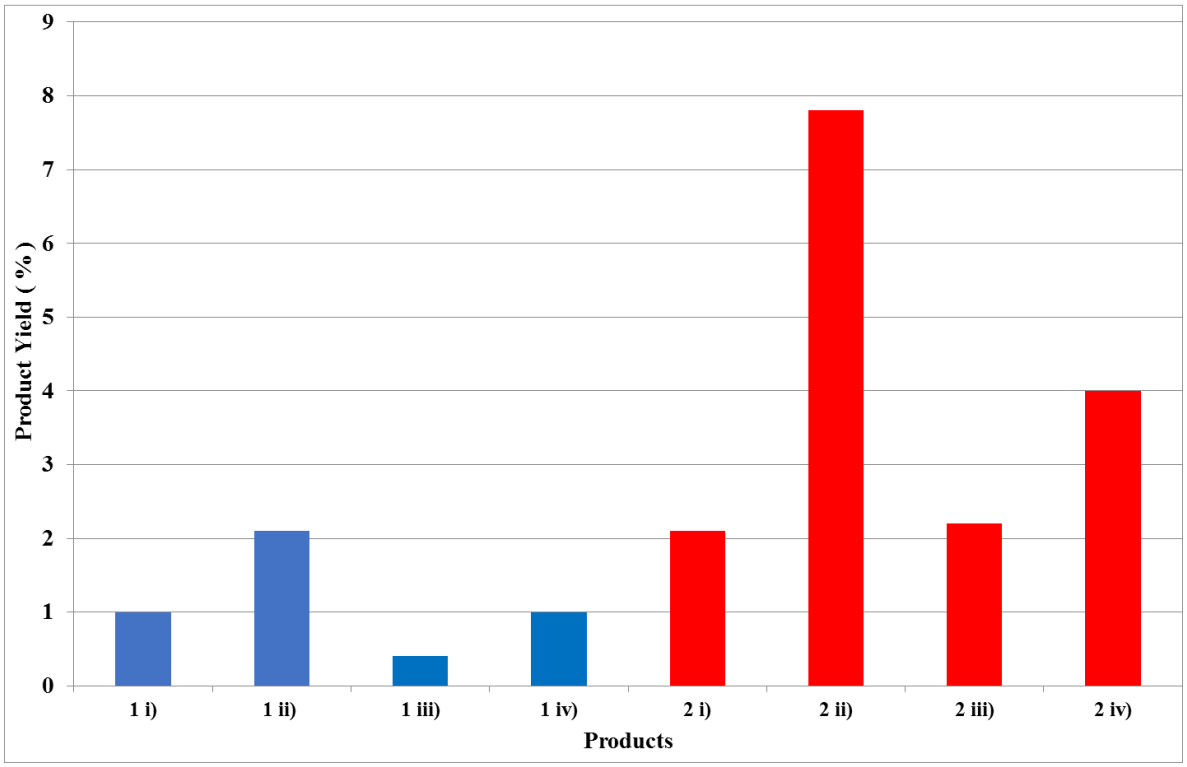

Figure 230: Comparison of product yield for individual and competitive hydrogenation of catechol, resorcinol and hydroquinone. Data taken at 17 % conversion of catechol, 13 % resorcinol and 15 % conversion of hydroquinone.

1 Cyclohexane i) Individual catechol ii) Competitive catechol + resorcinol + hydroquinone iii) Individual resorcinol iv) Individual hydroquinone

2 Cyclohexanol + Cyclohexanone i) Individual catechol ii) Competitive catechol + resorcinol + hydroquinone iii) Individual resorcinol iv) Individual hydroquinone

It is apparent that the total yield of the three HDO products from the individual hydrogenation reactions matches that formed during the competitive reaction. Therefore, the HDO product formation is not compromised, it is clearly a rate inhibition effect occurring rather than a blockage of a specific reaction pathway.

A visual representation of this pronounced effect on conversion in the individual and competitive environment is shown in Figure 231:

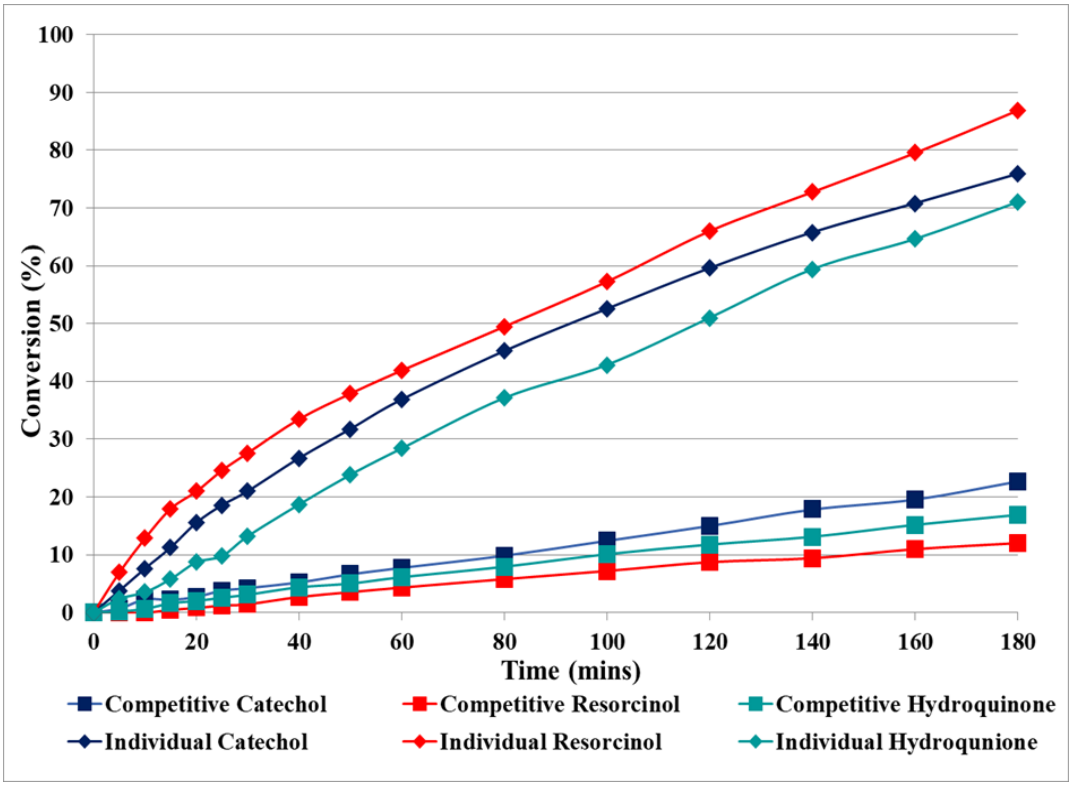

Figure 231: Individual and competitive hydrogenation conversions.

A significant decrease in activity for all three isomers is clearly present. This is postulated to be due to increased competition for available active sites on the catalyst due to a crowding effect from the presence of multiple substrates. It is also worth considering other factors such as steric and electronic factors and the mode of adsorption that may be responsible for suppressing activity. Looking at these factors individually: it may be that when all three substrates are trying to adsorb simultaneously on the active site a sterically inhibitive effect may occur. The effect of electronic factors between catalyst and substrate would be magnified due to the increased quantity of reactant present and again an inhibitive effect may arise. Although not immediately evident from our results, a change in mode of adsorption in the competitive environment may still occur and would result in a change in activity.

It is worth restating that across all pair and combinations tested, catechol had the highest reactivity whilst resorcinol recorded the lowest. This suggests a strength of adsorption order of catechol > hydroquinone > resorcinol, which in the case of catechol, correlates well with the order of reaction calculated: catechol > resorcinol > hydroquinone. The significant effect on reaction rates observed when more than one substrate is present again highlights the limitations of studying one single model compound as a route to understanding the processes required for the upgrading of a true bio-oil feed.

8.1.5 Deuteration Reactions

The effect of replacing hydrogen with deuterium was examined for the dihydroxybenzene isomers. A summary of each KIE calculated is shown in Table 38 below:

Table 38. Substrate KIE values.

Substrate	KIE
Catechol	0.6
Resorcinol	0.9
Hydroquinone	1.2

Looking at the values for each, it is apparent that catechol and resorcinol both exhibited a faster rate of reaction in the presence of deuterium, reflected in their inverse KIE figure. Hydroquinone gave a decreased rate under deuterated conditions and as such a positive KIE was calculated.

The literature in this area has given a range of measured KIE values. Hydrogen-deuterium studies of alkyl-substituted benzenes: toluene, ethylbenzene and propyl benzene, showed all three to have an inverse kinetic isotope effect, concluded to be due to the change in hybridisation of the carbon atom from sp^2 to sp^3 which takes place during the hydrogenation of the aromatic ring; an explanation which may apply to our inverse KIE values calculated for catechol and resorcinol. A study on xylenes hydrogenation also found a disparity amongst isomers, however in this instance the *ortho* isomer exhibited a positive KIE, and the *meta* and *para* isomers an inverse KIE. From their findings, they concluded the ortho-xylene must have a different rate-determining step from the *meta*- and *para*-xylene. [70] In our study, something similar may apply with both catechol and resorcinol having a different RDS from hydroquinone. Resorcinol and hydroquinone exhibiting a different effect with deuterium is out of step with previous results where resorcinol and hydroquinone have shown similar behaviour, this indicates that although resorcinol and hydroquinone have the same product distribution during standard hydrogenation, their behaviour differs under deuterated conditions.

To gain more information on the reaction mechanism in the presence of deuterium the KIE value for each product was calculated and is shown below in Table 39 for catechol:

Table 39. Catechol hydrogenation products KIE values.

Product	KIE
cis-1,2-Cyclohexanediol	0.8
trans-1,2-Cyclohexanediol	0.7
2-Hydroxycyclohexanone	0.8
Cyclohexanol	0.7
Cyclohexanone	0.7
Cyclohexane	0.7

From Table 39 it can be seen that the hydrogenated and HDO products all share an inverse KIE value between 0.7 and 0.8, in agreement with the overall inverse KIE calculated for catechol hydrogenation. The initial ring hydrogenated product, 2-hydroxycyclohexanone, undergoes a change in hybridisation from sp^2 (aromatic) to sp^3 (aliphatic) during the hydrogenation of catechol, which may explain the inverse KIE observed. These KIE product values for catechol are closely related to those calculated for resorcinol and shown below in Table 40:

Table 40. Resorcinol hydrogenation products KIE values.

Product	KIE
cis-1,3-Cyclohexanediol	0.7
trans-1,3-Cyclohexanediol	0.8
3-Hydroxycyclohexanone	0.7
Cyclohexanol	0.7
Cyclohexanone	0.7
Cyclohexane	1.5

This similarity between resorcinol and catechol is only apparent during these hydrogen-deuterium exchange reactions; their shared KIE values for the hydrogenated and HDO products, with the exception of cyclohexane, is of note and strongly indicates a shared pathway of formation from both isomers. The positive effect observed with cyclohexane suggests the reaction mechanism for the formation from resorcinol must be different to that of catechol. Analyses of hydroquinone product KIE values are shown in Table 41 below:

Table 41: Hydroquinone product KIE values.

Product	KIE
cis-1,4-Cyclohexanediol	1.1
trans-1,4-Cyclohexanediol	1.0
4-Hydroxycyclohexanone	1.1
Cyclohexanol	1.1
Cyclohexanone	1.1
Cyclohexane	1.2

All products from hydroquinone share a positive KIE value of 1.1 – 1.2, with the exception of *trans*-1,4-cyclohexanediol where no effect was calculated. The common value for all products indicates a shared route of formation for both hydrogenation and hydrogenolysis. It is clear that hydroquinone does not share the similarities observed between resorcinol and catechol, with all products registering a positive KIE. The significant differences between the product KIE values for hydroquinone and those from catechol and resorcinol correlate with what was observed with the overall KIE values, and again indicates individuality in the behaviour of hydroquinone. It should be stated, the cyclohexane KIE value is similar for both resorcinol and hydroquinone which suggests a possible shared route of formation solely for this HDO product. Whilst at this stage it is unclear the reasons behind the disparities between hydroquinone and that of resorcinol and catechol the results point to a potential adsorption effect. We have previously postulated that the three isomers can all adopt a flat mode of adsorption and much of our evidence points to this; however, these results open up the possibility that hydroquinone is the only isomer that adopts this flat mode of adsorption and catechol and resorcinol may in fact exhibit an inclined adsorption mode.

When the presence of deuterium during competitive reactions is studied, we again see a clear difference between reactions carried out in the individual and competitive environments. Looking at the combinations individually: when catechol and resorcinol are reacted together, catechol maintains its inverse KIE value whilst resorcinol now registers no effect in the presence of deuterium under this competitive environment. The product KIE values have also been calculated and these are shown in Table 42 below:

Table 42. Catechol and resorcinol competitive reaction product KIE values.

Product	KIE
cis-1,2-Cyclohexanediol	0.8
trans-1,2-Cyclohexanediol	1.0
2-Hydroxycyclohexanone	0.9
cis-1,3-Cyclohexanediol	0.7
trans-1,3-Cyclohexanediol	0.7
3-Hydroxycyclohexanone	0.8

As the HDO products, cyclohexanol, cyclohexanone and cyclohexane, can form from both catechol and resorcinol they are not included in the product KIE values. When comparison is made between the values obtained from individual and competitive environments the inverse KIE value recorded for each remained with exception to the *trans*-1,2-cyclohexanediol which now displayed no effect in the presence of deuterium. Catechol in the presence of hydroquinone shifts to a positive KIE overall suggesting a stronger influence on catechol hydrogenation from hydroquinone than that observed with resorcinol. This is further emphasised when studying the calculated product KIE values shown in Table 43:

Table 43: Catechol and hydroquinone competitive reaction product KIE values.

Product	KIE
cis-1,2-Cyclohexanediol	1.1
trans-1,2-Cyclohexanediol	1.1
2-Hydroxycyclohexanone	1.2
cis-1,4-Cyclohexanediol	1.1
trans-1,4-Cyclohexanediol	1.1
4-Hydroxycyclohexanone	1.2

The hydrogenated products from catechol have changed from inverse KIE values, whilst the hydrogenated products from hydroquinone have remained unchanged and positive, therefore, suggesting catechol is having no influence on hydroquinone reaction mechanism.

The competitive reaction of resorcinol and hydroquinone witnessed a change in hydroquinone KIE value from positive to inverse, whilst resorcinol remained inverse. The product KIE values calculated for this reaction are shown in Table 44 below:

Table 44. Resorcinol and hydroquinone competitive reaction product KIE values.

Product	KIE
cis-1,3-Cyclohexanediol	0.9
trans-1,3-Cyclohexanediol	0.9
3-Hydroxycyclohexanone	1.0
cis-1,4-Cyclohexanediol	0.8
trans-1,4-Cyclohexanediol	0.8
4-Hydroxycyclohexanone	0.9

The hydrogenated products from resorcinol remained inverse, with the exception of the initial hydrogenated product where no effect with deuterium was observed. The hydrogenated products from hydroquinone are now all registering an inverse KIE value compared with the positive effect found during individual hydrogenation. The change in the hydroquinone product KIE values observed only during the competitive reaction with resorcinol strongly suggests a change in the mechanism for hydroquinone hydrogenation when in the presence of resorcinol.

When all three isomers were reacted together in the presence of deuterium, catechol and resorcinol experienced a change in overall KIE from inverse to positive between individual and competitive hydrogenation, whilst hydroquinone remained positive. The product KIE values for this reaction are shown in Table 45 below:

Table 45. Catechol, resorcinol and hydroquinone competitive reaction product KIE values.

Product	KIE
cis-1,2-Cyclohexanediol	1.5
trans-1,2-Cyclohexanediol	1.5
2-Hydroxycyclohexanone	1.2
cis-1,3-Cyclohexanediol	0.4
trans-1,3-Cyclohexanediol	1.1
3-Hydroxycyclohexanone	0.6
cis-1,4-cyclohexanediol	1.2
trans-1,4-cyclohexanediol	0.8
4-hydroxycyclohexanone	1.6

Of the products pertaining to catechol, both the *cis* and *trans*-1,2-cyclohexanediol and the 2-hydroxycyclohexanone changed from an inverse to a positive KIE, in correlation with the overall positive KIE value recorded for catechol. This may be due to the presence of hydroquinone influencing the reaction mechanism of catechol as observed during the competitive reaction of both. The products from resorcinol remained unchanged and inverse, with the exception of the *trans*-1,3-cyclohexanediol which exhibited a change to a positive effect. A similar effect was observed with the products from hydroquinone - *cis*-1,4-cyclohexanediol and 4-hydroxycyclohexanone remained positive whilst the *trans*-1,4-cyclohexanediol experienced a change to an inverse KIE value. The general lack of change in the KIE values of the products from resorcinol and hydroquinone during the competitive reaction of all three substrates leaves the influence hydroquinone has on catechol product formation as the major factor in this environment.

Upon inspection of the product distributions no disparity between hydrogenation and deuteriation was observed, implying that although the KIE values may change during competitive reactions, the reaction routes of both hydrogenation and hydrogenolysis remain unaffected.

It is clear from these results that no trend emerges from our calculated KIE values, and in fact the picture is if anything less clear. We have already established that reactions in the competitive environment significantly influence rate; these results have shown us that mechanisms and specifically rate determining steps are also greatly affected. This increased level of complexity when combinations of isomers are tested in the presence of

deuterium furthers our belief that studying one single model compound, as a route to understanding a true bio-oil feed, may be of limited value.

Although the deuterium work was intended to improve our knowledge of the reaction mechanism, it seems it may have complicated it and as such, indicates that the hydrogenation mechanism for the dihydroxybenzenes may be more complex than previously thought.

8.1.6 Extended Runs

It is evident from the extended reaction results that the catalyst undergoes significant deactivation. This effect was most marked with hydroquinone resulting in a halving of conversion following the second addition of substrate. Catechol and resorcinol also showed significant deactivation with falls in conversion recorded of 80 to 50 % and 90 to 70 % respectively. Thermal analysis of the post reaction catalysts from the extended runs found greater levels of carbon laydown with catechol and resorcinol than with hydroquinone, indicating no correlation between catalyst deactivation and quantity of carbon laydown. Both behave independently of each other in agreement with the study of HDO of *para*-methyl guaiacol by Jackson *et al.* [21]

Analysis in greater detail of the TPO data show two distinct weight loss events below 473 K common to all three isomers. No concomitant evolution of carbon dioxide is detected suggesting these weight loss events may be due to the release of adsorbed solvent and starting material from the catalyst surface. This was confirmed by Soxhlet extraction performed on the post reaction catalyst used for resorcinol hydrogenation. TGA data for the untreated and the post extraction catalyst is shown below in Figures 232 and 233:

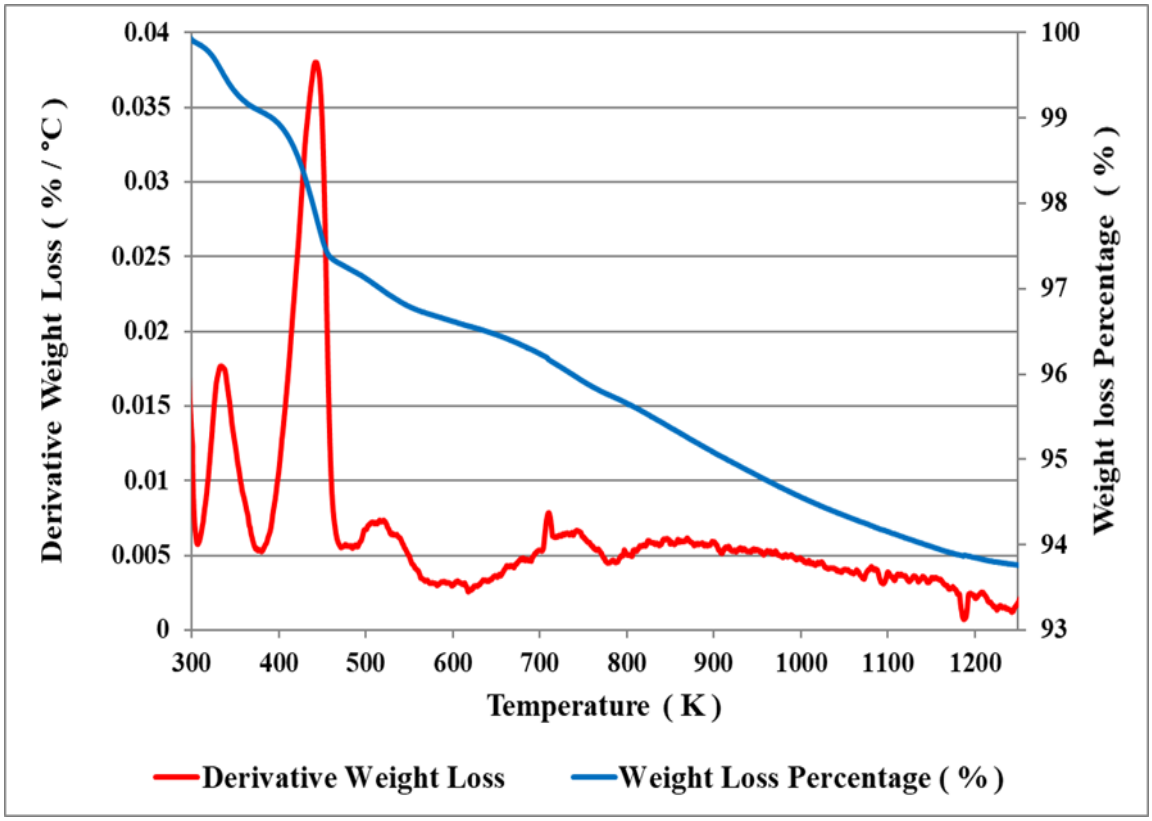

Figure 232. TGA of untreated Rh/SiO_2 catalyst after 3-hour resorcinol hydrogenation reaction.

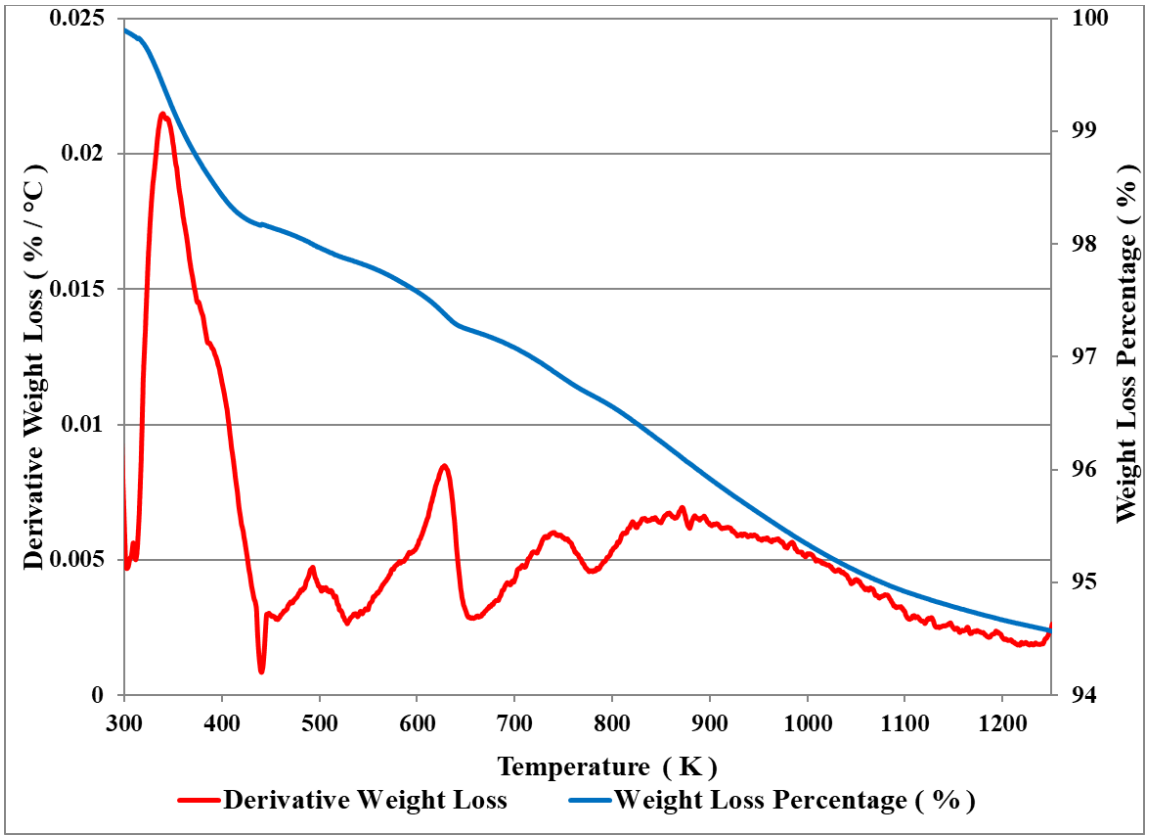

Figure 233. TGA of post Soxhlet extraction Rh/SiO_2 catalyst after 3-hour resorcinol hydrogenation.

From Figures 232 and 233 above it is clear the major weight loss event at 490 K is absent from the catalyst post Soxhlet extraction. Analysis by gas chromatography confirmed this to be the starting material.

The TPO data for catechol exhibits two further higher temperature (> 473 K) weight loss events with the associated evolution of carbon dioxide indicating the combustion of surface carbon species. Both resorcinol and hydroquinone registered an additional high temperature weight loss (~493 K), again associated with the release of carbon dioxide. The presence of three distinct high temperature weight loss events for both resorcinol and hydroquinone indicates the presence of more than one carbon species. It is likely that the lower weight loss event in this region (~493 K) unique to resorcinol and hydroquinone is a result of phenolic carbonaceous deposits on the catalyst surface, whilst the two higher temperature peaks shared by all three isomers are a result of the evolution of carbon. The aromatic nature of this carbon was confirmed through Raman spectroscopy indicating the presence of a weak G band at ~ 1600 cm^{-1}.

This difference between the carbon species present with resorcinol and hydroquinone against catechol is of real significance when compared with the product distributions for each. The occurrence of aromatic carbon on all three isomers is unsurprising, as the formation of cyclohexane in similar yields is common to all three. The presence of phenolic carbon only on the post reaction catalysts for resorcinol and hydroquinone correlates strongly with their higher yields of cyclohexanone and cyclohexanol. The favourability of catechol towards hydrogenation over hydrogenolysis may explain the lack of phenolic carbon on the post reaction catalyst.

The significant catalyst deactivation observed at the mild conditions we are operating at is unusual, however, with high levels of HDO occurring in addition to standard hydrogenation it is perhaps unsurprising. High levels of catalyst deactivation are a well-known problem with catalytic HDO, and it is of interest that despite operating at a temperature well below the standard conditions of >473 K it is still having a clear impact on our catalyst.

8.2 Cresol Isomers

8.2.1 Individual Hydrogenation

Hydrogenation of the individual substrates gave the following order of reactivity: *para*-> *meta*-> *ortho*-cresol, which is in agreement with a study by Wandas *et al*. over a Co-Mo catalyst. [107] However, in a study by Odebunmi and Ollis in 1982, also over a Co-Mo catalyst, an order of *meta*- > *para*- > *ortho*-cresol was recorded; the *ortho* isomer, however, was still found to have the least reactivity. [63-64,108] This lower reactivity for *ortho*-cresol has been reported in multiple other studies, with increased steric hinderance in the *ortho* position postulated as the reason behind this. [109,110] Our previously discussed belief that steric interactions play no role in the dihydroxybenzenes reactivity may not be applicable when one of the -OH groups is replaced with a $-CH_3$ group as with the cresols. In addition, the close proximity of the relatively bulky $-CH_3$ to the -OH group in the *ortho* position would have the greatest steric inhibitive effect, resulting in the lower reactivity observed across these studies. Less clear are the reasons behind the *para* isomer exhibiting the fastest rate of reaction, many have suggested a more favourable symmetrical arrangement can occur in the *para* position, however, our work on dihydroxybenzenes found the *para* isomer to be the least reactive despite a symmetrical arrangement far greater than that of *para*-cresol. Studies of the isomers of xylenes followed our order of reactivity with the *ortho* isomer again the slowest, as would be expected with the presence of two $-CH_3$ groups. [70] Although in this instance symmetry could be put forward as the reason for *para*-xylene exhibiting the fastest rate, our findings with dihydroxybenzenes suggest this cannot be definitively stated. These conflicting trends mean that we cannot say with any clarity whether or not symmetry plays a role in the higher reactivity found with *para*-cresol.

It has been accepted in the literature that the hydrogenation reactivity of alkyl substituted phenols (cresols) would be less than that of phenols due to the electronic effect on the aromatic rings related to the addition of alkyl substituents. However, comparison of our rate constant values against those recorded for phenol show that, with the exception of *ortho*-cresol, the cresols adopt a higher reactivity. In this instance, the addition of a methyl group and a double substituted aromatic has resulted in an increased rate of reaction. When we compare the rate constants with that calculated for the dihydroxybenzenes the cresols also exhibit a faster rate of reaction as shown in Table 46 below:

Table 46. Comparison of rate constants for cresol and dihydroxybenzene isomers.

Rate constant ($x10^{-3}min^{-1}$)			
	ortho	*meta*	*para*
Cresols	11.1	18.4	24.2
Dihydroxybenzenes	8.3	11.9	4.2

It can be seen from Table 46 that all isomers of cresol exhibit a faster rate of reaction than their comparable dihydroxybenzene isomer, with the slowest isomer of cresol (*ortho*) having a similar reactivity to the fastest dihydroxybenzene isomer (*meta*). This higher cresol reactivity may be a result of the presence of a single -OH group that can bond directly to the catalyst surface. Whilst we know from previous work on the hydrogenation of toluene that interaction between the $-CH_3$ group and the surface occurs, formation of a strong direct bond, as observed with hydroxyl groups, is unlikely to occur. [8] As such, different modes of adsorption between the cresols and dihydroxybenzenes are likely and would explain the disparity in their reactivities. Finally, it is worth looking at the effect of pKa on the reactivity of cresols. An order of 10.09 >10.26 >10.29 for *meta-*, *para-* and *ortho*-cresol respectively is documented; however, unlike the dihydroxybenzenes there is no correlation between this and isomer reactivity, indicating no effect of acid strength.

When we come to study the product distribution for each of the substrates, significant differences emerge when comparing mole fraction at the same conversion as shown in Figure 234:

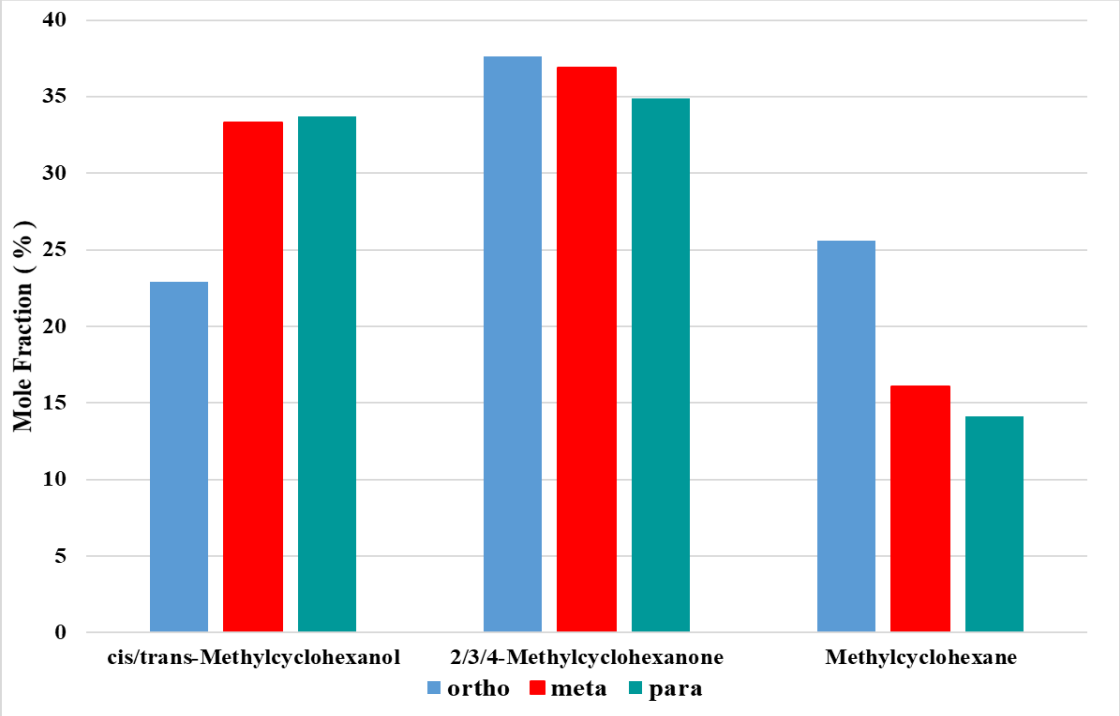

Figure 234. Product distribution for cresol isomers at ~ 90 % conversion.

It is apparent that *ortho*-cresol shows higher favourability towards HDO than *meta* and *para*-cresol, with 25 % mole fraction registered for the single HDO product, methylcyclohexane, against ~ 15 % for both *meta*- and *para*-cresol. This unique behaviour of the *ortho* isomer was reported previously in our section on dihydroxybenzene hydrogenation, however, on this occasion the *ortho* isomer shows enhanced HDO activity as against the reduced activity observed with *ortho*-dihydroxybenzene. The overall level of HDO is reduced from that observed with the dihydroxybenzenes a finding which when the substituents present are considered is unsurprising. [111] The replacement of a stabilizing, through both resonance and inductive effects, -OH group with that of a -CH_3 group which can stabilize only via inductive effects allows for less opportunity for formation of the intermediates necessary for HDO to occur.

The change from the *meta* and *para* isomers to the *ortho* isomer as the most favoured to undergo HDO is however, unexpected. We previously stated that we believe the close proximity of substituents in the *ortho* position could promote H-bonding and in turn hinder bond cleavage. The reason why this does not apply with the cresols is at this stage unclear. One possible explanation may be the differing modes of adsorption influencing the substrates ability to undergo HDO. The cresol isomers with a -CH_3 group would not adopt the flat mode of adsorption present with the dihydroxybenzenes, instead a non-planar mode of adsorption with the -CH_3 group pointing away from the surface and the -OH group bonded directly could exist. It is worth noting that although the main mode of adsorption

would be via the aromatic ring and the -OH group, interaction of the -CH_3 group and the surface will still occur, the extent and strength of which are unclear.

When we look at selectivity, the differences in favourability towards HDO and hydrogenation between the isomers is further emphasised. Figure 235 shows the selectivity of each product taken at ~ 70% conversion.

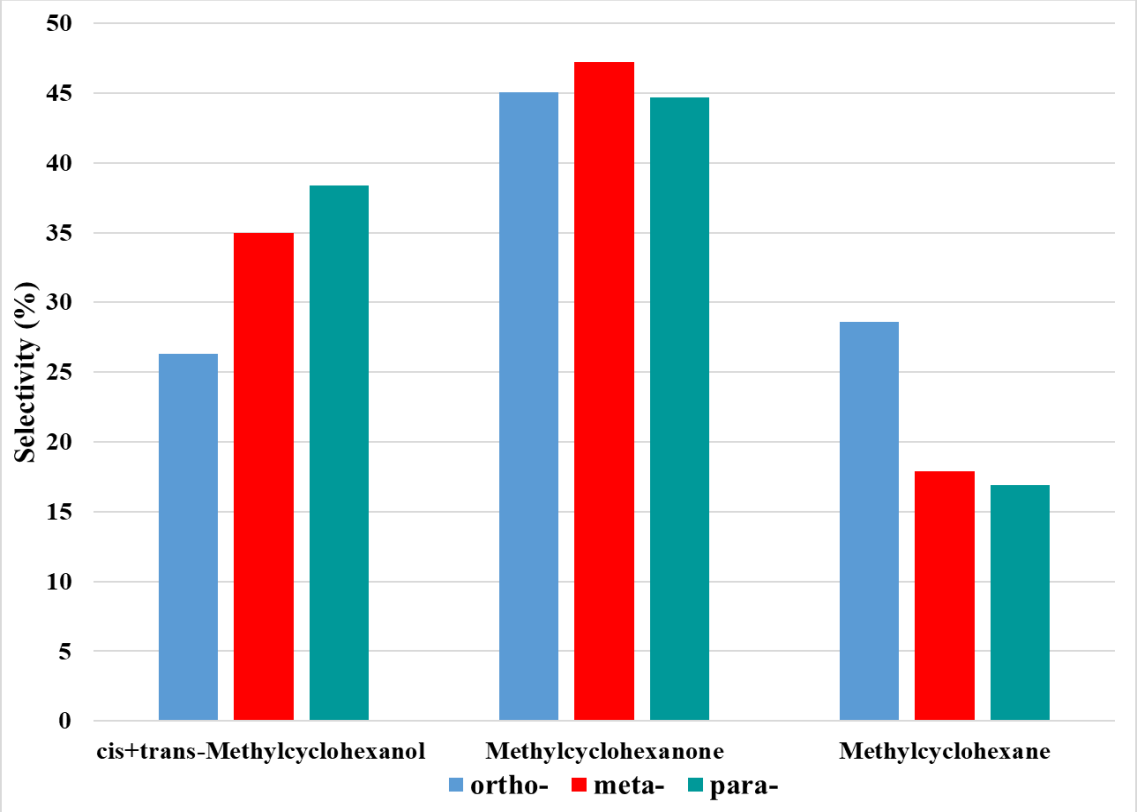

Figure 235. Product selectivity's calculated at ~ 70 % conversion of substrate.

From Figure 235 it is apparent that, with the exception of methylcyclohexanone, each of the products show differences in selectivity between the substrates. The *cis* and *trans*-methylcyclohexanol was clearly favoured by *meta*- and *para*-cresol with 35 % and 38 % selectivity recorded respectively against 26 % for *ortho*-cresol. This preference was reversed for the HDO product, methylcyclohexane, where *ortho*-cresol had ~ 30 % compared with ~ 15 % for *meta*- and *para*-cresol, reinforcing our belief that the nature of the *ortho*-cresol allows for HDO to take place more readily. As stated earlier, the selectivity towards methylcyclohexanone for each isomer was of a similar level at ~ 45 %, suggesting the position of the substituent plays no role in the formation of the initial hydrogenated product. It is worth stating that the position of the *ortho*-cresol, as the least reactive isomer yet the most likely to undergo HDO, indicates that no direct relationship between HDO and reactivity exists. This is in agreement with the dihydroxybenzenes where hydroquinone (*para*) had the lowest reactivity but the highest occurrence of HDO

and reiterates our understanding that a combination of specific properties of the substrate are vital in determining HDO favourability.

When favourability towards the *cis* and *trans* isomers is looked at individually further differences emerge between *ortho*, *meta* and *para*-cresol. The ratio of *cis*:*trans* for each isomer is shown in Figure 236:

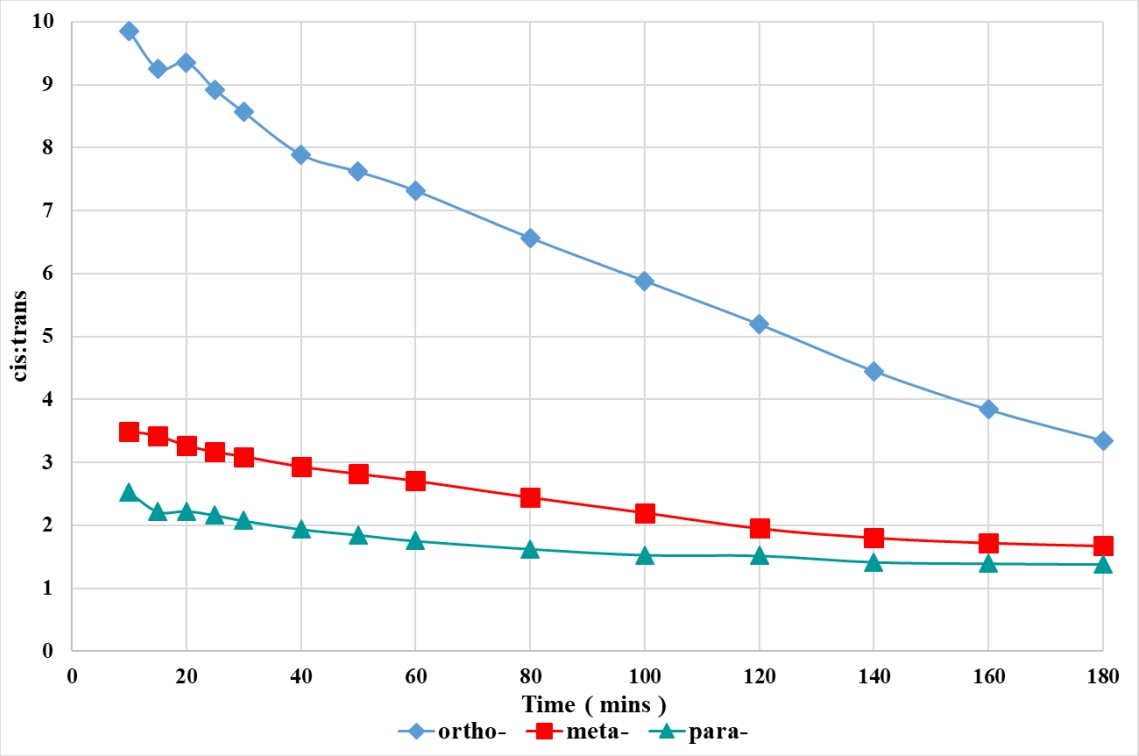

Figure 236. *cis*:*trans* Ratio for the cresol isomers with time.

From Figure 236 it is apparent that *ortho*-cresol shows a clear preference for the *cis* isomer, although as expected, a gradual shift towards the more thermodynamically favoured *trans* product is observed as the reaction proceeds. This preferential formation of the *cis* isomer is to be expected when our previously postulated view that *cis* formation can occur via both the initial enol intermediate and the ketone is considered. Formation of the trans isomer however, can only be via the ketone if no isomerization occurs. Steric constraints and the stability of the enol species dictate that within this group of substrates, the *ortho* position has the greatest selectivity towards the *cis* isomer, with an initial ratio of 10:1 *cis*:*trans*, against 2.5:1 and 3.5:1 respectively for the *meta* and *para* isomers. Similar behaviour was observed in a study of the xylene isomers, where all three showed a preference towards formation of the *cis* isomer, with *ortho*-xylene recording the highest *cis*:*trans* ratio. [70]

Looking in greater detail at the product mole fractions of *ortho*-cresol and *meta*-cresol as shown below in Figures 237 and 238:

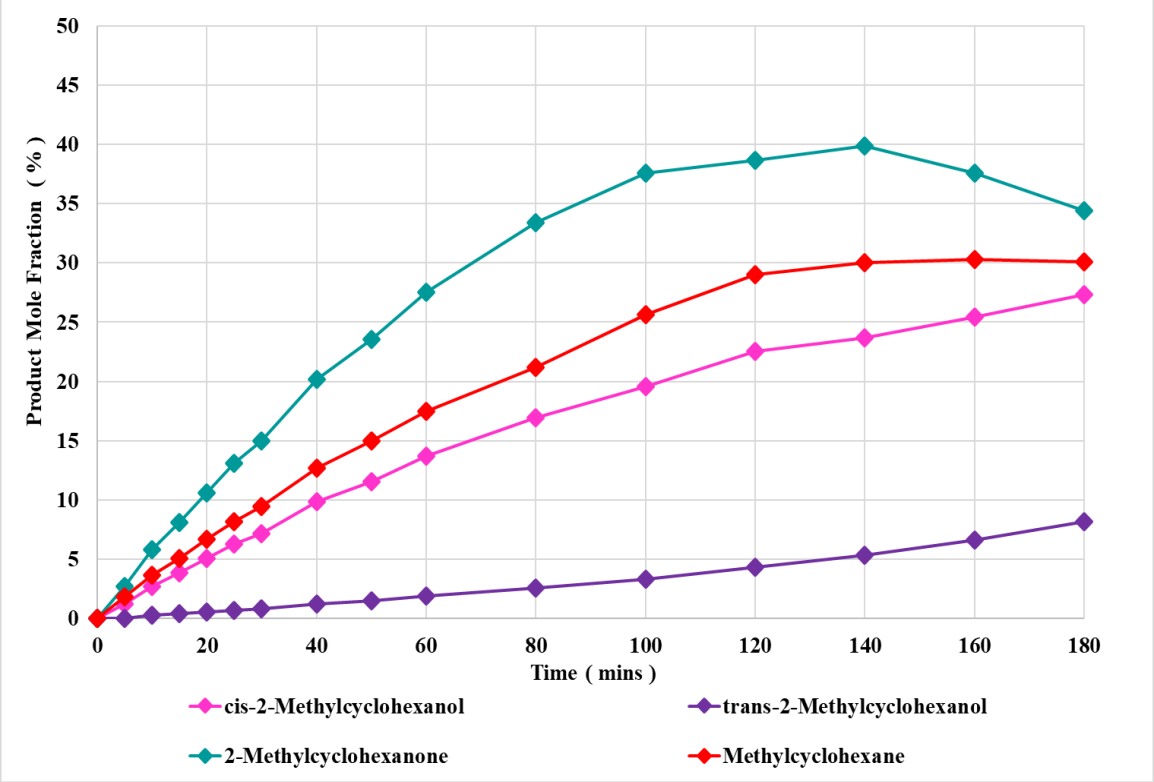

Figure 237. Product mole fraction plot for *ortho*-cresol hydrogenation, 323 K, 3 barg H_2 and 0.1 g Rh/SiO_2.

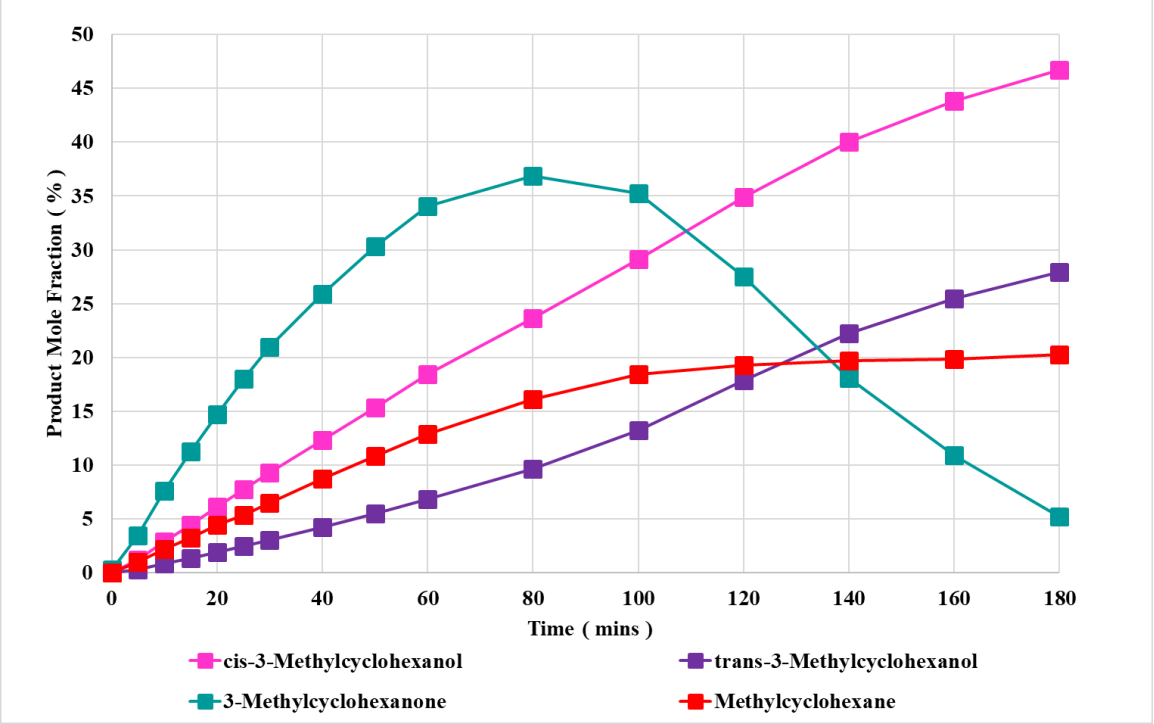

Figure 238. Product mole fraction plot for *meta*-cresol hydrogenation, 323 K, 3 barg H_2 and 0.1 g Rh/SiO_2.

We see that formation of all products, with the exception of *trans*-2-methylcyclohexanol and *trans*-3-methylcyclohexanol, occur from the outset of the reaction suggesting an independent, direct route for each. This idea has been previously postulated in our work on dihydroxybenzenes, and in a study on the hydrogenation of phenol. The nature of formation of the *trans* isomer however is less clear. In our earlier work on dihydroxybenzenes we confirmed, by the addition of solely *cis*-1,2-cyclohexanediol to the reactor, that formation did not occur through a desorption-readsorption mechanism from the *cis*-isomer. This reaction also confirmed the complete absence of deoxygenation activity, as no HDO products were detected. A similar investigation was carried out using a mixture of *cis*-2-methylcyclohexanol and *trans*-2-methylcyclohexanol and is shown in Figure 239:

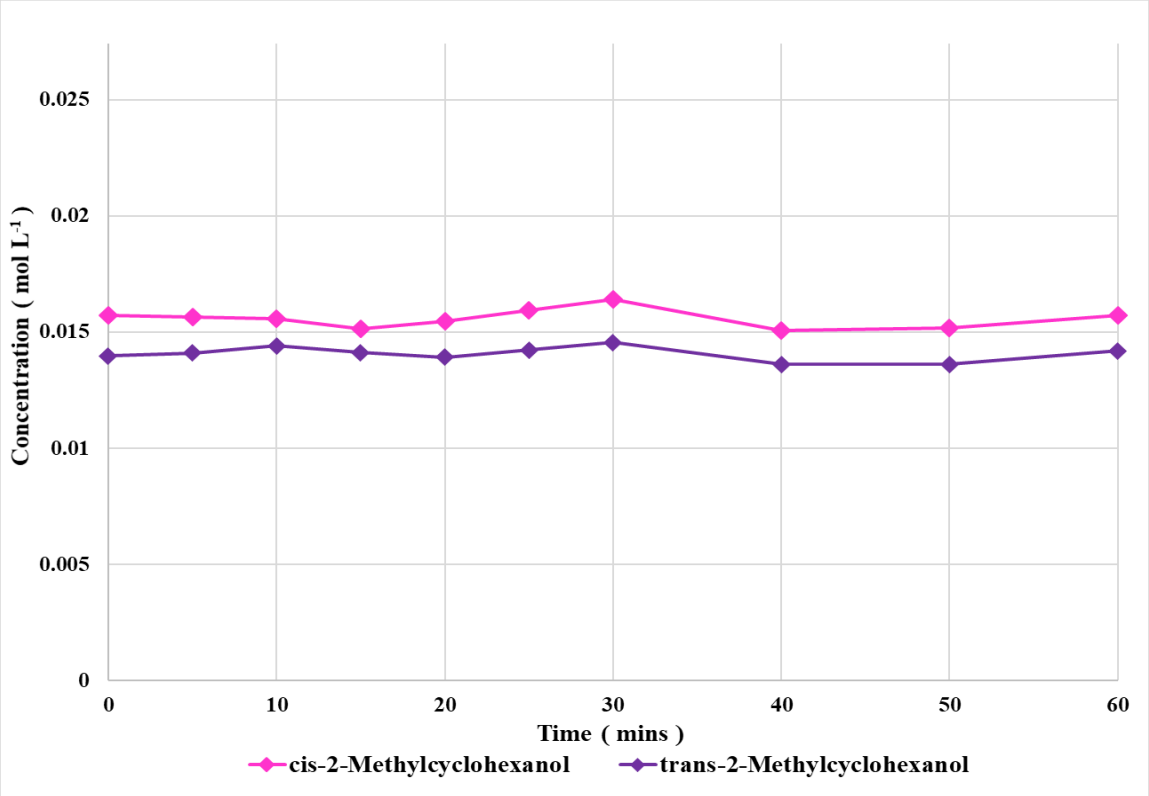

Figure 239. Reaction profile of *cis*-2-methylcyclohexanol + *trans*-2-methylcyclohexanol hydrogenation, 323 K, 3 barg H_2 and 0.1 g Rh/SiO_2.

From Figure 239 it is clear that *cis*/*trans* isomerization is absent, reiterating our belief that formation of the *trans* isomer can occur only via the ketone intermediate and not through isomerization. The absence of the HDO product, methylcyclohexane, adds additional support to our previously postulated idea that HDO does not occur via the hydrogenated products but instead directly from the aromatic substrate via reactive surface intermediates. These highly reactive intermediates are present only when the aromatic is available; phenol hydrogenation over the same catalyst found cyclohexane formation to cease after the

aromatic had been consumed. [59] Our findings with the cresols show similar behaviour as illustrated with *ortho*-cresol at 333K in Figure 240:

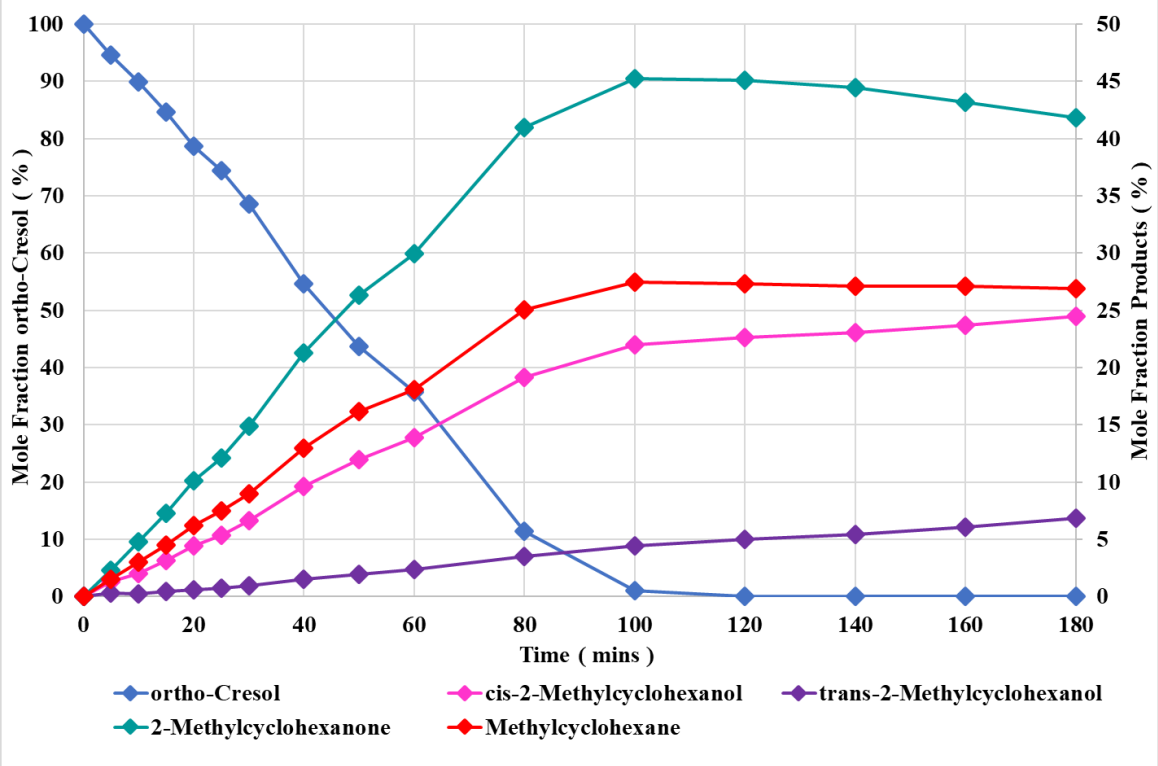

Figure 240. *ortho*-Cresol hydrogenation, 323 K, 3 barg H_2 and 0.1 g Rh/SiO_2.

A clear correlation exists between consumption of the aromatic and formation of the HDO product, methylcyclohexane, which maximises at 100 minutes in conjunction with full consumption of the aromatic and remains constant until end of reaction. As such, and in compatibility with our dihydroxybenzene findings, formation of HDO products must occur directly from the aromatic substrate via highly reactive surface intermediates; a finding in contrast to much of the literature where it is reported that the hydrogenated products undergo hydrogenolysis to produce the deoxygenated products. [7,8] The reaction scheme therefore proposed for the cresol isomers, using *para*-cresol as an example, is shown below in Figure 241:

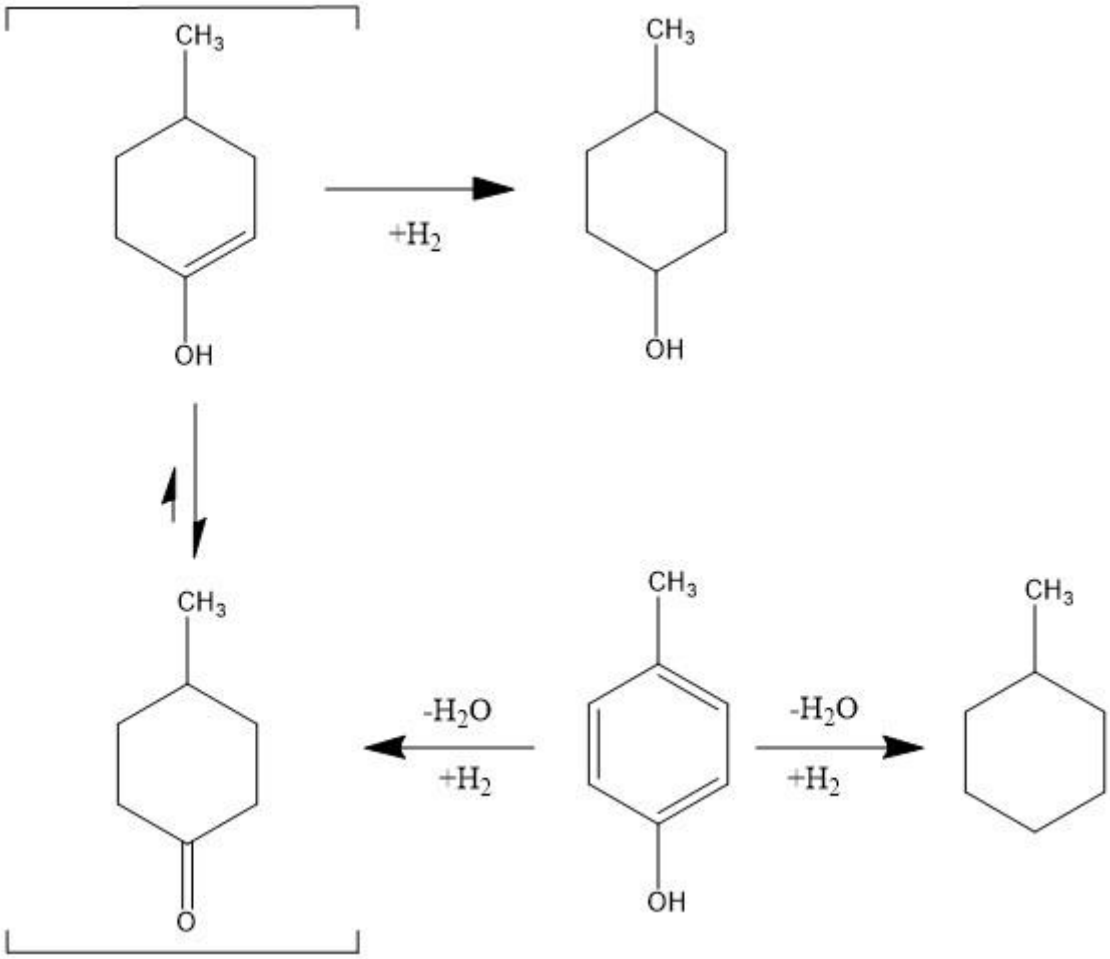

Figure 241. *para*-Cresol Reaction Scheme.

It is at this point worth restating the importance of high HDO activity under mild conditions. It is highly beneficial for the purpose of bio-oil upgrading that considerable amounts of oxygen are removed, and as such, the high selectivity particularly as outlined with *ortho*-cresol at ~ 30 % for methylcyclohexane is of real significance. In addition, interest in this product is growing continuously, predominantly in the petroleum sector, due to the growing environmental issues regarding removal of aromatics. [35]

8.2.2 Temperature Variations

As expected, all isomers of cresol showed an increase in rate with temperature, as summarised in Table 47 below:

Table 47. Rate constants of cresol isomers over temperature range.

Temperature (K)	***ortho*-: k ($x10^{-3}min^{-1}$)**	***meta*-: k ($x10^{-3}min^{-1}$)**	***para*-: k ($x10^{-3}min^{-1}$)**
303	9.1	11.6	8.6
313	10.0	12.7	12.4
323	11.1	18.4	24.2
333	18.0	26.0	39.4
343	24.6	41.0	43.6

From the calculated rate constants, it is clear that both *meta*- and *para*-cresol experienced the greatest effect with temperature; with a near 4-fold increase in rate over the 40 K temperature range for *meta*-cresol and a 5-fold increase for *para*-cresol. *ortho*-Cresol also exhibited a rate increase with temperature; however, this was less marked than seen with both *meta*- and *para*-cresol. The activation energies calculated followed the order: *para* > *meta* > *ortho* (37 > 34 > 29 $kJmol^{-1}$). The lower activation energy of the *ortho* isomer may be the result of a steric effect when adsorbed to the surface, however, the value does not differ greatly from that of the *meta* position where no steric inhibition would take place. This same order was documented previously by Odebunmi and Ollis over a Co-Mo catalyst, where the comparable values obtained were 37 > 27 > 23 $kJmol^{-1}$. [107] They suggested the low reactivity of the *ortho* isomer is due to steric effects and no explanation was given for the differences in activation energies of the three isomers. A comparison with the dihydroxybenzenes shows a different order in temperature dependence of resorcinol > hydroquinone ~ catechol (41 > 31 ~ 31 $kJmol^{-1}$). However, a similar study of xylenes hydrogenation over the same catalyst, found an activation energy order in accordance with ours of 42 > 27 > 25 $kJmol^{-1}$, for *para*, *meta* and *ortho* respectively. [70] It is of note that the *ortho* isomer registers the lowest activation energy regardless of substrate.

Over the temperature range measured the HDO product, methylcyclohexane, remained broadly constant for all three isomers. This was in contrast to the analogous HDO product of the dihydroxybenzenes, cyclohexane, which increased with temperature. It would be expected that hydrogenolysis would increase with temperature and why this does not occur with the cresols is not entirely clear. One possible explanation could be that, although we know hydrogenolysis occurs from the aromatic, two competing pathways for

hydrogenation and hydrogenolysis may still exist and any increase in temperature has an effect only on the pathway for hydrogenation. Examination of the effect of temperature on the initial and secondary hydrogenated products for *ortho*-cresol is shown in Figure 242:

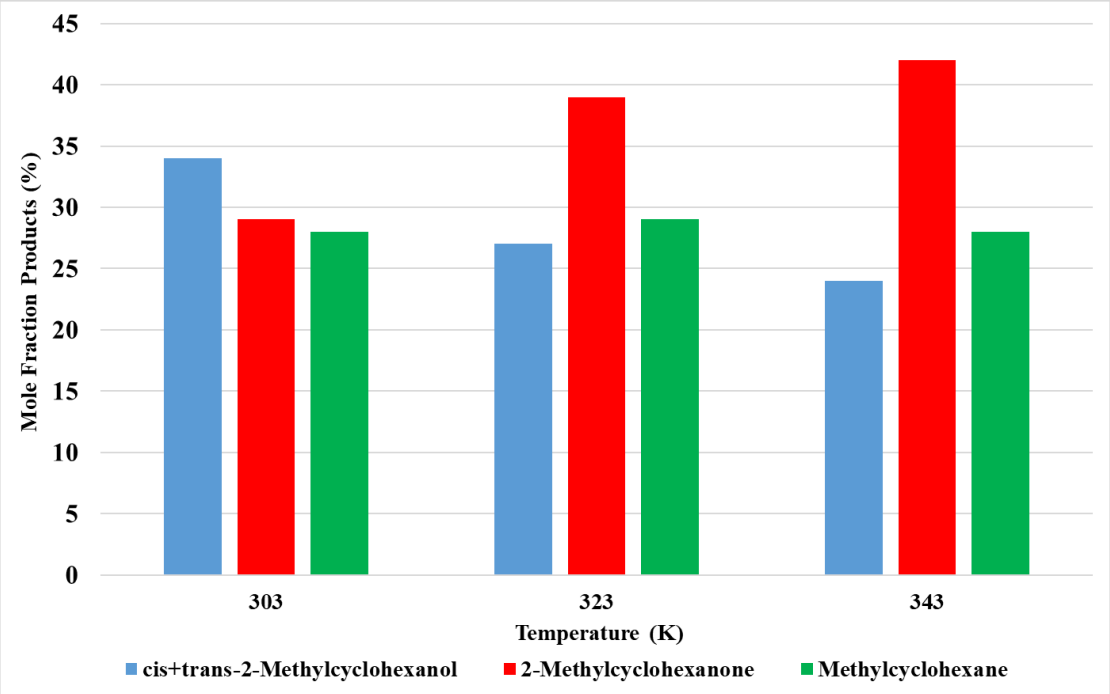

Figure 242. Product distribution at ~ 90 % conversion for *ortho*-cresol hydrogenation.

The increase in the initial hydrogenated product 2-methylcyclohexanone and concomitant decrease in the secondary hydrogenated products, *cis*+*trans*-2-methylcyclohexanol, are in line with what was observed with the dihydroxybenzenes. This suggests although there are differences in the effect of temperature on cresols and dihydroxybenzenes there is a commonality in the formation of both these sets of products.

Analysis of the *cis*:*trans* ratios taken for each substrate at the same conversion show selectivity is unaffected by temperature. From our previously postulated routes of formation for the *cis* and *trans* isomers this suggests no effect on the enol to keto tautomerization with temperature. A study on xylenes hydrogenation found the *trans* isomer to become more favoured with temperature; however, the difference between the hydrogenation of a ketone in our study against that of an aromatic ring with xylenes makes a direct comparison impossible. [70] A more appropriate comparison is to be found in our work on dihydroxybenzenes where the hydrogenation of a ketone occurs and again no temperature effect on the *cis*:*trans* ratio was observed. This suggests the positive effect temperature has on formation of the ketone is taking precedent over any *cis*:*trans* ratio effect.

8.2.3 Concentration Variations

The effect of concentration varied significantly between the cresol substrates: both *ortho* and *para*-cresol showed an enhanced rate with increased concentration whilst *meta*-cresol exhibited a marked decrease. The negative order of *meta*-cresol, -1.5, indicates a stronger adsorption to the catalyst surface than both *ortho* and *para* with their positive orders. When we look at the order of the dihydroxybenzene isomers we see that it is the *ortho* isomer that had the negative order with both *meta* and *para* exhibiting a positive ~ 0.5 order. This strongly suggests that orientation of the isomer has limited influence on the strength of adsorption, and it is dependent on the substituents attached to the aromatic ring.

In our previous work with the dihydroxybenzenes, we postulated the possibility of a link between strength of adsorption and hydrogenolysis, where catechol (-ve order) underwent the least hydrogenolysis and resorcinol and hydroquinone (+ve order) the greatest. Whilst these results show some correlation, they are not wholly compatible with this theory. It is true that *meta*-cresol with its negative order undergoes limited HDO, however, so does *para*-cresol and that displays a positive order. Once again, behaviour we see with one group of isomers cannot necessary be applied to another group.

The product distribution was found to be independent of concentration for both *ortho*- and *para*-cresol, in line with our findings for all isomers of dihydroxybenzene. *meta*-Cresol, however, again exhibited different behaviour with an increase in the *cis*+*trans*-3-methylcyclohexanol and a decrease in the 3-methycyclohexanone and methylcyclohexane with an increase in concentration. Whilst this behaviour is unique in our study, it has been recorded previously in anisole hydrogenation where it was found that cyclohexanol and cyclohexanone increased and methoxycyclohexane and cyclohexane decreased with an increase in concentration. [100]

8.2.4 Competitive Substrate Hydrogenation

When substrates were reacted in a competitive environment significantly different behaviour from that seen with the individual hydrogenation reactions occurred. Across all combinations of substrates, a marked decrease in rate was observed and a shift in order of reactivity from *para* > *meta* > *ortho* to *ortho* > *para* > *meta* witnessed; a change in order of reactivity also observed for the dihydroxybenzenes, in that instance from *meta* > *ortho* > *para* to *ortho* > *para* > *meta*. This shared order of isomer reactivity in the competitive environment for both cresols and dihydroxybenzenes indicates the most crucial factor may be the position of the substituents and its orientation to the catalyst surface rather than the nature of the substituent itself.

The effect of the competitive environment on each of the substrate combinations was studied and an example of the change in conversion for *ortho*- and *meta*-cresol is shown below:

Table 48. Individual and competitive conversion for *ortho*- and *meta*-cresol after 180 minutes.

Individual	**Conversion %**
ortho	100 % by 140 mins
meta	100 % by 120 mins
Competitive	**Conversion %**
ortho	74 %
meta	66 %

A clear effect on reactivity in the competitive environment is evident, neither isomer achieved full conversion by end of reaction and a shift to *ortho*-cresol registering the highest reactivity under competitive conditions occurred. When *ortho*- and *para*-cresol were reacted together, *ortho*-cresol was again found to have the higher reactivity, in contrast to individual hydrogenation where the reactivity of the *para* isomer was far greater. The conversion percentages of *ortho*- and *para*-cresol were similar to that recorded for the *ortho*- and *meta*-cresol reaction, suggesting a comparable effect from *ortho*-cresol on both other isomers under competitive conditions. Analysis of product distribution from both competitive reactions show that hydrogenation and HDO remain broadly constant, with any effect limited to reactivity.

The *meta*- and *para*-cresol competitive reaction showed the least inhibitive effect of all three pair combinations tested. This was in contrast to the comparative pair reaction with the dihydroxybenzenes, which exhibited the highest rate suppression. Unlike the decrease observed in hydrogenated products for both when reacted with *ortho*-cresol, product distributions for *meta*- and *para*-cresol remained similar to those observed for individual hydrogenation. This may suggest that *ortho*-cresol can access shared sites more readily than either *meta*- or *para*-cresol and in addition, opens up the possibility that a limited number of alternative sites may be available to solely *ortho*-cresol.

The competitive hydrogenation of *ortho*-, *meta*- and *para*-cresol showed a significant decrease in reactivity for all three substrates and a shift in order to *ortho* > *para* > *meta* from the *para* > *meta* > *ortho* observed during individual hydrogenation. The decrease in

measured rate constant was most marked with *para*-cresol which declined to $3.6x10^{-3}$ min^{-1} from the $24.2x10^{-3}$ min^{-1} registered during individual hydrogenation. These significant effects on reaction rate in the presence of more than one substrate have been discussed previously with the dihydroxybenzenes and again indicate increased competition for available active sites on the catalyst leading to a crowding effect. Analysis of product formation shows those hydrogenated from *ortho*- and *meta*-cresol, 2-methylcyclohexanone and 3-methylcyclohexanone, were formed initially, whilst that from *para*-cresol, 4-methylcyclohexanone, exhibited a slight delay in formation of around 10 minutes. This inhibitive effect on hydrogenation is not as pronounced as that observed for the comparable dihydroxybenzene competitive reaction. In that instance a delay in formation of 10 and 40 minutes occurred for the initial hydrogenated products from resorcinol and hydroquinone respectively. If as we believe, the strength of adsorption is greater with the dihydroxybenzenes when compared with that of the cresols, the increased extent of dihydroxybenzene interaction with the catalyst surface could explain this longer delay in product formation.

In addition to this suppression in reactivity, a change in the product distribution was observed when compared to individual hydrogenation. Product yield distribution of the shared HDO product, methylcyclohexane, and the hydrogenated products for both the individual and the *ortho*-, *meta*- and *para*-cresol competitive reactions are shown in Figures 243 and 244:

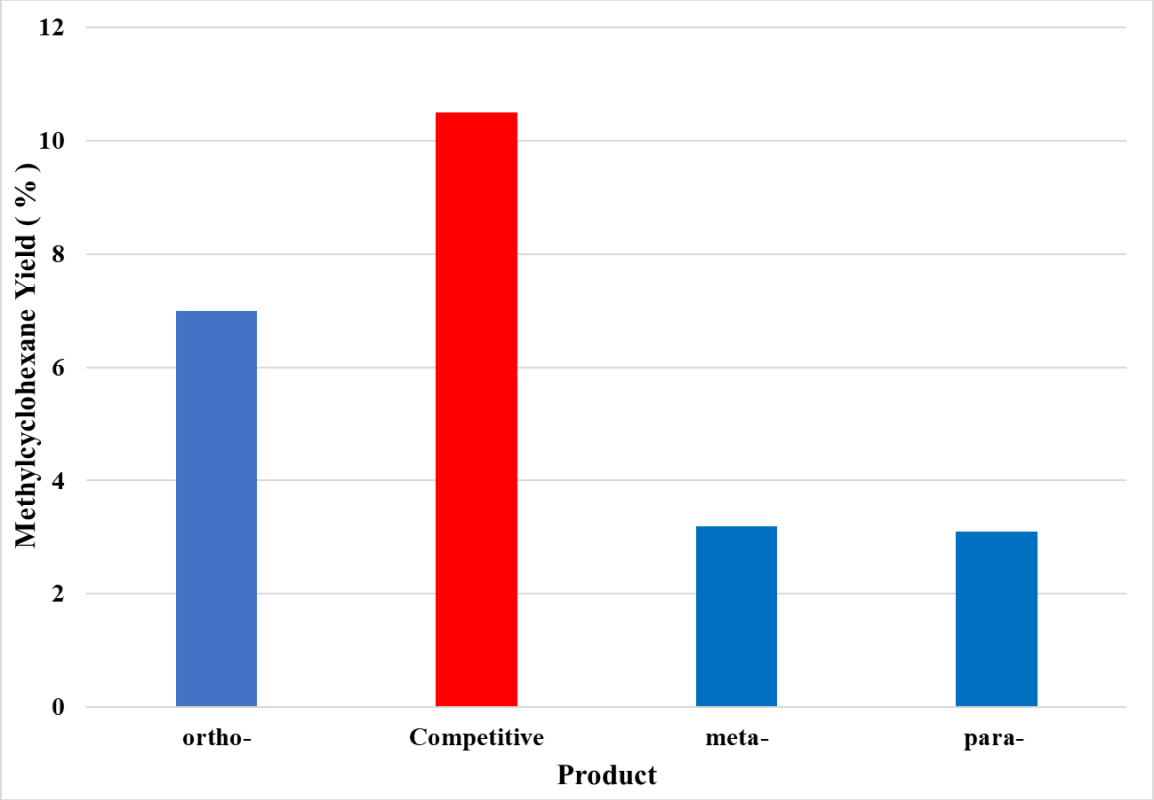

Figure 243. Comparison of methylcyclohexane yield for individual and competitive hydrogenation of *ortho*-, *meta*- and *para*-cresol. Data taken at 25 % conversion of *ortho*-, 19 % *meta*- and 20 % conversion of *para*-cresol.

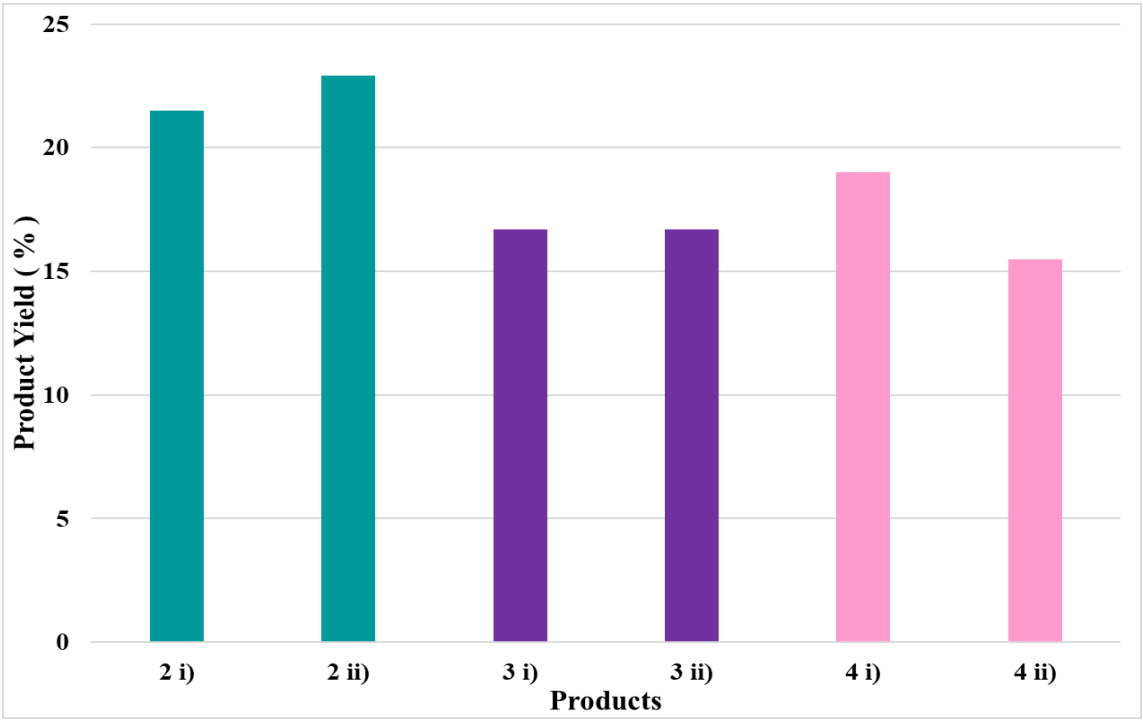

Figure 244. Comparison of product yield for individual and competitive hydrogenation of *ortho*-, *meta*- and *para*-cresol. Data taken at 25 % conversion of *ortho*-, 19 % *meta*- and 20 % conversion of *para*-cresol.

2 i) Individual ortho-cresol ii) Competitive ortho-cresol

3 i) Individual meta-cresol ii) Competitive meta-cresol

4 i) Individual para-cresol ii) Competitive para-cresol

Comparison of the combined methylcyclohexane product yield from the three individual hydrogenation reactions in Figure 243 shows a total of ~ 13% compared with ~ 10 % observed during the competitive reaction of all three. The ability of all three substrates to form the HDO product, methylcyclohexane, indicate that this suppression in activity of hydrogenolysis is a result of the increased competition for surface hydrogen in the presence of multiple substrates. Examination of the hydrogenated products from Figure 244 show an increase in those from *ortho*-cresol in accordance with what was observed during the pair combination reactions. Suppression of the products from *para*-cresol is evident whilst those from *meta*-cresol remain constant between both individual and competitive hydrogenation. This dominating behaviour of the *ortho* isomer in the competitive environment is similar to that observed with the dihydroxybenzenes, and again suggests the orientation of the *ortho* isomer allows for preferential access to the active sites on the catalyst.

The reasons behind these differences in behaviour of the isomers in a competitive environment is not entirely clear. In our work on the dihydroxybenzenes, where similar disparities were observed, we postulated that the presence of a negative order in substrate for catechol allowed it to outcompete resorcinol and hydroquinone when reacted together. This reasoning cannot be directly applied to the cresols where the best performing isomer in the competitive environment, *ortho*-cresol, registered a positive order in substrate and suggests order of reactivity is not influenced simply by strength of adsorption. Instead as previously stated, the nature of interactions between the aromatic and the catalyst surface, dependent on substituent ring position, is key to determining performance in the competitive environment; highlighted by the higher reactivity of the *ortho* isomer in both sets of substrates.

These significant effects on selectivity, coupled with those observed on rate for both cresols and dihydroxybenzenes in the competitive environment, highlight once more the limitations of studying a single model compound as a route to understanding the processes required for the upgrading of a true bio-oil feed.

8.2.5 Deuteration Reactions

The effect of replacing hydrogen with deuterium was examined for the cresol isomers. A summary of each KIE calculated is shown in Table 49 below:

Table 49. Substrate KIE values.

Substrate	KIE
ortho-	1.3
meta-	1.3
para-	2.0

Looking at the values for each, it is apparent that all isomers registered a decrease in reaction rate under deuterated conditions, reflected in their positive KIE value calculated for each.

We previously postulated in our section on dihydroxybenzenes, that the presence of an inverse KIE calculated for catechol and resorcinol may be a result of the change in hybridisation that occurs from sp^2 to sp^3 during aromatic hydrogenation. The absence of an overall inverse KIE value for the isomers of the cresol substrates indicates this change in hybridisation cannot be rate-determining for their hydrogenation and as such, shows different behaviour than that observed with the dihydroxybenzenes. The same positive KIE value recorded for all isomers of cresol indicates a similar bond may be being broken or formed in the RDS of their hydrogenation reaction. Comparison with the overall KIE values calculated for the dihydroxybenzene isomers show figures of: 0.6, 0.9 and 1.2 for the *ortho*, *meta* and *para* isomers respectively and points to no correlation between KIE value and position of substituent on the aromatic ring; instead KIE must be dependent on the nature of the substituent itself.

To gain more information on the reaction mechanism in the presence of deuterium, the KIE value for each product was calculated and is shown below in Table 50 for *ortho*-cresol:

Table 50. *ortho*-Cresol hydrogenated products KIE values.

Product	KIE
cis-2-Methylcyclohexanol	-
trans-2-Methylcyclohexanol	0.1
2-Methylcyclohexanone	1.0
Methylcyclohexane	1.4

It is apparent from Table 50 that no KIE value could be calculated for the *cis*-2-methylcyclohexanol hydrogenated product, a result of almost complete inhibition of formation in the presence of deuterium. It should be remembered, that during standard *ortho*-cresol hydrogenation the *cis* isomer was highly favoured. In the presence of deuterium, its level of formation is below our chromatography detection limit and as such, although we know a large primary KIE exists for *cis*-2-methylcyclohexanol, it is impossible to determine a value. We previously postulated two routes of formation for the *cis* isomer, through the enol and ketone intermediates, and it is clear that in the presence of deuterium neither can form the *cis* isomer. Whilst the enol route we believe exclusively forms the *cis* isomer the ketone intermediate is a route of formation for both *cis* and *trans* isomers.

The KIE product values for *meta*-cresol are shown below in Table 51:

Table 51. *meta*-Cresol hydrogenation products KIE values.

Product	KIE
cis-3-Methylcyclohexanol	1.1
trans-3-Methylcyclohexanol	1.2
3-Methylcyclohexanone	1.2
Methylcyclohexane	2.3

We can see that all products from resorcinol give a positive KIE value. In this instance, we see no inhibitive effect on the formation of the *cis*-3-methylcyclohexanol which adds weight to our earlier proposition that there may be a steric effect related to the *ortho*-position which inhibits the *cis*-2-methylcyclohexanol formation to below our detectable level. The increased distance between the two substituents in the *meta*- position would negate this steric effect. The KIE product values calculated for *para*-cresol are shown in Table 52:

Table 52. *para*-Cresol hydrogenation products KIE values.

Product	KIE
cis-4-Methylcyclohexanol	1.6
trans-4-Methylcyclohexanol	1.8
4-Methylcyclohexanone	1.2
Methylcyclohexane	1.2

As with *meta*-cresol, all products from *para*-cresol registered a positive KIE value. The similarity in behaviour of *meta*- and *para*-cresol in the presence of deuterium in contrast to the values for *ortho*-cresol indicates a different reaction mechanism must be occurring. The ketone product registering a positive KIE value is in strong contrast to the secondary inverse KIE value for the equivalent ketone product from the dihydroxybenzenes. This infers that different routes of formation of the initially formed ketone product exist between cresols and dihydroxybenzenes, and once again highlights that what can be applied to one set of substrates cannot be presumed for another. As with *meta*-cresol, no inhibition of either *cis* or *trans*-4-methylcyclohexanol was observed, and the measured KIE values were similar between both substrates. Here again, with the secondary hydrogenated products (*cis*+*trans*-methylcyclohexanol), we see this contrast in the behaviour of the *meta*- and *para*-cresol with that of the *ortho*-cresol. The suggestion is, that a shared route of formation exists for these products from *meta*- and *para*-cresol, one which differs from that from the *ortho*-cresol.

When we come to look at the effect of deuterium in the competitive environment, we see shifts in both overall and product KIE values from those calculated from individual reactions. Taking each combination individually, the reaction between *ortho*- and *meta*-cresol shows no effect observed in the KIE value of *ortho*-cresol, whilst meta-cresol changes from a positive to an inverse KIE. The product KIE values for this reaction are shown in Table 53 below:

Table 53. *ortho*- and *meta*-Cresol competitive reaction product KIE values.

Product	KIE
cis-2-Methylcyclohexanol	-
trans-2-Methylcyclohexanol	0.1
2-Methylcyclohexanone	0.8
cis-3-Methylcyclohexanol	0.9
trans-3-Methylcyclohexanol	0.9
3-Methylcyclohexanone	0.9

As the HDO product, methylcyclohexane, can form from both *ortho*- and *meta*-cresol it is not included in the table of product KIE values. Comparison of the effect on product KIE values between the individual and competitive environment were as follows: the initial hydrogenated product, 2-methylcyclohexanone, changed from no effect overall to an inverse KIE whilst 3-methylcyclohexanone now registered an inverse KIE from a positive KIE measured. As with the individual reaction of *ortho*-cresol, both secondary hydrogenated products remain unchanged; no *cis*-2-methylcyclohexanol was formed, and as such no KIE value calculated whilst *trans*-2-methylcyclohexanol remained small and inverse. In contrast, both secondary hydrogenated products from *meta*-cresol, *cis*-3-methylcyclohexanol and *trans*-3-methylcyclohexanol, showed a switch in KIE value from positive to inverse.

The combination of *ortho*-cresol and *para*-cresol showed a shift in overall KIE value for both: from positive to no effect for *ortho*-cresol and positive to inverse for *para*-cresol. The calculated product KIE values are shown in Table 54 below:

Table 54. *ortho*- and *para*-Cresol competitive reaction product KIE values.

Product	KIE
cis-2-Methylcyclohexanol	-
trans-2-Methylcyclohexanol	0.1
2-Methylcyclohexanone	0.8
cis-4-Methylcyclohexanol	0.8
trans-4-Methylcyclohexanol	0.7
4-Methylcyclohexanone	0.8

Again, we see a change in the initial hydrogenated product from *ortho*-cresol from no effect to an inverse KIE, whilst the secondary hydrogenated products remained unchanged from individual hydrogenation. This suggests the same effect on the initial hydrogenated product from *ortho*-cresol by both *meta*- and *para*-cresol, whilst no effect observed on the formation of the secondary hydrogenated products. The hydrogenated products from *para*-cresol all registered a change from positive to inverse, the same effect found for *meta*-cresol when reacted with *ortho*-cresol.

The pair combination of *meta*- and *para*-cresol resulted in a change in overall *meta*-cresol KIE value, from measured positive effect to an inverse effect, whilst no change in *para*-cresol was observed from the individual reaction. The product KIE values calculated are shown below in Table 55:

Table 55. *meta*- and *para*-Cresol competitive reaction product KIE values.

Product	KIE
cis-3-Methylcyclohexanol	0.4
trans-3-Methylcyclohexanol	0.8
3-Methylcyclohexanone	1.1
cis-4-Methylcyclohexanol	-
trans-4-Methylcyclohexanol	-
4-Methylcyclohexanone	1.0

It is apparent that the presence of *meta*-cresol had a significant effect on product formation of both the initial and secondary hydrogenated products from *para*-cresol. Significant suppression, to below detectable levels, of both *cis* and *trans*-4-methylcyclohexanol occurred, rendering the calculation of KIE values for both impossible; however, as stated previously with individual *ortho*-cresol if calculable, both would exhibit large primary values. This effect was not present for individual *para*-cresol or during the paired reaction with *ortho*-cresol, suggesting it is dependent on deuterium and the presence of *meta*-cresol. The initial hydrogenated product, 4-methylcyclohexanone, switched from a positive to no KIE value calculated. The secondary hydrogenated products from *meta*-cresol also exhibit a change from positive to an inverse KIE calculated for both *cis* and *trans* isomers, whilst the initial hydrogenated product remained unchanged and positive.

When all three substrates were reacted together in the presence of deuterium the following effect on overall KIE value from that of individual reactions was observed: o*rtho*-cresol

registered a change from a positive to no effect, *meta*-cresol moved to an inverse KIE from a positive effect and *para*-cresol remained positive across both environments. The product KIE values for this reaction are shown in Table 56 below:

Table 56. *ortho*-, *meta*- and *para*-Cresol competitive reaction product KIE values.

Product	KIE
cis-2-Methylcyclohexanol	-
trans-2-Methylcyclohexanol	0.3
2-Methylcyclohexanone	1.0
cis-3-Methylcyclohexanol	-
trans-3-Methylcyclohexanol	-
3-Methylcyclohexanone	1.0
cis-4-Methylcyclohexanol	0.4
trans-4-Methylcyclohexanol	-
4-Methylcyclohexanone	1.1

In this instance, we see for the first-time significant inhibition of the secondary hydrogenated products from *meta*-cresol, *cis*-3-methylcyclohexanol and *trans*-3-methylcyclohexanol, to below detectable levels and as such no KIE value could be calculated. As with the individual reaction of *meta*-cresol, no effect was observed on the secondary hydrogenated product, 3-methylcyclohexanone. The KIE values calculated for both secondary hydrogenated products from *ortho*-cresol remained consistent with those of the individual reaction; however, the 2-methycyclohexanone registered a change from having no effect to an inverse KIE. The initial hydrogenated product from *para*-cresol, 4-methylcyclohexanone, remained positive whilst a divergence in behaviour occurred with the secondary hydrogenated products: *cis*-4-methylcyclohexanol remained inverse whilst, in contrast to the inverse KIE measured during individual reaction, no KIE could be measured for the formation of *trans*-4-methylcyclohexanol. It is of note, that in the presence of deuterium, formation of the HDO product, methylcyclohexane, is delayed until 140 minutes reaction time. This is in contrast to the comparable hydrogenation reaction when methylcyclohexane formed from the outset and suggests significant competition for hydrogen during the majority of the reaction, why it begins to form after 140 minutes and becomes the second major product of the reaction is, however, unclear.

These findings show the addition of a third substrate further complicates our understanding of the behaviour of the cresol isomers in the competitive environment. For example, in this three-substrate combination we see complete suppression of the formation of *meta*-cresol secondary hydrogenated products. This does not occur in the individual *meta*-cresol reaction or either pair combination, and on the surface, it would seem unusual that no formation occurs when the same isomers are present. However, it may be that the combined influence of both *ortho*- and *para*-cresol is enough to completely inhibit formation of these secondary hydrogenated products from *meta*-cresol. This may in turn provide some insight into why both secondary hydrogenated products of *para*-cresol are completely absent during the *meta*- and *para*-cresol pair combination, however, when reacted as a three-substrate combination *cis*-4-methylcyclohexanol is present. It may be that the combined influence of the *ortho* and *para* isomers on secondary hydrogenated product formation from *meta*-cresol lessens the competition between *meta*- and *para*-cresol and allows *cis*-4-methylcyclohexanol formation to occur.

When looking at the individual and competitive combinations as a whole, it is clear that competition for active sites is taking place, however, the picture from this deuterated work is far from clear. What can be stated, is *ortho*-cresol exhibited the greatest reactivity and had a marked similarity in product KIE values across all combinations tested. This strongly suggests no effect from either competing isomer on product formation exists and may point to the possibility of alternative active sites available exclusively to the *ortho* isomer. It should be stated at this point that using substrate behaviour in the individual environment to predict the outcome of competitive reactions is extremely difficult, a problem exacerbated as each substrate is added.

To attempt to shed some light on this complex set of results, a sample from each individual deuterated reaction was taken after and analysed via NMR. The results for the *ortho*-cresol and *para*-cresol are shown in Figures 245-248:

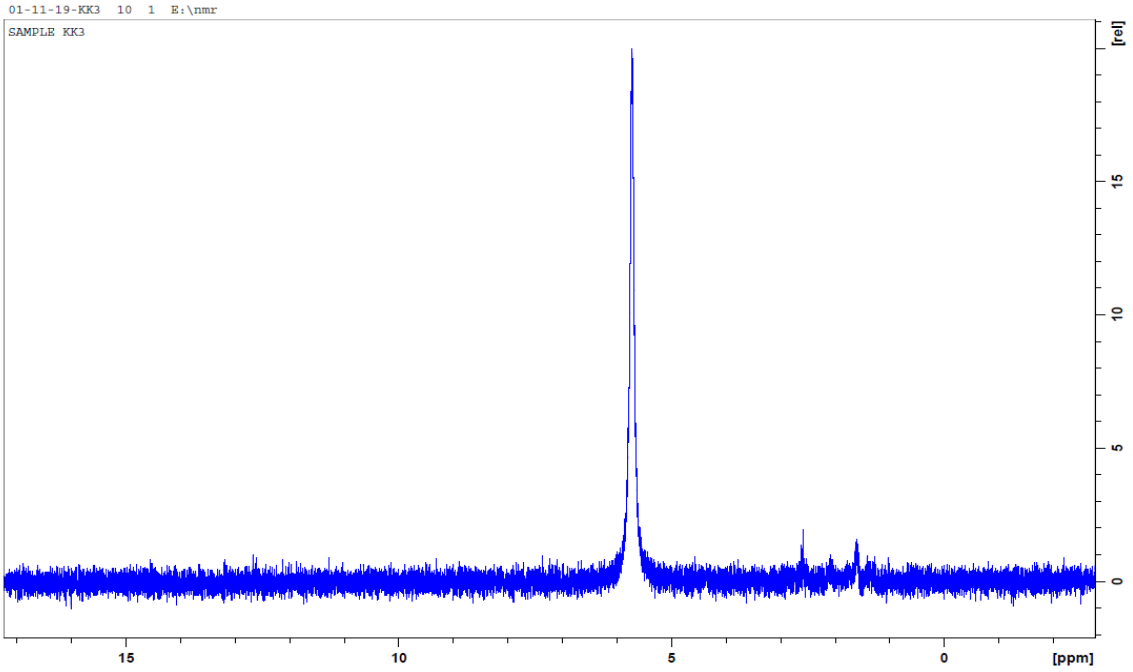

Figure 245. Deuterium NMR Data for ortho-cresol after 30-minute reaction time.

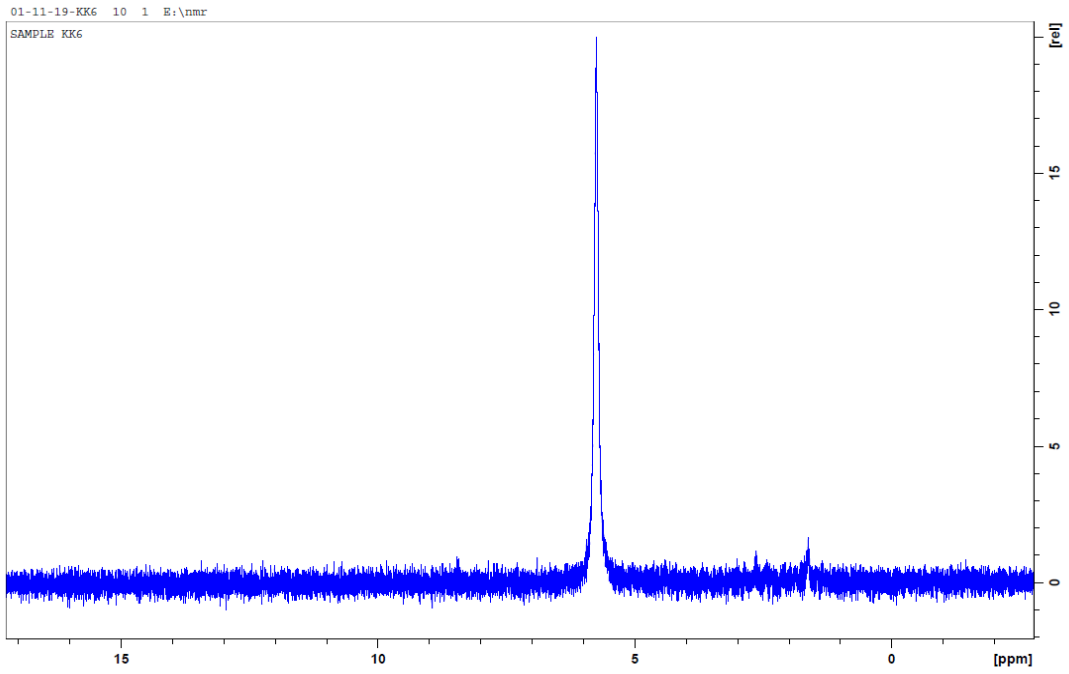

Figure 246. Deuterium NMR Data for para-cresol after 30-minute reaction time.

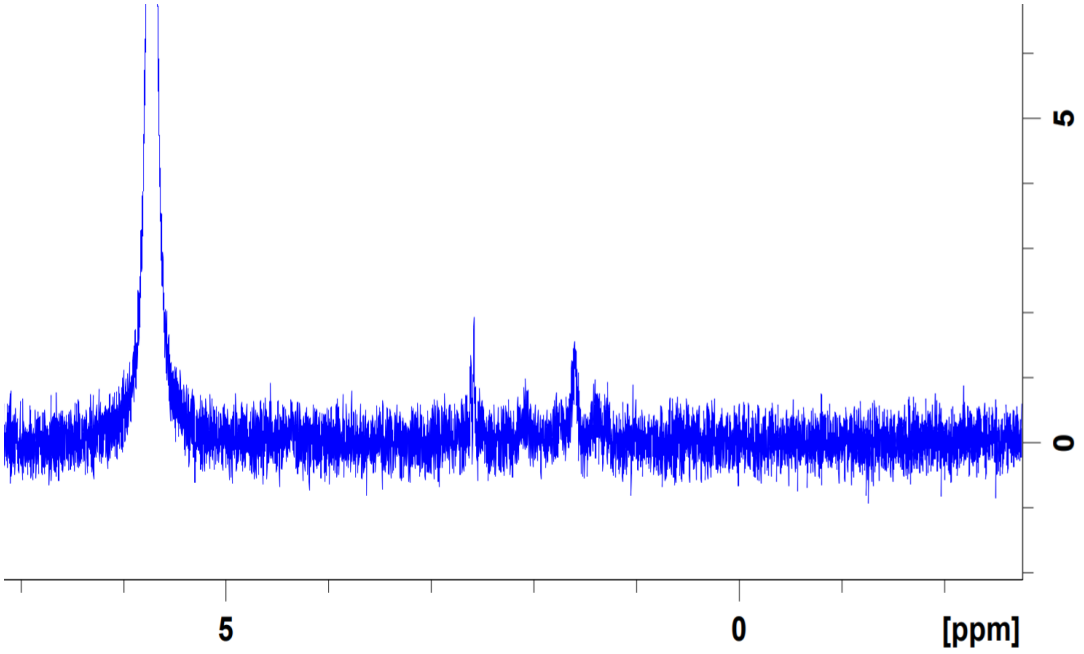

Figure 247. Focused Deuterium NMR Data for ortho-cresol after 30-minute reaction time.

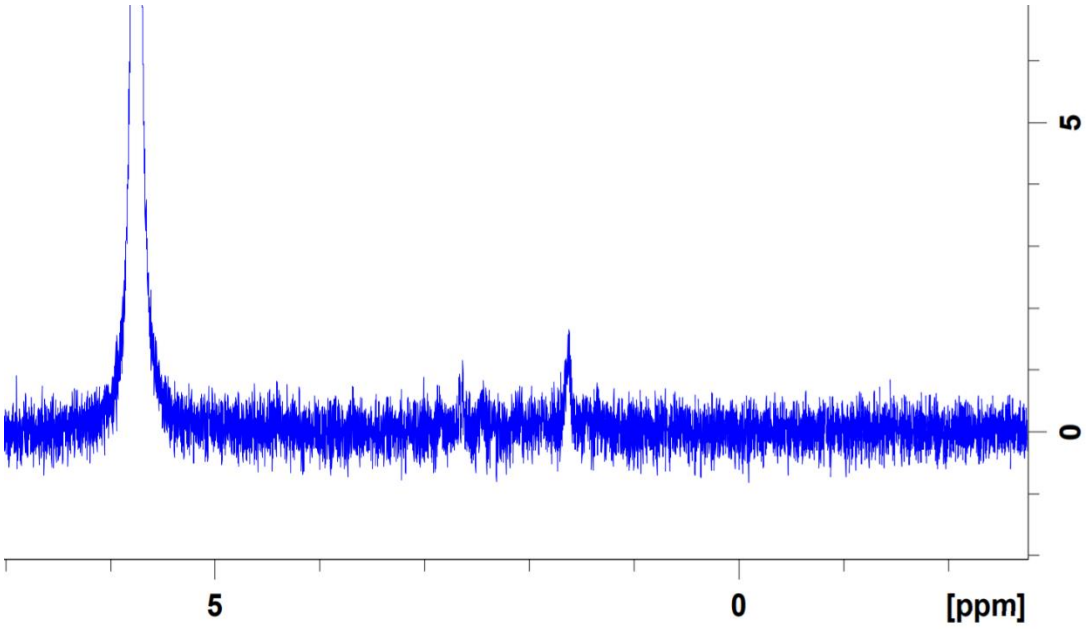

Figure 248. Focused Deuterium NMR Data for meta-cresol after 30-minute reaction time.

From Figures above, the peak at 5.7 ppm referring to the -OH group from isopropanol, suggests the solvent has exchanged with deuterium. The 5.7 ppm peak may also indicate hydrogen-deuterium exchange of the -OH group on the aromatic ring of both cresol isomers. Of greatest significance is the presence of an aromatic-CH_3 peak for *ortho*-cresol which is absent from the *para*-cresol spectrum. This clearly indicates that the CH_3 group of *ortho*-cresol is exchanging with deuterium and hence interacting with the catalyst surface,

something that cannot be said for *para*-cresol. Although methyl substituted aromatics interaction on the catalyst surface is widely thought to occur via the aromatic ring, Webb and Orozco, studying toluene adsorption, proposed that additional interaction with the -CH_3 group occurs. [92] We also know from previous toluene hydrogen-deuterium exchange experiments, over the same catalyst used in this work, that the -CH_3 group exchanges rapidly with deuterium, and for this to occur it must be interacting with the surface. [59]

This exchange of deuterium with the -CH_3 for the *ortho* isomer clearly points to the existence of a different mode of adsorption from that of the *para* isomer and the commonality of behaviour between the *meta*- and *para*-cresol allows us to state the same for *meta*-cresol. It could be that the *ortho* isomer is able to adopt a more planar mode of adsorption due to the interaction of both the -CH_3 and -OH groups with the catalyst surface. The lack of any -CH_3 interaction with *meta*- and *para*-cresol would point towards an inclined mode of adsorption. These results confirm the previously postulated belief that *ortho*-cresol can interact differently with the surface due to the orientation of the substituents and explains its dominance during competitive reactions. This could be also said to be independent of substituent, with similar dominant behaviour exhibited by the *ortho*- isomer during dihydroxybenzene competition.

Although the deuterium work has in some ways complicated the picture, we have of the mechanism for the hydrogenation of the cresol isomers, without this information we would be unaware of the following important observations:

- The marked decline in formation of the *cis*-2-methylcyclohexanol from *ortho*-cresol, to undetectable levels, suggests a clear primary KIE for its formation.
- The significant delay, until 140 minutes, in the formation of the HDO product, methylcyclohexane, when all three substrates were reacted together.
- Of greatest interest, however, has been the observed change in product KIE values between individual and competitive hydrogenation. The introduction of a second and third isomer into the reaction has significant implications on the mechanism and is not what would be expected prior to studying the competitive environment. This has further implications for the value of studying a single model compound as a route to understanding a true bio-oil feed.

8.2.6 Post Reaction Catalyst Characterization

Thermal analysis of the post reaction catalysts from each isomer found the greatest amount of carbon laydown associated with *ortho*-cresol, a result which in this instance could be due to its ability to undergo higher levels of HDO than both *meta* and *para*-cresol. This correlation between HDO and carbon laydown did not apply with the dihydroxybenzenes, where the *ortho* isomer registered the highest carbon laydown percentage but underwent the least HDO. A comparison of the percentage carbon deposition for each isomer of cresol and dihydroxybenzene is shown below in Table 57:

Table 57. Weight loss percentages associated with evolution of m/z 44.

	Cresols	Dihydroxybenzenes
ortho-	3.5 %	4 %
meta-	3 %	3.5 %
para-	3 %	3.5 %

It is evident that each isomer of cresol exhibits less weight loss associated with carbon dioxide evolution than its comparable dihydroxybenzene isomer. This is understandable when we consider the higher amount of oxygen present on the aromatic substrate of the dihydroxybenzenes, which is believed to give a greater affinity for carbon formation through polymerization reactions. [32]

Analysis in greater detail of the TPO data show one distinct weight loss event below 473 K common to all three isomers. No concomitant evolution of carbon dioxide is detected suggesting this weight loss event may be due to the release of adsorbed solvent from the catalyst surface. Three further high temperature weight loss events (>473 K) associated with the evolution of carbon dioxide, and indicating the combustion of surface carbon species, are present in all three substrates. Of these, the lower temperature peak at 490 K is a result of combustion of a single aromatic unit, similar in structure to the cresol substrate, trapped in the pores of the catalyst. The temperature of evolution is in accordance with the boiling points of the cresol substrates. TPO analysis of the post reaction dihydroxybenzene catalysts showed a shared temperature event in the same region; identified as the aromatic substrate through Soxhlet extraction. A second common temperature peak at 590 K is a result of the aromatic species moving towards a carbon species graphitic in nature. The highest of the shared evolution events > 690 K indicates combustion of fully graphitic carbon species from polynuclear aromatic residues on the catalyst surface. Although these

commonalties are present, unique aspects within the post reaction TPO profiles exist for all three substrates. An additional two weight loss events, associated with the evolution of carbon dioxide, are present in the *ortho*-cresol TPO. These may be indicative of the presence of a distinct carbon species resulting from the higher levels of HDO occurring during the *ortho*-cresol hydrogenation reaction. In addition, the higher temperature combustion event is significantly sharper for the *para*-cresol; a possible consequence of the combustion of a single specific carbon species, polynuclear in nature, and more readily formed due to the symmetrical arrangement of the *para* isomer.

As with our work on the dihydroxybenzenes, we observe significant carbon laydown on our catalyst at these mild conditions which as we previously expressed may seem unusual, however, again with high levels of HDO occurring in addition to standard hydrogenation it is perhaps unsurprising. These high levels of catalyst deactivation are a well-known problem with catalytic HDO, [35] and it is of interest that despite operating at a temperature well below the standard conditions of >473 K it is still having a clear impact on our catalyst for both sets of substrates.

8.3 Methoxyphenol Isomers

8.3.1 Individual Hydrogenation

Hydrogenation of the individual substrates gave the following order of reactivity: 3-methoxyphenol > 2-methoxyphenol > 4-methoxyphenol (*meta* > *ortho* > *para*). Literature on the reactivity of this group of isomers is sparse, and as such, no direct comparison with other studies can be made. Comparison with the other groups of substrates in our study, however, show an identical order with that found for the dihydroxybenzenes, whilst for the cresols an order of *para* > *meta* > *ortho* was recorded. This shared order in reactivity, only present when both substituent groups contain an oxygen atom, is noteworthy and indicates the nature of the substituent has a strong effect on the order of isomer activity within a group of substrates. Those arguments made previously for the dihydroxybenzenes explaining the higher reactivity of the *meta* isomer- the 'more favourable arrangement' due to the resonance structures and the reinforcing/cooperative effect that two EDG's in the *meta* position has on the aromatic ring- may again apply to the methoxyphenol isomers.

The presence of an aryl-ether bond (anisole-like) and an aryl-hydroxyl bond (phenol-like) in the methoxyphenol isomers allows for comparison of reactivity with both anisole and phenol. A study by Jackson *et al*. [100] recorded an order in calculated rate constants of anisole ($74.8 \times 10^{-3}\ min^{-1}$) >> phenol ($14.7 \times 10^{-3}\ min^{-1}$) > 4-methoxyphenol ($6.4 \times 10^{-3}\ min^{-1}$), with a significantly higher rate constant recorded for anisole. The rates of reactivity measured for both 2- and 3-methoxyphenol in this study were also found to be lower than those reported for anisole and phenol although in both instances the difference in recorded rate constant with that of phenol was minimal. It must be mentioned however, that we are comparing mono-substituted with di-substituted aromatic substrates. It is accepted in the literature that an increase in substituent results in a decrease in overall reactivity and as such the lower reactivity of the methoxyphenol isomers may be unsurprising. [116]

Comparison with the cresols and dihydroxybenzenes shows the reactivity of the methoxyphenols lies between both as shown in Table 58:

Table 58. Comparison of rate constants for methoxyphenol, cresol and dihydroxybenzene isomers.

Rate constant ($x10^3 min^{-1}$)			
	ortho	*meta*	*para*
Methoxyphenols	11.5	12.8	7.4
Cresols	11.1	18.4	24.2
Dihydroxybenzenes	8.3	11.9	4.2

Analysis of the comparable isomer reactivity for all three substrate groups show those of methoxyphenol to be higher than those of the dihydroxybenzenes. With the exception of the *ortho* isomer, the opposite was true for the cresols; most marked with the *para* isomer where the rate was over 3-times faster. This significantly higher reactivity observed with the cresols may be a result of the presence of a $-CH_3$ group and a single oxygen substituent. The presence of two oxygen substituents on the dihydroxybenzenes and methoxyphenols would allow a strong bond to be made with the catalyst surface via the two oxygen atoms. Whilst we know from our previous section the $-CH_3$ group does interact with the surface, formation of this strong direct bond would be unlikely to occur, and as such, the adsorption and desorption process during the catalytic cycle could occur more readily, resulting in a higher reactivity. The identical order of reactivity for the methoxyphenol and dihydroxybenzene isomers may point to a shared planar mode of adsorption through the previously mentioned surface interactions between the two oxygen substituents and the catalyst surface. The difference in order of reactivity for the cresols coupled with their significantly faster rates of reaction indicate, as previously postulated, the presence of a different, inclined, mode of adsorption when the methyl group is present. The effect of pKa on the reactivity of the methoxyphenol isomers shows further correlation with the dihydroxybenzene isomers. An order of 9.65 > 9.93 >10.16 for 3-, 2- and 4-methoxyphenol respectively is documented indicating that, as postulated for the dihydroxybenzenes, the acid strength may influence reactivity. Here again, the lower pKa value of the *meta* isomer allows for easier dissociation of the oxygen containing substituents resulting in enhanced reactivity on the surface of the catalyst. It is worth restating at this stage that no acid strength effect was present for the cresol isomers, and again indicates the nature of the substituents strongly affects reactivity.

Comparison of the product distribution for the methoxyphenol isomers at the same conversion shows significant differences. The cumulative mole fraction of the hydrogenated and HDO products are shown in Figure 249 below:

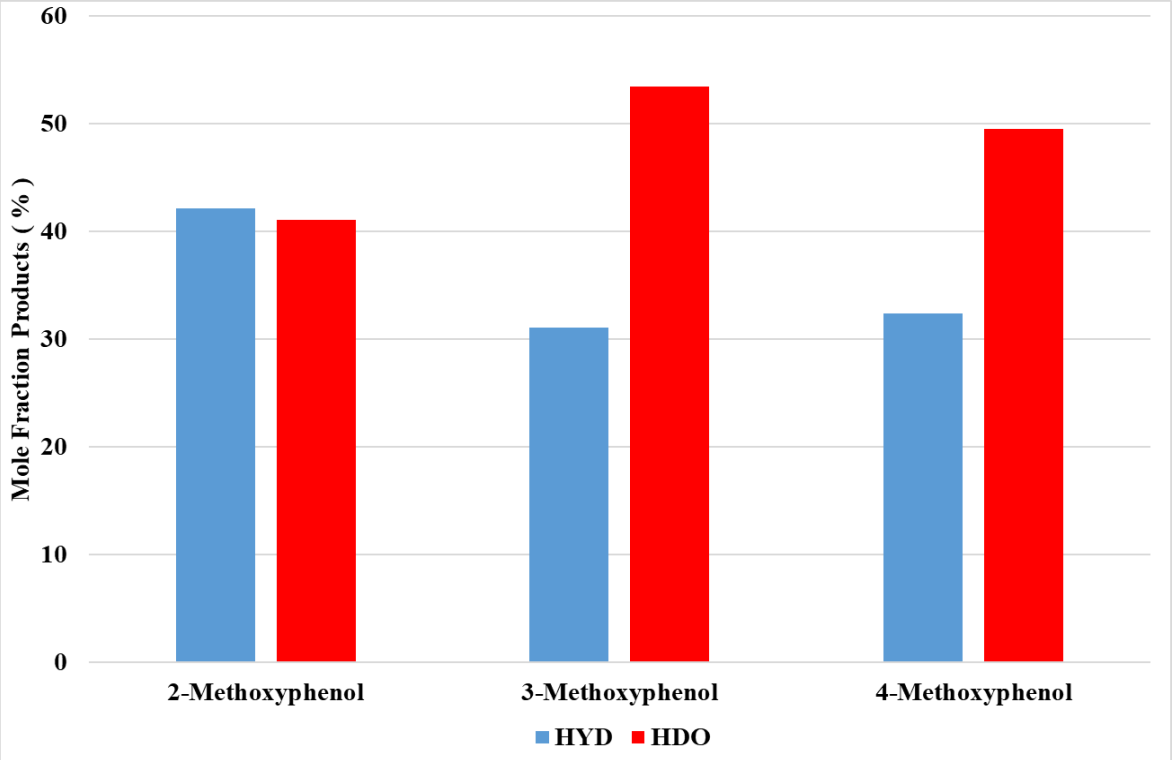

Figure 249. Hydrogenation versus hydrodeoxygenation at 80 % conversion of substrate.

It is clear from Figure 247 that 2-methoxyphenol favours hydrogenation and HDO equally, with a similar mole fraction total recorded for both. The 3- and 4-methoxyphenol show a clear preference towards HDO, again in agreement with what was recorded for the dihydroxybenzenes where the resorcinol and hydroquinone favoured HDO significantly more than catechol. As with order in reactivity the cresols show different behaviour to that observed for the methoxyphenols and dihydroxybenzenes; the *ortho* isomer in that instance exhibited the greatest favourability towards HDO. This again strongly suggests a clear adsorption/orientation effect on the catalyst surface dependent on substituent position and nature.

The overall level of HDO showed a slight increase from that observed with the dihydroxybenzenes with a cumulative HDO mole fraction of 45 % recorded for 3-methoxyphenol against 40 % for resorcinol at 70 % conversion. It would seem the presence of the methoxy group in addition to the hydroxyl group may result in an increase in promotion of HDO. A study of phenol and anisole showed a similar 5 % increase in HDO activity when moving from the hydroxy to the methoxy group with overall totals of

20 % and 25 % recorded for cyclohexane and methoxycyclohexane respectively. It should be noted that at the same conversion only 13 % HDO product mole fraction was recorded for the comparable cresol isomer. This, however, may be unsurprising due to the decreased opportunity for bond cleavage to occur as a result of the presence of only a single oxygen containing substituent.

Further differences in the product distribution between the three isomers are exposed when looking at the individual mole fraction percentages as shown in Figure 250 below:

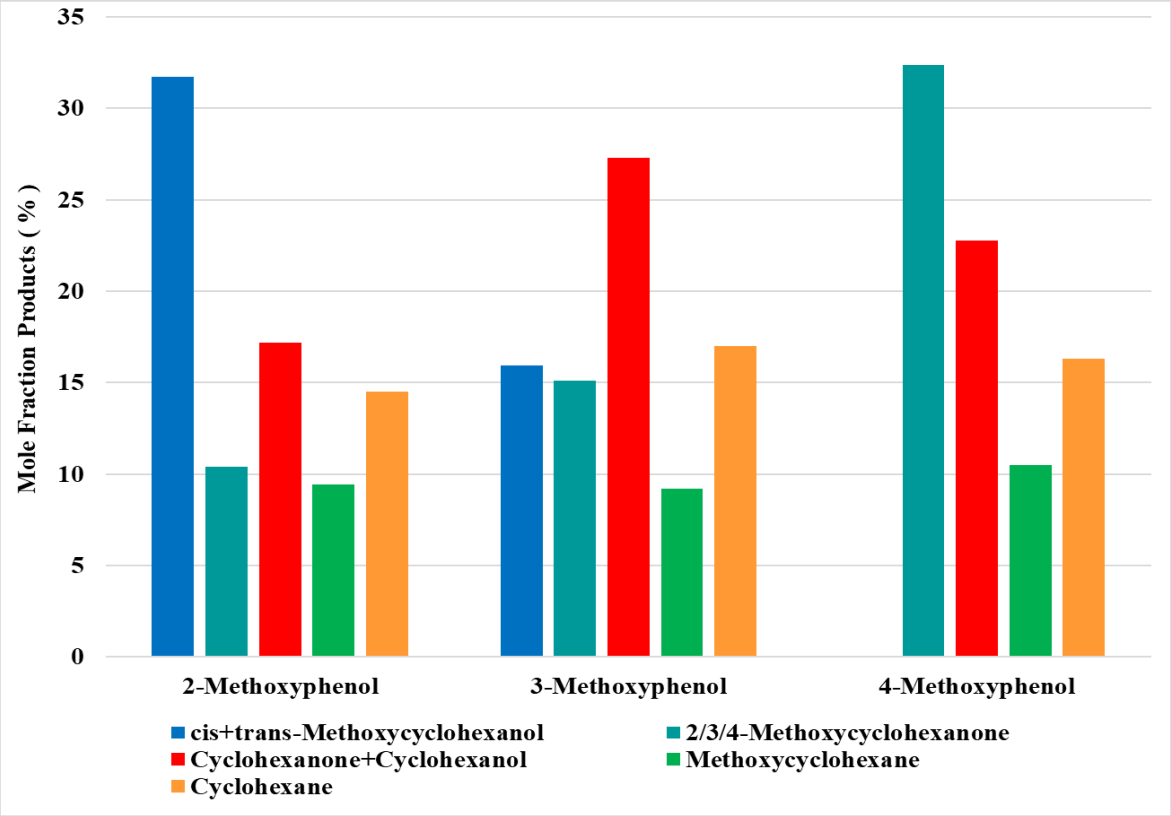

Figure 250. Product distribution for methoxyphenol isomers at ~ 80 % conversion.

It is apparent that the secondary hydrogenated products show the greatest disparity amongst the substrates. Most notable is the complete lack of any secondary hydrogenation from 4-methoxyphenol with only formation of the initial hydrogenated product, 4-methoxycyclohexanone, observed. Both 2- and 3-methoxyphenol underwent secondary hydrogenation with mole fraction percentages of 30 % and 15 % for their respective products. This failure of the *para* isomer to undergo secondary hydrogenation was not observed for either the dihydroxybenzenes or cresols. It was, however, reported from previous work on 4-methoxyphenol hydrogenation by Jackson *et al*. [100] The reason for this lack of subsequent hydrogenation is unclear; however, it cannot be related to substituent position as similar behaviour is not observed for hydroquinone and *para*-cresol and must be unique to the presence of the methoxy and hydroxyl group in the *para*

position. Could it be the relative bulkiness of the -OCH_3 group, specifically in the *para* position inhibits the ability of secondary hydrogenation to take place on the catalyst surface? One possible explanation may come from Jackson *et al*. [100] who postulated, in the previously mentioned study on 4-methoxyphenol hydrogenation, that the inability of 4-methoxycyclohexanone to undergo secondary hydrogenation was a result of its large cross-sectional area. Cleavage of the methoxy group, however, would allow for secondary hydrogenation of cyclohexanone to cyclohexanol to occur. Returning to Figure 248, examination of the individual mole fraction percentages of the HDO products show similar levels for both methoxycyclohexane and cyclohexane across all three isomers and suggests favourability towards their formation is independent of substituent position. This leads us on to the important area of how the formation of products occur during the hydrogenation of methoxyphenol.

For this purpose, we will focus on the product mole fraction graph, and that of each isomer is shown in Figures 251, 252 and 253:

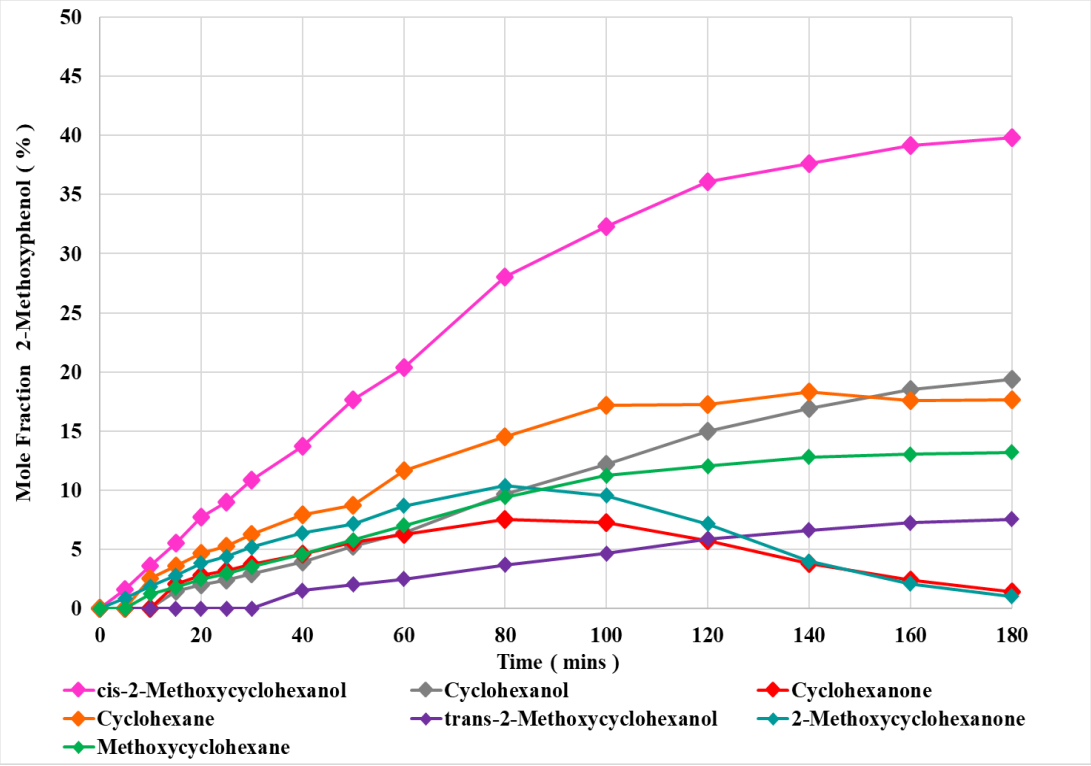

Figure 251. Product mole fraction graph of 2-methoxyphenol hydrogenation. Conditions, 323 K, 10 mmol, 3 barg.

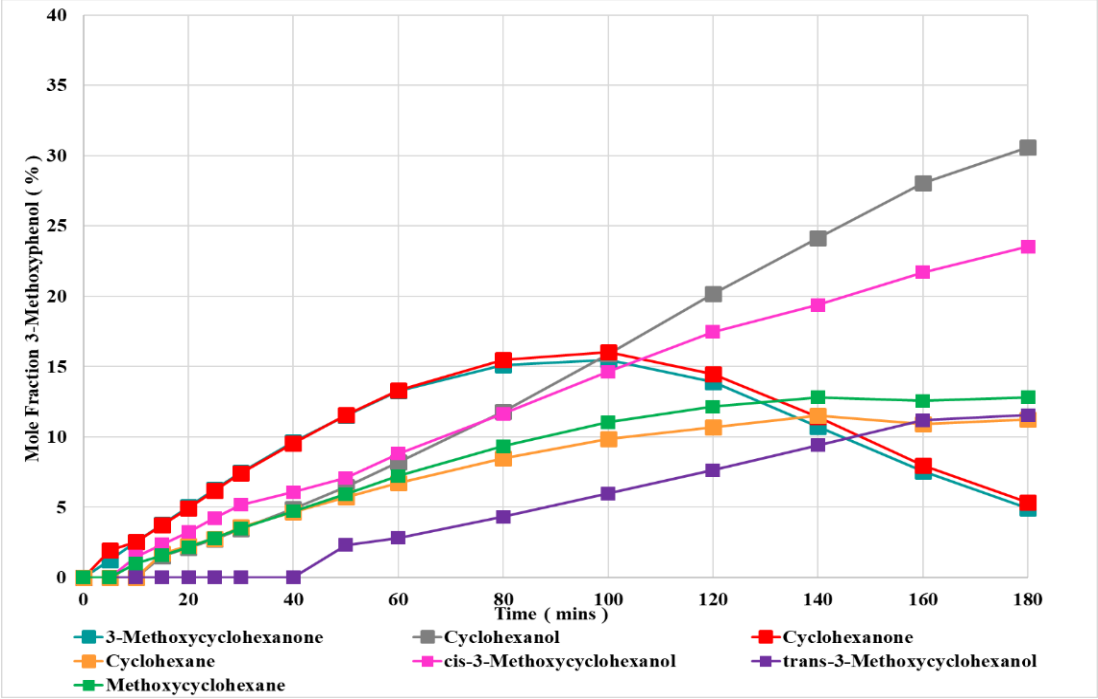

Figure 252. Product mole fraction graph of 3-methoxyphenol hydrogenation. Conditions, 323 K, 10 mmol, 3 barg.

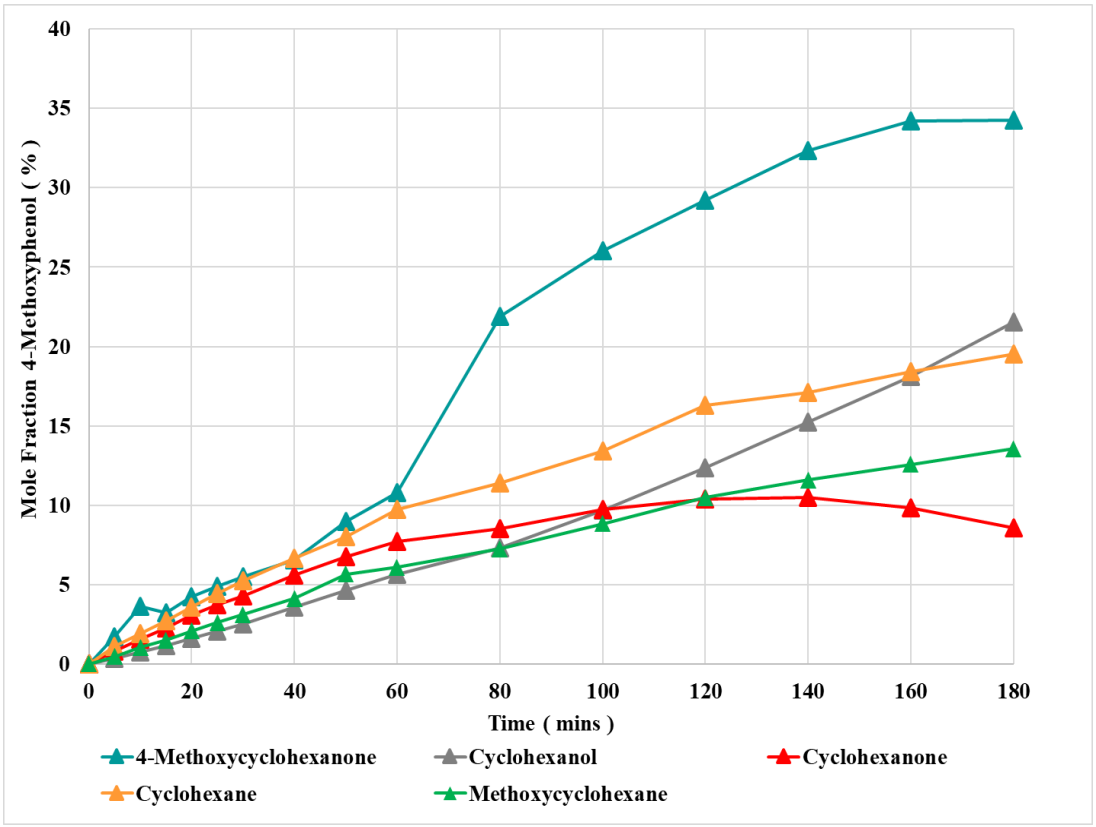

Figure 253. Product mole fraction graph of 4-methoxyphenol hydrogenation. Conditions, 323 K, 10 mmol, 3 barg.

It is evident from Figures 251 – 253 that a complex picture emerges when we look at product formation from the three substrates. Whilst certain similarities exist, many

important differences are evident. Most noteworthy of these is the significant delay in the formation of the majority of products from both 2- and 3-methoxyphenol, particularly pronounced with the *trans*-methoxycyclohexanol, with inhibition of 40 and 50 minutes respectively. This significant delay in the formation of multiple products is not evident for 4-methoxyphenol where all products are formed immediately, and neither was it present during dihydroxybenzene and cresol hydrogenation. The previously discussed differences in the ability of the isomers to undergo secondary hydrogenation may be the key to understanding why this effect is limited to 2- and 3-methoxyphenol. The formation of multiple products from both may cause a crowding effect on the catalyst surface whereby, as products are formed and undergo secondary hydrogenation, access to active sites becomes limited, and a resultant delay in product formation occurs. The presence of the initial hydrogenated product from both, 2/3-methoxycyclohexanone, from the outset of the reaction would add weight to this. The inability of the 4-methoxyphenol to undergo secondary hydrogenation and the resultant decrease in the number of products present in the system would lessen competition for active sites on the catalyst surface; hence no delay in product formation. A further similarity between 2- and 3-methoxyphenol is evident from the shared behaviour of their respective ketone products, 2/3-methoxycyclohexanone and cyclohexanone. An initial increase in formation followed by a clear decrease and concomitant increase in *cis*-2/3-methoxycyclohexanol and cyclohexanol, in conjunction with consumption of the aromatic, exists for both. This shared behaviour of the ketones independent of whether they have undergone sole hydrogenation, or hydrogenation and HDO shows the same adsorption and desorption process must be occurring on the catalyst surface. This implies that the presence of either a singly- or a doubly-substituted ketone does not affect this reaction.

Comparison of the relative mole fractions of cyclohexanone/cyclohexanol and methoxycyclohexane gives insight into the favourability towards either demethoxylation or dehydroxylation. Using 4-methoxyphenol to illustrate this, at 80 % conversion, the cumulative mole fraction of cyclohexanol and cyclohexanone was 23 % whilst it was 11 % for methoxycyclohexane, therefore, a 2:1 in favour of cleavage via demethoxylation. In our previous sections we proposed the formation of the HDO products occurred via highly reactive surface intermediates formed directly from the aromatic. To test if this theory is applicable to the methoxyphenol isomers, the hydrogenated product from 2-methoxyphenol, *cis*-2-methoxycyclohexanol, was added to the reactor and the result of this shown in Figure 254:

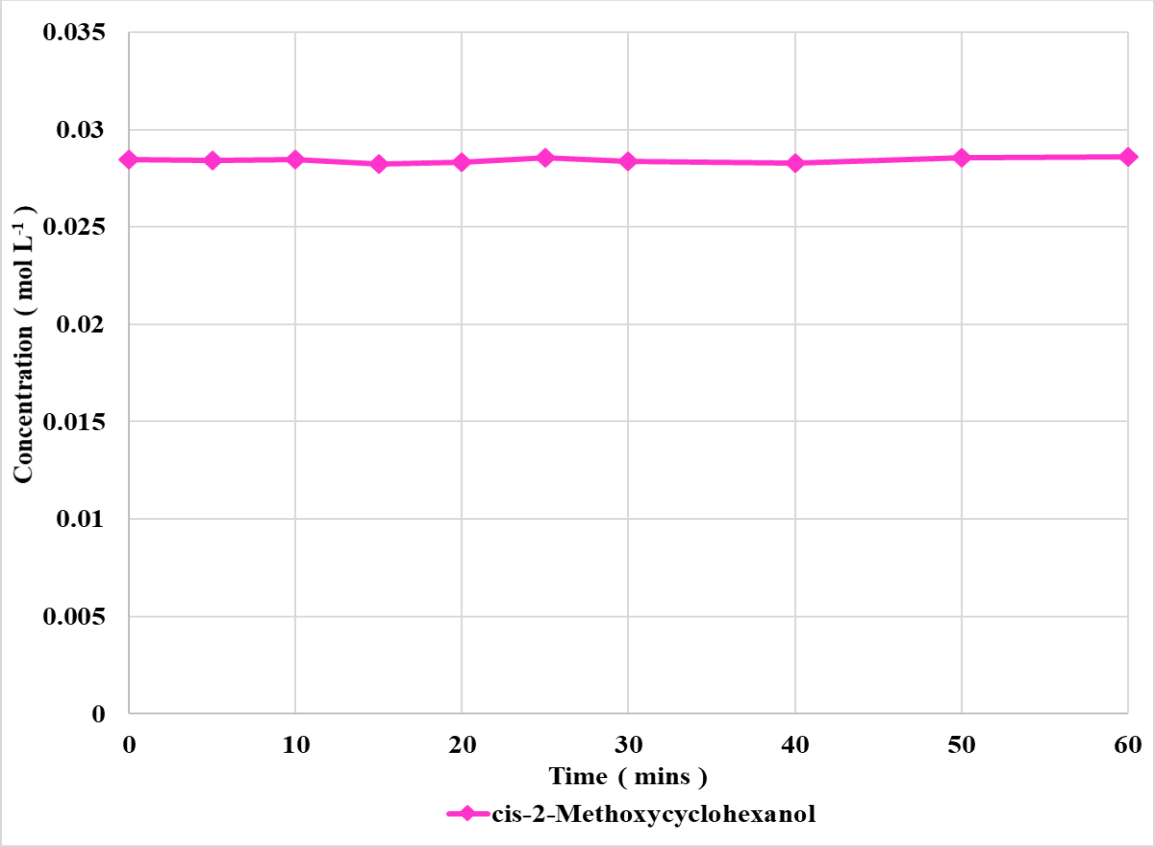

Figure 254. Reaction profile of cis-2-methoxycyclohexanol hydrogenation, 323 K, 3 barg H_2 and 0.1 g Rh/SiO_2.

The absence of any HDO products again indicates, that for HDO to occur the aromatic must be present and cannot take place via the hydrogenated products. The highly reactive intermediates via which we believe HDO occurs are only present when the aromatic is available. This has been shown previously with the dihydroxybenzenes and cresols where HDO formation ceased upon full consumption of the aromatic. Similar behaviour occurred with the methoxyphenols as evidenced for 2-methoxyphenol below:

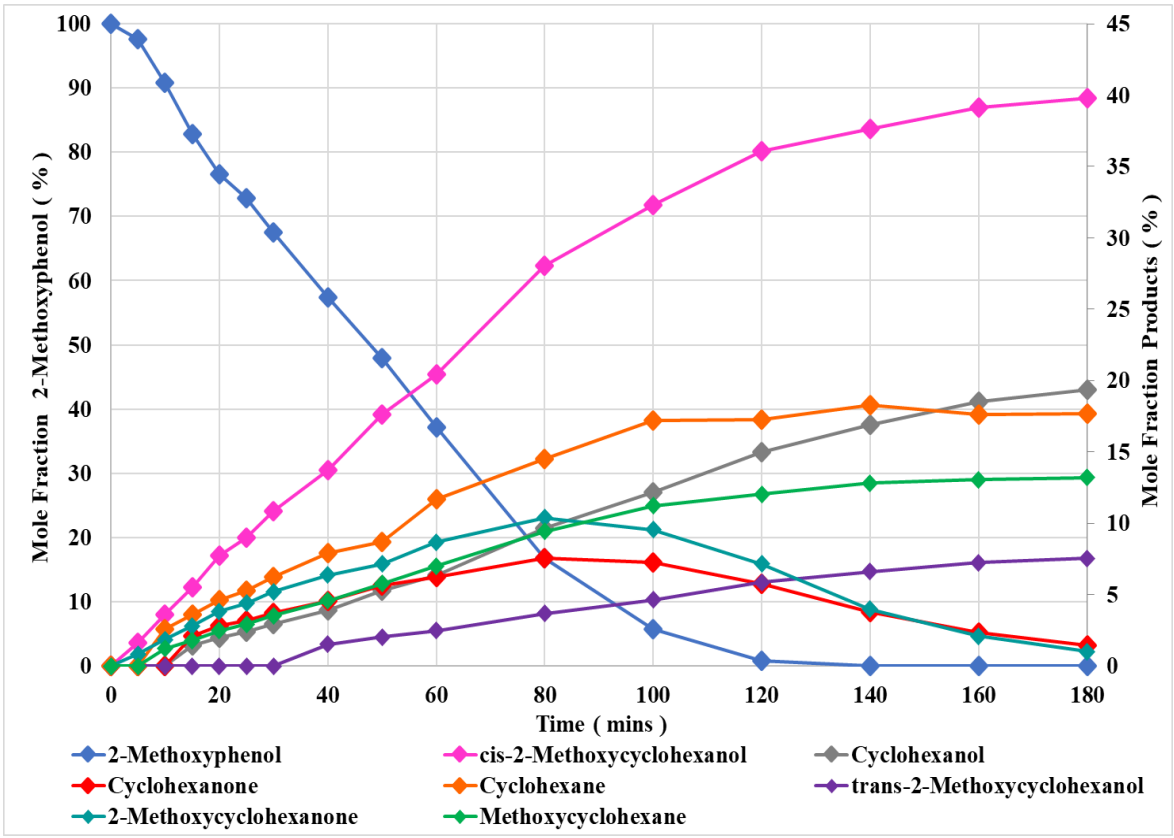

Figure 255. 2-Methoxyphenol hydrogenation, 323 K, 10 mmol.

The graph above shows this clear correlation between consumption of the aromatic and formation of the HDO products cyclohexane and methoxycyclohexane. It is clear that both products peak at around 140 minutes simultaneous to the aromatic being entirely used up and remain at a consistent level until end of reaction. This reiterates our belief that HDO product formation must occur directly from the aromatic substrate via highly reactive surface intermediates; a finding in contrast to much of the literature where it is reported that the hydrogenated products undergo hydrogenolysis to produce the deoxygenated products. The reaction scheme therefore proposed for the methoxyphenol isomers, using 4-methoxyphenol as an example, is shown in Figure 256:

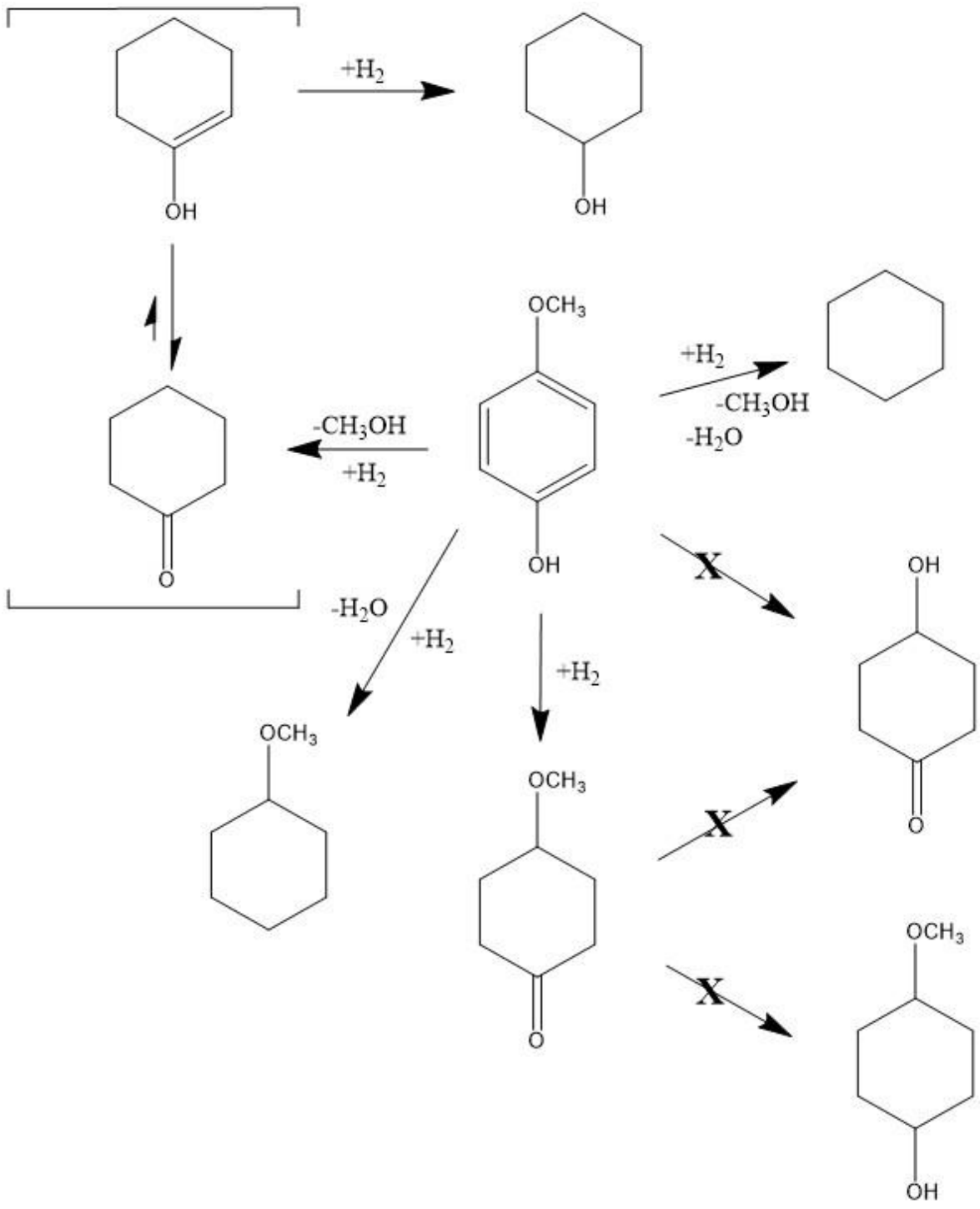

Figure 256. 4-Methoxyphenol Reaction Scheme.

8.3.2 Temperature Variations

As expected, all isomers of methoxyphenol showed an increase in rate with temperature, as summarised in Table 59 below:

Table 59. Rate constants of methoxyphenol isomers over temperature range.

Temperature (K)	**2-: k ($x10^{-3}min^{-1}$)**	**3-: k ($x10^{-3}min^{-1}$)**	**4-: k ($x10^{-3}min^{-1}$)**
303	8.5	9.1	6.0
313	11.4	11.1	6.6
333	25.7	37.1	15.2
343	42.7	45.2	24.2

The calculated rate constants above show a clear correlation on the effect of temperature on 2- and 3-methoxyphenol; both experience a near 5-fold increase in rate over the 40 K temperature range. Once again however, we see different behaviour from the 4-methoxyphenol with a less significant temperature effect present. The calculated activation energies followed the order: 3- > 4- > 2- methoxyphenol (41 > 38 > 35 $kJmol^{-1}$). It is of interest that despite 4-methoxyphenol exhibiting a moderately different effect with temperature, all three substrates give similar activation energies. The slightly lower figure expressed for 2-methoxyphenol is consistent with those of the comparable *ortho* isomers of the dihydroxybenzenes and cresols and may be a result of the previously hypothesized steric effect when adsorbed to the surface. Literature on the kinetic behaviour of these substrates is sparse, however, a study by Jackson *et al*. [100] found a similar activation energy for the 4-methoxyphenol.

A shift towards HDO was apparent for all three isomers as temperature was increased. This is outlined by the cumulative and individual mole fraction of the HDO and hydrogenated products for 3-methoxyphenol in Figures 257 and 258:

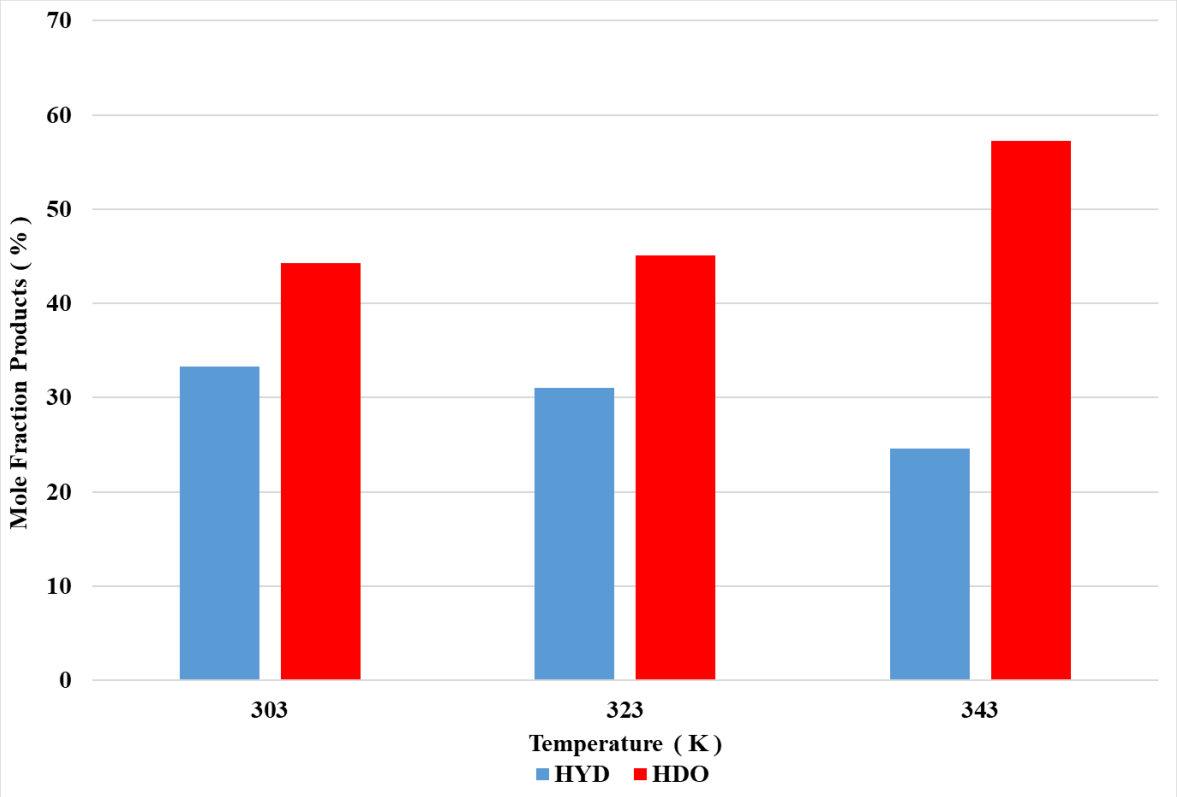

Figure 257. Comparison of hydrogenation and HDO at 80 % conversion of 3-methoxyphenol.

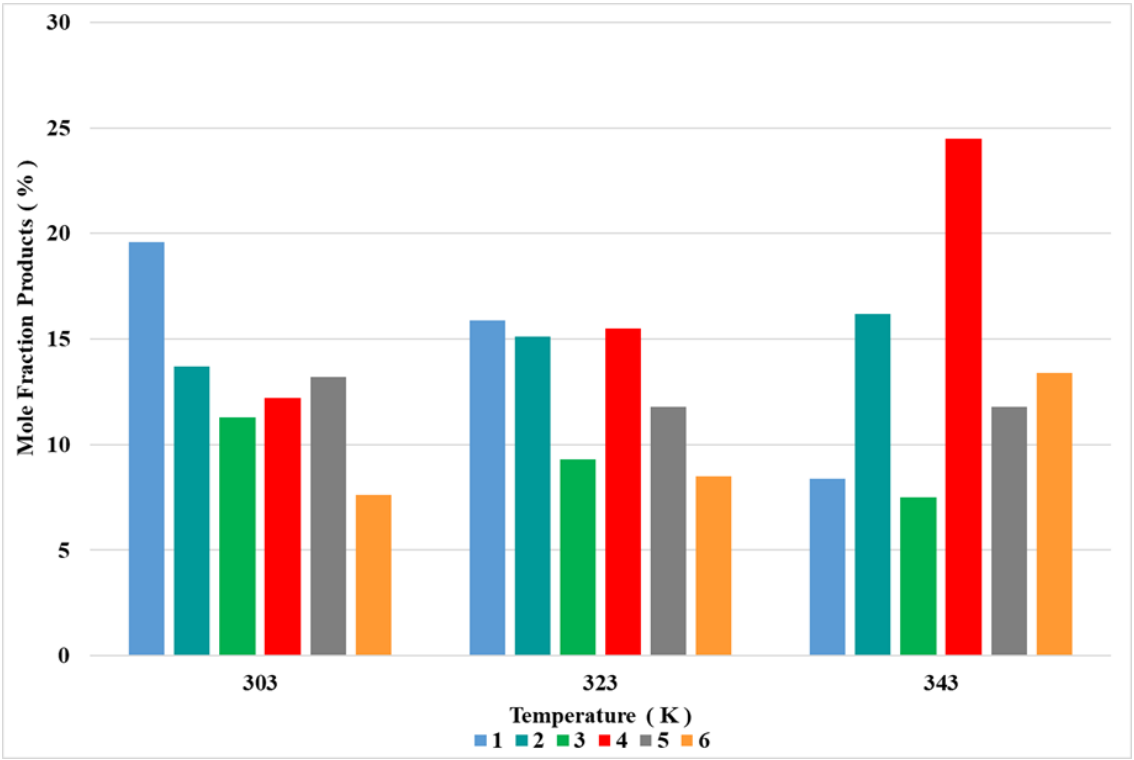

Figure 258. Mole fraction product distribution over temperature range for 3-methoxyphenol. 1=cis+trans-methoxycyclohexanol 2=methoxycyclohexanone 3=methoxycyclohexane 4=cyclohexanone 5=cyclohexanol 6=cyclohexane.

It is evident from Figure 257 that an overall increase in HDO and decrease in hydrogenation occurs with temperature an effect recorded previously with the dihydroxybenzenes. Again however, we see different behaviour with the cresols where HDO remained unaffected with temperature. From the individual product mole fractions in Figure 258 it is clear that, of the HDO products, cyclohexane and cyclohexanone, experienced the greatest effect from temperature; a near doubling in recorded mole fraction % for both. This correlates strongly with the dihydroxybenzenes where both these products showed a marked increase with temperature. The sole cresol HDO product, methylcyclohexane, remained constant over the temperature range measured. This is further evidence of the importance of substituent nature on HDO activity and indicates the replacement of an oxygen containing substituent with a methyl group negates any temperature effect on HDO.

Analysis of the *cis*:*trans* ratios taken for each substrate at the same conversion shows the effect on selectivity by temperature is limited to 2-methoxyphenol. Due to no formation of *cis*/*trans* hydrogenated products from 4-methoxyphenol, it is not included in the graph.

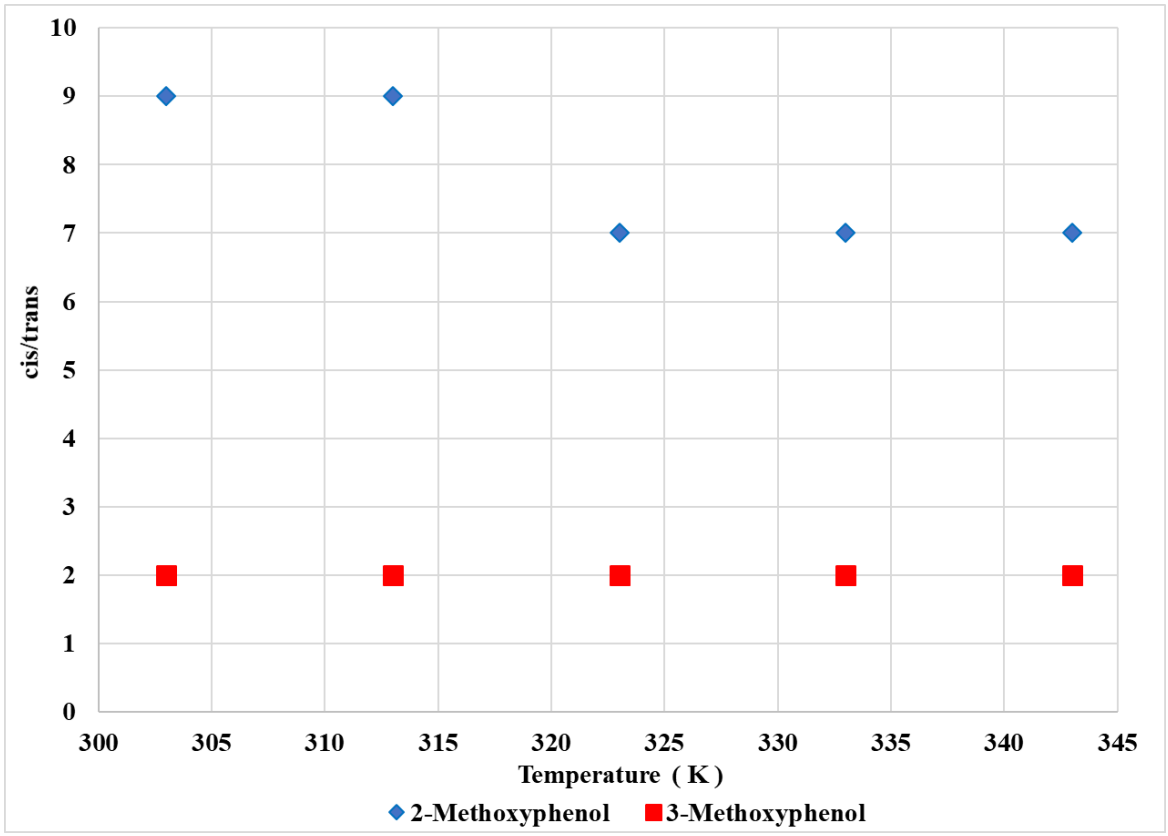

Figure 259. *cis*/*trans* Ratio of methoxyphenol isomers with temperature.

It can be seen from Figure 259 that the temperature effect on the *cis*/*trans* ratio of the 2-methoxyphenol is limited to the region between 313-323K where a decrease in *cis*/*trans*

ratio of 9:1 to 7:1 occurred; no further effect is present over the remainder of the measured temperature range. The absence of any temperature effect for the *cis*/*trans* ratio for 3-methoxyphenol is in keeping with what was found for all isomers of cresol and dihydroxybenzene. The reason for this unique behaviour of the 2-methoxyphenol is at this stage unclear; however, it may be a result of steric hindrance, whereby the bulky -OCH_3 group's close proximity to the -OH group makes formation of the *trans* isomer at elevated temperatures relatively more favourable than with the less sterically hindered 3-methoxyphenol. However, with this said, thermodynamically the *cis* isomer is more stable for the 3-methoxyphenol whilst for both the 2 and 4-methoxyphenol it is the *trans* isomer that is the more thermodynamically stable product making it all the more surprising we see this relationship.

8.3.3 Concentration Variations

All methoxyphenol substrates gave a positive order with concentration. Both 2- and 4-methoxyphenol gave a calculated order in substrate of 0.3 with 3-methoxyphenol recording a higher value of 0.8. Comparison with the dihydroxybenzene isomers show the *meta* and *para* isomers share an order of 0.5, with the *ortho* isomer behaving independently to give a negative order. The isomers of cresols showed a concentration effect slightly more akin to that of the methoxyphenol with the *ortho* and *para* isomers sharing a similar order; however, the *meta* isomer was significantly different in this instance and exhibited a clear negative order. These results taken together strongly suggest that substituent position on the strength of adsorption is limited, and instead order of substrate is dependent on the nature of the substituents attached on the aromatic ring.

Our previous work with the dihydroxybenzenes suggested a possible link between strength of adsorption and HDO activity. Our study into the effect of concentration with the cresol isomers, however, cast some doubt on this theory. Added together to what we now know from this work on the methoxyphenols, where 3- and 4-methoxyphenol undergo the most HDO, yet have different orders in substrate, we can now say that a direct link is unlikely to exist.

The product distribution was found to be independent of concentration for both 2- and 4-methoxyphenol in line with our findings for all isomers of dihydroxybenzene. However, 3-methoxyphenol exhibited different behaviour with a decrease in formation of *cis*+*trans*-3-methoxycyclohexanol and an increase in 3-methoxycyclohexanone with an increase in concentration; a similar relationship was found for the alcohol and HDO products, cyclohexanol and cyclohexanone. The unique behaviour of 3-methoxyphenol is analogous

to the comparative cresol isomer, *meta*-Cresol, where in that instance it was the sole isomer to show an effect on product distribution with an increase in concentration. This effect in concentration, limited to the product distribution of the *meta* isomers for both cresol and methoxyphenol, may be in some way related to their different orders in substrate when compared to the shared orders of their respective *ortho* and *para* isomers.

8.3.4 Competitive Substrate Hydrogenation

When substrates were reacted in a competitive environment significantly different behaviour from that observed with the individual hydrogenation reactions occurred as shown in Table 60:

Table 60. Competitive hydrogenation at 323 K, 3 barg and 10 mmol.

Reactant	First order rate constant, k (min^{-1}, $x10^{-3}$)				
	Single	2-/3-	2-/4-	3-/4-	2-/3-/4-
2-Methoxyphenol	11.5	10.6	3.8	-	6.6
3-Methoxyphenol	12.8	12.0	-	5.8	5.9
4-Methoxyphenol	7.4	-	4.7	4.7	6.4

This is in keeping with the marked changes we observed in behaviour between the individual and competitive environment for both cresols and dihydroxybenzenes. Again, as with those previous studies, we observed a decrease in rate for all substrate combination reactions. No clear trend emerges when we compare order of activity of the individual and competitive reactions. It can be seen that when reacted together, both 2- and 3-methoxyphenol show little change in reactivity from their individual reactions. However, when reacted individually with 4-methoxyphenol both registered a significant decrease in the calculated rate constants, clearly suggesting that the 4-methoxyphenol is having the greatest influence in the competitive environment. The existence of a strong competing effect between the 3- and 4-methoxyphenol isomers may not be particularly surprising with both having non-adjacent substituents and their product distributions showing a favouritism towards HDO. However, the fact that a similar suppression of 2-methoxyphenol when paired with 4-methoxyphenol exists suggests neither of these factors can be used to predict the outcome of these competitive reactions. When we look at the reaction combining all three isomers, we see that this significantly stronger influence from the 4-methoxyphenol no longer applies; all three register similar levels of reactivity. Whilst it could be said that the *ortho* isomer exhibits a slightly higher reactivity, which does correlate with previous all three substrate competitive reactions for the dihydroxybenzenes

and cresol isomers, the difference between all three isomers is negligible. Our previously stated view was, the position of substituents and the orientation to the catalyst surface rather than the nature of the substituent itself is key when determining reactivity during the competitive environment. These methoxyphenol results however do not lend any support to this view. A more appropriate postulation from the available evidence for this set of substrates is, increased competition for surface hydrogen when multiple substrates are present resulting in the decrease in reactivity observed in the competitive environment.

Previously, in our dihydroxybenzene study, we postulated the planar mode during individual hydrogenation could switch to a non-planar mode in the competitive environment, resulting in decreased activity. However, if all isomers changed adsorption mode under competitive conditions a greater decrease in activity during the 2- and 3-methoxyphenol combination would have been expected. Is it, that the 4-methoxyphenol inhibits the 2- and 3-methoxyphenol in a way that causes their adsorption mode to change and explains why suppression in activity occurs only in its presence?

When we come to look at product formation from the 3-substrate combination, we see a change in the hydrogenated products of all isomers, most marked with 3- and 4-methoxyphenol. HDO is unaffected. This is outlined in Figures 260 and 261:

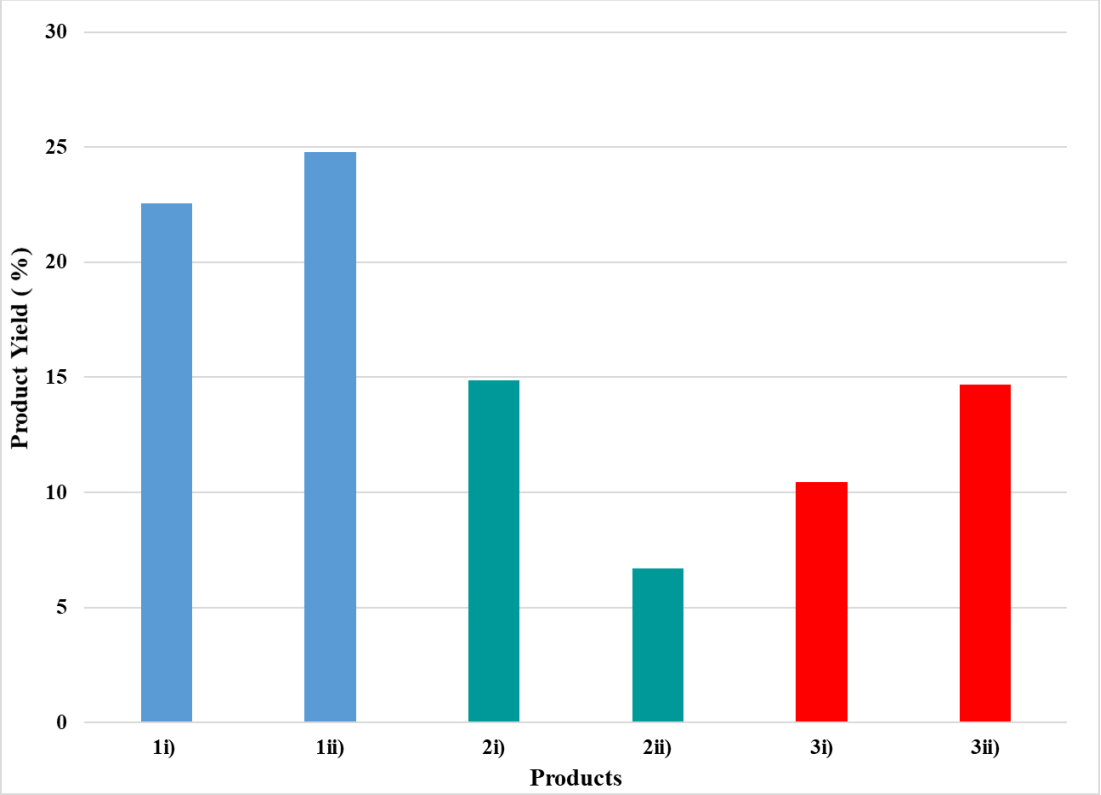

Figure 260. Comparison of product yield for individual and competitive hydrogenation of 2-, 3- and 4-methoxyphenol. Data taken at ~ 40 % conversion of all.

1 i) Individual 2-methoxyphenol ii) Competitive 2-methoxyphenol

2 i) Individual 3-methoxyphenol ii) Competitive 3-methoxyphenol

3 i) Individual 4-methoxyphenol ii) Competitive 4-methoxyphenol

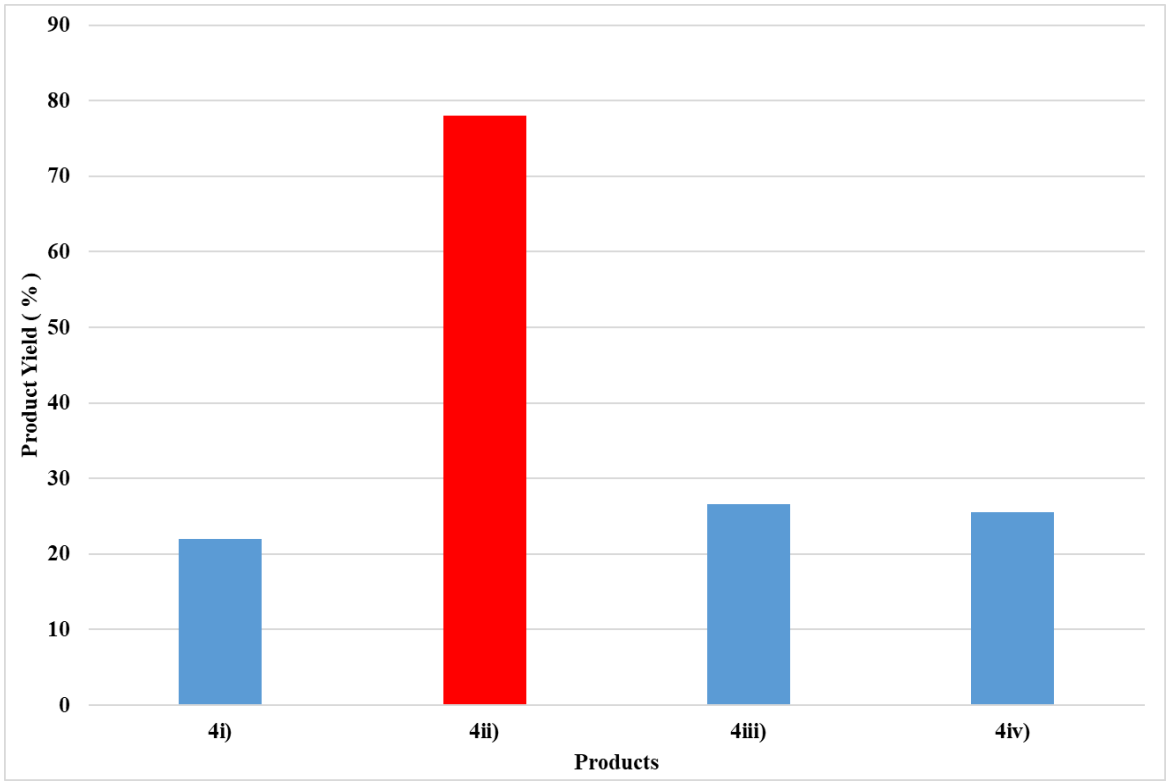

Figure 261. Comparison of product yield for the cumulative HDO products for individual and competitive hydrogenation of 2-, 3- and 4-methoxyphenol. Data taken at ~ 40 % conversion of all.

4 i) Individual 2-methoxyphenol ii) Competitive 2-, 3- and 4-methoxyphenol iii) Individual 3-methoxyphenol iv) Individual 4-methoxyphenol

From the Figures above it is clear that formation of hydrogenated products from both 3- and 4-methoxyphenol undergo significant change in the competitive environment with a clear decrease in those from 3-methoxyphenol and a marked increase in those from 4-methoxyphenol evident. A less pronounced increase was apparent for the hydrogenated products from 2-methoxyphenol. The reduction in hydrogenated products from 3-methoxyphenol was also registered during the competitive reaction of 2- and 3-methoxyphenol together. Although this pair combination exhibited the least suppression in reactivity, this effect on product distribution suggests some form of competition for active sites on the catalyst surface must be occurring. Regarding the increase in formation of the 4-methoxyphenol hydrogenated products, when reacted in the pair combinations this effect was not present and why the addition of the third substrate results in this, is unclear. The lack of effect on the formation of the HDO products in the competitive environment adds further weight to our belief that two independent pathways exist for hydrogenation and HDO.

As previously stated, a similar reactivity for all three isomers exists when reacted together. This lack of dominance of a single isomer throughout the competitive environment is out of sync with what was observed for both the cresols and dihydroxybenzenes; the *ortho* isomer in both these instances had a higher reactivity in all competitive situations. It is clear, that the significant similarities in behaviour shared between the dihydroxybenzenes and methoxyphenols in the individual environment do not extend to competitive situations.

Once again, these competitive reactions highlight the significant changes in substrate behaviour that can occur when even a single other similar substrate is present. The addition of a third exacerbates this further and hints strongly that availability of surface hydrogen becomes a major issue as substrate numbers increase. This brings significant implications for research involving the use of a single model compound as an exemplar of a mixed reaction feed.

8.3.5 Deuteration Reactions

The effect of replacing hydrogen with deuterium was examined for the methoxyphenol isomers. A summary of each KIE calculated is shown in Table 61 below:

Table 61. Substrate KIE values.

Substrate	KIE
2-Methoxyphenol	0.7
3-Methoxyphenol	0.7
4-Methoxyphenol	0.7

Looking at the values for each, it is apparent that all isomers exhibited a faster rate of reaction in the presence of deuterium, as reflected in their inverse KIE values; the only occasion in our study where the *para* isomer has witnessed an inverse effect. It is significant that, similar to the shared positive KIE value amongst the cresol isomers, all three isomers of methoxyphenol share an inverse KIE value which may indicate a shared RDS in their respective mechanisms of hydrogenation. The dihydroxybenzenes, however, must have a different RDS for the *ortho* and *meta* isomer from that of the *para* isomer, due to the differing KIE values across the isomers. It is of note that the value calculated for the methoxyphenol isomers is a similar value calculated for catechol. Does this suggest the rate determining step of methoxyphenol hydrogenation, independent of substituent position, is the same as that of the *ortho* isomer from the dihydroxybenzenes? However, with that said, these results overall indicate no comparable behaviour between the different

sets of substrates studied in relation to KIE values and instead point towards the nature of the substituent, rather than position on the aromatic ring, being fundamental in determining the effect of deuterium outcome.

Comparison with the overall calculated KIE value with that documented by Jackson *et al*. for 4-methoxyphenol shows agreement, whilst those of anisole and phenol were found to be 1.3 and 1.6 respectively, indicating independent behaviour from that of all methoxyphenol isomers. We previously postulated that the inverse KIE value for catechol and resorcinol may be result of the change in hybridisation that occurs from sp^2 to sp^3 during aromatic hydrogenation; an explanation that we propose may apply to the methoxyphenol isomers registering an overall inverse KIE value.

To gain more information on the reaction mechanism in the presence of deuterium, the KIE value for each product was calculated and is shown below in Table 62 for 2-methoxyphenol:

Table 62. 2-Methoxyphenol hydrogenated products KIE values.

Product	KIE
cis-2-Methoxycyclohexanol	0.7
trans-2-Methoxycyclohexanol	0.9
2-Methoxycyclohexanone	1.2
Cyclohexanol	0.9
Cyclohexanone	1.1
Methoxycyclohexane	0.9
Cyclohexane	1.2

The inverse KIE value expressed for both secondary hydrogenated products, *cis* and *trans*-2-methoxycyclohexanol is in agreement with the inverse KIE values calculated for the secondary hydrogenated products from catechol. The initial hydrogenated product, 2-methoxycyclohexanone, however, registered a positive KIE value, in contrast to the respective initial hydrogenated product from catechol which exhibited an inverse effect in deuterium. It can be stated that, although 2-methoxyphenol and catechol shared the same overall inverse KIE value the underlying rate determining step for formation of their initial hydrogenated product must be different and therefore fundamental to the nature of substituents present.

The product KIE values from 3-methoxyphenol were also calculated and shown in Table 63:

Table 63. 3-methoxyphenol hydrogenation products KIE values.

Product	KIE
cis-3-Methoxycyclohexanol	0.7
trans-3-Methoxycyclohexanol	0.8
3-Methoxycyclohexanone	1.1
Cyclohexanol	0.8
Cyclohexanone	1.1
Methoxycyclohexane	0.8
Cyclohexane	0.7

It can be seen a clear similarity in KIE effect was observed for the hydrogenated products of 3-methoxyphenol, with that of 2-methoxyphenol, with both secondary hydrogenated products registering an inverse effect and the initial hydrogenated products a positive effect. This suggests a similar hydrogenation route exists between 2- and 3-methoxyphenol. This similarity was continued with the HDO products, with the exception found with cyclohexane, where the positive effect found with 2-methoxyphenol was found to have an inverse effect with 3-methoxyphenol. This shows the rate determining step involved in the formation of cyclohexane must be different for 2- and 3-methoxyphenol, whilst the formation towards all other products must be similar. The difference found only with cyclohexane may be due to the steric hindrance related to the 2-methoxyphenol, where the bulky -OCH_3 group is in close proximity to the -OH group, may have an impact on the cleavage of both these groups not applicable when the isomer has the two substituents in the *meta* position.

The product KIE values were calculated for 4-methoxyphenol and shown in Table 64.

Table 64. 4-methoxyphenol hydrogenation products KIE values.

Product	KIE
4-Methoxycyclohexanone	0.8
Cyclohexanol	0.9
Cyclohexanone	0.9
Methoxycyclohexane	0.9
Cyclohexane	1.0

The initial hydrogenated product from 4-methoxyphenol, 4-methoxycyclohexanone, gives an inverse KIE, in contrast to the positive KIE observed for the comparable products from 2- and 3-methoxyphenol. It does however, agree with the initial hydrogenated products of the dihydroxybenzenes, where 2/3/4-hydroxycyclohexanone, gave the same KIE value and as such, our previous postulation, that this inverse value was a result of the change in hybridisation when the aromatic undergoes hydrogenation, could be applied to the 4-methoxycyclohexanone. These differences in KIE values of the initial hydrogenated products from 4-methoxyphenol to those of 2- and 3-methoxyphenol, shows further evidence of the unique behaviour of 4-methoxyphenol. This individualism may be a consequence of its inability to undergo subsequent hydrogenation to form the secondary hydrogenated products. Of the other products, cyclohexanol and methoxycyclohexane were in agreement with those found for 2- and 3-methoxyphenol, whilst the inverse KIE value for cyclohexanone was in disagreement. Uniquely, the HDO product, cyclohexane, showed no effect in the presence of deuterium.

When we look in greater detail at the KIE values calculated by Jackson *et al*. [100] for the 4-methoxyphenol products we find a reported inverse KIE value for the initial hydrogenated product, 4-methoxycyclohexanone, in agreement with ours. Comparison of the KIE values for the initial hydrogenated products from anisole and phenol show a positive KIE value for both, in accordance with our findings for 2- and 3-methoxyphenol. This correlation in KIE effect indicates similar behaviour, and further highlights the distinct behaviour of the 4-methoxyphenol. The suggestion must be that 4-methoxyphenol has a unique rate determining step.

These deuterium experiments have provided us with further insight into the reaction mechanism and highlighted otherwise unknown key differences between the isomers. We already knew the secondary hydrogenation step was completely inhibited for 4-methoxyphenol, with no formation of the *cis*/*trans*-4-methoxycyclohexanol observed. We

now know that formation of the initial hydrogenated product of 4-methoxyphenol also occurs in a different manner to that of 2- and 3-methoxyphenol. This may be a key piece of information in our understanding of why secondary hydrogenation does not take place for the 4-methoxyphenol.

8.3.6 Post Reaction Catalyst Characterization

Thermal analysis of the post reaction catalysts from each isomer found the greatest amount of carbon laydown associated with 3-methoxyphenol. On the surface this would tie in with the high level of HDO observed for this isomer; however, the 4-methoxyphenol, which undergoes similar levels of HDO, recorded the lowest weight loss associated with carbon laydown and as such a direct correlation between HDO and carbon laydown cannot be made. Perhaps unsurprising, in light of previous commonalties, this relationship was also absent in our work on dihydroxybenzenes; however, the cresols showed evidence of a link between isomer HDO and quantity of carbon present on the catalyst.

A comparison of the percentage carbon deposition for each isomer of methoxyphenol, dihydroxybenzene and cresol is shown below in Table 65:

Table 65. Weight loss percentages associated with evolution of m/z 44.

	Methoxyphenols	Dihydroxybenzenes	Cresols
ortho-	5 %	4 %	3.5 %
meta-	6 %	3.5 %	3 %
para-	3 %	3.5 %	3 %

From Table 65 it can be seen that, with the exception of the 4-methoxyphenol, the methoxyphenols have significantly higher levels of weight loss associated with carbon deposition than their comparable cresol and dihydroxybenzene isomers. Previously, when comparing dihydroxybenzenes and cresols we postulated that the presence of greater amounts of oxygen on the aromatic substrate was the reason behind the higher carbon percentage observed for dihydroxybenzenes. This is evidenced further by the methoxyphenols, where two oxygen and a methyl group are present, registering even greater levels of carbon associated weight loss. Again, we see this disparity in the behaviour of 4-methoxyphenol with its significantly lower levels of carbon laydown. In this instance this is unsurprising, the reduction in the number of products formed as a

consequence of the lack of secondary hydrogenation would result in less opportunity for the formation of carbon on the catalyst surface.

Analysis in greater detail of the TPO data show one distinct weight loss event below 473 K common to all three isomers. No concomitant evolution of carbon dioxide is detected suggesting this weight loss event may be due to the release of adsorbed solvent from the catalyst surface. Three further high temperature weight loss events (>473 K) associated with the evolution of carbon dioxide, indicating the combustion of surface carbon species, are present in all three substrates. Of these, the lower temperature peak < 500 K is a result of combustion of a single aromatic unit, similar in structure to the methoxyphenol substrate, trapped in the pores of the catalyst. The temperature of evolution is in accordance with the boiling points of the methoxyphenol substrates. TPO analysis of the post reaction dihydroxybenzene and cresol catalysts showed a shared temperature event in the same region; identified as the aromatic substrate through Soxhlet extraction. A second common temperature peak at > 500 K is a result of the aromatic species moving towards a carbon species graphitic in nature. The highest of the shared evolution events at 700 K indicates combustion of fully graphitic carbon species from polynuclear aromatic residues on the catalyst surface. The three substrates share commonalties as to the carbon species present, however again the 4-methoxyphenol shows a unique aspect. This higher temperature weight loss event > 800 K may be indicative of the presence of a distinct carbon species resulting from the higher levels of HDO occurring during the 4-methoxyphenol hydrogenation reaction. This unique weight loss event is similar to that observed with the *para* isomer of the cresols where it was postulated that it occurred as a consequence of the combustion of a single specific carbon species, polynuclear in nature, and more readily formed due to the symmetrical arrangement of the *para* isomer.

As with the dihydroxybenzenes and cresols, we see significant carbon laydown on our catalyst under mild conditions. Although this may seem unusual, it must be remembered that high levels of HDO in addition to standard hydrogenation are occurring and it is no surprise that the methoxyphenols showed both the highest levels of HDO and the greatest amount of carbon laydown of all substrates tested. Catalyst deactivation is a known problem with catalytic HDO, and it is of concern that despite operating at a temperature well below the standard conditions of >473 K it is still having a clear impact on our catalyst for all sets of substrates.

8.4 Combination of isomers

The reaction of the three *ortho* isomer substrates in the competitive environment, resulted in a decrease in reactivity similar to that recorded for the three-isomer combination in each set of substrates. The order of reactivity of 2-methoxyphenol ~ *ortho*-cresol > catechol observed during individual hydrogenation shifted to a shared rate of reactivity for all three *ortho* isomers when reacted together. This strongly suggests that no preference exists amongst the *ortho* isomers in this competitive situation. We know the nature and position of substituent has a significant effect on the hydrogenation activity in the individual environment, hence the higher reactivity of the *ortho* isomers of methoxyphenol and cresol than that of dihydroxybenzene. The removal of any variance in position of substituent indicates, that the uniform suppression in rate observed is a result of a separate factor, most probably increased competition for surface hydrogen on the catalyst surface. The product distributions were unaffected, it is clearly an effect on reactivity only.

Similar behaviour is observed when we look at the combination of the *meta* isomers, in this instance, however, although all three substrates give a comparable reactivity, *meta*-cresol does exhibit a slightly faster rate. Analysis of the *para* isomers showed near identical calculated rate constants for all three. As previously stated, each group of substrates showed marked differences in reactivity during their individual hydrogenation. This pattern of shared levels of reactivity within each isomer combination confirms our previous assertion that nature of substituent and ring position plays no role on reactivity in the competitive environment. An increased demand for limited surface hydrogen as organic substrate increases must be the only factor at play here; whether different substrates, or different isomers of the same substrate are combined, we see rates of reactivity suppressed to similar levels.

The effect of substituent position and nature on reactivity during individual hydrogenation should not be understated, however, we see again from these experiments that when we move to the competitive environment information garnered from individual reactions offers minimal assistance on what will occur. This has been a consistent factor throughout this study and strongly underlines our belief that the value of studying a single substrate to understand a true bio-oil feed is extremely limited.

9 Conclusions

The previously stated main objective of this thesis was to gain an understanding of the hydrogenation of oxygen-substituted aromatics, more specifically, the effect the nature and position of substituent has on reactivity and product distribution, with a view to discovering what favours HDO. Through carrying out multiple single compound and competitive reactions, we have gained significant insight into the complex behaviour that exists during the hydrogenation of these molecules and identified several factors that determine HDO favourability.

The individual hydrogenation of the dihydroxybenzene isomers gave an order in reactivity of: *meta* > *ortho* > *para*. The higher reactivity of the *meta* isomer is postulated to be a result of the reinforcing effect of two substituents, with electron donating properties, in the *meta* position to one another. Apart from *trans*-cyclohexanediol, all hydrogenated and HDO products formed from the outset of reaction suggesting a direct and independent route of product formation. The hydrogenated product, *cis*-cyclohexanediol, was found to be stable under standard reaction conditions, with no HDO products formed and no isomerization observed. This confirmed HDO does not take place on our catalyst without the presence of the aromatic substrate; further evidenced by the cessation in cyclohexane formation following the consumption of the aromatic under standard hydrogenation. Hydrogenation of the *cis*-cyclohexanediol gave clear insight into the previously undetermined route of *trans* isomer formation. No *trans*-cyclohexanediol was formed throughout this reaction, and as such, it was shown that the previously postulated route of formation, via desorption and readsorption of the *cis* isomer, does not exist for this system. Instead, it is proposed that the two isomers are formed independently- the *cis* isomer via both the ketone (hydroxycyclohexanone) and enol intermediates (highly reactive, unobserved), and the *trans* isomer via only the ketone intermediate as illustrated in Figure 262:

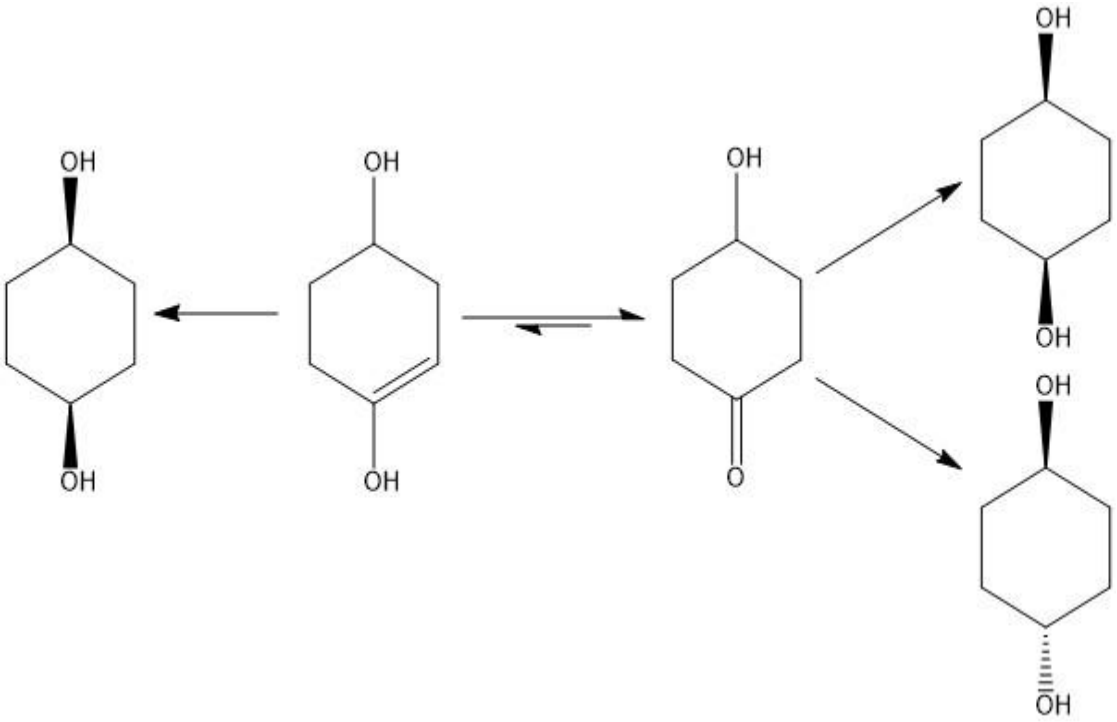

Figure 262. Formation of the *cis* and *trans* isomers.

Formation of the *trans* isomer - via initial formation of hydroxycyclohexanone followed by readsorption to the catalyst surface and subsequent desorption of the hydrogenated product– as outlined in this hypothesis, explains the delay observed solely for the *trans* isomer.

We have suggested that formation of the HDO products from the aromatic occur via highly reactive surface intermediates, with the position of substituent playing a major role in determining the favourability of an isomer towards HDO. The highest levels of HDO occurred with resorcinol and hydroquinone; a result of the greater number of HDO facilitating intermediates, containing a double-bond β-γ to a hydroxyl group, when the two hydroxyl groups are in the *meta* and *para* position. We postulate that mode of adsorption plays no role in dihydroxybenzene HDO favourability as when bonded through the two hydroxyl groups all isomers would adopt a planar mode of adsorption. Although HDO and hydrogenation are competing reaction pathways, temperature variation showed a commonality in behaviour of the products of both; the initial hydrogenated/HDO product (hydroxycyclohexanone/cyclohexanone) both increased with a concomitant decrease in the secondary hydrogenated/HDO products (*cis*/*trans*-cyclohexanediol/cyclohexanol) observed.

Competitive hydrogenation reactions for the dihydroxybenzene isomers resulted in a significant decrease in reactivity across all isomers and a shift in overall order in reactivity

to: *ortho* > *para* > *meta*. This decrease in reactivity is believed to be a result of competition for active sites on the catalyst surface. Catechol showed dominance in the competitive environment, concluded to be a consequence of its strength of adsorption which is reflected in its negative order in substrate for the reaction. From H/D exchange reactions, significantly different product KIE values were calculated for hydroquinone than for both resorcinol and catechol, indicating the existence of a different mode of adsorption for hydroquinone. Competitive H/D reactions recorded different product KIE values than those calculated under individual conditions, inferring that, in addition to the significant reduction in reactivity, changes in the mechanisms of product formation must occur in the competitive environment.

From TPO analysis of extended run spent catalysts we conclude no correlation exists between catalyst deactivation and the quantity of carbon laydown; hydroquinone exhibited the largest decrease in reactivity; however, the post reaction catalyst showed the lowest level of carbon laydown. TPO analysis highlighted the presence of phenolic carbon on the resorcinol and hydroquinone spent catalysts, this was absent from the catechol catalyst and is believed to be a result of their greater HDO activity.

The cresol isomers showed an order in isomer reactivity of: *para*- > *meta*- > *ortho*-cresol with the lower reactivity of the *ortho* isomer believed to be a result of steric hinderance between the methyl and hydroxyl group. Overall cresol reactivity was significantly higher than that of the dihydroxybenzenes as a result of the different mode of adsorption when only one substituent interacts directly with the catalyst surface, allowing for a faster adsorption/desorption process. Between cresol isomers, the *ortho* isomer showed the highest favourability towards HDO. H/D exchange reactions confirmed proton exchange with the methyl group occurred only when in the *ortho* position. The conclusion from this evidence of direct interaction between the methyl group and the catalyst surface must be that *ortho*-cresol adsorbs in a planar manner. The lack of exchange of the methyl groups in the *meta* and *para* isomers indicate an inclined mode of adsorption with the methyl groups pointing away from the surface.

The hydrogenated product (*cis*/*trans*-2-methylcyclohexanol) showed no HDO activity and no isomerization, and as with the dihydroxybenzenes, an independent and direct route from the aromatic species is proposed for product formation during cresol hydrogenation and HDO. In this instance, no link between strength of adsorption and HDO activity exists: *ortho*- and *para*-cresol both gave a positive order, however, *ortho*-cresol showed higher favourability towards HDO. A significant reduction in reactivity was again observed in the

competitive environment and a shift in reactivity to: *ortho* > *para* > *meta* recorded. This was the same order found for the dihydroxybenzene isomers during competitive hydrogenation and indicates that substituent position, rather than the nature of substituent, is the key factor when determining reactivity in the competitive environment.

Significantly, and in contrast to standard *ortho*-cresol hydrogenation, no *cis*-2-methylcyclohexanol was detected during the deuteration of *ortho*-cresol. It is clear that, in the presence of deuterium, neither of the postulated routes of formation for the *cis* isomer, through the enol and ketone intermediates, are available. The continued formation of *trans*-2-methylcyclohexanol indicates that availability of the ketone route may be determined by steric effects, with the addition of deuterium in place of hydrogen making formation of the *trans* isomer more attractive. TPO analysis on the spent, extended-run catalysts showed two additional weight loss events for the *ortho*-cresol, associated with the evolution of carbon dioxide and indicative of the presence of a distinct carbon species resulting from the higher levels of HDO occurring during the *ortho*-cresol hydrogenation reaction.

Hydrogenation of the methoxyphenol substrates gave an order in isomer reactivity of: *meta* > *ortho* > *para*. Notably, both order of reactivity and HDO isomer favourability was in accordance with that found for the dihydroxybenzenes and confirmed that the nature of substituent is fundamental in determining isomer behaviour during individual hydrogenation. The presence of two oxygen-bearing substituents in the methoxyphenol isomers would infer a shared planar mode of adsorption with that postulated for the dihydroxybenzenes. The contrast in behaviour and reactivity of the cresol substrates is a clear indication that the manner of surface adsorption is key in understanding the hydrogenation of these aromatic compounds.

Of great interest, was the absence of any secondary hydrogenation during 4-methoxyphenol hydrogenation; the only instance this was observed throughout our substrate study. We believe that the cross-sectional area of the 4-methoxycyclohexanone is larger than that of the other comparable products throughout this study. The adsorption/desorption kinetics when the bulky methoxy group and hydroxyl group are in the *para* position to one another may be the reason why we see this only with 4-methoxyphenol.

Competitive hydrogenation of methoxyphenol isomers found a significant reduction in reactivity and a shift in order to *ortho* > *para* > *meta*. It can be clearly stated that competition for active sites and surface hydrogen on the catalyst has a detrimental effect on

substrate reactivity. This is unsurprising if we assume Langmuir Hinshelwood kinetics, where the addition of a second [B] and third reactant [C] to the surface coverage equation of reactant [A], would result in the significant decrease in overall reactivity we observed. The clear decrease in reactivity and change in behaviour between the individual and the competitive environment has strong implications for the study of single bio-oil model compounds as a route to understanding the nature of complex bio-oil.

Competitive reactions of the comparable isomers from each substrate group gave similar calculated rate constants of ~ 3 – 4 $min^{-1}x10^{-3}$; comparable to those calculated for the three-isomer combination within each set of substrates. This uniform rate constant, independent of substituent nature and position confirms that competition for limited hydrogen and active sites on the catalyst surface is the major factor influencing reactivity in these competitive situations.

The methoxyphenol isomers recorded the most significant levels of carbon laydown which directly correlated with the nature of its substituent groups. As with both the dihydroxybenzenes and cresols, the extent of observed catalyst deactivation showed a clear correlation with the substituent present on the aromatic ring; increased oxygen content led to higher levels of carbon laydown. The occurrence of carbon laydown under these mild operating conditions highlights that catalyst deactivation is a serious concern during the HDO of bio-oil compounds, and is independent of operating conditions, instead is a consequence of the nature of the compounds present.

Our study of the individual and competitive hydrogenation of oxygen-substituted aromatics has increased our understanding of this important group of compounds in a number of key areas: confirmation of the presence of high levels of HDO under mild operating conditions; how nature and position of substituent affects HDO favourability; the route of product formation for both hydrogenation and HDO; the route of the *trans*-isomer formation; the significant effect on reactivity and the mechanism of product formation in the competitive environment and the occurrence of high levels of carbon laydown. It must be said, however that many questions still need to be answered for us to gain a complete understanding of the complex nature of oxygen-substituted aromatic hydrogenation.

10 Future Work

This study has given us a deeper understanding of oxygen-substituted aromatic hydrogenation; however, a complete picture of these complex reactions does not yet exist. A study of the effect of hydrogen would be particularly beneficial, in both gaining understanding into the relationship between surface hydrogen and reactivity, and to determine if product distribution is affected; in particular if HDO is promoted. Our postulation that the availability of surface hydrogen is fundamental to the significant reduction in reactivity we observe in the competitive environment would be tested if the hydrogen supply was increased during these reactions.

Throughout this study we have focused on a single Rh/SiO_2 catalyst, it would be of interest to ascertain if the high levels of HDO we observe is due to the characterstics of this particular catalyst. It would be of value to test Rh/SiO_2 catalysts with different metal particle sizes to determine what specific properties promote HDO. Further catalytic studies changing the active metal would confirm if this occurrence of HDO at our mild conditions is unique to rhodium.

11 References

[1] Bhatia, S., Hashim, S.S. Catalysts for Biomass Conversion. ACS Catalysis. 2013. (61), 57-77.

[2] He, Z., Wang, X. Catalysis for Sustainable Energy. 2012. (1), 28-52.

[3] Lange, J.P. Biofuels, Bioproducts and Biorefining. 2007, (1), 39-48.

[4] Mortensen, P.M., Grunwaldt, J.D., Jensen, P.A., Knudsen, K.G., Jensen, A.D. Applied Catalysis A: General. 2011. 407, (1–2), 1-19.

[5] Ruijven, B.V., Vuuren, D.P.V. Energy Policy. 2009. 37 (11), 4797–4808.

[6] Balat, M. Energy Conversion and Management. 2011. 52 (2), 795-1574.

[7] Saidi, M., Samimi, F., Karimipourfard, D., Nimmanwudipong, T., Gates, B.C., Rahimpour, M.R. Energy & Environmental Science. 2014. 7 (1), 103-129.

[8] Venderbosch, R.H., Ardiyanti, A.R., Wildschut, J, Oasmaa, A, Heeres, H.J. Journal of Chemical Technology and Biotechnology. 2010. 85 (5), 674-686.

[9] Elkasabia, Y, Mullen, C.A., Pighinelliab, A.L.M.T. Boateng, A.A. Fuel Processing Technology. 2014. 123, 11-18.

[10] Gunawan, R, Li, X, Lievens, C, Gholizadeh, M, Chaiwat, W, Hu, X, Mourant, D, Bromly, J. J, Bromly, Chun-Z,Li. Fuel. 2013. 111, 709-717.

[11] McKendry, P. Bioresource Technology. 2002. 83, 37-46.

[12] Kricka, W., Fitzpatrick, J., Bond, U. Advances in Applied Microbiology. 2015. 92, 89-125

[13] Isikgor, F.H., Becer, C.R. Polymer Chemistry. 2015, 6, 4497-4559.

[14] Campbell, M.M., Sederoff, R.R., Plant Physiology. 1996. 110 (1), 3-13.

[15] Venderbosch, R.H., Ardiyanti, A.R., Wildschut, J., Oasmaa, A. Chemical Technology and Biotechnology. 2010. 85 (5), 674-686.

[16] Ravanchi M.T., Sahebdelfar S. Handbook of Ecomaterials. 2019. 1965-1983.

[17] Reddy Kannapu, H.P., Mullen, C.A., Elkasabi, Y., Boateng, A.A. Fuel Processing Technology. 2015. 137, 220-228.

[18] Senol, O.I., Ryymin, E.M., Viljava, T.R., Krause, A.O.I. Journal of Molecular Catalysis A: Chemical. 2007. 277, 107-112.

[19] Kallury, R.K.M.R, Restivo, W.M., Tidwell, T.T., Boocock, D.G.B., Crimi, A., Douglas, J. Journal of Catalysis. 1985. 96, 535-543.

[20] Lødeng, R., Ranga, C., Rajkhowa, T., Alexiadis, V.I., Bjørkan, H., Chytil, S., Svenum, I.H., Walmsley, J., Thybaut. J.W. Biomass Conversion and Biorefinery. 2017. 7, 343-359.

[21] Bouxin, F., Zhang, X., Kings, I.N., Lee, A.F., Simmons, M.J.H., Wilson, K., Jackson, S.D. Applied Catalysis A. 2017. 539, 29-37.

[22] Boullosa-Eiras, S., Lødeng, R., Bergem, H., Stöcker, M., Hannevold, L., Blekkan, E.A. Catalysis Today. 2014. 223. 43-53.

[23] Elliott, D.C., Neuenschwander, G.G., Hart, T.R., Hu, J., Solana, A.E., Cao, C., D.G.B. Science in Thermal and Chemical Biomass Conversion, CPL Press, Newbury. 2006. 1536-1546.

[24] Cordero-Lanzac, T., Palos, R., Hita, I., Arandes, J.M., Rodríguez-Mirasol, J., Cordero, T., Bilbao, J., Castaño, P. Applied Catalysis B: Environmental. 2018. 239, 513-524.

[25] Alaba, P.A., and Sani, Y.M., and Mohammed, I.Y., and Daud, W.M.A.W. Reviews in Chemical Engineering. 2016, 32 (1), 71-91.

[26] Gutiérrez, A., Arandes, J.M., Castaño, P., Aguayo, A.T., Bilbao, J. Energy Fuels. 2011. 25, 8, 3389-3399.

[27] Furimsky, E., Massoth, F.E. Catalysis Today. 1999. 52, 381-495.

[28] He, Z., Wang, W. Catalysis for Sustainable Energy. 2013. 28-52.

[29] Elliott, D.C. Energy & Fuels. 2007. 21 (3), 1792-1815.

[30] McKendry, P. Bioresource Technology. 2002. 83 (1) 37-46.

[31] Laurent, E., Delmon, B. Journal of Catalysis. 1994. 146 (1), 281-285, 288-291.

[32] Popov, A., Kondratieva, E., Goupil, J.M., Mariey, L., Bazin, P., Gilson, J-P., Travert, A., Maugé, F. Journal of Physical Chemistry. 2010. 114 (37), 15661-15670.

[33] Nerozzi, F. Platinum Metals Review. 2012. 56 (4), 236-241.

[34] Stanislaus, A, Cooper, B.H. Catalysis Reviews-Science and Engineering. 1994. 36, 75-126.

[35] Furimsky, E. Applied Catalysis A: General. 2000. 199 (2), 147-306.

[36] Wenji, S., Liu, A.Y., Baráth, A.E., Zhao, A.C., Lercher, J.A. Green Chemistry. 2015. 17 (2), 1204-1218.

[37] Sabatier, P., Senderens, J.B. Ann. Chim. Phys. 1905. 4, 319–432.

[38] Kistiakowsky, G., Ruhoff, J.R., Smith, H.A., Vaughan, W.E. Journal of the American Chemical Society. 1936. 58(1), 137-145.

[39] Kistiakowsky, G., Ruhoff, J.R., Smith, H.A., Vaughan, W.E. Journal of American Chemical Society. 1936. 58(1),146-153.

[40] Schoenmaker-stolk, M.C., Verwijsj, J.W., Don, J.A., Scholten, J.F. Applied Catalysis. 1987. 29, 73-90.

[41] Siegel, S. "Advances in Catalysis". Academic Press, New York. 1966. p.123.

[42] Hartog, F., Zwietering, P. Journal of Catalysis. 1963. 2, 79-81.

[43] Keane, M., Patterson, P.M. Journal of the Chemical Society, Faraday Transactions. 1996. 92(8), 1413-1421.

[44] Mirodatos, C., Dalmon, J.A., Martin, G.A. Journal of Catalysis. 1987. 105, 405-415.

[45] Smeds, S., Salmi,T., Murzin, D. Applied Catalysis A. General. 1997. 150(115), 115-129.

[46] Donato, A., Neri, G, Pietropaolo, R. Journal of Chemical Technology and Biotechnology 1991, 51(2), 145-153.

[47] Velu, S., Kapoor, M.P., Inagaki, S., Suzuki, K. Applied Catalysis A. General. 2003. 245, 317–331.

[48] Wang,Y., Yao, J., Li, H., Su, D., Antonietti, M. Journal of the American Chemical Society. 2011. 133, 2362–2365.

[49] Coussemant, F., Jungers, J.C. Bull. Soc chim. beiges. 1950. 59, 295.

[50] Shuikin, N.I., Erivanskaya, L.A. Russ. Chem. Rev. 1960. 29, 309.

[51] Arunajatesan, V., McIntosh, S.L., Cruz, M., Renneke, R.F., Chen, B.S. Chemical & Industry. 2005. 104, 195–200.

[52] Smith, H., Stump, B.L. Journal of American Chemical Society. 1961. 83, 2739-2743.

[53] Scirè, S., Crisafulli, C., Maggiore, R., Minicò, S., Galvagno, S. Applied Surface Science. 1996. 93, 309–316.

[54] Taylor, D.R., Ludlum, K.H. Journal of Physical Chemistry.1972. 76, 2882–2886.

[55] Souza, P.M., Rabelo-Neto, R.C., Borges, L.E.P., Jacobs,G., Davis, B.H., Resasco, D.E., Noronha, F.B. ACS Catalysis. 2017. 7 (3), 2058-2073.

[56] Zhu, X., Nie, L., Lobban, L.L., Mallinson, R.G., Resasco, D.E. Energy Fuels. 2014. 28, 4104−4111.

[57] Watson, M.J. Johnson Matthey Technology. 2014. 58, 156−161.

[58] Zhong, J., Chen, J., Chen, L. Catalysis Science and Technology. 2014. 4 (10), 3675-3681.

[59] Alshehri, F. 2017: Ph. D. thesis, University of Glasgow.

[60] Rahaman, M., Vannice, M.A. Journal of Catalysis. 1991. 127, 251-266.

[61] Rahaman, M., Vannice, M.A., Journal of Catalysis. 1991. 127, 267-275.

[62] Stump, B.L. 1959: Ph. D. thesis, Univeristy of Tennessee.

[63] Odebunmi, E., Ollis, D.F. Journal of Catalysis. 1983. 80, 56-64.

[64] Odebunmi, E., Ollis, D.F. Journal of Catalysis. 1983. 80, 76-89.

[65] Song, W., Liu, A.Y., Baráth, E., Zhao, C., Lercher, J.A. Green Chemistry. 2015. 17, 1204-1218.

[66] Ouellette, R.J., Rawn, J.D. Principles of Organic Chemistry. 2015. 5, 133-162.

[67] Toppinen, S., Rantakyla, T-K., Salmi, T., Aittamaa, J. Industrial & Engineering Chemistry Research. 1996. 35 (12), 4424–4433.

[68] Toppinen, S., Rantakyla T-K., Salmi,T., Aittamaa, J, Industrial & Engineering Chemistry Research, 1997. 36 (6), 2101–2109.

[69] Rader, C.P., Smith, H.A., Journal of American Chemical Soceity. 1962. 84 (8), 1443-1449.

[70] Alshehri, F., Weinart, H.M., Jackson, S.D. Reaction Kinetics, Mechanisms and Catalysis. 2017. 122 (2), 699-714.

[71] Bond, G. Metal-Catalysed Reactions of Hydrocarbons. 2005. Springer.

[72] Bond, G., Wells, P.B. Academic Press, Inc,London and New York. 1965. 15, 4, p. 91.

[73] Rooney, J.J. Journal of Catalysis. 1963. 2 (53), 245-251.

[74] Siegel, S., Dunkel, M. Advances in Catalysis. 1957. 23 (4), 15-24.

[75] Massoth, F.E., Politzer, P.,Concha, M.C., Murray, J.S., Jakowski, J., Simon., J. 2006.

The Journal of Physical Chemistry B. 110 (29), 14283-14291.

[76] Shafaghat, H., Rezaei, P.S., Daud, W.M.A.W. Journal of Industrial and Engineering Chemistry. 2016, 35, 268-276.

[77] Nie, L., Resasco, D.E. Journal of Catalysis. 2014. 317, 22−29.

[78] Shin, E.J., Keane. M.A. Applied Catalysis B. 1998.18, 241-250.

[79] Shin, E.J., Keane. M.A. Catalysis Letters. 1999. 58, 141-145.

[80] Shin, E.J., Keane. M.A. Journal of Chemistry Technology Biotechnology. 2000, 75, 159-167.

[81] Romero, Y., Richard, F., Brunet, S. Applied Catalysis B-Environmental. 2010. 98, 213–223.

[82] Zanuttini, M.S., Lago, C.D.,Gross, M.S., Peralta, M.A., Querini, C.A. Industrail Engineering Chemical Research. 2017. 56, 22, 6419-6431.

[83] Li, K., Wang. R., Chen, Journal of Energy Fuels. 2011. 25, 854–863.

[84] Thompson, R.G. 1956: University of Tennessee.

[85] Liu, S., Wang, H., Smith, K.J., Kim, C. S. Energy Fuels. 2017. 31, 6, 6378-6388.

[86] Liu, X., An, W., Wang, A.Y., ,Turner, C.H., Resasco, D.E. Catalysis Science Technology. 2018. 8 (8), 2146-2158.

[87] Wang, X., Zhong, H. Catalysis for Sustainable Energy. 2013. 568, 84-91.

[88] Lin, Y-C., Li, C-L., Wan, H.P., Lee, H.T., Liu, C.F. Energy & Fuels. 2013. 25 (3), 890-896.

[89] Gutierrez, A., Kalia, R.K., Honkela, M.L., Slioor, R., Krause, A.O.I. Catalysis Today. 2009. 147 (3-4), 239-246.

[90] Farkas, A.,Farkas, L. Transactions of the Faraday Society. 1937. 33, 678-690, 837-844.

[91] Horiuti, J., Ogden, G., Polanyi, M. Transactions of the Faraday Society. 1934. 30, 663-665, 1164-1172.

[92] Orozco, J.M., Webb. G. Applied Catalysis. 1983. 6, 67-84.

[93] Harper, R.J., Kembal, C. Journal of the Chemical Society, Faraday Transactions. 1994. 4, 659-665.

[94] Williams, P., Than, C., Rabbani, S., Long, M.A., Garnett, J.L. Journal of Labelled Compounds and Radiopharmaceuticals. 1995, 36(1), 1-14.

[95] Sajiki, H., Aoki, F., Esaki, H., Maegawa, T., Hirota, K. Organic Letters. 2004. 6, 9, 1485-1487.

[96] Hamilton, C.A., Jackson, S.D., Kelly, G.J, Spence, R., Bruin D-de. Applied Catalysis A: General. 2002. 73, 77-82.

[97] Maximov, A., Zolotukhina, A., Murzin, V., Karakhanov, E., Rosenberg, E. ChemCatChem Catalysis. 2015. 7, 1197-1210.

[98] Suresh, S., Srivastava, V.V.C., Mishra, I.M. International Journal of Energy and Environmental Engineering. 2012, 3:32, 1-19.

[99] Bredenberg, J.B., Sarbak. Z. Chemical Technology Biotechnology. 1988. 42, 221-234.

[100] Alshehri, F., Feral1, C., Kirkwood, K., Jackson. S.D. Reaction Kinetics, Mechanisms and Catalysis. 2019, 8-18.

[101] Donato, A., Neri, G., Pietropaolo, R. Journal of Chemical Technology and Biotechnology. 1991, 51(2),145-153.

[102] Antonetti, C., Gallettia, A.M.R., Accorinti, P., Alini, S., Babini, P., Raabovac, K., Rozhko, E., Caldarelli, A., Righi, P., Cavani, F., Concepcion., P. Applied Catalysis A: General. 2013. 466, 21-31.

[103] Smith, H.A., Thompson. R.G. Advances of Catalysis. 1957. 9, 727-732.

[104] Aghapour, A.A, Moussavi, G, Yaghmaeian, K. Journal of Environmental Health Science and Engineering. 2013. 11(3).

[105] Smith, H.A. Annals of the New York Academy of Sciences. 1967. 145(1), 72-82.

[106] Abichndani, C.T., Jatkar, S.K.K. Journal of the Indian Institute Science. 1938. 126 417-441.

[107] Wandas, R., Surygala, J., Śliwka, E. Fuel. 1996. 75(6) 687-694.

[108] Odebunmi, E.O., Ollis. D.F. Journal of Catalysis. 1983. 80 65-75.

[109] Ding, X., Li, L.,Mei-Yu, H., Ying-Yan. J. Polymers for Advanced Technologies. 1999. 10, 116-119.

[110] Gonçalves, V.O.O., Brunet, S., Richard. F. Catalysis Letters. 2006. 146(8),1562-1573.

[111] Rylander, P. Catalytic Hydrogenation over Platinum Metals. 1967.

[112] Murzin, D., Smeds, S., Salmi, T. Reaction Kinetics and Catalysis Letters. 2000. 71(1), 47-54.